Державний вищий навчальний заклад
«Український державний хіміко-технологічний університет»
Міністерства освіти і науки України,

Львівський національний університет імені Івана Франка
Міністерства освіти і науки України

Кваліфікаційна наукова праця на правах наукової доповіді за сукупністю статей

Шмичкова Олеся Борисівна
(прізвище, ім'я, по батькові)

УДК 544.1;544.41, 544.47, 544.65:544.4, 541.13:541.183:541.138
(індекс)

ДИСЕРТАЦІЯ

Електрохімічне формування композитів на основі PbO_2
та їх електрокаталітичні властивості
(назва дисертації)

02.00.04 – фізична хімія
(шифр і назва спеціальності)

02 Хімічні науки
(галузь знань)

Подається на здобуття наукового ступеня доктора хімічних наук

Дисертація містить результати власних досліджень. Використання ідей, результатів і текстів інших авторів мають посилання на відповідне джерело

_____ О.Б. Шмичкова
(підпис, ініціали та прізвище здобувача)

Дніпро – 2022

АНОТАЦІЯ

Шмичкова О.Б. Електрохімічне формування композитів на основі PbO_2 та їх електрокаталітичні властивості. – Кваліфікаційна наукова праця на правах наукової доповіді за сукупністю статей.

Дисертація на здобуття наукового ступеня доктора хімічних наук за спеціальністю 02 Хімічні науки (02.00.04 – фізична хімія). – Державний вищий навчальний заклад «Український державний хіміко-технологічний університет», Дніпро. – Львівський національний університет імені І. Франка, Львів, 2022.

Метою роботи було встановлення загальних закономірностей отримання композитних електрокаталізаторів системи PbO_2-ПАР (полімер) заданого складу, виявлення впливу добавок у електроліт на закономірності осадження, склад, фізико-хімічні властивості, електрокаталітичну активність і селективність композитів у реакціях руйнування ароматичних забруднювачів.

Для одержання осадів плюмбум(IV) оксиду, що переважно складаються із α-фази, був рекомендований 1 М метансульфонатний електроліт, а для отримання покриттів, які складаються переважно із β-фази, – 0,1 М $Pb(NO_3)_2$ + 0.1 М HNO_3 або 0.1 М $Pb(CH_3SO_3)_2$ + 0.1 М CH_3SO_3H. Ці електроліти були вибрані як базові для подальших досліджень. Результати досліджень показали, що перспективнішим для створення композитних матеріалів є оксид, збагачений β-фазою. Наявність поверхнево-активних речовин в цих розчинах одночасно впливає на кінетику нуклеації, як α-, так і β-фази, але не приводить до суттєвої зміни фазового складу. Як правило, ПАР приводять до зменшення констант швидкостей нуклеації обох фаз PbO_2, що також вказує на блокування поверхні адсорбованими добавками.

В роботі перше вивчені закономірності впливу добавок ПАР та полімерів на нуклеацію PbO_2. Так, наприклад, виявлено, що і в нітратних, і в метансульфонатних електролітах за збільшення довжини карбонового ланцюга

аніонних ПАР із високою поверхневою активністю (натрію додецил сульфат та лаурет сульфат) та флуоровмісних спостерігається незначне зменшення вмісту α-фази PbO_2 в межах 10%. За цього мінімальний вміст спостерігається для покриттів PbO_2-натрію лауретсульфат та PbO_2-перфлуорогексансульфонат, що містять 16 та 8 атомів Карбону, відповідно.

Вперше запропоновано експрес-метод напівкількісної оцінки фазового складу покриттів, в основі якого лежить аналіз відновлення утворюваних осадів на інверсійній вольтамперограмі.

Проведено комплексні дослідження впливу аніонних ПАР на кінетику осадження PbO_2 вказують на пригнічення процесу внаслідок адсорбції. За цього ефект залежить як від природи ПАР, так і довжини флуоркарбонового ланцюга. Так, за збільшення довжини флуоркарбонового ланцюга ефект інгібування проявляється більше.

Введення в електроліт осадження ПАР впливає на кінетику електроосадження плюмбум(IV) оксиду, не змінюючи за цього механізму процесу в цілому. За низьких поляризацій процес реалізується із кінетичним контролем, а за високих – швидкість визначає дифузійна стадія доставки іонів плюмбуму до поверхні електрода. Наявність добавки викликає інгібування процесу електроосадження PbO_2 в результаті зменшення числа активних центрів за рахунок адсорбції поверхнево-активних речовин на поверхні зростаючого осаду. За цих умов за застосування в якості добавок ПАР утворюються композити металоксид-ПАР, в яких добавка за рахунок адсорбції впроваджується у зростаючий осад оксиду металу. Отримані дані можна адекватно пояснити на основі ряду гіпотез. З одного боку, всі отримані дані можна адекватно описати за допомогою класичної схеми електроосадження, коли на поверхні зростаючого PbO_2 відбувається адсорбція ПАР, а явище зміни вмісту поліелектроліту в покритті може бути викликане двома факторами: і) гетерогенним та іі) міграційним. З іншого боку, ми не можемо виключити, що не тільки кристалізація відбувається з перенасиченого шару розчину, але й утворюються колоїдні частинки в тій чи іншій кількості, які прилипають до

поверхні зростаючих кристалів. Механізм осадження PbO_2 це не виключає, оскільки проміжні продукти незакріплені, можуть перебувати і в об'ємі розчину і осідати на непровідні поверхні.

В дисертації встановлено вплив полімерів різної природи на кінетику електроосадження PbO_2. Показано, що на відміну від поверхнево-активних речовин, за наявності в електроліті полімера Nafon® спостерігається екстремальна залежність гетерогенної константи швидкості осадження від концентрації добавки, що обумовлено одночасним впливом на кінетику електроосадження ψ` потенціалу та параметру інгібування S.

За наявності в електроліті добавок ПАР та полімерів утворюються композитні покриття PbO_2-ПАР та PbO_2-полімер. Збільшення концентрації ПАР і полімерів в електроліті осадження приводить до росту їх вмісту композиті, що обумовлене збільшенням адсорбції. За однакових умов осадження кількість ПАР в композиті залежить від їх природи і зростає зі збільшенням довжини карбонового ланцюга. В цьому ж ряду зростає їх адсорбція на оксиді. За збільшення анодної густини струму кількість аніонних ПАР і поліелеткролітів, як правило, зростає. Виключенням є лауретсульфат натрію, який за збільшення густини струму (інтенсивності виділення кисню) за рахунок високої поверхневої активності частково перерозподіляється на межу розчин-повітря через газову флотацію. Збільшення температури та концентрації кислоти в електроліті приводить до збільшення вмісту добавок у композиті.

Для одержання композитів складу PbO_2-TiO_2-ПАР запропоновано використовувати суспензійні електроліти, де в якості частинок дисперсної фази виступає TiO_2, а в якості добавки – ПАР. Використання таких розчинів створює можливість одержання композиту зі збільшеною кількістю TiO_2 та ПАР, порівняно з подвійними системами.

Показано, що за використання у якості добавок ПАР і поліелектролітів, а також застосування агрегативно стабільних суспензійних електролітів із нанорозмірними частинками дисперсної фази та ПАР, можна отримувати новітні композитні матеріали (металоксид-ПАР, металоксид-полімер та

потрійні системи PbO_2-TiO_2-ПАР), що суттєво відрізняються за своїм складом. Варіювання складу електроліту осадження, густини струму і температури дозволяє змінювати вміст добавок у композитах від 1 до 18 мас.%, що дає змогу керовано впливати на морфологію, текстуру, фазовий склад, фізико-хімічні властивості, електрокаталітичну активність і селективність електрокаталізаторів на основі PbO_2 у цільових процесах.

В роботі встановлено, що на покритті, що складається практично із α-фази, перенапруга виділення кисню значно менше в результаті більшої гідратованості покриття порівняно з покриттям із більшим вмістом β-фази. Відмінності в кристалографічній орієнтації за фіксованого фазового складу плюмбум(IV) оксиду практично не впливають на кінетику виділення кисню. За характером впливу на реакцію виділення кисню, композитні матеріали з ПАР можна поділити на дві групи: такі, що зменшують перенапругу виділення кисню (з гідрогенкарбоновим ланцюгом) та такі, що збільшують перенапругу виділення кисню (з флуоркарбоновим ланцюгом). В останньому випадку це пов’язано, як і у випадку модифікування PbO_2 атомами Флуору, зі збільшенням міцності зв’язку кисеньвмісних радикалів із поверхнею електрода.

На прикладі модельних сполук було зроблено порівняння електрокаталітичної активності оксидних анодів SnO_2 та PbO_2. Так, було виявлено, що нітрофуразон руйнується ефективніше на PbO_2, завдяки великій кількості оксигеновмісних частинок, міцно зв’язаних із поверхнею оксиду, що характерно для плюмбум(IV) оксиду.

Разом із тим, за наявності хлорид-іонів в електроліті найбільша кількість гіпохлоритної кислоти, що бере участь у вторинних окисних процесах, виробляється на легованому SnO_2, що дозволяє досягти загальної швидкості процесу, зіставлюваної з PbO_2-анодами, та може бути цікавим з точки зору використання таких матеріалів для знезараження лікарняних стоків.

Показано, що SnO_2-електрод не є ефективним електрокаталізатором прямого електрохімічного окиснення забруднювачів, однак його застосування дозволяє на аноді одержати велику кількість гіпохлориту, а також певну

кількість кисню, що за відновлення на катоді приводить до синтезу гідроген пероксиду та утворення додаткової пероксенової системи.

Виявлено, що електрокаталітичну активність PbO_2 можна підвищити за рахунок утворення композитів металоксид-ПАР. Так, наприклад, за використання PbO_2-натрію додецилсульфату константа швидкості руйнування хлорамфеніколу збільшується в кілька разів.

Показано, що зміна фазового складу від α-до β- приводить до збільшення константи швидкості руйнування органічних речовин. За використання запропонованих композитних електрокаталізаторів швидкості руйнування ароматичних забруднювачів зростають у 1,4-2,4 рази. Найефективнішими для використання є електрокаталізатори з флуоровмісними ПАР та полімерами, а також потрійні системи PbO_2-TiO_2-ПАР.

Для інтенсифікації процесу електрохімічного руйнування ароматичних забруднювачів були запропоновані проточні системи з електрохімічним комірками коаксіального типу, що дозволило в 10 разів збільшити швидкість руйнування органічних сполук до досягнення ступеня перетворення в 95%. Враховуючи залежність швидкості руйнування органічних сполук від їх природи та складу композиту пропонується послідовно комбінувати окремі електрохімічні комірки в єдиний модуль.

Ключові слова: плюмбум(IV) оксид; композит; поверхнево-активна речовина; анодний процес; протокова система; фармацевтичний препарат.

ABSTRACT

Shmychkova O. Electrochemical formation of PbO_2-based composites and their electrocatalytic properties. – Scientific report on the basis of research publications.

The doctoral thesis on a specialty 02 Chemical Sciences (02.00.04 – physical chemistry). – Ukrainian State University of Chemical Technology, Dnipro. – Ivan Franko National University of Lviv, Lviv, 2022.

The main regularities of synthesis of PbO_2-surfactant (polymer) composites with a given composition have been established. The effect of additives in the electrolyte on the deposition regularities, composition, physicochemical properties, electrocatalytic activity and selectivity of composites in destruction of aromatic pollutants was identified.

A 1 M methanesulfonate electrolyte was recommended for the production of lead dioxide deposits, mainly consisting of the α-phase, and 0.1 M $Pb(NO_3)_2$ + 0.1 M HNO_3 or 0.1 M $Pb(CH_3SO_3)_2$ + 0.1 M CH_3SO_3H were recommended for the deposition of coatings consisting mainly of the β-phase. These electrolytes were selected as the basis for further research. The results of research have shown that β-phase enriched oxide is more promising for the creation of composite materials. The presence of surfactants in these solutions simultaneously affects the kinetics of nucleation of both α- and β-phases, but does not lead to a significant change in phase composition. As a rule, surfactants lead to a decrease in the rate constants of the nucleation of both phases of PbO_2, which also indicates the blocking of the surface by adsorbed additives.

The regularities of the influence of surfactants and polymers on PbO_2 nucleation are first studied. For example, it was found that there is a slight decrease in α-phase of PbO_2 (10% at the most) in both nitrate and methanesulfonate electrolytes with increasing the length of the carbon chain of anionic surfactants with high surface activity (sodium dodecyl sulfate and laureth sulfate) and fluorine-containing. Therefore, the minimum content is observed for PbO_2-sodium laureth sulfate and

PbO_2-perfluorohexanesulfonate coatings containing 16 and 8 carbon atoms, respectively.

For the first time, an express method of semi-quantitative assessment of the phase composition of coatings was proposed, which is based on the analysis of the composite reduction during the inversion voltammetry.

Comprehensive studies of the effect of anionic surfactants on the kinetics of PbO_2 deposition indicate the inhibition of the process due to adsorption. The effect depends on the nature of the surfactant and the length of the fluorocarbon chain. Thus, with increasing length of the fluorocarbon chain, the inhibitory effect is more pronounced.

The addition of surfactant in the deposition electrolyte affects the kinetics of lead dioxide electrodeposition, without changing the mechanism of the process as a whole. In the low polarizations area, the rate is determined by the kinetic stage of transfer of the second electron, whereas at the high polarizations the diffusion stage of delivery of lead ions to the electrode surface would be rate-determining. The addition of surfactant leads to inhibition of PbO_2 electrodeposition, because of the reduction of the number of active centers due the adsorption of surfactants on the surface of the growing oxide. Under these conditions, when surfactants are added to the deposition solution, metal oxide-surfactant composites are formed, in which the additive is introduced by adsorption into the growing deposit of metal oxide. The obtained data can be adequately explained on the basis of a number of hypotheses. On the one hand, all the data obtained can be adequately described using the classical electrodeposition scheme, when surfactant adsorption occurs on the surface of growing PbO_2, and the phenomenon of changes in surfactant/polyelectrolyte content in the coating can be caused by two factors: i) heterogeneous and ii) migratory. On the other hand, we cannot exclude that not only crystallization occurs from a supersaturated layer of solution, but also colloidal particles are formed in one or another quantity, that adhere to the surface of growing crystals. The mechanism of PbO_2 deposition does not exclude this, as intermediates are not fixed, can be in the solution bulk and settle on non-conductive surfaces.

The influence of polymers of different nature on the kinetics of PbO_2 electrodeposition has been established in the thesis. It is shown that in contrast to surfactants, there is an extreme dependence of the heterogeneous deposition rate constant on the additive concentration due to the simultaneous effect on electrodeposition kinetics both of ψ` potential and inhibition parameter S in the presence of Nafon® polymer.

Composites PbO_2-surfactant and PbO_2-polymer are formed in the presence of surfactant and polymer additives in the electrolyte. Increasing the concentration of surfactants and polymers in the deposition solution leads to an increase in their content in the composite, due to increased adsorption. Under the same deposition conditions, the content of surfactants in the composite depends on their nature and increases with increasing length of the carbon chain. In the same line, their adsorption on the oxide increases. As the anodic current density increases, the content of anionic surfactants and polymers tends to increase. The exception is sodium laureth sulfate, which with the increase in current density (intensity of oxygen evolution) is partially redistributed to the solution-air boundary through gas flotation due to high surface activity. Increasing the temperature and acid concentration in the electrolyte leads to an increase in the content of additives in the composite.

It is proposed to use suspension electrolytes, where TiO_2 acts as particles of the dispersed phase, and surfactants act as an additive in order to obtain triple systems PbO_2-TiO_2-surfactant. The use of such solutions allows one to obtain a composite with an increased amount of TiO_2 and surfactants, compared to dual systems.

It is shown that the use of surfactants and polymers, as well as the use of aggregatively stable suspension electrolytes with nanosized particles of dispersed phase and surfactants, one can get the novel composites (metal oxide-surfactant, metal oxide-polymer and ternary systems PbO_2-TiO_2-surfactant), which differ significantly in their composition. Variation in the composition of deposition electrolyte, current density and temperature allows one to change the content of additives in composites from 1 to 18 wt.%, that enables one to directly affect the

morphology, texture, phase composition, physicochemical properties, electrocatalytic activity and selectivity of PbO_2-based electrocatalysts in target processes.

The thesis finds that the overvoltage of oxygen evolution is much less on a coating consisting of almost α-phase, as a result of greater hydration of the coating compared to the coating with a higher content of β-phase. Differences in crystallographic orientation with a fixed phase composition of lead dioxide have virtually no effect on the kinetics of oxygen evolution. According to the nature of the effect on the oxygen evolution reaction, composite materials with surfactants can be divided into two groups: those that reduce the overvoltage of oxygen (with a hydrocarbon chain) and those that increase the overvoltage of oxygen (with a fluorocarbon chain). In the latter case, this is due, as in the case of modification of PbO_2 by fluorine atoms, with an increase in the strength of the bond of oxygen-containing radicals to the electrode surface.

The electrocatalytic activity of oxide anodes SnO_2 and PbO_2 was compared on the example of model compounds. Thus, nitrofurazone was found to be more efficiently oxidized on PbO_2 due to the large number of oxygen-containing particles strongly bounded to the oxide surface, which is characteristic of lead dioxide.

However, in the presence of chloride ions in the electrolyte, the largest amount of hypochlorous acid involved in secondary oxidative processes is produced on doped SnO_2, which allows one to achieve the overall process rate comparable to PbO_2 anodes, and may be interesting in terms of use such materials for disinfection of hospital effluents.

It has been shown that the SnO_2 electrode is not an effective electrocatalyst for direct electrochemical oxidation of pollutants, but its use as the anode allows one to obtain large amounts of hypochlorous acid and a certain amount of oxygen, which when reduced at the cathode leads to hydrogen peroxide synthesis and additional peroxene system.

It was found that the electrocatalytic activity of PbO_2 can be increased due to the formation of metal oxide-surfactant composites. For example, with the use of

PbO_2-sodium dodecyl sulfate, the rate of destruction of chloramphenicol increases in several times.

It is shown that the change of the phase composition from α-to β- leads to an increase in the rate constant of destruction of organic compounds. With the use of the proposed composites, the rate of destruction of aromatic pollutants increases by 1.4-2.4 times. Electrocatalysts with fluorine-containing surfactants and polymers, as well as ternary PbO_2-TiO_2-surfactant systems, are the most efficient to use.

Flow systems with electrochemical cells of coaxial type were proposed in order to intensify the process of electrochemical destruction of aromatic pollutants, which allowed tenfold increase in the rate of destruction of organic compounds and to achieve a degree of conversion of 95%. Given the dependence of the rate of destruction of organic compounds on their nature and the composition of the composite, it is proposed to consistently combine individual electrochemical cells into a single module.

Keywords: lead dioxide; composite; surfactant; anodic process; flow cell; pharmaceutical.

Список публікацій здобувача

Наукові праці, що розкривають основні наукові результати дисертації

1. **Shmychkova, O**.; Luk'yanenko, T.; Piletska, A.; etc. Electrocrystallization of lead dioxide: influence of early stages of nucleation on phase composition. J. Electroanal. Chem. **2015**, 746, 57-61. (входить до наукометричних баз, що індексуються Scopus, WoS). Видання віднесене до другого квартилю (**Q2**) відповідно до класифікації SCImago Journal. (*Особистий внесок здобувача: планування і проведення досліджень за використання інверсійної вольтамперометрії*, *аналіз початкових стадій кристалізації з адаптацією модельних уявлень про характер нуклеації плюмбум(*IV*) оксиду, узагальнення та інтерпретація результатів, підготовка рукопису до опублікування*. *Дисертанткою був запропонований експрес-метод напівкількісної оцінки*

фазового складу покриттів, в основі якого аналіз потенціалу піків відновлення утворюваних осадів на інверсійній вольтамперограмі).

2. **Shmychkova, O.**; Luk'yanenko, T.; Amadelli, R.; etc. Electrodeposition of Ni^{2+}-doped PbO_2 and physicochemical properties of the coating. J. Electroanal. Chem. **2016**, 774, 88–94. (входить до наукометричних баз, що індексуються Scopus, WoS). Видання віднесене до другого квартилю (**Q2**) відповідно до класифікації SCImago Journal. (*Особистий внесок здобувача: планування і проведення радіохімічних досліджень, узагальнення та інтерпретація результатів, підготовка рукопису до опублікування*).

3. **Шмычкова, О.Б.**; Лукьяненко, Т.В.; Величенко А.Б. Влияние ионов Ni^{2+} на электроосаждение PbO_2. *Вопр. химии и хим. технологии*. **2016**, 3(107). 40–46. (фахове видання). (*Особистий внесок здобувача: планування і проведення кінетичних досліджень, узагальнення та інтерпретація результатів, підготовка рукопису*).

4. **Shmychkova, O.**; Luk'yanenko, T.; Velichenko, A. The influence of early stages of PbO_2 nucleation on its phase composition. Chem. Met. Alloys. **2016**, № 3-4, 99–104. (фахове видання). (*Особистий внесок здобувача: узагальнення та інтерпретація результатів досліджень стосовно фазового складу покриттів*, *підготовка рукопису*).

5. **Шмычкова, О.Б.**; Лукьяненко, Т.В.; Гиренко, Д.В.; та ін. Влияние анионных добавок на закономерности электроосаждения диоксида свинца из нитратных электролитов. *Вопр. химии и хим. технологии*. **2016**, 4(108), 31–37. (фахове видання). (*Особистий внесок здобувача: планування і проведення експерименту, узагальнення та інтерпретація результатів, підготовка рукопису*).

6. **Shmychkova, O.B.**; Luk'yanenko, T.V.; Amadelli, R.; etc. Physicochemical properties of PbO_2 modified with nickel ions. Prot. Met. Phys. Chem. Surf. **2017**, 53, 68–74. (входить до наукометричних баз, що індексуються Scopus, WoS). Видання віднесене до третього квартилю (**Q3**) відповідно до класифікації

SCImago Journal. (*Особистий внесок здобувача: планування і проведення експерименту, інтерпретація результатів, підготовка рукопису*).

7. **Shmychkova, O.**; Luk'yanenko, T.; Velichenko, A. Lead dioxide electrocrystallization from nitrate and methanesulfonate electrolytes: the influence of various dopants on initial stages. ECS Transactions. 2017, 77(11), 1617–1623. (входить до наукометричних баз, що індексуються Scopus та WoS). (*Особистий внесок здобувача: планування і проведення експерименту, інтерпретація результатів, підготовка рукопису*).

8. **Shmychkova, O.**; Knysh, V.; Luk'yanenko, T.; etc. Electrodeposition of composite PbO_2–TiO_2 materials from colloidal methanesulfonate electrolytes. J. Solid State Electrochem. **2017**, 21, 537–544. (входить до наукометричних баз, що індексуються. Scopus, WoS). Видання віднесене до другого квартилю (**Q2**) відповідно до класифікації SCImago Journal. (*Особистий внесок здобувача: планування і проведення досліджень стосовно потрійних композитних систем* PbO_2-TiO_2-*ПАР, узагальнення та інтерпретація результатів, підготовка рукопису до опублікування)*.

9. **Shmychkova, O.**; Luk'yanenko, T.; Velichenko, A. The electrochemical oxidation of 4-nitroaniline and 4-nitrophenol on modified PbO_2-electrodes. Bull. Dnipr. Univ. Ser. Chem. **2017**, 25(1), 27–35. (входить до наукометричних баз, що індексуються WoS). (*Особистий внесок здобувача: планування і проведення експерименту, інтерпретація результатів, підготовка рукопису*).

10. **Shmychkova, O.**; Luk'yanenko, T.; Amadelli, R.; etc. The electrochemical oxidation of salicylic acid and its derivatives on modified PbO_2-electrodes. Bull. Dnipr. Univ. Ser. Chem. **2017**, 25(1), 36–44. (входить до наукометричних баз, що індексуються WoS). (*Особистий внесок здобувача: планування і проведення експерименту, узагальнення та інтерпретація результатів, підготовка рукопису*).

11. Velichenko, A.; Knysh, V.; Luk'yanenko, T.; **Shmychkova, O.** The composition and properties of composite PbO_2–TiO_2 materials electrodeposited from colloidal methanesulfonate electrolytes. Voprosy Khimii i Khimicheskoi Tekhnologii.

2017, 4, 14–20. (входить до наукометричних баз, що індексуються Scopus). (*Особистий внесок здобувача: інтерпретація результатів, підготовка рукопису*).

12. **Shmychkova, O.B.**; Knysh, V.A.; Luk'yanenko, T.V.; etc. Electrocatalytic processes on PbO_2 electrodes at high anodic potentials. Surf. Eng. Appl. Electrochem. **2018**, 54(1), 38–46 (входить до наукометричних баз, що індексуються Scopus та WoS). (*Особистий внесок здобувача: планування і проведення експерименту, узагальнення та інтерпретація результатів, підготовка рукопису (включаючи змістовний переклад).*

13. **Shmychkova, O.**; Luk'yanenko, T.; Dmitrikova, L.; etc. Modified lead dioxide for organic wastewater treatment: Physicochemical properties and electrocatalytic activity. J. Serb. Chem. Soc., **2019**, 84(2), 187–198. (входить у перелік видань, включених до наукометричних баз Scopus та WoS). (*Особистий внесок здобувача: планування і проведення експерименту, узагальнення та інтерпретація результатів, підготовка рукопису*).

14. Luk'yanenko, T.; **Shmychkova, O.**; Dmitrikova, L.; etc. The composition and electrocatalytic activity of composite PbO_2-surfactant electrodes. Voprosy Khimii i Khimicheskoi Tekhnologii. **2019**, 2019(5), 65–70. (входить у перелік видань, включених до наукометричних баз Scopus). Видання віднесене до третього квартилю (**Q3**) відповідно до класифікації SCImago Journal. (*Особистий внесок здобувача: планування і проведення експерименту, узагальнення та інтерпретація результатів, підготовка рукопису*).

15. Luk'yanenko, T.V.; **Shmychkova, O.B.**; Yanova, C.V.; etc. The synthesis and electrocatalytic activity of PbO_2-polyelectrolyte and PbO_2-surfactant composite coatings. J. Chem. Technol. **2019**, 27(1), 92–100. (входить у перелік видань, включених до наукометричних баз Scopus та WoS). (*Особистий внесок здобувача: планування і проведення експерименту, узагальнення результатів, підготовка рукопису*).

16. Velichenko, A.; Luk'yanenko, T.; **Shmychkova, O.** Morphology and phase composition of lead dioxide coatings: Influence of methanesulfonate ions. J. Energy

Storage. **2020**, 30, 101581 (входить до наукометричних баз, що індексуються Scopus та WoS). Видання віднесене до другого квартилю (**Q2**) відповідно до класифікації SCImago Journal. (*Особистий внесок здобувача: планування і проведення досліджень стосовно вибору оптимальних електролітів для електроосадження композитів із заданим фазовим складом, узагальнення та інтерпретація результатів, підготовка рукопису до опублікування)*.

17. Luk'yanenko, T.; **Shmychkova, O.**; Velichenko, A. PbO_2-surfactant composites: electrosynthesis and catalytic activity. J. Solid State Electrochem. **2020**, 24(4), 1045–1056. (входить до наукометричних баз, що індексуються Scopus та WoS). Видання віднесене до другого квартилю (**Q2**) відповідно до класифікації SCImago Journal. (*Особистий внесок здобувача: планування і проведення досліджень стосовно кінетики електроосадження та фізико-хімічних властивостей композитів* PbO_2*-натрію лауретсульфат, узагальнення та інтерпретація результатів, підготовка рукопису до опублікування)*.

18. Velichenko, A.; Luk'yanenko, T.; **Shmychkova, O.** Lead dioxide-SDS composites: design and properties. J. Electroanal. Chem. **2020**, 873, 114412 (входить до наукометричних баз, що індексуються Scopus та WoS). Видання віднесене до другого квартилю (**Q2**) відповідно до класифікації SCImago Journal. (*Особистий внесок здобувача: планування і проведення досліджень стосовно електросинтезу та застосування композитів* PbO_2*-натрію додецилсульфат, узагальнення та інтерпретація результатів, підготовка рукопису до опублікування)*.

19. Velichenko, A.; Luk'yanenko, T.; Shmychkova, O.; etc. Electrosynthesis and catalytic activity of PbO_2-fluorinated surfactant composites. J. Chem. Technol. Biotechnol. **2020**, 95(12), 3085–3092. (входить до наукометричних баз, що індексуються Scopus та WoS). Видання віднесене до другого квартилю (**Q2**) відповідно до класифікації SCImago Journal. (*Особистий внесок здобувача: планування і проведення досліджень щодо закономірностей синтезу композитів металоксид-ПАР із флуорокарбоновим ланцюгом, узагальнення та інтерпретація результатів, підготовка рукопису до опублікування)*.

20. Velichenko, A.; Luk'yanenko, T.; Nikolenko, N.; **Shmychkova, O.**; etc. Composite Electrodes PbO_2-Nafion®. J. Electrochem. Soc. **2020**, 167(6), 063501. (входить до наукометричних баз, що індексуються Scopus та WoS). Видання віднесене до першого квартилю (**Q1**) відповідно до класифікації SCImago Journal. (*Особистий внесок здобувача: планування і проведення досліджень стосовно встановлення закономірностей електроосадження та фізико-хімічних властивостей композитів металоксид-поліелектроліт, узагальнення та інтерпретація результатів, підготовка рукопису до опублікування)*.

21. **Shmychkova, O.**; Zahorulko, S.; Luk'yanenko, T.; etc. Electrochemical oxidation of chloramphenicol with lead dioxide–surfactant composites, Water Environ. Res. **2021**, 93(11) 2716–2726 (входить до наукометричних баз, що індексуються Scopus та WoS). Видання віднесене до третього квартилю (**Q3**) відповідно до класифікації SCImago Journal. (*Особистий внесок здобувача: планування експерименту стосовно електроокиснення модельної сполуки за використання електрокаталізатора* PbO_2*-натрію додецилсульфат у водних розчинах різного складу, узагальнення результатів, підготовка рукопису*).

22. Knysh, V; **Shmychkova, O.**; Luk'yanenko, T.; etc. Electrosynthesis and characterization of lead dioxide–perfluorobutanesulfonate composite, Voprosy Khimii i Khimicheskoi Tekhnologii, **2021**, 2021(5), 68–76. (входить до наукометричних баз, що індексуються Scopus). Видання віднесене до третього квартилю (**Q3**) відповідно до класифікації SCImago Journal. (*Особистий внесок здобувача: планування і проведення експерименту, узагальнення результатів, підготовка рукопису*).

23. **Shmychkova, O.**; Zahorulko, S.; Girenko, D.; etc. Material selection and optimization of conditions for electrooxidation of nitrofurazone: A comparative study of tin and lead dioxides. J. Electrochem. Soc., **2021**, 168(8), 086507. (входить до наукометричних баз, що індексуються Scopus та WoS). Видання віднесене до першого квартилю (**Q1**) відповідно до класифікації SCImago Journal. (*Особистий внесок здобувача: планування експерименту стосовно окиснення*

фурациліну як модельної сполуки за використання різних електродних матеріалів, узагальнення результатів, підготовка рукопису).

24. Velichenko, A.; **Shmychkova, O.**; Samiolo, L.; etc. Reduction of nitroaromatics on cadmium sulfide: further probing the electrochemical model of semiconductor photocatalysis. J. Solid State Electrochem. **2021**, 25(1), 85–92. (входить до наукометричних баз, що індексуються Scopus та WoS). Видання віднесене до другого квартилю (**Q2**) відповідно до класифікації SCImago Journal. (*Особистий внесок здобувача: планування експерименту стосовно вибору та можливості застосування фотокаталізаторів для окиснення нітроароматичних сполук, узагальнення та інтерпретація результатів, підготовка рукопису*).

25. Velichenko, A.B.; Luk'yanenko, T.V.; **Shmychkova, O.B.**; etc. New approaches to the creation of nanocomposite anode materials based on PbO_2: a review. Theor. Exp. Chem. **2021**, 57(5), 331–342. (входить до наукометричних баз, що індексуються Scopus та WoS). Видання віднесене до третього квартилю (**Q3**) відповідно до класифікації SCImago Journal. (*Особистий внесок здобувача: запропоновано оригінальний підхід до створення новітніх нанокомпозитних анодних матеріалів на основі плюмбум(*IV*) оксиду*, *узагальнення результатів, підготовка рукопису*).

26. **Shmychkova, O.**; Girenko, D.; Velichenko, A. Noble metals doped tin dioxide for sodium hypochlorite synthesis from low concentrated NaCl solutions. J. Chem. Tech. Biotech. **2022**, 97(4), 903–913. (входить до наукометричних баз, що індексуються Scopus та WoS). Видання віднесене до другого квартилю (**Q2**) відповідно до класифікації SCImago Journal. (*Особистий внесок здобувача: планування експерименту стосовно дослідження матеріалів для електрохімічного синтезу кисеньвмісних окисників, що утворюються в процесі електролізу водних розчинів різного складу, узагальнення результатів рентгенівської фотоелектронної спектроскопії, підготовка рукопису*).

Публікації, що засвідчують апробацію матеріалів дисертації

1. **Shmychkova, O.**; Luk’yanenko, T.; Velichenko, A. Kinetic regularities of lead dioxide electrocrystallization. In ECS Meeting*: abstracts*, Honolulu, Hawaii (USA), 2016, 3594. (*Здобувач встановила закономірності електрокристалізації*, *підготувала тези до друку)*.

2. **Shmychkova, O.**; Luk’yanenko, T.; Velichenko, A. The influence of ionic dopants on initial stages of lead dioxide electrocrystallisation. *Перспективні матеріали та процеси в технічній електрохімії*: монографія / В. З. Барсуков, Ю. В. Борисенко, О. А. Букет, В. Г. Хоменко; за заг. ред. В. З. Барсукова. – К.: КНУТД, 2016. – С. 199-204. ISBN 978-966-7972-61-5. (*Здобувач встановила закономірності електрокристалізації*, *виступила з доповіддю на конференції*).

3. **Шмичкова, О.**; Лук'яненко, Т.; Величенко, О. Складові малоізношувані аноди з активним шаром на основі PbO_2. В матеріалах Всеукр. наук.-практ. конф. [*«Актуальні проблеми хім. та хім. технол.»*, К.: НУХТ, 2016, 35–36. (*Здобувач здійснила електрохімічний синтез електродів*, *підготувала тези до друку)*.

4. **Shmychkova, O.**; Luk’yanenko, T.; Velichenko, A. Influence of early stages of PbO_2 nucleation on the phase compostion. In proceedings XIII Intern. conf. on crystal chem. of intermetallic compounds: abstracts, Lviv, 2016, 109. (*Здобувач вивчила нуклеацію покриттів*, *виступила з доповіддю на конференції*).

5. **Шмичкова, О.Б.**; Лук’яненко, Т.В. Електрохімічна руйнація токсичних органічних речовин ароматичної природи − забруднювачів водного середовища. В матеріалах XX міжнар. наук.-техн. конф. [«*Технологія*-2017»], Сєвєродонецьк, 2017, 147–149. (*Здобувач спланувала та провела експеримент*, *підготувала тези до друку)*.

6. **Шмичкова, О.Б.**; Манзюк, М.В.; Мурашевич, Б.В. Електрохімічне окиснення саліцилової кислоти на модифікованих PbO_2-анодах. В матеріалах VIII міжнар. наук.-техн. конф. [«*Хімія та сучасні технології*»], Дніпро, 2017, 56–57. (*Здобувач спланувала та провела експеримент*, *виступила з доповіддю на конференції*).

7. **Shmychkova, O.**; Luk’yanenko, T.; Knysh, V. Electrochemical oxidation of toxic organic aromatic substances. In Promising materials and processes in applied electrochemistry: monograph / editor-in-chief V. Z. Barsukov. – Kyiv: KNUTD, 2017. – Part. – P. 207-213. (ISBN 978-966-7972-79-0). (*Здобувач спланувала та провела експеримент*, *виступила з доповіддю на конференції*).

8. **Shmychkova, O.**; Luk'yanenko, T.; Velichenko, A. Lead dioxide electrocrystallization from nitrate and methanesulfonate electrolytes: the influence of various dopants on initial stages. In ECS Meet. Abstr. – 2017 MA2017-01(38): 1807. (*Здобувач встановила закономірності електрокристалізації*, *підготувала тези до друку)*.

9. **Shmychkova, O.**; Luk’yanenko, T.; Velichenko, A. The influence of various dopants on initial stages of lead dioxide electrocrystallization from nitrate and methanesulfonate electrolytes. In Lead-*Acid Batteries LABAT’2017*, Albena: LabatScience, 2017, 257–290. (входить до наукометричних баз, що індексуються **Scopus**). (*Здобувач встановила закономірності електрокристалізації*, *підготувала тези до друку)*.

10. **Shmychkova, O.**; Luk’yanenko, T.; Velichenko, A. Lead dioxide based oxide-surfactant composites. In ECS Meeting: abstracts, Atlanta, GA (USA), 2019, 826. (*Здобувач вивчила властивості покриттів* PbO_2-*ПАР*, *підготувала тези до друку)*.

11. **Шмичкова, О.Б.**; Лук’яненко, Т.В.; Книш, В.О.; та ін. Вплив флуоровмісних поверхнево-активних речовин та поліелектролітів на закономірності електроосадження PbO_2. В *Електрохімія сьогодення: здобутки, проблеми, перспективи*: збірник наукових праць IX Українського з’їзду з електрохімії за участю закордонних вчених, причвячений 90 річниці від дня заснування Інституту загальної та неогрганічної хімії ім В.І. вернадського НАН України, Київ, 2021, 42–43. (*Здобувач встановила вплив довжини флуорокарбонового ланцюга на властивості композитів*, *виступила з доповіддю на конференції*).

ЗМІСТ

ПЕРЕЛІК УМОВНИХ ПОЗНАЧЕНЬ, СИМВОЛІВ, ОДИНИЦЬ, СКОРОЧЕНЬ І ТЕРМІНІВ

ВС – вихід за струмом

ДВНЗ УДХТУ – Державний вищий навчальний заклад “Український державний хіміко-технологічний університет”

ККМ – критична концентрація міцелоутворення

НАН України – Національна академія наук України

ОДЕ – обертовий дисковий електрод

ПАГ – поліаміногуанідин

ПАР – поверхнево-активна речовина

ПЕ – поліелектроліт

РВК – реакція виділення кисню

РФС – рентген фотоелектронна спектроскопія

СЕМ – скануюча електронна мікроскопія

ЦВА – циклічна вольтамперограма

EDX – Energy Dispersive X-ray Spectroscopy (енергетично-дисперсійна рентгенівська спектроскопія)

SLES – натрію лауретсульфат

SDS – натрію додецилсульфат

ВСТУП

Створення матеріалів із заданими функціональними властивостями є основним завданням сучасної фізичної хімії та хімічного матеріалознавства. Електрохімічні методи відрізняються від існуючих своєю дешевизною та умовною безреагентністю, завдяки чому для реалізації процесів немає потреби в створенні інфраструктури та в постачанні реактивів в місця обробки стічних вод.

Можливість застосування тих або інших оксидних систем за високих анодних потенціалів визначатиметься їх відповідністю загальним експлуатаційним вимогам, що висуваються до електродів і забезпечують високу швидкість та селективність цільового процесу. Відсутність універсального анодного матеріалу вимагає створення нових підходів до управління функціональними властивостями каталізатора.

У загальному випадку електрокаталітична активність електрода залежить від досить великого числа факторів, які можна об'єднати в дві великі групи: хімічні (які визначаються складом матеріалу) і структурні (що визначаються будовою). Взагалі, для оцінки електрокаталітичної активності матеріалу структурні та хімічні фактори необхідно розділити, що зробити вкрай важно, оскільки ці фактори є взаємозалежними. Структура матеріалу, як правило, пов’язана з його хімічним складом. Так, наприклад, зміна хімічного складу покриття приводитиме до зміни морфології, фазового складу, текстури.

На жаль, не існує можливостей створення універсального анодного матеріалу, який можна використати для всіх процесів. Оптимальна стратегія під час розробки нових анодів полягає у виборі базового матеріалу, що задовольняє загальним експлуатаційним вимогам (задовільна електропровідність, тривалий ресурс роботи, доступність і прийнятна вартість), із наступним створенням на його основі активного шару електрокаталізатора відповідно до вимог конкретних цільових процесів (висока електрокаталітична активність і

селективність). Таким матеріалом може бути PbO_2, який, як відомо, є одним із найбільш широко застосовуваних електрокаталізаторів для реакцій, що реалізуються за участі кисеньвмісних радикалів.

За високих анодних потенціалів більшість процесів, таких як виділення кисню і озону, окиснення неорганічних і органічних речовин, проходять через початкову стадію утворення кисеньвмісних частинок радикального типу, адсорбованих на поверхні електрода. Оскільки такі процеси описуються механізмами, що включає як мінімум одну однакову стадію, зокрема, першу стадію утворення адсорбованих гідроксил-радикалів, їх умовно об'єднують в одну велику групу, яка називається реакціями з перенесенням кисню.

Беручи до уваги таке розмаїття процесів, потрібно певним чином впливати на швидкість цільового процесу. Не завжди вдається селективно впливати тільки на один процес, оскільки вони не являються повністю незалежними. Типовими процесами, що реалізуються у водних розчинах на фоні виділення кисню, є окиснення органічних сполук і синтез сильних окисників (озон і гіпохлоритна кислота, тощо), які сильно залежать від природи каталізатора. Зміна швидкості навіть одного з цих процесів впливатиме на селективність цільового процесу.

Спроби прогнозування каталітичної активності змішаних чи модифікованих оксидів до сих пір не мали успіху. Необхідно відзначити, що інформативність різноманітних кореляцій між швидкістю реакції та фізико-хімічними властивостями електрокаталізатора є досить низькою. Це зумовлено низкою обставин, зокрема, відсутністю достовірної інформації про механізми реакцій та природу лімітуючих стадій, що реалізуються на різних електродах. Іншою перепоною є відсутність експериментальної можливості виділення впливу лише одного фактора в чистому вигляді навіть за проходження реакцій за однаковим механізмом. Наприклад, практична неможливість відокремлення хімічних та структурних факторів один від одного вимагає отримання достовірних експериментальних даних про закономірності проходження досліджуваних процесів за різних умов, і вплив умов формування

електрокаталізатора з його фізико-хімічні властивості, тобто. виникає класична тріада: умови отримання – склад та властивості матеріалу – електрокаталітична активність.

Вирішення цієї проблеми значно ускладнюється як відсутністю єдиної теорії електрокаталізу, так і методології керованого синтезу електрокаталізаторів із високою електрокаталітичною активністю та селективністю в цільових процесах. Таким чином, виконання даної роботи є необхідним і актуальним.

Зв'язок роботи з науковими програмами, планами, темами. Робота виконана автором особисто на кафедрі фізичної хімії ДНВЗ «Український державний хіміко-технологічний університет» впродовж 2014-2022 років, згідно з планами науково-дослідних робіт ДВНЗ «Український державний хіміко-технологічний університет», завданнями держбюджетних науково-дослідних робіт Міністерства освіти і науки України: «Нанокомпозиційні оксидні електрокаталізатори для процесів окиснення за участю оксигенвмісних радикалів»; номер держреєстрації 0112U002062 (2012-2014 рр.); «Фізико-хімічні методи одержання функціональних матеріалів», номер держреєстрації 0114U002802 (2014-2018 рр.); «Керований синтез металоксидних матеріалів із прогнозованими властивостями», номер держреєстрації 0115U003160 (2015-2017 рр.); «Композиційні каталізатори комбінованого типу в проточних системах для застосування в зонах локальних конфліктів», номер держреєстрації 0116U001490 (2016-2018 рр.); «Електрохімічна руйнація токсичних органічних речовин ароматичної природи – забруднювачів водного середовища», номер державної реєстрації 0116U006896 (2016-2018 рр.); «Керований електрохімічний синтез композиційних матеріалів металоксид-поверхнево-активна речовина», номер державної реєстрації 0118U003397 (2018-2020 рр.); «Каталітичне руйнування залишків фармацевтичних препаратів у проточних системах», номер державної реєстрації 0121U109529 (2021-2022 рр.) та Національного фонду досліджень України «Умовно безреагентні

системи обробки лікарняних стоків», номер державної реєстрації 0120U104861 (2020-2021 рр.).

Мета і задачі дослідження. Мета роботи – встановлення загальних закономірностей отримання композитних електрокаталізаторів системи PbO_2-ПАР (полімер) заданого складу, виявлення впливу добавок у електроліт на закономірності осадження, склад, фізико-хімічні властивості, електрокаталітичну активність і селективність композитів у реакціях руйнування ароматичних забруднювачів.

Для досягнення мети необхідно вирішити наступні задачі:

− виявити вплив ПАР та полімерів різної природи на закономірності електрокристалізації та кінетику електроосадження PbO_2;

− встановити закономірності утворення композитів металоксид-ПАР і металоксид-полімер і визначити фактори керування складом композитів;

− оцінити вплив хімічного складу на фізико-хімічні властивості матеріалів на основі PbO_2, а також електрокаталітичну активність і селективність у процесах окиснення за високих анодних потенціалів;

− визначити оптимальний склад електролітів та умови електролізу для ефективного руйнування ароматичних забруднювачів.

Вирішення цих задач сприятиме розвитку теорії електрокаталізу та дозволить розробити композитні матеріали металоксил-ПАР та металокисд-полімер для практичного використання в процесах руйнування ароматичних забруднювачів.

Об'єкт дослідження: електрокаталітичні процеси, що проходять на композитних електрокаталізаторах на основі PbO_2 за високих анодних потенціалів із участю кисеньвмісних частинок.

Предмет дослідження: кінетичні закономірності електроосадження композитів PbO_2-ПАР (полімер), фізико-хімічні властивості отриманих матеріалів, закономірності виділення кисню та окиснення органічних сполук на досліджуваних композитах.

Методи дослідження: стаціонарна, циклічна, інверсійна вольтамперометрія, вольтамперометрія з лінійною розгорткою потенціалу, хронопотенціометрія, хроноамперометрія, метод електродного імпедансу, метод обертового дискового електрода (вивчення кінетики електрохімічних процесів); фотоколориметрія, флуоресцентна та спектрофотометрія в УФ та видимій областях, атомно-абсорбційна спектроскопія, високоефективна рідинна хроматографія (аналіз складу розчинів); скануюча електронна та атомно-силова мікроскопії, рентгенівська дифракція, енергодисперсійна рентгенівська та фотоелектронна спектроскопія (характеристика морфології, структури та хімічного складу оксидних покриттів); статистичний метод (обчислення та статистична обробка результатів).

Наукова новизна одержаних результатів. У роботі вперше отримані комплексні дані про вплив поверхнево-активних речовин і полімерів на кінетику електрохімічного формування матеріалів на основі PbO_2. Запропоновано експрес-метод напівкількісної оцінки фазового складу тонких шарів оксиду, що утворюється на металічному колекторі струму, в основі якого аналіз відновлення утворюваних осадів на інверсійній вольтамперограмі.

Вперше вивчено кінетику осадження композитів за наявності в електроліті осадження ПАР, показано, що ефект інгібування осадження PbO_2 проявляється більше зі збільшенням довжини флуор-карбонового ланцюга. Вперше виявлено нетиповий ефект збільшення константи швидкості гетерогенної реакції окиснення Pb^{2+} залежно від концентрації полімера в розчині, пов'язаний із одночасною дією потенціала в площині локалізації активованого комплекса і параметра інгібування.

Уперше встановлені фактори керування складом композитних матеріалів PbO_2-ПАР, PbO_2-полімер, PbO_2-TiO_2-ПАР. Вивчено вплив складу композитів на реакцію виділення кисню. Отримано систематичні дані стосовно окиснення вибраних лікарських препаратів і сполук фенольного типу.

Практичне значення одержаних результатів. Розроблені електрокаталізатори новітнього типу PbO_2-ПАР, PbO_2-полімер, PbO_2-TiO_2-ПАР.

Для інтенсифікації процесу руйнування ароматичних забруднювачів запропоновано використання електрокаталізаторів в проточних системах, що дозволяє скоротити час перетворення в 10 разів.

Створено наукові та експериментальні основи технології отримання композитних матеріалів металоксид-ПАР, металоксид-полімер, PbO_2-TiO_2-ПАР.

Особистий внесок здобувача. Здобувач особисто здійснила пошук і аналіз наукової літератури за темою дисертації. Визначила та обґрунтувала методи наукових досліджень. Автором самостійно здійснено більшість експериментальних досліджень, статистичну обробку отриманих даних. Спільно з чл.-кор. НАН України, д.х.н., професором О. Б. Веліченком поставлено мету та задачі дослідження, сплановано експериментальні дослідження, проаналізовано отримані результати, сформульовано висновки. Автор висловлює йому свою глибоку вдячність. Частину експериментальних досліджень було виконано в Університеті Ферари (Італія) в відділенні Інституту органічного синтезу та фотокаталізу Національної Ради з досліджень (ISOF-CNR) у рамках програми Міністерства освіти і науки України № 221250 «Навчання, стажування, підвищення кваліфікації студентів, аспірантів, науково-педагогічних та педагогічних працівників за кордоном». Під час здійснення цих досліджень науково-консультативну допомогу надавав професор Росано Амаделлі (керівник відділення ISOF-CNR в Університеті Ферари). Дослідження за використання методів рентгенівського спектрального аналізу були проведені в міжфакультетській науково-навчальній лабораторії рентгеноструктурного аналізу та центрі колективного користування науковим обладнанням “Лабораторія матеріалознавства інтерметалічних сполук”, що є структурними підрозділами Львівського національного університету імені Івана Франка. Тут консультаційну допомогу з інтерпретації отриманих результатів надавали акад. НАН України, д.х.н., проф. Р. Є. Гладишевський , к.х.н. та доцент П.Ю. Демченко. Здобувач висловлює подяку співавторами публікацій: професорам д.х.н. Т.В. Лук’яненко, д.х.н. М.В. Ніколенку, д.х.н. Д.В. Гиренку; доцентам к.х.н. Л.В. Дмітріковій та к.х.н. В.О. Книш. Автор брала участь у

формулюванні наукового напряму, постановці мети і завдань, виконання експериментальних досліджень, інтерпретації результатів кваліфікаційної роботи на здобуття наукового ступеня доктора філософії Загорулько Світлани Юріївни. З наукових праць, опублікованих у співавторстві, в дисертаційній роботі використано тільки ті ідеї та здобутки, що являються особистим внеском здобувача.

Апробація результатів дисертації. Основні результати дисертації доповідались і обговорювались на XX, міжнар. наук.-техн. конф. «Технологія-2017», Сєвєродонецьк, 2017; V міжнар. конф. студентів, аспірантів та молодих вчених «Хімія та хімічні технології», Київ, 2014; Lead-Acid Batteries LABAT'2017, Golden Sands, 2017 (входить у перелік видань, включених до наукометричних баз Scopus); VIII міжнар. конф. студ., аспір. та мол. вчених «Хімія та сучасні технології», Дніпро, 2017; ECS Meeting: abstracts Honolulu, Hawaii, 2016, New Orlean, LA, 2017, Atlanta, GA, 2019 (USA); Всеукр. наук.-практ. конф. «Актуальні проблеми хім. та хім. технол.», Київ, 2016; XIII Intern. conf. on crystal chem. of intermetallic compounds, Lviv, 2016; IX Українському з'їзді з електрохімії Київ, 2021.

Публікації. За матеріалами дисертації опубліковано 37 наукових робіт, із них 3 у наукових фахових виданнях України, 23 у зарубіжних наукових журналах, проіндексованих міжнародною наукометричною базою даних Scopus та/або WoS та 11 тез доповідей на наукових конференціях різного рівня. В цих роботах наявні 11 публікацій, які розкривають основні результати дисертації, у виданнях, віднесених до першого і другого квартилів (Q1 і Q2) та 4 публікації у виданнях, віднесених до третього квартилю (Q3), відповідно до класифікації SCImago Journal.

Структура дисертації. Дисертаційна робота є кваліфікаційною науковою працею на правах наукової доповіді за сукупністю статей, викладена на 283 друкованих сторінках та має наступні основні структурні елементи: вступ, огляд літератури, матеріали та методи досліджень, аналіз і узагальнення результатів досліджень (викладено в 5 розділах), висновки, перелік

використаних джерел. Розділами дисертації є публікації здобувача наукового ступеня в журналах високого рівня. Список використаної літератури включає 797 найменувань, з них 58 – за виключенням джерел, наведених у публікаціях здобувача. Робота без урахування наведеного в публікаціях містить 3 таблиці та 33 рисунки та схеми.

РОЗДІЛ 1
ОГЛЯД ЛІТЕРАТУРИ

Велика кількість публікацій присвячена дослідженням мікромодифікованих діоксидносвинцевих покриттів із поліпшеними характеристиками. Утворення таких матеріалів відбувається шляхом використання іонних добавок, що впроваджуються в оксид під час його електроосадження шляхом іонного обміну. До того ж добавки підбираються за ознакою спорідненості іонних розмірів і зарядів. У загальному випадку вміст іонних добавок в електроосадженому PbO_2 менше, ніж 1 мас.%. Підвищення кількості добавки приводить до утворення композиційних PbO_2-матеріалів, які додатково містять оксиди (утворені за участі іонної добавки) в якості окремої фази. Спосіб формування композитного матеріалу за рахунок використання іонних добавок є обмеженим, оскільки в цьому випадку потенціали формування оксиду матриці та частинок дисперсної фази мають бути близькими, що важко реалізувати на практиці. Частіше такі матеріали одержують із суспензійних електролітів, де в якості частинок дисперсної фази використовують частинки металів або їх сполуки (оксиди, гідроксиди, карбіди), а також органічні речовини – поверхнево-активні речовини (ПАР), поліелектроліти та полімери. Головною проблемою такого способу електроосадження композитів є агрегативна нестійкість суспензійних електролітів навіть за нанорозмірних частинок дисперсної фази, а також зміна їх складу впродовж навіть незначного терміну зберігання. За використання цих розчинів процес осадження може бути реалізований тільки в умовах перемішування, що приводить до значних флуктуацій складу та товщини покриттів, особливо у випадку використання складнопрофільних колекторів струму. Таким чином, найбільш цікавими для практичного застосування під час одержання різноманітних композитних матеріалів на основі PbO_2 є агрегативно стійкі суспензійні електроліти, у складі яких знаходяться нанорозмірні частинки оксидів в якості дисперсної фази, або ПАР та полімери. Такі системи є доволі перспективними, а дослідження в

цьому напрямі не були систематизовані в інших публікаціях на відміну від одержання мікромодифікованих і композитних матеріалів на основі PbO_2 з класичних суспензійних електролітів. Значна увага також буде приділена новітнім композитам системи PbO_2-ПАР (полімер).

Основні результати розділу опубліковано в огляді автора [1].

DOI 10.1007/s11237-022-09709-6
Theoretical and Experimental Chemistry, Vol. 57, No. 5, November, 2021 (Ukrainian Original Vol. 57, No. 5, September-October, 2021)

NEW APPROACHES TO THE CREATION OF NANOCOMPOSITE ANODE MATERIALS BASED ON PbO_2: A REVIEW

A. B. Velichenko, T. V. Luk'yanenko, O. B. Shmychkova, and V. O. Knysh UDC 541.138; 544.653.1

An original approach to the creation of new nanocomposite anode materials based on PbO_2 and to the processes of composite formation due to the influence of selective adsorption of valve metal oxides and different types of surfactants on both electrochemical and colloid-chemical processes in the near-electrode zone is considered. It is shown that variation of deposition electrolyte composition, current density, and temperature allows one to change the content of additives in composites and to provide control of morphology, texture, phase composition, physicochemical properties, electrocatalytic activity, and selectivity of electrocatalysts based on PbO_2 in target processes.

Keywords: *anode materials, electrodeposition, nanocomposites, PbO_2, suspension electrolytes, surfactants, polyelectrolyte.*

INTRODUCTION

Directed synthesis of new or modified functional materials with predicted properties is one of the most important tasks of chemical materials science. Despite a variety of existing methods for obtaining materials, electrochemical ones are the most attractive both in terms of synthesis control and cost-effectiveness. This applies, in particular, to the production of various oxide electrocatalysts. Requirements for anode materials can be divided into two groups: general operational (developed surface, satisfactory electrical conductivity, long service life, availability, and reasonable cost) and specific used in particular target process (electrocatalytic activity and selectivity) [1].

Unfortunately, there is no possibility of creating a universal anode material that can be used in all technologies considering the latter. An optimal strategy in the development of new anodes includes the selection of base material that meets the general operational requirements, followed by the formation of an active layer of electrocatalyst on its basis in accordance with the particular process requirements. Electrochemical modification and/or formation of a composite coating appears to be the most rational approach to changing the electrocatalytic activity and selectivity of base coating. PbO_2-based materials attract a great deal of attention of researchers due to satisfactory corrosion resistance, low cost, and high electrocatalytic activity in reactions that are carried out at high anode potentials [2].

Aqueous perchlorate, acetate, borofluoride, lead, and nitrate solutions of Pb(II) are used as the most common basic electrolytes for deposition of PbO_2-based materials. At the same time, traditional electrolytes used in deposition of Pb(IV) oxide-based materials have numerous disadvantages such as inability to change texture, morphology, and phase composition of deposits in a wide range, as well as to obtain coatings of considerable thickness with satisfactory mechanical properties. Over the last few decades, there is a practical possibility of using methanesulfonic acid-based electrolytes that are characterized by

Ukrainian State University of Chemical Technology, Dnipro, Ukraine. E-mail: velichenko@ukr.net. Translated from Teoretychna ta Eksperymentalna Khimiya, Vol. 57, No. 5, pp. 284-293, September-October, 2021. Received September 2, 2021; accepted October 25, 2021.

0040-5760/21/5705-0331

unique properties, such as specific adsorption on metal oxides, as well as the effect on water structure and nature of adsorbed oxygen-containing particles in the surface layer at high anode potentials [3, 4], thus providing new opportunities for controlled synthesis of PbO_2-based materials of a given chemical and phase composition with the required functional properties [2, 5, 6]. It should be noted that it seems logical to implement technology innovations using modern chemistry approaches considering the presence of only industrial production of lead batteries in Ukraine.

A large number of publications are devoted to a study of micro modified lead-dioxide coatings with improved characteristics [7-24]. The formation of such materials requires the use of ionic additives that are introduced into oxide during its electrodeposition by ion exchange. In addition, additives are selected on the basis of ionic size and charge affinity. In general, the content of ionic additives is less than 1 wt.% in electrodeposited PbO_2. The increase in the amount of additive leads to the formation of composite PbO_2 materials, which additionally contain oxides (formed with the participation of ionic additives) as a separate phase [25]. The deposition method of composite material is limited when using ionic additives, since the deposition potentials of oxide matrix and particles of a dispersed phase must be close in this case, which is difficult to implement in practice. Usually, such materials are obtained using suspension electrolytes, where metal particles or their compounds (oxides, hydroxides, and carbides) are used as particles of the dispersed phase [26-36], as well as organic substances, such as surfactants, polyelectrolytes, and polymers [37 -40].

The main issue of electrodeposition of composites includes aggregate instability of suspension electrolytes even with nanosized particles of the dispersed phase and changes in their composition during a short service life. The deposition process can be realized only under mixing conditions when using these solutions, which leads to significant fluctuations in the composition and thickness of coatings, especially in the case of complex profile current collectors. Therefore, aggregatively stable suspension electrolytes are the most interesting for practical application in the production of various PbO_2-based composite materials, which contain nanosized oxide particles as dispersed phase [41], or surfactants and polymers. Since these systems are quite promising, they are the subject of this review. Research in this area has not been systematized in other publications in contrast to the production of PbO_2-based micro modified and composite materials using traditional suspension electrolytes. The latest composites of PbO_2-surfactant (polymer) system attract a great deal of attention.

SUSPENSION ELECTROLYTES WITH HIGH AGGREGATE STABILITY

The colloid-chemical properties of suspension solutions were studied in order to create electrolytes with high aggregate stability, in which the dispersed phase particles were obtained directly in solution by Ti(IV)-isopropylate hydrolysis [42]. The sizes of colloidal TiO_2 particles do not differ and are 12 nm in solutions of nitric and methanesulfonic acids of 0.1 mol/dm^3. It should be noted that their size does not change over time, and solutions retain aggregate stability for a long time.

According to the potentiometric measurements, the pH_0 of TiO_2 is 5.6 in nitrate medium, which is much less when compared to particles of commercial titanium(IV) oxide (6.4). Such data indicate a difference in the particle properties obtained by hydrolysis, their smaller size and charge in acid solution when compared to commercial materials. The pH_0 is shifted to the alkaline region by 0.3 units in the presence of methanesulfonate ions, which indicates the specific adsorption nature of $CH_3SO_3^-$ ions [42, 43]. The dispersed phase particles are positively charged regardless of the acid nature at a concentration of 0.1 mol/dm^3. It should be noted that the increase in the acid concentration (both nitric and methanesulfonic) to 1 mol/dm^3 leads to a significant increase in particle size with gradual sedimentation.

The addition of lead nitrate or methanesulfonate at a concentration of 0.1 mol/dm^3 to the solution increases particle size of the dispersed phase by 2 nm, which does not change over time during a long period of storage. However, a further increase in the concentration of Pb^{2+} ions to 0.5 mol/dm^3 leads to the destruction of colloidal solutions due to an increase in their size and sedimentation, which is caused by adsorption of Pb^{2+} ions on TiO_2 particles [41-43].

There is a significant increase in particle size (more than an order of magnitude) when sodium dodecyl sulfate is added to the solution. Thus, the particle size increases and reaches 179 nm in the first day of investigation. Despite such a significant increase in the particle size, solutions partially retain aggregate stability for several days. The observed effect is caused by the adsorption of sodium dodecyl sulfate on oxide [27].

Therefore, nitrate and methanesulfonate suspension electrolytes with a concentration of acid and Pb^{2+} ions of 0.1 mol/dm^3 aggregate stability, as well as an average particle size of 14 nm of the dispersed phase, are of significant interest for the production of Pb(IV) oxide-based composite materials.

ELECTROCRYSTALLIZATION OF PbO_2-BASED SYSTEMS

Crystallization process kinetics and crystal structure nature of the formed oxide depend on nucleation rate, linear crystallization rate, and their ratio. These parameters can be determined by current transients of electrodeposition process of PbO_2. According to Gonzalez–Garcia's conception, it is possible to determine the nucleation nature by analyzing the initial stages of crystallization [44, 45]. The ratio of the maximum current to the quasi-stationary value indicates the predominant geometric shape of the formed nuclei. The difference in peak and plateau currents of a chronoamperogram indicates the ratio between constants of nucleation rates to the electrode surface in the parallel and perpendicular directions. Three main geometric shapes of nuclei are considered in the formation of oxides: hemispheroid, cone, and cylinder. The conical shape of crystals is preferable when analyzing crystallization of Pb(IV) oxide using nitrate electrolytes on the surface of glassy carbon [46-48].

The Abyaneh kinetic model was chosen to describe the initial formation steps of a new phase of Pb(IV) oxide [49-53] since it provides a more complete description and concept of the growth mechanism of the new phase of lead(IV) oxide and allows one to determine the kinetic parameters of nucleation for α- and β-phase. This model provides a good description of the crystallization process under kinetic control of the initial formation stages of the new PbO_2 phase. The growing part of a current transient is insensible to the crystal growth geometry, thus determining the kinetic parameters of 2D nucleation of nuclei. The formation of two phases (α and β) is possible in the process of electrodeposition of Pb(IV) oxide. Coating electrodeposition begins with the formation of the α-phase, and only then the formation of the β-phase or the deposition of two phases occurs simultaneously. The crystallization of Pb(IV) oxide is realized via a progressive mechanism using methanesulfonate electrolytes at all deposition potentials.

The predominant growth of one phase over another is possible depending on the composition of an electrolyte, as well as complete overlap and absorption of growing sites of one phase [54-56]. The formation of one of the phases detains behind the other. The nature of the delayed phase depends on deposition conditions. There is a slight predominance in growth of the α-phase of PbO_2 at low polarization. The α-phase begins to detain in growth in the case of high polarization, while there is an overlap and absorption of the growing sites of the α-phase by β-phase crystals on the surface of an electrode. Analysis of the data obtained in nitrate and methanesulfonate electrolytes showed significant differences in deposition currents despite the similar concentration of lead ions in the solution. This unusual effect can probably be explained by the change in the nature of discharged particles. The electrode surface will receive a more positive charge when deposition potential is increased, which should contribute to the fixation of particles with the opposite sign on the surface. The change in particle charge should facilitate the crystallization of Pb(IV) oxide on the positively charged electrode surface in the case of methanesulfonate electrolytes when compared to nitrate solutions. The nature of nucleation is progressive in all cases. However, cylinder is the predominant form of crystals in 2D nucleation in the case of methanesulfonate electrolyte, while the formation of crystals occurs in the form of cones for nitrate electrolyte. Thus, the nucleation constants of the α- and β-phases of PbO_2 differ slightly for nitrate electrolyte, while there is a predominance in the formation of the α-phase of PbO_2 in the case of methanesulfonate electrolyte (Table 1).

It should be noted that the electrode material on which oxides are deposited and the preparation of its surface before deposition of coating significantly affects the processes of crystal formation. Comparison of the parameters of the initial stages of crystallization of the process was performed on a platinum electrode and on the Pb(IV) oxide surface. There is an increase in the intensity of deposition current during deposition of Pb(IV) oxide on a PbO_2 supporter; at the same time, a very short induction period of crystallization is also observed. Stationary deposition current can be seen on the chronoamperogram after 40 s, the value of which coincides in both cases. Crystallization occurs according to the progressive mechanism described in

TABLE 1. Parameters of Initial Stages of Pb(IV) Oxide Crystallization

Deposition electrolyte	t_α, s	K_α, mol·m^{-2}·s^{-4}	t_β, s	K_β, mol·m^{-2}·s^{-4}
0.1 M $Pb(NO_3)_2$ + 1 M HNO_3	0.84	$4.34 \cdot 10^{-5}$	1.95	$3.85 \cdot 10^{-4}$
0.1 M $Pb(NO_3)_2$ + 1.0 M HNO_3 + $3 \cdot 10^{-5}$ M SDS	3.03	$3.26 \cdot 10^{-6}$	7.87	$1.1 \cdot 10^{-5}$
0.1 M $Pb(NO_3)_2$ + 1.0 M HNO_3 + $7 \cdot 10^{-5}$ M SDS	2.35	$1.08 \cdot 10^{-5}$	6.31	$3.3 \cdot 10^{-5}$
0.1 M $Pb(CH_3SO_3)_2$ + 1 M CH_3SO_3H	0.88	$1.23 \cdot 10^{-5}$	1.07	$7.44 \cdot 10^{-7}$
0.1 M $Pb(CH_3SO_3)_2$ + 1 M CH_3SO_3H + $3 \cdot 10^{-5}$ M SDS	1.51	$6.38 \cdot 10^{-6}$	2.81	$1.04 \cdot 10^{-5}$
0.1 M $Pb(CH_3SO_3)_2$ + 1 M CH_3SO_3H + $7 \cdot 10^{-5}$ M SDS	0.84	$1.38 \cdot 10^{-6}$	1.08	$8.22 \cdot 10^{-6}$

Note. SDS is sodium dodecyl sulfate, $C_{12}H_{25}O_4SNa$.

[45] for all studied cases. Cylinder is the predominant form of crystals in 2D nucleation on the surface of Pb(IV) oxide, while the formation of nuclei in the form of cones is possible in the case of platinum.

Crystallization also occurs according to the progressive mechanism in the presence of surfactants in methanesulfonate electrolytes. The progressive mechanism changes to instantaneous for nitrate electrolytes when surfactant concentration is increased [57-59]. Hemispheroid is the predominant form of crystals in 2D nucleation in the presence of additives in nitrate electrolytes, while cylinder is the predominant form of crystals in the case of methanesulfonate electrolytes. The main parameters of Pb(IV) oxide crystallization depending on the presence of surfactants in electrolytes are given in Table 1.

Studies of the PbO_2 electrocrystallization regularities were also performed in nitrate and methanesulfonate suspension electrolytes containing Ti(IV) oxide particles [60, 61]. The nature of the chronoamperograms is determined by electrode potential.

A long induction period is observed in the case of nitrate electrolyte at low polarization (E = 1.4 V), which is followed by a very slow increase in current reaching a stationary value. This indicates a slow accumulation of intermediates and kinetic control of crystallization process of Pb(IV) oxide. An increase in polarization by 50 mV (E = 1.45 V) leads to a sharp decrease in the duration of the induction period. A blurred maximum (I_p) is observed on the I-t curve until steady current (I_s) is reached, which indicates the appearance of diffusion complications during crystallization. A slight difference between I_p and I_s indicates a mixed diffusion-kinetic control of crystallization process. There is almost no induction period on the chronoamperograms during the transition to high polarization (E = 1.55 V). There is a maximum current that is several times higher than the I_s value. There is a clear diffusion control of oxide crystallization process in this case. The main parameters of crystallization of Pb(IV) oxide-based composite are given in Table 2. According to the obtained data, the β-phase is predominant in growth during crystallization from suspension electrolytes. It should be noted that the ratio between the α- and β-phase growth depends on the electrode polarization. This effect of the dispersed phase particles is probably due to the imposed geometry of TiO_2 crystals, which are considered as additional crystallization sites.

The main parameters of Pb(IV) oxide crystallization using methanesulfonate suspension electrolytes with different number of particles of the dispersed phase are given in Table 3. The crystallization rate of Pb(IV) oxide increases on the platinum electrode in the presence of colloidal TiO_2; while the content of the latter increases up to 1 g/L. The effect of dispersed phase particles is insignificant when the concentration is above 2 g/L. The β-phase is predominant in growth in all studied cases. It should be noted that the ratio between kinetic growth constants of the α- and β-phase crystals changes depending on the number of particles of the dispersed phase. The observed effect can be caused by several factors: the first one is associated with an increase in the actual area of electrode (the appearance of additional sites where PbO_2 crystallization can take place); the second one is associated with an increase in the surface concentration of lead ions due to the adsorption of the latter on TiO_2. The formation of additional reaction sites is also possible, in which adsorbed oxygen-containing particles such as OH_{ads} can participate in PbO_2 formation [62].

TABLE 2. Parameters of Initial Stages of Pb(IV) Oxide Crystallization Using Suspension Electrolyte

E, V	t_α, s	K_α, mol·m^{-2}·s^{-4}	t_β, s	K_β, mol·m^{-2}·s^{-4}
1.4	1.24	$3.58\cdot10^{-7}$	3.64	$2.1\cdot10^{-6}$
1.45	1.05	$8.56\cdot10^{-7}$	2.76	$7.3\cdot10^{-6}$
1.55	0.39	$1.08\cdot10^{-6}$	1.22	$1.18\cdot10^{-5}$
1.55	0.73	$3.52\cdot10^{-6}$	2.92	$1.47\cdot10^{-5}$

Note. 1-3 are 0,1 M HNO_3 + 0,1 M $Pb(NO_3)_2$ + 5 g/dm^3 TiO_2; 4 is 0,1 M $Pb(CH_3SO_3)_2$ + 0,1 M CH_3SO_3H + 5 g/dm^3 TiO_2.

TABLE 3. Parameters of Initial Stages of Pb(IV) Oxide Crystallization Using Methanesulfonate Electrolytes (E = 1.6 V)

Deposition electrolyte	t_α, s	K_α, mol·m^{-2}·s^{-4}	t_β, s	K_β, mol·m^{-2}·s^{-4}
0.1 M $Pb(CH_3SO_3)_2$ + 0.1 M CH_3SO_3H	0.54	$3.4\cdot10^{-5}$	1.65	$1.02\cdot10^{-4}$
0.1 M $Pb(CH_3SO_3)_2$+ 0.1 M CH_3SO_3H + 0.5 g/L TiO_2	1.06	$2.16\cdot10^{-4}$	1.42	$4.18\cdot10^{-4}$
0.1 M $Pb(CH_3SO_3)_2$ + 0.1 M CH_3SO_3H + 1 g/L TiO_2	0.84	$9.4\cdot10^{-5}$	1.25	$2.96\cdot10^{-5}$
0.1 M $Pb(CH_3SO_3)_2$ + 0.1 M CH_3SO_3H + 2 g/L TiO_2	0.84	$3.8\cdot10^{-5}$	1.24	$1.64\cdot10^{-5}$
0.1 M $Pb(CH_3SO_3)_2$ + 0.1 M CH_3SO_3H + 3 g/L TiO_2	0.98	$2.84\cdot10^{-5}$	1.36	$2.94\cdot10^{-5}$
0.1 M $Pb(CH_3SO_3)_2$ + 0.1 M CH_3SO_3H + 4 g/L TiO_2	0.81	$2.46\cdot10^{-5}$	1.14	$8.47\cdot10^{-5}$
0.1 M $Pb(CH_3SO_3)_2$ + 0.1 M CH_3SO_3H + 5 g/L TiO_2	0.92	$3.7\cdot10^{-6}$	1.42	$2.17\cdot10^{-5}$

CHARACTERISTICS OF ELECTRODEPOSITION OF PbO_2-BASED COMPOSITES IN THE PRESENCE OF ADDITIVES

The most complete kinetic scheme of electrooxidation of Pb^{2+} ions, which explained the whole set of available experimental data within a single mechanism, was proposed in [62-65]. The mechanism of Pb(IV) oxide formation is shown in the form of a four-stage kinetic scheme

$$H_2O \rightarrow OH^{\cdot}_{ads} + H^+ + e^-, \quad (1)$$

$$Pb^{2+} + OH^{\cdot}_{ads} \rightarrow Pb(OH)^{2+}, \quad (2)$$

$$Pb(OH)^{2+} + H_2O \rightarrow Pb(OH)_2^{2+} + H^+ + e^-, \quad (3)$$

$$Pb(OH)_2^{2+} \rightarrow PbO_2 + 2H^+. \quad (4)$$

Primarily, the first electron is transferred with the formation of $OH^{\cdot}_{ads}$ oxygen-containing particles on the electrode surface by anodic ionization of water (1). Then these particles react with lead ions in the next chemical stage (2), forming Pb(III) oxygen-containing intermediate that is not fixed on the electrode surface, which is further (3) oxidized with the transfer of the second electron. Soluble intermediate compounds of tetravalent lead accumulate as a result of this reaction, which decompose in the last stage (4) with the formation of Pb(IV) oxide [63].

The limiting stage of the PbO_2 electrodeposition process is mostly determined by several factors: deposition potential (current density) and electrode surface state, concentration of Pb^{2+} ions in solution, and hydrodynamic conditions of the process. Kinetic control of the process is usually realized at low anode polarization ($E \leq 1.6$ V). The electrodeposition rate is limited by the Pb(II) delivery stage to the electrode surface during transition to the high anodic polarization region ($E \geq 1.6$ V).

The main differences between nitrate solutions and suspension electrolytes based on them include overvoltage reduction in anode process. The obtained data show the effect of Ti(IV) oxide nanoparticles on the characteristics of PbO_2 electrocrystallization and are consistent with the results of electrocrystallization. The increase in the electrodeposition rate in suspension electrolytes is caused by adsorption of lead ions on Ti(IV) oxide. As a result, there is an additional transport mechanism of Pb^{2+} ions to the electrode surface and crystallization of Pb(IV) oxide, which can additionally occur in the bulk of the near-electrode region. This can formally be considered an increase in the specific surface area of electrode. The possibility of formation of additional reaction sites should be considered, consisting of oxygen-containing particles such as $OH^{\cdot}_{ads}$, which are located on the TiO_2 surface and can participate in the formation of PbO_2 [62]:

$$TiO_2 - OH + OH^{\cdot} = TiO_2 - O^{\cdot} + H_2O. \quad (5)$$

This mechanism provides description of the obtained experimental results on electrodeposition of Pb(IV) oxide using nitrate and methanesulfonate suspension electrolytes, and explains the process rate increase in the presence of dispersed phase particles that do not have their own electrochemical activity, such as TiO_2. The obtained data also expand the previously proposed colloid-electrochemical formation mechanism of composite coatings, which is based on the formation of colloidal PbO_2 particles in the near-electrode region [61].

The dependence of the rate constant of the second electron transfer stage on the concentration of Nafion® polymer additive is extreme in the electrolyte [66, 67]. The maximum is observed at a polyelectrolyte concentration of $3 \cdot 10^{-3}$%, where the rate constant reaches a value of $33 \cdot 10^{-4}$ m/s. The rate constant increases by almost an order of magnitude when compared to the electrolyte, which does not contain additives (Table 4). It is necessary to analyze the effect of adsorption on the process rate in order to explain this nonstandard dependence, which can be described by an equation [66].

$$\frac{i_\theta}{i_{\theta=0}} = (1 - \theta) \exp(-S\theta) \exp\left[-\frac{(z + \beta n)F\Delta\psi'(\theta)}{RT}\right]. \quad (6)$$

The decrease in the potential value in the localization plane of ψ' active complex will increase the rate of the charge transfer stage, which is observed in reality at low concentrations of polymer additive in electrolyte. The ψ' value is able to significantly decrease and even become negative when adsorbing anionic polyelectrolyte on the electrode surface by recharging the electric double layer; which is proved by the change in electrokinetic potential of PbO_2 from positive to negative when Nafion® is added to the electrolyte. It should be noted that the increase in the rate constant is not a common effect and is observed only for anionic polyelectrolyte due to the significant negative charge on the polyelectrolyte molecule.

The inhibition parameter S reflects both electrostatic and chemical interaction of the activated complex with the adsorption layer. A further increase in the volume concentration of additive in the electrolyte leads to an increase in the degree of filling of the electrode surface и with adsorbed Nafion®, thus reducing the rate of the charge transfer stage by blocking the active sites. An inhibitory effect is observed when using anionic surfactants as additives (Table 4) [57-59].

TABLE 4. Pd^{2+} Electro-oxidation Reaction Rate Constants in the Presence of Anionic Surfactants

Composition of deposition electrolyte	Reaction rate constant, $k_s \cdot 10^4$, m/s
0.1 M HNO_3 + 0.1 M Pb^{2+}	4.1
0.1 M HNO_3 + 0.1 M Pb^{2+} + 0.00003 M SDS	4.0
0.1 M HNO_3 + 0.1 M Pb^{2+} + 0.00007 M SDS	4.0
0.1 M HNO_{3i} + 0.1 M Pb^{2+} + 0.0002 M SDS	3.8
0.1 M HNO_3 + 0.1 M Pb^{2+} + 0.00003 M $C_{16}H_{29}O_6SNa$	3.9
0.1 M HNO_3 + 0.1 M Pb^{2+} + 0.00005 M $C_{16}H_{29}O_6SNa$	3.8
0.1 M HNO_3 + 0.1 M Pb^{2+} + 0.0001 M $C_{16}H_{29}O_6SNa$	3.7
0.1 M HNO_3 + 0.1 M Pb^{2+} + 0.00003 M $C_4F_9O_3SK$	3.8
0.1 M HNO_3 + 0.1 M Pb^{2+} + 0.0003 M $C_4F_9O_3SK$	3.6
0.1 M HNO_3 + 0.1 M Pb^{2+} + 0.003 M $C_4F_9O_3SK$	3.5

COMPOSITION OF PbO_2-BASED COMPOSITE MATERIALS DEPENDING ON ELECTRODEPOSITION CONDITIONS

According to the proposed kinetic scheme (1)-(5), which describes the electrodeposition of Pb(IV) oxide using suspension electrolytes, there is a high probability of introduction of dispersed phase particles into a growing precipitate with the formation of a composite material. The composite is a PbO_2 matrix in which additive particles are dispersed.

Formation models and mechanisms of a composite coating have been developed for suspension electrolytes that contain particles of a dispersed phase of micron size [26]. Most theories involve the delivery of particles of the dispersed phase to the electrode surface and their inclusion in the composite coating by one of four possible options: electrophoresis, mechanical capture, adsorption, and convective diffusion. There have been few attempts to obtain Pb(IV) oxide-based composite coatings using suspension electrolytes that contain submicron and micron-size dispersed phase particles [27-35]. Such suspension electrolytes are not aggregatively stable, and therefore, the deposition is carried out under conditions of convective diffusion.

Systems with suspension electrolytes of aggregate stability containing nanosized titanium(IV) oxide as dispersed phase particles have been considered [42, 43]. The TiO_2 content in a composite is determined by delivery stages of dispersed phase particles from the electrolyte bulk to the electrode surface by means of diffusion and/or migration and their interaction with the anode surface. The electrode surface charge is positive, since the value of the zero charge potential of lead(IV) oxide in 0.1 M HNO_3 is 0.9 ± 10.1 V (SCE) at deposition potentials greater than 1.5 V. Despite the positive charge of TiO_2 in electrolyte, dispersed phase particles are included in the growing coating, which may indicate a small contribution of the migration component and electrostatic repulsion in the near-electrode region.

The curve describing the content of the dispersed phase in the composite depending on current density can be divided into two regions (Fig. 1). In the first one, the deposition process of Pb(IV) oxide is controlled by the kinetic stage; at the same time, the current increases when the potential is higher [43]. This increases the capture probability of colloidal TiO_2 particles, while its content increases in the composite (Fig. 1, region I). In the second one, the TiO_2 content remains almost constant in coating as soon as the deposition rate reaches the limit value in the diffusion region (Fig. 1, region II).

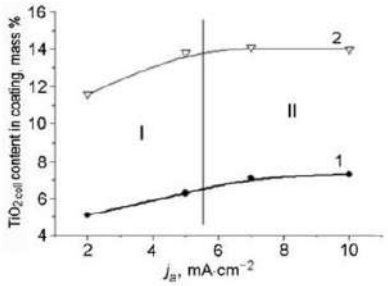

Fig. 1. The amount of TiO_2 in the composite coating depending on anode current density in electrolytes: 0.1 M $Pb(NO_3)_2$ + 0.1 M HNO_3 + 5.0 g/dm^3 $TiO_{2\,coll}$ (1); 0.1 M $Pb(CH_3SO_3)_2$ + 0.1 M CH_3SO_3H + 5.0 g/dm^3 $TiO_{2\,coll}$ (2).

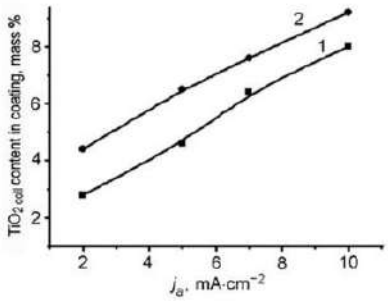

Fig. 2. The amount of TiO_2 in the composite coating depending on anode current density in coatings deposited from electrolytes: 0.1 M $Pb(NO_3)_2$ + 0.1 M HNO_3 + 2 g/L $TiO_{2\,coll}$ + $3\cdot10^{-4}$ M $C_{12}H_{25}SO_4Na$ (1); 0.1 M $Pb(NO_3)_2$ + 0.1 M HNO_3 + 5 g/L $TiO_{2\,coll}$ + $3\cdot10^{-4}$ M $C_{12}H_{25}SO_4Na$ (2).

It should be noted that the replacement of nitrate electrolyte with methanesulfonate leads to a significant increase in the content of TiO_2 under other identical conditions (Fig. 1). The observed effect is caused by a decrease in the charge of discharged particles and a decrease in the electrode surface due to the adsorption of methanesulfonate ions.

A similar effect, but less pronounced, is observed when anionic surfactant (sodium dodecyl sulfate) is added to nitrate suspension electrolyte. The adsorption of surfactants on the surface of electrode and particles of the dispersed phase leads to a decrease in the positive charge similar to methanesulfonate electrolytes. Thus, the forces of electrostatic repulsion decrease, which make it difficult to introduce particles of the dispersed phase into the composite. In this case, the negatively charged TiO_2-surfactant particles move to the positively charged anode under the action of electrophoretic forces, where they are included in the growing coating. The content of Ti(IV) oxide particles increases in composite material in the presence of surfactants when current density is increased (Fig. 2); however, the concentration of Ti(IV) oxide does not reach the limit value in the coating. In this case, TiO_2 is delivered not only by diffusion but also by migration, the rate of which increases continuously when polarization is increased.

According to the obtained data (Figs. 2 and 3), an increase in the concentration of Ti(IV) oxide in deposition electrolyte leads to an increase in its content in the composite. The observed effect is caused by the increase in the concentration gradient of oxide particles of the dispersed phase when its content is increased in suspension electrolyte. A similar situation is observed in

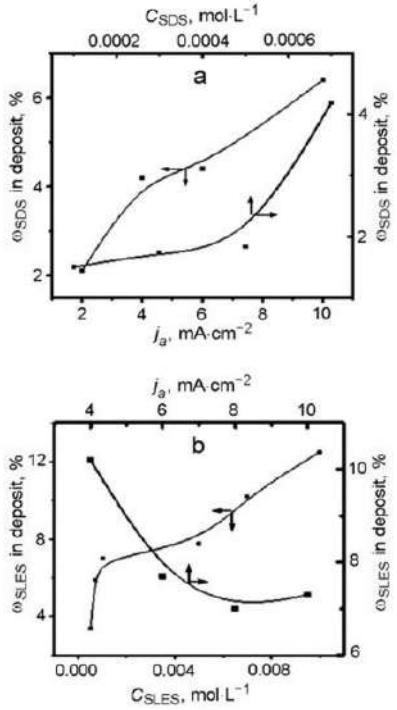

Fig. 3. Dependence of the amount of additive in the composite on its concentration in the deposition electrolyte and current density: a) $C_{12}H_{25}O_4SNa$ (SDS); b) $C_{16}H_{29}O_6SNa$ (SLES).

methanesulfonate electrolytes. For example, its content is 7% in the composite when the concentration of TiO_2 is 2 g/L in electrolyte, while it is 14% at 5 g/L (anode current density 10 mA/cm^2).

There is also an increase in the number of dispersed phase particles in coating when the solution temperature is increased. For example, the content of the dispersed phase particles is 27% in the composite obtained from methanesulfonate electrolyte at a temperature of 55°C; while it is only 15% when using nitrate (concentration of TiO_2 is 5.0 g/dm^3 in suspension electrolyte, anode current density is 10 mA/cm^2). The observed effect of increased content of titanium(IV) oxide in the composite when temperature is increased is caused by a decrease in the electrolyte viscosity, which facilitates the diffusion of the dispersed phase particles to the electrode surface. According to the obtained data, the content of TiO_2 in composites obtained from methanesulfonate electrolytes under similar conditions significantly exceeds the values that can be obtained using nitrate solutions.

Composites are formed when surfactants and polyelectrolytes are used as additives [68]. The increase in the concentration of surfactants and polymers in deposition electrolyte leads to an increase in their content in the composite (Figs. 3 and 4), which is caused by the increase in adsorption. Under the similar deposition conditions, the amount of surfactants in the composite depends on their nature and increases in the following sequence: $C_4F_9SO_3K < C_{12}H_{25}O_4SNa < C_{16}H_{29}O_6SNa$. Their adsorption on oxide increases in the same sequence. The number of anionic surfactants and polyelectrolytes, as a rule, increases when anode current density is increased. The exception is sodium laureth sulfate, which is partially redistributed to the solution-air boundary through gas flotation when the current density is increased (oxygen evolution intensity) due to high surface activity.

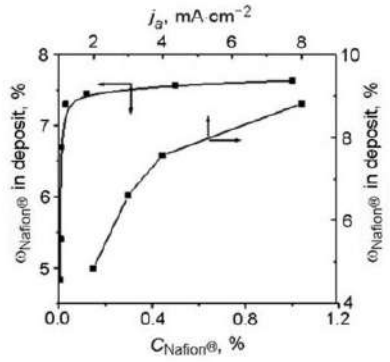

Fig. 4. Dependence of the amount of Nafion® in the composite on the concentration of additive in the deposition electrolyte and current density.

TABLE 5. Effect of Deposition Conditions on Nafion® Content in PbO_2

Deposition conditions	Nafion® in PbO_2, mass %
0.1 M HNO_3 + 0.1 M Pb^{2+} + 0,05% Nafion®	7.6
1 M HNO_3 + 0.1 M Pb^{2+} + 0,05% Nafion®	10.2
2 M HNO_3 + 0.1 M Pb^{2+} + 0.05% Nafion®	13.1
3 M HNO_3 + 0.1 M Pb^{2+} + 0.05% Nafion®	16.9

Note. The deposition temperature is 25°C; $j_a = 4$ mA/cm^2.

The increase in temperature and acid concentration in electrolyte leads to an increase in the content of additives in the composite (Table 5) [68].

Therefore, it is possible to obtain composite materials that differ significantly in their composition when using surfactants and polyelectrolytes as additives, as well as aggregatively stable suspension electrolytes with nanosized particles of the dispersed phase. The change in deposition electrolyte composition, current density, and temperature allows one to alter the content of additives in composites from 1 to 27%, thus, affecting morphology, texture, phase composition, physicochemical properties, electrocatalytic activity, and selectivity of PbO_2-based electrocatalysts in target processes.

REFERENCES

1. S. Trasatti, *Electrochim. Acta*, **29**, No. 11, 1503-1512 (1984).
2. X. Li, D. Pletcher, and F. C. Walsh, *Chem. Soc. Rev.*, **40**, 3879-3894 (2011).
3. A. P. Sandoval, M. F. Suarez-Herrera, V. Climent, et al., *Electrochem. Commun.*, **50**, 47-50 (2015).
4. M. D. Gernon, M. Wu, Th. Buszta, et al., *Green Chem.*, **1**, 127-140 (1999).
5. A. B. Velichenko, R. Amadelli, E. V. Gruzdeva, et al., *J. Power Sources*, **191**, 103-110 (2009).

6. A. Velichenko, T. Luk'yanenko, and O. Shmychkova, *J. Energy Storage*, **30**, Art. 101581 (2020).
7. A. Velichenko, T. Luk'yanenko, L. Dmitrikova, et al., *J. Serb. Chem. Soc.*, **84**, No. 2, 187-198 (2019).
8. A. B. Velichenko, D. V. Girenko, S. V. Kovalyov, et al., *J. Electroanal. Chem.*, **454**, Nos. 1-2, 205-210 (1998).
9. A. B. Velichenko, R. Amadelli, G. L. Zucchini, et al., *Electrochim. Acta*, **45**, 4341-4350 (2000).
10. D. Rosestolato, R. Amadelli, and A. B. Velichenko, *J. Solid State Electrochem.*, **20**, No. 4, 1181-1190 (2016).
11. A. B. Velichenko, R. Amadelli, E. A. Baranova, et al., *J. Electroanal. Chem.*, **527**, 56-64 (2002).
12. R. Amadelli and A. B. Velichenko, *J. Serb. Chem. Soc.*, **66**, No. 11-12, 835-845 (2001).
13. O. Shmychkova, T. Luk'yanenko, A. Velichenko, et al., *Electrochim. Acta*, **111**, 332-338 (2013).
14. O. Shmychkova, S. Zahorulko, D. Girenko, et al., *J. Electrochem. Soc.*, **168**, Art. 086507 (2021).
15. O. Shmychkova, T. Luk'yanenko, and R. Amadelli, *J. Electroanal. Chem.*, **717-718**, 196-201 (2014).
16. O. B. Shmychkova, T. V. Luk'yanenko, L. V. Dmitrikova, et al., *Prot. Met. Phys. Chem. Surf.*, **50**, No. 2, 218-222 (2014).
17. O. B. Shmychkova, T. V. Luk'yanenko, A. B. Velichenko, et al., *Prot. Met. Phys. Chem. Surf.*, **50**, No. 4, 493-498 (2014).
18. O. Shmychkova, T. Luk'yanenko, A. Yakubenko, et al., *Appl. Catal. B*, **162**, 346-351 (2015).
19. A. B. Velichenko, S. V. Kovalyov, A. N. Gnatenko, et al., *J. Electroanal. Chem.*, **454**, 203-208 (1998).
20. R. Amadelli, L. Armelao, E. Tondello, et al., *Appl. Surf. Sci.*, **142**, 200-203 (1999).
21. K. L. Pamplin and D. C. Johnson, *J. Electrochem. Soc.*, **143**, 2119-2125 (1996).
22. O. Shmychkova, T. Luk'yanenko, R. Amadelli, et al., *J. Electroanal. Chem.*, **774**, 88-94 (2016).
23. O. Shmychkova, T. Luk'yanenko, R. Amadelli, et al., *Prot. Met. Phys. Chem. Surf.*, **53**, No. 1, 68-74 (2017).
24. S. Zahorulko, O. Shmychkova, T. Luk'yanenko, et al., *Mater. Today Proc.*, **6**, 242-249 (2019).
25. S. Cattarin, I. Frateur, P. Guerriero, et al., *Electrochim. Acta*, **45**, 2279-2288 (2000).
26. S. Cattarin and M. Musiani, *Electrochim. Acta*, **52**, 2796-2805 (2007).
27. A. B. Velichenko, V. A. Knysh, T. V. Luk'yanenko, et al., *Mater. Chem. Phys.*, **131**, 686-693 (2012).
28. A. Velichenko, V. Knysh, T. Luk'yanenko, et al., *Chem. Chem. Technol.*, **6**, No. 2, 123-133 (2012).
29. M. Musiani, *Chem. Commun.*, **21**, 2403-2404 (1996).
30. M. Musiani, F. Furlanetto, and P. Guerriero, *J. Electroanal. Chem.*, **440**, 131-138 (1997).
31. M. Musiani and P. Guerriero, *Electrochim. Acta*, **44**, 1499-1507 (1998).
32. R. Bertoncello, F. Furlanetto, P. Guerriero, et al., *Electrochim. Acta*, **44**, 4061-4068 (1999).
33. M. Musiani, F. Furlanetto, and R. Bertoncello, *J. Electroanal. Chem.*, **465**, 160-167 (1999).
34. R. Bertoncello, S. Cattarin, I. Frateur, et al., *J. Electroanal. Chem.*, **492**, 145-149 (2000).
35. M. Musiani, *Electrochim. Acta*, **45**, 3397-3402 (2000).
36. M. Ghaemi, E. Ghafouri, and J. Neshati, *J. Power Sources*, **157**, 550-562 (2006).
37. T. C. Wen, M. G. Wei, and K. L. Lin, *J. Electrochem. Soc.*, **137**, 2700-2702 (1990).
38. C. N. Ho and B. J. Hwang, *J. Electroanal. Chem.*, **377**, 177-190 (1994).
39. B. J. Hwang and K. L. Lee, *J. Appl. Electrochem.*, **26**, 153-159 (1996).
40. X. Li, H. Xu, and W. Yan, *J. Alloy Compd.*, **718**, 386-395 (2018).
41. R. Amadelli., L. Samiolo, A. B. Velichenko, et al., *Electrochim. Acta*, **54**, 5239-5245 (2009).
42. A. B. Velichenko, V. A. Knysh, T. V. Luk'yanenko, et al., *Theor. Exp. Chem.*, **52**, No. 2, 127-131 (2016).
43. V. Knysh, T. Luk'yanenko, O. Shmychkova, et al., *J. Solid State Electrochem.*, **21**, No. 2, 537-544 (2017).
44. J. Gonzalez-Garcia, J. Iniesta, E. Exposito, et al., *Thin Solid Films*, **352**, 49-56 (1999).
45. J. Gonzalez-Garcia, F. Gallud, J. Iniesta, et al., *New J. Chem.*, **25**, 1195-1198 (2001).
46. M. Y. Abyaneh, V. Saez, J. Gonzalez-Garcia, et al., *Electrochim. Acta*, **55**, 3572-3579 (2010).
47. J. Gonzalez-Garcia, F. Gallud, J. Iniesta, et al., *J. Electrochem. Soc.*, **147**, 2969-2974 (2000).
48. J. Gonzalez-Garcia, F. Gallud, J. Iniesta, et al., *Electroanalysis*, **13**, 1258-1264 (2001).
49. M. Y. Abyaneh, *J. Electroanal. Chem.*, **586**, 196-203 (2006).
50. M. Y. Abyaneh, *J. Electrochem. Soc.*, **154**, No. 1, D5-D12 (2007).
51. M. Y. Abyaneh, *J. Electroanal. Chem.*, **530**, 82-88 (2002).
52. M. Y. Abyaneh and S. Fletcher, *J. Electroanal. Chem.*, **530**, 89-95 (2002).

53. M. Y. Abyaneh, *J. Electroanal. Chem.*, **530**, 96-104 (2002).
54. O. Shmychkova, T. Luk'yanenko, and A. B. Velichenko, *ECS Trans.*, **77**, No. 11, 1617-1623 (2017).
55. O. Shmychkova, T. Luk'yanenko, A. Piletska, et al., *J. Electroanal. Chem.*, **746**, 57-61 (2015).
56. A. B. Velichenko, O. B. Shmychkova, T. V. Luk'yanenko, et al., *Prot. Met. Phys. Chem. Surf.*, **51**, N4, 593-599 (2015).
57. A. Velichenko, T. Luk'yanenko, O. Shmychkova, et al., *J. Chem. Technol. Biotechnol.*, **95**, N 12, 3085-3092 (2020).
58. A. Velichenko, T. Luk'yanenko, and O. Shmychkova, *J. Electroanal. Chem.*, **873**, Art. 114412 (2020).
59. T. Luk'yanenko, O. Shmychkova, and A. Velichenko, *J. Solid State Electrochem.*, **24**, No. 4, 1045-1056 (2020).
60. A. Velichenko, V. Knysh, O. Shmychkova, et al., *Vopr. Khim. Khim. Tekhnol.*, 4, 14-20 (2017).
61. V. A. Knysh, T. V. Luk'yanenko, P. Yu. Demchenko, et al., *Prot. Met. Phys. Chem. Surf.*, **54**, No. 6, 1038-1046 (2018).
62. A. B. Velichenko, R. Amadelli, and V. A. Knysh, *J. Electroanal. Chem.*, **632**, 192-196 (2009).
63. A. B. Velichenko, D. V. Girenko, and F. I. Danilov, *J. Electroanal. Chem.*, **405**, 127-132 (1996).
64. A. B. Velichenko, R. Amadelli, A. Benedetti, et al., *J. Electrochem. Soc.*, **149**, C445-C449 (2002).
65. A. B. Velichenko, E. A. Baranova, D. V. Girenko, et al., *Russ. J. Electrochem.*, **39**, 615-621 (2003).
66. A. B. Velichenko, T. V. Luk'yanenko, N. V. Nikolenko, et al., *Russ. J. Electrochem.*, **43**, 118-120 (2007).
67. A. B. Velichenko and D. Devilliers, *J. Fluorine Chem.*, **128**, 269-276 (2007).
68. A. Velichenko, T. Luk'yanenko, N. Nikolenko, et al., *J. Electrochem. Soc.*, **167**, No. 6, Art. 063501 (2020).

*В огляді розглянуто оригінальний підхід до створення новітніх нанокомпозитних анодних матеріалів на основі плюмбум(*IV*) оксиду, що полягав в одночасному управлінні процесом утворення композиту, його складом та властивостями за рахунок впливу селективної адсорбції оксидів вентильних металів та різних типів ПАР, як на електрохімічні процеси, що проходять на поверхні електроду, так і колоїдно-хімічні в навколоелектродній зоні. Використання багатокомнонентних добавок із селективним впливом кожного компонента на різні процеси суттєво збільшило можливості управління складом та властивостями оксидних композитних матеріалів порівняно з їх модифікуванням добавками іонів та іншими оксидами або неметалічними матеріалами. Наявність ПАР в таких системах може виконувати як самостійну функцію зміни властивостей композиту за рахунок їх включення в об'єм композита та модифікації поверхні, так і допоміжну – змінювати колоїдно-хімічні властивості частинок дисперсної фази, що утворюються в навколоелектродній зоні та беруть участь у формуванні композитного матеріалу. Показано, що варіювання складу електроліту осадження, густини струму та температури дозволяє змінювати вміст добавок у композитах від 1 до 27 %, що дає змогу керовано впливати на морфологію, текстуру, фазовий склад, фізико-хімічні властивості, електрокаталітичну активність і селективність електрокаталізаторів на основі* PbO_2 *у цільових процесах*.

РОЗДІЛ 2
МАТЕРІАЛИ ТА МЕТОДИ ДОСЛІДЖЕНЬ

2.1 Матеріали досліджень

Для виконання роботи були використані реактиви кваліфікації «хч», «чда» та двічі дистильована вода з електропровідністю 1,6 мкСм $см^{-1}$. Поверхнево-активні речовини (полімери), модельні органічні сполуки було придбано в фірмі ALSI Ltd, яка є офіційним дистриб'ютором компанії Merck. Реактиви мали кваліфікацію ACS – найвищий ступінь чистоти, що задовольняє вимогам Американського хімічного товариства (American Chemical Society, ACS). Внутрішньолабораторний контроль якості та чистоти реактивів проводився відповідно до вимог ДСТУ 2216-93.

Гравіметричні вимірювання виконували на лабораторних електронних аналітичних вагах моделі ESJ-200-4, pH електролітів контролювали за допомогою універсального іономіру ЕВ-74.

Електроліти готували з розчинів відомих концентрацій шляхом відбору аліквоти зі подальшим розведенням водою до необхідного об'єму. Для отримання анодів з активним покриттям на основі плюмбум(IV) оксиду як базовий електроліт осадження використовували розчини наступного складу, моль/$дм^3$: $Pb(CH_3SO_3)_2$ / $Pb(NO_3)_2$ – 0,1; CH_3SO_3H / HNO_3– 0,1. Залежно від завдання експерименту концентрації метансульфонатної/ нітратної кислоти та її солі варіювали в межах 0,1–1 моль/$дм^3$. Поверхнево-активні речовини та поліелектроліти додавали в електроліт осадження в вигляді водних розчинів невисоких концентрацій. Оскільки за високих концентрацій поверхнево-активної речовини склад електроліту суттєво змінювався під час осадження, була обрана концентрація, за якої на ізотермі адсорбції можна отримати 100% ступінь заповнення поверхні, коли склад електроліту не змінювався.

Полімерну добавку Nafion® вводили з 5% водно-спиртового розчину (суміш низькомолекулярних аліфатичних спиртів, що містить 15-20% води), приготованого з порошку іонообмінної мембрани Nafion® 117 (Aldrich).

Реакцію виділення кисню на немодифікованому та модифікованому плюмбум(IV) оксиді вивчали у сульфатному розчині та розчині $HClO_4$. Процеси окиснення органічних речовин вивчали у сульфатному розчині.

Кінетику електроосадження плюмбум(IV) оксиду вивчали на Pt або Au дисковому електроді, змонтованому в тефлоновому корпусі. Площа диска – 0,196 $см^2$. Вибір електрода обумовлений його низькою швидкістю окиснення та руйнування за високих анодних потенціалів. Оскільки електрокаталітична активність платини у більшості анодних процесів, що проходять за участі хемосорбованих кисеньвмісних частинок, значною мірою визначається способом підготовки поверхні електрода [2], попередньо вивчали поведінку електрода у фоновому електроліті.

Перед кожним експериментом поверхню електрода обробляли у свіжоприготовленій суміші (1:1) концентрованих H_2SO_4 та H_2O_2 [3]. Подібна методика попередньої підготовки дозволяла стабілізувати стан поверхні електрода, яка під дією сильного окисного середовища окиснюється до певного стану (заданий фазовий і хімічний склад поверхневих оксидів), що визначає задовільну відтворюваність результатів під час реєстрації циклічних вольтамперограм у фоновому розчині (0,1 М кислота). Як допоміжний електрод використовували платиновий дріт. Електроосадження плюмбум(IV) оксиду вивчали в метансульфонатних/ нітратних електролітах, що містили 0,1 М CH_3SO_3H/ HNO_3; 0,01 М $Pb(CH_3SO_3)_2$ / $Pb(NO_3)_2$ та добавку залежно від завдань експерименту.

Покриття були осаджені за анодної густини струму 4$мА/см^2$ і температури 25 ºС. Товщина покриттів становила ~ 50 мкм. Платинований титан було використано в якості колектора струму. Перед нанесенням платинового покриття титанові пластини готували за наступною методикою.

Поверхню обробляли механічним способом. Знежирювали в 5 М КОН впродовж 12 годин. Ретельно промивали бідистильованою водою. Протравлювали в киплячому розчині 6 М HCl впродовж 20 хв. Ретельно промивали бідистильованою водою. Платинове покриття наносили катодно за густини струму 10 мА/см^2 та температури 80 ºС з розчину цис-динітродиамінплатини(II) в аміаці. За таких умов вихід за струмом осадження платини становив близько 30%. Кількість платини на титановому колекторі складала близько 2 мг/см^2 видимої поверхні електрода. Вміст осадженої платини контролювали гравіметрично.

Як базовий покривний розчин для піролітичного нанесення покриттів на основі SnO_2 використовувався еквімолярний розчин $SnCl_4$ в н-C_4H_9OH. Для його приготування 5 см^3 $SnCl_4$ розчиняли за охолодження в 15 см^3 н-бутанолу. Для нанесення модифікованого покриття в 1 см^3 даного базового розчину вводилися добавки у відповідних кількостях у вигляді $H_2PtCl_6 \cdot 6H_2O$, $PdCl_2$, попередньо розчинених в невеликій кількості концентрованої хлоридної кислоти. Шари наносилися пензлем із подальшою сушкою за температури 80-90ºС впродовж 10 хвилин. Після сушіння поверхня набувала коричнево-бурого відтінку. Далі відбувалася термічна обробка анода в муфельній печі 5 хв за температури 450 ºС. Після нанесення 10 шарів проводили фінішну термообробку за 500 ºС впродовж 60 хвилин.

Електроокислення органічних сполук проводили за анодної густини струму j_a=50-80 мА/см^2. Об’єм аноліту становив 130 см^3. Анолітом служили водні розчини речовини наступного складу: сульфатний розчин (0,5 М Na_2SO_4)+$2 \cdot 10^{-4}$ М органічної речовини (pH 6,6), католітом – сульфатний розчин. Як катод використовували сталеву пластинку або дріт, анод – композитні покриття на основі PbO_2. Площа електродів становила 2,5 см^2.

2.2 Методи досліджень

2.2.1 Фізичні методи досліджень

Морфологію поверхні електроосадженого плюмбум(IV) оксиду досліджували методом скануючої електронної мікроскопії (SEM) з використанням растрового електронного мікроскопа LEICA S360, що працює зі вторинними електронами та оснащеного приставкою для рентгенівського мікроаналізу (EDAX, енергетично-дисперсійна рентгенівська спектроскопія) зі використанням Nanoscope Dimension 3100 AFM з Nanoscope III, контрольованого програмним забезпеченням.

Рентгенівські дифрактограми PbO_2 були записані Advance Bruker D8 або PHILIPS PW3710 дифрактометрами з Cuk_α джерелом рентгенівського випромінювання. Запис показань проводили за 30 кВ, 20 мкА зі швидкістю обертання детектора 2 град/хв за безперервного режиму запису. Для рентгенофазових досліджень і визначення елементного складу, проводили аналіз зразків PbO_2 товщиною 20, 1000 і 2000 мкм, які було осаджено на Ti-Pt підложку. У випадку товщини покриттів більш ніж 20 мкм на рентгенограмах досліджуваних зразків сигнал матеріалу підложки не виявляли.

Рентгенівський фазовий аналіз проводили за допомогою програм Powdercell і STOE Winxpow (version 3.03. Stoe & Cie Gmbh, Darmstadt, Germany 2010) методом порівняння рентгенівських профілів одержаних експериментальних дифрактограм між собою та з теоретичними дифрактограмами відомих фаз системи. Для зразків з високим ступенем кристалічності структура була уточнена за методом Рітвельда з використанням програми Fullprof.2k (версія 5.40).

Розрахунки параметрів мікроструктури (розміри доменів когерентного розсіювання (у першому наближенні – розмір зерен фази) і внутрішні напруження) для зерен фази поверхневого шару електродів в ізотропному наближенні проведено методами інтегральної ширини дифракційних максимумів, з використанням процедури опису профілю максимумів

апроксимацією Войта за допомогою алгоритмів пакета програм Winplotr. Інструментальна складова приладу виділена за первинним пучком.

Зразки PbO_2 також були досліджені методом порошкової рентгенівської дифракції за допомогою STOE STADI P автоматичного дифрактометра з лінійним PSD детектором (режим трансмісії, 2θ/ω-сканування; Cu $K\alpha_1$ випромінювання, германієвий (1 1 1) монохроматор; 2 θ-діапазон $6{,}000 \leq 2\theta \leq 102{,}945°$ 2θ із кроком 0.015° 2θ; PSD (position sensitive detector – позиційно-чутливий детектор) крок 0,480° 2θ, час сканування 50 с/крок).

Елементний склад електроосаджених покриттів визначали на рентгеноспектральному електронно-зондовому мікроаналізаторі Superprobe 733 (JEOL, Japan). Для визначення елементного складу були проаналізовані зразки PbO_2, товщиною 50 мкм, які осаджували на Ti/Pt підложку.

Поверхня покриттів була також досліджена методом рентгенівської фотоелектронної спектроскопії за допомогою PHI 5000 спектрометра з використанням монохроматичного AlKα випромінювання або надвисоковакуумного скануючого зондового мікроскопа JSPM-4610 з роздільною здатністю 0,14 нм за горизонталлю та 0,01 нм за вертикаллю. Величина енергії зв'язку для C(1s) становила 284,8 (±0,3) еВ. Граничний залишковий тиск у колоні мікроскопа не перевищував $3{,}0 \cdot 10^{-8}$ Па.

2.2.2 Електрохімічні вимірювання

Для електрохімічних вимірювань використовувався потенціостат EG&G з програмним забезпеченням EG&G. Усі вимірювання проводили в деаерованому аргоном розчині H_2O/CH_3CN (80:20 об/об) з використанням перхлорату натрію (0,2 моль $дм^{-3}$) як допоміжного електроліту.

УФ-видимі спектри розчинів отримували на спектрофотометрі Kontron (Uvikon 943) з використанням 1-мм кварцової кювети.

Спектри фотолюмінесценції реєстрували на спектрофлуориметрі Jobin Yvon Spex Fluoromax II (фотопомножувач Hamamatsu R3896) із використанням зразків плівки CdS, відлитої на кварцових підкладках.

Експерименти за опромінення (10 мВт $см^{-2}$) проводили на кварцовій ртутній лампі середнього тиску Helios Q400 Ital з використанням відсікаючого фільтра ($\lambda > 400$ нм).

2.2.3 Фізико-хімічні методи аналізу

Реакцію виділення кисню було досліджено методами квазістаціонарної поляризації та імпедансної спектроскопії за допомогою контрольованого комп'ютерним програмним забезпеченням потенціостату EG&G Princeton Applied Research, модель 273A та синхронізуючого підсилювача Amplifier, модель 5210. PbO_2 було осаджено на платинову проволоку (0.13 $см^2$). Обробку отриманих експериментальних даних здійснювали за допомогою комп'ютерної програми Boucamp's equivalent circuit simulation та ZsimpWin 3.21 софту.

Зміну концентрації органічної речовини під час електролізу визначали шляхом відбору проб (об'ємом 5 $см^3$) з певною періодичністю та вимірюванням оптичної густини розчину в УФ і видимій області (область довжин хвиль 200-570 нм). Спектри поглинання розчинів, що містять органічні речовини, були отримані зі використанням спектрофотометрів ULAB 108UV або Uvikon.

Аналіз продуктів окиснення органічних речовин здійснювали методом рідинної хроматографії за допомогою контрольованого комп'ютерним програмним забезпеченням високоефективного рідинного хроматографа Shimadzu RF-10A xL, оснащеного ультрафіолетовим діод-матричним детектором. Розділова хроматографічна колонка для зверненої фази: Discovery® C18 діаметром 3,9 мм, довжиною 300 мм. Рухома фаза: буферний розчин двозаміщеного кислого калію ортофосфата [с (KH_2PO_4) = 0,0125 моль/$дм^3$] + ацетонітрил (90 об'ємних частин + 10 об'ємних частин). Швидкість

потоку 0,8 $см^3$/хв. Ультрафіолетове детектування за 250 нм, видиме – за 380 нм. Обсяг проби, що впорскується 10 $мм^3$.

Похибки вимірювань вираховували за допомогою статистичної обробки результатів спостережень відповідно до вимог ДСТУ 2681-94. Оцінку істинного значення вимірюваної величини, невизначеності похибки результатів прямих вимірів проводили відповідно до ДСТУ ISO/IEC Guide 98-4:2018.

2.3 Статистична обробка результатів

Устаткування мало нормовані метрологічні характеристики та своєчасно калібрувалося.

Дані для лінеаризованих графіків обробляли методом найменших квадратів [4], що вимагає, щоб сума квадратів відхилень експериментальних точок від кривої була найменшою. Для прямих було знайдено рівняння, у тому числі визначено константи. Достовірними вважалися дані, для яких коефіцієнт кореляції становив понад 0,99.

Калібрувальні графіки обробляли програмою обробки даних калібрувальних (градуювальних) графіків згідно з ДСТУ ISO 8466-1-2001 та ДСТУ ISO 8466-2-2001 [5, 6].

Для визначення необхідної кількості вимірювань та оцінки достовірності отриманих експериментальних даних результати опрацьовували за допомогою методів математичної статистики [7].

Достовірність отриманих результатів та обґрунтованість зроблених висновків підтверджується комплексним використанням набору сучасних методик, відтворюваністю експериментального матеріалу, широким поданням результатів на наукових конференціях, семінарах, їх опублікуванням у виданнях, віднесених до першого і другого квартилів (Q1 і Q2), відповідно до класифікації SCImago Journal.

РОЗДІЛ 3
ЕЛЕКТРОЛІТИ ОСАДЖЕННЯ

3.1 Вибір оптимального базового складу електроліту для отримання модифікованих покриттів і композитів

У якості найпоширеніших базових електролітів осадження матеріалів на основі PbO_2 використовують водні перхлоратні, ацетатні, борфлуоридні, плюмбатні та нітратні розчини Pb(II). Разом із тим традиційні електроліти, які використовують для осадження матеріалів на основі плюмбум(IV) оксиду мають велику кількість різноманітних недоліків. Вони не дозволяють змінювати в широких межах текстуру, морфологію та фазовий склад депозитів, а також отримувати осади значної товщини зі задовільними механічними властивостями. В останні кілька десятиліть з'явилась практична можливість використання електролітів на основі метансульфонової кислоти, яка має унікальні властивості, що обумовлено специфічною адсорбцією на оксидах металів, а також впливом на структуру води та природу адсорбованих кисеньвмісних частинок в поверхневому шарі за високих анодних потенціалів [8, 9]. Все це створює нові можливості керованого синтезу матеріалів на основі PbO_2 заданого хімічного і фазового складу з необхідними функціональними властивостями [10-12]. Необхідно зауважити, що в обставинах, коли в Україні залишилось промислове виробництво лише свинцевих акумуляторів, логічним виглядає впровадження у їхню технологію інновацій з використанням підходів сучасної хімії.

У загальному випадку електрокаталітична активність електрода залежить від досить великого числа факторів, які можна об'єднати в дві великі групи: хімічні (які визначаються складом матеріалу) і структурні (що визначаються будовою). Взагалі, для оцінки електрокаталітичної активності матеріалу структурні та хімічні фактори необхідно розділити, що зробити вкрай важно, оскільки вони діють одночасно. Зміна хімічного складу покриття приводитиме

до зміни морфології, фазового складу, текстури. І це є однією із проблем електрокаталізу.

В своїх дослідженнях ми зробили спробу розділити ці фактори: структурні та хімічні. Щоб виділити структурний фактор потрібно мати уявлення про закономірності кристалізації плюмбум оксиду.

Для дослідження початкових стадій осадження плюмбум оксиду отримані хроноамперограмми на Pt-ДЕ. Типова I-t крива осадження PbO_2 може бути умовно розділена на кілька характерних ділянок: стрибок струму в початковий період поляризації електрода, що відповідає зарядженню подвійного електричного шару; індукційний період, зумовлений часом, необхідним для початку фазоутворення; максимум струму, обумовлений зменшенням концентрації електроактивних частинок в навколоелектродному просторі та досягнення квазістаціонарного значення струму. Як випливає з хроноамперограмм, отриманих з нітратного і метансульфонатного електролітів, незважаючи на однакову концентрацію іонів плюмбуму в розчині, спостерігаються суттєві відмінності в струмах осадження, що є нестандартним ефектом. Цей незвичайний ефект, імовірно, може бути пояснений зміною природи частинок, що розряджаються. За збільшення потенціалу осадження поверхня електрода здобуватиме усе більш позитивний заряд, що повинно сприяти закріпленню на поверхні частинок протилежного знаку. Зміна заряду частинок у випадку метансульфонатних електролітів порівняно з нітратними розчинами повинна полегшити кристалізацію плюмбум(IV) оксиду на позитивно зарядженій поверхні електрода.

Під час електроосадження як кінетичні закономірності процесу кристалізації, так і характер кристалічної структури утворюваного оксиду залежать від швидкості нуклеації, швидкості лінійної кристалізації та їх співвідношення. Ці параметри можна визначити з транзієнтів процесу електроосадження плюмбум оксиду. Аналізуючи початкові стадії кристалізації, згідно з модельними уявленнями Гонсалеса-Гарсії [13, 14], можна припустити характер нуклеації. Відношення максимального струму до квазістаціонарного

значення вказує на переважаючу геометричну форму ядер, які утворюються. Різниця у струмах піку та плато хроноамперограми також дозволяє робити висновок про відношення між константами швидкостей нуклеації в напрямах паралельно та перпендикулярно до поверхні електрода. Під час формування оксидів розглядають три основні геометричні форми ядер такі як, напівсфероїд, конус і циліндр. Під час аналізу кристалізації плюмбум(IV) оксиду з нітратних електролітів на поверхні скловуглецю віддають перевагу конусоподібній формі кристалів [15-17].

Для опису початкових стадій формування нової фази плюмбум(IV) оксиду була обрана кінетична модель Аб'єна [18-22], оскільки вона дає повніший опис і уявлення про механізм росту нової фази плюмбум(IV) оксиду та дозволяє визначити кінетичні параметри нуклеації як для α- так і для β-фази. Ця модель задовільно описує процес кристалізації саме за кінетичного контролю початкових стадій формування нової фази PbO_2. Зростаюча частина транзієнта струму нечутлива до геометрії росту кристалу, що дозволяє визначити кінетичні параметри 2D нуклеації ядер. В процесі електроосадження плюмбум(IV) оксиду можливе формування одночасно двох фаз (α і β). Електроосадження покриття починається з формування α-фази, і тільки потім відбувається утворення β-фази або осадження двох фаз одночасно. За всіх потенціалів осадження кристалізація плюмбум(IV) оксиду з метансульфонатних електролітів відбувається за прогресивним механізмом.

Проте і тут ми стикнулися із низкою проблем, оскільки наявність двох лінійних ділянок на графіку свідчить про одночасне осадження двох фаз PbO_2, до того ж утворення однієї фази помітно відстає від іншої. В залежності від складу електроліту можлива як перевага росту однієї фази над іншою, так і повне перекривання та поглинання центрів росту однієї фази [23-25]. Природа запізнюваної фази залежить від умов осадження. За низьких поляризацій спостерігається незначна перевага росту α-фази PbO_2. У випадку високих поляризацій α-фаза починає відставати в рості, та на поверхні електрода

відбувається перекривання та поглинання центрів росту α-фази кристалами β-фази.

Виходячи із результатів цих досліджень, ми обрали склад електролітів та умови осадження покриттів, що необхідні для вивчення структурного фактора. Як бачимо за осадження з 0,1 М $Pb(CH_3SO_3)_2$+1,0 М CH_3SO_3H електроліту покриття переважно складається з α-фази, а за осадження з 0,1 М $Pb(NO_3)_2$+1,0 М HNO_3, навпаки, переважно з β. В кислих розчинах взагалі досить складно отримати покриття, що складалося лише б із однієї фази. З 0,1 М HNO_3/ CH_3SO_3H + 0,01 М $Pb(NO_3)_2$/ $(CH_3SO_3)_2Pb$ електролітів, незважаючи на різний хімічний склад, утворюються покриття із однаковим фазовим складом і текстурою. Тому виникає потреба в швидкому методі напівкількісного прогнозування фазового складу покриттів без проведення рентгенівського аналізу. Нами був запропонований такий метод [24]. Він досить перспективний для визначення фазового складу тонких плівок, оскільки покриття не товсте, за використання рентгенівської дифракції із невеликим кутом опромінення на дифрактограмі проявляються також і рефлекси підкладки, а зняти таке покриття для порошкової рентгенівської дифракції немає можливості. Як було показано дослідженнями з використанням інверсійної вольтамперометрії, відновлення осадів, отриманих з метансульфонатних електролітів (α-фаза), відбувається за меншого потенціалу, ніж для покриттів, осаджених з нітратного розчину (β-фаза) [24].

Як результат були вибрані склади розчинів осадження, що ми використовували як базові. Ми вибрали електроліт із невисоким вмістом α-фази, оскільки введення у такий розчин добавок суттєво не впливає на фазовий склад покриттів. Ми не використовували електроліт, з якого осаджуються покриття повністю з α-фази, оскільки, як було встановлено раніше, покриття такого типу містить велику кількість катіонних вакансій та в значному ступені гідратовані. І як будь-яке гідратоване покриття в умовах анодної поляризації піддаватиметься електрохімічному розчиненню та рекристалізації з часом.

Незважаючи на досить високу електрокаталітичну активність матеріалів на основі PbO_2 в реакціях перенесення кисню, їх практичне застосування ще не вийшло за межі лабораторних масштабів через труднощі створення розмірно стабільних електродів цього типу. Основною проблемою є суттєві відмінності в механічних властивостях металічої підкладки та плюмбум оксиду, неможливість отримати покриття товщиною більше 50 мкм з низькими внутрішніми напруженнями, а також дифузія кисню через PbO_2 до титанової підкладки та подальше її окиснення, що приводить до блокування оксиду титану. Слід також зазначити, що покриття на основі PbO_2, отримані з нітратних електролітів, характеризуються значними внутрішніми напруженнями і тому під час роботи зазнають значного механічного руйнування. За високої густини струму та високого електричного опору на міжфазній межі оксиду металу можна спостерігати локальний розігрів електрода, що через відмінності коефіцієнтів лінійного розширення металу та оксиду призводить до відриву покриття від підкладки. Більшість із цих проблем можна вирішити за використання метансульфонатного електроліту.

Утворення плюмбум оксиду відбувається одночасно з виділенням кисню. Оскільки вихід за струмом зменшується зі збільшенням потенціалу осадження PbO_2, діапазон потенціалів, у якому реакція утворення PbO_2 є переважним процесом, малий. На рисунку 3.1 можна побачити типову залежність виходу за струмом від густини струму.

Залежність екстремальна, що пов’язано з одночасним процесом утворення плюмбум оксиду та виділенням кисню. За низької густини струму, коли швидкість утворення PbO_2 невелика, оксидне покриття не суцільне впродовж тривалого часу, тому що реакція виділення кисню може відбуватися на ділянках, що містять платину та її фазові оксиди, де перенапруга РВК значно нижча, ніж на PbO_2. Збільшення густини струму сприяє швидкому заповненню поверхні платинового електрода плюмбум оксидом, підвищується перенапруга РВК і вихід за струмом наближається до 100%. Таким чином, в області I, де вихід за струмом збільшується зі збільшенням густини струму, процес

одночасно проходить нібито на двох електродах, платиновому та плюмбум оксиді, з поступовим повним переходом до останнього.

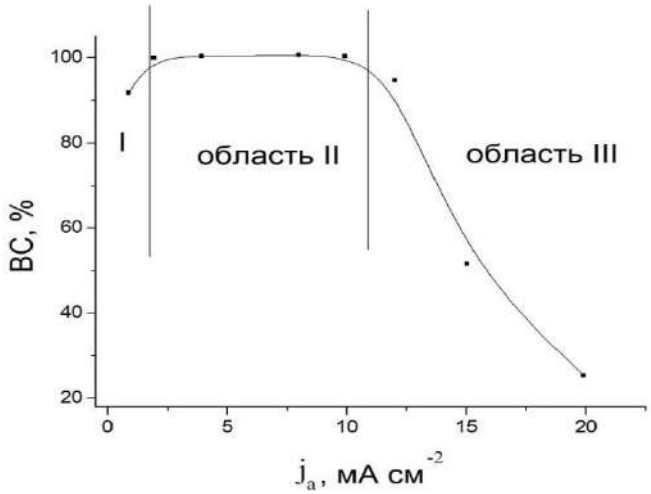

Рис. 3.1 Залежність виходу за струмом PbO_2 від густини струму в 0,1 М $Pb(CH_3SO_3)_2$ + 0,1 М CH_3SO_3H.

В області II кривої вихід за струмом становить 100% і не залежить від густини струму, оскільки кисень ще не виділяється на PbO_2 через високу перенапругу. Ділянка III кривої демонструє швидке падіння виходу за струмом через те, що струм осадження плюмбум оксиду досягає граничного значення, тоді як швидкість виділення кисню зростає експонентно. Оскільки перенапруга виділення кисню на PbO_2 практично не залежить від складу електроліту, єдиний спосіб розширити діапазон густин струму із 100% виходом – це збільшення граничного струму осадження плюмбум оксиду шляхом збільшення концентрації сполук плюмбуму в розчині або перемішуванням електроліту, що можна зробити за використання метансульфонатного електроліту.

Виходячи з вище викладеного, ми пропонуємо використовувати електроліти наступного складу 0,1 М $Pb(NO_3)_2$+ 0,1 М HNO_3 / 0,1 М $(CH_3SO_3)_2Pb$ + 0,1 М CH_3SO_3H. Покриття осаджувані з цих електролітів, близькі за фазовим складом, спостерігаються деякі відмінності в кристалографічній орієнтації. З метансульфонатних розчинів можна отримувати товсті покриття. До того ж метансульфонова кислота – екологічно безпечний електроліт. ЇЇ солі

більше розчинні порівняно зі солями мінеральних кислот. В залежності від задач експерименту ми можемо використовувати ті або інші електроліти, можемо обирати, коли необхідно використати нітратний електроліт, а коли необхідно досягти високих швидкостей осадження – використовувати висококонцентрований метансульфонатний електроліт, в якому широкий діапазон густин струму дозволяє забезпечити криючу здатність.

В більшості випадків структурні фактори не є превалюючими. Кардинально структура не змінюється, тому представляє інтерес за однакового фазового складу впливати на хімічний склад. Тут розглянемо модель Рючі (рис. 3.2).

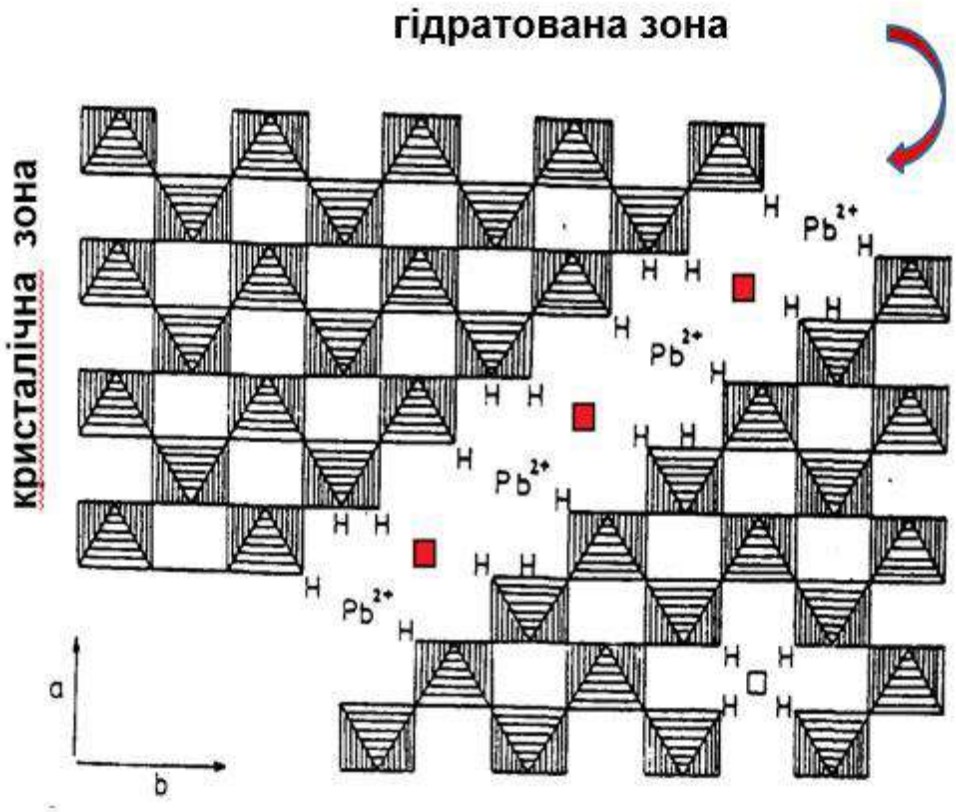

Рис. 3.2 Схематичне зображення дефіциту катіонів у PbO_2, спроєктоване на (001) площину [26].

Як відомо, на поверхні плюмбум оксиду локалізовані дві зони: гідратована, що складається з іонів Pb^{2+}, асоційованих з відповідною кількістю гідроксил-іонів і кристалічна, в якій іони Pb^{4+} у вузлах кристалічної решітки пов'язані з

іонами кисню O^{2-}. Хімічний склад описується формулою $Pb^{4+}_{(1-x-y)}Pb^{2+}_{y}O^{2-}_{(2-4x-2y)}OH^{-}_{(4x+2y)}$. Заміна іонів плюмбуму як в гідратованій, так і в кристалічній зонах викликатиме не тільки зміну кількості кисеньвмісних частинок в кожній із зон, але і їх енергій зв'язку, що в свою чергу приводитиме до зміни електрокаталітичної активності матеріалу. В цілому мікромодифіковані діоксидносвинцеві системи доволі широко вивчені. І раніше був виявлений каталітичний ефект нікелю. Проте накопичені емпіричні дані ніхто не намагався пояснити. Чому такі зміни відбуваються?

Ми виявили цікавий ефект поступового зменшення, а потім збільшення вмісту нікелю в покритті в залежності від густини струму осадження (рис. 3.3).

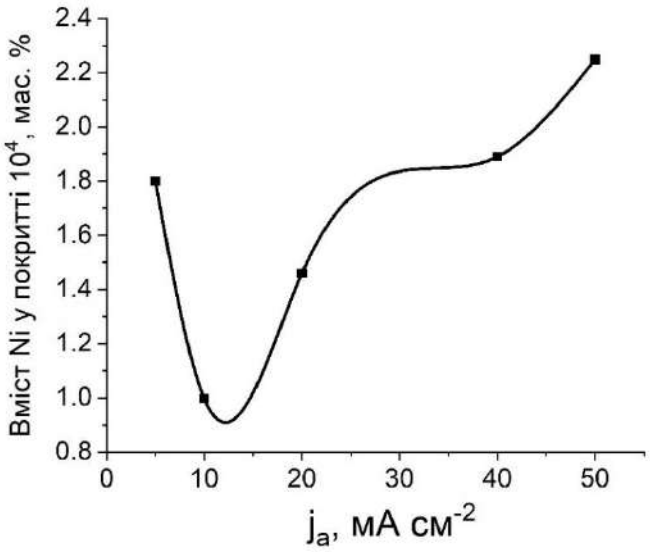

Рис. 3.3 Вміст нікелю в PbO_2-покритті залежно від густини струму осадження

Початкова ділянка пояснюється тим, що відбувається відштовхування між іонами Ni^{2+} та іонами плюмбуму, потім вміст добавки збільшується за рахунок утворення сполук тривалентного нікелю, що термодинамічно можливо. В процесі росту PbO_2 вони легко можуть замінити іони Pb^{4+} в кристалічній решітці, утворюючи змішані оксидно-гідроксидні сполуки типу NiOOH. Такий обмін допустимий, виходячи з близькості радіусів іонів Ni^{3+} та Pb^{4+} Для балансу

заряду відбуватиметься добір гідроксильних груп. Непрямим доказом утворення таких сполук є результат радіохімічних вимірювань (рис. 3.4) і дані рентген фотоелектронної спектроскопії (рис. 3.5).

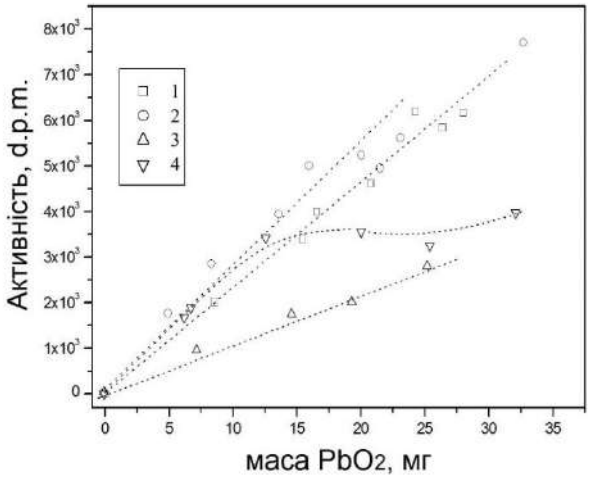

Рис. 3.4 Радіохімічне вимірювання активності тритію у PbO_2, осадженому за 296 (1; 2) або 338 К (3; 4) з електролітів: 1; 3 – 0,1 М HNO_3 + 0,1 М $Pb(NO_3)_2$; 2; 4 – 0,1 М HNO_3 + 0,1 М $Pb(NO_3)_2$+ 0,01 М $Ni(NO_3)_2$

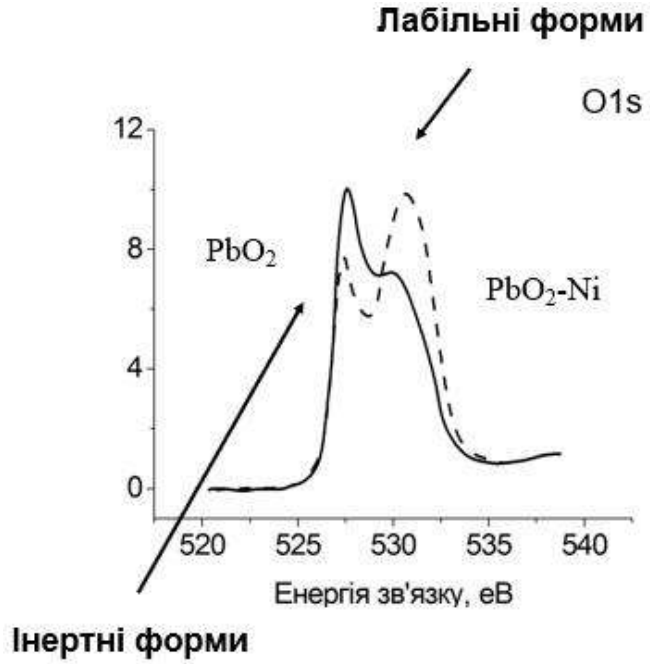

Рис. 3.5 Структура O 1 s рівня ядра у PbO_2, отриманого з розчинів: 1 – 0,1 М HNO_3 + 0,1 М $Pb(NO_3)_2$; 2 – 0,1 М HNO_3 + 0,1 М $Pb(NO_3)_2$ + 0,01 М $Ni(NO_3)_2$

Найбільші зміни на РФС спектрах спостерігаються в O1s області. Отримані спектри характеризуються двома піками: один за більш низької енергії зв'язку відноситься до міцно зв'язаного кисню кристалічної решітки, тоді як за більш високої енергії зв’язку – до слабко зв’язаних кисеньвмісних частинок (гідроксидні групи, адсорбовані кисеньвмісні частинки і вода). Добавки іонів впливають на ступінь гідроксилювання поверхневого шару оксиду, викликають зміни у фазовому складі покриття, приводячи до зменшення вмісту α-фази. Раніше передбачалося, що іони нікелю знаходяться в гідратованій зоні оксиду у вигляді гідроксиду. Проте, якщо б це припущення відповідало дійсності на РФС спектрі не спостерігалося б змін. А ми спостерігаємо на спектрі одночасне зменшення кількості інертних кисеньвмісних частинок, і збільшення лабільних.

Потрібно зауважити, що використання мікромодифікованих систем має один суттєвий недолік. Скоріше за все такі іони концентруються в поверхневому шарі оксиду, їх кількість менше 1 мас.%, впродовж роботи відбуватиметься перерозподіл частинок на поверхні, і електрод стане працювати іншим способом, ще і за виділення кисню відбуватиметься підкислення розчину. З нашої точки зору перспективнішим є використання композитів, де компоненти досить рівномірно розподіляються в усьому об’ємі покриття.

Основні результати розділу опубліковано в роботах автора [12, 23, 24, 27-33].

Journal of Electroanalytical Chemistry 746 (2015) 57–61

Contents lists available at ScienceDirect

Journal of Electroanalytical Chemistry

journal homepage: www.elsevier.com/locate/jelechem

Electrocrystallization of lead dioxide: Influence of early stages of nucleation on phase composition

O. Shmychkova [a], T. Luk'yanenko [a], A. Piletska [a], A. Velichenko [a,*], R. Gladyshevskii [b], P. Demchenko [b], R. Amadelli [c]

[a] Ukrainian State University of Chemical Technology, 8, Gagarin Ave., 49005 Dniepropetrovsk, Ukraine
[b] Lviv National Ivan Franko University, 6, Kirila i Mephodiya Str., 79005 Lviv, Ukraine
[c] Istituto per la Sintesi Organica e la Fotoreattivita – Consiglio Nazionale delle Recerche (ISOF – CNR), Dipartimento di Chimica, Universita di Ferrara, via L. Borsari, 46, 44121 Ferrara, Italy

ARTICLE INFO

Article history:
Received 16 January 2015
Received in revised form 21 March 2015
Accepted 27 March 2015
Available online 28 March 2015

Keywords:
Lead dioxide
Methanesulfonate electrolyte
Nucleation and growth
Phase composition

ABSTRACT

It has been revealed that coatings obtained from methanesulfonate bath at investigated conditions (10 mA cm^{-2}; pH = 1.0) are almost entirely composed of α-phase. It was found that the gradual transition from α- to β-phase in the coating occurs in the presence of additives in deposition electrolytes. It was proposed to use charge coming on the formation of nuclei as the correlation parameter to predict the phase composition of obtained lead dioxide deposits. Electrocrystallization of PbO_2 begins with the formation of a monolayer on the electrode surface, then the formation and growth of three-dimensional nuclei takes place. The simultaneous formation of α and β phases results in the presence of two linear areas on the plot of $(j - j_1)^{1/3}$ vs. time for the progressive growth of crystals. The formation of one phase is noticeably lagged behind the other. At layer-by-layer crystallization and significant lagging of one of phases may occur ingesting of growing centers of one phase by another. The type of lagging phase depends on the nature of electrolyte: for nitrate bath it is β, for methanesulfonate – α.

1. Introduction

Electrodes based on lead dioxide doped by ionic additives are known to be of great interest for investigation owing to tailoring solid state properties as well as electrocatalytic activity of PbO_2 [1–7]. Particular attention should be paid to ionic additives in high oxidation states +3, and +4 (compared to places of cation vacancies of lead dioxide, in which Pb^{2+}-ions are known to be localized). It is recognized [8–11], that there are two zones on the lead dioxide surface: crystal (PbO_2) and hydrated [$PbO(OH)_2$], that are in equilibrium and are capable to exchange cations and anions with the ions present in the bulk. Lead ions replacement both in hydrated and crystal zone would cause not only the change of amount of oxygen-containing particles in each zone, but their binding energies, that in turn will change the electrocatalytic activity of materials. The radii of the ions [12] in the oxidation state +2, +3 (Bi^{3+} – 1.03; Ce^{3+} – 1.02; Sn^{2+} – 1.18 Å) are close to ionic radius of Pb^{2+} (1.19 Å), ions in a higher oxidation state +4 and +5 (Bi^{5+} – 0.76; Ce^{4+} – 0.87; Sn^{4+} – 0.69 Å) are close to the ionic radius of Pb^{4+} (0.78 Å). The ionic radius of F^- (1.33 Å) is close to radii of OH^- (1.37 Å) or O^{2-} (1.40 Å). Hence, lead ion substitution on them is possible in both zones. This was the criterion for choosing of dopants.

In the present work we examine early stages of electrocrystallization of PbO_2 from methanesulfonate electrolytes that contain various ionic additives (Bi^{3+}, Ce^{3+}, Sn^{4+}, $[NiF_6]^{2-}$, $[SnF_6]^{2-}$) and identify correlations between the deposition conditions and phase composition of coatings. It should be pointed out that such data is currently absent in the literature.

2. Experimental

All chemicals were reagent grade. Electrodeposition regularities of doped lead dioxide were studied on a Pt disk electrode (Pt-DE, 0.19 cm^2) by steady-state voltammetry, chronoamperometry. The Pt-DE surface was treated, before use, by the procedure described in [13]. Such preliminary treatment permits to achieve a reproducible surface. Voltammetry measurements were carried out in a standard temperature-controlled three-electrode cell. All potentials were recorded and reported vs. $Ag/AgCl/KCl_{(sat.)}$.

* Corresponding author.
E-mail address: velichenko@ukr.net (A. Velichenk).

http://dx.doi.org/10.1016/j.jelechem.2015.03.031
1572-6657/

The inversion voltamperometry was used for estimation of the deposition regularities of lead dioxide both in nitrate and methanesulfonate electrolytes. The method consisted in the accumulation of pre-analyzed oxide on the working electrode by the electrolysis at a controlled potential and its subsequent electrochemical dissolving under the linearly changing potential.

Electrodeposition of lead dioxide was studied in the methanesulfonate/nitrate electrolytes that contained 1 M CH_3SO_3H/HNO_3, 0.01 M $Pb(CH_3SO_3)_2/Pb(NO_3)_2$ and 0.01 M additive ($Bi(NO_3)_3$, $Ce(NO_3)_3$, $(CH_3COO)_4Sn$, $K_2[NiF_6]$, $K_2[SnF_6]$) depending on purposes of the experiments.

In other section of experiments platinized titanium was used as substrate. Titanium sheet was treated as described in [13] before platinum layer depositing. Lead dioxide coatings were electrodeposited at anodic current density 10 mA cm^{-2} and temperature (282 ± 2) K or (298 ± 2) K. The coating thickness was ~50 μm.

X-ray powder diffraction data were collected on a STOE STADI P automatic diffractometer [14] equipped with linear PSD detector (transmission mode, $2\theta/\omega$-scan; Cu $K\alpha_1$ radiation, curved germanium (1 1 1) monochromator; 2θ-range $6000 \leqslant 2\theta \leqslant 102{,}945°$ 2θ with step 0.015° 2θ; PSD step 0.480° 2θ, scan time 50 s/step).

Qualitative and quantitative phase analysis was performed using the PowderCell program [15]. For selected samples with relatively high degree of crystallinity the Rietveld refinement was carried out using FullProf.2k (version 5.40) program [16,17].

3. Results and discussions

3.1. Early stages of nucleation and growth of lead dioxide

Current transients for PbO_2 deposition on Pt disk electrode were obtained for investigation of initial stages lead dioxide electrodeposition from methanesulfonate electrolytes. A typical j–t curve of PbO_2 deposition is shown on Fig. 1. Observed transient can be divided on several characteristic regions [18]: the current density step in the initial period of electrode polarization corresponding to charging of the double electrical layer; induction period corresponding to the time required for beginning of the phase formation; maximum current density due to a decrease in the concentration of electroactive species in the near electrode space and the achievement of a quasi-stationary current density. The type of transient is determined by the electrode potential. At low polarizations (E = 1.55 V) the biggest induction period with a further stretched maximum of current is observed. Increasing of an anodic polarization leads to a substantial decreasing of the induction period and to increasing of current maximum.

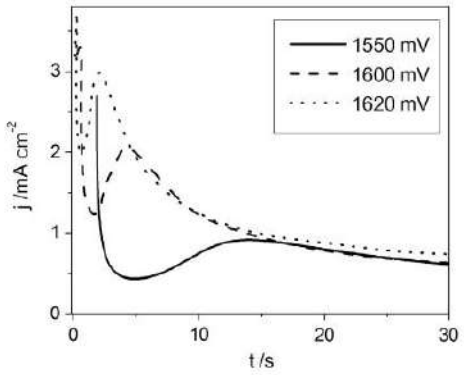

Fig. 1. Current transients for PbO_2 deposition on Pt disk electrode from 0.01 M $Pb(CH_3SO_3)_2$ + 1 M CH_3SO_3H at different deposition potentials.

A linear relationship between the natural logarithm of the induction time of crystallization and the applied potential with negative slope is observed both for nitrate and methanesulfonate electrolytes (Fig. 2). Such dependence shows that the electrocrystallization of PbO_2 begins with the formation of a monolayer on the entire surface of the electrode, and then the formation and growth of nuclei occurs. Growth of lead dioxide occurs through layer-by-layer crystallization, so each following layer is formed on the renewed surface.

According to transients obtained from nitrate and methanesulfonate electrolytes (Fig. 3), one can conclude that despite the same concentration of lead ions in solution, there are significant differences in currents of the deposition that is an unusual effect caused, probably, by adsorption of negatively charged lead methanesulfonate complexes on positively charged electrode [19].

Lead dioxide formation takes place at constantly renewed surface. Particles like $Pb(CH_3SO_3)_2$, $Pb(CH_3SO_3)^+$ or $Pb(CH_3SO_3)_3^-$ can be adsorbed on the growing oxide surface from the bulk. According to [19] data, three lead(II)-methanesulfonate complexes are characterized as being the predominant species, thus particles like $Pb(CH_3SO_3)_2$ and $Pb(CH_3SO_3)_3^-$ can be in the surface layer. With the potential growth the electrode surface will become redundant positively charged, that would promote the binding of particles with the opposite sign on the surface. Complex compounds with a neutral or negative charge, adsorbed on the surface, would

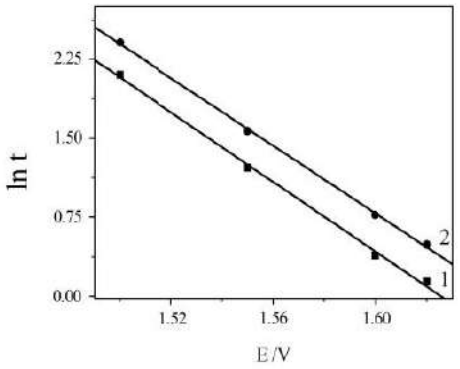

Fig. 2. Plot of the natural logarithm of the induction period of crystallization vs. potential for methanesulfonate (1) and nitrate (2) electrolytes.

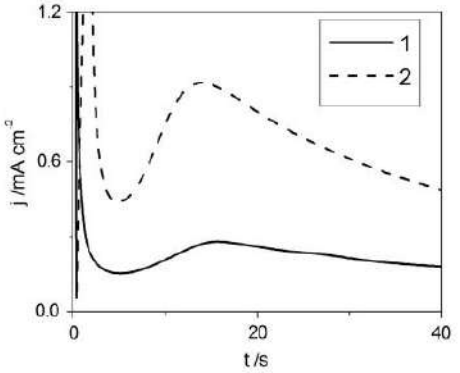

Fig. 3. Current transients for PbO_2 deposition at 1.55 V on Pt disk electrode from different electrolytes: (1) 0.01 M $Pb(NO_3)_2$ + 1 M HNO_3; (2) 0.01 M $Pb(CH_3SO_3)_2$ + 1 M CH_3SO_3H.

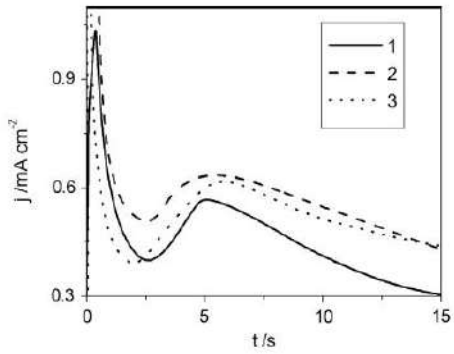

Fig. 4. Current transients for PbO_2 deposition on Pt disk electrode at 1620 mV from electrolytes: (1) 0.01 M $Pb(CH_3SO_3)_2$ + 1 M CH_3SO_3H (1) + 0.01 M Bi^{3+}; (2) (1) + 0.001 M Ce^{3+}; (3) (1) + 0.01 M Sn^{4+}.

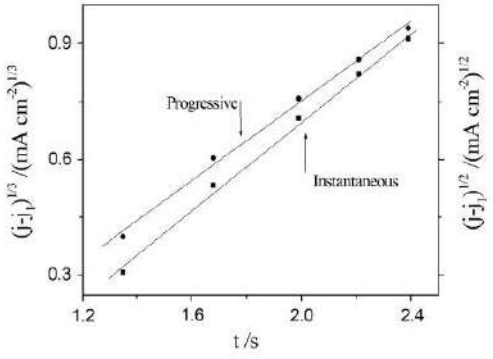

Fig. 5. Plots of $(j-j_1)^{1/3}$ and $(j-j_1)^{1/2}$ vs. time for a transient recorded during the electrocrystallization of PbO_2 from a solution of 0.01 M $Pb(CH_3SO_3)_2$ + 1 M CH_3SO_3H at an applied potential of 1.62 V.

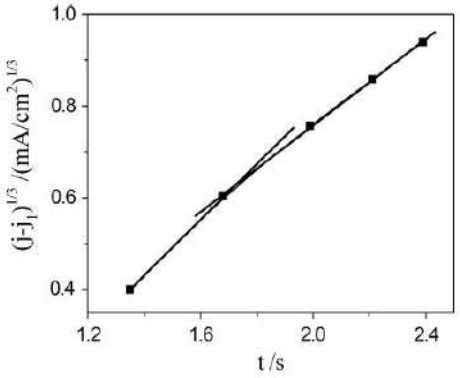

Fig. 6. Analysis of plot of $(j-j_1)^{1/3}$ vs. time for a transient recorded during the electrocrystallization of PbO_2 from a solution of 0.01 M $Pb(CH_3SO_3)_2$ + 1 M CH_3SO_3H at an applied potential of 1.62 V.

facilitate the lead dioxide crystallization on a positively charged electrode surface. Similar phenomena for the processes occurring in the limiting current region have been described in [20].

It is clear from transients (Fig. 4) that an increase of a current delay corresponding to the induction time can be observed if ionic

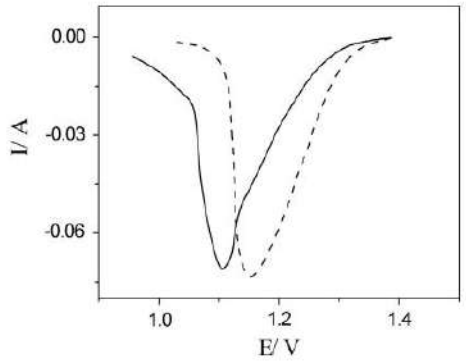

Fig. 7. Inversion voltammograms cathodic branches (scan range 1.4–0.6 V) in 1 M $HClO_4$ lead dioxide previously deposited on Pt electrode from solutions containing 0.1 M $Pb(CH_3SO_3)_2$ + 1 M CH_3SO_3H (—), 0.1 M $Pb(NO_3)_2$ + 1 M HNO_3 (--). ν = 50 mV/s.

Table 1
The phase composition of lead dioxide coatings depending on deposition conditions.*

Solution	T (K)	Content (w.%)/ α-PbO_2/β-PbO_2
0.1 M $Pb(NO_3)_2$ + 1 M HNO_3 (N)	282	36/64
N	298	25/75
N	313	17/83
N	333	15/85
0.1 M $Pb(NO_3)_2$ + 0.11 M HNO_3	298	14/86
0.1 M $Pb(CH_3SO_3)_2$ + 0.11 M CH_3SO_3H	298	17/83
0.1 M $Pb(CH_3SO_3)_2$ + 1 M CH_3SO_3H (M)	282	59/41
M	298	90/10
M	313	83/17
M	333	33/67
M + 0.001 M Bi^{3+}	282	65/35
M + 0.01 M Bi^{3+}	282	5/95
M + 0.001 M Ce^{3+}	298	83/17
M + 0.003 M Ce^{3+}	298	19/81
M + 0.01 M Sn^{4+}	298	44/56
M + 0.01 M $[SnF_6]^{2-}$	298	0/100
M + 0.01 M $[NiF_6]^{2-}$	298	38/62

* Samples are deposited at j = 10 mA/cm^2.

dopants are present in the deposition bath. This indicates difficulties in the initial stages of the phase formation of lead dioxide.

For the analysis of obtained transients we used the model, described in [18], and calculated current densities for instantaneous and progressive nucleation. Fig. 5 represents the plots of $(j-j_1)^{1/3}$ and $(j-j_1)^{1/2}$ vs. time for a transient obtained at 1620 mV.

At this potential difference between instantaneous and progressive nucleation is not apparent. Plot of $(j-j_1)^{1/2}$ vs. t deviates from linearity and curve downwards indicating that $(j-j_1)$ is proportional to t to the powers smaller than 2, and the plot of $(j-j_1)^{1/3}$ vs. t has a slight tendency to curve downwards indicating that $(j-j_1)$ is proportional to t to the powers slightly less than 3. But, in accordance with results, obtained for nitrate bath in [18], it may be assumed that our experimental data also follows more closely the plot of $(j-j_1)^{1/3}$ vs. t.

The existence of two linear parts in the plot of $(j-j_1)^{1/3}$ vs. t (Fig. 6) indicates the simultaneous deposition of two phases of PbO_2, and the formation of one phase is noticeably lagged behind the other. The type of lagging phase depends on the nature of electrolyte: for nitrate bath it is β, for methanesulfonate – α.

Moreover, as has been shown by investigations using inversion voltamperometry, the reduction of deposits obtained from the

Table 2
Lattice parameters of lead dioxide coatings depending on nature of electrolyte.

Sample description	Lattice parameters, Å (α/β)			Reliability factors
	a	*b*	*c*	R_I/R_P, R_{WP}, R_{EXP}
0.1 M $Pb(CH_3SO_3)_2$ + 1 M CH_3SO_3H	4.9888(3)/4.95222(8)	5.9415(4)/–	5.4529(3)/3.38184(10)	0.0510 0.0488/0.0800, 0.105, 0.0716
0.1 M $Pb(NO_3)_2$ + 1 M HNO_3	4.9854(6)/4.94871(5)	5.9429(7)/–	5.4544(5)/3.37931(6)	0.0503 0.0339/0.0703, 0.0954, 0.0597

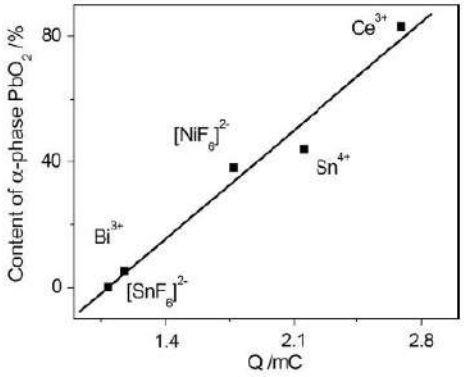

Fig. 8. α-Phase PbO_2 content vs. electricity, that is coming on the formation of two dimensional nuclei at early stages of nucleation and growth of oxide.

methanesulfonate bath (α-phase) occurs at a lower potential than such for coatings deposited from nitrate bath (β-phase, Fig. 7).

3.2. Texture and phase composition

Data about morphology of deposits are described in detail in our previous publications [4–6]. Let's focus on the phase composition of investigated deposits.

As has been determined by X-ray powder diffraction all of our investigated samples contain two phases: α-PbO_2 (structure type $Fe_2N_{0.94}$, space group *Pbcn*) and β-PbO_2 (structure type TiO_2 rutile, space group $P4_2/mnm$). The difference was observed only in the ratio of these two phases and also in the degree of crystallinity (Table 1).

No significant differences in the unit cell dimensions were found between the two electrolytes (Table 2). The peak intensities are rather low. This confirms probably the decreasing of the size of crystals of lead dioxide formed at higher current densities. However, it should be noted that such an effect is possible when water entrapment by porous structure of lead dioxide takes place, as shown in [21]. The temperature of deposition also provides a significant influence on the phase composition. It is shown [1], that with the temperature growth the content of β-phase in lead dioxide deposit increases. We observed a similar effect when the temperature rises from 298 to 313 K.

Individual phases consist of compounds formed by dopants have not been detected in none of investigated samples. Taking into account their low content in the deposit, even in the case of formation of such phases, their amount would be clearly insufficient to detect by X-ray diffraction. However, a whole number of indirect data, in particular differences in the phase composition and the crystallographic orientation of the individual faces indicate the possibility of incorporating of ionic additives into crystal lattice instead of Pb(IV).

According to obtained data one can conclude that the nature of depositing electrolyte considerably influences on the phase composition of lead dioxide coatings and on crystallographic orientations of individual faces.

Table 3
Standard thermodynamic values for Pb(IV) oxides.

Value	α-PbO_2	β-PbO_2
ΔH^0_{298} (kJ/mol)	−265.8	−276.6
ΔS^0_{298} (J/mol K)	92.5	76.4
ΔG^0_{298} (kJ/mol)	−299.5	−219.3

Thus, lead dioxide deposited from nitrate bath mainly composed of β-phase [1,2], whereas coatings obtained from methanesulfonate bath are almost entirely composed of α-phase.

The temperature of deposition influences on the phase composition of PbO_2-coatings. Thus, an increase of temperature leads to the growth of β-phase in the coating. At the same time, the rising of temperature also increases the peaks intensity on the diffractogram. The latter, probably, indicates an increase in crystal size. Differences in the phase composition of obtained materials have been also detected as changing pH of the solution. Thus, the growth of pH from 1.0 to 5.0 leads to an increase of β-phase content in the coating.

A similar effect makes the addition of dopants in deposition electrolytes. It has been found that the content of β-phase of PbO_2 increases in the next line of additives: $Ce^{3+} < Sn^{4+} < [NiF_6]^{2-} < Bi^{3+} < [SnF_6]^{2-}$, wherein the presence in the deposition electrolyte of latter complex ion leads to the formation of the deposit completely represented by β-phase of PbO_2.

It should be pointed out that in the line involved, values of $(j - j_1)^{1/3}$ for progressive nucleation increase, the induction time decrease and the content of β-phase in the deposit grows. At layer-by-layer crystallization and significant lagging of one of phases may occur ingesting of growing centers of one phase by another.

According to obtained results one can conclude that investigated factors (temperature, pH, current density, presence of dopants in the electrodeposition solutions) lead to changes in surface charge, namely, they make its charge more positive, which in turn leads to an increase in the content of β-phase in the coating.

In connection with such significant differences in the phase composition of coatings the comparison of kinetic parameters of nucleation of modified lead dioxide and α-phase content in coatings is seemed to be of considerable interest.

Subsequently, to study the influence effect of dopants on the deposition regularities of lead dioxide from methanesulfonate electrolytes the initial stages of growth and electrocrystallization of PbO_2 in the presence of these ions in the deposition electrolyte have been investigated. An increase of the current delay corresponding to the induction period, when dopants are present in the electrolyte, indicates the difficulties in the initial stages of the phase formation of lead dioxide.

Regions on transients corresponding to early growth of nuclei, when they are growing, by majority, as isolated centers and have not yet overlapped [19] (so-called two-dimensional crystal growth) have been analyzed. Because the configuration of peaks

on transients (Fig. 4) differs one from each other, it seems more appropriate to evaluate the amount of electricity coming on the formation of crystals at the initial stages of growth instead of the current of crystallization. The amount of electricity was calculated by integrating of the peak area on obtained transients and then the dependence between this value and the content of the alpha phase in the coating (according to data listed in Table 1) has been built.

As shown by the results of studies a number of crystals with orthorhombic lattice is proportional to the charge (integrated peak area) coming on formation of two-dimensional nuclei (Fig. 8). Thus, these results indicate that such phenomenon can be used as the correlation parameter to predict the phase composition of materials involved.

Moreover, according to the reference data [22] (Table 3), the thermodynamic potential of the formation of α-phase PbO_2 is lower than of the β-phase PbO_2, hence at a fixed deposition potential the formation of two-dimensional cluster with orthorhombic lattice is more favorable thermodynamically.

This in turn suggests that the phase composition is largely influenced not by the nature of the substrate but by kinetic difficulties in initial stages of crystallization depending on the composition of the deposition electrolyte.

4. Conclusions

According to obtained data one can conclude that the nature of depositing electrolyte considerably influences on the phase composition of lead dioxide coatings and on crystallographic orientations of individual faces. Coatings obtained from methanesulfonate bath are almost entirely composed of α-phase. It was found for the first time that addition of dopants in deposition electrolytes leads to growth of β-phase content in deposits. Charge coming on the formation of two dimensional nuclei can be used as the correlation parameter to predict the phase composition of obtained lead dioxide deposits.

References

[1] X. Li, D. Pletcher, F.C. Walsh, Electrodeposited lead dioxide coatings, Chem. Soc. Rev. 40 (2011) 3879.

[2] C.T.J. Low, D. Pletcher, F.C. Walsh, The electrodeposition of highly reflective lead dioxide coatings, Electrochem. Commun. 11 (2009) 1301.

[3] Y. Liu, H. Liu, Comparative studies on the electrocatalytic properties of modified PbO_2 anodes, Electrochim. Acta 53 (2008) 5077.

[4] O. Shmychkova, T. Luk'yanenko, A. Velichenko, L. Meda, R. Amadelli, Bi-doped PbO_2 anodes: electrodeposition and physico-chemical properties, Electrochim. Acta 111 (2013) 332.

[5] O. Shmychkova, T. Luk'yanenko, A. Velichenko, R. Amadelli, Electrodeposition of Ce-doped PbO_2, J. Electroanal. Chem. 706 (2013) 86.

[6] O. Shmychkova, T. Luk'yanenko, R. Amadelli, A. Velichenko, Physico-chemical properties of PbO_2-anodes doped with Sn^{4+} and complex ions, J. Electroanal. Chem. 717–718 (2014) 196.

[7] A.B. Velichenko, R. Amadelli, E.V. Gruzdeva, T.V. Luk'yanenko, F.I. Danilov, Electrodeposition of lead dioxide from methanesulfonate solutions, J. Power Sources 191 (2009) 103.

[8] P. Ruetschi, R. Giovanoli, On the presence of OH^- ions, Pb^{2+} ions and cation vacancies in PbO_2, Power Sources 13 (1991) 81.

[9] D. Pavlov, I. Balkanov, T. Halachev, P. Rachev, Hydration and amorphization of active mass PbO_2 particles and their influence on the electrical properties of the lead-acid battery positive plate, J. Electrochem. Soc. 136 (11) (1989) 3189.

[10] D. Pavlov, I. Balkanov, The PbO_2 particle: exchange reactions between ions of the electrolyte and the PbO_2 particles of the lead-acid battery positive active mass, J. Electrochem. Soc. 139 (1992) 1830.

[11] D. Pavlov, The lead-acid battery lead dioxide active mass – a gel-crystal system with proton and electron conductivity, J. Electrochem. Soc. 139 (1992) 3075.

[12] N.N. Greenwood, A. Earnshaw, Chemistry of Elements, Pergamon Press Ltd., Oxford, New York, Toronto, Sydney, Paris, Frankfurt, 1985 (p. 1542).

[13] A.B. Velichenko, D.V. Girenko, S.V. Kovalyov, A.N. Gnatenko, R. Amadelli, F.I. Danilov, Lead dioxide electrodeposition and its application: influence of fluoride and iron ions, J. Electroanal. Chem. 454 (1998) 203.

[14] STOE WinXPOW, version 3.03, Stoe & Cie GmbH, Darmstadt, 2010.

[15] W. Kraus, G. Nolze, PowderCell for Windows (version 2.4), Federal Institute for Materials Research and Testing, Berlin, 2000.

[16] J. Rodriguez-Carvajal, Recent developments of the program FULLPROF, commission on powder diffraction (IUCr), Newsletter 26 (2001) 12.

[17] T. Roisnel, J. Rodriguez-Carvajal, WinPLOTR: a windows tool for powder diffraction patterns analysis, Mater. Sci. Forum 378–381 (2001) 118.

[18] M.Y. Abyaneh, V. Saez, J. Gonzalez-Garcia, T.J. Mason, Electrocrystallization of lead dioxide: analysis of the early stages of nucleation and growth, Electrochim. Acta 55 (2010) 3572.

[19] M.D. Capelato, J.A. Nobrega, E.F.A. Neves, Complexing power of alkanesulfonate ions: the lead-methanesulfonate system, J. Appl. Electrochem. 25 (1995) 408.

[20] A.B. Velichenko, T.V. Luk'yanenko, N.V. Nikolenko, R. Amadelli, F.I. Danilov, Nafion effect on the lead dioxide electrodeposition kinetics, Russ. J. Electrochem. 43 (2007) 118.

[21] D.J. Payne, R.G. Egdell, D.S.L. Law, Experimental and theoretical study of the electronic structures of α-PbO_2 and β-PbO_2, J. Mater. Chem. 17 (2007) 267.

[22] C. Daniel, J.O. Besenhard, Handbook of Battery Materials, second ed., Wiley-VCH, 2011 (p. 1023).

Journal of Electroanalytical Chemistry 774 (2016) 88–94

Contents lists available at ScienceDirect

Journal of Electroanalytical Chemistry

journal homepage: www.elsevier.com/locate/jelechem

Electrodeposition of Ni^{2+}-doped PbO_2 and physicochemical properties of the coating

O. Shmychkova [a], T. Luk'yanenko [a], R. Amadelli [b], A. Velichenko [a,*]

[a] Ukrainian State University of Chemical Technology, 8, Gagarin Ave., 49005 Dniepropetrovsk, Ukraine
[b] ISOF-CNR u.o.s Ferrara c/o Dipartimento di Scienze Chimiche e Farmaceutiche, Universita di Ferrara, via L. Borsari, 46–44121, Ferrara, Italy

ARTICLE INFO

Article history:
Received 15 March 2016
Received in revised form 12 May 2016
Accepted 13 May 2016
Available online 14 May 2016

Keywords:
Lead dioxide
Nitrate electrolyte
Electrodeposition kinetics
Nickel ions
Chemical composition

ABSTRACT

The kinetics of PbO_2 electrodeposition from nitrate electrolytes containing nickel ions, and the influence of deposition conditions on the physicochemical properties of obtained materials, have been investigated. This study reveals that the mechanism of Ni^{2+}/PbO_2 electrodeposition is not in conflict with that of PbO_2 formation in the absence of foreign species that we described earlier. Accordingly, electrochemical formation of PbO_2 occurs in four stages, two of which are electron transfer steps while the other two are chemical reactions involving formation and decay of soluble intermediates consisting of 3 and 4-valent lead species. We observed an inhibition of Pb^{2+} electrooxidation in the presence of Ni^{2+} that is attributable to partial blocking of the active surface sites by the adsorbed foreign cations. Interestingly though, blocked active sites that inhibit the growth of PbO_2 show, at the same time, a high activity for O_2 evolution. Changing of the electrolyte composition and conditions of electrodeposition of PbO_2 (deposition potential, temperature and pH) significantly influences the physicochemical properties of the PbO_2 deposits. In particular, the phase and chemical composition, the crystallographic orientation, the content of structural water and the nature of adsorbed oxygen-containing particles on the electrode surface. Concerning the last point, bearing direct relevance to the electrocatalytic properties, we noted that Ni^{2+}/PbO_2 electrodes feature a significant increase in the amount of labile oxygen intermediates on the electrode surface which are responsible of a high electrocatalytic activity in the O_2 evolution reaction.

1. Introduction

The development of methods for the direct synthesis of new materials with specific properties is one of the priorities of modern science [1,2]. Despite a fairly large number of methods for the synthesis of oxide materials, electrochemical methods are considered among the most promising ones because of their ease of implementation and relatively small energy losses compared to sol-gel, CVD and PVD techniques. By a suitable choice of electrolysis regimes, electrolyte composition and subsequent electrochemical and/or thermal treatment [3,4], this method offers great opportunities to control the thickness of deposits and improve their adhesion to the current collector; additionally, mechanical and physicochemical properties of materials such as chemical and phase composition, morphology and texture can often be advantageously tailored.

A typical representative of this type of materials is lead(IV) oxide (PbO_2), which is widely used in the electrochemical energetics (lead-acid batteries, Red-Ox flow batteries for energy storages, asymmetric supercapacitors) [5,6], as well as anode in various electrochemical applications including electroplating, ozone generation, synthesis of inorganic and organic compounds, electrochemical degradation of toxic organic substances in the wastewater and in seawater electrolysis [7–9].

A notable advantage of PbO_2 compared to other oxide systems is the possibility of engineering its bulk and surface properties, during electrosynthesis in suitable media, in order to meet specific requirements in terms of composition and physicochemical properties [10–12]. Typical disadvantages are unsatisfactory mechanical properties and instability of certain functional properties under prolonged or cyclic electrolysis. The latter prevents the development of new advanced technologies of electrochemical energy conversion and electrolysis of aqueous solutions using thick (several millimeters) oxide layers on metal, oxide or carbon-composite polymer matrix.

Having in mind that the challenge in PbO_2 research is to obtain an electrochemically active and durable material, in this work we report and discuss the electrodeposition of PbO_2 from a Ni^{2+}-containing medium.

Although methanesulfonate is becoming the most popular electrolyte for PbO_2 electro-synthesis [13], we chose nitrate electrolytes because they are cheaper, easier to prepare and work with; their regeneration presents no particular difficulties, and PbO_2 obtained in this medium has satisfactory mechanical properties. In addition, we

* Corresponding author.
E-mail address: velichenko@ukr.net (A. Velichenko).

http://dx.doi.org/10.1016/j.jelechem.2016.05.017
1572-6657/

wanted to avoid the possible influence of the anion in an assessment of peculiarities of Ni^{2+} effects; in this respect, the known specific adsorption of the methanesulfonate anion on oxides [14] would complicate the analysis of electrochemical results.

Electrodeposition conditions and the electrolyte composition, in particular, are known to dramatically affect both the physicochemical properties and the electrocatalytic activity of the resulting deposits [10–12]. Despite the large number of publications, each system is unique because the presence of additives leads to alteration of various material properties. Unlike coatings obtained by Xia et al. [15], our system can be defined as micromodified since the content of the modifying element is not more than 0.01 wt.%. One of the objects of our work was to develop such a micromodified system with given electrocatalytic properties by changing the quantity of surface adsorbed oxygen species.

The mechanism analysis of PbO_2 electrodeposition is based on the following reaction scheme described in the literature [10,16–20]:

$$H_2O \rightarrow OH^{\bullet}_{ads} + H^+ + e^- \quad (1)$$

$$Pb^{2+} + OH^{\bullet}_{ads} \rightarrow Pb(OH)^{2+} \quad (2)$$

$$Pb(OH)^{2+} + H_2O \rightarrow Pb(OH)_2{}^{2+} + H^+ + e^- \quad (3)$$

$$Pb(OH)_2^{2+} \rightarrow PbO_2 + 2H^+. \quad (4)$$

2. Material and methods

All chemicals were reagent grade. Electrodeposition regularities of doped lead dioxide were studied on a Pt rotating disk electrode (Pt-RDE, 0.19 cm^2) by steady-state voltammetry, chronoamperometry. For the RDE experiments the voltammetry system SVA-1BM was used. The potential scan rate was varied within 1 ÷ 100 mV/s depending on purposes of the experiments. Before each experiment, the electrode surface was treated with a freshly prepared mixture (1:1) of concentrated H_2SO_4 and H_2O_2 [16]. This preliminary treatment technique permits to stabilize the electrode surface, which under the action of strong oxidizing medium is oxidized to a certain state (defined phase and chemical composition of the surface oxides), which determines the satisfactory reproducibility in taking of cyclic voltammograms in the background electrolyte (0.1 M HNO_3). Voltammetry measurements were carried out in a standard temperature-controlled three-electrode cell.

Electrodeposition of lead dioxide was studied in the nitrate electrolytes that contained 1 M HNO_3, 0.02 M $Pb(NO_3)_2$ and 0.01 M $Ni(NO_3)_2$. In other experiments platinized titanium sheet was used. Titanium sheet was treated as described in [17] before platinum layer depositing. Lead dioxide coatings were electrodeposited at anodic current density 4 mA cm^{-2} and temperature (293 ± 2) K. The determination of modifying additive in anodic material was carried out with Grafite furnace atomic adsorption spectroscope (GF-AAS) model Analyst 800. Increasing of the concentration of the ionic dopant in the deposition electrolyte leads to an increase of the content of modifying element in lead dioxide. The content of the ion additives in the oxide usually does not exceed 0.01 wt.%.

Lead dioxide anodes surface morphology was studied by scanning electron microscopy (SEM) with SEM-106I microscope and by X-ray diffraction with Advance Bruker D8 diffractometer.

For the radiochemical measurement TriCarb 300C Packard equipment was used. After deposition from solutions enriched by ^3H_2O, deposits were weighed and then dissolved in 5 cm^3 of a solution containing 20 cm dm^{-3} of concentrated acetic acid and 10 cm dm^{-3} of hydrogen peroxide. Then the activity of resulting solutions was measured by scintillation.

In research by secondary ion mass spectrometry (SIMS), the sample was bombarded by O^{2+} ions (10 keV). Sprayed sample particles were accumulated and analyzed with Balzer QMA 400 analyzer.

XPS studies were carried out on a PHI 5000 spectrometer using monochromatic AlKα radiation for excitation. The BE value of C(1 s), due to adventitious carbon and residual solvent is 285.0 (± 0.3) eV.

Oxygen evolution reaction was investigated by steady-state polarization and impedance spectroscopy on computer controlled EG & G Princeton Applied Research potentiostat model 273 A and lock-in Amplifier model 5210. PbO_2 was deposited on Pt wire (0.13 cm^2). The comparison of the theoretical equivalent circuit with experimentally determined data was performed by a graphical method. All potentials were recorded and reported vs. $Ag/AgCl/KCl_{(sat.)}$.

3. Results and discussion

3.1. Electrodeposition kinetics of PbO_2-Ni-anodes

Cyclic voltammograms (CV) obtained in the presence of Ni^{2+} ions in the solution are slightly different from the curves for the platinum electrode in a solution containing no added foreign ions. The main differences between CVs obtained in the presence of additives are a decrease of the current peak height for cathodic PbO_2 reduction and the increase of anodic current on the exponential part of the curve. The observed effects indicate an increase in the rate of oxygen evolution reaction and inhibition of the reaction of Pb^{2+} electrooxidation.

An increase of the RDE angular velocity causes a decrease of the CV peak of PbO_2 reduction regardless of the scanning potentials range; this, too, indicates a decrease of the reaction rate of Pb^{2+} oxidation (Fig. 1). In the absence of ionic dopants in the electrolyte the character of the anode current in the exponential part of CV is determined by the potential scan range. In so-called "short" cycles, when the electrode is covered with an ultrathin film of PbO_x (potential scanning range 1.0–1.6 V), the anodic current in the exponential part of the curve decreases with increasing of the angular velocity irrespective of the nature of ionic additive [10,16,18].

In the case that the proposed mechanism is true, an induction period for PbO_2 crystal phase nucleation should be observed that increases with an increase of the angular velocity. Experimental verification was performed with chronoamperometry (Fig. 2). As expected, an increase of the electrode angular velocity leads to an increase of the induction

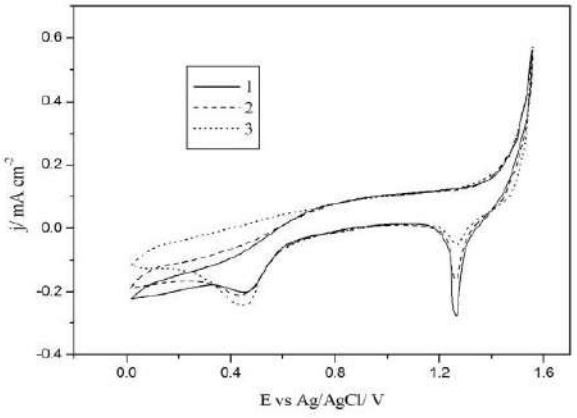

Fig. 1. Cyclic voltammograms of Pt-RDE in 1M HNO_3 + 0.02 M $Pb(NO_3)_2$, additionally containing 0.01M Ni^{2+}, obtained at different electrode's angular velocities (rpm): 1–0; 2–350; 3–960. V = 100 mV/s.

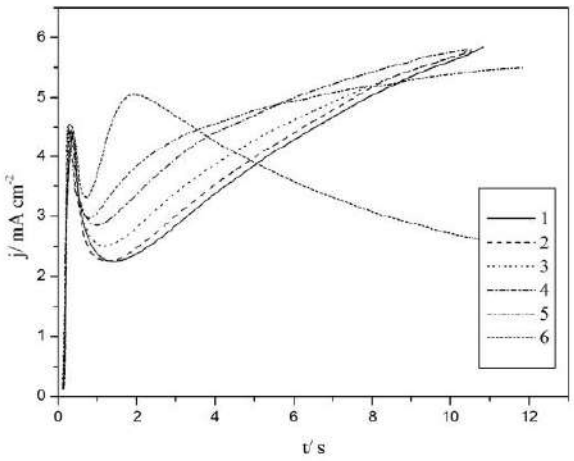

Fig. 2. Current transients for PbO_2 deposition on Pt disk electrode from 1M HNO_3 + 0.02 M $Pb(NO_3)_2$, additionally containing 0.01 M $Ni(NO_3)_2$, at 1.6 V and different electrode's angular velocities (rpm): 1–3900; 2–3100; 3–1900; 4–960; 5–350; 6–0.

period due to a decrease of the amount of the more mobile surface intermediates. So, PbO_2 electrodeposition in the presence of Ni^{2+} in the electrolyte is probably limited by the second electron transfer step and occurs with the participation of soluble lead intermediates.

Since PbO_2 formation at high potentials (more positive than 1.7 V) is controlled by the diffusion of Pb^{2+} ions to the electrode surface, I-E curves for total and partial current were measured to characterize the processes taking place in this potential range. When anodic polarization grows (at potentials higher than 1.75) a limiting current of PbO_2 deposition can be observed (Fig. 3). In the examined potential range, the measured partial current of PbO_2 electrodeposition depends on the electrode angular velocity. Such results confirm diffusion control of the process at high anodic polarizations.

For a quantitative description of observed effects, the values of the apparent heterogeneous rate constants (k) for anodic Pb^{2+} oxidation were calculated according to the Koutecky-Levich equation from intercepts of $1/I–1/\omega^{1/2}$ plots (Table 1). It is noted that the presence of ionic additives in different concentrations has no significant effect on the rate

Table 1
Apparent heterogeneous rate constants of lead dioxide formation (E = 1.8 V).

Deposition solution	$k \cdot 10^4$, m s^{-1}
1 M HNO_3 + 0.02 M $Pb(NO_3)_2$	6.0
1 M HNO_3 + 0.02 M $Pb(NO_3)_2$ + 0.01 Ni^{2+}	5.5
1 M HNO_3 + 0.02 M $Pb(NO_3)_2$ + 0.02 Ni^{2+}	5.5

of the process, which is in agreement with the CV data and steady-state polarization investigations.

The observed inhibition of the reaction of Pb^{2+} ions oxidation in the presence of Ni^{2+} is apparently related to partial blocking of the active sites on the surface of the growing PbO_2 due to adsorption of the foreign cation. At the same time, it is likely that the same active sites that block the thickening of the PbO_2 layer show high activity for the simultaneous oxygen evolution reaction.

For an estimation of the effect of ion additives on the O_2 process, we analyzed the overall polarization curves (Fig. 3). In the presence of Ni^{2+} in the solution the total current (sum of processes of divalent lead ions oxidation and oxygen evolution) increases, whereas the measured partial current for PbO_2 electrodeposition decreases. This is a clear manifestation of enhanced oxygen evolution reaction efficiency.

As seen in Fig. 4, the current efficiency of PbO_2 formation decreases with the increase of deposition potential, due to an increase of O_2 evolution reaction rate at the limiting current of deposition of lead dioxide. As mentioned above in the text, an increase of the concentration of Ni^{2+} has no noticeable effect on the process of Pb(II) electrooxidation.

According to [17,19,20], adsorption of Ni^{2+} on the electrode surface increases the amount of labile oxygen-containing particles and reduces the amount of inert oxygen-containing particles. Since according to the literature [21] O_2 evolution on PbO_2 is most likely controlled by an electrochemical desorption step, an increase of the amount of labile oxygen-containing particles (with low bond strength with the electrode surface) should lead to an increase in the reaction rate, which is indeed confirmed by experimental data (Figs. 3, 4). In this case the observed lower oxidation rate of Pb^{2+}, is probably due to a decrease of the amount of inert oxygen-containing particles involved in PbO_2 formation.

In order to verify earlier assumptions about the possibility of adsorption of Ni^{2+} on the PbO_2 we carried out adsorption measurements using a PbO_2 powder in the absence of polarization were carried out. Experimentally, a linear relationship is observed in plots of the inverse of the amount of adsorbed Ni^{2+} vs. the inverse of its solution concentration

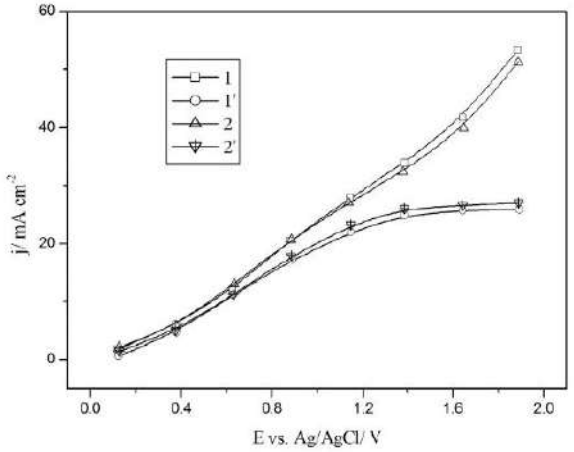

Fig. 3. Steady-state polarization curves for total (1, 2) and partial (1′,2′) electrodeposition current on Pt-RDE in 1 M HNO_3 + 0.02 M $Pb(NO_3)_2$, additionally containing X M $Ni(NO_3)_2$, where X: 1, 1′ – 0; 2, 2′ – 0.01.

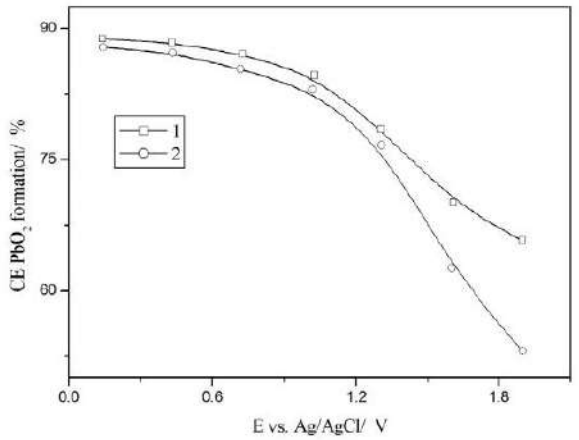

Fig. 4. Current efficiency of PbO_2 formation on Pt disk electrode versus the deposition potential in 1M HNO_3, additionally containing: 1–0.02 M $Pb(NO_3)_2$; 2–0.02 M $Pb(NO_3)_2$ + 0.01 M $Ni(NO_3)_2$.

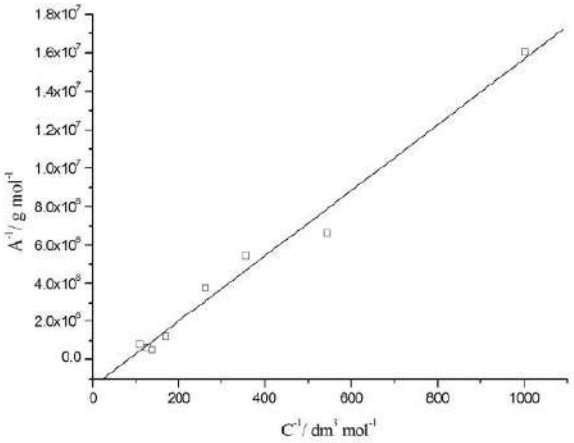

Fig. 5. Inverse of the amount of adsorbed Ni^{2+} vs. the inverse of its solution concentration of Ni^{2+} from 0.1 M HNO_3, additionally containing $Ni(NO_3)_2$.

(Fig. 5) indicating that adsorption is satisfactorily described by the Langmuir isotherm. The values of limiting adsorption, the equilibrium adsorption constant and the adsorption energy (ΔG_{ads}) of -17.6 kJ mol^{-1} were calculated from this plot. These data indicate a weak specific adsorption of nickel cations on lead dioxide [22].

Since the potentials of the PbO_2 electrodeposition is much higher than the steady-state potential at which adsorption measurements were carried out, it was necessary to confirm experimentally the possibility of adsorption of Ni^{2+} at potentials in the range where formation of PbO_2 occurs. We did this by examining the dependence of the electrical double layer capacity (C_{dl}) on potential for PbO_2 electrode in the background electrolyte (0.1 M HNO_3), in the absence and in the presence of Ni^{2+}. Data obtained by impedance measurement (Fig. 6) show that C_{dl} for the electrode in the background electrolyte remains substantially constant over the entire range of investigated potentials. The presence of Ni^{2+} ions in the solution causes a significant decrease of C_{dl} at low polarization; but, at potentials higher than 1.6 V, it increases and tends to a value closer to that measured in the background electrolyte.

This behavior suggests adsorption of cations at potentials at which PbO_2 grows as well as formation of some amounts of nickel oxide on the surface and in the bulk of PbO_2. These data suggest the same nature of the adsorption of Ni^{2+} ions at a steady-state potential and at potentials of PbO_2 formation. However, the increase of influence of the

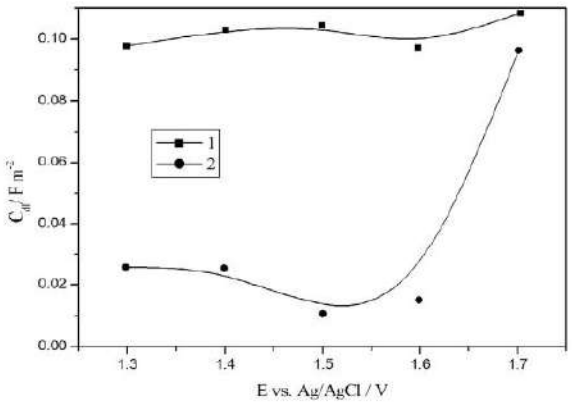

Fig. 6. Double electric layer capacity versus potential of lead dioxide electrode in electrolytes: 1–0.1 M HNO_3; 2–0.1 M HNO_3 + 0.01 M $Ni(NO_3)_2$.

electrostatic factor with increasing of electrode polarization that reduces adsorption of Ni^{2+} should be noted. In contrast to the lead dioxide, nickel oxides are semiconductors, and are characterized by significantly lower capacity due to the existence of a space-charge region [23]. It should be noted, that C_{dl} values at the potential up to 1.6 V remain virtually unchanged.

To further confirm the hypothesis of an invariance of Pb^{2+} electrooxidation mechanism in the presence of the foreign cation ions, we again resorted to electrode impedance technique, which has undeniable advantages compared with other relaxation methods in cases where it is necessary to study the kinetics of multistage electrode processes, including parallel routes, and accountable the absorption of electrochemical reactions participants.

Parameters that were extracted using the equivalent electrical circuit (given in Scheme, Appendix A) as described in [24] are given in Table 2. However, for the Ni^{2+} the form of an electric circuit at 1.3 V was not set, because in diagnostic coordinates C_p-$(R_p)^{-1}$ the frequency dependence mode is not described by a straight equation, therefore, in this case, the equivalent electrical circuit varies and can include frequency dependent elements, namely, the Warburg impedance, the selection of which by inverse division method is difficult.

Since the electrical circuit prepared on the basis of the model representations and that one synthesized from the experimental data, match, it can be concluded that electrodeposition of lead dioxide from nitrate electrolytes actually occurs through the proposed scheme given in [10, 16–20] and the presence of additive does not result in a change of the mechanism of the process.

3.2. The influence of electrodeposition conditions on physicochemical properties of the deposits

The electrodeposition of lead dioxide from nitrate electrolytes occurs on a positively charged electrode surface (the point of zero charge is 0.87 ± 0.1 V, $pH_0 = 4.7$). Since Ni^{2+} has a significant positive charge, it is most likely that their incorporation into the growing oxide occurs through the mechanism of ion exchange on cation vacancies sites bearing a local negative charge. The content of the dopant should depend not only on the total charge of the electrode surface (electrode potential), but also on the charge of the foreign ion, which can vary because of hydration or complexation.

In the presence of added Ni^{2+} the variation of the solution pH and temperature results in a change of the content of the modifying element in the oxide bulk (Table 3). Since under our experimental conditions the hydrolysis of Ni^{2+} is impossible, an effective way to increase the amount of Ni^{2+} inside PbO_2 is to reduce the positive surface charge, which can be achieved by lowering the deposition current density or by using a porous substrate. Alternatively, the positive charge of the doping cation can be reduced by formation of complexes such as $[Ni(OH)_xF_y]^n$, where the ligands are fluoride anions [16,18,25]. The simultaneous presence in the solution of Ni^{2+} and fluoride leads to a significant increase in the amount of modifying elements in the oxide [12].

From a general point of view, it is interesting to note that there are various methods of inclusion of cationic additives in electrochemically synthesized oxides [16–18,25]:

Table 2
Parameters of experimental electric circuit equivalent to the impedance of lead dioxide electrodeposition from the electrolyte, containing Ni^{2+} ions and without additive.

E*/V	R_s/Ω	R_1/Ω	R_2/Ω	R_3/Ω	$C_{dl}\cdot10^7$/F	$C_1\cdot10^6$/F	$C_2\cdot10^5$/F
PbO_2							
1.20	64	1010	154	166	6.0	4.0	10.0
1.30	64	1000	500	222	4.0	30.0	70.0
PbO_2-Ni							
1.20	62	1000	167	240	6.0	3.0	7.0

* Potentials are reported vs. $Ag/AgCl/KCl_{(sat.)}$; electrode area is 0.13 cm^2.

i) Occlusion of the electrolyte. This event is highly improbable since compact nonporous coatings are deposited in our experimental conditions.

ii) Nickel oxide phase formation by co-electrodeposition with lead dioxide. If this mechanism is operative, the thermodynamic potential of a new phase cannot exceed potentials of PbO_2 electrodeposition. In this case, the content of the modifying element should increase or remain invariant upon increasing the applied potential, as the electrodeposition of lead dioxide in our conditions takes place under diffusion control at currents close to the limiting current [16–18,25–27].
In most cases equilibrium potentials of Ni^{2+} ions oxidation is high enough to make it possible its occurrence in parallel with the formation of lead dioxide [28]:

$$Ni^{2+} + 2H_2O - 2e = NiO_2 + 4H^+,\ E_0 = 1.593 - 0.1182pH - 0.0295\lg a_{Ni}^{2+} \quad (1)$$

$$2Ni^{2+} + 3H_2O - 2e = Ni_2O_3 + 6H^+,\ E = 1.753 - 0.1773pH - 0.0591\lg a_{Ni}^{2+} \quad (2)$$

$$3Ni^{2+} + 4H_2O - 2e = Ni_3O_4 + 8H^+,\ E = 1.977 - 0.2364pH - 0.0886\lg a_{Ni}^{2+} \quad (3)$$

One can note that under certain conditions the formation NiO_2 is thermodynamically possible. However, the latter possibility is not supported by experimental data which rather show a decrease in the nickel content with increasing anodic current density in the entire range of deposition potentials.

iii) Substitution of lead ions on nickel cations by ion exchange mechanism. According to experimental data obtained by the radioactive tracer technique (described below), the mechanism of lead dioxide modification by nickel ions encloses at least two steps: chemisorption of cations on PbO_2 and their subsequent inclusion into the bulk through ion exchange with Pb^{2+} in hydrated or Pb^{4+} ions in crystalline zones of the oxide [10].

Oxygen evolution processes, the oxidation of lead and growth of the oxide film, accompanied by the destruction of the anode material, mainly occur on lead dioxide electrodes at high anodic polarization [29].

The analysis of steady-state polarization curves for O_2 evolution (Fig. 7) has shown that the Tafel slope reduces from 0.120 V for 1.6 M $(NH_4)_2SO_4$ to 0.08 V for solutions containing Ni^{2+} ions. The obtained data indicate that nickel ions cause a change in the mechanism as observed earlier in the case of iron ions [16–18,25].

The corrosion rate of non-modified electrode in the background solution at an anode current density of 500 mA cm^{-2} is 80 g m^{-2} h^{-1}. The presence of nickel ions in the electrolyte leads to a decrease in the degradation rate of the electrodes: 78 and 59 g m^{-2} h^{-1} at 0.001 M and 0.01 M concentration of Ni^{2+}, respectively.

Changes in the corrosion rate of electrodes in different electrolytes are known to be associated mainly with the change of the protective film content (ratio α- and β-PbO_2) and its structural and mechanical properties (porosity, internal stress, coefficient of thermal expansion etc.) [30]. Since the decrease of thickness of the protective layer in the presence of Ni^{2+} in solution will hardly contribute to the formation of oxide films with good shielding properties, an explanation of the decrease in dissolution rate of anodes based on this approach is not feasible. Probably, in some cases, the effect of these factors is not determinant.

We think that the presence of Ni^{2+} in a solution leads to the formation on the anode surface of chemisorbed complexes with low bond strength OH_{ads}. This reduces the number of inert oxygen-containing particles and thus decreases the rate of destruction of the anode material. Such particles, according to [25], are capable of interacting with surface metal atoms, weakening their binding to the lattice enough as to favor their transition into the solution as an oxygen-containing complex. Subsequently, these decompose into some ionic species or molecular poorly soluble compounds (e.g., metal oxides or hydroxides). Increasing of the dissolution rate of the oxide leads to an increase in the number of defects and pores in the protective film, which in turn facilitates the mechanical destruction of the anode material.

Thus, processes of the oxygen evolution, the formation of oxide film and destruction of lead dioxide anode occur through the common step, i.e., the anodic oxidation of water with formation of chemisorbed OH-radicals [17,31]. It is possible to influence each of the processes involved by somehow changing the number of labile and inert oxygen-containing particles on the anode surface.

Data about the surface morphology of the PbO_2-based materials was obtained by scanning electron microscopy. As follows from results, PbO_2 and PbO_2-Ni are virtually identical in morphology (Appendix B).

Let's consider the influence of electrodeposition conditions on the chemical composition of lead dioxide. As it is known, in almost all cases, there are deviations from the ideal stoichiometry of PbO_2 [32], and the actual chemical formula of PbO_2 was experimentally established by detection of Pb(II) [33] and structural water [16] within the lattice. Investigations have also confirmed that there is a

Table 3
The influence of deposition conditions on the dopant content in PbO_2.

Deposition conditions $j_a = 4$ mA cm^{-2}; T = 298 K	Content of Ni^{2+}, wt.%
(N)* + 0.01 M $Ni(NO_3)_2$	0.0011
(N) + 0.02 M $Ni(NO_3)_2$	0.0022
(N) + 0.05 M $Ni(NO_3)_2$	0.0050
(N) + 0.01 M $Ni(NO_3)_2$, $j_a = 2$ mA cm^{-2}	0.0061
(N) + 0.01 M $Ni(NO_3)_2$, $j_a = 10$ mA cm^{-2}	0.0009
(N) + 0.01 M $Ni(NO_3)_2$, porous sheet	0.0205
(N) + 0.01 M $Ni(NO_3)_2$, T = 338 K	0.0033
0.1 M $Pb(NO_3)_2$ + 0.5 M HNO_3 + 0.01 M $Ni(NO_3)_2$	0.0027
0.1 M $Pb(NO_3)_2$ + 1 M HNO_3 + 0.01 M $Ni(NO_3)_2$	0.0106
(N) + 0.01 M $Ni(NO_3)_2$ + 0.01 M NaF	0.0022
(N) + 0.01 M $Ni(NO_3)_2$ + 0.02 M NaF	0.0123

* (N) means 0.1 M $Pb(NO_3)_2$ + 0.1 M HNO_3.

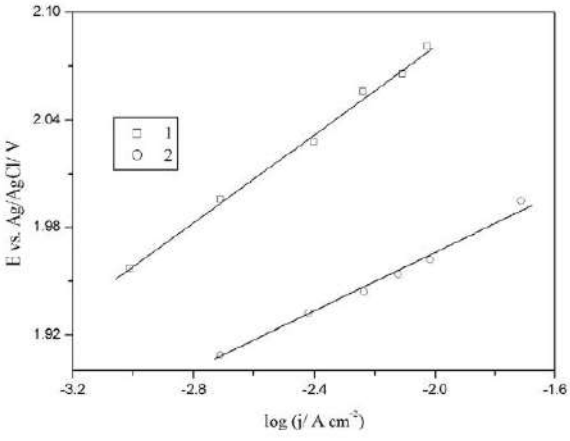

Fig. 7. Steady-state polarization curves in 1.6 M $(NH_4)_2SO_4$ of PbO_2 (1) and PbO_2-Ni (2).

relationship between the hydrogen content in PbO_2 and its electrochemical activity. However, there are few [34] studies in the literature on the impact of conditions of lead dioxide electrodeposition on the content of structural water in the resulting deposit, and this complicates studies directed at the electrochemical synthesis of PbO_2 with a given electrocatalytic activity. In this connection, we made an attempt to evaluate the influence of electrodeposition conditions of PbO_2 on the chemical composition of the resulting deposits; in particular, the content of structural water.

Data on the amount of water in PbO_2 at different thicknesses of deposits were obtained by radioactive tracer technique, using tritium water $3H_2O$. The results indicate a correlation between the amount of structural water and allotropic form of oxide, in particular, α-PbO_2 contains more water than β-PbO_2, which is consistent with the results obtained by the high resolution transmission electron spectroscopy [16, 33,34]. Different crystal structure of α- and β-PbO_2 leads to differences in the number of cation vacancies in the oxide and, as a result, the amount of water of crystallization.

The influence of deposition conditions on the phase composition of electrodeposited lead dioxide was studied by X-ray diffraction. As described in [16], in some cases the phase composition of lead dioxide may depend on the thickness of deposits. To avoid this undesirable effect all measurements were performed on samples with fixed thickness (corresponding to about 35 mg cm^{-2}). It should be noted that, except for the beta(200) line, we did not notice any change in the character and intensity of the diffraction pattern peaks with the change in the angle of X-rays to the sample surface, and with changing of the coating thickness. This indicates a homogeneous distribution of the various phases and crystals with different crystallographic orientation in lead dioxide obtained at our conditions (Appendix C).

A series of radiochemical measurements were performed for the estimation of the influence of Ni^{2+} on the content of the internal water, as well as for confirmation of earlier assumptions about the location of the modifying ions and way they are included into the growing oxide. In order to gain insights, we prepared deposits at room temperature and at elevated temperatures in the presence and in the absence of the cationic additive. It should be noted that irrespective of the localization of modifying cation, its influence on internal water content (tritium activity) would be determined, basically, by its charge. In particular, if the charges of ion additive and exchangeable Pb^{2+} cation in hydrated zone of oxide will be the same, this should not change the amount of internal water in oxide. An example is Ni^{2+}/ PbO_2 obtained at 1.5 V and room temperature, when nickel is in the in form of Ni^{2+} because electrochemical oxidation can be neglected. Replacement of Pb^{2+} by Ni^{2+} in the hydrated zones of the oxide will not cause deprotonation of hydroxyl group to compensate the excess positive charge of the ionic additive, and tritium activity should not change, as observed experimentally (Fig. 8). However, at elevated temperatures, the presence of Ni^{2+} in the solution brings about, as in the case of Fe^{3+} ions [35,36], an increase of the tritium activity because Ni^{2+} ions substitute Pb^{4+} in the lattice sites (crystalline zone of oxide) by an ion exchange mechanism that leads to protonation of O^{2-} in the crystalline lattice with formation of OH^- for compensation of the negative charge excess. In this case tritium activity will increase (Fig. 8).

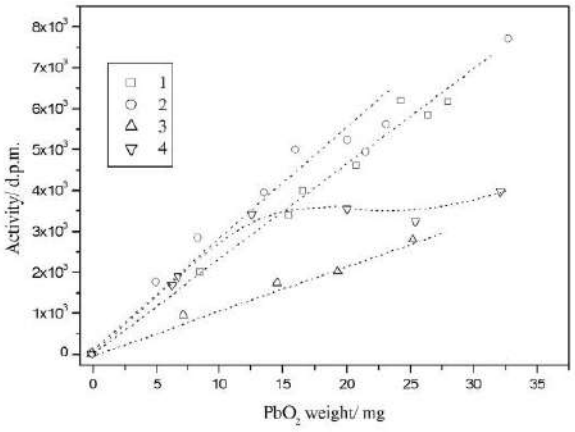

Fig. 8. Radiochemical measurement of tritium activity of PbO_2, deposited at 296 (1; 2) or 338 K (3; 4) from electrolytes: 1; 3–0.1 M HNO_3 + 0.1 M $Pb(NO_3)_2$; 2; 4–0.1 M HNO_3 + 0.1 M $Pb(NO_3)_2$ + 0.01 M $Ni(NO_3)_2$. j_a = 4 mA cm^{-2}.

Thus, the radiochemical measurements confirm our assumptions about the mechanism of Ni^{2+} inclusion in the growing lead dioxide. Cationic additives approach the electrode surface by the diffusion, are chemisorbed onto the electrode surface and are finally included in the oxide bulk by ion exchange with Pb^{2+} in a hydrated (room temperature) or Pb^{4+} crystalline (elevated temperature) zone of oxide. The change of the internal water content is due to the protonation or deprotonation of oxygen-containing particles for compensation of excess charges.

The pattern obtained by secondary ion mass spectrometry (negative ion mass spectra) confirmed the presence of water and hydroxyl particles not only on the surface but also in the bulk of lead dioxide (not shown). It should be noted that the amount of hydroxyl groups on the surface is significantly higher than in the bulk that is caused by adsorption of OH^- on the oxide surface [2,37].

X-ray photoelectron spectroscopy (XPS) data show that the Pb $4f_{7/2}$ peak falls at 137.4 eV and can be consequently assigned to Pb(IV) in PbO_2 [36]. The peak width of 1.75 eV, and its symmetry also favor the location of lead on the oxide surface mainly in the mentioned form; the content of other lead compounds is not more than a few wt.%.

According to [25], the position of the O1s XPS signal is a good indicator of the nature of chemisorbed oxygen-containing particles on lead dioxide. In the present case, the binding energy of oxygen in PbO_2 (527.7–528.6 eV) is slightly different from the binding energy of the inert (strongly bounded) adsorbed oxygen-containing particles (528.9 eV [36]), while the binding energy of the labile oxygen (530.2 eV [36]), as well as hydroxyl groups and water molecules 531.0–533.0 eV [38] is much higher. Such large differences in binding energies allow the experimental detection of labile chemisorbed oxygen-containing particles on the lead dioxide surface.

Modification of PbO_2 by Ni^{2+} leads to a significant increase in the number of labile oxygen-containing surface species (Fig. 9). Such changes in the surface concentration of adsorbed oxygen-containing particles on the electrode is expected to affect the electrocatalytic activity of anodes, which is known to depend on chemical (the composition of the

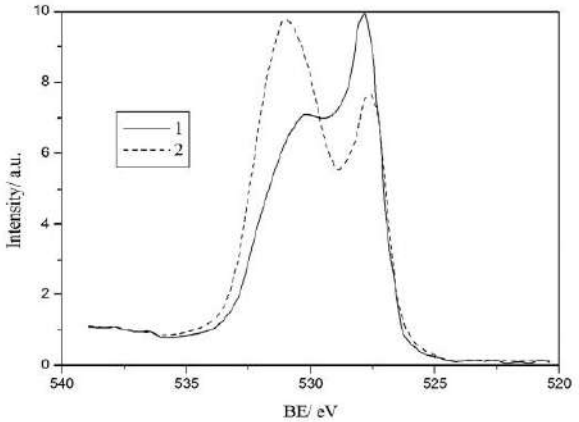

Fig. 9. O 1 s core level structure in PbO_2 obtained at j_a = 4 mA cm^{-2} from solutions: 1–0.1 M HNO_3 + 0.1 M $Pb(NO_3)_2$; 2–0.1 M HNO_3 + 0.1 M $Pb(NO_3)_2$ + 0.01 M $Ni(NO_3)_2$.

material) and geometrical factors such as the structure and morphology. Unfortunately, due to the low content of the modifying elements we were unable to identify the nature of surface nickel compounds by XPS.

Modification of lead dioxide by Ni^{2+} also reduces the oxygen evolution overpotential, but in this case we did not observe Tafel slope decrease with increasing of Ni^{2+} content in the oxide. This permit to assume that the reaction of electrochemical desorption (the second electron transfer) [39] remains the rate-limiting step. Since PbO_2 modification by Ni^{2+} leads to a significant increase in the amount of labile surface oxygen-containing species, an increase in the catalytic activity of the oxide in respect to the oxygen evolution reaction is quite natural.

4. Conclusions

The formation of PbO_2 occurs in four stages (1)–(4), two of which are electrochemical step electron transfer and the other two are chemical stages involving the formation and decay of soluble intermediates 3 and 4-valent lead. The first step is the first electron transfer with the formation on the electrode surface of oxygen-containing particles such as OH_{ads}, which are formed by the anode ionization of water. Then, in the subsequent chemical step these particles react with lead ions with formation at the electrode surface of a mobile oxygen-containing intermediate of Pb(III) such as $Pb(OH)^{2+}$, which is subsequently oxidized with the second electron transfer. As a result of this reaction soluble tetravalent lead intermediates (such as $Pb(OH)_2^{2+}$) evolving to PbO_2 in the last step.

The observed inhibition effect of Pb^{2+} oxidation in the presence of Ni^{2+}, is apparently related to partial blocking of the active sites on the surface of the growing lead dioxide, due to cation adsorption on the electrode. Changing of the electrolyte composition and conditions of electrodeposition of PbO_2 (deposition potential, temperature and pH) significantly influences the physicochemical properties of PbO_2 based materials, particularly the phase and chemical composition, the crystallographic orientation, the content of structural water and the nature of adsorbed oxygen-containing particles on the electrode surface. Modification of PbO_2 by Ni^{2+} leads to a significant increase in the amount of weakly bonded surface oxygen-containing particles, which is identified as the reason for the observed enhancement of the electrocatalytic activity of Ni^{2+} /PbO_2 electrodes.

Appendix A. Supplementary data

Supplementary data to this article can be found online at http://dx.doi.org/10.1016/j.jelechem.2016.05.017.

References

[1] X. Li, D. Pletcher, F.C. Walsh, Electrodeposited lead dioxide coatings, Chem. Soc. Rev. 40 (2011) 3879.
[2] R. Vargas, C. Borras, J. Mostany, B.R. Scharifker, Electrocatalysis of the anodic oxygen transfer reaction, Bol. Acad. Cienc. Fis. Mat. Nat. 71 (2011) 37.
[3] C.T.J. Low, D. Pletcher, F.C. Walsh, The electrodeposition of highly reflective lead dioxide coatings, Electrochem. Commun. 11 (2009) 1301.
[4] Y. Liu, H. Liu, Comparative studies on the electrocatalytic properties of modified PbO_2 anodes, Electrochim. Acta 53 (2008) 5077.
[5] A. Oury, A. Kirchev, Y. Bultel, Potential response of lead dioxide/lead(II) galvanostatic cycling in methanesulfonic acid: a morphologico-kinetics interpretation, J. Electrochem. Soc. 160 (2013) A148.
[6] M.G. Verde, K.J. Carroll, Z. Wang, A. Sathrum, Y.S. Meng, Achieving high efficiency and cyclability in inexpensive soluble lead flow batteries, Energy Environ. Sci. 6 (2013) 1573.
[7] B.P. Chaplin, Critical review of electrochemical advanced oxidation processes for water treatment applications, Environ. Sci.: Processes Impacts 16 (2014) 1182.
[8] R. Vargas, C. Borras, D. Mendez, J. Mostany, B.R. Scharifker, Electrochemical oxygen transfer reactions: electrode materials, surface processes, kinetic models, linear free energy correlations, and perspectives. A review, J. Solid State Electrochem. 20 (2016) 875.
[9] O. Shmychkova, T. Luk'yanenko, A. Yakubenko, R. Amadelli, A. Velichenko, Electrooxidation of some phenolic compounds at Bi-doped PbO_2, Appl. Catal. B 162 (2015) 346.
[10] O. Shmychkova, T. Luk'yanenko, A. Velichenko, L. Meda, R. Amadelli, Bi-doped PbO_2 anodes: electrodeposition and physico-chemical properties, Electrochim. Acta 111 (2013) 332.
[11] O. Shmychkova, T. Luk'yanenko, A. Velichenko, R. Amadelli, Electrodeposition of Ce-doped PbO_2, J. Electroanal. Chem. 706 (2013) 86.
[12] O. Shmychkova, T. Luk'yanenko, R. Amadelli, A. Velichenko, Physico-chemical properties of PbO_2-anodes doped with Sn^{4+} and complex ions, J. Electroanal. Chem. 717-718 (2014) 196.
[13] F.C. Walsh, C. Ponce de Leon, Versatile electrochemical coatings and surface layers from methanesulfonic acid, Surf. Coat. Technol. 259 (2014) 676.
[14] M.D. Capelato, J.A. Nobrega, E.F.A. Neves, Complexing power of alkanesulfonate ions: the lead-methanesulfonate system, J. Appl. Electrochem. 25 (1995) 408.
[15] Y. Xia, Q. Dai, J. Chen, Electrochemical degradation of aspirin using a Ni doped PbO_2 electrode, J. Electroanal. Chem. 744 (2015) 117.
[16] A.B. Velichenko, D.V. Girenko, S.V. Kovalyov, A.N. Gnatenko, R. Amadelli, F.I. Danilov, Lead dioxide electrodeposition and its application: influence of fluoride and iron ions, J. Electroanal. Chem. 454 (1998) 203.
[17] A.B. Velichenko, R. Amadelli, A. Benedetti, D.V. Girenko, S.V. Kovalyov, F.I. Danilov, Electrosynthesis and physicochemical properties of PbO_2, J. Electrochem. Soc. 149 (2002) C445.
[18] A.B. Velichenko, R. Amadelli, G.L. Zucchini, D.V. Girenko, F.I. Danilov, Electrosynthesis and physicochemical properties of Fe-doped lead dioxide electrocatalysts, Electrochim. Acta 45 (2000) 4341.
[19] A.B. Velichenko, D.V. Girenko, F.I. Danilov, Electrodeposition of lead dioxide at an Au electrode, Electrochim. Acta 40 (1995) 2803.
[20] A.B. Velichenko, D.V. Girenko, F.I. Danilov, The mechanism of lead dioxide electrodeposition on a platinum electrode, Russ. J. Electrochem. 33 (1996) 96.
[21] D. Pavlov, B. Monahov, D. Petrov, Influence of Ag as alloy additive on the oxygen evolution reaction on Pb/PbO_2 electrode, J. Power Sources 85 (2000) 59.
[22] N.V. Nikolenko, Surface properties of calcite: Adsorption model with orbital control, Adsorpt. Sci. Technol. 19 (2001) 237.
[23] S. Trasatti, G. Lodi, Properties of Conductive Transition Metal Oxides with Rutile-Type Structure. Electrodes of Conductive Metallic Oxides. Part A, Elsevier, Amsterdam, 1980 301.
[24] A.B. Velichenko, E.A. Baranova, D.V. Girenko, R. Amadelli, S.V. Kovalev, F.I. Danilov, Mechanism of electrodeposition of lead dioxide from nitrate solutions, Russ. J. Electrochem. 39 (2003) 615.
[25] A.B. Velichenko, D. Devilliers, Electrodeposition of fluorine-doped PbO_2, J. Fluor. Chem. 128 (2007) 269.
[26] O.B. Shmychkova, T.V. Luk'yanenko, A.B. Velichenko, R.E. Gladyshevskii, P.Y. Demchenko, R. Amadelli, The influence of deposition conditions on phase composition of lead dioxide-based materials, Prot. Met. Phys. Chem. Surf. 51 (2015) 593.
[27] O. Shmychkova, T. Luk'yanenko, A. Pilerska, A. Velichenko, R. Gladyshevskii, P. Demchenko, R. Amadelli, Electrocrystallization of lead dioxide: influence of early stages of nucleation on phase composition, J. Electroanal. Chem. 746 (2015) 57.
[28] M. Pourbaix, Atlas of Electrochemical Equilibria in Aqueous Solutions, NACE, Houston, 1976 (458 pp.).
[29] C. Saez, P. Canizares, J. Llanos, M.A. Rodrigo, The treatment of actual industrial wastewaters using electrochemical techniques, Electrocatalysis 4 (2013) 252.
[30] I. Petersson, E. Ahlberg, B. Berghult, Parameters influencing the ratio between electrochemically formed α- and β-PbO_2, J. Power Sources 76 (1998) 98.
[31] F.I. Danilov, A.B. Velichenko, Electrocatalytic activity of anodes in reference to Cr(III) oxidation reaction, Electrochim. Acta 38 (1993) 437.
[32] W.-H. Yang, W.-T. Yang, X.-Y. Lin, Preparation and characterization of a novel Bi-doped PbO_2 electrode, Acta Phys. -Chim. Sin. 28 (2012) 831.
[33] P. Ruetschi, R. Giovanoli, On the presence of OH^- ions, Pb^{2+} ions and cation vacancies in PbO_2, Power Sources 13 (1991) 81.
[34] R. Amadelli, L. Samiolo, A.B. Velichenko, An electrochemical and radiotracer investigation on lead dioxide: influence of the deposition current and temperature, J. Serb. Chem. Soc. 78 (2013) 2099.
[35] R. Amadelli, A.B. Velichenko, E. Tondello, L. Armelao, S. Daolio, M. Fabrizio, Ion bombardment of PbO_2 films: water influence of cluster production, Int. J. Mass Spectrom. 179-180 (1998) 309.
[36] R. Amadelli, L. Armelao, E. Tondello, S. Daolio, M. Fabrizio, C. Pagura, A. Velichenko, A SIMS and XPS study about ions influence on electrodeposited PbO_2 films, Appl. Surf. Sci. 142 (1999) 200.
[37] D. Pech, T. Brousse, D. Belanger, D. Guay, EQCM study of electrodeposited PbO_2: investigation of the gel formation and discharge mechanisms, Electrochim. Acta 54 (2009) 7382.
[38] C.D. Wanger, W.M. Riggs, L.E. Davis, J.F. Moulder, G.E. Muilenberg, Handbook of X-ray Photoelectron Spectroscopy, Perkin-Elmer Corp., Physical Electronics Division, Eden Prairie, Minnesota, USA, 1995 (190 pp.).
[39] R. Amadelli, A. Maldotti, A. Molinari, F.I. Danilov, A.B. Velichenko, Influence of the electrode history and effects of the electrolyte composition and temperature on O_2 evolution at β-PbO_2 anodes in acid media, J. Electroanal. Chem. 534 (2002) 1.

ECS Transactions, 77 (11) 1617-1623 (2017)
10.1149/07711.1617ecst ©The Electrochemical Society

Lead dioxide electrocrystallization from nitrate and methanesulfonate electrolytes: the influence of various dopants on initial stages

O. Shmychkova, T. Luk'yanenko, A. Velichenko

Ukrainian State University of Chemical Technology, 8, Gagarin Ave., 49005 Dnipro, Ukraine

Integrated data about the influence of dopants with different nature on crystallization rate constants and crystal shape have been presented in this work. It was obtain that there is an increase of current delay, corresponding to the induction period on chronoamperometric curves in the presence of cationic additives in the deposition electrolyte that indicates difficulties in initial stages of lead dioxide phase formation. The crystallization occurs through the progressive mechanism. The preferred geometric shape of formed crystals at 2D nucleation from electrolytes containing cationic additives is cone. And upon crystallization from electrolytes containing complex ions additives geometric shape changes on a cylinder. For nitrate electrolytes there is a change in the mechanism from progressive on instantaneous at high concentrations of added surfactants. The preferred form of crystals at 2D nucleation in the presence of surfactant additives in nitrate electrolytes is semi-spheroid, and in the case of methanesulfonate electrolytes cylinder becomes the preferred form of crystals. In the case of suspension electrolytes at 2D nucleation the formation of three main forms of crystals is possible depending on the polarization.

Introduction

Properties of electrodeposited lead dioxide depend on the composition of the electrolyte and deposition conditions (1–3). Various ions or dispersed particles added in the electrolyte affect regularities of lead dioxide electrodeposition (4–8). It is also known (9–12), that additives in the deposition electrolyte can distort the shape of crystals due to changing of the surface energy of the growing crystal faces or their incorporation into the crystal, thereby disturbing the crystallization process.

In the present work we examine early stages of electrocrystallization of PbO_2 from methanesulfonate electrolytes that contain various ionic additives (Bi^{3+}, Ce^{3+}, Sn^{4+}, $(NiF_6)^{2-}$, $(SnF_6)^{2-}$, sodium dodecyl sulfate (SDS), colloid of TiO_2). Integrated data about the influence of dopants with different nature on crystallization rate constants and crystal shape are presented in this work. It should be pointed out that such data is currently absent in the literature.

Experimental

ECS Transactions, 77 (11) 1617-1623 (2017)

All chemicals were reagent grade. Electrodeposition regularities of lead dioxide both in nitrate and methanesulfonate electrolytes were studied on Pt disk electrode (Pt-DE, 0.19 cm^2) by steady-state voltammetry, chronoamperometry. The Pt-DE surface was treated, before use, by the procedure described in (8). Such preliminary treatment permits to achieve a reproducible surface. Voltammetry measurements were carried out in a standard temperature-controlled three-electrode cell. All potentials were recorded and reported vs. Ag / AgCl / KCl $_{(sat.)}$.

Electrodeposition of lead dioxide was studied in the methanesulfonate / nitrate electrolytes that contained 1 M CH_3SO_3H / HNO_3, 0.01 M $Pb(CH_3SO_3)_2$ / $Pb(NO_3)_2$ and 0.01 M additive ($Bi(NO_3)_3$, $Ce(NO_3)_3$, $(CH_3COO)_4Sn$, $K_2[NiF_6]$, $K_2[SnF_6]$); SDS of two different concentrations 3×10^{-5} and 7×10^{-5} mol dm^{-3}; 0.5–5 g dm^{-3} $TiO_{2(colloid)}$ depending on purposes of experiments.

Results and discussion

As one can see, there is an increase of current delay, corresponding to the induction period on chronoamperometric curves (Fig. 1) in the presence of cationic additives in the deposition electrolyte. This indicates difficulties in initial stages of lead dioxide phase formation.

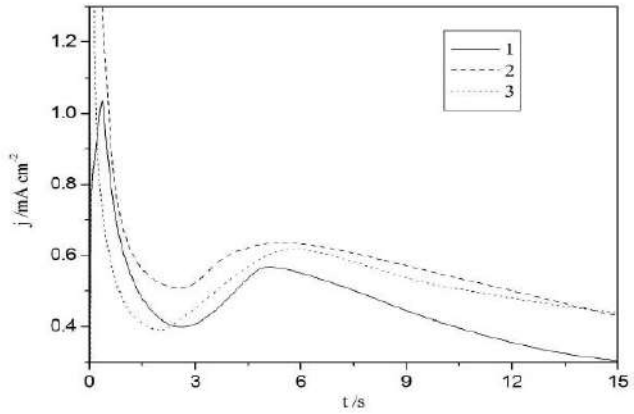

Figure 1. Current-time transients obtained at PbO_2 deposition on Pt electrode at 1620 mV from next solutions: 1 – 0.01 M $Pb(CH_3SO_3)_2$+1 M CH_3SO_3H (1)+0.01 M Bi^{3+}; 2 – (1)+0.001 M Ce^{3+}; 3 – (1)+0.01 M Sn^{4+}.

During electrodeposition both kinetic regularities of the crystallization process and the nature of the crystal structure of formed oxide depend on the nucleation rate, i.e. the rate of formation of crystal nuclei, linear crystallization velosity and their ratio. These paremeters can be determined from current transients of the process of lead dioxide electrodeposition (13–15).

For all the above cases, the crystallization occurs through the progressive mechanism. The preferred geometric shape of formed crystals at 2D nucleation from electrolytes containing cationic additives is cone. And upon crystallization from electrolytes containing complex ions additives geometric shape changes on a cylinder.

ECS Transactions, 77 (11) 1617-1623 (2017)

The main parameters of the crystallization of lead dioxide from electrolytes containing ionic additives are presented in the Table 1.

TABLE 1. Parameters of initial stages of lead dioxide electrocrystallization*

Deposition electrolyte	t_α	K_α	t_β	K_β
0.01 M $Pb(CH_3SO_3)_2$+1 M CH_3SO_3H+0.01 M Bi^{3+}	2.17	9.20×10^{-6}	4.71	4.1×10^{-5}
0.01 M $Pb(CH_3SO_3)_2$+1 M CH_3SO_3H+0.001 M Ce^{3+}	2.40	2.12×10^{-6}	4.40	8.95×10^{-8}
0.01 M $Pb(CH_3SO_3)_2$+1 M CH_3SO_3H+0.01 M Sn^{4+}	1.56	2.06×10^{-5}	4.41	6.28×10^{-7}
0.01 M $Pb(CH_3SO_3)_2$+1 M CH_3SO_3H+0.01 M $[NiF_6]^{2-}$	0.02	4.61×10^{-5}	0.05	9.78×10^{-7}
0.01 M $Pb(CH_3SO_3)_2$+1 M CH_3SO_3H+0.01 M $[SnF_6]^{2-}$	0.64	3.92×10^{-6}	1.99	5.32×10^{-5}

*In this table K_α (mol m^{-2} s^{-1}) – rate constant for growth of α-phase crystals in a direction, perpendicular to the electrode surface; t_α(s) – time, corresponding to the beginning of α-phase formation.
K_β (mol m^{-2} s^{-1}) – rate constant for growth of β -phase crystals in a direction, perpendicular to the electrode surface; t_β (s) – time, corresponding to the beginning of β -phase formation

As one can conclude from obtained data, the presence of cations in the deposition electrolyte alters the ratio between α- and β-phase crystallization constants in different amount. Thus, in the presence of the complex ion $[SnF_6]^{2-}$ the growth of β-phase dominates. For other cationic additives the prevalence of α-phase growth is observed. It should also be noted, that the presence of complex nickel and tin fluoride ions reduces the beginning of nucleation. Most clearly this effect is observed for $[NiF_6]^{2-}$ ion.

It is known (7), that the surfactant additive has a significant effect on the kinetics of lead dioxide electrodeposition, without changing the mechanism of the process. It has been also found that it is incorporated into the growing coating through adsorption on PbO_2 crystals. That in turn will lead to changes in initial stages of the crystallization. It is known (16), that surfactant additives selectively adsorbed on certain faces, usually parallel to faces, reducing the growth rate of these faces, and thereby altering the shape of growing crystals. For more detailed analysis of surfactant additives influence on the initial stages of the crystallization current-time transients from electrolytes, containing SDS of two different concentrations 3×10^{-5} and 7×10^{-5} mol dm^{-3} were obtained.

The analysis of obtained transient revealed that in the case of methanesulfonate electrolytes the crystallization proceeds according to the progressive mechanism. For nitrate electrolytes there is a change in the mechanism from progressive on instantaneous at high concentrations of surfactants. The preferred form of crystals at 2D nucleation in the presence of additives in nitrate electrolytes is semi-spheroid, and in the case of methanesulfonate electrolytes cylinder becomes the preferred form of crystals. The main parameters of crystallization of lead dioxide in the presence of surfactants are presented in the Table 2.

TABLE 2. Parameters of initial stages of lead dioxide electrocrystallization in the presence of surfactants in the deposition electrolyte

Deposition electrolyte	t_α	K_α	t_β	K_β
0.1 M $Pb(NO_3)_2$+1.0 M HNO_3+ 3×10^{-5} SDS	3.03	3.26×10^{-6}	7.87	1.10×10^{-5}
0.1 M $Pb(NO_3)_2$+1.0 M HNO_3+ 7×10^{-5} SDS	2.35	1.08×10^{-5}	6.30	3.30×10^{-5}
0.1 M $Pb(CH_3SO_3)_2$+ 1 M CH_3SO_3H + 3×10^{-5} SDS	1.50	6.38×10^{-6}	2.80	1.04×10^{-5}
0.1 M $Pb(CH_3SO_3)_2$+ 1 M CH_3SO_3H + 7×10^{-5} SDS	0.84	1.38×10^{-6}	1.08	8.22×10^{-6}

As has been shown in (8), the presence of TiO_2 particles during the electrodeposition of PbO_2 produces range of composite materials with a various content of dispersed phase in the deposit that allows one to control physico-chemical, electrocatalytical and photocatalytical properties of the coating.

The investigation of regularities of PbO_2 electrodeposition was carried out from nitrate and methanesulfonate electrolytes, containing colloidal titanium dioxide. The system is resistant to sedimentation for a long time even in the presence of relatively

ECS Transactions, 77 (11) 1617-1623 (2017)

high concentrations of lead nitrate. Such systems do not fracture spontaneously over time and are the perfect model to assess the influence of valve metal particles on the initial stages of lead dioxide crystallization.

As it has been seen from Fig. 2, the type of transient is determined by the electrode potential. In the case of nitrate electrolyte at low polarizations (E=1400 mV) prolonged induction period is observed with a further very slow increase of current and reaching of quasi-stationary current.

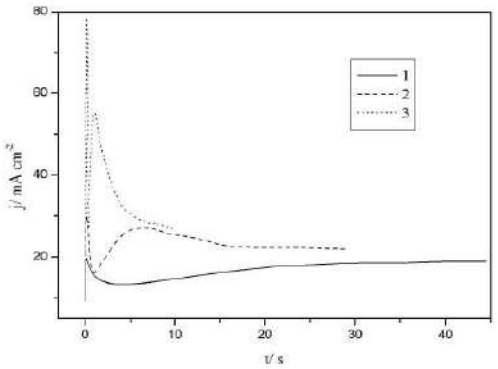

Figure 2. Current-time transients obtained at PbO_2 deposition on Pt electrode from 0.1 M HNO_3+0.1 M $Pb(NO_3)_2$ + 5 g dm^{-3} $TiO_{2(colloid)}$ at different potentials, mV: 1–1400; 2–1450; 3–1550

Such type of transient points the slow accumulation of intermediate products and the kinetic control of lead dioxide crystallization. The increasing of polarization on 50 mV (E=1450) results in a sharp decrease of the induction period. The diffuse maximum of current (I_p) is observed on the j-t curve up to reaching the quasi steady-state current (I_s), indicating the occurrence of diffusion difficulties in the crystallization. A slight difference between I_p and I_s indicates a mixed diffusion-kinetic control of the crystallization process. At the high polarization (E=1550 mV) induction period is virtually absent on transient, but there is a maximum current that is several times greater than I_s value. In this case, one can see a clear occurrence of the diffusion control of oxide crystallization process.

At 1400 mV the nucleation of suspension electrolytes proceeds through the progressive mechanism. The geometric shape of crystals is differs at 2D nucleation in the case of suspension electrolytes and depends on the polarization of the electrode. Thus, depending on the polarization, the formation of three main forms of crystals is possible. At low polarization (E=1400 mV) it is a semi-spheroid, that is the geometric shape, demanding less energy inputs in the formation of crystals of the new phase. With an increase of polarization on 50 mV change in crystal form on tapered takes place, and at high polarizations (E=1550 mV), the formation of cylinder crystals may occur. The main parameters of lead dioxide crystallization at different potentials are presented in the Table 3.

TABLE 3. Parameters of initial stages of lead dioxide electrocrystallization depending on the electrode polarization

E/ mV	t_α	K_α	t_β	K_β
		Nitrate electrolyte		
1400	1.24	3.58×10^{-7}	3.64	2.10×10^{-6}

ECS Transactions, 77 (11) 1617-1623 (2017)

1450	1.05	8.56×10^{-7}	2.76	7.30×10^{-6}
1550	0.39	1.08×10^{-6}	1.22	1.18×10^{-5}
	Methanesulfonate electrolyte			
1550	0.73	3.5×10^{-6}	2.92	1.47×10^{-5}
1620	0.41	1.04×10^{-6}	2.04	2.96×10^{-6}

As one can conclude from the data obtained at the crystallization from suspension electrolytes the growth of β-phase is predominant. Only the ratio between the growths of α- and β-phase depends on the polarization of the electrode. This effect of the dispersed phase is likely due to imposed geometry of TiO_2 crystals that become apparently additional crystallization centers.

In the case of methanesulfonate electrolyte the type of transient is also depend on the electrode polarization.

At low polarization the nucleation is instantaneous, and at high it is progressive. The preferred form of crystals at 2D nucleation at low polarization is a semi-spheroid (the simplest form), at high – is cone. The main parameters of lead dioxide crystallization from methanesulfonate electrolytes are presented in the Table 3.

Current transients, obtained at E=1500 mV from nitrate electrolyte and an electrolyte, additionally containing colloidal particles of titanium dioxide, are shown on Fig. 3. According to observed data, during the deposition from the electrolyte, containing colloid of TiO_2, one can see the two-fold reduction of the induction period, also as an increasing of the value of a quasi steady-state current, and the appearance of a clearly expressed peak current with less polarization time.

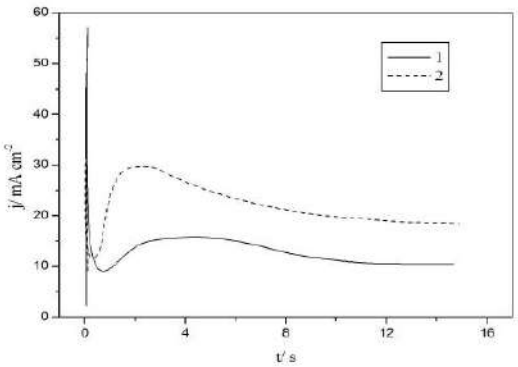

Figure 3. Current-time transients obtained at PbO_2 deposition on Pt electrode at 1550 mV from next electrolytes: 1– 0.1M HNO_3+0.1 M $Pb(NO_3)_2$; 2– 0.1M HNO_3+0.1 M $Pb(NO_3)_2$ + 5 g dm^{-3} $TiO_{2(colloid)}$

Probably, observed effects are due to the appearance of new centers of lead dioxide crystallization such as colloidal TiO_2 particles on the surface of the platinum electrode. In general, a presence in the solution of electrochemically inert valve metal oxide particles facilitates the crystallization of lead dioxide on the metal electrode. As a consequence, the preferred geometric shape of crystals at 2D nucleation is a cone, in some cases, a semi-spheroid can be formed. The main parameters of lead dioxide crystallization in the presence of colloidal TiO_2 in the solution are presented in the Table 4.

ECS Transactions, 77 (11) 1617-1623 (2017)

TABLE 4. Parameters of initial stages of lead dioxide electrocrystallization from solutions additionally contained $TiO_{2\ (colloid)}$

Deposition electrolyte	t_α	K_α	t_β	K_β
0.1M $Pb(NO_3)_2$ + 0.1M HNO_3	0.68	3.10×10^{-6}	1.45	6.57×10^{-5}
0.1M $Pb(NO_3)_2$+0.1M HNO_3+0.5 g dm^{-3} TiO_2	0.39	1.08×10^{-6}	1.22	1.18×10^{-5}
0.1M Pb^{2+}+0.1M CH_3SO_3H	0.54	3.40×10^{-5}	1.65	1.02×10^{-4}
0.1M Pb^{2+}+0.1M CH_3SO_3H +0.5 g dm^{-3} TiO_2	1.06	2.16×10^{-4}	1.42	4.18×10^{-4}
0.1M Pb^{2+}+0.1M CH_3SO_3H + 1 g dm^{-3} TiO_2	0.84	9.40×10^{-5}	1.25	2.96×10^{-5}
0.1M Pb^{2+}+0.1M CH_3SO_3H + 2 g dm^{-3} TiO_2	0.84	3.80×10^{-5}	1.24	1.64×10^{-5}
0.1M Pb^{2+}+0.1M CH_3SO_3H + 3 g dm^{-3} TiO_2	0.98	2.84×10^{-5}	1.36	2.94×10^{-5}
0.1M Pb^{2+}+0.1M CH_3SO_3H + 4 g dm^{-3} TiO_2	0.81	2.46×10^{-5}	1.14	8.47×10^{-5}
0.1M Pb^{2+}+0.1M CH_3SO_3H + 5 g dm^{-3} TiO_2	0.90	3.70×10^{-6}	1.40	2.17×10^{-5}

As one can conclude from obtained data, the rate of lead dioxide crystallization on Pt electrode (E=1620 mV) grows in the presence of colloidal TiO_2 up to the 1 g dm^{-3} concentration of latter. At concentrations above 2 g dm^{-3} the effect of the dispersed phase particles is negligible. The growth of β-phase is predominant in all cases. Depending on the amount of the dispersed phase particles varies only the ratio between kinetic constants of the crystal growth of α- and β-phase. The observed effect may be due to several reasons: the first is related to the increase of the real electrode surface (the appearance of additional centers (particles of valve metal oxide), that can be sites of PbO_2 crystallization), the second is associated with an increase of the surface concentration of lead ions, due to the adsorption of lead ions on TiO_2. Also, the formation of additional reaction centers consisting of oxygen-containing particles such as $OH^{\bullet}_{ads}$ that are located on TiO_2 surface of and can participate in the formation of PbO_2 may occur.

Conclusions

The process of coating formation of lead dioxide begins with the formation of α-phase crystals. After a certain period of time, the formation of β-phase crystals takes place. Wherein, the α- and β-phases can be formed simultaneously. Predominance in the growth of one or the other phase is determined by the ratio between the kinetic constants of the crystal growth of α- and β-phase.

In all cases involved the crystallization of lead dioxide from methanesulfonate electrolytes proceeds through the progressive mechanism. A preferred form of formed crystals at 2D nucleation in the case of electrolytes, based on nitric acid is a cone, and electrolytes, based on methanesulfonic acid is a cylinder.

For nitrate electrolytes there is a change in the mechanism from progressive on instantaneous at high concentrations of added surfactants. The preferred form of crystals at 2D nucleation in the presence of surfactant additives in nitrate electrolytes is semi-spheroid, and in the case of methanesulfonate electrolytes cylinder becomes the preferred form of crystals.

The geometric shape of crystals is differs at 2D nucleation in the case of suspension electrolytes and depends on the polarization of the electrode. Thus, at low polarization (E=1400 mV) it is a semi-spheroid, with an increase of polarization on 50 mV change in crystal form on tapered takes place, and at high polarizations (E=1550 mV), the formation of cylinder crystals may occur.

References

ECS Transactions, 77 (11) 1617-1623 (2017)

1. R. Vargas, C. Borras, D. Mendez, J. Mostany and B. R. Scharifker, *J. Solid State Electrochem.*, **20** 875 (2016).
2. B. P. Chaplin, *Environ. Sci.: Processes Impacts*, **16** 1182 (2014).
3. X. Li, D. Pletcher and F. C. Walsh, *Chem. Soc. Rev.*, **40** 3879 (2011).
4. O. Shmychkova, T. Luk'yanenko, A. Velichenko, L. Meda and R. Amadelli, *Electrochim. Acta*, **111** 332 (2013).
5. V. Knysh, T. Luk'yanenko O. Shmychkova, R. Amadelli and A. Velichenko, *J. Solid State Electrochem.*, **21** 537 (2017).
6. O. Shmychkova, T. Luk'yanenko, R. Amadelli and A. Velichenko, *J. Electroanal. Chem.* **774** 88 (2016).
7. A. B. Velichenko, T. V. Luk'yanenko, N. V. Nikolenko, R. Amadelli and F.I. Danilov, *Russ. J. Electrochem.*, **43** 118 (2007).
8. A. B. Velichenko, V. A. Knysh, T. V. Luk'yanenko, Y.A. Velichenko and D. Devilliers, *Mat. Chem. Phys.* **131** 686 (2012).
9. T. P. Moffat, J. E. Bonevich, W. H. Huber, A. Stanishevsky, D. R. Kelly, G. R. Stafford, D. Josell, *J. Electrochem. Soc.*, **147** 4524 (2000).
10. M. G. Verde, K.J. Carroll, Z. Wang, A. Sathrum and Y. S. Meng, *Energy Environ. Sci.*, **6** 1573 (2013).
11. D. Qian, B. Xu, M. Chi and Y. S. Meng, *Phys. Chem. Chem. Phys.*, **16** 14665(2014).
12. T. Grygar, F. Marken, U. Schroder and F. Scholtz, *Collect. Chech. Chem. Commun.*, **67** 163 (2002).
13. M. Y. Abyaneh, V. Saez, J. Gonzalez-Garcia and T. J. Mason, *Electrochim. Acta* **55** 3572 (2010).
14. M. Y. Abyaneh in *Developments in electrochemistry: science inspired by Martin Fleischmann*, D. Pletcher, Z.-Q. Tian and D. E. Williams, Editors, John Wiley & Sons, Ltd, Chichester, UK (2014).
15. V. Saez, E. Marchante, M. I. Diez, M. D. Esclapez, P. Bonete, T. Lana-Villarreal, J. Gonzalez-Garcia and J. Mostany, *Mat. Chem. Phys.*, **125** 46 (2011).
16. R. Munoz-Espi, Y. Mastai, S. Gross and K. Landfester, *Cryst. Eng. Comm.*, **15** 2175 (2013).

J Solid State Electrochem
DOI 10.1007/s10008-016-3394-1

ORIGINAL PAPER

Electrodeposition of composite PbO_2–TiO_2 materials from colloidal methanesulfonate electrolytes

V. Knysh[1] · T. Luk'yanenko[1] · O. Shmychkova[1] · R. Amadelli[2] · A. Velichenko[1]

Received: 23 May 2016 / Revised: 7 September 2016 / Accepted: 9 September 2016

Abstract The influence of particles of colloidal titanium dioxide on the morphology and structure of lead dioxide electrodeposits has been investigated. The presence of colloidal TiO_2 particles (at levels of up to 1 g dm^{-3}) in the electrolyte leads to an increase in the rate of lead dioxide formation, and a higher TiO_2 content in the deposits. The electrodeposition of lead dioxide from colloidal dispersions containing particles of valve metal oxides is considered via an eleven-stage kinetic scheme.

Keywords Nanocomposite PbO_2–TiO_2 materials · Methanesulfonate electrolyte · Electrodeposition kinetics · Phase composition

Introduction

Dimensionally stable lead dioxide anodes obtained by the electrodeposition of PbO_2 are known to be widely used in industrial technologies [1–3]. The preparation of compact and unstrained PbO_2 deposits from suspension methanesulfonate ($CH_3SO_3^-$) electrolytes containing dispersed particles of inert oxides is of great interest. Electrochemical methods for the synthesis of oxide materials are considered to be more promising than sol–gel, CVD, and PVD techniques due to smaller energy losses [4, 5]. These electrochemical methods allow the thickness of the deposits to be controlled and permit enhanced substrate adhesion. Features such as its easy scalability and the ability to process different-sized workpieces in simple tank cells using aqueous electrolytes are examples of the versatility and simplicity of electrodeposition. These features, and the ability to control the current density and time in order to tailor the deposit thickness and morphology [6], should be contrasted with the need for special vacuum chambers and gases in PVD and CVD.

While maintaining the basic properties of PbO_2, the compositions and physicochemical properties of composite materials of this type can vary widely. As mentioned previously [7, 8], suspension nitrate electrolytes are considered to be the most promising electrolytes for producing composites with TiO_2 nanoparticles, as they are stable with respect to aggregation and thus do not require mechanical mixing during the coating process (achieved by electrodeposition). However, using nitrate electrolytes, it is not possible to obtain coatings thicker than 100 μm which are also sufficiently mechanically stable. In this regard, in the work described in the present paper, the possibility of electrodepositing nanocomposite PbO_2–TiO_2 materials from suspension methanesulfonate electrolytes was considered. It has previously been shown [8] that PbO_2 coatings up to 2 mm thick with satisfactory mechanical properties can be prepared in these media, but data on the possibility of obtaining stable TiO_2 suspensions in methanesulfonate electrolytes are absent from the literature, so there is also no information on PbO_2 composite materials prepared using this approach. The development of such systems is complicated by a lack of information on the kinetics of the electrolytic plating of PbO_2 in the presence of valve metal oxides, which may be included in the growing oxide matrix. In most cases, the estimation of the kinetic parameters of electrochemical processes that occur in suspension electrolytes is a difficult task due to the instability of such systems over time. In this regard, the influence of the dispersed phase on the

✉ A. Velichenko
velichenko@ukr.net

[1] Ukrainian State University of Chemical Technology, 8, Gagarin Ave., 49005 Dniepropetrovsk, Ukraine

[2] ISOF-CNR u.o.s Ferrara c/o Dipartimento di Scienze Chimiche e Farmaceutiche, Universita di Ferrara, via L. Borsari, 46-44121 Ferrara, Italy

Published online: 27 September 2016

kinetics of PbO_2 electrodeposition was investigated in electrolytes containing colloidal titanium dioxide. As has been shown previously [9, 10], such systems are stable over time and do not require continuous stirring.

In the work reported here, we investigated the electrodeposition kinetics of PbO_2-based composite materials from methanesulfonate electrolytes containing TiO_2 nanoparticles, as well as the physicochemical properties of the coatings. As has been pointed out by Li et al. [11], the modification of β-PbO_2 by TiO_2 particles can have two effects: (i) an increase in the density of the materials and a reduction in internal pressure, which favorably affects the service life of the electrodes, and (ii) a synergistic interaction between the two oxides. Considering these results and those discussed herein, we envisage that the obtained composite materials may also have interesting prospective applications as photocatalysts for the destruction of organic contaminants.

Materials and methods

All chemicals were reagent grade. The electrodeposition characteristics of doped lead dioxide were studied on a Pt plate in a sealed glass (0.145 cm^2) by steady-state voltammetry and chronoamperometry. The Pt electrode surface was treated before use, employing the procedure described in [12]. This preliminary treatment allowed us to achieve a reproducible surface. Voltammetry measurements were carried out in a standard temperature-controlled three-electrode cell. All potentials were recorded and are reported vs. $Ag/AgCl/KCl_{(sat)}$.

The electrodeposition of lead dioxide was studied in methanesulfonate/nitrate electrolytes that contained 0.1 M CH_3SO_3H/HNO_3 and 0.1 M $Pb(CH_3SO_3)_2/Pb(NO_3)_2$.

Another set of experiments utilized platinized titanium sheet, which was treated as described in [13] before platinum layer deposition. Suspension electrolytes containing TiO_2 as a dispersed phase were prepared by the hydrolysis of Ti(IV) isopropylate [7, 9]. The particle size of the titanium dioxide in solution was measured by turbidimetric analysis. Since the exponent of the wavelength for the sols involved was equal to 4.0, the Rayleigh equation was used to calculate the particle size. During the formation of a titanium oxyhydroxide sol, it initially tends to form the crystal lattice of anatase, so the refractive index of anatase (2.550) and its density of 3.95 g cm^{-3} were used in the calculation. The refractive index of the aqueous medium is 1.332.

The results of our previous investigations [7, 8] showed that it is possible to produce suspension electrolytes with aggregative stability based on sols of titanium dioxide formed through the hydrolysis of titanium isopropylate. In those investigations we also identified the optimum conditions to obtain electrolytes with high aggregative stability, including a pH of 1, a Pb^{2+} salt concentration of 0.1 M, and a TiO_2 sol particle size of ≤14 nm.

The surface morphology was investigated by scanning electron microscopy (SEM) using a Leica (Wetzlar, Germany) S360 microscope. X-ray powder diffraction data were collected on a STOE (Darmstadt, Germany) STADI P automatic diffractometer [14] equipped with a linear PSD detector (transmission mode, $2\theta/\omega$-scan; Cu $K\alpha_1$ radiation; curved germanium (1 1 1) monochromator; $6.000 \le 2\theta \le 102.945°$; 2θ step size $0.015°2\theta$; PSD step size $0.480°2\theta$; scan time 50 s/step).

Qualitative and quantitative phase analysis was performed using the PowderCell program [15]. For selected samples with relatively high degrees of crystallinity, Rietveld refinement was carried out using the FullProf.2 k (version 5.40) program [16].

Results and discussion

The kinetics of PbO_2 electrodeposition in both nitrate and methanesulfonate electrolytes containing colloidal TiO_2 nanoparticles were studied and compared. These systems resist sedimentation for a long time, even in the presence of a relatively high concentration of Pb^{2+} at low pH. Such systems do not collapse spontaneously over time, and represent the perfect model to assess the influence of particles on the kinetics of PbO_2 electrodeposition.

In order to develop highly stable suspensions in electrolytes, we first investigated the chemical properties of the colloidal media. Results show that the sizes of the colloidal TiO_2 particles in both 0.1 M nitric and methanesulfonic acids are essentially identical—about 12 nm; this is about 2 nm larger than that measured in the absence of electrolytes. It should also be noted that the particle size does not change over time, and the dispersions remain very stable. Notably, however, we found that the presence of Pb^{2+} at a concentration of 0.5 M leads to sedimentation of the colloidal dispersion, likely due to an increase in particle size. According to [8, 17], the cations are adsorbed on the TiO_2 particles, increasing the positive charge of those particles, which leads to a loss of stability.

An important step in the electrosynthesis of PbO_2-based materials with given properties is to establish the laws that regulate the electrocrystallization during the initial stages of the process. To do this, chronoamperometric curves on a platinum electrode were recorded; typical results for j-t are reported in Fig. 1. The observed transient can be divided into several characteristic regions [18]: (i) the current density step during the initial period of electrode polarization, corresponding to the charging of the double electrical layer; (ii) an induction period corresponding to the time required for PbO_2 phase formation to start; and then (iii) the appearance of a current density maximum due to a decrease in the concentration of the

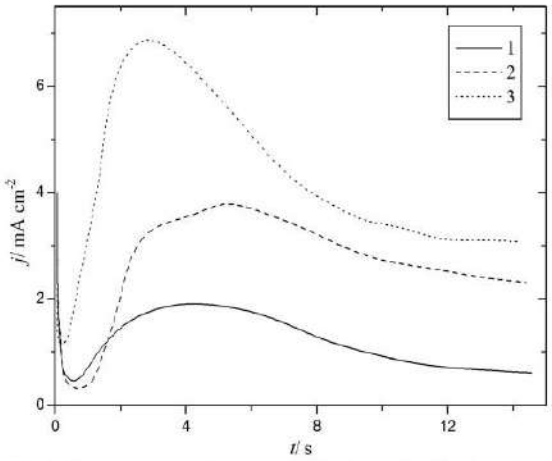

Fig. 1 Chronoamperometric curves obtained on a Pt disk electrode at 1.5 V for the following electrolytes: *1* 0.1 M $Pb(NO_3)_2$ + 0.1 M HNO_3; *2* 0.1 M $Pb(NO_3)_2$ + 0.1 M CH_3SO_3H; *3* 0.1 M $Pb(CH_3SO_3)_2$ + 0.1 M CH_3SO_3H

electroactive species near the electrode, before the process reaches a quasi-steady state at longer times.

According to transients obtained from nitrate and methanesulfonate electrolytes (see Fig. 1), it can be concluded that, despite the presence of the same concentration of Pb^{2+} in solution, the deposition current intensities for these electrolytes are significantly different, which is an unusual effect. Increasing the $CH_3SO_3^-$ ion concentration leads to a significant reduction in the induction period and causes a marked increase in the deposition current, indicating that the rate of PbO_2 phase formation is initially enhanced. This phenomenon is likely due to either the formation of lead methanesulfonate complexes such as $[Pb(CH_3SO_3)]^+$ with a low positive charge [19, 20] or the specific adsorption of such complexes on the positively charged electrode [21, 22], as evidenced by its zero-point pH shift of 0.3 units into the acid region.

The electrocrystallization model proposed by Abyaneh and Gonzalez-Garcia [22, 23] was selected as appropriate for investigating the initial stages of the formation of a new PbO_2 phase, as it provides a rather comprehensive description and a means for understanding phase formation, in the sense that it allows the kinetic parameters for nucleation to be determined for both the α and β phases from an analysis of current–time transients. The nucleation of PbO_2 occurs through the progressive mechanism in both methanesulfonate and nitrate electrolytes [22, 23]. However, cylindrical crystals grow in the methanesulfonate electrolyte whereas conical crystal formation occurs in the nitrate electrolyte. Increasing the $CH_3SO_3^-$ ions in the deposition bath changes the ratio between the α- and β-phase crystallization constants; in particular, β-phase growth predominates in the nitrate electrolyte, ($K_\beta = 1.45 \times 10^{-5}$ mol m^{-2} s^{-1}). Upon increasing the content of $CH_3SO_3^-$ ions in the electrolyte, the ratio between the constants K_α and K_β is reduced and the growth of the α phase is facilitated.

The content of dispersed-phase particles in a suspension electrolyte significantly influences the initial stages of crystallization. Chronoamperometric curves obtained in a methanesulfonate electrolyte that additionally contained various amounts of valve metal oxides are shown in Fig. 2. In all cases, the nucleation is progressive; the preferred shape of the crystals is a cone or, in some cases, a semispheroid. The main parameters of PbO_2 crystallization under these conditions are presented in Table 1.

One can conclude from the data obtained that the rate of PbO_2 crystallization on a Pt electrode (E = 1.62 V) increases in the presence of concentrations of colloidal TiO_2 of up to 1 g dm^{-3}; above this concentration the rate decreases until finally there is no further effect above 2 g dm^{-3}. The growth of the β phase predominates in all cases. In the suspensions, only the ratio between the kinetic constants of crystal growth for the α and β phases changes in a way that depends on the amount of dispersed particles. This observed effect may be caused by an increase in the surface area of the electrode (due to the appearance of additional centers—particles of valve metal oxides that can act as sites for PbO_2 crystallization) and an increase in the surface concentration of Pb^{2+} ions due to their adsorption on TiO_2. It is noteworthy that additional reaction centers consisting of oxygen-containing particles such as $OH^{\bullet}_{ads}$ that are located on the TiO_2 surface can form and participate in PbO_2 formation [9].

On the other hand, increasing the content of TiO_2 in the deposition bath will inhibit the process as active sites will be blocked due to the shielding of the electrode surface by semiconducting TiO_2. Factors exerting opposite effects act

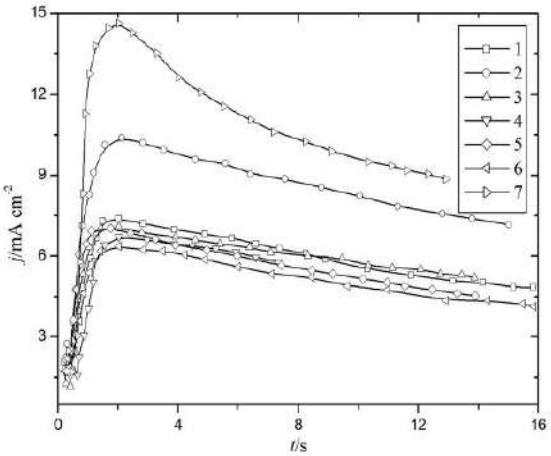

Fig. 2 Chronoamperometric curves obtained at PbO_2 deposition on a Pt electrode at 1.62 V from 0.1 M $Pb(CH_3SO_3)_2$ + 0.1 M CH_3SO_3H + X g dm^{-3} TiO_2, where X is: *1*, 0; *2*, 0.5; *3*, 1; *4*, 2; *5*, 3; *6*, 4; *7*, 5

simultaneously, giving rise to a pronounced dependence of the crystallization rate on the content of dispersed-phase particles in the electrolyte.

It is known that a change of conditions during electrodeposition results in the formation of a coating with completely new physicochemical properties. We thus considered the influence of the deposition conditions on the morphology of the PbO_2 deposit. Electrodeposition from a methanesulfonate bath leads to significant changes in the morphology of the coating (Fig. 3a). In this case, a polycrystalline deposit is formed, the surface of which is a mixture of randomly oriented crystals (Fig. 3b). As can be seen from the SEM data, the presence of TiO_2 nanoparticles brings about a substantial reduction in the size of the PbO_2 crystals. Moreover, the surface appears to be inhomogeneous, with two clearly identifiable areas consisting, respectively, of crystals with a predominance of PbO_2 and regions that are richer in TiO_2 which expand as the amount of TiO_2 is increased. Apparently, the formation of PbO_2 takes place at both the electrode surface already covered with PbO_2 and at TiO_2 particles near the electrode surface. Hindered crystallization on the surface of TiO_2 hampers the growth of large, well-defined, oriented crystals [24], resulting in a composite material consisting of a PbO_2 matrix with submicron and nanoscale crystals that incorporate TiO_2 particles.

As mentioned above, electrodeposited PbO_2 is a polycrystalline material consisting of a mixture of α and β phases. Inclusion of the dispersed particles leads to significant changes in the phase content of the composite coating; depending on the deposition conditions, the ratio of α-PbO_2 to β-PbO_2 and the rate constant during the initial stage of crystallization can change drastically (Table 2). In particular, the content of the α phase first increases and then decreases (Table 2), likely due to the changing conditions for PbO_2 nucleation, in good agreement with the data obtained for the initial stages of crystallization reported in Fig. 2.

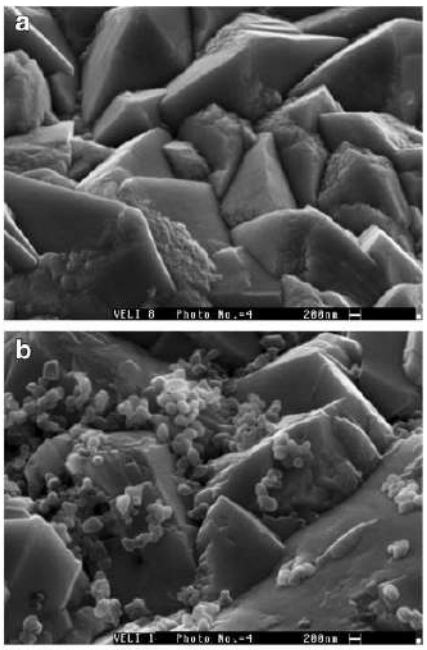

Fig. 3 SEM micrographs of coatings obtained, at $j_a = 10$ mA cm^{-2}, from the following solutions: *a* 0.1 M $Pb(CH_3SO_3)_2 + 0.1$ M CH_3SO_3H; *b* 0.1 M $Pb(CH_3SO_3)_2 + 0.1$ M $CH_3SO_3H + 5.0$ g dm^{-3} TiO_2 (colloidal)

In the electrodeposition of the composites from suspensions, solution stirring has a considerable influence on the TiO_2 content in the coating as well as on the phase composition of the PbO_2 matrix. In the context of convection diffusion, there is a pronounced influence of the dispersed-phase concentration that conditions the content of α-PbO_2 in particular. A comparison of the X-ray

Table 1 Parameters for the initial stage of lead dioxide electrocrystallization from solutions additionally containing TiO_2 (colloid)[a]

Deposition electrolyte	t_α	K_α	t_β	K_β
0.1 M $Pb(NO_3)_2 + 0.1$ M HNO_3	0.68	3.10×10^{-6}	1.45	6.57×10^{-5}
0.1 M $Pb(NO_3)_2 + 0.1$ M $HNO_3 + 0.5$ g dm^{-3} TiO_2	0.39	1.08×10^{-6}	1.22	1.18×10^{-5}
0.1 M Pb^{2+}+0.1 M CH_3SO_3H	0.54	3.40×10^{-5}	1.65	1.02×10^{-4}
0.1 M Pb^{2+}+0.1 M CH_3SO_3H +0.5 g dm^{-3} TiO_2	1.06	2.16×10^{-4}	1.42	4.18×10^{-4}
0.1 M Pb^{2+}+0.1 M $CH_3SO_3H + 1$ g dm^{-3} TiO_2	0.84	9.40×10^{-5}	1.25	2.96×10^{-5}
0.1 M Pb^{2+}+0.1 M $CH_3SO_3H + 2$ g dm^{-3} TiO_2	0.84	3.80×10^{-5}	1.24	1.64×10^{-5}
0.1 M Pb^{2+}+0.1 M $CH_3SO_3H + 3$ g dm^{-3} TiO_2	0.98	2.84×10^{-5}	1.36	2.94×10^{-5}
0.1 M Pb^{2+}+0.1 M $CH_3SO_3H + 4$ g dm^{-3} TiO_2	0.81	2.46×10^{-5}	1.14	8.47×10^{-5}
0.1 M Pb^{2+}+0.1 M $CH_3SO_3H + 5$ g dm^{-3} TiO_2	0.90	3.70×10^{-6}	1.40	2.17×10^{-5}

[a] In this table, K_α (mol m^{-2} s^{-1}) is the rate constant for the growth of α-phase crystals in a direction perpendicular to the electrode surface; t_α (s) is the time at which α-phase formation begins; K_β (mol m^{-2} s^{-1}) is the rate constant for the growth of the β-phase crystals in a direction perpendicular to the electrode surface; t_β (s) is the time at which β-phase formation begins

Table 2 Influence of the deposition electrolyte on the phase composition of lead dioxide

Deposition electrolyte	Proportion of the PbO_2 phase (%)	
	α	β
(M)[a]	17	83
(M), stirring	16	84
(M) + 2 g dm^{-3} TiO_2	57	42
(M) + 2 g dm^{-3} TiO_2, stirring	76	24
(M) + 5 g dm^{-3} TiO_2	34	66
(M) + 5 g dm^{-3} TiO_2, stirring	23	77

[a] *(M)* refers to 0.1 M $Pb(CH_3SO_3)_2$ + 0.1 M CH_3SO_3H. Coatings were deposited at j_a = 10 mA cm^{-2}, T = 298 K

diffraction pattern of unmodified PbO_2 (Fig. 4a) with that of the coating obtained from an electrolyte containing 5 g dm^{-3} TiO_2 (Fig. 4b) reveals differences in the crystallographic orientation of PbO_2. Specifically, in the latter case, the peak corresponding to the α phase is significantly more intense. In contrast, decreases in the intensities of the other peaks and appreciable peak broadening are observed (Fig. 4b), which may indicate a reduction in the size of the PbO_2 crystals with increasing proportion of TiO_2 in the sample.

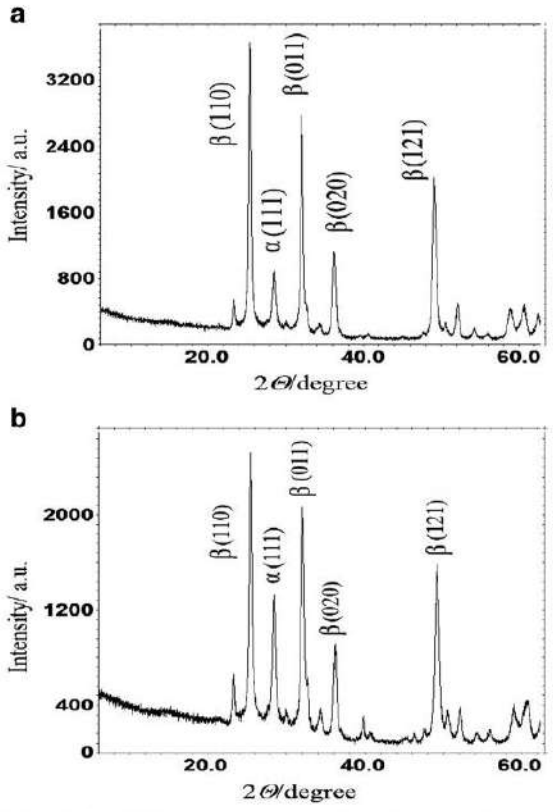

Fig. 4 X-ray diffractograms of composite materials obtained, at j_a = 10 mA cm^{-2}, from the following solutions: *a* 0.1 M $Pb(CH_3SO_3)_2$ + 0.1 M CH_2SO_3H; *b* 0.1 M $Pb(CH_3SO_3)_2$ + 0.1 M CH_3SO_3H + 5.0 g dm^{-3} TiO_2 (colloidal)

Cyclic voltammograms (CV) were obtained on a platinum electrode in both true solutions and colloid dispersions to study the process of PbO_2–TiO_2 electrodeposition. The CV method is quite convenient for investigating the process of Pb^{2+} electrodeposition that takes place simultaneously with oxygen evolution because, at the reverse sweep, this method can be used to determine the amount of lead dioxide formed on the electrode from the charge passed for the cathodic reduction of the preformed PbO_2 [25]. There are several characteristic regions of the CV curve (potential scanning interval 0–1.6 V) (Fig. 5). The anodic branch of the curve, at potentials higher than 1.4 V, features exponential current growth corresponding to the simultaneous oxidation of Pb^{2+} oxidation and evolution of oxygen. It should be noted that the forward and reverse scan cycles on the CV curve do not coincide. The observed hysteresis indicates a change in the degree of coverage of the platinum electrode by PbO_2, which, in turn, leads to a change in the overpotential of anodic processes, in that PbO_2 crystallization on the Pt electrode covered with a thin porous layer of PbO_2 will be easier.

In the cathodic branch of the curve, a current peak due to lead dioxide reduction can be observed at potentials between 0.9 and 0.95 V. It should be noted that the formation of PbO_2 proceeds at the same time as the evolution of oxygen. Thus, the current efficiency decreases as the PbO_2 deposition potential increases; the potential range in which PbO_2 formation is the predominant process is thus rather small. This fact makes it difficult to investigate the reaction that leads to PbO_2

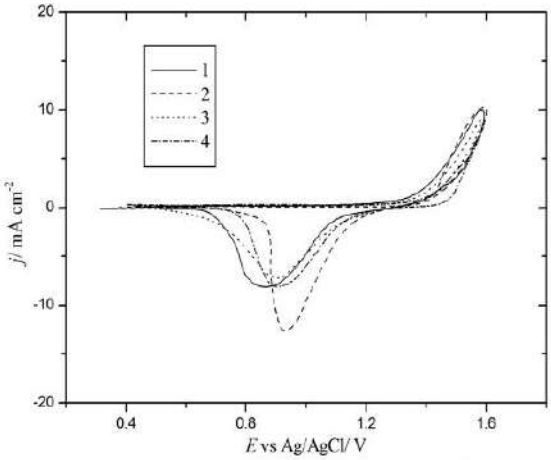

Fig. 5 Cyclic voltammograms obtained on Pt (0.1962 cm^2) in 0.1 M $Pb(CH_3SO_3)_2$ + 0.1 M CH_3SO_3H, additionally containing X g dm^{-3} TiO_2 nanoparticles, where X is *1*, 0; *2*, 0.5; *3*, 1.0; *4*, 5.0

formation, because the anodic current (recorded on the CV) corresponds to the overall rate of a process that includes several reactions. Therefore, to investigate the influence of hydrodynamic and other factors on the process of PbO_2 electrodeposition, it has been proposed that the peak area for the cathodic reduction of PbO_2 should be used as the criterion, as it reflects the rate of partial oxidation of Pb^{2+}. The validity of this method was confirmed in several experiments. Since it is established [25] that the cathodic peak charge (integrated area) is proportional to the amount of PbO_2 electrodeposited, these parameters can be used to assess the PbO_2 electrodeposition rate.

CV curves recorded on Pt electrodes in $CH_3SO_3^-$ solutions without and with colloidal TiO_2 particles differ significantly (Fig. 5). The main differences are an increase in the overpotential of the anodic process, which is especially pronounced in the reverse cycle of the CV (5 g dm^{-3} TiO_2), and a substantial increase in the cathodic peak corresponding to lead dioxide reduction (0.5 g dm^{-3} TiO_2). The results are in satisfactory agreement with chronoamperometric data, and are possibly explained by facilitated PbO_2 crystallization due to the availability of the additional active sites provided by TiO_2. Indeed, a significant increase in the peak cathodic current is observed which reflects PbO_2 reduction at the composite coating. However, increasing the TiO_2 content in the deposition electrolyte inhibits the process, seemingly because active sites are blocked due to the shielding of the electrode surface by semiconducting TiO_2.

In order to gain further insight into the influence of colloidal TiO_2 on the kinetics of PbO_2 electrodeposition, we recorded steady-state polarization curves (Fig. 6). These curves take

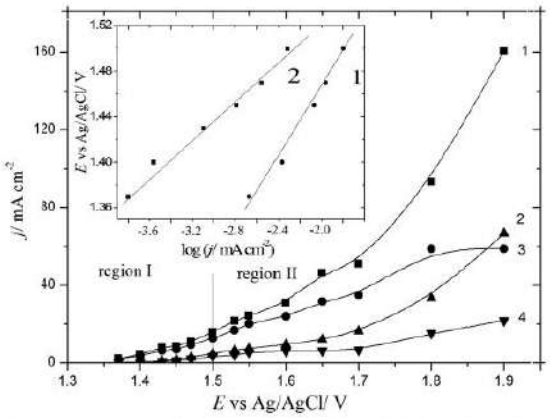

Fig. 6 Steady-state polarization curves for the total (*1*, *2*) and partial (*3*, *4*) PbO_2 electrodeposition currents on a Pt electrode from solutions of 0.1 M $Pb(CH_3SO_3)_2$ + 0.1 M CH_3SO_3H (*1*, *3*) and 0.1 M $Pb(CH_3SO_3)_2$ + 0.1 M CH_3SO_3H + 5 g dm^{-3} $TiO_{2\ (coll)}$ (*2*, *4*). *Inset*: *E* vs. log *j* plots for lead dioxide deposition at the lower potential range in solutions of 0.1 M $Pb(CH_3SO_3)_2$ + 0.1 M CH_3SO_3H (*1*) and 0.1 M $Pb(CH_3SO_3)_2$ + 0.1 M CH_3SO_3H + 5 g dm^{-3} $TiO_{2\ (coll)}$ (*2*)

into account both the total (O_2 evolution and Pb^{2+} oxidation) and the partial Pb^{2+} electrooxidation processes [9].

The current efficiency and partial current of PbO_2 deposition ($I_{Pb(II)}$) were determined by polarizing the electrode at a chosen potential above 1.4 V for between 30 s and 5 min (depending on the potential value) and coulometrically measuring the total charge passed during electrolysis (Q). Subsequently, the charge (Q_{red}) passed for the cathodic reduction of the preformed PbO_2 was also measured coulometrically, in the background electrolyte, in the potential range from an established anodic potential up to 0.8 V. As shown earlier [9, 25], at slow sweep rates, quantitative reduction of PbO_2 occurs for thin oxide films. For relatively thick films, the adequacy of this method was confirmed by gravimetric experiments that show a direct proportionality between charge and amount of PbO_2 deposited, as reported in the publications cited above. Then, in all cases, the data enable the current efficiency and partial current for PbO_2 electrodeposition to be evaluated.

The partial Pb^{2+} oxidation current ($I_{Pb(II)}$) is determined as described earlier [9, 10] from the PbO_2 reduction charge passed divided by the electrolysis time at an established anodic potential. The current efficiency for PbO_2 formation was calculated from the reduction charge divided by the total charge.

In the lower potential range ($E < 1.5$ V), plots of E vs log(j, in mA cm^{-2}), obtained from I–E curves, are linear ($r = 0.99$, Fig. 6, inset), indicating that the PbO_2 electrodeposition process is kinetically controlled [25]. A limiting current for PbO_2 electrodeposition is observed at $E > 1.5$ V, which decreases as the amount of TiO_2 particles in the suspension is increased. The coefficient b in the Tafel equation decreases from 0.1236 (see Fig. 6, inset, curve 1) to 0.0761 V (see Fig. 6, inset, curve 2). Once more, these results can be explained by the presence of the valve oxides in the coating, which partially block the electrode surface.

It is known that the substrate on which the deposition occurs plays a significant role in the formation of coatings [6]. Thus, we investigated the influence of deposition on PbO_2 itself by recording the total polarization curves on a PbO_2 electrode in electrolytes additionally containing colloidal TiO_2. As depicted in Fig. 7, in the diffusion control region, the limiting current of PbO_2 deposition is reduced in the presence of the dispersed phase. The differences between the anodic currents at the platinum and the PbO_2 electrodes are seemingly caused by the different natures of the substrates.

To sum up briefly, the presence of a relatively small amount of TiO_2 in the electrolyte leads to an increase in the formation rate of PbO_2 (deposition electrolyte with TiO_2) and a decrease in the deposition rate as the concentration of the dispersed phase in the deposition electrolyte is increased further. We underline that, despite some

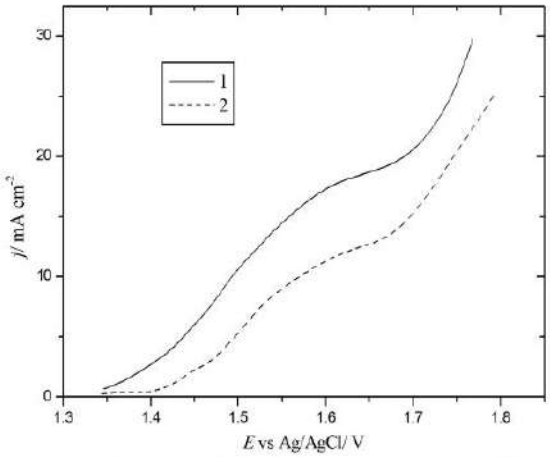

Fig. 7 Steady-state polarization curves for the total PbO_2 electrodeposition current on a PbO_2 electrode (0.8483 cm^2) in solutions of 0.1 M $Pb(CH_3SO_3)_2$ + 0.1 M CH_3SO_3H (*1*) and 0.1 M $Pb(CH_3SO_3)_2$ + 0.1 M CH_3SO_3H + 5 g dm^{-3} $TiO_{2\ (coll)}$ (*2*)

quantitative differences in the deposition and crystallization rates, the mechanisms of PbO_2 deposition in true nitrate and methanesulfonate solutions are essentially the same [25, 26]. In principle, it therefore seems appropriate to adapt the same mechanistic formalism to processes that take place in TiO_2 suspensions of those electrolytes [25, 26]. The kinetic scheme for a process that takes into account both the complexation and the formation of electroactive particles on the TiO_2 nanoparticles can be represented as follows:

$$H_2O \rightarrow OH^{\cdot} + H^+ + e^- \quad (1)$$

$$TiO_2\text{–}OH + OH^{\cdot} \rightarrow TiO_2\text{–}O^{\cdot} + H_2O \quad (2)$$

$$\left[Pb(CH_3SO_3)_n\right]^{(2-n)+} + OH^{\cdot}{}_{ads} \rightarrow \left[Pb(CH_3SO_3)_n(OH)\right]^{(2-n)+} \quad (3)$$

$$TiO_2\left[Pb(CH_3SO_3)_n\right]^{(2-n)+} + OH^{\cdot}{}_{ads} \rightarrow TiO_2\left[Pb(CH_3SO_3)_n(OH)\right]^{(2-n)+} \quad (4)$$

$$TiO_2\text{–}O^{\cdot} + TiO_2\left[Pb(CH_3SO_3)_n\right]^{(2-n)+} \rightarrow \left[TiO_2\text{–}O^{\cdot}\right]\left[Pb(CH_3SO_3)_n\right]^{(2-n)+} \quad (5)$$

$$\left[Pb(CH_3SO_3)_n(OH)\right]^{(2-n)+} + H_2O \rightarrow \left[Pb(CH_3SO_3)_n(OH)_2\right]^{(2-n)+} + H^+ + e^- \quad (6)$$

$$\left[TiO_2\right]\left[Pb(CH_3SO_3)_n(OH)\right]^{(2-n)+} + H_2O \rightarrow \left[TiO_2\right]\left[Pb(CH_3SO_3)_n(OH)_2\right]^{(2-n)+} + H^+ + e^- \quad (7)$$

$$\left[TiO_2\text{–}O^{\cdot}\right]\left[Pb(CH_3SO_3)_n\right]^{(2-n)+} + H_2O \rightarrow \left[TiO_2\text{–}O^{\cdot}\right]\left[Pb(CH_3SO_3)_n(OH)\right]^{(2-n)+} + H^+ + e^- \quad (8)$$

$$\left[Pb(CH_3SO_3)_n(OH)_2\right]^{(2-n)+} \rightarrow PbO_2 + n(CH_3SO_3)^- + 2H^+ \quad (9)$$

$$\left[TiO_2\right]\left[Pb(CH_3SO_3)_n(OH)_2\right]^{(2-n)+} \rightarrow TiO_2\text{–}PbO_2 + n(CH_3SO_3)^- + 2H^+ \quad (10)$$

$$\left[TiO_2\text{–}O^{\cdot}\right]\left[Pb(CH_3SO_3)_n(OH)\right]^{(2-n)+} \rightarrow TiO_2\text{–}PbO_2 + n(CH_3SO_3)^- + H^+ \quad (11)$$

Steps (1), (3), (6), and (9) occur in true methanesulfonate and nitrate (for which $n = 0$) solutions without a dispersed phase, and take place on the electrode surface. All remaining steps are implemented only in suspension electrolytes, where Pb^{2+} ions or their complexes can be adsorbed on the dispersed-phase particles. Note that all of these stages are stacked in the previously proposed kinetic scheme consisting of four stages [25, 26].

The first step is electron transfer with the formation of the electrode surface or on particles of the dispersed-phase oxygen containing radicals such as OH• or O•, which are formed by the anodic ionization of water in steps (1)–(2). Then, in the subsequent chemical steps (3)–(5), these particles react with lead ions Pb^{2+} or with methanesulfonate complexes of lead, forming a mobile oxygen-containing intermediate at the electrode surface. This intermediate is oxidized and the second electron is transferred in steps (6)–(8). The final chemical reactions involve the formation and decay of soluble intermediates consisting of lead species with valences of 3 and 4 and PbO_2 formation.

The electrode surface state, deposition potential, lead ion concentration, and hydrodynamic conditions are known to largely determine the nature of the rate-determining step in lead dioxide electrodeposition. As a rule, at low anodic polarizations ($E < 1.6$ V), the reactions will be under kinetic control, whereas at high polarizations, the transport of Pb^{2+} ions to the electrode surface will be the rate-determining step [25].

Conclusions

As can be concluded from the results obtained, the presence of colloidal TiO_2 in the solution increases the rate of lead dioxide crystallization on a platinum electrode. On the other hand, increasing the content of titanium dioxide in the deposition electrolyte inhibits the process because the active sites are blocked due to the shielding of the electrode surface by the n-type semiconductor (TiO_2).

The inclusion of the dispersed phase in the PbO_2 leads to significant changes in the phase content of the composite coating. Depending on the deposition conditions, the α-PbO_2 content comprises 16–76 % of the total PbO_2 content.

The 11-stage mechanism described above not only allows the experimental results obtained upon the electrodeposition of lead dioxide from nitrate and methanesulfonate colloidal electrolytes to be described satisfactorily, but it also helps to explain the increase in the rate of deposition in the presence of dispersed-phase particles that are not electrochemically active. The data also point to an extension of the previously proposed colloidal–electrochemical formation mechanism of composite coatings that involves the formation of colloidal PbO_2 particles in the zone near to the electrode.

References

1. Li X, Pletcher D, Walsh FC (2011) Electrodeposited lead dioxide coatings. Chem Soc Rev 40:3879–3894
2. Chaplin BP (2014) Critical review of electrochemical advanced oxidation processes for water treatment applications. Environ Sci: Processes Impacts 16:1182–1283
3. Vargas R, Borras C, Mendez D, Mostany J, Scharifker BR (2016) Electrochemical oxygen transfer reactions: electrode materials, surface processes, kinetic models, linear free energy correlations, and perspectives. J Solid State Electrochem 20:875–893
4. Low CTJ, Wills RGA, Walsh FC (2006) Electrodeposition of composite coatings containing nanoparticles in a metal deposit. Surf Coat Tech 201:371–383
5. Walsh FC, Ponce de Leon C (2014) A review of the electrodeposition of metal matrix composite coatings by inclusion of particles in a metal layer: an established and diversifying coatings technology. Trans IMF 92:83–98
6. Ponce de Leon C, Walsh FC (2014) Versatile electrochemical coatings and surface layers from methanesulfonic acid. Surf Coat Tech 259:676–697
7. Amadelli R, Samiolo L, Velichenko AB, Knysh VA, Luk'yanenko TV, Danilov FI (2009) Composite PbO_2-TiO_2 materials deposited from colloidal electrolyte: electrosynthesis, and physicochemical properties. Electrochim Acta 54:5239–5245
8. Velichenko AB, Knysh VA, Luk'yanenko TV, Velichenko YA, Devilliers D (2012) Electrodeposition PbO_2-TiO_2 and PbO_2-ZrO_2 and its physicochemical properties. Mater Chem Phys 131:686–693
9. Velichenko AB, Amadelli R, Knysh VA, Luk'yanenko TV, Danilov FI (2009) Kinetics of lead dioxide electrodeposition from nitrate solutions containing colloidal TiO_2. J Electroanal Chem 632:192–196
10. Velichenko AB, Amadelli R, Gruzdeva EV, Luk'yanenko TV, Danilov FI (2009) Electrodeposition of lead dioxide from methanesulfonate solutions. J Power Sources 191:103–110
11. Li G, Qu J, Zhang X, Ge J (2006) Electrochemically assisted photocatalytic degradation of Acid Orange 7 with β-PbO_2 electrodes modified by TiO_2. Wat Res 40:212–220
12. Shmychkova O, Luk'yanenko T, Amadelli R, Velichenko A (2014) Physico-chemical properties of PbO_2-anodes doped with $Sn^{4+}$and complex ions. J Electroanal Chem 717–718:196–201
13. Shmychkova O, Luk'yanenko T, Velichenko A, Amadelli R (2013) Electrodeposition of Ce-doped PbO_2. J Electroanal Chem 706:86–92
14. STOE (2010) WinXPOW version 3.03. STOE & Cie GmbH, Darmstadt
15. Kraus W, Nolze G (2000) PowderCell for Windows (version 2.4). Federal Institute for Materials Research and Testing, Berlin
16. Rodriguez-Carvajal J (2001) Recent developments of the program FULLPROF. IUCr CPD Newslett 26:12–19
17. Velichenko AB, Knysh VA, Luk'yanenko TV, Danilov FI, Devilliers D (2009) PbO_2–TiO_2 composite electrodes. Prot Met Phys Chem Surf 45:327–332
18. Shmychkova O, Luk'yanenko T, Piletska A, Velichenko A, Gladyshevskii R, Demchenko P, Amadelli R (2015) Electrocrystallization of lead dioxide: influence of early stages of nucleation on phase composition. J Electroanal Chem 746:57–61
19. Capelato MD, Nobrega JA, Neves EFA (1995) Complexing power of alkanesulfonate ions: the lead–methanesulfonate system. J Appl Electrochem 25:408–411
20. Li S, Qian W, Tao F-M (2007) Ionic dissociation of methanesulfonic acid in small water clusters. Chem Phys Lett 438:190–195
21. Sandoval AP, Suarez-Herrera MF, Climent V, Feliu JM (2015) Interaction of water with methanesulfonic acid on Pt single crystal electrodes. Chem Commun 50:47–50
22. Abyaneh MY, Saez V, Gonzalez-Garcia J, Mason TJ (2010) Electrocrystallization of lead dioxide: analysis of the early stages of nucleation and growth. Electrochim Acta 55:3572–3579
23. Gonzalez-Garcia J, Gallud F, Iniesta J, Montiel V, Aldaz A, Lasia A (2000) Kinetics of electrocrystallization of PbO_2 on glassy carbon electrodes. Partial inhibition of the progressive three-dimensional nucleation and growth. J Electrochem Soc 147:2969–2974
24. Cattarin S, Frateur I, Guerriero P, Musiani M (2000) Electrodeposition of PbO_2 + CoO_x composites by simultaneous oxidation of Pb^{2+} and Co^{2+} and their use as anodes for O_2 evolution. Electrochim Acta 45:2279–2288
25. Shmychkova O, Luk'yanenko T, Velichenko A, Meda L, Amadelli R (2013) Bi-doped PbO_2 anodes: electrodeposition and physicochemical properties. Electrochim Acta 111:332–338
26. Shmychkova O, Luk'yanenko T, Amadelli R, Velichenko A (2016) Electrodeposition of Ni^{2+}-doped PbO_2 and physicochemical properties of the coating. J Electroanal Chem 774:88–94

Journal of Energy Storage 30 (2020) 101581

Contents lists available at ScienceDirect

Journal of Energy Storage

journal homepage: www.elsevier.com/locate/est

Morphology and phase composition of lead dioxide coatings: Influence of methanesulfonate ions

A. Velichenko*, T. Luk'yanenko, O. Shmychkova

Ukrainian State University of Chemical Technology, 8, Gagarina Ave., 49005 Dnipro, Ukraine

ARTICLE INFO

Keywords:
Lead dioxide
Methanesulfonic electrolyte
Phase composition
Sodium methanesulfonate

ABSTRACT

Depending on the concentration of methanesulfonate in the electrolyte and the hydrodynamic conditions of the process, it is possible to synthesize high-quality films up to 2 mm thickness, free from internal stresses, with reliable adhesion to the substrate in the current density range of 2–180 mA cm^{-2}. The change in the composition of the methanesulfonate electrolyte and the deposition conditions affect the phase composition of lead dioxide. The main difference from oxides obtained from nitrate solutions is the significant α-phase content, which can vary from 17 to 90%. The deposits are polycrystalline and are characterized by smaller crystals. All the results obtained by the X-ray diffraction method are in satisfactory agreement with the scanning electron microscopy data.

1. Introduction

Many applications of lead acid batteries have been found, and they are still in a widespread use as car batteries or a backup power. The main advantages of this type of battery are its low cost, simple and well-known technological process, almost 100% effective recycling, and low self-discharge. The disadvantages include a limited number of full charge/discharge cycles, a need of storing in charged condition and a high mass caused by a low specific energy in relation to newer battery types, among which the soluble lead redox flow battery is recognized as of particular interest. It makes use of the variable oxidation states of lead, namely Pb, Pb(II) and Pb(IV). Electrolytes are designed either from lead oxide, lead carbonate or aqueous lead methanesulfonate, and methanesulfonic acid [1].

The synthesis of new electrode materials with valuable functional properties is considered as one of the urgent challenges of modern electrochemistry [2,3]. One should have a clear understanding of the correlation between the chemical and phase composition of the surface layers of electrode and kinetics of the reactions proceeding on it. In modern electrochemical technologies, much attention is given to the development of anode materials consisting of various metal oxides. Conductive metal oxides (α- and β-PbO_2, γ-MnO_2, IrO_2, etc.) can be used to obtain the dimensionally stable anodes (DSA®) [4,5].

It should be noted that in some cases the surface of the oxide material has catalytic properties in relation to the reactions proceeding on it. Significant acceleration of the reaction of electrochemical oxygen evolution will reduce the voltage on the electrochemical cell during electrolysis, which, certainly of interest to practice [6,7]. Also, some oxide materials have selectivity with respect to the reactions proceeding on them, which allows one to minimize the undesirable processes during electrolysis.

Anodic electrocrystallization is widely used to produce various modifications of metal oxides [8,9]. However, materials obtained by electrolysis often do not meet the requirements for their stability and selectivity. It makes researchers to look for new approaches to methods for the modification of oxide materials used in applied electrochemistry.

Dimensionally stable lead dioxide anodes (DSA), obtained by electrodeposition of PbO_2, are known to be widely used in industrial technology [10–12]. Despite the rather high electrocatalytic activity of the lead(IV) oxide-based materials in the oxygen-transfer reactions, which take place at high anode potentials, their practical application has not yet gone beyond the laboratory scale due to the difficulty in creating DSA of this type [10]. The main problem is the significant differences in the mechanical properties of the metal substrate and lead oxide, the inability to obtain a coating thickness of more than 50 μm with low internal stresses, as well as the diffusion of oxygen through PbO_2 to titanium substrate and subsequent its oxidation followed by titanium(IV) oxide blocking (n-type semiconductor). It should also be noted that coatings based on PbO_2 obtained from nitrate electrolytes are characterized by significant internal stresses and therefore undergo considerable mechanical degradation during operation [13–15]. The

* Corresponding author.
E-mail address: velichenko@ukr.net (A. Velichenko).

https://doi.org/10.1016/j.est.2020.101581
Received 10 April 2020; Received in revised form 2 May 2020; Accepted 25 May 2020

rate of mechanical destruction of the oxide layer of the composite dimensionally stable anode is proportional to the intensity of oxygen evolution. It should be noted that at high current densities and high electrical resistance at the interfacial metal-oxide boundary, local heating of the electrode can be observed, which, due to differences in the coefficients of linear expansion of the metal and the oxide, results in the detachment of the coating from the substrate. A lot of these problems can be solved by the use of methanesulfonate electrolytes. Methanesulfonic acid (MSA), as an environmentally friendly electrolyte, has been considered to used in the metal finishing industry due to its chemical stability and excellent solubilisation of metal salts [16,17] Coatings obtained from methanesulfonic bath are characterized by high electrical conductivity, ease of production and low cost, as well as electrochemical and chemical stability in various solutions [18,19]. It is noteworthy that the base oxide displays the high electrocatalytic activity in reactions occurring at high anode potentials (oxidation of toxic organic substances, ozone evolution) [10,12]. Nevertheless, most of the studies are devoted to deposition kinetics or applied aspects related to the operation of electrodes in flow batteries [20–22]. Practically no attention was paid to the study of the parameters affecting the current efficiency, namely, the concentration of methanesulfonate ions and the density of the deposition current. Also, the influence of electrolysis parameters and methanesulfonic acid concentration on the physicochemical properties that are important from the point of view of the mechanical properties and electrochemical behavior of the coatings remained beyond attention. In this connection, herein we present a thorough study of the influence of deposition conditions on the structure and phase composition of the PbO_2 formed by electrodeposition from methanesulfonic acid media.

2. Material and methods

All chemicals were reagent grade. The regularities of lead dioxide electrodeposition were studied on a Pt rotating disk electrode (Pt-RDE, 0.19 cm^2) by steady-state voltammetry. For the RDE experiments the voltammetry system SVA-1BM was used. The potential scan rate was varied within 1 ÷ 100 mV/s depending on purposes of the experiments. Before each experiment, the electrode surface was treated with a freshly prepared mixture (1:1) of concentrated H_2SO_4 and H_2O_2 [9]. This preliminary treatment technique permits to stabilize the electrode surface, which under the action of strong oxidizing medium is oxidized to a certain state (defined phase and chemical composition of the surface oxides), which determines the satisfactory reproducibility in taking of cyclic voltammograms in the background electrolyte (0.1 M CH_3SO_3H). Voltammetry measurements were carried out in a standard temperature-controlled three-electrode cell. Temperature was maintained 25 ± 1 °C. All potentials were recorded and reported vs. Ag / AgCl / KCl $_{(sat.)}$.

Lead dioxide anodes surface morphology was studied by scanning electron microscopy (SEM) with Tescan Vega 3 LMU with energy-dispersive X-ray microanalyzer Oxford Instruments Aztec ONE with X-Max^{N}20 detector. X-Ray powder diffraction (XRPD) data were collected in the transmission mode on a STOE STADI P diffractometer with Cu $K\alpha_1$-radiation, curved Ge (1 1 1) monochromator on primary beam, $2\theta/\omega$-scan, angular range for data collection 20.000–110.225 °2θ with increment 0.015, linear position sensitive detector with step of recording 0.480 °2θ and times per step 75–300 s, U = 40 kV, I = 35 mA, T = 298 K. A calibration procedure was performed utilizing SRM 640b (Si) and SRM 676 (Al_2O_3) NIST standards. Preliminary data processing and X-ray qualitative phase analysis were performed using STOE WinXPOW and PowderCell program packages. Crystal structures of the phases were refined by the Rietveld method with the program FullProf.2k, applying a pseudo-Voigt profile function and isotropic approximation for the atomic displacement parameters, together with quantitative phase analysis.

The determination of current efficiency of lead dioxide deposition was done according to the method described in detail in our previous publication [23] by measuring coulometrically the total charge (Q) passed during electrolysis. Subsequently, the charge passed for the cathodic reduction (Q_{red}) of the pre-formed PbO_2 was also measured coulometrically, in the background electrolyte. As has been shown earlier [24–26], at slow sweep rates, quantitative reduction of PbO_2 takes place for thin oxide films. For relatively thick films, the adequacy of this method was confirmed by gravimetric experiments that show a direct proportionality between charge and amount of deposited PbO_2, as reported in the above cited publications. The current efficiency (CE) for PbO_2 formation was calculated from the reduction charge divided by the total charge according to the following formula:

$$CE = \frac{Q_{red}}{Q} \cdot 100\%$$

In order to evaluate the effect of the composition of the active layer on the lifetime of the anodes, accelerated resource tests were performed in 1 M H_2SO_4 at an anode current density of 500 mA cm^{-2}. Preheating the electrolyte to 40–50 °C during the anode process resulted in more severe test conditions. The lifetime of the electrodes is a time of continuous polarization, during which the potential is practically unchanged. The sharp increase in potential indicates the failure of the electrode, even if there is no significant mechanical damage to the active coating. It is considered impossible to operate such an electrode because of the significant increase in voltage on the cell.

3. Results and discussion

The formation of lead dioxide proceeds simultaneously with the oxygen evolution [8,9]. Since the current efficiency decreases with increasing of PbO_2 deposition potential, the potential range in which the reaction of PbO_2 formation is the predominant process is small. The dependence of PbO_2 CE on various factors is important for selecting the optimal electrolyte composition and deposition conditions. A typical dependence of CE on the current density is shown in Fig. 1. The dependence is extreme, which is associated with the simultaneous proceeding of lead(IV) oxide formation and oxygen evolution.

At low current densities, when the rate of formation of the lead(IV) oxide is negligible, the oxide coating is not continuous for a long time, so that the oxygen evolution reaction (OER) can occur on the oxide-free portions of the platinum, where the OER overvoltage is substantially lower than on PbO_2. The increase in current density contributes to the fast filling of the platinum electrode surface with the lead(IV) oxide, the OER overvoltage increases and CE approaches 100%. Thus, in the area I, where the CE increases with increasing current density, the process

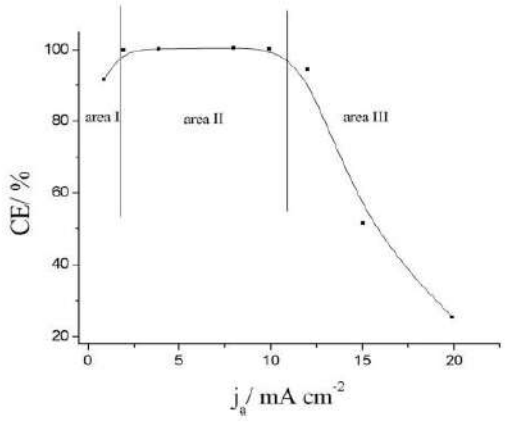

Fig. 1. Current efficiency of PbO_2 vs. current density in 0.1 M Pb $(CH_3SO_3)_2$ + 0.1 M CH_3SO_3H.

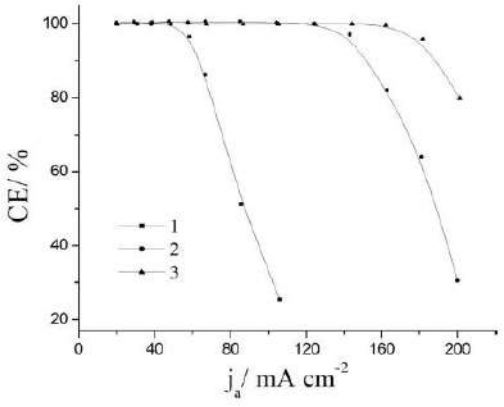

Fig. 2. Current efficiency of PbO_2 vs. current density in various electrolytes: 1 – 0.5M $Pb(CH_3SO_3)_2$ + 0.1 M CH_3SO_3H; 2 – 1.0 M $Pb(CH_3SO_3)_2$ + 0.1 M CH_3SO_3H; 3 – 1.0 M $Pb(CH_3SO_3)_2$ + 0.1 M CH_3SO_3H with mixing.

simultaneously proceeds allegedly on two electrodes, platinum and lead dioxide, with a gradual complete transition to the latter. In the area II of the curve (see Fig. 1), the current efficiency is 100% and does not depend on the current density, since oxygen has not yet released on PbO_2 due to the high overvoltage. The area III of the curve shows a rapid fall in the CE due to the fact that the deposition current of the lead dioxide reaches a limit value, while the rate of oxygen evolution increases exponentially.

Since OER overvoltage on PbO_2 is virtually independent of the composition of the electrolyte, the only way to extend the current density range for 100% CE is to increase the limiting current of lead dioxide deposition by increasing the concentration of lead compounds in solution or mixing the electrolyte.

According to the data obtained (Fig. 2), increasing the concentration of lead methanesulfonate allows one to significantly expand the range of current densities at which led dioxide with 100% current efficiency can be obtained. An additional effect can also be obtained by mixing the electrolyte (see Fig. 2). It should be noted that the change in the concentration of methanesulfonic acid in the electrolyte in the concentration range from 0.05 to 2.0 M practically does not affect the CE, which is probably due to the same effect of acidity both on the electrodeposition of PbO_2 and OER.

Having in mind that in soluble lead-acid redox flow battery the presence of 100% current efficiency is essential, we conducted our studies in the galvanostatic mode. During the deposition of lead dioxide in the whole investigated current density range, where the CE is about 100%, high-quality deposits up to 2 mm thick with low internal stresses and reliable adhesion to the metal substrate (Ti/Pt) are obtained, which may be of potential interest to use as electrocatalytic layer components of DSA®. The presence of internal stresses in the samples was determined by the wafer curvature method described in detail in the review [27].

Although the investigated electrolytes did not contain dopants that could lead to a change in the chemical composition of lead dioxide [9], the effect of the solution composition and deposition conditions on the phase composition and the physicochemical properties of the coatings obtained should not be excluded. Particularly important in this regard are surface morphology and texture, as they are one of the most important structural factors affecting the electrocatalytic activity of anodes in oxygen transfer reactions [12].

As follows from the SEM data, PbO_2 obtained from nitrate bath is a set of large polycrystalline blocks with a slightly pronounced predominant orientation (Fig. 3a). While the use of methanesulfonate media allows one to obtain PbO_2, which differs significantly in morphology (Fig. 3b) and represented by randomly oriented nano- and submicron crystals.

It should be noted that when using methanesulfonate electrolytes, the morphology of the deposited lead dioxide is determined mainly by the deposition conditions and composition of the solution. An increase in current density (Fig. 3c) as well as deposition temperature leads to the appearance of polycrystalline blocks with a well-defined predominant orientation. With increasing acidity of the electrolyte, the crystals became smaller (Fig. 3d).

According to the literature data [28], the formation of complex compounds of different stoichiometry, such as $[PbCH_3SO_3^+]$, $[Pb(CH_3SO_3)_2]$, $[Pb(CH_3SO_3)_3^-]$ is possible in lead-methansulfonate medium. Since the formation of PbO_2 proceeds on a constantly renewable surface, complex particles can be adsorbed from the solution bulk on the surface of the growing oxide. These particles are probably involved in the oxidation of lead(II), and the differences in their adsorption on the electrode surface lead to different effects, in particular reduces crystal size. It should be noted that in nitrate electrolytes, such an effect is not clearly apparent.

And secondary effect that with an increase in potential, the surface of the electrode will have a more positive charge, which should also help to fix negative and neutral charged particles on the surface. Subsequently, complex compounds on the surface most likely undergo electrochemical transformations with the formation of PbO_2.

SEM/EDAX experiments were performed to evaluate the amount and distribution of elements in electrodeposited composite. The data obtained have shown the presence Pb, O on the surface. The analysis has not detected the sulphur peak.

Lead dioxide can exist in both amorphous and crystalline forms [29]. Two of its allotropic forms are known: α-PbO_2, characterized by an elemental rhombic cell, and β-PbO_2, a tetragonal lattice of the rutile type. As shown in [30], these forms differ greatly in crystal size and mechanical properties. α-PbO_2 synthesized as relatively large, approximately 1 μm, closely adjacent crystals, it is chemically more stable, usually used in lead-acid batteries [31]; β-PbO_2 – in the form of small needle crystals with a size of 0.03-0.5 μm, weakly bonded to each other [13]. Due to the tight packing of crystals, α-PbO_2 has a more compact structure in comparison with β-PbO_2 [32], which is a porous structure that provides a larger active surface area [33]. Usually, electrodeposited coating is often composed of different phase structures of α-/β-PbO_2 [34].

We conducted X-ray powder diffraction method in order to investigate the effect of electrolyte composition and deposition conditions on the phase composition of electrodeposited PbO_2 and its texture. As one can see from the data obtained (Table 1), the addition of sodium methanesulfonate (NaMS) to the nitrate electrolyte results in an almost threefold increase in the α-phase content of the coating, which is then practically unchanged in the range from 0.5 to 1.2 M NaMs and remains of about 43%.

The observed effect indicates that the amount of methanesulfonate ions in the phase formation process has a greater effect on the adsorption than on the complexation. As has been shown in our previous publication [35], at such concentration ratio of ligand and lead ions, even at maximum NaMS concentrations in solution, almost a quarter of Pb^{2+} ions remains free, and the complex formed is predominantly a single charge cation. However, the 0.1 M NaMS concentration in the electrolyte is quite sufficient to achieve the maximum adsorption.

As one can see from the X-ray powder diffraction data, in the presence of 0.1 M NaMS in the nitrate electrolyte, the coating texture changes slightly. The reflexes of the same faces occurred in the PbO_2 coatings obtained from nitrate and methanesulfonate bathes, however, the intensity of some of them changes when methanesulfonate ions added into solution. There is a significant increase in the intensity of the reflection (110) $2\theta = 23.30$ and (111) $2\theta = 28.50$ for the α-phase, as well as the decrease in the intensity of the reflection (110) $2\theta = 25.40$; (011) $2\theta = 31.90$; (020) $2\theta = 36.20$ and (121) $2\theta = 49.10$ for the β-

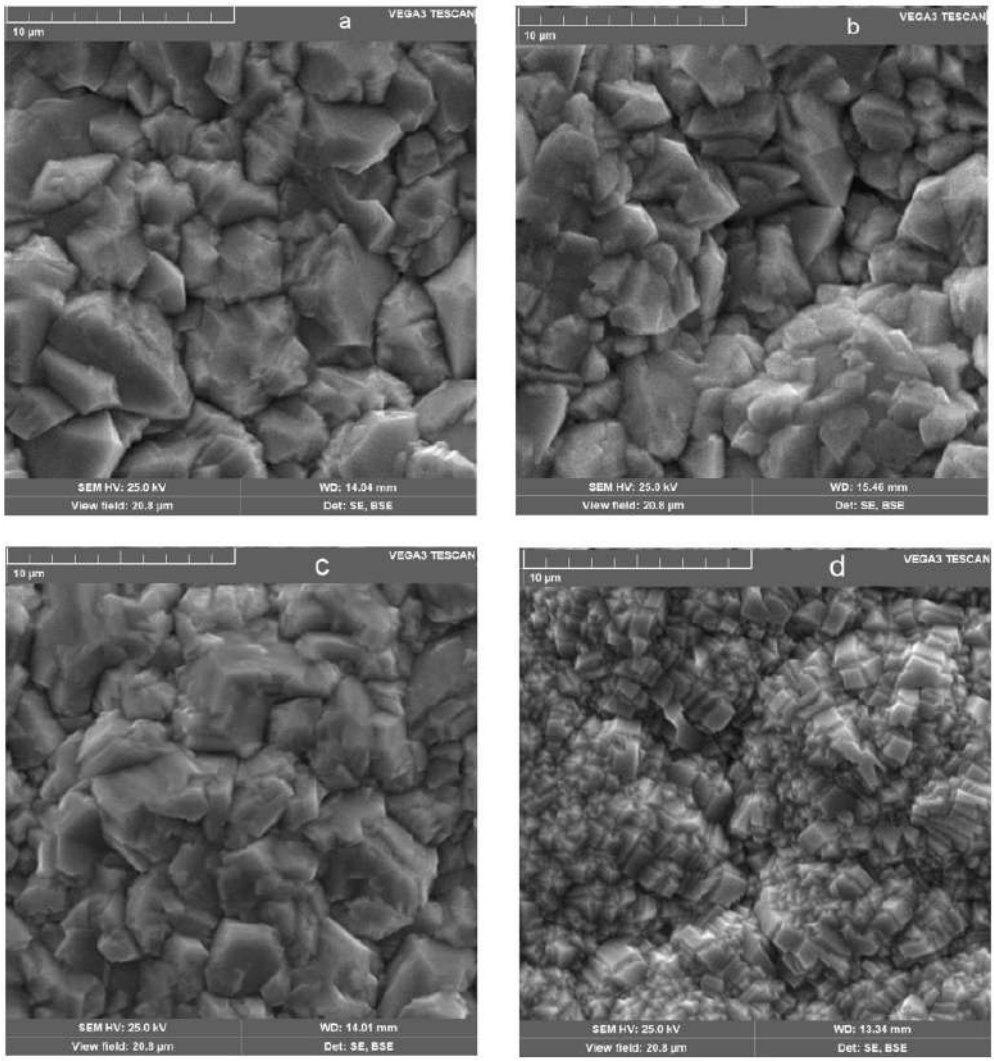

Fig. 3. SEM micrographs of lead dioxide, obtained at $j_a = 5$ mA cm^{-2} (t = 25 °C) from next solutions: a – 0.1 M $Pb(NO_3)_2$ + 0.1 M HNO_3; b – 0.1 M $Pb(CH_3SO_3)_2$ + 0.1 M CH_3SO_3H; from 0.1 M $Pb(CH_3SO_3)_2$ + 0.1 M CH_3SO_3H at $j_a = 10$ mA cm^{-2}, t = 25 °C (c) 0.1 M $Pb(CH_3SO_3)_2$ + 1 M CH_3SO_3H at $j_a = 5$ mA cm^{-2}, t = 25 °C (d).

Table 1
Phase composition of PbO_2 depending on methanesulfonate concentration in mixed deposition electrolyte.

Electrolyte	α-PbO_2/%	β- PbO_2/%
0.1 M $Pb(NO_3)_2$ + 1 M HNO_3 (N)	15.5	84.5
(N) + 0.1 M NaMS	41.2	58.8
(N) + 0.4 M NaMS	40.2	59.8
(N) + 0.5 M NaMS	43.3	56.7
(N) + 0.6 M NaMS	43.8	56.2
(N) + 1.2 M NaMS	43.8	56.2

phase.

As one can see from the data presented in Fig. 4, the change in the concentration of sodium methanesulfonate from 0.2 to 1.2 M practically does not affect the texture of the coatings obtained at 5 mA cm^{-2} and 25 °C, which is in full accordance with the data of the X-ray phase analysis (see Table 1). All deposits are polycrystalline. The maximum intensities are observed for the reflections (110) $2\theta = 25.40$; (011) $2\theta = 31.90$ and (121) $2\theta = 49.10$ for β-phases, and (111) $2\theta = 28.50$ for α-phases.

Further investigations were performed in methanesulfonate electrolytes that did not contain nitrate ions at higher current densities that were about 10 mA cm^{-2}. Under these conditions, the current efficiency of lead dioxide is still 100%, but the deposition rate is higher, which allows one even to obtain a coating of considerable thickness for an acceptable time with 0.1 M methanesulfonate content. The effect of the thickness (deposition time) of the coating is considered of great interest on its phase composition. Some influence of the nature of the substrate on texture and phase composition should be considered when synthesizing coatings of small thickness. However, this phenomenon is revealed for a short time, as then the deposition occurred on lead dioxide.

According to the obtained results (Table 2), the phase composition of the coatings changes with increasing coating thickness, the line of

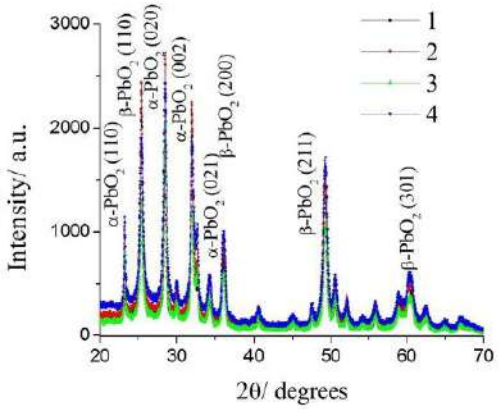

Fig. 4. X-Ray diffractograms of PbO_2-coatings, electrodeposited at j_a = 5 mA cm^{-2} and 25 °C from next solutions: 0.1 M $Pb(NO_3)_2$ + 1.0 M HNO_3 + X M NaMS, where 1 – 0.2; 2 – 0.4; 3 – 0.6; 4 – 1.2.

Table 2
Phase composition of PbO_2 depending on the coating thickness.

Electrolyte	α-PbO_2/%	β- PbO_2/%
0.1 M $Pb(MS)_2$ + 0.1 M MSA; 50 μm	17	83
0.1 M $Pb(MS)_2$ + 0.1 M MSA; 500 μm	21	79
0.1 M $Pb(MS)_2$ + 1 M MSA; 50 μm	90	10
0.1 M $Pb(MS)_2$ + 1 M MSA; 500 μm	60	40

this change depends on the content of methanesulfonic acid in the electrolyte.

For example, at low acidity (0.1 M), the coating is mainly composed of the β-phase and is slightly different from the oxide synthesized from nitrate solutions (see Table 1). The tenfold increasing of the coating thickness (up to 500 μm) leads to a slight decrease in the β-phase content (by 4%), so, for systems of this type, a change in the phase composition with increasing coating thickness can be neglected. The texture of the obtained coatings is also practically the same. A significantly different situation is observed when deposition proceeds from electrolytes with a high concentration of methanesulfonic acid (1.0 M). First of all, it should be noted that 90% of such coating consists of α-phase.

As been suggested in [34], during the nucleation depending on the composition of electrolyte may occur either the predominance of one phase over another or ingesting of growing centres of one phase by another. The formation of one phase is noticeably lagged behind the other. The type of lagging phase depends on the deposition conditions: at low polarizations there is a slight predominance of the growth of α-phase of PbO_2; at high polarization α-phase becomes stunted, and there is overlap and ingesting of formed α-phase growth centers by β-phase crystals on the surface of the electrode. In all cases, the type of nucleation is progressive. However, the preferred form of crystals at 2D nucleation in the case of methanesulfonate electrolyte is the cylinder, and in the nitrate electrolyte the crystal formation occurs in the form of cones, which is consistent with literature [36]. Rate constants of nucleation of α and β-phases of PbO_2 in the nitrate electrolyte differ slightly, and in the case of methanesulfonate electrolyte there is a predominance of α- phase forming [35].

With changing of the nature of the acid in the deposition electrolyte kinetic parameters of initial crystallization steps also change. In particular, the nucleation is reduced. Nature of acid changes the ratio between α- and β-phase crystallization constants in different amount. Thus, in the presence of nitric acid the growth of β-phase is noticeably predominant. In the case of methanesulfonate ion there is predominance in α-phase growth. It should also be noted, that when the electrolyte contains only ions Pb^{2+} and $CH_3SO_3^-$ ions in the ratio equal to 10 the α-phase growth prevails in 20 times. This effect of changing of kinetic parameters of 2D nucleation of lead dioxide probably will affect the 3D crystallization of the coating and as a consequence the phase composition of the coating [35]. It should be noted, that a substrate on which oxide is deposited, and its surface pretreatment prior the plating plays a significant role in the nucleation of crystals.

The phase composition of the coatings is significantly different for methanesulfonate and mixed nitrate-methanesulfonate electrolytes even at the same concentration of methanesulfonate ions and the acidity of the solutions. This indicates a significant effect of nitrate ions on the crystallization of lead dioxide also in mixed nitrate-methanesulfonate electrolytes. Although their significance is not completely understood, since nitrate ions do not form complex compounds and cannot be specifically adsorbed on the electrode surface. Possibly, the differences lie in the nature of the intermediate Pb(III) and Pb(IV) compounds, which are formed during the lead dioxide electrodeposition, which naturally reflects on the phase composition and physicochemical properties of coating.

The tenfold increasing of the coating thickness for deposits obtained from 1 M methanesulfonate bath results in a significant decrease in the α-phase content (up to 60%). However, further increase of the coating thickness up to 1000 μm does not change the phase composition of the coatings. The texture of the coatings with increasing their thickness also remains practically unchanged (Fig. 5). In this case, the intensities of (110) 2θ = 25.40; (011) 2θ = 31.90 and (121) 2θ = 49.10 for β-phases reflections significantly increase, which leads to growth in the content of the latter.

As follows from obtained data (Table 3) an increase in the acidity, both in nitrate and methanesulfonate electrolytes, leads to growth of the α-phase content.

However, at 0.1 M acid concentration, the phase composition of coatings obtained from nitrate and methanesulfonate electrolytes differs slightly. A major reason is a slight difference in the composition of the electroactive lead particles. About 60% of lead compounds are in the form of Pb^{2+} at ratio of methanesulfonate and lead ions 3:1, and the complex compounds are represented mainly by a single charged cation.

The revealed differences are probably due to the specific adsorption of methanesulfonate ions on the lead dioxide. With increasing concentration of methanesulfonic acid, not only the acidity increases, but also the methanesulfonate lead ions ratio grows, which at 1 M concentration is already 1:2:1. Under these conditions, the α-phase becomes

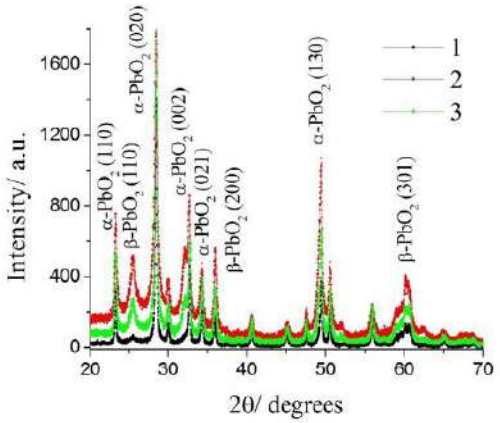

Fig. 5. X-Ray diffractograms of PbO_2-coatings with different thickness, electrodeposited at j_a = 10 mA cm^{-2} and 25 °C from 0.1 M $Pb(MS)_2$ + 1.0 M MSA, where 1 –50; 2 – 500; 3 – 1000 μm.

Table 3
Phase composition of PbO_2 depending on the electrolyte acidity.

Electrolyte	α-PbO_2/%	β- PbO_2/%
0.1 M $Pb(NO_3)_2$ + 0.1 M HNO_3	13.6	86.4
0.1 M $Pb(NO_3)_2$ + 0.25 M HNO_3	6.2	93.8
0.1 M $Pb(NO_3)_2$ + 0.5 M HNO_3	19.1	80.9
0.1 M $Pb(NO_3)_2$ + 1 M HNO_3	25.0	75.0
0.1 M $Pb(MS)_2$ + 0.1 M MSA	17.0	83.0
0.1 M $Pb(MS)_2$ + 0.25 M MSA	50.1	49.9
0.1 M $Pb(MS)_2$ + 0.5 M MSA	74.1	25.9
0.1 M $Pb(MS)_2$ + 1 M MSA	90.0	10.0

the main phase of the lead dioxide obtained from the methanesulfonate medium. The acidity most likely affects the composition and structure of the intermediate oxygen-containing Pb(III) and Pb(IV) species, which are formed in steps (2) and (3) during PbO_2 electrodeposition according to the mechanism, described in [35]:

$$H_2O \rightarrow OH^{\cdot}_{ads} + H^+ + e^- \quad (1)$$

$$[Pb(CH_3SO_3)_n]^{(2-n)+} + OH_{ads} \rightarrow [Pb(CH_3SO_3)_n(OH)]^{(2-n)+} \quad (2)$$

$$[Pb(CH_3SO_3)_n(OH)]^{(2-n)+} + H_2O \rightarrow [Pb(CH_3SO_3)_n(OH)_2]^{(2-n)+} + H^+ + e^- \quad (3)$$

$$[Pb(CH_3SO_3)_n(OH)_2]^{(2-n)+} \rightarrow PbO_2 + n(CH_3SO_3)^- + 2H^+ \quad (4)$$

The initial step of the process is the electrooxidation of water with the formation of oxygen-containing radicals of $OH^{\cdot}_{ads}$ type on the electrode surface (1). Considering the water concentration in aqueous solutions and the fact that the hydroxylation of the electrode surface occurs at much lower potentials than the processes of oxygen evolution and oxidation of lead compounds, this stage is fast. Then follows the chemical stage of oxidation of $[Pb(CH_3SO_3)]_n^{(2n)+}$ by oxygen-containing radicals $OH^{\cdot}_{ads}$ (2) with the formation of the unfixed on the electrode surface Pb(III) hydroxo complex $[Pb(CH_3SO_3)_n(OH)]^{(2-n)+}$, which is subsequently (3) oxidized in the electrochemical stage of charge transfer. In the last stage of the process, the hydroxo complexes of tetravalent lead decay by chemical mechanism with the formation of lead dioxide (4).

The above mentioned $[Pb(CH_3SO_3)]_n^{(2n)+}$ and $[Pb(CH_3SO_3)_n(OH)]^{(2-n)+}$ intermediates are directly involved in the crystallization of PbO_2, so their composition and charge are reflected in both the crystallization regularities and the phase composition of coatings. Reducing the acidity will promote the deprotonation of hydroxyl groups, which will facilitate the formation of lead dioxide.

As follows from the X-ray diffractograms (Fig. 6), the textures of each series of coatings obtained from methanesulfonate and nitrate solutions vary slightly, however, depending on the intensities and half-widths of the peaks, the dependence of the crystal size versus the acid content passes through the maximum.

The investigation of the effect of deposition conditions (current density, temperature and mixing) on the phase composition and texture of deposited lead dioxide is also of considerable interest. The variation of anode current density in the range of 2–10 mA cm^{-2} during the electrodeposition of PbO_2 from methanesulfonate bath has almost no effect on the phase composition of PbO_2 in contrast to nitrate solutions [8,30].

However, changes in temperature in both methanesulfonate and nitrate bath lead to an increase in the β-phase content: from 10 till 67% and from 75 till 86 %, respectively when increasing temperature from 25 till 60 °C.

Further increase in temperature in both media results in growing intensity of the peaks of almost all reflections of the polycrystalline coating, reducing the semi-width of peaks, which indicates an increase in the crystal size. Partially, the observed effect may be associated with an increase in the rate of diffusion of oxygen-containing Pb(III) and Pb (IV) species, followed by their inclusion in the growing matrix on the film surface.

Mixing of methanesulfonate electrolyte results in an increase of α-phase content by 6% (up to 27%) with virtually unchanged coating texture. There is a decrease in the intensity of the main reflections under the stirring, but the coating is characterized by a high degree of crystallinity.

As a substrate, Ti/Pt was used in the work. According to the data obtained, the lifetime of such anodes is about 20 h. It should be noted that usually lead dioxide electrodes are operated at current densities of 20–50 mA cm^{-2}. In such operating modes, the life of the electrodes in comparison with the data obtained in the accelerated tests will increase from 10 to 100 times, which is caused by a significant decrease in the rate of mechanical fracture and heating of the transition layer. However, even in this case, the result obtained cannot be considered satisfactory for the construction of industrial anodes. Variation of the coating thickness in the range of 20–2000 μm did not lead to a significant change in the life of the work. It should be noted that the Ti/Pt without active lead oxide coating served under the same conditions for less than an hour. Violation of the integrity of the lead dioxide coating due to the appearance of cracks and through porosity leads to rapid passivation of the substrate due to its oxidation and increased transient resistance. A similar effect, only more elongated in time, will detect the possible diffusion of oxygen to the substrate through the oxide of the active coating.

In this regard, the need to address the problem of the transition layer comes to the fore, as it is one of the main factors affecting the life of the DSA in real operating conditions. We have attempted to solve these problems by using a transitional platinum-containing layer obtained by the combined electrochemical-pyrolytic method, which can significantly increase the anode life of the accelerated test mode.

Thus, the maximum lifetime of the anodes was about 105 h compared to 8 h for the Ebonex®-based substrate [37] and 20 h for the traditional anode fabricated on the Ti/Pt, i.e. 12 and 5 times increase in service life, respectively.

4. Conclusions

Having in mind the potential impact on the bond strength of oxygen-containing radicals adsorbed on the electrode surface, such structural parameters as the texture and phase composition of PbO_2-based materials may be important. These factors can also secondarily affect the chemical composition of the PbO_2 surface by changing the number and nature of cationic vacancies, as well as the nature and surface concentration of oxygen-containing compounds. Unlike nitrate solutions, the use of methanesulfonate electrolytes of different composition allows one change of phase composition of the coating over a wide range. First of all, it should be noted that the addition of 0.1 M sodium methanesulfonate to the nitrate electrolyte leads to an increase in the content of α-phase from 15 to 41%. Further increase in the concentration of NaMs practically does not affect the phase composition of the coating. However, changing the ratio between allotropic forms does not lead to the emergence of new crystallographic orientations of the α- and β-phases. All deposits are polycrystalline. The maximum intensities are shown for the reflections (110) 2θ = 25.40; (011) 2θ = 31.90 and (121) 2θ = 49.10 for β-phase, and (111) 2θ = 28.50 for α-phase.

Increasing the current density from 5 to 10 mA cm^{-2} has virtually no effect on the phase composition and texture of the coatings, while increasing the acid content of both nitrate and methanesulfonate solutions from 0.1 M to 1.0 M leads to a significant increase in the amount of α-phase in the coating up to 25 and 90% respectively. It should be noted that at low acidity, the phase composition of PbO_2 synthesized from nitrate and methanesulfonate electrolytes is practically no different. However, at 1.0 M concentration of acid in mixed nitrate-methanesulfonate electrolytes, the maximum amount of α-phase is only

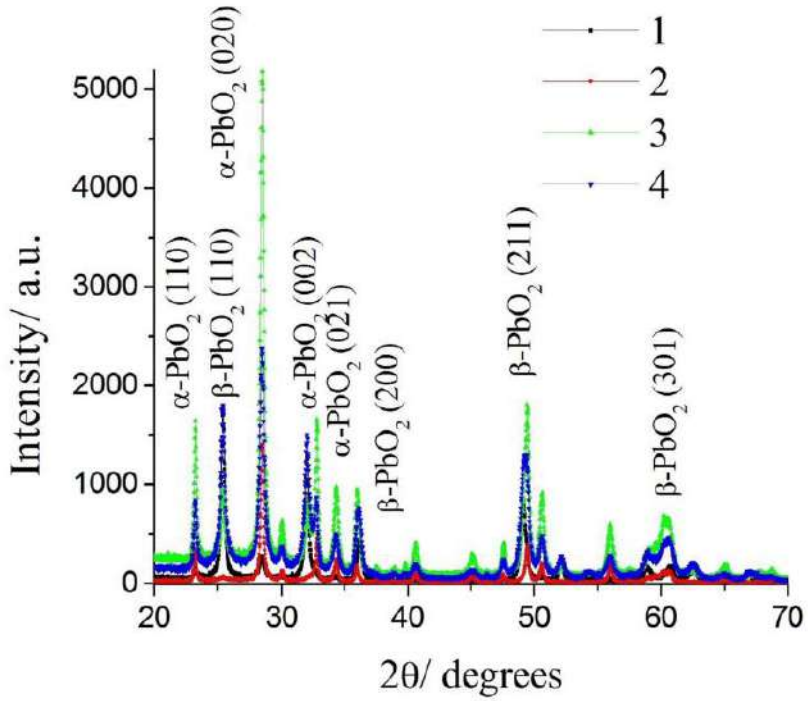

a

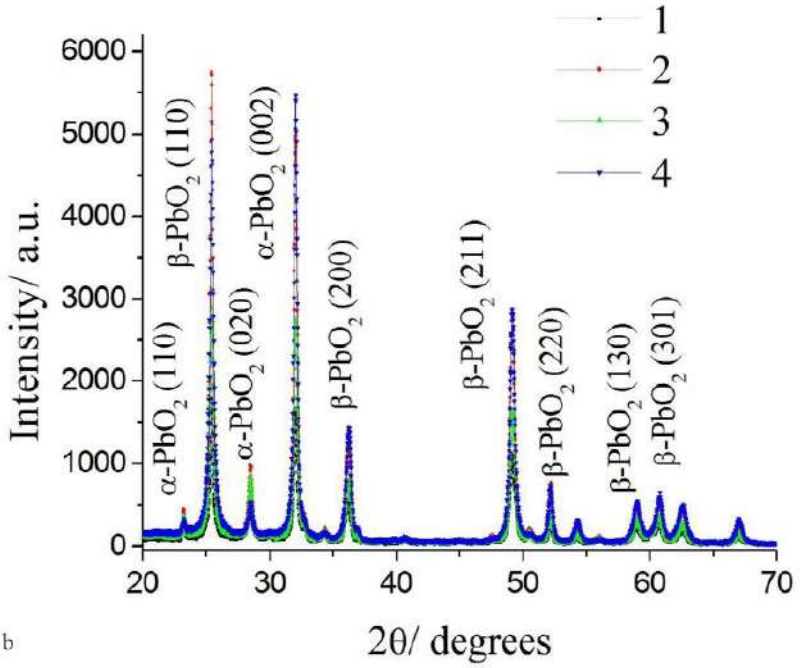

b

Fig. 6. X-Ray diffractograms of PbO_2-coatings, electrodeposited at j_a = 10 mA cm^{-2} and 25 °C from next solutions: a – 0.1 M $Pb(MS)_2$ + X M MSA; b – 0.1 M $Pb(NO_3)_2$ + X M HNO_3, where X is 1 – 0.1; 2 –0.25; 3 – 0.5; 4 – 1.0.

44%, which is 2 times lower compared to the methanesulfonate electrolyte with the same concentration of lead and methanesulfonate ions. Since the nitrate ion is not adsorbed on the electrode surface and does not form complex compounds with Pb^{2+}, the sole presence of sodium ion solution may be the only effect. The latter may affect the coordination of water and its structure in the near electrode layer or the hydration of methanesulfonate ions, which in turn may affect the nature of the oxygen-containing radicals involved in the formation of PbO_2.

It should take into account that the nature of the substrate may have some influence on texture and phase composition during deposition of coatings of small thickness. This effect is present for a short time, since then the deposition is carried out on the lead dioxide. The phase composition of the coatings changes with increasing thickness of the coating, the line of this change depends on the content of methanesulfonic acid in the electrolyte. At low concentration (0.1 M), the tenfold increasing of the coating thickness (up to 500 μm) leads to a slight decrease in the β-phase content (by 4%), i.e., for systems of this type, the change in phase composition with increasing coating thickness can be neglected. The texture of the obtained coatings is also practically the same. A significantly different situation is observed during deposition from electrolytes with a high concentration of methanesulfonic acid (1.0 M). The tenfold increasing of the coating thickness results in a significant decrease in the α-phase content (up to 60%). However, further increase of the coating thickness up to 1000 μm does not change the phase composition of the coatings. The texture of the coatings with increasing their thickness also remains virtually unchanged.

An increase in the temperature of the methanesulfonate electrolytes leads to an increase in the β-phase content. Mixing the methanesulfonate electrolyte results in an increase of the α-phase content by 6% (up to 27%) with virtually unchanged texture of the coatings. There is a decrease in the intensity of the main reflections under stirring, but the coating is characterized by a high degree of crystallinity.

Thus, the main influence on the phase composition of PbO_2 obtained from methanesulfonate electrolytes is the concentration of methanesulfonic acid. Changing its concentration in solution from 0.1 M to 1.0 M makes it possible to increase the amount of α-phase in the coating from 17 to 90%.

Funding

This work was supported by Ministry of Education and Science of Ukraine.

CRediT authorship contribution statement

A. Velichenko: Supervision, Writing - review & editing. **T. Luk'yanenko:** Conceptualization, Methodology, Investigation. **O. Shmychkova:** Data curation, Writing - original draft.

Declaration of Competing Interest

The authors declare that they have no known competing financial interests or personal relationships that could have appeared to influence the work reported in this paper.

Acknowledgements

The authors are indebted to Laboratory of Material Science and Intermetallic compounds (Ivan Franko Lviv National University) for help in the discussion of obtained results.

References

[1] M. Krishna, E.J. Fraser, R.G.A. Wills, F.C. Walsh, Developments in soluble lead flow batteries and remaining challenges: an illustrated review, J. Energy Storage 15 (2018) 69–90 https://doi.org/10.1016/j.est.2017.10.020.
[2] F.C. Walsh, C.T.J. Low, A review of developments in the electrodeposition of tin-copper alloys, Surf. Coat. Tech. 304 (2016) 246–262 https://doi.org/10.1016/j.surfcoat.2016.06.065.
[3] C. Ponce de Leon, F.C. Walsh, Versatile electrochemical coatings and surface layers from aqueous methanesulfonic acid, Surf. Coat. Tech. 259 (2014) 676–697 http://dx.doi.org/10.1016/j.surfcoat.2014.10.010.
[4] S. Chou, F. Cheng, J. Chen, Electrodeposition synthesis and electrochemical properties of nanostructured γ-MnO_2 films, J. Power Sour. 162 (2006) 727–734 https://doi.org/10.1016/j.jpowsour.2006.06.033.
[5] S. Chai, G. Zhao, Y. Wang, Y. Zhang, Y. Wang, Y. Jin, X. Huang, Fabrication and enhanced electrocatalytic activity of 3D highlyordered macroporous PbO_2 electrode for recalcitrant pollutant incineration, Appl. Catal., B 147 (2014) 275–286 https://doi.org/10.1016/j.apcatb.2013.08.046.
[6] C. Zhao, H. Yu, Y. Li, X. Li, L. Ding, L. Fan, Electrochemical controlled synthesis and characterization of well-aligned IrO_2 nanotube arrays with enhanced electrocatalytic activity toward oxygen evolution reaction, J. Electroanal. Chem. 688 (2013) 269–274 https://doi.org/10.1016/j.jelechem.2012.08.032.
[7] S. Fierro, T. Nagel, H. Baltruschat, Ch. Comninellis, Investigation of the oxygen evolution reaction on Ti/IrO_2 electrodes using isotope labelling and on-line mass spectrometry, Electrochem. Commun. 9 (2007) 1969–1974 https://doi.org/10.1016/j.elecom.2007.05.008.
[8] A.B. Velichenko, R. Amadelli, E.V. Gruzdeva, T.V. Luk'yanenko, F.I. Danilov, Electrodeposition of lead dioxide from methanesulfonate solutions, J. Power Sour. 191 (2009) 103–110 https://doi.org/10.1016/j.jpowsour.2008.10.054.
[9] O. Shmychkova, T. Luk'yanenko, R. Amadelli, A. Velichenko, Electrodeposition of Ni^{2+}-doped PbO_2 and physicochemical properties of the coating, J. Electroanal. Chem. 774 (2016) 86–94 https://doi.org/10.1016/j.jelechem.2016.05.017.
[10] X. Li, D. Pletcher, F.C. Walsh, Electrodeposited lead dioxide coatings, Chem. Soc. Rev 40 (2011) 3879–3894 https://doi.org/10.1039/C0CS00213E.
[11] B.P. Chaplin, Critical review of electrochemical advanced oxidation processes for water treatment applications, Environ. Sci.: Process. Impacts 16 (2014) 1182–1203 https://doi.org/10.1039/C3EM00679D.
[12] R. Vargas, C. Borras, D. Mendez, J. Mostany, B.R. Scharifker, Electrochemical oxygen transfer reactions: electrode materials, surface processes, kinetic models, linear free energy correlations, and perspectives. A review, J Solid State Electrochem. 20 (2016) 875–893, https://doi.org/10.1007/s10008-015-2984-7.
[13] S.P. Tong, C.A. Ma, H. Feng, A novel PbO_2 electrode preparation and its application in organic degradation, Electrochim. Acta 53 (2008) 3002–3006 https://doi.org/10.1016/j.electacta.2007.11.011.
[14] Y. Zheng, W. Su, S. Chen, X. Wu, X. Chen, Ti/SnO_2–Sb_2O_5–RuO_2/α-PbO_2/β-PbO_2 electrodes for pollutants degradation, Chem. Eng. J. 174 (2011) 304–309 https://doi.org/10.1016/j.cej.2011.09.035.
[15] Y. Chen, H. Li, W. Liu, Y. Tu, Y. Zhang, W. Han, L. Wang, Electrochemical degradation of nitrobenzene by anodic oxidation on the constructed TiO_2-NTs/SnO_2-Sb/PbO_2 electrode, Chemosphere 113 (2014) 48–55 https://doi.org/10.1016/j.chemosphere.2014.03.122.
[16] L.N. Bengoa, P. Pary, M.S. Conconi, W.A. Egli, Electrodeposition of Cu-Sn alloys from a methanesulfonic acid electrolyte containing benzyl alcohol, Electrochim. Acta 256 (2017) 211–219 https://doi.org/10.1016/j.electacta.2017.10.027.
[17] B. Jin, D.B. Dreisinger, A green electrorefining process for production of pure lead from methanesulfonic acid medium, Sep. Purif. Technol. 170 (2016) 199–207 https://doi.org/10.1016/j.seppur.2016.06.050.
[18] B. Yu, R. Xu, Y. Li, J. Zhang, Z. Qin, Study of Pb(II) effect on electrosynthesis of lead dioxide in more environmentally electrolyte of methanesulfonic acid, Int. J. Electrochem. Sci 12 (2017) 8059–8069 https://doi.org/10.20964/2017.09.28.
[19] B. Yu, R. Xu, S. He, Z. Qin, W. Wang, Preparations and performances testing of α/β-PbO_2 phase compositions prepared in methanesulfonic acid in order to provide more appropriate environmentally sustainable electrodes, Electrochem 87 (4) (2019) 197–203 https://doi.org/10.5796/electrochemistry.18-00066.
[20] J. Dong, X. Wu, Y. Chen, N. Brandon, X. Li, J. Yang, J. Yu, W. Zhang, Y. Hu, W. Yu, J. Wang, S. Liang, J. Hu, H. Hou, B. Liu, C. Yang, A study on Pb^{2+}/Pb electrodes for soluble lead redox flow cells prepared with methanesulfonic acid and recycled lead, J. Appl. Electrochem. 46 (2016) 861–868 https://doi.org/10.1007/s10800-016-0980-y.
[21] J. Wei, X. Wu, An in-depth study of lead dioxide formation in nitrate and methanesulfonate solutions by in situ analysis and numerical model, J. Energy Storage 28 (2020) 101308https://doi.org/10.1016/j.est.2020.101308.
[22] J. Wei, Y. Gu, Z. Guo, C. Deng, M. Xie, J. Li, R. Xiong, Y. Xue, L. Wang, H. Zhao, X. Wu, EQCM study of hydrated PbO_2 content and its influence on cycling performance of lead-acid batteries, J. Energy Storage 21 (2019) 706–712 https://doi.org/10.1016/j.est.2019.01.015.
[23] O. Shmychkova, T. Luk'yanenko, A. Velichenko, L. Meda, R. Amadelli, Bi-doped PbO anodes: electrodeposition and physico-chemical properties, Electrochim Acta 111 (2013) 332–338 https://doi.org/10.1016/j.electacta.2013.08.082.
[24] A.B. Velichenko, D.V. Girenko, S.V. Kovalyov, A.N. Gnatenko, R. Amadelli, F.I. Danilov, Lead dioxide electrodeposition and its application: influence of fluoride and iron ions, J. Electroanal. Chem. 454 (1998) 203–208 https://doi.org/10.1016/S0022-0728(98)00256-3.
[25] A.B. Velichenko, D.V. Girenko, F.I. Danilov, Electrodeposition of lead dioxide at an Au electrode, Electrochim. Acta 40 (1995) 2803–2807 https://doi.org/10.1016/0013-4686(95)00257-F.
[26] A.B. Velichenko, D.V. Girenko, F.I. Danilov, Mechanism of lead dioxide electrodeposition, J, Electroanal. Chem. 405 (1996) 127–132 https://doi.org/10.1016/0022-0728(95)04401-9.
[27] G. Abadias, E. Chason, J. Keckes, M. Sebastiani, G.B. Thompson, E. Barthel,

G.L. Doll, C.E. Murray, Ch.H. Stoessel, L. Martinu, Review Article: Stress in thin films and coatings: Current status, challenges, and prospects, J.Vac. Sci. Technol. A 36 (2018) 020801https://doi.org/10.1116/1.5011790.

[28] M.D. Capelato, J.A. Nobrega, E.F.A. Neves, Complexing power of alkanesulfonate ions: the lead-methanesulfonate system, J. Apl. Electrochem. 25 (1995) 408–411 https://doi.org/10.1007/BF00249661.

[29] M.E. Herron, D. Pletcher, F.C. Walsh, A combined electrochemical and in-situ X-ray diffraction study of the cycling of well-defined lead dioxide layers on platinum, J. Electroanal. Chem. 332 (1-2) (1992) 183–197 https://doi.org/10.1016/0022-0728(92)80350-D.

[30] A.B. Velichenko, D. Devilliers, Electrodeposition of fluorine-doped lead dioxide, J. Fluorine Chem 128 (2007) 269–276 https://doi.org/10.1016/j.jfluchem.2006.11.010.

[31] P. Gao, Y. Liu, X. Bu, M. Hu, Y. Dai, X. Gao, L. Lei, Solvothermal synthesis of a-PbO from lead dioxide and its electrochemical performance as a positive electrode material, J. Power Sour. 242 (2013) 299–304 https://doi.org/10.1016/j.jpowsour.2013.05.077.

[32] U. Casellato, S. Cattarin, M. Musiani, Preparation of porous PbO_2 electrodes by electrochemical deposition of composites, Electrochim. Acta 48 (2003) 3991–3998 https://doi.org/10.1016/S0013-4686(03)00527-9.

[33] I. Sires, C.T.J. Low, C. Ponce-de-Leon, F.C. Walsh, The deposition of nanostructured β-PbO_2 coatings from aqueous methanesulfonic acid for the electrochemical oxidation of organic pollutants, Electrochem. Commun. 12 (1) (2010) 70–74 https://doi.org/10.1016/j.elecom.2009.10.038.

[34] O. Shmychkova, T. Luk'yanenko, A. Pileiska, A. Velichenko, R. Gladyshevskii, P. Demchenko, R. Amadelli, Electrocrystallization of lead dioxide: Influence of early stages of nucleation on phase composition, J. Electroanal. Chem. 746 (2015) 57–61 https://doi.org/10.1016/j.jelechem.2015.03.031.

[35] T. Luk'yanenko, A. Velichenko, V. Knysh, O. Shmychkova, Influence of methanesulfonate ions on electrooxidation of Pb(II), Voprosy Khimii i Khimicheskoi Tekhnologii 4 (2018) 27–35 https://udhtu.edu.ua/public/userfiles/file/VHHT/2018/4/Luk'yanenko.pdf.

[36] M.Y. Abyaneh, Modelling diffusion controlled electrocrystallisation processes, J. Electroanal. Chem 586 (2006) 196–203 https://doi.org/10.1016/j.jelechem.2005.10.004.

[37] T. Luk'yanenko, O. Shmychkova, V. Knysh, A. Velichenko, Design and properties of dimensionally stable anodes on Ebonex® substrate, Voprosy Khimii i Khimicheskoi Tekhnologii 6 (2019) 121–127 https://doi.org/10.32434/0321-4095-2019-127-6-121-127.

*Таким чином, для одержання осадів плюмбум(*IV*) оксиду, що переважно складаються із α-фази, був рекомендований 1 М метансульфонатний електроліт, а для отримання покриттів, які складаються переважно із β-фази,* – 0,1 *М* $Pb(NO_3)_2$ + 0.1 M HNO_3 *або* 0.1 M $Pb(CH_3SO_3)_2$ + 0.1 M CH_3SO_3H. *Ці електроліти були вибрані як базові для подальших досліджень. Результати досліджень показали, що перспективнішим для створення композитних матеріалів є оксид, збагачений β-фазою. Наявність поверхнево-активних речовин в цих розчинах одночасно впливає на кінетику нуклеації, як α-, так і β-фази, але не приводить до суттєвої зміни фазового складу. Як правило, ПАР приводять до зменшення констант швидкостей нуклеації обох фаз* PbO_2*, що також вказує на блокування поверхні адсорбованими добавками.*

Вперше вивчені закономірності впливу добавок ПАР та полімерів на нуклеацію PbO_2. *Так, наприклад, виявлено, що і в нітратних, і в метансульфонатних електролітах за збільшення довжини карбонового ланцюга аніонних ПАР із високою поверхневою активністю* (*натрію додецил сульфат та лаурет сульфат*) *та флуоровмісних спостерігається незначне зменшення вмісту α-фази* PbO_2 *в межах 10%. За цього мінімальний вміст спостерігається для покриттів* PbO_2*-натрію лауретсульфат та* PbO_2*-перфлуорогексансульфонат, що містять 16 та 8 атомів Карбону, відповідно.*

Вперше запропоновано експрес-метод напівкількісної оцінки фазового складу покриттів, в основі якого лежить аналіз відновлення утворюваних осадів на інверсійній вольтамперограмі. Він досить перспективний для визначення фазового складу тонких плівок, оскільки покриття не товсте, за використання рентгенівської дифракції із невеликим кутом опромінення на дифрактограмі проявляються також і рефлекси підкладки, а зняти таке покриття для порошкової рентгенівської дифракції немає можливості. Дослідженнями з використанням інверсійної вольтамперометрії показано, що відновлення осадів, отриманих з метансульфонатних електролітів (α-фаза), відбувається за меншого потенціалу, ніж для покриттів, осаджених з нітратного розчину (β-фаза).

РОЗДІЛ 4
КОМПОЗИТИ PbO_2-ПАР: ЗАКОНОМІРНОСТІ ОСАДЖЕННЯ ТА ВЛАСТИВОСТІ ПОКРИТТІВ

4.1 Вплив аніонних ПАР із високою поверхневою активністю

Найбільш цікавими для практичного застосування під час одержання різноманітних композитних матеріалів на основі PbO_2 є електроліти, у складі яких знаходяться ПАР та полімери. В дослідженнях для нас цікавішими були композити із аніонними ПАР. Оскільки поверхня PbO_2 заряджена позитивно, то катіонні ПАР робитимуть її ще позитивнішою, що приведе до блокування останньої. Для нас це небажаний ефект. Як свідчать літературні дані, неіногенні ПАР також не мають суттєвого впливу на склад покриття та його властивості [34]. Тоді як використання в якості добавок до електроліту осадження аніонних ПАР, які внаслідок адсорбції не сильно інгібуватимуть електроосадження, а навпаки, будуть впроваджуватися в оксид і утворювати композит, представляє інтерес. Тут потрібно зазначити, що ми застосовували електроліти із невеликою концентрацією ПАР, що означає використання дійсних розчинів. За таких концентрацій ми ще не досягаємо ККМ, більш того ПАР із іонами плюмбуму не утворюють комплексних сполук та асоціатів.

Нами були вибрані аніонні ПАР із високою поверхневою активністю, такі як натрію лаурет сульфат додецил сульфат, та ПАР із низькою поверхневою активністю, що містять у своєму складі флуорид-іони. Гідрофобність F-C хвоста набагато більша, ніж у H-C. Тут є ніша для досліджень, оскільки такі електроди за рахунок гідрофобізації поверхні здатні впливати на енергію зв’язку кисеньвмісних частинок. Згідно з літературними даними такий ефект створюватиме умови для більшої реакційної здатності в реакціях окиснення органічних сполук. В цьому випадку для нас представляло інтерес з’ясування впливу довжини флуор-карбонового ланцюга на властивості покриття. З полімерів ми досліджували аніонний полімер Nafion® та катіонний

поліаміногуанідин. Відомості про такі композити в літературі практично відсутні. Тому ми пропонуємо матеріали новітнього типу.

Розглянемо закономірності осадження PbO_2 за наявності в електроліті осадження ПАР та полімерів. На типових циклічних вольтамперограмах анодна гілка кривої (рис. 4.1, 4.2) за потенціалів вище 1,4 В характеризується експонентним ростом струму, що відповідає одночасним реакціям окислення плюмбуму(II) та виділення кисню.

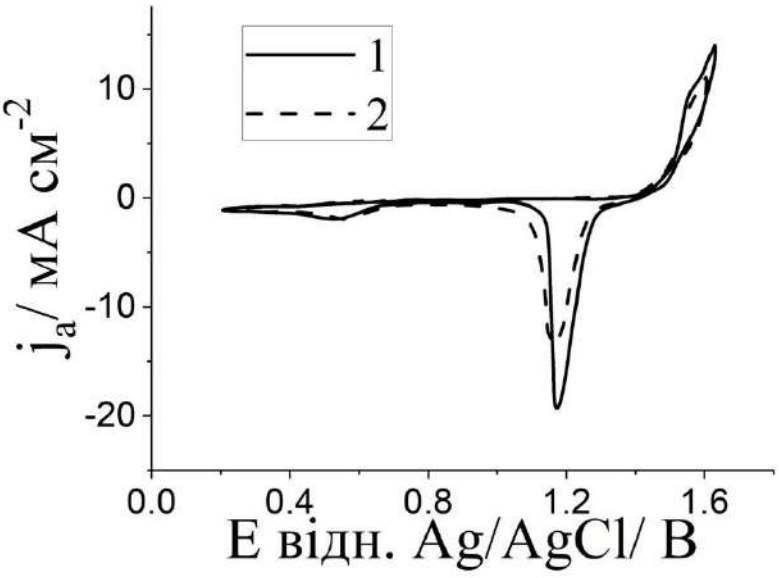

Рис. 4.1 Циклічні вольтамперограми (діапазон потенціалів сканування 0,0 1,6 В) на платиновому електроді в розчинах 0,01 М $Pb(NO_3)_2$ + 0,1 М HNO_3 (1) + 3×10^{-4} М натрію лауретсульфату (2). v=20 мВ/с

На катодній гілці кривої можна спостерігати пік струму за рахунок відновлення плюмбум оксиду за потенціалів між 1,0 і 1,2 В. Додавання до електроліту осадження аніонних поверхнево-активних речовин приводить до незначного пригнічення осадження PbO_2 (див. рис. 4.1, 4.2). Як можна побачити з рисунку, маса золотого електрода збільшується на анодній гілці ЦВА через осадження плюмбум оксиду (рис. 4.3). Менша маса покриття, отриманого за наявності ПАР у розчині, підтверджує пригнічення електроосадження PbO_2 через добавку аніонних ПАР.

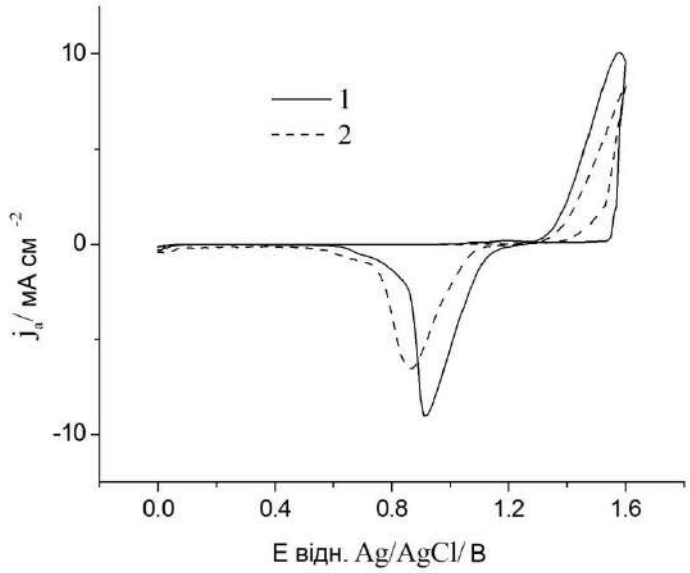

Рис. 4.2 Циклічні вольтамперограми (діапазон потенціалів сканування 0,0 1,6 В) на золотому електроді в розчинах 0,01 М $Pb(NO_3)_2$ + 0,1 М HNO_3 (1) + 7×10^{-4} М натрію додецилсульфату (2). v=50 мВ/с

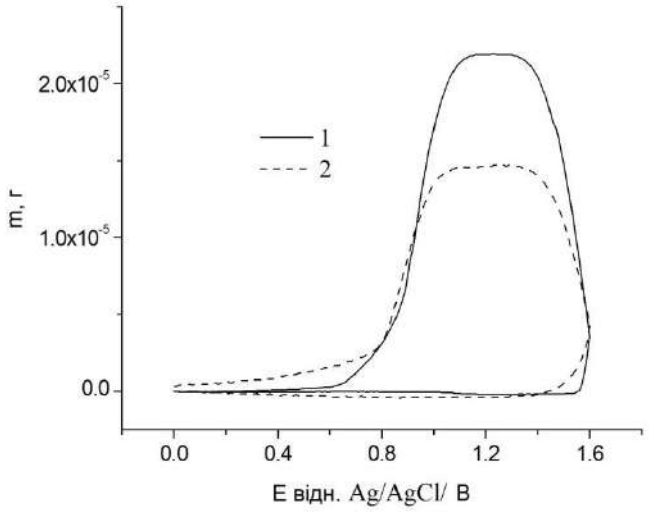

Рис. 4.3 Зміна маси золотого електрода під час реєстрації ЦВА (рис. 4.2) за електроосадження плюмбум(IV) оксиду з різних електролітів: 1 – 1,0 М HNO_3 + 0,01 М $Pb(NO_3)_2$; 2 – 1,0 М HNO_3 + 0,01 М $Pb(NO_3)_2$ + 7×10^{-4} М натрію додецил сульфату.

Незначне гальмування процесу електроокислення Pb^{2+} спостерігається на стаціонарних кривих j-E, отриманих як для повного процесу (виділення кисню та осадження PbO_2), так і для парціального процесу електроокислення Pb(II) (рис. 4.4). В області низької поляризації (область I) залежності потенціалу E від логарифму густини струму log j, побудованої з кривих j-E лінійні (r = 0,99), що вказує на кінетичний контроль процесу електроосадження.

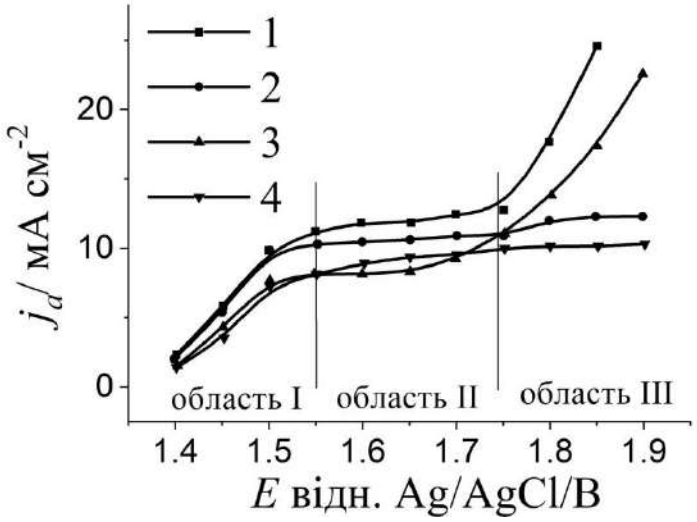

Рис. 4.4 Стаціонарні поляризаційні криві для загального (1,2) та парціального (3,4) струмів процесу електроосадження PbO_2 на платиновому електроді в розчинах 0,01 M $Pb(NO_3)_2$ + 0,1 M HNO_3 (1,3) та 0,01 M $Pb(NO_3)_2$ + 0,1 M HNO_3 + 0,0003 M SLES (2,4)

Кількість електронів, які беруть участь у кінетичній стадії, визначали за допомогою вольтамперометрії з лінійною розгорткою потенціалу згідно з рівнянням Делахея.

$$i=3{,}00\cdot10^5\cdot n\cdot(\beta n_\beta)^{1/2}\cdot D^{1/2}\cdot c\cdot S\cdot\upsilon^{1/2} \qquad (4.1)$$

Характерним значенням у цьому методі є пік анодного струму на кривій j-E, значення якого залежить від швидкості розгортки потенціалу (рис. 4.5). Як

можна побачити, зі збільшенням швидкості розгортки потенціалу анодний пік зміщується у бік збільшення Е, що вказує на незворотний перенос електронів.

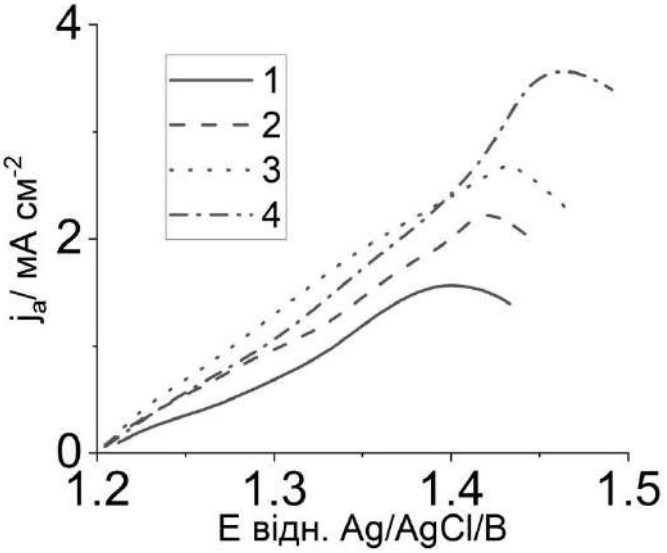

Рис. 4.5 Анодні вольтамперограми за різних швидкостей розгортки потенціалу, мВ/с: 1 – 20; 2 – 50; 3 – 100; 4 – 200 в розчині 0,01 М $Pb(NO_3)_2$ + 0,1 М HNO_3 + 3×10^{-4} М натрію лауретсульфат

Як випливає з наведеного рівняння, залежність потенціалу піку від логарифма швидкості розгортки потенціалу повинна бути лінійною і з її нахилу можна розрахувати коєфіцієнт перенесення електронів βn_β досліджуваного процесу.

$$E_p=E^\circ–RT/\ \beta n_\beta\ F\ [0{,}78–\ln k_s+\ln(D\beta n_\beta F\upsilon\ /RT)^{1/2}] \qquad (4.2)$$

З цього рівняння βn_β = RT/2bF, де b – кутовий коєфіцієнт залежності E_p–ln υ.

Коефіцієнт перенесення залишається майже незмінним (β = 0,4) за наявності поверхнево-активної речовини в електроліті осадження. Розрахована кількість електронів в елементарній стадії дорівнювала одиниці, що підтверджує, що утворення PbO_2-це стадійний процес переносу заряду.

Зі збільшенням анодної поляризації (область III) на стаціонарній поляризаційній кривій спостерігається граничний струм осадження плюмбум оксиду (див. рис. 4.1, 4.2). У досліджуваному діапазоні потенціалів значення виміряних парціальних струмів електроосадження плюмбум оксиду лінійно залежать від швидкості обертання електрода, підкоряючись рівнянню Левича (коефіцієнт кореляції r = 0,99) (рис. 4.6).

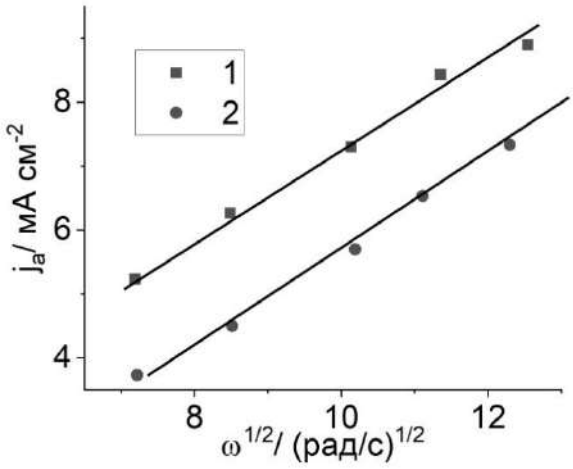

Рис. 4.6 Густина анодного струму (E = 1,8 В) від квадратного кореня швидкості обертання Pt-ОДЕ в розчині 0,01 М $Pb(NO_3)_2$ + 0,1 М HNO_3 (1) + 3×10^{-4} М натрію лауретсульфат (2)

Отримані дані свідчать про дифузійний контроль процесу за високих анодних поляризацій.

4.2 Вплив флуоровмісних ПАР та довжини їх флуор-карбонового ланцюга

За наявності флуоровмісних ПАР в електроліті осадження також спостерігається пригнічення утворення PbO_2 (рис. 4.7). За збільшення довжини карбонового ланцюга цей ефект проявляється більше (рис. 4.8).

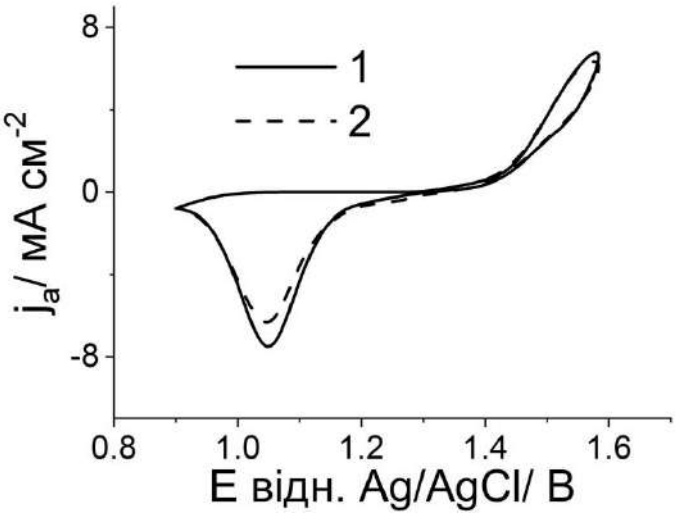

Рис. 4.7 Циклічні вольтамперограми (діапазон потенціалів сканування 0,0 1,6 В) на платиновому електроді в розчинах 0,01 М $Pb(NO_3)_2$ + 0,1 М HNO_3 (1) + 3×10^{-3} М $C_4F_9SO_3K$ (2). v=50 мВ/с

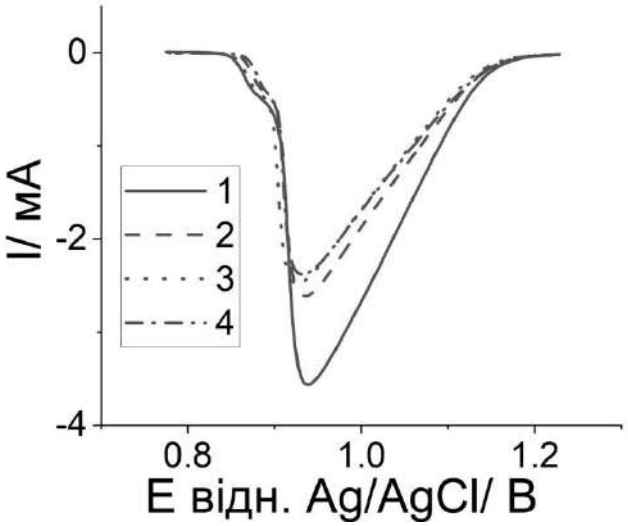

Рис. 4.8 Катодні гілки ЦВА у розчинах 0,01 М $Pb(NO_3)_2$+ 0,1 М HNO_3 (1) + Х М $C_6F_{13}SO_3K$, де Х 3×10^{-5} (2) 3×10^{-4} (3) і 3×10^{-3} (4)

Гетерогенні константи швидкості були розраховані за рівнянням Коутецьки-Левича (рівн. 4.3). Результати показують, що наявність ПАР у розчині осадження приводить до того, що гетерогенна константа швидкості дещо зменшується.

$$\frac{1}{I} = \frac{1}{nkFSc_0} + \frac{1}{0.62nFSD^{2/3}\nu^{-1/6}c_0} \cdot \frac{1}{\varpi^{1/2}} \qquad (4.3)$$

Зі збільшенням довжини карбонового ланцюга таке інгібування проявляється більше. За досягнення певної довжини флуор-карбонового ланцюга константи перестають змінюватись (табл. 4.1).

Таблиця 4.1

Гетерогенні константи швидкості утворення PbO_2 у різних електролітах

Склад електроліту осадження	$k \times 10^4$, м/с
0,1 M HNO_3 + 0,1 M Pb^{2+}	4,1
0,1 M HNO_3 + 0,1 M Pb^{2+} + $3,0\times10^{-5}$ M SDS	4,0
0,1 M HNO_3 + 0,1 M Pb^{2+} + $2,0\times10^{-4}$ M SDS	3,8
0,1 M HNO_3 + 0,1 M Pb^{2+} + $5,0\times10^{-4}$ M SLES	3,8
0,1 M HNO_3 + 0,1 M Pb^{2+} + $1,0\times10^{-3}$M SLES	3,7
0,1 M HNO_3 + 0,1 M Pb^{2+} + $3,0\times10^{-5}$ M $C_4F_9O_3SK$	3,8
0,1 M HNO_3 + 0,1 M Pb^{2+} + $3,0\times10^{-4}$ M $C_4F_9O_3SK$	3,6
0,1 M HNO_3 + 0,1 M Pb^{2+} + $3,0\times10^{-3}$ M $C_4F_9O_3SK$	3,5
0,1 M HNO_3 + 0,1 M Pb^{2+} + $3,0\times10^{-4}$ M $C_6F_{13}O_3SK$	2,8
0,1 M HNO_3 + 0,1 M Pb^{2+} + $3,0\times10^{-4}$ M $C_8F_{17}O_3SK$	2,8
0,1 M HNO_3 + 0,1 M Pb^{2+} + $3,0\times10^{-3}$ % Nafion®	33

Основні результати розділу опубліковано в роботах автора [35-39].

ISSN 0321-4095, Voprosy khimii i khimicheskoi tekhnologii, 2019, No. 5, pp. 65-70 65

UDC 544.653.2

T. Luk'yanenko [a], O. Shmychkova [a], L. Dmitrikova [b], L. Borschevich [c], A. Velichenko [a]

THE COMPOSITION AND ELECTROCATALYTIC ACTIVITY OF COMPOSITE PbO_2–SURFACTANT ELECTRODES

[a] Ukrainian State University of Chemical Technology, Dnipro, Ukraine
[b] State Institution «Dnipropetrovsk Medical Academy of the Ministry of Health of Ukraine», Dnipro, Ukraine
[c] Oles Honchar Dnipro National University, Dnipro, Ukraine

It is shown that anionic surfactants, sodium laureth sulphate in particular, are included in electrodeposited lead dioxide. The content of organic substance in the composite coating can vary from 3.4 to 12.5 wt.%. The change in deposition conditions (temperature, pH and anodic current density) allows controlling the content of surfactant in the resulting oxide. The electocatalytic activity of the materials involved was investigated in respect to the oxygen evolution reaction and the electrochemical oxidation of 4-chlorophenol. The calculated value of Tafel slope is 229 mV dec^{-1} for non-modified PbO_2, while it is 178 mV dec^{-1} for composite of PbO_2 with 10.2 wt.% of sodium laureth sulfate. According to absorption spectra, the initial solution of 4-chlorophenol is characterized by two peaks at 220 and 280 nm. At first, the electrolysis leads to a decrease in the peak at 220 nm, a slight increase of the peak at 280 nm and the appearance of the plateau at 240–270 nm. This is caused by a decrease in the concentration of 4-chlorophenol and accumulation of benzoquinone in the solution. A further increase in the electrolysis duration results in the disappearance of the peaks at 220 and 280 nm and the reduction of the plateau at 240–270 nm due to a decrease in the concentrations of both 4-chlorophenol and benzoquinone. Already after 4 hours of electrolysis, the aromatic compounds are completely destroyed with the formation of only aliphatic electrolysis products (mainly maleic acid), that was evidenced by high performance liquid chromatography. The processes of electrooxidation of 4-chlorophenol on lead dioxide and PbO_2-based composite materials proceed qualitatively in the same way and differ only in the rate.

Keywords: nitrate electrolyte, lead dioxide, 4-chlorophenol, sodium laureth sulfate, electrooxidation.

DOI: 10.32434/0321-4095-2019-126-5-65-70

Introduction

The development of methods for directed synthesis of new materials with specified properties is known to be the one of the priorities of modern science [1,2]. At the same time, the great attention is paid to various electrochemical methods in connection with the simplicity of their implementation, low cost equipment and the ability to control the composition and properties of the materials obtained by changing the electrolysis regimes and the composition of electrolytes. Methods for the electrochemical synthesis of oxide composites are of considerable interest among others [3–5].

Lead dioxide is considered to be an exceptionally successful object in this regard because of its following specific features: (i) it is formed at high anodic polarization by the electrodeposition from aqueous Pb(II) solutions; (ii) its physicochemical properties and electrocatalytic activity can be altered by the modification with various additives during the electrodeposition [6,7]; and (iii) PbO_2 has a high electrical conductivity, is chemically stable in both acidic and alkaline media and is characterized by a rather high basic electrocatalytic activity towards most anodic reactions [8,9].

Composite materials based on lead dioxide and containing surfactants are of considerable interest

for research, since while maintaining the basic properties of PbO_2, the composition, physicochemical properties, and electrocatalytic activity of such materials can vary widely [10,11]. At the same time, there is a lack of information regarding the effect of surfactants on the characteristics of electrodeposition of materials based on lead dioxide, especially the physicochemical properties of the oxides obtained and their electrocatalytic activity. In this connection, the effect of sodium laureth sulfate (SLES) on the PbO_2 chemical composition and electrocatalytic activity was investigated in this work.

Material and methods

All chemicals were reagent grade. Lead dioxide was electrodeposited from nitrate electrolytes that contained 0.1 M HNO_3 and 0.1 M $Pb(NO_3)_2$.

Platinized titanium was used as a sheet. It was treated as described in ref. [6] before platinum layer depositing. The content of SLES ($CH_3(CH_2)_{11}(OCH_2CH_2)_nOSO_3Na$), depending on purposes of the experiment, varied within the range of $1\cdot10^{-6}$ to 0.01 M. Electrolyte compositions and conditions of the deposition of composite coatings were selected hereby that in all cases the current efficiency of lead dioxide deposition was about 100%.

Oxygen evolution reaction was investigated by steady-state polarization using computer controlled EG & G Princeton Applied Research potentiostat (model 273A) in 1 M H_2SO_4. All potentials were recorded and reported vs. Ag/AgCl/KCl(sat.) reference electrode.

The electrooxidation of organic compounds was carried out in a divided cell at j_a=50 mA cm^{-2}. The volume of anolyte was 130 cm^3. Solution containing phosphate buffer (0.25 M Na_2HPO_4+0.1 M KH_2PO_4)+10^{-4} M organic compound (pH 6.55) was used as an anolyte; phosphate buffer served as a catholyte. Stainless steel was used as a cathode. Composite PbO_2–SLES electrodes were used as anodes. Electrode surface area was 2.5 cm^2.

The change of the concentration of the organic substance during the electrolysis was measured by sampling (volume of 5 cm^3) at regular intervals and measuring the absorbance of the solution in the ultraviolet and visible region (wavelength range of 200–350 nm) using a Kontron Uvikon 940 spectrometer.

Analyses of the reaction products were conducted by high performance liquid chromatography (HPLC) using a Shimadzu RF-10A xL instrument equipped with a Ultraviolet SPD-20AV detector and a 30 cm Discovery® C18 column.

Results and discussion

In some cases, small amounts of ionic additives are incorporated into the growing oxide, forming micromodified materials based on lead dioxide [5–8,10]. On this basis, it should be assumed that the addition of organic substances would also affect the electrodeposition, composition and properties of oxide materials. It should be noted that at present, the addition of organic substances (most often surfactants and polyelectrolytes) are widely used in electroplating processes for the production of metals and alloys [12,13]. Additives can be used for various purposes, affecting both the technological parameters of the electroplating of metals and the properties of the resulting coatings. An extensive amount of publications is devoted to these investigations, in which various aspects of the use of additives of organic substances in the processes of electrodeposition of metals are considered in detail [12,13].

In contrast to the above processes, there is almost no information in the literature about the effect of polyelectrolytes and surfactants on regularities of the electrodeposition and physicochemical properties of the resulting oxide materials.

It was established that anionic surfactants, SLES in particular, are included in the growing lead dioxide. The content of organic substance in the coating can vary from 3.4 to 12.5 wt.%, a surfactant-oxide composite being formed (Table 1).

Table 1

Dependence of SLES content in PbO_2 on its concentration in the deposition electrolyte 0.1 M HNO_3+0.1 M $Pb(NO_3)_2$+X M $C_{16}H_{29}O_6SNa$*

X, M	Content, wt.%
0.0005	3.4
0.0007	5.9
0.001	7.0
0.005	7.8
0.007	10.2
0.01	12.5

Note: * – coatings are deposited at 4 mA cm^{-2}.

The content of the additive in the composite can be controlled by changing the composition of the solution and electrolysis conditions. Surface effects are caused by the adsorption of additives both on the lead dioxide surface and on the colloidal PbO_2 particles formed in the near-electrode zone [10]. It should be noted that the obtained experimental data on the influence of the deposition conditions and the composition of the solution on the content of the additive in the composite coating are in good qualitative agreement with the influence of these factors on the adsorption of substances on lead

ISSN 0321-4095, Voprosy khimii i khimicheskoi tekhnologii, 2019, No. 5, pp. 65-70 67

Table 2

The influence of pH and the deposition temperature on SLES content in PbO_2 (j_a=4 mA cm^{-2})

Electrolysis conditions	Content, wt.%
0.1 M HNO_3+0.1 M $Pb(NO_3)_2$+0.007 M SLES, T=298 K	10.2
0.3 M HNO_3+0.1 M $Pb(NO_3)_2$+0.007 M SLES, T=298 K	3.2
1 M HNO_3+0.1 M $Pb(NO_3)_2$+0.007 M SLES, T=298 K	3.0
0.1 M HNO_3+0.1 M $Pb(NO_3)_2$+0.007 M SLES, T=323 K	3.0
0.1 M HNO_3+0.1 M $Pb(NO_3)_2$+0.007 M SLES, T=343 K	2.8

dioxide, i.e. an increase in adsorption leads to an increase in the content of surfactants in PbO_2 (an increase in the concentration of the additive or a positive charge of oxide due to a decrease in the pH of the solution or an increase in the anodic current density).

An increase in the deposition temperature and acid concentration in deposition electrolyte also leads to an increase in the content of surfactant in lead dioxide (Table 2).

The electrocatalytic activity of the obtained materials was investigated in respect to the oxygen evolution reaction and the electrooxidation of 4-chlorophenol.

It should also be assumed that oxide-surfactant composite materials will differ significantly in electrocatalytic activity in respect to lead dioxide. Since at high anodic potentials the vast majority of electrochemical processes occur with the participation of oxygen-containing particles adsorbed on the electrode (so-called oxygen transfer reactions), it is convenient to evaluate the nature of the effects by the determination of oxygen evolution overpotential.

The observed change in the electrochemical properties of lead dioxide-based composite materials with respect to the oxygen evolution reaction is mainly because of the change in the chemical properties of the oxide surface, leading to a change in the bond strength of oxygen-containing particles chemisorbed on the electrode [5–8]. As it is seen from the obtained data (Fig. 1), modification of lead dioxide by SLES leads to an increase in oxygen evolution overvoltage.

In this way, the Tafel slope is 229 mV dec^{-1} on non-modified PbO_2, while it is 178 mV dec^{-1} at 10.2 wt.% SLES content (Fig. 2). As one can conclude from the calculated results, the Tafel slope significantly exceeds the theoretical value, which indicates a decrease in the degree of filling of oxygen-containing particles on the surface of the electrode, probably due to blocking by sulfate ions. This effect was described in detail in previous publication [14]. A decrease in the slope in the case of PbO_2–SLES

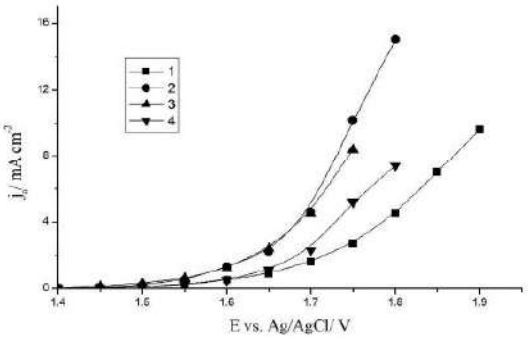

Fig. 1. Steady-state polarization curves of oxygen evolution in 1 M H_2SO_4 on the following electrodes: PbO_2 (1); PbO_2–3.2 wt.% SLES (2); PbO_2–7 wt.% SLES (3); PbO_2–10.2 wt.% SLES (4)

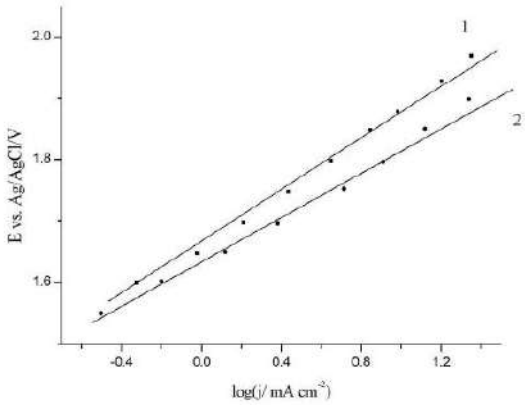

Fig. 2. Tafel plots (1 M H_2SO_4) for lead dioxide anodes electrodeposited from the following solutions: (1) – 0.1 M $Pb(NO_3)_2$+0.1 M HNO_3; (2) – 0.1 M $Pb(NO_3)_2$+0.1 M HNO_3+0.0007 M SLES

denotes an increase in the degree of filling of lead dioxide by oxygen-containing radicals, which are directly involved in the electrochemical stages of oxygen evolution. The most likely, surfactants on the electrode surface are mediators in the process of oxygen evolution and inhibit the surface blocking by sulfate ions on such materials.

Phenolic compounds, 4-chlorophenol in particular, and anode materials, based on lead dioxide, were selected to evaluate the electrocatalytic activity of the materials involved in the oxidation of organic substances. Since processes of electrooxidation of phenolic compounds on various electrodes are rather well studied, the focus can only be aimed on clarifying the role of anode material.

According to the literature [15], a highly large number of intermediate products are formed during the anodic oxidation of 4-chlorophenol. The main intermediate products include benzquinone and maleic acid.

A simple and convenient way to estimate the electrocatalytic activity of an electrode material in the investigation of phenol oxidation is the disappearance time of aromatic intermediates which can be determined from the UV spectra of solutions at different electrolysis time.

The initial solution of 4-chlorophenol is characterized by two peaks at 220 and 280 nm (Fig. 3). At first, the electrolysis shows a decrease in the peak at 220 nm, as well as a slight increase in the peak at 280 nm and the appearance of the plateau at 240–270 nm which is caused by a decrease in the concentration of 4-chlorophenol and accumulation of benzoquinone in the solution. A further increase in the time of electrolysis leads to the disappearance of the peaks at 220 and 280 nm, as well as the reduction of the plateau at 240–270 nm due to a decrease in the concentrations of both 4-chlorophenol and benzoquinone. Already after 4 hours of electrolysis, the aromatic compounds are completely destroyed with the formation of only aliphatic electrolysis products (mainly maleic acid), that was evidenced by HPLC [15].

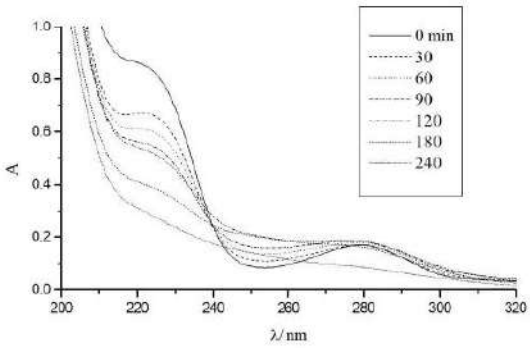

Fig. 3. The electronic absorption spectra of 0.5 M Na_2SO_4+0.1 mM 4-chlorphenol+phosphate buffer solution at different electrolysis duration on the PbO_2–10.2 wt.% SLES anode

As was shown earlier [5–8,15], the modification of the lead dioxide results in a significant increase in its electrocatalytic activity with respect to reactions involving oxygen-adsorbed particles on the electrode. In this regard, we investigated the electrooxidation of 4-chlorophenol on composite anodes based on lead dioxide containing different amount of surfactant (Fig. 4). It should be noted that the processes of electrooxidation of 4-chlorophenol on lead dioxide and PbO_2-based composite materials proceed qualitatively in the same way and differ only in the rate. This suggests the invariance of the mechanism of 4-chlorophenol oxidation on different materials which makes it possible to correctly compare their electrocatalytic activity with respect to the reaction involved.

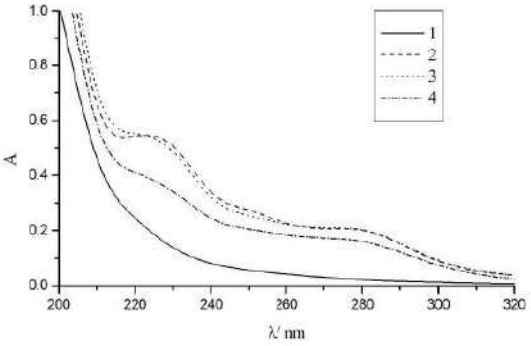

Fig. 4. The electronic absorption spectra of 0.5 M Na_2SO_4+0.1 mM 4-chlorphenol+phosphate buffer solution after 180 min of electrolysis on the PbO_2 (1); PbO_2–3.2 wt.% SLES (2); PbO_2–7 wt.% SLES (3); PbO_2–10.2 wt.% SLES (4) anodes

Conclusions

Anionic surfactants, SLES in particular, are included in the electrodeposited lead dioxide. The content of organic substance in the surfactant-oxide composite can vary from 3.4 to 12.5 wt.%. An increase in the temperature and acid concentration in deposition electrolyte leads to an increase in the content of surfactant in lead dioxide-based composite.

The electocatalytic activity of the materials involved was investigated in respect to oxygen evolution reaction and the oxidation of 4-chlorophenol. The calculated value of Tafel slope is 229 mV dec^{-1} on non-modified PbO_2, while it is 178 mV dec^{-1} on 10.2 wt.% SLES-PbO_2. A decrease of the slope in the case of PbO_2–SLES denotes an increase in the degree of filling of lead dioxide by oxygen-containing radicals, which are directly involved in the electrochemical stages of oxygen

evolution. The most likely, surfactants on the electrode surface play the role of mediators in the process of oxygen evolution and inhibit the surface blocking by sulfate ions on such materials. The processes of electrooxidation of 4-chlorophenol on lead dioxide and PbO_2-based composite materials proceed qualitatively in the same way and differ only in the rate.

Thus, lead dioxide based surfactant-oxide composite coatings are of great interest because of high electrocatalytic activity in respect to oxygen transfer reactions.

Acknowledgements

Authors gratefully acknowledge the financial supports of the Ministry of Education and Science of Ukraine.

REFERENCES

1. *Electrochemical* oxygen transfer reactions: electrode materials, surface processes, kinetic models, linear free energy correlations, and perspectives / Vargas R., Borras C., Mendez D., Mostany J., Scharifker B.R. // J. Solid State Electrochem. – 2016. – Vol.20. – P.875-893.

2. *Developments* in soluble lead flow batteries and remaining challenges: An illustrated review / Krishna M., Fraser E.J., Wills R.G.A., Walsh F.C. // J. Energy Storage. – 2018. – Vol.15. – P.69-90.

3. *Wu W., Huang Z.-H., Lim T.-T.* Recent development of mixed metal oxide anodes for electrochemical oxidation of organic pollutants in water // Appl. Catal. A. – 2014. – Vol.480. – P.58-78.

4. *Application* of TiO_2-nanotubes/PbO_2 as an anode for the electrochemical elimination of Acid Red 1 dye / Santos J.E.L., de Moura D.C., da Silva D.R., Panizza M., Martinez-Huitle C.A. // J. Solid State Electrochem. – 2019. – Vol.23. – P.351-360.

5. *Electrodeposition of* composite PbO_2–TiO_2 materials from colloidal methanesulfonate electrolytes / Knysh V., Luk'yanenko T., Shmychkova O., Amadelli R., Velichenko A. // J. Solid State Electrochem. – 2017. – Vol.21. – P.537-544.

6. *Electrodeposition of* Ni^{2+}-doped PbO_2 and physicochemical properties of the coating / Shmychkova O., Luk'yanenko T., Amadelli R., Velichenko A. // J. Electroanal. Chem. – 2016. – Vol.774. – P.88-94.

7. *Physico-chemical* properties of PbO_2-anodes doped with $Sn^{4+}$and complex ions / Shmychkova O., Luk'yanenko T., Amadelli R., Velichenko A. // J. Electroanal. Chem. – 2014. – Vol.717-718. – P.196-201.

8. *Electrooxidation of* some phenolic compounds at Bi-doped PbO_2 / Shmychkova O., Luk'yanenko T., Yakubenko A., Amadelli R. Velichenko A. // Appl. Catal. B. – 2015. – Vol.162. – P.346-351.

9. *Single* and coupled electrochemical processes and reactors for the abatement of organic water pollutants: a critical review / Martinez-Huitle C.A., Rodrigo M.A, Sires I., Scialdone O. // Chem. Rev. – 2015. – Vol.115. – P.13362-13407.

10. *Nafion* effect on the lead dioxide electrodeposition kinetics / Velichenko A.B., Luk'yanenko T.V., Nikolenko N.V., Amadelli R., Danilov F.I. // Russ. J. Electrochem. – 2007. – Vol.43. – P.118-120.

11. *Li X., Xu H., Yan W.* Effects of twelve sodium dodecyl sulfate (SDS) on electro-catalytic performance and stability of PbO_2 electrode // J. Alloy Compd. – 2017. – Vol.718. – P.386-395.

12. *Hollow* functional materials derived from metal–organic frameworks: synthetic strategies, conversion mechanisms, and electrochemical applications / Cai Z.-X., Wang Z.-L., Kim J., Yamauchi Y. // Adv. Mater. – 2019. – Vol.31. – Article No. 1804903.

13. *A review* of the synthesis and applications of polymer-nanoclay composites / Guo F., Aryana S., Han Y., Jiao Y. // Appl. Sci. (Switzerland). – 2018. – Vol. 8. – Article No. 1696.

14. *Influence* of the electrode history and effects of the electrolyte composition and temperature on O_2 evolution at β-PbO_2-anodes in acid media / Amadelli R., Maldotti A., Molinari A., Danilov F.I., Velichenko A.B. // J. Electroanal. Chem. – 2002. – Vol.534. – P.1-12.

15. *Electrooxidation* of 4-clorphenol on modified lead dioxide anodes / Shmychkova O., Luk'yanenko T., Dmitrikova L., Velichenko A. // Voprosy Khimii i Khimicheskoi Tekhnologii. – 2018. – No. 3. – P.50-57.

Received 15.04.2019

СКЛАД ТА ЕЛЕКТРОКАТАЛІТИЧНА АКТИВНІСТЬ КОМПОЗИЦІЙНИХ ЕЛЕКТРОДІВ PbO_2–ПОВЕРХНЕВО-АКТИВНА РЕЧОВИНА

Т. Лук'яненко, О. Шмичкова, Л. Дмітрікова, Л. Борщевич, О. Величенко

Показано, що аніонні поверхнево-активні речовини, зокрема натрію лауретсульфат, включаються до електроосадженого плюмбум(IV) оксиду. Вміст органічної речовини в композиційному покритті «поверхнево-активна речовина-оксид» може варіюватися від 3,4 до 12,5 мас.%. Зміна умов осадження (температура, pH і анодна густина струму) дозволяє контролювати вміст поверхнево-активної речовини в одержуваному композиті. Встановлено електрокаталітичну активність досліджених матеріалів у реакції виділення кисню та окиснення 4-хлорфенолу. Розраховане значення тафелівського нахилу становить 229 мВ/дек для немодифікованого PbO_2 та 178 мВ/дек для PbO_2, що містить 10,2 мас.% натрію лауретсульфату. Як випливає зі спектрів поглинання, вихідний розчин хлорфенолу характеризується двома піками при 220 і 280 нм. Протягом електролізу спостерігається зменшення піка при 220 нм, а також невелике збільшення піка при 280 нм і поява плато при 240–270 нм, що викликано зменшенням концентрації 4-хлорфенолу і накопиченням бензохінону в розчині. Подальше збільшення тривалості електролізу приводить до зникнення піків при 220 і 280 нм, а також до зменшення плато при 240–270 нм в результаті зниження концентрацій як 4-хлорфенолу, так і

бензохінону. Вже після 4 годин електролізу ароматичні сполуки повністю руйнуються з утворенням виключно аліфатичних продуктів (в основному, малеїнової кислоти), про що свідчать дані високоефективної рідинної хроматографії. Процеси електроокиснення 4-хлорфенолу на плюмбум(IV) оксиді та композиційних матеріалах на основі PbO_2 відбуваються якісно однаково та відрізняються лише швидкістю.

Ключові слова: нітратний електроліт, плюмбум(IV) оксид, 4-хлорфенол, натрію лауретсульфат.

THE COMPOSITION AND ELECTROCATALYTIC ACTIVITY OF COMPOSITE PbO_2–SURFACTANT ELECTRODES

T. Luk'yanenko [a,], O. Shmychkova [a], L. Dmitrikova [b], L. Borschevich [c], A. Velichenko [a]*

[a] **Ukrainian State University of Chemical Technology, Dnipro, Ukraine**

[b] **State Institution «Dnipropetrovsk Medical Academy of the Ministry of Health of Ukraine», Dnipro, Ukraine**

[c] **Oles Honchar Dnipro National University, Dnipro, Ukraine**

[*] **e-mail: tluk@ukr.net**

It is shown that anionic surfactants, sodium laureth sulphate in particular, are included in electrodeposited lead dioxide. The content of organic substance in the composite coating can vary from 3.4 to 12.5 wt.%. The change in deposition conditions (temperature, pH and anodic current density) allows controlling the content of surfactant in the resulting oxide. The electocatalytic activity of the materials involved was investigated in respect to the oxygen evolution reaction and the electrochemical oxidation of 4-chlorophenol. The calculated value of Tafel slope is 229 mV dec^{-1} for non-modified PbO_2, while it is 178 mV dec^{-1} for composite of PbO_2 with 10.2 wt.% of sodium laureth sulfate. According to absorption spectra, the initial solution of 4-chlorophenol is characterized by two peaks at 220 and 280 nm. At first, the electrolysis leads to a decrease in the peak at 220 nm, a slight increase of the peak at 280 nm and the appearance of the plateau at 240–270 nm. This is caused by a decrease in the concentration of 4-chlorophenol and accumulation of benzoquinone in the solution. A further increase in the electrolysis duration results in the disappearance of the peaks at 220 and 280 nm and the reduction of the plateau at 240–270 nm due to a decrease in the concentrations of both 4-chlorophenol and benzoquinone. Already after 4 hours of electrolysis, the aromatic compounds are completely destroyed with the formation of only aliphatic electrolysis products (mainly maleic acid), that was evidenced by high performance liquid chromatography. The processes of electrooxidation of 4-chlorophenol on lead dioxide and PbO_2-based composite materials proceed qualitatively in the same way and differ only in the rate.

Keywords: nitrate electrolyte; lead dioxide; 4-chlorophenol; sodium laureth sulfate; electrooxidation.

REFERENCES

1. Vargas R., Borras C., Mendez D., Mostany J., Scharifker B.R. Electrochemical oxygen transfer reactions: electrode materials, surface processes, kinetic models, linear free energy correlations, and perspectives. *Journal of Solid State Electrochemistry*, 2016, vol. 20, pp. 875-893.

2. Krishna M., Fraser E.J., Wills R.G.A., Walsh F.C. Developments in soluble lead flow batteries and remaining challenges: an illustrated review. *Journal of Energy Storage*, 2018, vol. 15, pp. 69-90.

3. Wu W., Huang Z.-H., Lim T.-T. Recent development of mixed metal oxide anodes for electrochemical oxidation of organic pollutants in water. *Applied Catalysis A: General*, 2014, vol. 480, pp. 58-78.

4. Santos J.E.L., de Moura D.C., da Silva D.R., Panizza M., Martinez-Huitle C.A. Application of TiO_2-nanotubes/PbO_2 as an anode for the electrochemical elimination of Acid Red 1 dye. *Journal of Solid State Electrochemistry*, 2019, vol. 23, pp. 351-360.

5. Knysh V., Luk'yanenko T., Shmychkova O., Amadelli R., Velichenko A. Electrodeposition of composite PbO_2–TiO_2 materials from colloidal methanesulfonate electrolytes. *Journal of Solid State Electrochemistry*, 2017, vol. 21, pp. 537-544.

6. Shmychkova O., Luk'yanenko T., Amadelli R., Velichenko A. Electrodeposition of Ni^{2+}-doped PbO_2 and physicochemical properties of the coating. *Journal of Electroanalytical Chemistry*, 2016, vol. 774, pp. 88-94.

7. Shmychkova O., Luk'yanenko T., Amadelli R., Velichenko A. Physico-chemical properties of PbO_2-anodes doped with Sn^{4+} and complex ions. *Journal of Electroanalytical Chemistry*, 2014, vol. 717-718, pp. 196-201.

8. Shmychkova O., Luk'yanenko T., Yakubenko A., Amadelli R. Velichenko A. Electrooxidation of some phenolic compounds at Bi-doped PbO_2. *Applied Catalysis B: Environmental*, 2015, vol. 162, pp. 346-351.

9. Martinez-Huitle C.A., Rodrigo M.A, Sires I., Scialdone O. Single and coupled electrochemical processes and reactors for the abatement of organic water pollutants: a critical review. *Chemical Reviews*, 2015, vol. 115, pp. 13362-13407.

10. Velichenko A.B., Luk'yanenko T.V., Nikolenko N.V., Amadelli R., Danilov F.I. Nafion effect on the lead dioxide electrodeposition kinetics. *Russian Journal of Electrochemistry*, 2007, vol. 43, pp. 118-120.

11. Li X., Xu H., Yan W. Effects of twelve sodium dodecyl sulfate (SDS) on electro-catalytic performance and stability of PbO_2 electrode. *Journal of Alloys and Compounds*, 2017, vol. 718, pp. 386-395.

12. Cai Z.-X., Wang Z.-L., Kim J., Yamauchi Y. Hollow functional materials derived from metal–organic frameworks: synthetic strategies, conversion mechanisms, and electrochemical applications. *Advanced Materials*, 2019, vol. 31, article no. 1804903.

13. Guo F., Aryana S., Han Y., Jiao Y. A review of the synthesis and applications of polymer–nanoclay composites. *Applied Sciences*, 2018, vol. 8, article no. 1696.

14. Amadelli R., Maldotti A., Molinari A., Danilov F.I., Velichenko A.B. Influence of the electrode history and effects of the electrolyte composition and temperature on O_2 evolution at β-PbO_2 anodes in acid media. *Journal of Electroanalytical Chemistry*, 2002, vol. 534, pp. 1-12.

15. Shmychkova O., Luk'yanenko T., Dmitrikova L., Velichenko A. Electrooxidation of 4-clorphenol on modified lead dioxide anodes. *Voprosy Kimii i Kimicheskoi Tekhnologii*, 2018, no. 3, pp. 50-57.

Journal of Solid State Electrochemistry
https://doi.org/10.1007/s10008-020-04572-8

ORIGINAL PAPER

PbO_2-surfactant composites: electrosynthesis and catalytic activity

T. Luk'yanenko[1] · O. Shmychkova[1] · A. Velichenko[1]

Received: 16 September 2019 / Revised: 19 March 2020 / Accepted: 20 March 2020

Abstract
The electrodeposition of PbO_2 from sodium laureth sulfate-containing medium has been investigated. It has been established that at low anodic polarizations, second electron transfer step is rate determining, whereas at high anodic polarizations, such step is diffusion transport of lead ions to the electrode surface. The presence of sodium laureth sulfate in the deposition electrolyte leads to a slight inhibition of the deposition of lead dioxide. It has been found that the morphology and structure of composite materials differs significantly from lead dioxide. With an increase in the additive content in the composite, there is a transition from large-grained deposits to materials with submicron and nano-sized crystals. It is shown that anionic surfactants, sodium laureth sulfate in particular, are included in the growing lead dioxide. The content of organic substance in the oxide can vary from 3.2 to 12.5 wt.%, forming a surfactant-oxide composite coating. The electrocatalytic activity of the materials involved was investigated with respect to oxygen evolution reaction and the oxidation of 4-chlorophenol. The calculated value of Tafel slope is 229 on non-modified PbO_2, while on 10.2 wt.% sodium laureth sulfate-PbO_2, it is 178 mV/dec. According to absorption spectra, the initial solution of chlorophenol is characterized by two peaks at 220 and 280 nm. At first, the electrolysis shows a decrease in the peak at 220 nm, as well as a slight increase in the peak at 280 nm and the appearance of the plateau at 240–270 nm, which is caused by a decrease in the concentration of 4-chlorophenol and accumulation of benzoquinone in the solution. A further increase in the time of electrolysis leads to the disappearance of the peaks at 220 and 280 nm, as well as the reduction of the plateau at 240–270 nm due to a decrease in the concentrations of both 4-chlorophenol and benzoquinone. Already after 4 h of electrolysis, the aromatic compounds are completely destroyed with the formation of only aliphatic electrolysis products (mainly maleic acid), which was evidenced by high performance liquid chromatography. The processes of electrooxidation of 4-chlorophenol on lead dioxide and PbO_2-based composite materials proceed qualitatively in the same way and differ only in the rate.

Keywords Lead dioxide · Nitrate electrolyte · Surfactant · Electrodeposition · Adsorption

Introduction

Composite electrochemical coatings play a special role in solving problems of improving the surface of metals and oxide coatings, giving it special, in particular adsorption, catalytic and anticorrosion properties. Composites are heterophasic systems obtained by an electrochemical process and consisting of a metal/oxide matrix and a relatively uniformly distributed dispersed phase from particles of any nature, ranging in size from nanoscale to micrometer order [1–3]. Using additives of different nature in the synthesis of composite coatings allows one to modified metal matrix for a variety of purposes. In addition to improving the strength characteristics, a significant increase in the corrosion resistance of coatings, an improvement in their electrocatalytic activity, and a change in conductivity can be achieved [4, 5]. The noted features of the materials open up to researchers the prospects for creating composite layers of a special purpose: in machine building and instrument making, radio electronics, electrical engineering, and other branches of science and technology.

However, most composites have been developed on a metal base with inert oxide included to improve mechanical properties. Materials of this type do not have a prospect for their use as catalysts. At the same time, oxide electrocatalysts (based on PbO_2, SnO_2, Co_3O_4, and RuO_2) [6–8] and photocatalysts (based on TiO_2) [9, 10] have been proposed, but their use is possible only for a few processes for the

✉ A. Velichenko
velichenko@ukr.net

[1] Physical Chemistry Department, Ukrainian State University of Chemical Technology, Dnipro, Ukraine

Published online: 13 April 2020

destruction of toxicants in the wastewater, mainly due to the secondary chemical oxidation by oxidants formed at the anode.

Composite materials based on lead dioxide, containing surfactants, are of considerable interest for research, since while maintaining the basic properties of PbO_2, the composition, physicochemical properties, and electrocatalytic activity of such materials can vary widely. A noticeable effect on the morphology and physicochemical properties is observed with the addition of some surfactants into the electrolyte [11]. The addition of surfactants such as Tween 80, Triton X-100, and sodium dodecyl sulfate (SDS) increases the content of α-PbO_2. It should be noted that if the deposition is carried out with stirring of the electrolyte, the effect of SDS is counteracted.

Despite significant research efforts in this area, there are still presently a number of technical and theoretical issues that require development and explanation. The synthesis of some types of composite coatings with given properties is to a certain extent hampered by the insufficient study of complex microprocesses proceeding during the formation of coatings. There is no unambiguous connection, for example, between the electrokinetic properties of particles of the dispersed phase and their co-sedimentation with oxides. The behavior of additives largely depends on the composition of the electrolyte, i.e., on the nature and structure of the molecules and ions adsorbed on the surface of the particles. Therefore, a change in the surface properties of particles is considered an important factor in the regulation of the process of formation of composite materials. The chemical behavior in deposition solutions of polyelectrolytes and surfactants that are promising for codeposition with metal oxide coatings is not studied.

By analogy with the processes of metal electrodeposition, the additives of organic substances to the deposition electrolyte of oxides must meet several basic requirements:

- Adsorb to the surface of the oxide
- Have electrochemical stability at the deposition potentials of the oxide coating
- Influence the electrodeposition and the properties of the materials obtained

Since electrodeposition of lead dioxide takes place at high anodic potentials, at which most organic compounds oxidize at a sufficiently high rate, the choice of additives is a significant problem. We chose sodium laureth sulfate (SLES, formula $CH_3(CH_2)_{11}(OCH_2CH_2)_nOSO_3Na$) that is known as anionic detergent and surfactant found in many personal care products. Chemical formula is $C_{16}H_{29}SO_6Na$. In this work, we report and discuss the electrodeposition of PbO_2 from a SLES-containing medium, physicochemical properties, and electrocatalytic activity of obtained materials.

Materials and methods

All chemicals were reagent grade. Electrodeposition kinetics of doped lead dioxide was studied on a Pt rotating disk electrode (Pt-RDE, 0.19 cm^2) by steady-state voltammetry and chronoamperometry. For the RDE experiments, the voltammetry system SVA-1BM was used. The potential scan rate was varied within 1 ÷ 100 mV/s depending on purposes of the experiments. Before each experiment, the electrode surface was treated with a freshly prepared mixture (1:1) of concentrated H_2SO_4 and H_2O_2 [12]. This preliminary treatment technique permits to stabilize the electrode surface, which under the action of strong oxidizing medium is oxidized to a certain state (defined phase and chemical composition of the surface oxides), which determines the satisfactory reproducibility in taking of cyclic voltammograms in the background electrolyte (0.1 M HNO_3). Voltammetry measurements were carried out in a standard temperature-controlled three-electrode cell. Temperature was maintained 298 ± 1 K. All potentials were recorded and reported vs. Ag/AgCl/KCl $_{(sat.)}$.

Electrodeposition was studied in 0.1 M HNO_3 + 0.01 M $Pb(NO_3)_2$. Surfactant was added into the deposition electrolyte as aqueous solutions with 0.0003 M concentration.

Lead dioxide anodes surface morphology was studied by scanning electron microscopy (SEM) with Stereoscan 440 LEO microscope. X-ray powder diffraction data were collected on a STOE STADI P automatic diffractometer equipped with linear PSD detector (transmission mode, $2\theta/\omega$-scan; Cu $K\alpha_1$ radiation, curved germanium (1 1 1) monochromator; 2θ-range $6.000 \leq 2\theta \leq 102.945$ °2θ with step 0.015 °2θ; PSD step 0.480 °2θ, scan time 50 s/step).

Qualitative and quantitative phase analysis was performed using the PowderCell program. For selected samples with relatively high degree of crystallinity, the Rietveld refinement was carried out using FullProf.2k (version 5.40) program.

The electrical conductivity of the coatings was investigated by the strip method. It is a variation of the contact method for measuring electrical conductivity, which consists in measuring the resistance of a coating that is in direct contact with measuring electrodes [13]. The electrode strip is equilibrated with the appropriate medium and placed on a flat or cylindrical non-conducting surface. Measuring electrodes are brought either to the edges of the strip, or one is fixed, and the other moves along the strip.

The sign of the electrokinetic potential was determined by an electrophoretic method [14]. Electrophoresis was performed in a U-shaped tube. External potential difference was applied to titanium electrodes. Colloid system consisted of finely dispersed PbO_2 particles and the surfactant.

Experimental

The method for the determination of high molecular weight aliphatic acids [15] was adapted for the determination of the concentration of surfactants in aqueous solutions. Such method consists in the formation of an associate of a high-molecular anion and a dye, followed by extraction into a non-aqueous medium. The content of organic substance was determined photocolorimetrically after extraction of the ionic associate with chloroform. Ten milliliters of distilled water was placed in a separatory funnel, and 2 ml of a 0.1% aqueous solution of methylene blue was injected. Then, 1 ml of the test solution was injected and shaken for 2 min with 15 ml of chloroform. The organic phase was filtered through cotton wool, and the optical density was measured at 650 nm using a photoelectric colorimeter. To determine surfactants in composite coatings of known mass, the latter were anodically dissolved at a current density of 2 mA cm^{-2} in 30 ml of 0.1 M HCl. Then, the concentration of additives was determined in solution by the above method.

Adsorption measurements were carried out on 0.5 g of PbO_2 powder (Merck) in 0.1 M HCl solutions containing various amounts of additive. It should be noted that the measurements were carried out in the presence of an indifferent electrolyte (0.1 M KCl), which screened the electrostatic field of the oxide surface. The time to establish the adsorption equilibrium was 24 h. Concentration of organic substances during the adsorption measurements was determined by the method described above. Surface tension of surfactant solutions was measured by the method of maximum pressure in a gas bubble [16].

Platinized titanium was used as a sheet during investigation of electrocatalytic activity of materials. It was treated as described in [12] before platinum layer depositing. The content of SLES depending on purposes of the experiment varied within 5×10^{-5} to 5×10^{-4} M. Electrolyte compositions and conditions of the deposition of composite coatings were selected hereby that in all cases, the current efficiency of lead dioxide deposition was about 100%.

Oxygen evolution reaction was investigated by steady-state polarization on computer-controlled EG&G Princeton Applied Research potentiostat model 273A in 1 M H_2SO_4.

The electrooxidation of organic compounds was carried out in divided cell at $j_a = 50$ mA cm^{-2}. The volume of anolyte was 130 cm^3. Solution, containing phosphate buffer (0.25 M $Na_2HPO_4 + 0.1$ M KH_2PO_4) + 10^{-4} M organic compound (pH = 6.55), was used as anolyte and phosphate buffer as catholyte. Stainless steel was used as cathode. Composite PbO_2-SLES electrodes were used as anodes. Electrode surface area was 2.5 cm^2.

The changing of the concentration of the organic substance during the electrolysis was measured by sampling (volume of 5 cm^3) at regular intervals and measuring the optical density of the solution in the ultraviolet and visible region (wavelength range 200–350 nm) using a Kontron Uvikon 940 spectrometer.

Analyses of the reaction products were conducted by high-performance liquid chromatography (HPLC) using a Shimadzu RF-10A xL instrument equipped with an Ultraviolet SPD-20AV detector and a 30-cm Discovery® C18 column.

Results and discussion

The regularities of electrodeposition of PbO_2-SLES composites

We carried out adsorption measurements on PbO_2 powder in the absence of polarization. The pH of zero charge in nitric acid is 7.2. The value is quite large; in the studied electrolytes, the pH of the solution is approximately 1; surfactant concentration (0.0003 M) is much lower than acid concentration (0.1 M), and there is an excess of a positive charge on the surface, imposed by a large acid concentration. In fact, the adsorption of surfactant does not significantly affect the surface charge; there is no recharging of the surface and a cardinal change in charge. We studied the adsorption process at such surfactant concentrations that were used in deposition electrolytes. As one can see from the experimental data (Table 1), with increasing concentration from 5×10^{-5} to 5×10^{-4} M, the adsorption value increases from 2.3×10^{-7} to 8.0×10^{-7} mol g^{-1}. As a result of potentiometric measurements (not shown), it was established that the adsorption of SLES on PbO_2 is accompanied by a shift of the zero charge point of the oxide to a region of higher pH. This suggests that the adsorption of surfactant at $pH < pH_0$ is not only due to the electrostatic attraction of the surfactant to the positively charged surface of lead dioxide, but also, apparently, as a result of some specific interaction. This hypothesis is well-supported by the data on the adsorption material balance [17]. The obtained data indicate the weak chemical adsorption of surfactant on lead dioxide [18], which is confirmed by a slight displacement of the pH_0 of the oxide, which is 0.71 ± 0.1 V in 0.1 M HNO_3 [19].

To understand the processes occurring during the formation of coatings, it is first necessary to assess the state of the

Table 1 Parameters of SLES adsorption on lead dioxide

Concentration of surfactant 10^4/M	A 10^7/ mole g^{-1}
0.5	2.3
1.0	4.5
3.0	6.3
5.0	8.0

surfactant in the deposition electrolyte. For this purpose, the dependences of the surface tension of the solution on the concentration of additive in the electrolyte were studied. The high surface activity was observed for sodium laureth sulfate (Fig. 1a). The value of the critical micelle concentration (CMC) in 0.1 M $Pb(NO_3)_2 + 0.1$ M HNO_3 solution is rather large and amounts to 0.00562 M. In this work, we used such surfactant concentrations at which the deposition electrolytes remained true solutions.

Since oxygen evolution proceeds simultaneously with the formation of lead dioxide, a decrease in the equilibrium concentration of the surfactant in the solution due to its adsorption at the liquid-gas interface can be observed. To estimate this decrease, the surface excess of the surfactant was calculated from the curves $\sigma = f(c)$ (see Fig. 1a), using the Gibbs equation [18]. The isotherm of adsorption of SLES on the liquid-gas interface is shown in Fig. 1b. As one can conclude from the above curves, sodium laureth sulfate exhibits high surface activity.

In order to ascertain whether the selected substance has electrochemical stability at the deposition potentials of PbO_2 coating, cyclic voltammograms were obtained on a Pt-electrode in a 0.1 M HNO_3 background electrolyte that additionally contained SLES (potential scan area 0–1.6 V). It was found that anionic surfactant SLES does not exhibit electrochemical activity in the investigated potential range.

In typical cyclic voltammograms, the anodic branch of the curve (Fig. 2), at potentials higher than 1.4 V, features an exponential current growth corresponding to the simultaneous reactions of lead(II) oxidation and oxygen evolution. In the cathodic branch of the curve, a current peak due to lead dioxide reduction can be observed at potentials between 1.0 and 1.2 V [20]. The addition to the deposition electrolyte of anionic surfactants results in a slight inhibition of PbO_2 deposition.

The synthesis of PbO_2 from various electrolytes has been the subject of a rather large number of publications [21]. Fleischmann et al. were the first who propose the theory of nucleation and early growth of lead dioxide [22]. The mechanism of deposition of lead dioxide proposed as a result of these studies [23, 24] described the nucleation of new-phase nanocenters as an initial stage, then instantaneous and progressive nucleation, two- and three-dimensional growth, and overlapping growing centers, thickening during delayed stages of charge transfer or mass transfer [21]. These suggestions were developed by researchers from several groups [25–27]. In particular, Johnson et al. [28] by investigations on RRDE proved the formation of a hydrated form of Pb(IV), and later, the formation of soluble intermediate oxygen-containing products of Pb(III), capable of further electrochemical transformations, was shown in the works of Velichenko et al. [29, 30].

We carried out an analysis of mechanism of lead dioxide electrodeposition according to the following reaction scheme described in our earlier publications [31]:

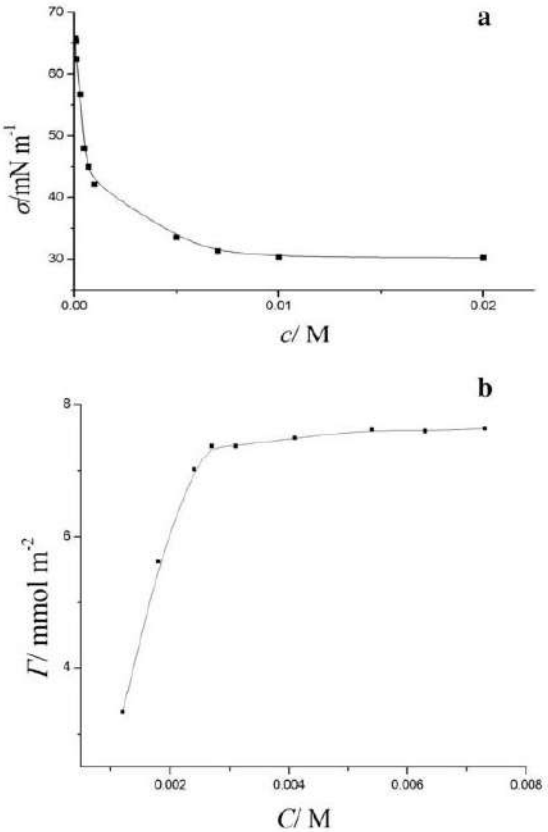

Fig. 1 The isotherm of surface tension (**a**) and the surface surplus at the liquid-gas interface (**b**) of SLES solutions

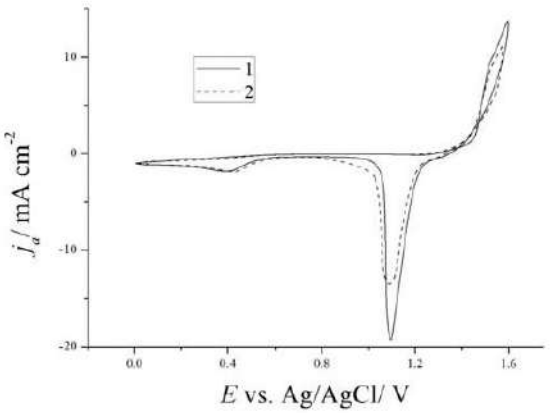

Fig. 2 Cyclic voltammograms (scan range 0.0 to 1.6 V) on Pt in solutions containing 0.01 M $Pb(NO_3)_2 + 0.1$ M HNO_3 (1) + 0.0003 M SLES (2). $\nu = 20$ mV/s

$$H_20 \rightarrow OH_{ads}^{\cdot} + H^+ + e^- \quad (1)$$

$$Pb^2 + OH_{ads} \rightarrow Pb(OH)^{2+} \quad (2)$$

$$Pb(OH)^2 + H_2O \rightarrow Pb(OH)_2^{2+} + H^+ + e^- \quad (3)$$

$$Pb(OH)_2^{2+} \rightarrow PbO_2 + 2H^+ \quad (4)$$

Since we synthesize composites from nitrate electrolytes, we establish the regularities of deposition in order to identify differences (if any) during deposition from nitrate electrolytes that additionally contain surfactants. We did not see significant differences in the electrodeposition regularities. In addition, the phase composition (see in the next paragraph) of the coatings obtained by deposition from electrolytes containing surfactant and not containing it does not differ radically; therefore, we considered it possible to use the mechanism involved.

In our later works, it was shown that such a mechanism is applicable to a wide range of electrolytes (both nitrate and methanesulfonate), including those containing ionic dopants [12, 20, 32], colloidal TiO_2 [10, 33], and polyelectrolytes [17].

The electrode surface state, deposition potential, lead ion concentration, and hydrodynamic conditions are known to significantly determine the nature of limiting stage of the lead dioxide electrodeposition. As a rule, at the low anodic polarizations ($E < 1.6$ V), reactions will be under the kinetic control, whereas at the high polarizations, a Pb^{2+} ion transport to the electrode surface will be the rate-determining stage.

If step (2) is slow and steps (3) and (4) are fast, an increase in the electrode rotation rate does not result in changes in either the anodic or cathodic current of the CV curves. Such an effect is realized with very low polarizations in the range of cycling potentials of 1–1.45 V.

If step (3) is slow and steps (2) and (4) are fast, one should expect a drop in both the current of the cathodic peak and the anode current in the exponential segment with an increase in the electrode rotation rate. These effects are due to the fact that $Pb(OH)^{2+}$ particles formed by reaction (2), which are not able to be oxidized electrochemically, are partially released into the electrolyte bulk (near-electrode zone). The fall of the cathode and anode currents with an increase in the electrode rotation rate was observed on "short cycles," and also noted earlier in Johnson's works [28].

If step (4) is slow and step (3) is fast, oxygen-containing Pb(IV) species formed in step (3), under the convective diffusion, can be partially removed from the electrode surface and decay with the formation of PbO_2 outside its surface [28]. The height of the cathode peak decreases with increasing rotation rate of the electrode.

If step (4) is slow and step (2) is fast, with an increase in the electrode rotation rate, a sharp decrease in the peak current of the cathode reduction of PbO_2 (the amount of formed lead dioxide) will be observed with a slight decrease in the anode current. The latter is due to the additional removal from the electrode surface of the reaction product (3) $Pb(OH)_2^{2+}$ because of the slow step (4) and/or the slow crystallization process that follows, which in turn will lead to a significant decrease in the amount of deposited PbO_2. In this case, lead dioxide can be deposited on Teflon holder around the disk, which was observed in this work, and was also described earlier by Johnson [28] during the deposition of PbO_2 from perchlorate electrolytes.

Chronoamperograms were obtained on a Pt disk electrode to investigate the initial stages of deposition of lead dioxide in the presence of surfactant in solution. A typical j-t curve of PbO_2 deposition (Fig. 3) can be characterized by several features and fully consistent with the chronoamperograms obtained and described in detail by Saez et al. [34] during the deposition of lead dioxide on glassy carbon from nitrate bath under the kinetic control of process. During electrodeposition, both kinetic regularities of the crystallization process and the nature of the crystal structure of formed oxide depend on the nucleation rate, i.e., the rate of formation of crystal nuclei, linear crystallization rate, and their ratio. These parameters can be determined from current transients of the process of lead dioxide electrodeposition [27, 35–37].

The electrocrystallization model, proposed by Abyaneh [30], was selected as appropriate for investigation of initial stages of the formation of a new phase of lead dioxide, since it gives a more complete description and understanding of the growth mechanism of a new phase of lead dioxide and allows one to determine the kinetic parameters of nucleation for both α- and β-phases by analysis of current-time transients. According to model suggestions of authors [35], one can establish the nature of the nucleation (instantaneous or progressive) by comparing the ratio I_{max} and I_{plato}. Also, the ratio of the maximum current to the deposition current shows a preferred geometric shape of formed nuclei.

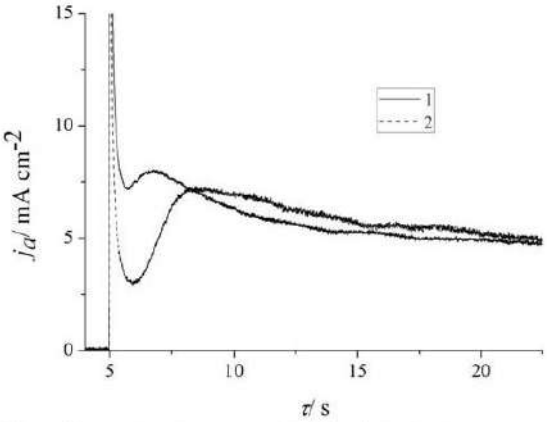

Fig. 3 Chronoamperogramms on Pt disk electrode at E = 1.45 V, obtained during PbO_2 deposition from solutions containing 0.01 M $Pb(NO_3)_2$ + 0.1 M HNO_3 (1) + 0.0003 M SLES (2)

It should be noted that rising portion of the current transient is insensitive to the geometry of the crystal growth, and it allows one to determine the kinetic parameters of 2D nucleation. Further formation of a crystalline deposit, when 3D nucleation is considered, at the determination of the kinetic parameters of the formation of a new phase, the geometry of the nuclei should be taken into account.

After investigation of initial stages of PbO_2 electrodeposition from nitrate electrolyte, it was established that process proceeds by progressive mechanism of nucleation. The preferred form of crystals at 2D nucleation from methanesulfonate electrolytes is a cone [38]. The main parameters of PbO_2 crystallization from nitrate solutions that additionally contain surfactant are presented in Table 2.

As one can conclude from the obtained results, there are no significant changes in nucleation in the presence of surfactant. One expected effect, which we have observed, is a slight inhibition due to surface inhibition by adsorbed surfactant molecules, which has been also observed in cyclic voltammograms. We do not observe qualitative differences in transients during prolonged deposition. A similar effect is known to be observed in the presence of polyelectrolytes and during the deposition of metals in the presence of surfactants [17].

The data obtained are in satisfactory agreement with the data obtained by the groups of Abyaneh et al. and Gonzalez-Garsia et al. during the deposition of lead dioxide on glassy carbon [27, 35–37].

The electrocrystallization of PbO_2 begins with the formation of a monolayer over the entire surface of the electrode, and only then is there a formation and growth of 3D nuclei. The growth of lead dioxide occurs through crystallization layer by the next layer, so each consequent layer is formed on the renewed surface, as has been shown in our previous work on nucleation of lead dioxide from methanesulfonate electrolytes [39].

A slight inhibition of Pb^{2+} electrooxidation process is observed on steady-state j-E curves obtained for both the total process (oxygen evolution and PbO_2 deposition) and the partial Pb(II) electrooxidation process in the presence of surfactant in the deposition electrolyte (Fig. 4), which is in satisfactory agreement with chronoamperometric data. In the low polarization region (area I, see Fig. 4), the dependences of the potential E on the logarithm of the current density log j

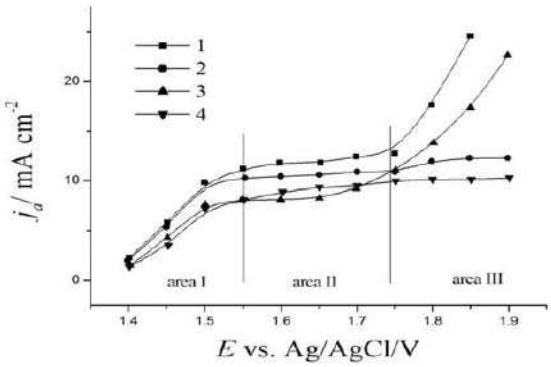

Fig. 4 Steady-state polarization curves for total (1,2) and partial (3,4) PbO_2 electrodeposition current on Pt in solutions 0.01 M $Pb(NO_3)_2$ + 0.1 M HNO_3 (1,3) and 0.01 M $Pb(NO_3)_2$ + 0.1 M HNO_3 + 0.0003 M SLES (2,4)

constructed from j-E curves are linear (r = 0.99) and indicate a kinetic control of the electrodeposition process, as in the case of ion additives [12, 20, 21]. Deposition of lead dioxide is observed on the Teflon holder, at some distance from the platinum disk, also in the presence of surfactant in the electrolyte.

The number of electrons that take part in the kinetic stage was determined from linear potential sweep voltammetry measurements according to Delahay equation [12], as described in the literature for analogous conditions [38]. The characteristic value in this method is the peak of the anode current on the j-E curve, the value of which depends on the potential sweep rate (Fig. 5), both for reversible and irreversible processes. With increasing potential sweep rate, the anode peak shifts in the direction of increasing E, which indicates irreversible electron transfer. The transfer coefficient remains almost unchanged ($\alpha = 0.4$) when the surfactant is present in the deposition electrolyte. The calculated number of electrons in the elementary stage was one, confirming that PbO_2 formation is a multistep charge transfer which involves consecutive two one-electron steps, as outlined in [12], both in the absence and in the presence of added SLES.

With an increase in the anodic polarization (area III, see Fig. 4), the limiting current of deposition of lead dioxide is observed on the stationary polarization curve. In the investigated range of potentials, the values of the measured partial currents of electrodeposition of lead dioxide depend on the rotation rate of the

Table 2 Parameters of initial stages of lead dioxide electrocrystallization

Deposition electrolyte	t_α	K_α	t_β	K_β
0.01 M $Pb(NO_3)_2$ + 0.1 M HNO_3	5.71	2.44×10^{-6}	6.43	3.95×10^{-7}
0.01 M $Pb(NO_3)_2$ + 0.1 M HNO_3 + 0.0003 M SLES	5.98	2.63×10^{-6}	7.56	3.84×10^{-7}

In this table, K_α (mol m^{-2} s^{-1})—rate constant for growth of α-phase crystals in a direction, perpendicular to the electrode surface; t_α(s)—time, corresponding to the beginning of α-phase formation; K_β (mol m^{-2} s^{-1}) – rate constant for growth of β-phase crystals in a direction, perpendicular to the electrode surface; t_β (s) – time, corresponding to the beginning of β-phase formation

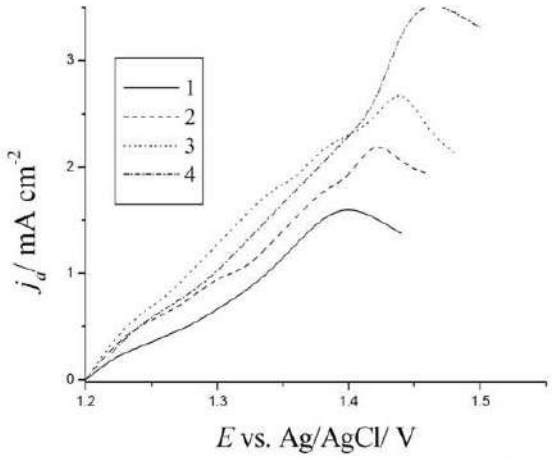

Fig. 5 Anodic voltammograms on Pt disk electrode in 0.01 M $Pb(NO_3)_2$ + 0.1 M HNO_3 + 0.0003 M SLES at different potential sweep rates, mV/s: 1—20, 2—50, 3—100, 4—200

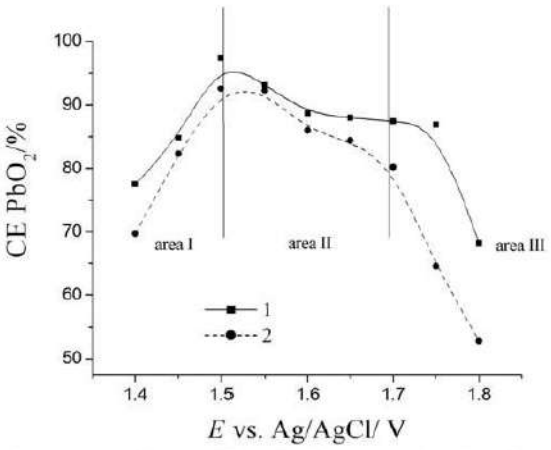

Fig. 7 Current efficiency of lead dioxide vs. potential of deposition, where 1—non modified PbO_2; 2—PbO_2–3.2 wt.% SLES

electrode, obeying the Levich equation (Fig. 6, correlation factor r = 0.99). The data obtained indicate diffusion control of the process at high anodic polarizations [12, 20, 29].

Apparent heterogeneous rate constants were calculated according to the Koutecky-Levich equation [12, 38] from intercepts of $1/I$ vs. $1/\omega^{1/2}$ plots. Results show that the presence of SLES in the deposition solution causes the apparent heterogeneous rate constant to decrease slightly from 4.1×10^{-4} (without surfactant) to 3.7×10^{-4} m s^{-1}. These results are in agreement with the voltammetry data (see Fig. 2) discussed above.

When the surfactant is present in the solution, the current efficiency (CE) of lead dioxide somewhat decreases due to the inhibition of the PbO_2 formation reaction (Fig. 7).

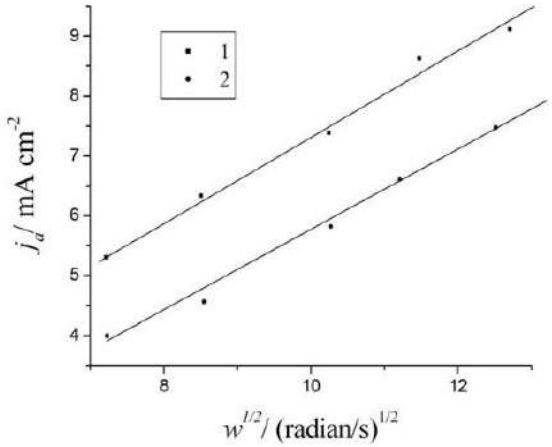

Fig. 6 Dependence of the anode current density value (E = 1.8 V) on the square root of Pt-RDE rotation rate in solutions containing 0.01 M $Pb(NO_3)_2$ + 0.1 M HNO_3 (1) + 0.0003 M SLES (2)

The data obtained can be adequately explained on the basis of a number of hypotheses. On the one hand, all the obtained data can be adequately described using classical electrodeposition scheme (1)–(4), when surfactant adsorption occurs on the surface of growing PbO_2, and the phenomenon of changing in the polyelectrolyte content in the coating can be caused by two factors: (i) heterogeneous and (ii) migratory. On the other hand, we cannot exclude that not only crystallization occurs from the supersaturated layer of the solution, but also colloidal particles are formed in some quantity that adhere to the surface of the growing crystals, as observed in the case of synthesis of PbO_2-TiO_2 composites [33].

It should be noted that it is possible that all the described effects can be realized simultaneously with different contributions that do not contradict the obtained experimental data.

Influence of deposition conditions on the chemical composition of lead dioxide-based composite materials

It has been established that additives [12, 20, 32, 40, 41], and anionic surfactants in particular [11], are included in the growing lead dioxide. An increase in the concentration of the surfactant additive in the deposition electrolyte, as a rule, leads to an increase in the content of the additive in lead dioxide [11, 17]. Thus, with an increase in the concentration of surfactant in solution from 5×10^{-5} to 5×10^{-4} M, its content in the coating increases from 3.2 to 12.5 wt.%. The observed effect is probably due to the adsorption of surfactant on lead dioxide, which also increases with increasing concentration. The content of the additive in the coating is likely to be determined by both thermodynamic parameters (equilibrium adsorption on lead dioxide) and kinetic factors (by the ratio of the rates of adsorption and desorption of surfactant at the time of

formation of the deposit). Generally, as the anodic current density increases the content of anionic surfactant in the coating due to an increase in the Coulomb attraction force between the positively charged electrode surface and the negatively charged anionic surfactant, this in turn leads to an increase in the adsorption and in content of surfactant in the oxide [17]. However, sodium laureth sulfate is an exception since its content in the coating decreases with increasing anodic current density. Thus, with a fixed surfactant content in the solution, with an increase in the deposition current density from 4 to 10 mA cm^{-2}, its content in the coating decreases from 10.2 to 7.0 wt.%. In this case, at the solution-air interface, the formation of foam is visually observed whose amount is proportional to the intensity of oxygen evolution (increases with increasing current density). This effect is unusual. An increase in the anode current density is accompanied by an increase in the current efficiency of molecular oxygen, which in turn creates favorable conditions for the redistribution of surfactant at the solid-liquid and liquid-gas interfaces. In fact, under conditions of increasing anode current density, effective surfactant removal to another interface leads to depletion of the near-electrode zone by surfactant and consequently to decrease of its content in the coating.

Physicochemical properties of PbO_2-SLES composites

Lead dioxide, deposited from nitrate electrolytes, is a polycrystalline formation consisting of a mixture of α- and β-phases of different crystallographic orientation, with the latter predominating (Fig. 8). The main orientations of the β-phase are (110), (011), (220), and (130), and the α-phases are (111). As described in [12], in some cases, the phase composition of the lead dioxide coatings may depend on the thickness of the coating. In order to avoid this undesirable effect, all measurements were performed on samples with a fixed coating thickness (35 mg cm^{-2}). At the same time, it should be noted that we did not observe a change in the nature of the diffractogram and the intensity of the peaks both when the angle of X-ray radiation changes to the sample surface and when the thickness of the coating changes. This indicates a uniform distribution of various phases and crystals of different crystallographic orientations in the lead dioxide coatings obtained under the conditions studied.

As follows from X-ray diffraction patterns (see Fig. 8), surfactant additive has a significant impact on the structure of lead dioxide. The β (110) and α (111) facets practically disappear, but β (022) additionally appears. In fact, composite materials are β-PbO_2, containing the X-ray amorphous phase of the surfactant. With an increase in the additive content in the composite, a decrease in the intensities of almost all faces is observed, which probably indicates a decrease in the size of lead dioxide crystals with an increase in the fraction of X-ray amorphous phases. It should be noted, however, that a decrease

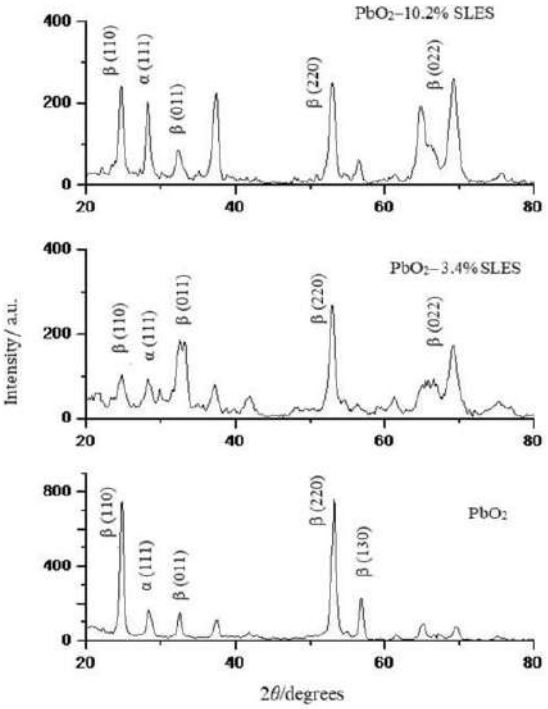

Fig. 8 X-ray diffractograms of PbO_2-SLES composite materials containing 0; 3.2 and 10.2 wt.% of SLES

in the intensity of the peaks cannot unambiguously indicate an increase in the amount of the crystalline phase since a similar effect on diffractograms can also be observed when water is captured by the porous structure of lead dioxide [10, 17].

The surface of non-modified sample is homogeneous and large-crystalline (Fig. 9a). With a surfactant concentration up to 3%, several zones with different surface morphology can be distinguished (Fig. 9b): the central zone, in which there are large sharp crystals (their size is several micrometers), and the peripheral zone, containing only small crystals of submicron size. When the surfactant content in the composite is 10%, the surface looks more or less uniform. The surface is like a two-layer, when larger crystals of submicron size are covered with very small nano-sized crystals that have a spindle-shaped form. It should be noted that a similar morphology of coatings was observed during the synthesis of PbO_2 from colloidal solutions containing TiO_2 [33]. One can observe a surface effect, when polycrystalline blocks did not have time to form due to different adsorption rates. During the growth of large crystals, organics are adsorbed on them all the time and further gradually grows into these crystals; zones with different areas (polycrystalline blocks and small crystals) can change during the electrolysis.

An X-ray microanalysis (Fig. 9c) of these two zones was carried out. The two spectra are strictly identical. Only Pb and

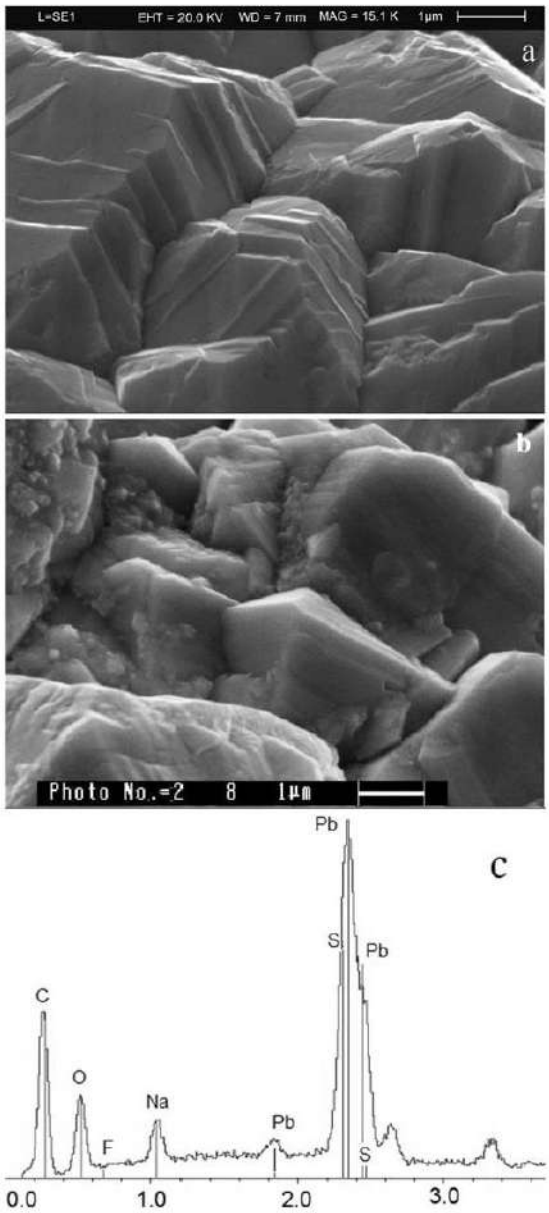

Fig. 9 SEM micrographs of non-doped PbO_2 (**a**) PbO_2–3.2 wt.% SLES (**b**) and EDX spectrum (**c**) of coating surface

O are visible (very few impurities). EDX spectra did not show an independent sulfur peak, probably due to the fact that its position practically coincides with the peak of lead in oxide. For a composite containing the maximum amount of sodium laureth sulfate, a distinct carbon peak appears on the EDX spectra. It should be noted that the maximum signal intensity is observed in areas covered by nano-sludge. However, EDX technique allows one to measure the local content of elements on different parts of the surface and very much depends on the surface morphology; such a picture can be the result of different specific surfaces of these areas.

Lead dioxide has high electrical conductivity of metallic nature, due to the deviation from the stoichiometric composition in the direction of decreasing the oxygen content and the transition of a part of Pb^{4+} ions to Pb^{2+} [42]. On this basis, the electrical conductivity of materials based on lead dioxide should depend on both their chemical composition and method of synthesis. The electrical conductivity of the obtained composite materials was measured by the strip method. Both the nature and the content of the additive in the composite have a significant effect on the measured value.

So, for example, the electrical conductivity of the Ti–Pt–PbO_2-10.2 wt.% SLES material is reduced by more than 3.7 times compared to pure PbO_2. The values are 49 and 13.4 Ω^{-1} cm^{-1} for PbO_2 and PbO_2-10.2% $C_{16}H_{29}O_6SNa$, respectively. The data obtained suggest that in composite materials with a high content of additives, oxide nanocrystals are surrounded by surfactant molecules, that is, the latter act as a kind of binder. The obtained data are also indirect confirmation of the mechanism proposed by us for the anodic formation of composite oxide materials.

Electrocatalytic activity of PbO_2-surfactant coatings

Having in mind that the processes of oxidation of organic substances and the oxygen evolution in most cases precede simultaneously, we investigated the dependence of the overvoltage of the oxygen evolution reaction on the electrodes involved.

According to the mechanism proposed by D. Pavlov et al. [43], oxygen evolution occurs at active sites located in a hydrous layer on PbO_2 [44]. As proven by Trasatti and Lodi [45], if oxygen evolution reaction (OER) is limited by a second electron transfer (electrochemical desorption), an increase of bond strength of chemisorbed oxygen will lead to an increase of OER overvoltage.

According to our results (Fig. 10), oxygen overpotential on PbO_2-surfactant coatings increases, as was observed in the case of bismuth [20, 44, 46]. In this way, on non-modified PbO_2, the Tafel slope is 229, while at 10.2 wt.% SLES content, it is 178 mV/dec (not shown). As one can conclude from calculated results, the slope significantly exceed the theoretical value, which indicates a decrease in the degree of surface coverage by oxygen-containing particles, probably due to blocking by sulfate ions. Such an effect was described in detail in previous publication [47]. Slope decreasing in the case of PbO_2-SLES denotes the increasing of lead dioxide surface coverage by oxygen-containing radicals, which are directly involved in the electrochemical stages of oxygen evolution. Most likely, surfactants on the electrode surface play the role

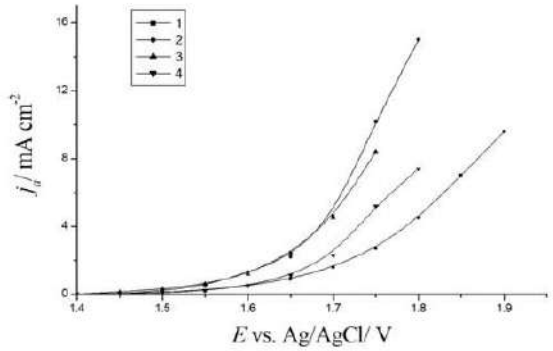

Fig. 10 Steady-state polarization curves of oxygen evolution in 1 M H_2SO_4 on next electrodes: PbO_2 (1); PbO_2–3.2 wt.% SLES (2); PbO_2–7 wt.% SLES (3); PbO_2–10.2 wt.% SLES (4)

of mediators in the process of oxygen evolution and inhibit the surface blocking by sulfate ions on such materials.

Phenolic compounds, in particular 4-chlorophenol, were selected for estimation of electrocatalytic activity of the composites involved in oxidation of organic compounds.

According to the literature [48], a rather large number of intermediate products are formed during the anodic oxidation of 4-chlorophenol. The main intermediate products include benzoquinone and maleic acid.

The initial solution of chlorophenol is characterized by two peaks at 220 and 280 nm (Fig. 11). At first, the electrolysis shows a decrease in the peak at 220 nm, as well as a slight increase in the peak at 280 nm and the appearance of the plateau at 240–270 nm, which is caused by a decrease in the concentration of 4-chlorophenol and accumulation of benzoquinone in the solution. A further increase in the time of electrolysis leads to the disappearance of the peaks at 220 and 280 nm, as well as the reduction of the plateau at 240–270 nm due to a decrease in the concentrations of both 4-chlorophenol and benzoquinone. Already after 4 h of electrolysis, the aromatic compounds are

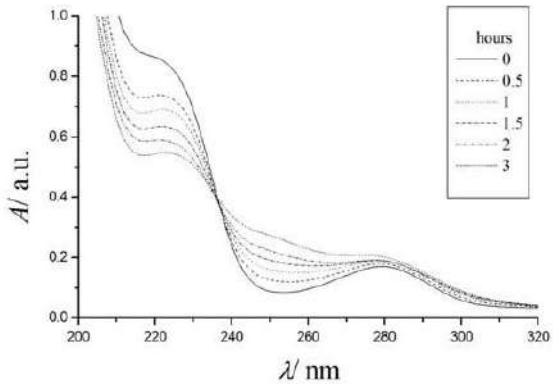

Fig. 11 The electronic absorption spectra of 0.5 M Na_2SO_4 + 0.1 mM 4-chlorphenol + phosphate buffer solution at different electrolysis duration on the PbO_2–3.2 wt.% SLES anode

completely destroyed with the formation of only aliphatic electrolysis products (mainly maleic acid), which was evidenced by HPLC [48].

Conclusions

The addition of surfactants has a significant impact on the kinetics of lead dioxide electrodeposition, without changing the mechanism of the process. In this way, at low anodic polarizations, second electron transfer stage is rate determining, whereas at high anodic polarizations, such stage is diffusion transport of the lead ions to the electrode surface. The presence of sodium laureth sulfate in the deposition electrolyte leads to a slight inhibition of the deposition of lead dioxide.

The content of the additive in lead dioxide is determined mainly by its adsorption on the oxide. An increase in the adsorption of additive due to an increase in its concentration in the solution and an increase in electrostatic attraction leads to the enrichment of the composite material with organic substance.

The morphology and structure of composite materials differs significantly from lead dioxide. With an increase in the additive content in the composite, there is a transition from large-grained deposits to materials with submicron and nanosized crystals. The content of organic substance in the oxide can vary from 3.2 to 12.5wt.%, forming a surfactant-oxide composite coating.

The electrocatalytic activity of the materials involved was investigated with respect to oxygen evolution reaction and the oxidation of 4-chlorophenol. The calculated value of Tafel slope is 229 on non-modified PbO_2, while on 10.2 wt.% SLES-PbO_2, it is 178 mV/dec. Slope decreasing in the case of PbO_2-SLES denotes the increasing of lead dioxide infilling degree by oxygen-containing radicals, which are directly involved in the electrochemical stages of oxygen evolution. Most likely, surfactants on the electrode surface play the role of mediators in the process of oxygen evolution and inhibit the surface blocking by sulfate ions on such materials. The processes of electrooxidation of 4-chlorophenol on lead dioxide and PbO_2-based composite materials proceed qualitatively in the same way and differ only in the rate.

Thus, lead dioxide-based surfactant-oxide composite coatings are of great interest because of high electrocatalytic activity with respect to oxygen evolution reaction.

Acknowledgments The authors are indebted to Rossano Amadelli (Universita' degli Studi di Ferrara) for help in the discussion of obtained results.

Compliance with ethical standards

Conflict of interest The authors declare that they have no conflict of interest.

References

1. Bi Q, Guan W, Gao Y, Cui Y, Ma S, Xue J (2019) Study of the mechanisms underlying the effects of composite intermediate layers on the performance of Ti/SnO_2-Sb-La electrodes. Electrochim Acta 306:667–679
2. Du H, Duan G, Yang N, Liu J, Tang Y, Pang R, Chen Y, Wan P (2018) Fabrication of Ga_2O_3–PbO_2 electrode and its performance in electrochemical advanced oxidation processes. J Solid State Electrochem 22(12):3799–3806
3. Pereyra J, Martinez MV, Barbero C, Bruno M, Acevedo D (2019) Hydrogel-graphene oxide nanocomposites as electrochemical platform to simultaneously determine dopamine in presence of ascorbic acid using an unmodified glassy carbon electrode. J Compos Sci 3: 1–14
4. Vargas R, Borras C, Mendez D, Mostany J, Scharifker BR (2016) Electrochemical oxygen transfer reactions: electrode materials, surface processes, kinetic models, linear free energy correlations, and perspectives. A review. J Solid State Electrochem 20:875–893
5. Santos JEL, de Moura DC, da Silva DR, Panizza M, Martinez-Huitle CA (2019) Application of TiO_2-nanotubes/PbO_2 as an anode for the electrochemical elimination of acid red 1 dye. J Solid State Electrochem 23:351–360
6. Labbe F, Asset T, Chatenet M, Ahmad Y, Guerin K, Metkemeijer R, Berthon-Fabry S (2019) Activity and durability of platinum-based electrocatalysts with tin oxide–coated carbon aerogel materials as catalyst supports. Electrocatalysis 10:156–172
7. Wang G, Zhang L, Zhang J (2012) A review of electrode materials for electrochemical supercapacitors. Chem Soc Rev 41(2):797–828
8. Berenguer R, Quijada C, La Rosa-Toro A, Morallon E (2019) Electro-oxidation of cyanide on active and non-active anodes: designing the electrocatalytic response of cobalt spinels. Sep Purif Technol 208:42–50
9. Pouladvand I, Asl SK, Hoseini MG, Rezvani M (2019) Characterization and electrochemical behavior of Ti/TiO_2–RuO_2–IrO_2–SnO_2 anodes prepared by sol–gel process. J Sol-Gel Sci Technol 89:553–561
10. Velichenko AB, Knysh VA, Luk'yanenko TV, Velichenko YA, Devilliers D (2012) Electrodeposition PbO_2-TiO_2 and PbO_2-ZrO_2 and its physicochemical properties. Mater Chem Phys 131:686–693
11. Li X, Xu H, Yan W (2017) Effects of twelve sodium dodecyl sulfate (SDS) on electro-catalytic performance and stability of PbO_2 electrode. J Alloys Compd 718:386–395
12. Shmychkova O, Luk'yanenko T, Amadelli R, Velichenko A (2016) Electrodeposition of Ni^{2+}-doped PbO_2 and physicochemical properties of the coating. J Electroanal Chem 774:88–94
13. Boyes W (2010) Instrumentation reference book, 4th edn. Elsevier, Amsterdam, Boston, Heidelberg, London, New York, Oxford, Paris, San Diego, San Francisco, Singapore, Sydney, Tokyo
14. Li D (2008) Encyclopedia of microfluidics and nanofluidics. Springer Boston MA
15. Robinson JW, Frame EMS, Frame GM II (2005) Undergraduate instrumental analysis, 6th edn. Marcel Dekker, New York
16. Adamson AW, Gast AP (1997) Physical chemistry of surfaces, 6th edn Wiley Interscience
17. Velichenko AB, Luk'yanenko TV, Nikolenko NV, Amadelli R, Danilov FI (2007) Nafion effect on the lead dioxide electrodeposition kinetics. Russ J Electrochem 43:118–120
18. Nikolenko NV, Esajenko EE (2005) Surface properties of synthetic calcium hydroxyapatite. Adsorpt Sci Technol 23:543–553
19. Campbell SA, Peter LM (1991) Detection of soluble intermediates during deposition and reduction of lead dioxide. J Electroanal Chem 306:185–194
20. Shmychkova O, Luk'yanenko T, Velichenko A, Meda L, Amadelli R (2013) Bi-doped PbO_2 anodes: electrodeposition and physicochemical properties. Electrochim Acta 111:332–338
21. Li X, Pletcher D, Walsh FC (2011) Electrodeposited lead dioxide coatings. Chem Soc Rev 40:3879–3894
22. Fleischmann M, Liler M (1958) The anodic oxidation of solutions of plumbous salts. Part 1. The kinetics of deposition of α-lead dioxide from acetate solutions. Trans Faraday Soc 54:1370–1381
23. Fleischmann M, Thirsk HR (1959) The potentiostatic study of the growth of deposits on electrodes. Electrochim Acta 1:146–160
24. Fleischmann M, Mansfield JR, Thirsk HR, Wilson HGE, Wynne-Jones L (1967) The investigation of the kinetics of electrode reactions by the application of repetitive square pulses of potential. Electrochim Acta 12:967–982
25. The electrochemistry of lead / [ed. AT Kuhn]. – New York: Academic Press, 1979
26. Abyaneh MY, Fleischmann M, Del Giudice E (2009) The investigation of nucleation using microelectrodes: I. the ensemble averages of the times of birth of the first nucleus. Electrochim Acta 54: 879–887
27. Abyaneh MY, Saez V, Gonzalez-Garcia J, Mason TJ (2010) Electrocrystallization of lead dioxide: analysis of the early stages of nucleation and growth. Electrochim Acta 55:3572–3579
28. Chang H, Johnson DC (1989) Electrocatalysis of anodic oxygen-transfer reaction. Chronoamperometric and voltammetric studies of the nucleation and electrodeposition of β-lead dioxide at a rotated gold disk electrode in acidic media. J Electrochem Soc 136:17–22
29. Velicheko AB, Girenko DV, Danilov FI (1995) Electrodeposition of lead dioxide at an Au electrode. Electrochim Acta 40:2803–2807
30. Velicheko AB, Girenko DV, Danilov FI (1996) Mechanism of lead dioxide electrodeposition. J Electroanal Chem 425(1):127–132
31. Velichenko AB, Baranova EA, Girenko DV, Amadelli R, Kovalyov SV, Danilov FI (2003) Mechanism of electrodeposition of lead dioxide from nitrate solutions. Russ J Electrochem 39:615–621
32. Shmychkova O, Luk'yanenko T, Amadelli R, Velichenko A (2014) Physico-chemical properties of PbO_2-anodes doped with $Sn^{4+}$and complex ions. J Electroanal Chem 717-718:196–201
33. Knysh V, Luk'yanenko T, Shmychkova O, Amadelli R, Velichenko A (2017) Electrodeposition of composite PbO2-TiO2 materials from colloidal methanesulfonate electrolytes. J Solid State Electrochem 21:537–544
34. Saez V, Marchante E, Diez MI, Esclapez MD, Bonete P, Lana-Villarreal T, Gonzalez Garcia J, Mostany J (2011) A study of the lead dioxide electrocrystallization mechanism on glassy carbon electrodes. Part I: experimental conditions for kinetic control. Mater Chem Phys 125:46–54
35. Abyaneh MY (2014) Electrocrystallization: modeling and its application, in Developments in electrochemistry: science inspired by Martin Fleischmann (eds D Pletcher, Z-Q Tian and DE Williams), John Wiley & Sons, Ltd, Chichester, UK https://doi.org/10.1002/9781118694404.ch3
36. Gonzalez-Garcia J, Gallud F, Iniesta J, Montiel V, Aldaz A, Lasia A (2000) Kinetics of electrocrystallization of PbO_2 on glassy carbon electrodes. Partial inhibition of the progressive three-dimensional nucleation and growth. J Electrochem Soc 147:2969–2974
37. Gonzalez-Garcia J, Gallud F, Iniesta J, Montiel V, Aldaz A, Lasia A (2001) Kinetics of electrocrystallization of PbO_2 on glassy carbon electrodes. Influence of the electrode rotation. Electroanalysis 13: 1258–1264
38. Luk'yanenko T, Velichenko A, Knysh V, Shmychkova O (2018) Influence of methanesulfonate ions on electrooxidation of Pb(II). Voprosy Khimii i Khimicheskoi Tekhnologii 4:27–35
39. Shmychkova O, Luk'yanenko T, Piletska A, Velichenko A, Gladyshevskii R, Demchenko P, Amadelli R (2015) Electrocrystallization of lead dioxide: influence of early stages of nucleation on phase composition. J Electroanal Chem 746:57–61

40. Nunez M (2007) Trends in electrochemistry research. Nova Publ Inc, N-Y
41. Ghasemi S, Mousavi MF, Shamsipur M (2007) Electrochemical deposition of lead dioxide in the presence of polyvinylpyrrolidone. A morphological study. Electrochim Acta 53:459–467
42. Ruetschi P, Giovanoli R (1991) On the presence of OH^- ions, Pb^{2+} ions and cation vacancies in PbO_2. Power Sources 13:81–97
43. Pavlov D, Monahov B, Petrov D (2000) Influence of Ag as alloy additive on the oxygen evolution reaction on Pb/PbO_2 electrode. J Power Sources 85:59–62
44. Shmychkova O, Luk'yanenko T, Dmitrikova L, Velichenko A (2019) Modified lead dioxide for organic wastewater treatment: physico-chemical properties and electrocatalytic activity. J Serb Chem Soc 84:187–198
45. Trasatti S, Lodi G (1981) Electrodes of conductive metallic oxides. Part B, Elsevier, Amsterdam, Holland
46. Shmychkova O, Luk'yanenko T, Yakubenko A, Amadelli R, Velichenko A (2015) Electrooxidation of some phenolic compounds at Bi-doped PbO_2. Appl Catal B 162:346–351
47. Amadelli R, Maldotti A, Molinari A, Danilov FI, Velichenko AB (2002) Influence of the electrode history and effects of the electrolyte composition and temperature on O_2 evolution at β-PbO_2-anodes in acid media. J Electroanal Chem 534:1–12
48. Shmychkova O, Luk'yanenko T, Dmitrikova L, Velichenko A (2018) Electrooxidation of 4-clorphenol on modified lead dioxide anodes. Voprosy Khimii i Khimicheskoi Tekhnologii 3:50–57

Journal of Electroanalytical Chemistry 873 (2020) 114412

Contents lists available at ScienceDirect

Journal of Electroanalytical Chemistry

journal homepage: www.elsevier.com/locate/jelechem

Lead dioxide-SDS composites: Design and properties

A. Velichenko *, T. Luk'yanenko, O. Shmychkova

Ukrainian State University of Chemical Technology, 8, Gagarina Ave., 49005 Dnipro, Ukraine

ARTICLE INFO

Article history:
Received 8 May 2020
Received in revised form 24 June 2020
Accepted 25 June 2020
Available online 7 July 2020

Keywords:
Lead dioxide
Nitrate electrolyte
Sodium dodecyl sulfate
Electrodeposition
Adsorption

ABSTRACT

The electrodeposition of PbO_2 from a sodium dodecyl sulphate-containing medium has been investigated. The presence of sodium dodecyl sulfate in the deposition electrolyte leads to a slight inhibition of the deposition of lead dioxide. It has been found that the morphology and structure of composite materials differs significantly from lead dioxide. With an increase in the additive content in the composite, there is a transition from large-grained deposits to materials with submicron and nano-sized crystals. It is shown that anionic surfactants, sodium dodecyl sulfate in particular, are included in the growing lead dioxide. The changing in deposition conditions (temperature, pH and anodic current density) allows one to control the content of surfactant in the resulting oxide. It is possible to obtain a surfactant-oxide composite with the content of organic substance in the oxide up to 5.4 wt%. The electocatalytic activity of the materials involved was investigated in respect to oxygen evolution reaction and the oxidation of 4-chlorophenol. Oxygen overpotential on PbO_2-SDS coatings decreases in comparison to non-modified sample because of a decrease in the degree of filling of oxygen-containing particles on the surface of the electrode, probably due to blocking by sulfate ions. The 4-chlorophenol oxidation rate is significantly increased on PbO_2-SDS composites. Thus, already after 90 min of electrolysis on composites, contained 2 and 4.2 wt% SDS, all aromatic intermediates are destroyed, and only aliphatic acids are found in the solution.

1. Introduction

Development of methods for the direct synthesis of new materials with predicted properties is recognized as one of the priority issues of modern science [1,2]. Among other coatings composite materials are the most promising ones, since changing their composition allows one to control the functional properties over a wide range due to the dispersed phase particles of composites with different nature. Despite the large number of synthesis methods, electrochemical are considered to be the most promising due to their ease of implementation and relatively low energy losses compared to sol-gel and other technologies [3,4]. This method opens wide opportunities for influencing the composition and properties of materials by changing the conditions of the electrolysis and the composition of the electrolyte. Typical materials of this type are lead(IV) and manganese(IV) oxides, which, due to their simplicity of electrochemical production, high corrosion resistance and relatively low cost, are widely used in electrocatalysis, electroplating and electrochemical energy (lead-acid batteries, soluble lead redox flow battery, asymmetric supercapacitors, primary and secondary current sources) [5–9].

The main focus of researchers was to explore the possibilities of synthesis of highly dispersed systems using porous current collectors, which is extremely important for the use of the obtained materials as efficient electrocatalysts and in electrochemical energy [10]. The main obstacle in obtaining such systems is the extremely uneven current distribution in the porous substrate, which results in blocking the deposition in the interior space of the 3D matrix [11].

Currently, additives of organic substances (most often surfactants and polyelectrolytes) are widely used in galvanic processes for the production of metals and alloys [12,13]. Additives can be used for various purposes, influencing both the technological parameters of metal electrodeposition processes and the properties of the resulting coatings.

Herein we proposed to use anionic surfactant sodium dodecyl sulfate (SDS) to influence the electrodeposition process and properties of oxide materials, namely lead dioxide. Since its electrodeposition takes place at high anodic potentials, at which most organic compounds oxidize at a sufficiently high rate, the choice of additives is a significant problem. SDS, or sodium lauryl sulfate is one of the synthetic anionic surfactants, a product that consists of approximately 70% sodium dodecyl sulfate and 30% sodium tetradecyl sulfate, with the formula of $CH_3(CH_2)_{11}OSO_3Na$, has been used in many cleaning products; in pharmaceutical and food products, as well as in industrial and laboratory applications [14].

Despite some successes, extensive and largely empirical methods of creating new modified and composite materials are observed, so in most cases it is not about controlled synthesis of oxide materials. Most likely, at this stage of research, it should be noted the accumulation of unsystematic experimental data in the absence of even empirical correlation parameters.

* Corresponding author.
E-mail address: velichenko@ukr.net. (A. Velichenko).

http://dx.doi.org/10.1016/j.jelechem.2020.114412
1572-6657/

The influence of surfactants on the regularities of electrodeposition of oxides, their composition and properties has been described in only a few publications [15–18].

In this work we report and discuss the electrodeposition of PbO_2 from a SDS-containing medium, physico-chemical properties and electrocatalytic activity of obtained materials.

2. Material and methods

All chemicals were reagent grade. Bidistilled tap water with electrolytic conductivity 1.6 μS/cm was used to prepare solutions. Electrodeposition regularities of doped lead dioxide were studied on an Au disk electrode (Au-DE, 1 cm^2) by steady-state voltammetry, chronoamperometry. The voltammetry system SVA-1BM was used. The potential scan rate was varied within 1–50 mV s^{-1} depending on purposes of the experiments. Before each experiment, the electrode surface was treated with a freshly prepared mixture (1:1) of concentrated H_2SO_4 and H_2O_2 [19]. This preliminary treatment technique permits to stabilize the electrode surface, which under the action of strong oxidizing medium is oxidized to a certain state (defined phase and chemical composition of the surface oxides), which determines the satisfactory reproducibility of cyclic voltammograms in the background electrolyte (0.1 M HNO_3). Voltammetry measurements were carried out in a standard temperature-controlled three-electrode cell. Change in the mass of the gold electrode under galvanostatic conditions was carried out gravimetrically with quartz microbalances. All potentials were recorded and reported vs. Ag / AgCl / KCl $_{(sat.)}$.

The determination of current efficiency and partial current of lead dioxide deposition was done according the method described in details in our previous publication [20]. Lead dioxide was electrodeposited from nitrate electrolytes that contained 1.0 M HNO_3, 0.01 M $Pb(NO_3)_2$. Surfactant was added into the deposition electrolyte as aqueous solutions with 7×10^{-4} M concentration. Since at low concentrations of surfactant, the composition of the electrolyte will significantly change during deposition, the concentration was chosen at which, according to the adsorption isotherm, one can obtain the 100% degree of surface filling, when the electrolyte composition will not change if the surfactant has been consumed.

Lead dioxide anodes surface morphology was studied by scanning electron microscopy (SEM) with Stereoscan 440 LEO microscope. X-Ray powder diffraction (XRPD) data were collected in the transmission mode on a STOE STADI P diffractometer with Cu $K\alpha_1$-radiation, curved Ge (111) monochromator on primary beam, $2\theta/\omega$-scan, angular range for data collection 20.000–110.225°2θ with increment 0.015, linear position sensitive detector with step of recording 0.480°2θ and times per step 75–300 s, U = 40 kV, I = 35 mA, T = 298 K. A calibration procedure was performed utilizing SRM 640b (Si) and SRM 676 (Al_2O_3) NIST standards. Preliminary data processing and X-ray qualitative phase analysis were performed using STOE WinXPOW and PowderCell program packages. Crystal structures of the phases were refined by the Rietveld method with the program FullProf.2 k, applying a pseudo-Voigt profile function and isotropic approximation for the atomic displacement parameters, together with quantitative phase analysis.

The method for the determination of high molecular weight aliphatic acids [21] was adapted for the determination of the concentration of surfactant in aqueous solutions. Such method consists in the formation of an associate of a high-molecular anion and a dye, followed by extraction into a non-aqueous medium. The content of organic substance was determined photocolorimetrically after extraction of the ionic associate with chloroform. 10 ml of distilled water was placed in a separatory funnel and 2 ml of a 0.1% aqueous solution of methylene blue was injected. Then, 1 ml of the test solution was injected and shaken for 2 min with 15 ml of chloroform. The organic phase was filtered through cotton wool and the optical density was measured at 650 nm using a CPC-2 colorimeter. To determine surfactants in composite coatings of known mass, the latter were anodically dissolved at a current density of 2 mA cm^{-2} in 30 ml of 0.1 M HCl. Then the concentration of additives was determined in solution by the above method.

Adsorption measurements were carried out on 0.5 g of PbO_2 powder (Merck) in 0.1 M HCl solutions containing various amounts of additive. The measurements were carried out in the presence of an indifferent electrolyte (0.1 M KCl), which screened the electrostatic field of the oxide surface. The time to establish the adsorption equilibrium was 24 h.

Adsorption parameters were calculated using the Frumkin equation [22]:

$$Bc = \frac{\theta}{1-\theta}\exp(-2\alpha\theta)$$

where B is adsorption constant;

θ – surface coverage;

α – interaction parameter.

Platinized titanium was used as a sheet during investigation of electrocatalytic activity of materials. It was treated accordingly before platinum layer depositing [23].

Oxygen evolution reaction was investigated by steady-state polarization on computer controlled EG & G Princeton Applied Research potentiostat model 273A in 1 M H_2SO_4.

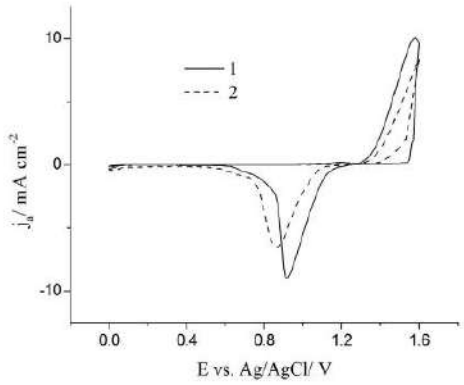

Fig. 1. Cyclic voltammogram on Au-electrode in solutions: 1–1.0 M HNO_3 + 0.01 M $Pb(NO_3)_2$; 2–1.0 M HNO_3 + 0.01 M $Pb(NO_3)_2$ + 7×10^{-4} M. Potential scan rate 50 mV s^{-1}.

Table 1
Parameters of initial stages of lead dioxide electrocrystallization[a].

Deposition electrolyte 0.01 M $Pb(NO_3)_2$ + 1.0 M HNO_3	t_α	K_α	t_β	K_β
+ 3×10^{-4} SDS	3.03	3.26×10^{-6}	7.87	1.10×10^{-5}
+ 7×10^{-4} SDS	2.35	1.08×10^{-5}	6.31	3.30×10^{-5}

[a] In this table K_0 (mol $m^{-2} s^{-1}$) – rate constant for growth of α-phase crystals in a direction, perpendicular to the electrode surface; t_α(s) – time, corresponding to the beginning of α-phase formation; K_β (mol $m^{-2} s^{-1}$) – rate constant for growth of β-phase crystals in a direction, perpendicular to the electrode surface; t_β (s) – time, corresponding to the beginning of β-phase formation.

Table 2
Effect of SDS concentration on the kinetic parameters of PbO_2 electrodeposition.

Electrodeposition solution	α	Apparent heterogeneous rate constant k 10^8 / m s^{-1}
1.0 M HNO_3 + 0.01 M $Pb(NO_3)_2$	0.4	4.1
1.0 M HNO_3 + 0.01 M $Pb(NO_3)_2$ + 3×10^{-5} M $C_{12}H_{25}O_4SNa$	0.5	4.0
1.0 M HNO_3 + 0.01 M $Pb(NO_3)_2$ + 7×10^{-4} M $C_{12}H_{25}O_4SNa$	0.5	3.9
1.0 M HNO_3 + 0.01 M $Pb(NO_3)_2$ + 2×10^{-3} M $C_{12}H_{25}O_4SNa$	0.4	3.8

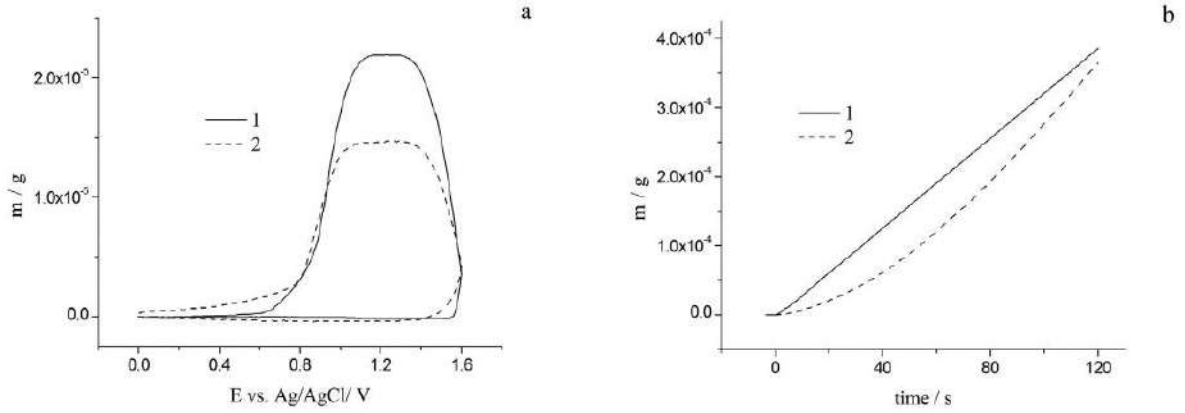

Fig. 2. Change in the mass of the gold electrode during CVA (Fig. 1) (a) and under galvanostatic conditions (j_a = 5 mA cm^{-2}) (b) during the electrodeposition of lead dioxide from various electrolytes: 1–1.0 M HNO_3 + 0.01 M $Pb(NO_3)_2$; 2–1.0 M HNO_3 + 0.01 M $Pb(NO_3)_2$ + 7 × 10^{-4} M SDS.

The electrooxidation of organic compounds was carried out in divided cell at j_a = 50 mA cm^{-2}. The volume of anolyte was 130 cm^3. Solution, containing phosphate buffer (0.25 M Na_2HPO_4 + 0.1 M KH_2PO_4) + 10^{-4} M organic compound, (pH = 7.0) was used as anolyte; phosphate buffer as catholyte. Stainless steel was used as cathode. Composite PbO_2-fluoropolymer electrodes were used as anodes. Electrode surface area was 2.5 cm^2.

The changing of the concentration of the organic substance during the electrolysis was measured by sampling (volume of 5 cm^3) at regular intervals and measuring the optical density of the solution in the ultraviolet and visible region (wavelength range 200–350 nm) using a Kontron Uvikon 940 spectrometer.

Analyses of the reaction products were conducted by high performance liquid chromatography (HPLC) using a Shimadzu RF-10A xL instrument equipped with an Ultraviolet SPD-20AV detector and a 30 cm Discovery® C18 column.

3. Results and discussions

The mechanism of lead dioxide electrodeposition is presented by a four stages kinetic scheme [18–20]. The mechanism has been modified from the first version [24], where insoluble oxygen-containing Pb(IV) intermediates were proposed, through ones involving the oxygen-containing Pb(IV) species proposed by Chang and Johnson [25], and the oxygen-containing Pb (III) intermediate suggested by Velichenko et al. [26], who afterwards proved the existence of both oxygen-Pb(III) and oxygen-Pb(IV) soluble

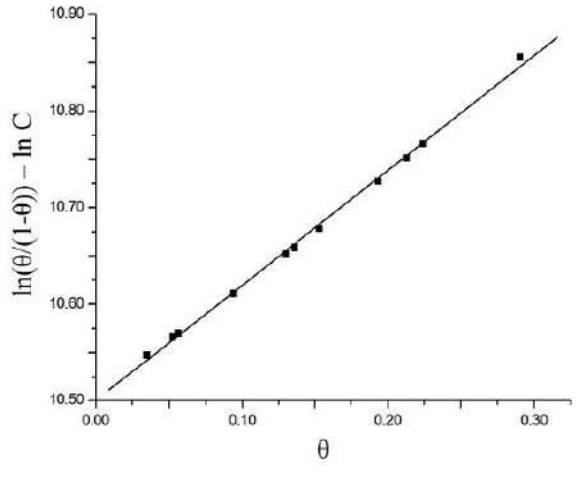

Fig. 3. The Frumkin isotherm of $C_{12}H_{25}SO_4Na$ adsorption on PbO_2. θ and C means surface coverage and equilibrium concentration, respectively.

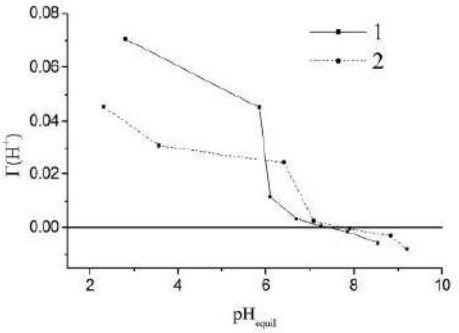

Fig. 4. PbO_2 (0.5 g) potentiometric titration results. The concentration of sodium dodecylsulfate is 0 (1) and 7 × 10^{-4} M (2).

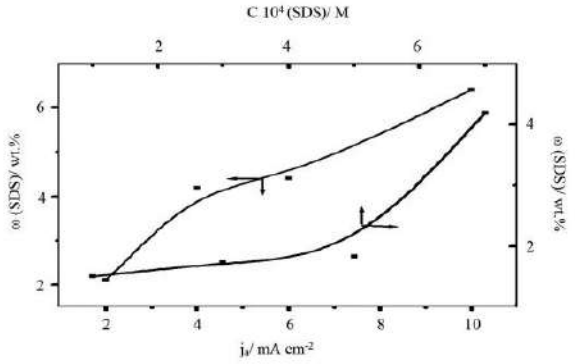

Fig. 5. Effect of anodic current density and SDS concentration in the electrolyte on its content in the lead dioxide deposit.

Table 3
Effect of nitric acid concentration on the additive content in the composite material (j_a = 4 mAcm^{-2}).

Electrodeposition solution	Content of SDS/ wt%
0.1 M HNO_3 + 0.1 M Pb^{2+} + 7 × 10^{-4} M $C_{12}H_{25}O_4SNa$	4.2
0.5 M HNO_3 + 0.1 M Pb^{2+} + 7 × 10^{-4} M $C_{12}H_{25}O_4SNa$	4.8
1 M HNO_3 + 0.1 M Pb^{2+} + 7 × 10^{-4} M $C_{12}H_{25}O_4SNa$	5.4

intermediates [27]:

$$H_2O \rightarrow OH_{ads} + H^+ + e^- \quad (1)$$

$$Pb^{2+} + OH_{ads} \rightarrow Pb(OH)^{2+} \quad (2)$$

$$Pb(OH)^{2+} + H_2O \rightarrow Pb(OH)_2^{2+} + H^+ + e^- \quad (3)$$

$$Pb(OH)_2^{2+} \rightarrow PbO_2 + 2H^+ \quad (4)$$

At low anodic polarizations (E < 1.6 V), kinetic control of the process is realized. At high anodic polarizations (E > 1.6 V), the rate of electrodeposition is limited by the stage of Pb(II) delivery to the electrode surface.

It has been shown in our recent publications [16–18] that surfactant additives significantly affect the kinetics of electrodeposition of lead(IV) oxide without altering the mechanism of the process. It was also found that the surfactants in the electrolyte deposition are included in the growing coating, adsorbed on PbO_2 crystals, which in turn leads to changes in the initial stages of crystallization. It is known [28] that surfactants are selectively adsorbed on certain faces, usually parallel to the faces, reducing the growth rate of these faces, and thus changing the shape of the growing crystals.

In order to get a more detailed analysis of the effect of the surfactant on the initial stages of crystallization, current transients on Au electrode were obtained in the presence of SDS in the deposition solution. Two different concentrations were investigated. These are 3 and 7 × 10^{-4} M. j-t Curve of PbO_2 deposition (not shown) can be characterized by several features and fully consistent with the transients obtained and described in detail by Saez et al. [29].

It was found that crystallization proceeds by a progressive mechanism. There is a change in the progressive mechanism to instantaneous at high concentrations of surfactant. The predominant form of crystals at 2D nucleation in the presence of additives in nitrate electrolytes is a hemispheroid. The main parameters of crystallization of the lead(IV) oxide, depending on the presence of surfactant in the electrolytes of deposition are given in Table 1:

In order to ascertain whether the selected substance has electrochemical stability at the deposition potentials of PbO_2 coating cyclic voltammograms were obtained on an Au-electrode in a 1.0 M HNO_3 background electrolyte that additionally contained SDS (potential scan area 0–1.6 V). It was found that anionic surfactant SDS does not exhibit electrochemical activity in the investigated potential range.

In typical cyclic voltammogram, the anodic branch of the curve (Fig. 1), at potentials higher than 1.4 V, features an exponential current growth corresponding to the simultaneous reactions of lead(II) oxidation and oxygen evolution. In the cathodic branch of the curve, a current peak due to lead dioxide reduction can be observed at potentials between 0.8 and 1.2 V [20]. The addition to the deposition electrolyte of anionic surfactant results in a slight inhibition of PbO_2 deposition.

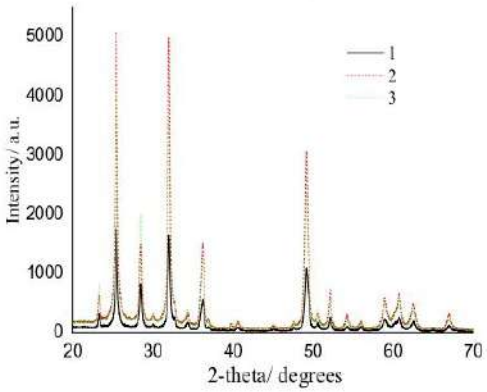

Fig. 6. XRD patterns of composite materials, obtained from 1.0 M HNO_3 + 0.1 M Pb $(NO_3)_2$ + X M SDS, where X is 0 (1); 3 × 10^{-5} (2) and 7 × 10^{-4}(3).

The number of electrons that take part in the kinetic stage was determined from linear potential sweep voltammetry measurements according to Delahay equation [19]. The transfer coefficient (α) remains almost unchanged when the surfactant is present in the deposition electrolyte (Table 2). The calculated number of electrons in the elementary stage was one, confirming that PbO_2 formation is a multistep charge transfer which involves consecutive two one-electron steps, as outlined in [19], both in the absence and in the presence of added SDS.

Apparent heterogeneous rate constants were calculated according to the Koutecky-Levich equation [19] from intercepts of $1/I$ vs. $1/\omega^{1/2}$ plots. Results show that the presence of SDS in the deposition solution causes the apparent heterogeneous rate constant to decrease slightly (see Table 2). These results are in agreement with the voltammetry data (see Fig. 1) discussed above.

As one can see from Fig. 2, the mass of the gold electrode increases on the anodic branch of the CV because of lead dioxide deposition. The smaller mass of the coating obtained in the presence of surfactant in solution confirms the inhibition of the PbO_2 electrodeposition because of SDS additive.

Adsorption measurements were performed on a lead dioxide powder at zero charge potential [30]. As one can see from the experimental data, the adsorption of surfactant is satisfactorily described by the Frumkin isotherm (Fig. 3, correlation factor 0.999). The value of interaction parameter calculated from above mentioned dependence is 1.00 that evidences the slight interaction between adsorbed molecules. The value of the energy of adsorption interaction ($-\Delta G$) for $C_{12}H_{25}SO_4Na$ is 35.6 kJ mole^{-1}, which indicates the specific character of adsorption.

Table 4
Phase composition and crystallographic data of coatings.

Sample description	Content (mass %) α-PbO_2 / β-PbO_2	Phase	Lattice parameters, Å			Reliability factors
			a	*b*	*c*	R_I / R_P, R_{WP}, R_{EXP}
0.1 M $Pb(NO_3)_2$ + 1 M HNO_3	13.6(2) / 86.4(7)	α-PbO_2	4.9886(10)	5.9524(11)	5.4600(8)	0.0508
		β-PbO_2	4.9522(3)	–	3.38217(18)	0.0200 /0.0734, 0.101, 0.0760
0.1 M $Pb(NO_3)_2$ + 1 M HNO_3 +3 × 10^{-5} M SDS	18.6(2) / 81.4(6)	α-PbO_2	4.9398(8)	5.9493(9)	5.4629(7)	0.0521
		β-PbO_2	4.9563(3)	–	3.3840(2)	0.0202 /0.0682, 0.0924, 0.0678
0.1 M $Pb(NO_3)_2$ + 1 M HNO_3 + 7 × 10^{-4} M SDS	26.7(2) / 73.3(6)	α-PbO_2	4.9921(6)	5.9483(7)	5.4625(6)	0.0350
		β-PbO_2	4.9562(3)	–	3.3838(2)	0.0219 /0.0699, 0.0940, 0.0712

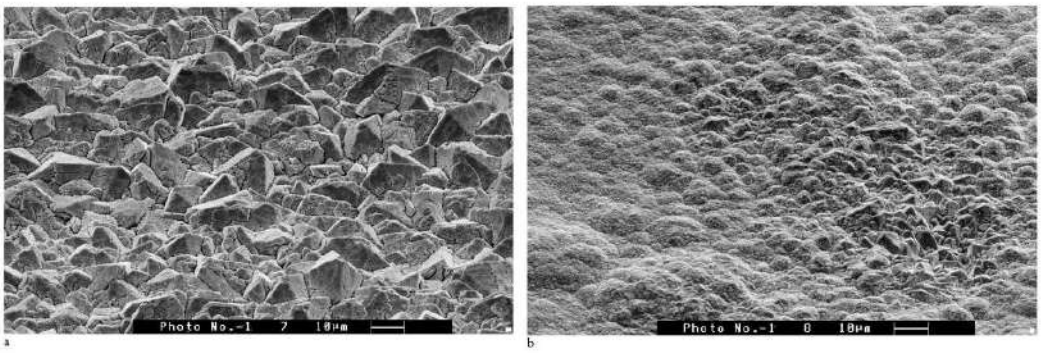

a b

Fig. 7. SEM micrographs of PbO_2-SDS composite materials: a – 1.5, b – 4.5 wt% $C_{12}H_{25}SO_4Na$.

As a result of potentiometric measurements (Fig. 4), it was established that the adsorption of $C_{12}H_{25}SO_4Na$ on PbO_2 is accompanied by a shift of the zero charge potential of the oxide to a region of higher pH. This suggests that adsorption proceeds without the participation of functional groups of both a surfactant and the oxide surface. The obtained data indicate the weak chemical adsorption of surfactant on lead dioxide [31], that is confirmed by a slight displacement of the zero charge potential of the oxide, which is 0.71 ± 0.1 V in 1.0 M HNO_3 [32].

The critical micelle concentration (CMC) of SDS was determined in order to establish whether micellization is present in the solution Its value in 0.1 M $Pb(NO_3)_2$ + 1.0 M HNO_3 solution amounts to 0.002 M. This is also confirms that all the working electrolytes were true solutions.

It was found that during electrodeposition of PbO_2 in the presence of $C_{12}H_{25}SO_4Na$ in the electrolyte, the additive is included in the growing deposit with the formation of a composite oxide-surfactant coating.

An increase in the surfactant concentration in the deposition electrolyte leads to the growth of the additive content in lead dioxide (Fig. 5). The observed effect is probably because of the adsorption of surfactant on lead dioxide, which also increases with increasing concentration. The content of the additive in the coating is likely to be determined by both thermodynamic parameters (the value of equilibrium adsorption on lead dioxide) and kinetic factors (the ratio of the rates of surfactant adsorption and desorption at the time of coating formation).

With increasing anode current density, the content of anionic surfactant in the deposit increases (see Fig. 5). This is explained by an increase in the Coulomb attraction forces between the positively charged surface of the electrode and the negatively charged anionic surfactant, which in turn leads to an increase in adsorption and, as a result, to an increase in the amount of additive in the oxide.

An increase in acid concentration in the deposition electrolyte also leads to an increase in the content of surfactant additive in lead dioxide (Table 3).

Thus, the introduction of additive into the growing coating of lead dioxide can be due to both volumetric and surface effects. Volume effects are negligible and will not affect the increase in the concentration of additives in the near-electrode zone. Surface effects are because the adsorption of additives both on the surface of lead dioxide electrode and on oxygen-containing lead particles formed in the near electrode zone [18,33]. It should be noted that the obtained experimental data on the influence of the deposition conditions and the composition of the solution on the additive content in the composite coating are in good qualitative agreement with the influence of these factors on the adsorption of substance on lead dioxide, i.e. an increase in adsorption leads to an increase in the content of surfactant in PbO_2 (an increase in the concentration of the additive or a positive oxide charge due to a decrease in the pH of the solution or an increase in the anode current density).

Lead dioxide is known to exist in both amorphous and crystalline forms [34]. Two of its allotropic forms are known: α-PbO_2, characterized by an elemental rhombic cell, and β-PbO_2, a tetragonal lattice of the rutile type. These forms differ greatly in crystal size and mechanical properties [35]. α-PbO_2 is known to have a more compact structure in comparison with β-PbO_2 [36]. Usually, electrodeposited coating is often composed of different phase structures of α − /β-PbO_2 [37].

We conducted X-ray powder diffraction method in order to investigate the effect of sodium dodecyl sulfate on the phase composition of electrodeposited PbO_2 and its texture. The XRPD data detected that all investigated samples contain two phases: α-PbO_2 (structure type $Fe_2N_{0.94}$, space group *Pbcn*) and β-PbO_2 (structure type TiO_2 rutile, space group $P4_2/mnm$). The difference is observed only in the ratio of these two phases and also in the degree of crystallinity (Table 4). Typical powder pattern of modified sample is shown in Fig. 6. As one can see from the data obtained, the addition of SDS to the nitrate electrolyte results in an almost twofold increase in the α-phase content of the coating.

As it is known, the surface of lead dioxide is a set of large polycrystalline blocks with a slightly pronounced preferential orientation. The inclusion of SDS in lead dioxide leads to a significant change in the morphology of the coating (Fig. 7).

Sample with 1.5 wt% SDS exhibits several zones with different surface morphologies: the central zone, in which large crystals are located (their size is several micrometers) and the peripheral one, containing only small crystals of submicron sizes. When the surfactant content in the composite is 4.5 wt%, the surface looks more or less homogeneous. The surface is, as it were, two-layer, when larger crystals of submicron sizes are coated with very small crystals of nanoscale having a spindle-shaped shape.

X-ray microanalysis of the surface of samples containing sodium dodecyl sulfate was performed in order to determine the amount and distribution of elements in electrodeposited composites (Fig. 8). Only Pb and O are visible (very few impurities). EDX spectra did not show an independent sulfur peak, probably due to the fact that its position practically coincides with the peak of lead in oxide. For a composite containing the maximum amount of sodium dodecyl sulfate, a distinct carbon peak appears on the EDX spectra. It should be noted that the maximum signal intensity is observed in areas covered by nanodeposit.

The electrocatalytic activity of the composites involved was investigated in respect to the oxygen evolution and oxidation of organic substances.

It is believed that there are some deviations from the ideal stoichiometry of PbO_2 that is imputed to the occurrence of lead cation disorder in the crystallographic structure, with cation vacancies forming interfaces (internal surfaces) between crystallographically ordered areas [38]. Each missing Pb^{4+} ion would be compensated by Pb^{2+} and OH^- ions, and the chemical composition is described by the formula $Pb^{4+}_{(1-x-y)}Pb^{2+}_{y}O^{2-}_{(2-4x-2y)}OH^-_{(4x+2y)}$. Especially in the case of electrochemically deposited films, the coefficients x and y can have high values [38].

The modification of lead dioxide very strongly affects the properties of the material and depends on the places where these additives are included in the oxide matrix, as has been shown in our earlier work [39].

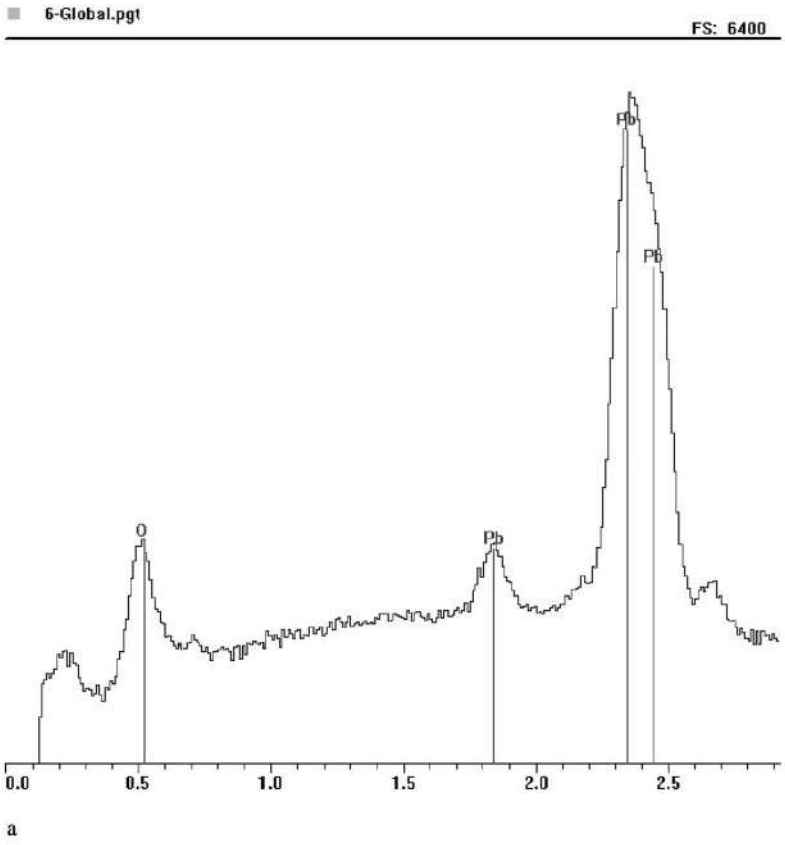

Fig. 8. EDX spectra obtained for PbO_2-SDS composite materials: a – 1.5, b – 4.5 wt% $C_{12}H_{25}SO_4Na$.

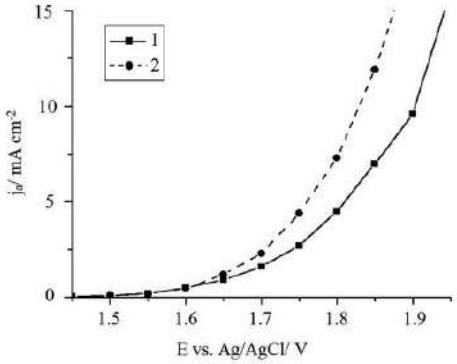

Fig. 9. Steady state polarization curves of oxygen evolution in 1 M H_2SO_4 (Scan rate 1 mV s^{-1}, t = 25°C) on PbO_2-electrodes, containing SDS, wt%: 0 (1), 4.2 (2). Coating electrodeposited on Ti/Pt sheet.

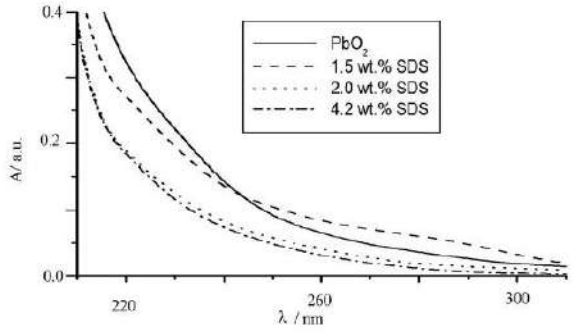

Fig. 10. Electronic absorption spectra of solutions (0.5 M Na_2SO_4 + phosphate buffer, pH = 7.0) with 0.1 mM initial concentration of 4-chlorophenol after 90 min of electrolysis on PbO_2, containing various amount of SDS.

The rate of oxygen evolution process can change because of nature and amount of additive [19,20,23,40]. Such change mainly depends on changes in chemical properties of oxide surface that, in turn, leads to bond strength change of oxygen-containing particles chemisorbed on the electrode surface.

Pavlov et al. [41] proposed the mechanism according to which the oxygen evolution occurs at active sites located in a hydrous layer on PbO_2. It is recognized that oxygen evolution reaction (OER) is limited by a second electron transfer (electrochemical desorption) [42] and depends on bond strength of oxygen-containing particles chemisorbed on the surface. Thus, an increase of bond strength of chemisorbed oxygen will lead to an increase of OER overvoltage [43].

According to obtained results (Fig. 9), oxygen overpotential on PbO_2-surfactant coatings decreases, as was observed in the case of cerium [23,40]. As one can conclude from calculated results, tafel slope significantly exceed the theoretical value, which indicates a decrease in the degree of filling of oxygen-containing particles on the surface of the electrode, probably due to blocking by sulfate ions.

It should be noted that during the modification of lead dioxide with various ions [19,20,23,40], surfactants [16–18,44], polymers [33], valve metal oxides [45], we did not find a direct relationship between the overvoltage of oxygen evolution and the degradation capability of the electrode material. So, for example, on PbO_2, modified with Co^{2+} [46], the overvoltage of oxygen evolution is lower than on a pure electrode, and the service life of the modified sample significantly exceeds the unmodified one. The modification of lead dioxide with TiO_2 has the same effect [45]. In this work, even in the processes of prolonged electrolysis, the modified sample in terms of stability was similar to the unmodified sample (constant potential over time, the absence of visible products of electrode destruction in the cell).

Phenolic compounds, in particular, 4-chlorophenol, was selected for estimation of electrocatalytic activity of the composites involved in oxidation of organic compounds. Such choice was due to the possibility of carrying out of kinetic investigations over the initial substance, since Beer–Lambert law maintains a linear relationship between absorbance and concentration of 4-chlorophenol (y = 1375.6x + 0.06097; r = 0,994). The main intermediate products formed during the anodic oxidation of 4-chlorophenol include benzquinone and maleic acid [47].

As has been shown in our recent publications [18,33], the initial solution of chlorophenol both on non-modified and modified electrodes is characterized by two peaks at 230 and 280 nm. At first, the electrolysis shows a decrease in the peak at 220 nm, as well as a slight increase in the peak at 280 nm and the appearance of the plateau at 240–270 nm, which is caused by a decrease in the concentration of 4-chlorophenol and accumulation of benzoquinone in the solution. A further increase in the time of electrolysis leads to the disappearance of the peaks at 220 and 280 nm, as well as the reduction of the plateau at 240–270 nm due to a decrease in the concentrations of both 4-chlorophenol and benzoquinone. Already after 4 h of electrolysis, the aromatic compounds are completely destroyed with the formation of only aliphatic electrolysis products (mainly maleic acid), that was evidenced by HPLC [18,23]. The 4-chlorophenol oxidation rate is significantly increased on PbO_2-SDS composites. Thus, already after 90 min of electrolysis on composites, contained 2 and 4.2 wt% SDS, all aromatic intermediates are destroyed, and only aliphatic acids are found in the solution (Fig. 10).

4. Conclusions

The addition of sodium dodecyl sulfate has a significant impact on the kinetics of lead dioxide electrodeposition, without changing the mechanism of the process. The presence of SDS in the deposition electrolyte leads to a slight inhibition of the deposition of lead dioxide.

The content of the additive in lead dioxide is determined mainly by its adsorption on the oxide. An increase in the adsorption of additive due to an increase in its concentration in the solution and an increase in electrostatic attraction (an increase in the anodic current density and the acid content in the deposition electrolyte) leads to the enrichment of the composite material with organic substance. It is possible to obtain a surfactant-oxide composite coating with the content of organic substance in the oxide up to 5.4 wt%.

The morphology and structure of composite materials differs significantly from lead dioxide. With an increase in the additive content in the composite, there is a transition from large-grained deposits to materials with submicron and nano-sized crystals.

Oxygen overpotential on PbO_2-SDS coatings decreases in comparison to non-modified sample because of a decrease in the degree of filling of oxygen-containing particles on the surface of the electrode, probably due to blocking by sulfate ions. The 4-chlorophenol oxidation rate is significantly increased on PbO_2-SDS composites. Thus, already after 90 min of electrolysis on composites, contained 2 and 4.2 wt% SDS, all aromatic intermediates are destroyed, and only aliphatic acids are found in the solution.

The authors declare that they have no conflict of interest.

Funding

This work was supported by Ministry of Education and Science of Ukraine.

Declaration of Competing Interest

The authors declare that they have no known competing financial interests or personal relationships that could have appeared to influence the work reported in this paper.

References

[1] F.C. Walsh, Modern developments in electrodes for electrochemical technology and the role of surface finishing, T. I. Met. Finish 97 (1) (2019) 28–42, https://doi.org/10.1080/00202967.2019.1551277.

[2] Y. Yang, M. Luo, W. Zhang, Y. Sun, X. Chen, S. Guo, Metal surface and interface energy electrocatalysis: fundamentals, performance, engineering and opportunities, Chem. 4 (9) (2018) 2054–2083, https://doi.org/10.1016/j.chempr.2018.05.019.

[3] M. Velicky, P.S. Toth, From two-dimensional materials to their heterostructures: an electrochemist's perspective, Appl. Mater. Today 8 (2017) 68–103, https://doi.org/10.1016/j.apmt.2017.05.003.

[4] F.C. Walsh, L.F. Arenas, C. Ponce de Leon, Developments in electrode design: structure, decoration and applications of electrodes for electrochemical technology, J. Chem. Technol. Biotechnol. 93 (11) (2018) 3073–3090, https://doi.org/10.1002/jctb.5706.

[5] X. Li, D. Pletcher, F.C. Walsh, Electrodeposited lead dioxide coatings, Chem. Soc. Rev. 40 (2011) 3879–3894, https://doi.org/10.1039/COCS00213E.

[6] M. Krishna, E.J. Fraser, R.G.A. Wills, F.C. Walsh, Developments in soluble lead flow batteries and remaining challenges: an illustrated review, J. Energy Storage 15 (2018) 69–90, https://doi.org/10.1016/j.est.2017.10.020.

[7] P. Perret, Z. Khani, T. Brousse, D. Belanger, D. Guay, Carbon/PbO_2 asymmetric supercapacitor based on methanesulfonic acid electrolyte, Electrochim. Acta 56 (24) (2011) 8122–8128, https://doi.org/10.1016/j.electacta.2011.05.125.

[8] A.R.C. Bredar, A.L. Chown, A.R. Burton, B.H. Farnum, Electrochemical impedance spectroscopy of metal oxide electrodes for energy applications, ACS Appl. Energy Mater. 3 (1) (2020) 66–98, https://doi.org/10.1021/acsaem.9b01965.

[9] T. Iwai, M. Murakami, S. Takai, T. Yabutsuka, T. Yao, Chemical transformation of PbO_2 due to local cell reaction on the cathode of lead acid battery, J. Alloys Compd. 780 (2019) 85–89, https://doi.org/10.1016/j.jallcom.2018.11.248.

[10] L. Lu, J.Th.M. De Hosson, Y. Pei, Three-dimensional micron-porous graphene foams for lightweight current collectors of lithium-sulfur batteries, Carbon 144 (2019) 713–723 doi:10.1016/j.carbon.2018.12.103.

[11] K. Lee, A. Mazare, P. Schmuki, One-dimensional titanium dioxide nanomaterials: nanotubes Chem, Rev. 114 (19) (2014) 9385–9454 doi:10.1021/cr500061m.

[12] Z.-X. Cai, Z.-L. Wang, J. Kim, Y. Yamauchi, Hollow functional materials derived from metal–organic frameworks: synthetic strategies, conversion mechanisms, and electrochemical applications, Adv. Mater. 31 (2019) 1804903 doi:10.1002/adma.201804903.

[13] F. Guo, S. Aryana, Y. Han, Y. Jiao, A review of the synthesis and applications of polymer–nanoclay composites, Appl. Sci. 8 (2018) 1696 doi:10.3390/app8091696.

[14] C. Cao, Z. Cao, P. Yu, Yu. Zhao, Genome-wide identification for genes involved in sodium dodecyl sulfate toxicity in Saccharomyces cerevisiae, BMC Microbiol. 20 (2020) 34, https://doi.org/10.1186/s12866-020-1721-2.

[15] X. Li, H. Xu, W. Yan, Effects of twelve sodium dodecyl sulfate (SDS) on electro-catalytic performance and stability of PbO_2 electrode, J. Alloys Compd. 718 (2017) 386–395, https://doi.org/10.1016/j.jallcom.2017.05.147.

[16] T. Luk'yanenko, O. Shmychkova, L. Dmitrikova, L. Borschevich, A. Velichenko, The composition and electrocatalytic activity of composite PbO_2-surfactant electrodes, Voprosy khimii i khimicheskoi tekhnologii 5 (2019) 65–70, https://doi.org/10.32434/0321-4095-2019-126-5-65-70.

[17] T.V. Luk'yanenko, O.B. Shmychkova, C.V. Yanova, N.I. Krivonosova, A.B. Velichenko, The synthesis and electrocatalytic activity of PbO_2-polyelectrolyte and PbO_2-surfactant composite coatings, J. Chem. Technol. 27 (1) (2019) 92–100, https://doi.org/10.15421/081910.

[18] T. Luk'yanenko, O. Shmychkova, A. Velichenko, PbO_2-surfactant composites: electrosynthesis and catalytic activity, J. Solid State Electrochem. (2020) https://doi.org/10.1007/s10008-020-04572-8.

[19] O. Shmychkova, T. Luk'yanenko, R. Amadelli, A. Velichenko, Electrodeposition of Ni^{2+}-doped PbO_2 and physicochemical properties of the coating, J. Electroanal. Chem. 774 (2016) 88–94, https://doi.org/10.1016/j.jelechem.2016.05.017.

[20] O. Shmychkova, T. Luk'yanenko, A. Velichenko, L. Meda, R. Amadelli, Bi-doped PbO_2 anodes: electrodeposition and physico-chemical properties, Electrochim. Acta 111 (2013) 332–338, https://doi.org/10.1016/j.electacta.2013.08.082.

[21] J.W. Robinson, E.M.S. Frame, G.M. Frame II in Undergraduate instrumental analysis, seventh ed Marcel Dekker CRC Press, New York, 2014.

[22] B. Damaskin, Adsorption of Organic Compounds on Electrodes, Plenum Press, Springer, US, NY, 1971.

[23] O.B. Shmychkova, T.V. Luk'yanenko, R. Amadelli, A.B. Velichenko, PbO_2 anodes modified by cerium ions, Prot. Met. Phys. Chem. Surf. 50 (2014) 493–498, https://doi.org/10.1134/S2070205114040169.

[24] M. Fleischmann, M. Liler, The anodic oxidation of solutions of plumbous salts. Part 1. The kinetics of deposition of α-lead dioxide from acetate solutions, Trans. Faraday Soc. 54 (1958) 1370–1381, https://doi.org/10.1039/TF9585401370.

[25] H. Chang, D.C. Johnson, Electrocatalysis of anodic oxygen-transfer reaction. Chronoamperometric and voltammetric studies of the nucleation and electrodeposition of β-lead dioxide at a rotated gold disk electrode in acidic media, J. Electrochem. Soc. 136 (1989) 17–22, https://doi.org/10.1149/1.2096581.

[26] A.B. Velichenko, D.V. Girenko, F.I. Danilov, Mechanism of lead dioxide electrodeposition, J. Electroanal. Chem. 405 (1–2) (1996) 127–132, https://doi.org/10.1016/0022-0728(95)04401-9.

[27] A.B. Velichenko, E.A. Baranova, D.V. Girenko, R. Amadelli, S.V. Kovalev, F.I. Danilov, Mechanism of electrodeposition of lead dioxide from nitrate solutions, Russ. J. Electrochem. 39 (2003) 615–621, https://doi.org/10.1023/A:1024101210790.

[28] R. Inguanta, S. Piazza, C. Sunseri, Growth and characterization of ordered PbO_2 nanowire arrays, J. Electrochem. Soc. 155 (2008) K205–K210, https://doi.org/10.1149/1.2988728.

[29] V. Saez, E. Marchante, M.I. Diez, M.D. Esclapez, P. Bonete, T. Lana-Villarreal, J. Gonzalez Garcia, J. Mostany, A study of the lead dioxide electrocrystallization mechanism on glassy carbon electrodes. Part I: Experimental conditions for kinetic control, Mater. Chem. Phys. 125 (2011) 46–54, https://doi.org/10.1016/j.matchemphys.2010.08.069.

[30] N.V. Nikolenko, Surface properties of calcite: Adsorbtion model with the orbital control, Adsorpt. Sci. Technol. 19 (3) (2001) 237–244, https://doi.org/10.1260/026361701494123.

[31] N.V. Nikolenko, E.E. Esajenko, Surface properties of synthetic calcium hydroxyapatite, Adsorpt. Sci. Technol. 23 (2005) 543–553, https://doi.org/10.1260/026361705775212466.

[32] S.A. Campbell, L.M. Peter, Detection of soluble intermediates during deposition and reduction of lead dioxide, J. Electroanal. Chem. 306 (1991) 185–194, https://doi.org/10.1016/0022-0728(91)85230-M.

[33] A. Velichenko, T. Luk'yanenko, N. Nikolenko, O. Shmychkova, P. Demchenko, R. Gladyshevskii, Composite electrodes PbO_2-Nafion®, J. Electrochem. Soc. 167 (2020), 063501. https://doi.org/10.1149/1945-7111/ab805f.

[34] M.E. Herron, D. Pletcher, F.C. Walsh, A combined electrochemical and in-situ X-ray diffraction study of the cycling of well-defined lead dioxide layers on platinum, J. Electroanal. Chem. 332 (1–2) (1992) 183–197, https://doi.org/10.1016/0022-0728(92)80350-D.

[35] A.B. Velichenko, D. Devilliers, Electrodeposition of fluorine-doped lead dioxide, J. Fluor. Chem. 128 (2007) 269–276, https://doi.org/10.1016/j.jfluchem.2006.11.010.

[36] U. Casellato, S. Cattarin, M. Musiani, Preparation of porous PbO_2 electrodes by electrochemical deposition of composites, Electrochim. Acta 48 (2003) 3991–3998, https://doi.org/10.1016/S0013-4686(03)00527-9.

[37] O. Shmychkova, T. Luk'yanenko, A. Piletska, A. Velichenko, R. Gladyshevskii, P. Demchenko, R. Amadelli, Electrocrystallization of lead dioxide: influence of early stages of nucleation on phase composition, J. Electroanal. Chem. 746 (2015) 57–61, https://doi.org/10.1016/j.jelechem.2015.03.031.

[38] P. Ruetschi, R. Giovanoli, On the presence of OH^- ions, Pb^{2+} ions and cation vacancies in PbO_2, Power Sources 13 (1991) 81–97.

[39] R. Amadelli, L. Armelao, E. Tondello, S. Daolio, M. Fabrizio, C. Pagura, A. Velichenko, SIMS and XPS study about ions influence on electrodeposited PbO_2 films, Appl. Surf. Sci. 142 (1999) 200–203, https://doi.org/10.1016/S0169-4332(98)00707-7.

[40] O. Shmychkova, T. Luk'yanenko, A. Velichenko, R. Amadelli, Electrodeposition of Ce-doped PbO_2, J. Electroanal. Chem. 706 (2013) 86–92, https://doi.org/10.1016/j.jelechem.2013.08.002.

[41] D. Pavlov, B. Monahov, D. Petrov, Influence of Ag as alloy additive on the oxygen evolution reaction on Pb/PbO_2 electrode, J. Power Sources 85 (2000) 59–62, https://doi.org/10.1016/S0378-7753(99)00383-3.

[42] S. Trasatti, G. Lodi, Electrodes of Conductive Metallic Oxides. Part B, Elsevier, Amsterdam, Holland, 1981.

[43] O. Shmychkova, T. Luk'yanenko, L. Dmitrikova, A. Velichenko, Modified lead dioxide for organic wastewater treatment: physico-chemical properties and electrocatalytic activity, J. Serb. Chem. Soc. 84 (2019) 187–198, https://doi.org/10.2298/JSC180712091S.

[44] A. Velichenko, T. Luk'yanenko, O. Shmychkova, L. Dmitrikova, Electrosynthesis and catalytic activity of PbO_2-fluorinated surfactant composites, J. Chem. Technol. Biotechnol. (2020)https://doi.org/10.1002/jctb.6483.

[45] A. Velichenko, V. Knysh, O. Shmychkova, T. Luk'yanenko, The composition and properties of composite PbO_2-TiO_2 materials electrodeposited from colloidal methanesulfonate electrolytes, Voprosy Khimii i Khimicheskoi Tekhnologii 4 (2017) 14–20.

[46] R. Amadelli, A. Velichenko, Lead dioxide electrodes for high potential anodic processes, J. Serb. Chem. Soc. 66 (2001) 835–845, https://doi.org/10.2298/jsc0112835a.

[47] O. Shmychkova, T. Luk'yanenko, L. Dmitrikova, A. Velichenko, Electrooxidation of 4-clorphenol on modified lead dioxide anodes, Voprosy Khimii i Khimicheskoi Tekhnologii 3 (2018) 50–57, https://doi.org/10.32434/0321-4095-2019-126-5-65-70.

68 ISSN 0321-4095, Voprosy khimii i khimicheskoi tekhnologii, 2021, No. 5, pp. 68-76

UDC 544.1;544.41,544.47,544.65:544.4,541.138/.138.3

V. Knysh [a], O. Shmychkova [a], T. Luk'yanenko [a], L. Dmitrikova [b], A. Velichenko [a]

ELECTROSYNTHESIS AND CHARACTERIZATION OF LEAD DIOXIDE–PERFLUOROBUTANESULFONATE COMPOSITE

[a] Ukrainian State University of Chemical Technology, Dnipro, Ukraine
[b] Dnipro State Medical University, Dnipro, Ukraine

The effect of potassium perfluorobutanesulfonate on the kinetic features of electrodeposition of lead dioxide from methanesulfonate electrolytes has been investigated. The introduction of $C_4F_9SO_3K$ into the lead dioxide deposition electrolyte leads to insignificant inhibition of the Pb^{2+} electrooxidation process, while the mechanism of the process does not change. A composite coating is formed upon deposition of coatings from electrolytes containing surfactants. The surface of a composite material consists of a mixture of clearly expressed large crystalline blocks with sharp angles and small crystals. Energy dispersive X-ray analysis revealed the satisfactory distribution of modifying elements in the entire sample bulk, and not only on the coating surface. It was shown that the electrocatalytic activity of lead dioxide–perfluorobuthanesulfonate composite differs from the undoped sample. The oxygen evolution reaction slightly decelerates on a PbO_2–$C_4F_9SO_3K$ composite. The Tafel slopes in 1 M $HClO_4$ calculated from these curves plotted in semilogarithmic coordinates are 136 and 145 mV dec^{-1} for undoped sample and lead dioxide-surfactant composite, respectively. The reaction of electrochemical oxidation of p-chlorophenol is characterized by the pseudo-first order kinetics with respect to the initial compound. The use of doped $C_4F_9SO_3K$ lead dioxide as an anode leads to the inhibition of the process of oxygen evolution and an almost one and a half higher rate of electrochemical conversion of 4-chlorophenol to aliphatic compounds.

Keywords: lead dioxide, methanesulfonate electrolyte, surfactant, electrodeposition, 4-chlorophenol.

DOI: 10.32434/0321-4095-2021-138-5-68-76

Introduction

Development of methods for direct synthesis of new materials with predicted properties is one of the priority challenges of modern electrochemistry [1]. It should be noted that the fabrication of composite materials is recognized to be the most promising method due to possibility to change the functional properties in a wide range by variations in the nature of dispersed phase [2]. Despite the large number of methods for the synthesis of composite materials, electrochemical ones are considered the most promising due to the simplicity of their implementation and relatively small energy losses as compared with sol-gel method and other techniques [3]. This method opens wide opportunities for influencing the composition and properties of materials by changing the conditions of electrolysis and electrolyte composition. Lead (IV) and manganese (IV) oxides are known as typical representatives of such materials, which due to the simplicity of their electrochemical synthesis, high corrosion resistance and relatively low cost are widely used in electrocatalysis, electroplating and electrochemical energy, lead-acid batteries, flowing redox energy storage devices, asymmetric supercapacitors, and primary and secondary current sources [4]. The inclusion of fluorinated compounds in the metal-oxide matrix ensures anti-static, anti-adhesive, and anti-corrosion properties and at the same time, they retain the following properties of the metal-oxide: high electrical conductivity, resistance to mechanical wear and good adhesion to the substrate.

Per- and polyfluoroalkyl substances are synthetic organofluorine chemical compounds that have several fluorine atoms attached to an alkyl chain.

As such, they contain at least one perfluoroalkyl moiety, $C_nF_{2n}-$ [5]. Fluorinated surfactants can reduce the surface tension of water to a value that is half that which can be obtained using hydrocarbon surfactants [6]. This ability is due to the lipophobic nature of fluorocarbons, since fluorinated surfactants tend to concentrate at the liquid–air interface [7]. They are not as sensitive to London dispersion force, which contributes to lipophilicity, since the electronegativity of fluorine reduces the polarizability of surfactants with a fluorinated surface.

However, in nitrate electrolytes it is not possible to produce coatings with a thickness of over 100 μm, which possess a satisfactory mechanical stability. In this regard, in the present paper, the possibility of electrodeposition of PbO_2-fluorinated surfactant composites from methanesulfonate electrolytes has been considered. Methanesulfonic acid is a green acid with a remarkably high solubility of majority of metals including lead, making it an interesting leaching agent for metals. It is safer and less toxic than the mineral acids (HCl, H_2SO_4, HNO_3) and intensively employed for leaching metals from primary and secondary sources [8]. It has previously been shown [9], that PbO_2 coatings up to 2 mm thick with satisfactory mechanical properties can be prepared in these media.

Therefore, in this work, we studied the kinetics of electrodeposition of lead dioxide in the presence of potassium perfluorobutanesulfonate as a dopant in methanesulfonate electrolyte and determined the electrocatalytic activity of the fabricated oxide materials.

Materials and methods

All chemicals were reagent grade. Kinetics of electrodeposition of doped lead dioxide was studied on a Pt rotating disk electrode (Pt–RDE, 0.19 cm^2) by steady-state voltammetry and chronoamperometry. For the RDE experiments, the voltammetry system SVA–1BM was used. The potential scan rate was varied within the range of 1 to 100 mV s^{-1} depending on purposes of the experiments. Before each experiment, the electrode surface was treated with a freshly prepared mixture (1:1) of concentrated H_2SO_4 and H_2O_2 [9]. Such preliminary treatment technique permits to stabilize the electrode surface and provides the reproducibility of cyclic voltammograms in a supporting electrolyte (0.11 M CH_3SO_3H). Voltammetry measurements were carried out in a standard temperature-controlled three-electrode cell. Temperature was maintained at 25±1°C. All potentials were recorded and reported vs. Ag/AgCl/KCl(sat.) reference electrode.

Electrodeposition was studied in 0.11 M CH_3SO_3H+0.01 M $Pb(CH_3SO_3)_2$ solution. Surfactant was added into the deposition electrolyte as aqueous solutions (0.0003 M). Due to low concentrations of surfactant, the composition of the electrolyte may significantly change during deposition; therefore, the concentration of surfactant was chosen at which, according to the adsorption isotherm, a 100% degree of surface filling is observed, which ensures that the electrolyte composition will not significantly change even if the surfactant is consumed.

The current efficiency and partial current of lead dioxide deposition ($I_{Pb(II)}$) were determined according to method described in detail previously [10].

Surface morphology of lead dioxide anodes was studied by scanning electron microscopy (SEM) with Stereoscan 440 LEO microscope. X-ray powder diffraction (XRPD) data were collected in the transmission mode on a STOE STADI P diffractometer with the following setup: Cu $K_{\alpha 1}$-radiation, curved Ge (1 1 1) monochromator on primary beam, 2θ/ω-scan, angular range for data collection of 20.000–110.225° 2θ with increment of 0.015, linear position sensitive detector with the step of recording of 0.480° 2q and times per step of 130–250 s, U=40 kV, I=30 mA, and T=294 K. A calibration procedure was performed utilizing SRM 640b (Si) and SRM 676 (Al_2O_3) NIST standards. Preliminary data processing and X-ray qualitative phase analysis were performed using STOE WinXPOW and PowderCell program packages. Crystal structures of the phases were refined by the Rietveld method with the program FullProf.2k, using a pseudo-Voigt profile function and isotropic approximation for the atomic displacement parameters, together with quantitative phase analysis. Microstructural parameters (i.e., size of coherently diffracting domains accepted as average apparent crystallite size D, and average maximum strain ε) were identified by isotropic line broadening analysis using simplified integral breadth methods for reflections with maximal intensities: (110) for α-PbO_2 and (111) for β-PbO_2.

The determination of the concentration of surfactant in aqueous solutions was conducted according to the procedure described elsewhere [10]. Adsorption measurements were carried out using 0.5 g of PbO_2 powder (Merck) in 0.1 M HCl solutions containing various amounts of additive. The measurements were performed in the presence of an indifferent electrolyte (0.1 M KCl), which screened the electrostatic field of the oxide surface. The time to establish the adsorption equilibrium was 24 hours. Adsorption parameters were calculated using the

Frumkin equation [11].

Platinized titanium was used as a sheet during investigation of electrocatalytic activity of materials. It was treated accordingly before platinum layer depositing [9].

Oxygen evolution reaction was investigated by steady-state polarization on computer controlled EG & G Princeton Applied Research potentiostat model 273A in 1 M H_2SO_4.

The electrooxidation of organic compounds was carried out in a divided cell at j_a=50 mA cm^{-2}. The volume of anolyte was 130 cm^3. Solution containing phosphate buffer (0.25 M Na_2HPO_4+0.1 M KH_2PO_4)+$2\cdot10^{-4}$ M organic compound (pH 6.55) was used as anolyte; phosphate buffer served as catholyte. Stainless steel was used as cathode. Composite PbO_2–surfactant electrodes were used as anodes. Electrode surface area was 2.5 cm^2.

The change of the concentration of the organic substance during the electrolysis was measured by sampling (volume of 5 cm^3) at regular intervals and measuring the absorbance of the solution in the ultraviolet and visible region (the wavelength range of 200–350 nm) using a Kontron Uvikon 940 spectrometer.

Analyses of the reaction products were conducted by high performance liquid chromatography (HPLC) using a Shimadzu RF-10A xL instrument equipped with an Ultraviolet SPD-20AV detector and a 30 cm Discovery® C18 column.

Results and discussion

The introduction of $C_4F_9SO_3K$ into the lead dioxide deposition electrolyte leads to insignificant inhibition of the Pb^{2+} electrooxidation process, while the mechanism of the process does not change. This mechanism was described and discussed in detail in our previous publication [10], where lead dioxide–surfactant composites were deposited from a nitrate medium.

Chronoamperograms were obtained on a Pt disk electrode in order to investigate the initial stages of deposition of lead dioxide in the presence of perfluorobutanesulfonate in solution. A typical j–t curve of PbO_2 deposition can be characterized by several features and fully consistent with the transients recorded and described in detail by Abyaneh et al. [12] during the electrocrystallization of PbO_2 onto a vitreous carbon electrode from nitrate solutios and in our previous paper [13] concerning the initial stages of lead dioxide nucleation. The electrocrystallization model proposed by Abyaneh and Gonzalez-Garcia [12] was selected as appropriate one for investigation of initial stages of the formation of a new PbO_2 phase. This model gives a rather complete description and provides means for understanding phase formation, in the sense that it allows determining kinetic parameters of nucleation for both α- and β-phases from an analysis of current–time transients. It was previously shown that such model is appropriable for both methanesulfonate and nitrate electrolytes [13]. The main parameters of lead dioxide crystallization from methanesulfonate electrolyte (Table 1) were calculated based on the model [12] for progressive mechanism with simultaneous formation of α- and β-phases of PbO_2.

In accordance to [13], one can observe either the predominance of one phase over another or ingesting of growing centers of one phase by another, depending on the composition of electrolyte. The formation of one phase is noticeably lagged behind the other. In present work, there is a slight predominance of the growth of β-phase of PbO_2 both for undoped sample and for lead dioxide–surfactant composite. Phase growth is inhibited by a surfactant due to surface blocking, which does not contradict existing models of electrocrystallization [13].

On the one hand, the mechanism of electrodeposition can be adequately described using the classical four-stage scheme of electrodeposition [9,10], according to which surfactant adsorption occurs on the surface of growing PbO_2, and the change in the surfactant content in the coating can be caused by two factors: (i) heterogeneous and (ii) migratory. On the other hand, we cannot exclude that not only crystallization occurs from a supersaturated solution bulk, but also colloidal particles are formed which adhere to the surface of growing crystals. It should be noted that it is possible

Table 1

Parameters of initial stages of lead dioxide electrocrystallization*

Deposition electrolyte	t_α / s	K_α / mol m^{-2} s^{-1}	t_β / s	K_β / mol m^{-2} s^{-1}
0.1 M Pb^{2+}+0.1 M CH_3SO_3H	0.54	$3.40\cdot10^{-5}$	1.65	$1.02\cdot10^{-4}$
0.1 M Pb^{2+}+0.1 M CH_3SO_3H+$3\cdot10^{-4}$ $C_4F_9SO_3K$	0.57	$4.46\cdot10^{-5}$	1.88	$0.82\cdot10^{-4}$

Note: K_α is the rate constant of growth of α-phase crystals in a direction perpendicular to the electrode surface; t_α is time corresponding to the beginning of α-phase formation; K_β is the rate constant of growth of β-phase crystals in a direction perpendicular to the electrode surface; t_β is the time corresponding to the beginning of β-phase formation.

that all the described effects can be realized simultaneously with different contributions. All these hypotheses do not contradict the obtained experimental data.

Adsorption measurements were performed on a lead dioxide powder at zero charge potential [14]. The adsorption of surfactant is satisfactorily described by the Frumkin isotherm (correlation factor 0.996). The value of interaction parameter calculated from above mentioned dependence is unity, which evidences a slight interaction between adsorbed molecules. The value of the energy of adsorption interaction ($-\Delta G$) is 33.2 kJ mol^{-1}, indicating the specific character of adsorption. The adsorption of $C_4F_9SO_3K$ on PbO_2 is accompanied by a shift of pH_0 (zero charge pH) of the oxide to a region of higher value: from 7.4 for naked PbO_2 to 7.6 for PbO_2–2 wt.% $C_4F_9SO_3K$, which was discussed in detail in our previous publication [10].

The effect of deposition conditions (current density, temperature, and concentration of dopants in the electrolyte) on the composition of lead dioxide–surfactant composites, fluorine-containing surfactants in particular were investigated in works

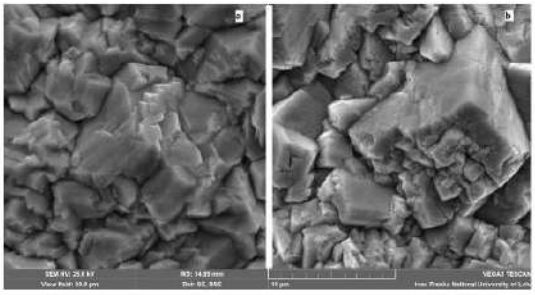

Fig. 1. SEM images of composite surfaces obtained from the following solutions: a – 0.1 M $Pb(CH_3SO_3)_2$+0.11 M CH_3SO_3H; b – 0.1 M $Pb(CH_3SO_3)_2$+0.11 M CH_3SO_3H+0.0003 M $C_4F_9SO_3K$

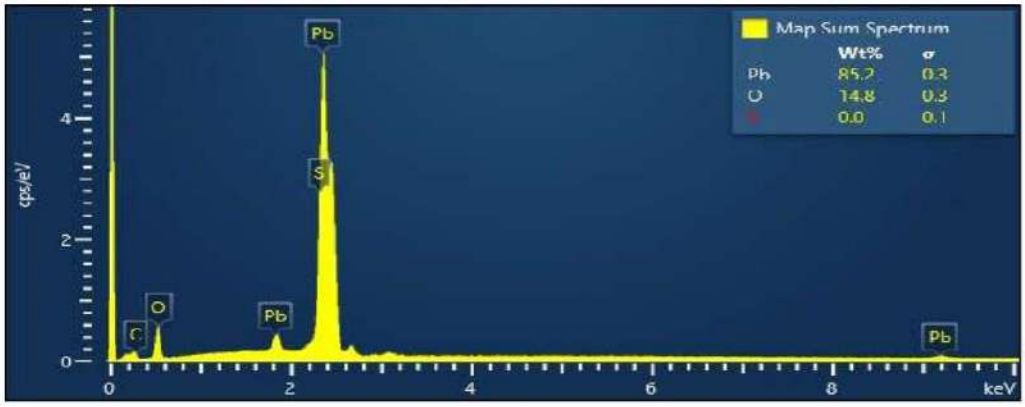

a

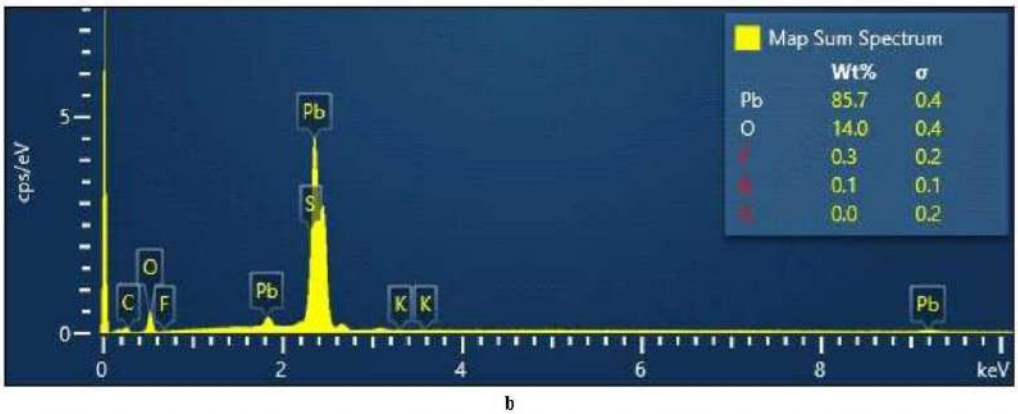

b

Fig. 2. EDX spectra of composites obtained from the following solutions: a – 0.1 M $Pb(CH_3SO_3)_2$+0.11 M CH_3SO_3H; b – 0.1 M $Pb(CH_3SO_3)_2$+0.11 M CH_3SO_3H+0.0003 M $C_4F_9SO_2K$

[9,10]. It was found that the surfactant content in the composite weakly depends on its concentration in the deposition electrolyte. At high surfactant concentrations in the electrolyte, the active centers of oxide are blocked by the surfactant, which leads to a decrease in electrical conductivity and deterioration of the mechanical properties. Low surfactant concentrations in the electrolyte deposition have weak effect on the catalytic activity of the coating. Having in mind these effects, the optimal concentration of perfluorobutanesulfonate in solution was chosen. At this concentration, the content of surfactant in the resulting coating was 2 wt.%.

The inclusion of surfactants in a growing coating led to a change in the texture and structure of the resulting film [10]. Surface morphology of the investigated samples is depicted in Fig. 1.

As can be seen, large crystalline blocks with sharp angles and small crystals are clearly expressed in the case of lead dioxide–perfluorobutanesulfonate

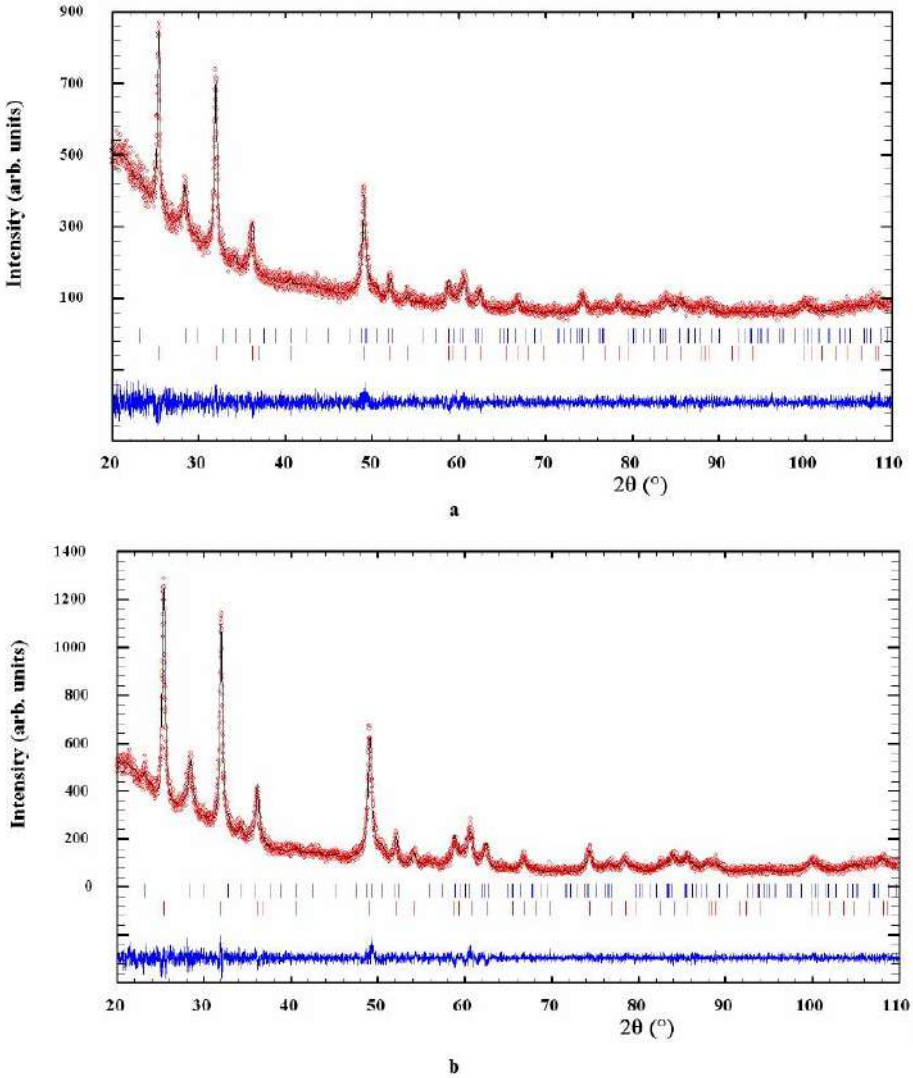

Fig. 3. Observed and calculated X-ray powder profiles for composite surfaces obtained from the following solutions: a – 0.1 M $Pb(CH_3SO_3)_2$+0.11 M CH_3SO_3H; b – 0.1 M $Pb(CH_3SO_3)_2$+0.11 M CH_3SO_3H+0.0003 M $C_4F_9SO_3K$. Experimental data (circles) and calculated profile (solid line through the circles) are presented together with the calculated Bragg positions (vertical ticks) and difference curve (bottom solid line). Upper ticks: α-PbO_2, bottom ticks: β-PbO_2

composite, which is typical of lead dioxide–surfactant coatings deposited from nitrate electrolytes [10] (Fig. 1,b). The surface of the unmodified sample is more ordered, large and small crystals are evenly distributed (Fig. 1,a).

SEM/EDAX experiments (Fig. 2) were performed to evaluate the amount and distribution of chemical elements in a electrodeposited composite. Low peaks corresponding to O and F indicate a satisfactory distribution of modifying elements in the entire sample bulk, and not only on the coating surface. In addition, it was not possible to detect the sulfur peak due to proximity of the very intense lead peak.

All investigated samples contain two phases (as detected by XRPD): α-PbO_2 (structure type $Fe_2N_{0.94}$, space group *Pbcn*) and β-PbO_2 (structure type TiO_2 rutile, space group $P4_2/mnm$). The difference is observed only in the ratio of these two phases and also in the degree of crystallinity (Fig. 3, Table 2).

As one can see, both investigated samples have the higher β-phase amount, which is twice bigger than α-phase amount. The presence of surfactant leads to small fluctuations in the phase composition of the resulting coatings.

It is widely recognized [15] that oxide surface consists of crystal (PbO_2) and hydrated [$PbO(OH)_2$] zones which are in equilibrium, and the latter is a rather open structure which can exchange cations and anions. From the point of view of the phase composition, no obvious changes are observed in the crystalline zone of the oxide, but this does not exclude changes in the composition of the oxide in the hydrated zone, which could explain the electrocatalytic activity of the coatings involved. Such phase composition (as XPRD investigation provides information about crystal phase) is an indirect confirmation that the main changes in the composition occur in the hydrated zone of the oxide.

The electrocatalytic activity of lead dioxide deposited from a methanesulfonic solution containing surfactant was studied both in the oxygen evolution

Table 2

Phase composition, crystallographic data and microstructural parameters of the investigated samples

Sample description	Phase	Content (wt.%)	Lattice parameters, Å			Unit cell volume, Å^3	Reliability factors R_I/R_P, R_{WP}, R_{EXP}, χ^2	D, Å/ε*
			a	b	c	V		
PbO_2	α-PbO_2	33(6)	4.997(4)	5.963(5)	5.457(4)	162.6(2)	0.0613	184/0.0085
	β-PbO_2	67(4)	4.9588(10)	–	3.3862(7)	83.27(3)	0.0356/0.0615, 0.0812, 0.0839, 0.94	247/0.0071
PbO_2–$C_4F_9KO_3S$	α-PbO_2	38(7)	5.000(3)	5.955(4)	5.453(3)	162.38(18)	0.0308	131/0.0120
	β-PbO_2	62(4)	4.9578(6)	–	3.3847(5)	83.195(19)	0.0229/0.0589, 0.0773, 0.0773, 1.0	227/0.0077

Note: meaning of parameters see in Materials and methods section.

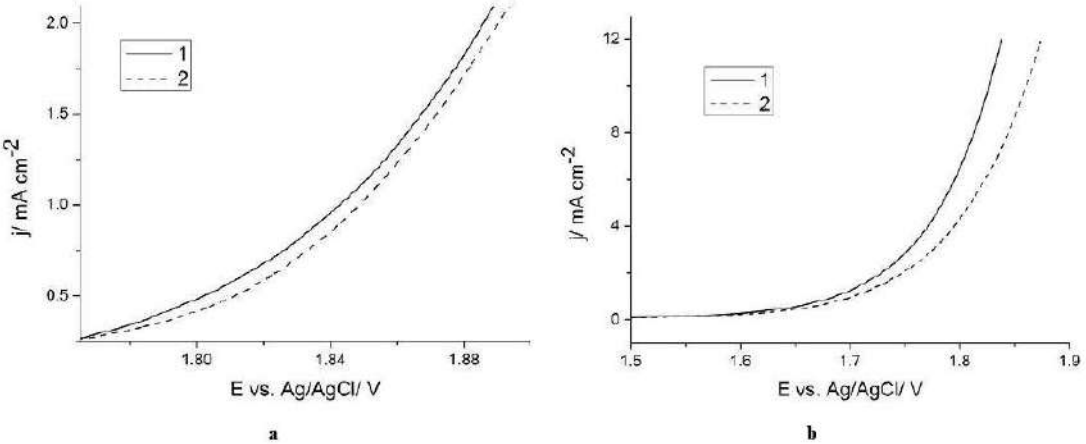

Fig. 4. Steady state polarization curves of oxygen evolution in 1 M $HClO_4$ (a) and phosphate buffer (b) (scan rate 1 mV s^{-1}, t=25°C) on PbO_2 electrodes deposited from the following solutions: 0.1 M $Pb(CH_3SO_3)_2$+0.11 M CH_3SO_3H (1); 0.1 M $Pb(CH_3SO_3)_2$+0.11 M CH_3SO_3H+0.0003 M $C_4F_9SO_3K$ (2). Coating were electrodeposited on Ti/Pt sheet

reaction and in the oxidation of 4-chlorophenol. As follows from the steady state polarization curves (Fig. 4), the oxygen evolution reaction slightly decelerates on a PbO_2–$C_4F_9SO_3K$ composite. The Tafel slopes were calculated from these curves plotted in semilogarithmic coordinates: they are 136 and 145 mV dec^{-1} for undoped sample and lead dioxide–surfactant composite in 1 M $HClO_4$, respectively; and 140 and 157 mV dec^{-1} in phosphate buffer, respectively.

Two processes occur in the investigated solutions: (i) oxygen evolution and (ii) oxidation of the organic compound, which proceeds at the limiting current density due to a relatively low concentration of 4-chlorophenol. The oxygen evolution is an undesirable side process; so one should be interested in the factors inhibiting this process. The kinetics of oxygen evolution on lead dioxide has been well studied by Pavlov et al. [15]. In order to increase the selectivity of the target process (oxidation of 4-chlorophenol), it is necessary to increase the Tafel slope of the oxygen evolution process, since this process is limited by the charge transfer stage, and the target oxidation process of the organic compound is controlled by diffusion kinetics. This effect can be achieved by modifying the lead dioxide surface with perfluorobutanesulfonate.

The inhibition of oxygen evolution and an increase in the Tafel slope in the case of a lead dioxide–perfluorobuthanesulfonate sample is probably due to the blocking of the surface by the surfactant, as is observed in sulfate solutions. The shift of the oxygen evolution potential to the region of lower potentials on both samples in a buffer solution is associated with a change in the electrolyte pH.

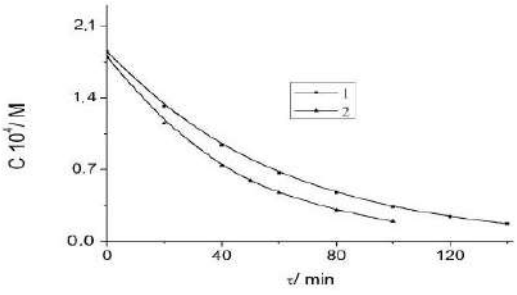

Fig. 5. Time dependences of 4-chlorophenol concentration during the electrochemical oxidation on the following electrodes: 1 – PbO_2; 2 – PbO_2–$C_4F_9SO_3K$

Fig. 5 shows dependences concentration of 4-chlorophenol versus time during the electrochemical oxidation. Plotting them in the corresponding coordinates reveals the pseudo first order of the reaction with respect to the initial compound.

As it was established earlier, the rate of oxidation of organic compounds increases significantly in the case of modification of lead dioxide with a fluorinated surfactant [10] or a polymer [9]. The same effect is observed in the present work. Thus, the conversion rate of 4-chlorophenol on lead dioxide–perfluorobuthanesulfonate composite is 1.3 times higher than on unmodified sample (Table 3).

Table 3

The rate of 4-chlorophenol oxidation on the composites involved

Anode	Apparent heterogeneous rate constant $\times 10^2$ min^{-1}
PbO_2	1.7
PbO_2–$C_4F_9SO_3K$	2.2

HPLC data indicated that the aromatic compounds are completely destroyed with the formation of only aliphatic electrolysis products (in particular, maleic acid) after 2 hours of electrolysis on an unmodified PbO_2-anode. It should be noted that even using the unmodified film synthesized from methanesulfonic medium allows destroying the 4-chlorophenol 2 times faster than in the case of coating synthesized from nitrate medium [10].

Conclusions

The kinetics of lead dioxide electrodeposition from a methanesulfonate medium does not differ from that observed obtained in a nitrate medium. As concern the nucleation of coatings, there is a slight predominance of the growth of β-phase of PbO_2 both for undoped sample and for lead dioxide surfactant composite. Phase growth is inhibited by surfactant due to surface blocking, which does not contradict existing models of electrocrystallization. The adsorption of surfactant is satisfactorily described by the Frumkin isotherm and is accompanied by a shift of the zero-charge pH of the oxide to a region of higher values. The morphology of the composites involved differs when the perfluorobuthanesulfonate is added to the deposition electrolyte. Thus, large crystalline blocks with sharp angles and small crystals are clearly expressed on the surface of lead dioxide–perfluorobutanesulfonate composite. It has been observed that both investigated samples have the higher β-phase amount, which is twice bigger than α-phase amount. The presence of surfactant leads to small fluctuations in the phase composition of the resulting coatings. The oxygen evolution potential on lead dioxide–surfactant composite is higher than

on undoped film. It was established that apparent heterogeneous rate constant of 4-chlorophenol on lead dioxide–perfluorobuthanesulfonate composite is 1.3 times higher than on unmodified sample.

Funding

This work was supported by Ministry of Education and Science of Ukraine (grant number 0121U109529).

REFERENCES

1. *Walsh F.C.* Modern developments in electrodes for electrochemical technology and the role of surface finishing // Trans. Inst. Met. Finish. – 2019. – Vol.97. – No. 1. – P.28-42.

2. *Velicky M., Toth P.S.* From two-dimensional materials to their heterostructures: an electrochemist's perspective // Appl. Mater. Today. – 2017. – Vol.8. – P.68-103.

3. *Walsh F.C., Arenas L.F., Ponce de Leon C.* Developments in electrode design: structure, decoration and applications of electrodes for electrochemical technology // J. Chem. Technol. Biotechnol. – 2018. – Vol.93. – No. 11. – P.3073-3090.

4. *Developments* in soluble lead flow batteries and remaining challenges: an illustrated review / Krishna M., Fraser E.J., Wills R.G.A., Walsh F.C. // J. Energy Storage. – 2018. – Vol.15. – P.69-90.

5. *Perfluoroalkyl* and polyfluoroalkyl substances in the environment: terminology, classification, and origins / Buck R.C., Franklin J., Berger U., Conder J.M., Cousins I.T., de Voogt P., et al. // Integr. Environ. Assess. Manage. – 2011. – Vol.7. – No. 4. – P.513-541.

6. *Short-chain* and long-chain fluorosurfactants in firefighting foam: a review / Peshoria S., Nandini D., Tanwar R.K., Narang R. // Environ. Chem. Lett. – 2020. – Vol.18. – P.1277-1300.

7. *Fluoro-* vs hydrocarbon surfactants: why do they differ in wetting performance? / Kovalchuk N.M., Trybala A., Starov V., Matar O., Ivanova N. // Adv. Colloid Interface Sci. – 2014. – Vol.210. – P.65-71.

8. *Methanesulfonic* acid: a sustainable acidic solvent for recovering metals from the jarosite residue of the zinc industry / Palden T., Onghena B., Regadio M., Binnemans K. // Green Chem. – 2019. – Vol.21. – P.5394-5404.

9. *Composite* electrodes PbO_2-Nafion® / Velichenko A., Luk'yanenko T., Nikolenko N., Shmychkova O., Demchenko P., Gladyshevskii R. // J. Electrochem. Soc. – 2020. – Vol.167. – No. 6. – Art. No. 063501.

10. *Electrosynthesis* and catalytic activity of PbO_2-fluorinated surfactant composites / Velichenko A., Luk'yanenko T., Shmychkova O., Dmitrikova L. // J. Chem. Technol. Biotechnol. – 2020. – Vol.95. – No. 12. – P.3085-3092.

11. *Damaskin B.* Adsorption of organic compounds on electrodes. – New York: Plenum Press, Springer, 1971.

12. *Electrocrystallization* of lead dioxide: analysis of the early stages of nucleation and growth / Abyaneh M.Y., Saez V., Gonzalez-Garcia J., Mason T.J. // Electrochim. Acta. – 2010. – Vol.55. – No. 10. – P.3572-3579.

13. *Electrocrystallization* of lead dioxide: influence of early stages of nucleation on phase composition / Shmychkova O., Luk'yanenko T., Piletska A., Velichenko A., Gladyshevskii R., Demchenko P., et al. // J. Electroanal. Chem. – 2015. – Vol.746. – P.57-61.

14. *Nikolenko N.V.* The surface properties of calcite: an adsorption model with orbital control // Adsorp. Sci. Technol. – 2001. – Vol.19. – No. 3. – P.237-244.

15. *Monahov B., Pavlov D., Petrov D.* Influence of Ag as alloy additive on the oxygen evolution reaction on Pb/PbO_2 electrode // J. Power Sources. – 2000. – Vol.85. – No. 1. – P.59-62.

Received 01.06.2021

ЕЛЕКТРОСИНТЕЗ І ХАРАКТЕРИСТИКА КОМПОЗИТУ СВИНЕЦЬ(IV) ОКСИД–ПЕРФТОРБУТАНСУЛЬФОНАТ

В. Книш, О. Шмичкова, Т. Лук'яненко, Л. Дмітрікова, О. Величенко

Досліджено вплив калій перфлуоробутансульфонату на кінетичні закономірності електроосадження свинець(IV) оксиду з метансульфонатних електролітів. Введення $C_4F_9SO_3K$ в електроліт осадження свинець(IV) оксиду приводить до незначного пригнічення процесу електроокислення Pb^{2+}, при цьому механізм процесу не змінюється. З електролітів, що містять поверхнево-активну речовину, утворюється композитне покриття. Поверхня композитного матеріалу складається з суміші чітко виражених великих кристалічних блоків із гострими кутами та дрібних кристалів. Енергодисперсійний рентгенівський аналіз показав задовільний розподіл модифікуючих елементів у всьому об'ємі зразка, а не тільки на поверхні покриття. Показано, що електрокаталітична активність композиту свинець(IV) оксид–перфлуоробутансульфонат відрізняється від немодифікованого зразка. На композиті PbO_2–$C_4F_9SO_3K$ реакція виділення кисню трохи сповільнюється. Тафелівські нахили в 1 М $HClO_4$, розраховані за цими кривими, побудованим в логарифмічних координатах, становлять 136 і 145 мВ/дек для немодифікованого зразка і композиту, відповідно. Реакція електрохімічного окислення п-хлорфенолу характеризується кінетикою псевдопершого порядку за вихідною сполукою. Використання модифікованого $C_4F_9SO_3K$ свинець(IV) оксиду як анода приводить до пригнічення процесу виділення кисню і в півтора рази вищого значення швидкості електрохімічного перетворення 4-хлорфенолу в аліфатичні сполуки.

Ключові слова: свинець(IV) оксид, метансульфонатний електроліт, поверхнево-активна речовина, електроосадження, 4-хлорфенол.

ELECTROSYNTHESIS AND CHARACTERIZATION OF LEAD DIOXIDE–PERFLUOROBUTANESULFONATE COMPOSITE

*V. Knysh [a], O. Shmychkova [a, *], T. Luk'yanenko [a], L. Dmitrikova [b], A. Velichenko [a]*

[a] **Ukrainian State University of Chemical Technology, Dnipro, Ukraine**

[b] **Dnipro State Medical University, Dnipro, Ukraine**

[*] **e-mail: lesiandra08@gmail.com**

The effect of potassium perfluorobutanesulfonate on the kinetic features of electrodeposition of lead dioxide from methanesulfonate electrolytes has been investigated. The introduction of $C_4F_9SO_3K$ into the lead dioxide deposition electrolyte leads to insignificant inhibition of the Pb^{2+} electrooxidation process, while the mechanism of the process does not change. A composite coating is formed upon deposition of coatings from electrolytes containing surfactants. The surface of a composite material consists of a mixture of clearly expressed large crystalline blocks with sharp angles and small crystals. Energy dispersive X-ray analysis revealed the satisfactory distribution of modifying elements in the entire sample bulk, and not only on the coating surface. It was shown that the electrocatalytic activity of lead dioxide–perfluorobuthanesulfonate composite differs from the undoped sample. The oxygen evolution reaction slightly decelerates on a PbO_2–$C_4F_9SO_3K$ composite. The Tafel slopes in 1 M $HClO_4$ calculated from these curves plotted in semilogarithmic coordinates are 136 and 145 mV dec^{-1} for undoped sample and lead dioxide–surfactant composite, respectively. The reaction of electrochemical oxidation of p-chlorophenol is characterized by the pseudo-first order kinetics with respect to the initial compound. The use of doped $C_4F_9SO_3K$ lead dioxide as an anode leads to the inhibition of the process of oxygen evolution and an almost one and a half higher rate of electrochemical conversion of 4-chlorophenol to aliphatic compounds.

Keywords: lead dioxide; methanesulfonate electrolyte; surfactant; electrodeposition; 4-chlorophenol.

REFERENCES

1. Walsh FC. Modern developments in electrodes for electrochemical technology and the role of surface finishing. *Trans Inst Met Finish*. 2019; 97: 28-42. doi: 10.1080/00202967.2019.1551277.

2. Velicky M, Toth PS. From two-dimensional materials to their heterostructures: an electrochemist's perspective. *Appl Mater Today*. 2017; 8: 68-103. doi: 10.1016/j.apmt.2017.05.003.

3. Walsh FC, Arenas LF, Ponce de Leon C. Developments in electrode design: structure, decoration and applications of electrodes for electrochemical technology. *J Chem Technol Biotechnol*. 2018; 93: 3073-3090. doi: 10.1002/jctb.5706.

4. Krishna M, Fraser EJ, Wills RGA, Walsh FC. Developments in soluble lead flow batteries and remaining challenges: an illustrated review. *J Energy Storage*. 2018; 15: 69-90. doi: 10.1016/j.est.2017.10.020.

5. Buck RC, Franklin J, Berger U, Conder JM, Cousins IT, de Voogt P, et al. Perfluoroalkyl and polyfluoroalkyl substances in the environment: terminology, classification, and origins. *Integr Environ Assess Manage*. 2011; 7: 513-541. doi: 10.1002/ieam.258.

6. Peshoria S, Nandini D, Tanwar RK, Narang R. Short-chain and long-chain fluorosurfactants in firefighting foam: a review. *Environ Chem Lett*. 2020; 18: 1277-1300. doi: 10.1007/s10311-020-01015-8.

7. Kovalchuk NM, Trybala A, Starov V, Matar O, Ivanova N. Fluoro- vs hydrocarbon surfactants: why do they differ in wetting performance? *Adv Colloid Interface Sci*. 2014; 210: 65-71. doi: 10.1016/j.cis.2014.04.003.

8. Palden T, Onghena B, Regadio M, Binnemans K. Methanesulfonic acid: a sustainable acidic solvent for recovering metals from the jarosite residue of the zinc industry. *Green Chem*. 2019; 21: 5394-5404. doi: 10.1039/C9GC02238D.

9. Velichenko A, Luk'yanenko T, Nikolenko N, Shmychkova O, Demchenko P, Gladyshevskii R. Composite electrodes PbO_2-Nafion®. *J Electrochem Soc*. 2020; 167(6): 063501. doi: 10.1149/1945-7111/ab805f.

10. Velichenko A, Luk'yanenko T, Shmychkova O, Dmitrikova L. Electrosynthesis and catalytic activity of PbO_2-fluorinated surfactant composites. *J Chem Technol Biotechnol*. 2020; 95: 3085-3092. doi: 10.1002/jctb.6483.

11. Damaskin B. *Adsorption of organic compounds on electrodes*. New York: Springer; 1971.

12. Abyaneh MY, Saez V, Gonzalez-Garcia J, Mason TJ. Electrocrystallization of lead dioxide: analysis of the early stages of nucleation and growth. *Electrochim Acta*. 2010; 55: 3572-3579. doi: 10.1016/j.electacta.2009.12.021.

13. Shmychkova O, Luk'yanenko T, Piletska A, Velichenko A, Gladyshevskii R, Demchenko P, et al. Electrocrystallization of lead dioxide: influence of early stages of nucleation on phase composition. *J Electroanal Chem*. 2015; 746: 57-61. doi: 10.1016/j.jelechem.2015.03.031.

14. Nikolenko NV. The surface properties of calcite: an adsorption model with orbital control. *Adsorp Sci Technol*. 2001; 19(3): 237-244. doi: 10.1260/0263617011494123.

15. Monahov B, Pavlov D, Petrov D. Influence of Ag as alloy additive on the oxygen evolution reaction on Pb/PbO_2 electrode. *J Power Sources*. 2000; 85: 59-62. doi: 10.1016/S0378-7753(99)00383-3.

Research Article

SCI

Received: 26 March 2020 Revised: 8 May 2020 Accepted article published: 17 May 2020 Published online in Wiley Online Library: 7 June 2020

(wileyonlinelibrary.com) DOI 10.1002/jctb.6483

Electrosynthesis and catalytic activity of PbO_2-fluorinated surfactant composites

Alexander Velichenko,[a*] Tatiana Luk'yanenko,[a] Olesia Shmychkova[a] and Larisa Dmitrikova[b]

Abstract

BACKGROUND: The effect of the potassium salt of nonafluorobutanesulfonic acid ($C_4F_9SO_3K$) on the kinetic regularities of electrodeposition of lead dioxide (PbO_2) from nitrate electrolytes has been investigated. Obtained results concerning synthesis and physicochemical properties can contribute substantially to a fundamental understanding of the relationship between coating structure and catalytic activity, important to all fields of catalysis.

RESULTS: The introduction of $C_4F_9SO_3K$ into the PbO_2 deposition electrolyte leads to insignificant inhibition of the Pb^{2+} electrooxidation process, whereas the mechanism of the process does not change. Upon deposition of coatings from electrolytes containing surfactants, a composite coating is formed. Depending on the electrolyte composition and electrolysis conditions, the surfactant content in the composite can vary from 2.00 ± 0.05 to 17.00 ± 0.05 wt%. The inclusion of surfactants in the coating composition with subsequent overgrowth with PbO_2 leads to a decrease in the size of PbO_2 crystals and prevents the formation of polycrystalline blocks. The composite material is a PbO_2 matrix with submicron and nanoscale crystals into which surfactant particles are embedded.

CONCLUSION: It was shown that the electrocatalytic activity of composite PbO_2-surfactant materials depends on the nature and content of the latter in the composite. The use of PbO_2 doped with $C_4F_9SO_3K$ as an anode leads to an inhibition of the process of oxygen evolution and an almost three-fold increase in the rate of electrochemical conversion of 4-chlorophenol to aliphatic compounds.

Keywords: lead dioxide; nitrate electrolyte; surfactant; electrodeposition; 4-chlorophenol

INTRODUCTION

Design and application of various coatings are now employed extensively in modern electrochemical technology.[1–3] Composite coatings, including metal oxide coatings, are one of the most promising issues for modifying the surface properties of various materials.[4,5] A well-known and obvious advantage of composite coatings is that their properties and parameters can be changed directionally by varying the composition of the coating and the ratio of its constituent components.

Electrolysis opens up great opportunities in controlling the structure and the properties of deposited oxide films, accordingly. The development of composite electrochemical coatings based on metal oxides with the inclusion of dopants of various natures, including surfactants should be considered as the one of main directions of electrocatalysis.[6]

Among composite coatings, metal oxide-polymer coatings in which fluorinated compounds are used as a dopant component are of particular interest.[7] The inclusion of fluorinated compounds in the metal-oxide matrix gives antistatic, anti-adhesive and anticorrosion properties while retaining the inherent properties of the metal oxide, including high electrical conductivity, resistance to mechanical wear and good adhesion to the substrate.

Electrodeposited lead dioxide (PbO_2) has a number of valuable benefits that facilitate its use as a platinum (Pt) substitute in a various processes of electrochemical synthesis.[8] These features include chemical resistance in aggressive solutions, high electrical conductivity of the metal type, the ability to create composite materials and ease of preparation.

The addition of polyelectrolytes (long-chain polymers with charged functional groups) into the electrolyte deposition leads to significant changes in the electrodeposition regularities, the physicochemical properties of oxides and the electrocatalytic activity of the obtained electrode materials.[9,10] As was shown in a number of our previous works, the presence of fluorine (F) ions[11] and the Nafion® polyelectrolyte[12, 13] in the deposition electrolyte affects the properties of the obtained PbO_2, in particular, changing its morphology, texture and electrocatalytic activity in oxygen transfer reactions. From this point of view, investigation of the influence of potassium salt of nonafluorobutanesulfonic acid ($C_4F_9SO_3K$) on the properties of synthesized PbO_2 is of significant interest, because $C_4F_9SO_3K$ is an intermediate surfactant between small fluoride ion and the large polyelectrolyte Nafion®.

* Correspondence to: A Velichenko, Ukrainian State University of Chemical Technology, 8, Gagarina Ave., 49005 Dnipro, Ukraine. E-mail: velichenko@ukr.net

a Ukrainian State University of Chemical Technology, Dnipro, Ukraine

b Dnipropetrovsk State Medical Academy, Dnipro, Ukraine

For polyelectrolytes, in particular for Nafion®,[12] significant changes were observed both in the electrodeposition regularities and in the electrocatalytic activity of the resulting electrode materials. It is obvious that modification with surfactants, because some of them are monomers of polyelectrolytes, also should lead to a change in the kinetics of deposition, and, as a consequence, to a change in their properties.

Herein we used $C_4F_9SO_3K$ as an additive in the PbO_2 deposition electrolyte. We chose a surfactant containing F and a fluorosulfonic acid residue as substituents. This surfactant contains substituents similar to Nafion®, and, in fact, is its monomer. The oxidation of compounds of this type at high anodic potentials is practically excluded. Because the selected additive is an anionic surfactant, then most likely it will be adsorbed on the positively charged surface of the growing oxide. It should be noted that in the literature there is practically no information on the effect of surfactants on the electrodeposition regularities of metal oxides.[14] Therefore, in this work, we studied the regularities of electrodeposition of PbO_2 in the presence of nonafluorobutanesulfonic acid in the potassium salt solution as a modifying additive, as well as the electrocatalytic activity of the obtained oxide materials.

The obtained results concerning synthesis and physicochemical properties can contribute substantially to a fundamental understanding of the relationship between the coating composition, structure and catalytic activity, important to all fields of catalysis.

MATERIALS AND METHODS

All chemicals were reagent grade. Electrodeposition kinetics of doped PbO_2 were studied on a Pt rotating disk electrode (Pt-RDE, 0.19 cm^2) by steady-state voltammetry and chronoamperometry. For the RDE experiments the voltammetry system SVA-1BM was used. The potential scan rate was varied within 1–100 mV s^{-1} depending on the purposes of the experiments. Before each experiment, the electrode surface was treated with a freshly prepared mixture (1:1) of concentrated sulfuric acid (H_2SO_4) and hydrogen peroxide (H_2O_2).[15] This preliminary treatment technique permits the stabilization of the electrode surface and determines the reproducibility of cyclic voltammograms in the background electrolyte (0.1 mol L^{-1} HNO_3). Voltammetry measurements were carried out in a standard temperature-controlled three-electrode cell. Temperature was maintained at 298 ± 1 K. All potentials were recorded and reported *versus* silver/silver/potassium chloride [Ag/AgCl/KCl $_{(sat.)}$].

Electrodeposition was studied in 0.1 mol L^{-1} nitric acid (HNO_3) + 0.01 mol L^{-1} lead nitrate [$Pb(NO_3)_2$]. Surfactant was added into the deposition electrolyte as an aqueous solutions with 0.003 mol L^{-1} concentration. Because at low concentrations of surfactant, the composition of the electrolyte will significantly change during deposition, a concentration was chosen at which, according to the adsorption isotherm, one can obtain 100% surface filling, when the electrolyte composition will not change if the surfactant has been consumed.

The determination of current efficiency and partial current of PbO_2 deposition [$I_{Pb(II)}$] was done according to the method described in detail previously.[16]

Becuase PbO_2 electrodeposition proceeds simultaneously with an oxygen evolution reaction, for determination of partial PbO_2 electrodeposition current [$I_{Pb(II)}$] and current efficiency [CE_{PbO_2}] of the PbO_2 total charge and charge that passed on the reduction of obtained deposit were measured[16]:

$$CE_{PbO_2} = Q_{red}/Q$$

$$I_{PbO_2} = Q_{red}/\tau,$$

where Q and Q_{red} are charges passed through the electrolytic cell and passed on the reduction of PbO_2 coating, respectively, and τ is electrolysis time upon state potential.

For finding out the surfactant influence on PbO_2 electrodeposition kinetics values of the apparent heterogeneous rate constants (k) for anodic Pb(II) oxidation were calculated according to the Koutecky–Levich equation:

$$\frac{1}{I} = \frac{1}{nkFSc_0} + \frac{1}{0.62nFSD^{2/3}\nu^{-1/6}c_0}\cdot\frac{1}{\omega^{1/2}},$$

where n is the number of electrons transferred in the half reaction, S is the electrode area (cm^2), ω is the angular velocity of electrode rotation (rad s^{-1}), ν is the solution kinematic viscosity (Pa s) and other terms have their conventional electrochemical significance.[17]

The surface morphology of the PbO_2 anodes was studied by scanning electron microscopy (SEM) with a Leica/Cambridge Stereoscan 440 LEO microscope/ UK.

The method for the determination of high molecular weight aliphatic acids[18] was adapted for the determination of the concentration of surfactant in aqueous solutions. This method involves the formation of an associate of a high-molecular anion and a dye, followed by extraction into a nonaqueous medium. The content of organic substance was determined photocolorimetrically after extraction of the ionic associate with chloroform. Ten millilitres of distilled water were placed in a separatory funnel and 2 mL of 0.1% aqueous solution of methylene blue was injected. Then, 1 mL of the test solution was injected and shaken for 2 min with 15 mL chloroform. The organic phase was filtered through cotton wool and the optical density measured at 650 nm using a CPC-2 colorimeter/ Sergiev Posad/ Russian Federation. To determine surfactants in composite coatings of known mass, the latter were cathodically dissolved at a current density of 2 mA cm^{-2} in 30 mL of 0.1 mol L^{-1} HCl. Then the concentration of additives was determined in solution by the above method.

Adsorption measurements were carried out on 0.5 g PbO_2 powder (Merck) in 0.1 mol L^{-1} hydrochloric acid (HCl) solutions containing various amounts of additive. The measurements were carried out in the presence of an indifferent electrolyte (0.1 mol L^{-1} KCl), which screened the electrostatic field of the oxide surface. The time to establish the adsorption equilibrium was 24 h.

Adsorption parameters were calculated using the Frumkin equation[19]:

$$Bc = \frac{\theta}{1-\theta}\exp(-2\alpha\theta),$$

where B is the adsorption constant, θ is the surface coverage, α is an interaction parameter and c is the equilibrium concentration.

For aqueous solutions, when the concentration of solute is small and is expressed in mol L^{-1},

$B = 0,018\exp(-\Delta G/RT)$,where ΔG is free adsorption energy.

The surface tension of surfactant solutions was measured by the method of maximum pressure in a gas bubble.[20] Platinized titanium was used as a sheet during investigation of the

electrocatalytic activity of materials. It was treated accordingly before Pt layer deposition.[21]

The O_2 evolution reaction was investigated by steady-state polarization on a computer-controlled EG & G Princeton Applied Research potentiostat model 273A/ Ametek/UK in 1 mol L^{-1} H_2SO_4.

The electro-oxidation of organic compounds was carried out in divided cell at j_a = 50 mA cm^{-2}. The volume of anolyte was 130 cm^3. Solution containing phosphate buffer (0.25 mol L^{-1} Na_2HPO_4 + 0.1 mol L^{-1} KH_2PO_4) + 10^{-4} mol L^{-1} organic compound (pH = 6.55) was used as anolyte; phosphate buffer was the catholyte with a stainless steel cathode. Composite PbO_2-surfactant electrodes were used as anodes. The electrode surface area was 2.5 cm^2.

The changing concentration of the organic substance during electrolysis was measured by sampling (5 cm^3 volumes) at regular intervals and measuring the optical density of the solution in the UV-visible region (wavelength range 200–350 nm) using a Kontron Uvikon 940 spectrometer/ Kontron Instruments/ Plaisir/ France.

Analyses of the reaction products were conducted by high performance liquid chromatography (HPLC) using a Shimadzu RF-10A xL instrument/ Shimadzu/ Japan equipped with an Ultraviolet SPD-20AV detector and a 30-cm Discovery® C18 column.

All of the experiments were repeated twice at least in order to achieve satisfactory reproducibility. All instruments had normalized metrological characteristics and were calibrated. The data for the linearized plots were processed using the least squares method, which requires that the sum of the squared deviations of the experimental points from the curve be the smallest. For straight lines, equations were found from which constants were determined. Reliable data were considered for which the correlation factor was >0.99. Calibration plots were processed by a data processing program for calibration plots. The results were processed using mathematical statistics methods in order to determine the required number of measurements and assess the reliability of the obtained experimental data. The reliability of the results and the validity of the conclusions were confirmed by the integrated use of a set of modern techniques, reproducibility of experimental material.

RESULTS AND DISCUSSIONS

Several characteristic regions could be distinguished in cyclic voltammograms (CV, potential scan area 0.9–1.6 V; Fig. 1). An exponential increase in the anode current was observed in the anode region at potentials from 1.4 V due to the simultaneous Pb(II) oxidation and oxygen evolution reactions. There was a maximum current on the cathode branch at potentials between 1.0 and 1.1 V, due to the PbO_2 reduction reaction:[22]

$$PbO_2 + 4H^+ \rightarrow Pb^{2+} + 2H_2O + 2e^-.$$

When $C_4F_9SO_3K$ was added to the electrolyte, the peak of cathodic reduction of PbO_2 decreased slightly (see Fig. 1), which indicates a slight inhibition in the rate of PbO_2 formation. Moreover, with an increase in the concentration of surfactant in the deposition electrolyte, the effect of inhibiting Pb^{2+} oxidation was not apparent. The number of electrons that take part in the kinetic stage are determined from linear potential sweep voltammetry measurements according to Delahay equation,[16] as described in the literature for analogous conditions.[23,24] The

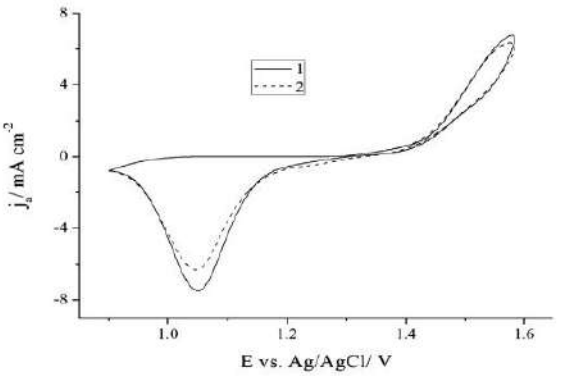

Figure 1 Cyclic voltammograms (scan range 0.9–1.6 V) on Pt in solutions containing 0.01 mol L^{-1} $Pb(NO_3)_2$ + 0.1 mol L^{-1} HNO_3 (1) + 0.003 mol L^{-1} $C_4F_9SO_3K$ (2). v = 50 mV s^{-1}.

transfer coefficient remained almost unchanged ($\alpha = 0.42 \pm 0.1$) when the surfactant was present in the deposition electrolyte. The calculated number of electrons in the elementary stage was 1.0 ± 0.1, confirming that PbO_2 formation is a multistep charge transfer which involves two consecutive one-electron stages, as outlined in the following kinetic scheme:

$$H_2O \rightarrow OH_{ads}^{\cdot} + H^+ + e^- \quad (1)$$

$$Pb^{2+} + OH_{ads}^{\cdot} \rightarrow Pb(OH)^{2+} \quad (2)$$

$$Pb(OH)^{2+} + H_2O \rightarrow Pb(OH)_2^{2+} + H^+ + e^- \quad (3)$$

$$Pb(OH)_2^{2+} \rightarrow PbO_2 + 2H^+ \quad (4)$$

This mechanism has been modified from the first version, proposed by Fleischmann and Liler,[25] where insoluble oxygen-containing Pb(IV) intermediates were proposed, involving the presence of several soluble intermediates such as the oxygen-containing Pb(IV) species proposed by Chang and Johnson,[26] and the oxygen-containing Pb(III) intermediate suggested by Velichenko *et al.*,[27] who afterwards proved the existence of both oxygen-Pb(III) and oxygen-Pb(IV) soluble intermediates.[28]

As a rule, at low anodic polarizations (E < 1.55 V) reactions will be under kinetic control, whereas at the high polarizations Pb^{2+} ion transport to the electrode surface will be the rate-determining stage.

Steady-state polarization curves are shown in Fig. 2. These curves take into account the partial Pb(II) electro-oxidation process, in the absence and in the presence of surfactant.[16,23,24] In the lower potential range, plots of E *versus* log j are linear (r = 0.99) indicating that the PbO_2 electrodeposition process is controlled kinetically. The limiting diffusion current of the partial oxidation of Pb^{2+} ions is reached at deposition potentials above 1.8 V. One can observe some decrease in the rate of PbO_2 formation in the presence of added surfactant from these curves.

Apparent heterogeneous rate constants were calculated according to the Koutecky–Levich equation[17,29] from intercepts of $1/I$ *versus* $1/\omega^{1/2}$ plots. Results show that the presence of $C_4F_9SO_3K$ in the deposition solution caused the apparent heterogeneous rate constant to decrease slightly from $(4.06 \pm 0.1) \times 10^{-4}$ to $(3.28 \pm 0.1) \times 10^{-4}$ ms^{-1} as the concentration of dopant increases from 0 to 0.003 mol L^{-1}. These results

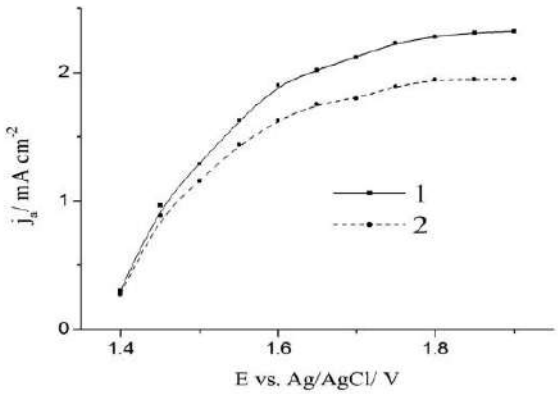

Figure 2 Steady-state polarization curves for partial PbO_2 electrodeposition current on Pt disk electrode in solutions containing 0.01 mol L^{-1} $Pb(NO_3)_2$ + 0.1 mol L^{-1} HNO_3 (1) + 0.003 mol L^{-1} $C_4F_9SO_3K$ (2).

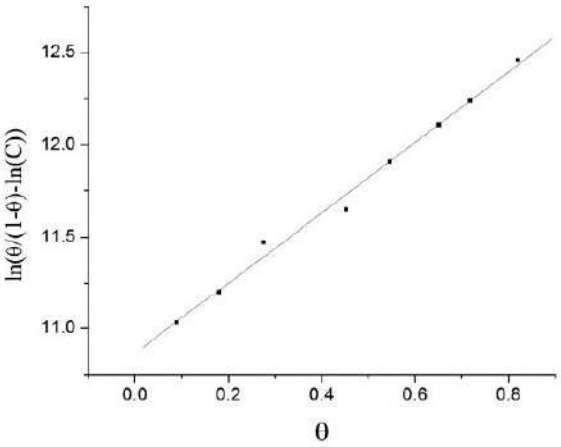

Figure 4 The Frumkin isotherm of $C_4F_9SO_3K$ adsorption on PbO_2. θ and C, surface coverage and equilibrium concentration, respectively.

are in agreement with the voltammetry data (see Fig. 1) discussed above in this section.

Figure 3 shows the dependences of the current efficiency (CE) of PbO_2 formation obtained from stationary polarization curves. The CE of PbO_2 decreased when surfactants were added to the solution, whereas the inhibition effect was insignificant with an increase in the concentration of surfactant. The observed effect is probably due to a decrease in the number of active centres on the electrode surface.

Adsorption measurements were performed on a PbO2 powder at zero charge potential.[30] As one can see from the experimental data, the adsorption of surfactant is satisfactorily described by the Frumkin isotherm (Fig. 4, correlation factor 0.996). The value of interaction parameter calculated from the Frumkin equation is 1.00 ± 0.05 that suggests the slight interaction between adsorbed molecules. The value of the energy of adsorption interaction ($-\Delta G$) for potassium perfluorobutanesulfonate is 33.20 ± 0.01 kJ mol^{-1}, which indicates the specific character of adsorption.

As a result of potentiometric measurements (Fig. 5), it was established that the adsorption of $C_4F_9SO_3K$ on PbO_2 was accompanied by a shift of the pH_0 (zero charge pH) of the oxide to a region of higher value. This suggests that adsorption proceeds without the participation of functional groups of both a surfactant and the oxide surface. This hypothesis is well-supported by the data on the adsorption material balance.[11] The obtained data indicate the weak chemical adsorption of surfactant on lead dioxide,[31] that is confirmed by a slight displacement of the pH_0 of the oxide.[32]

The critical micelle concentration (CMC) of $C_4F_9SO_3K$ was determined in order to establish whether micellization is present in the solution. Its value in 0.1 mol L^{-1} $Pb(NO_3)_2$ + 0.1 mol L^{-1} HNO_3 solution was rather large and amounted to 0.020 ± 0.001 mol L^{-1}. This also confirmed that all the working electrolytes were true solutions.

It was found that during electrodeposition of PbO_2 in the presence of $C_4F_9SO_3K$ in the electrolyte, the additive was included in the growing deposit with the formation of a composite oxide-surfactant coating. Thus, it was found that an increase in the concentration of surfactant does not affect its content in the coating. The latter was *c.* 2.00 ± 0.05 wt% when the concentration of

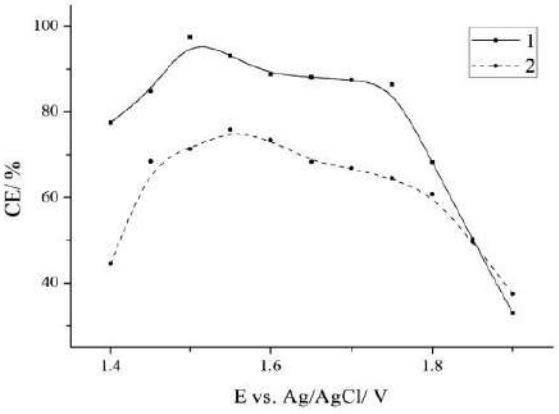

Figure 3 Current efficiency of lead dioxide *versus* potential of deposition in solutions containing 0.01 mol L^{-1} $Pb(NO_3)_2$ + 0.1 mol L^{-1} HNO_3 (1) + 0.003 mol L^{-1} $C_4F_9SO_3K$ (2).

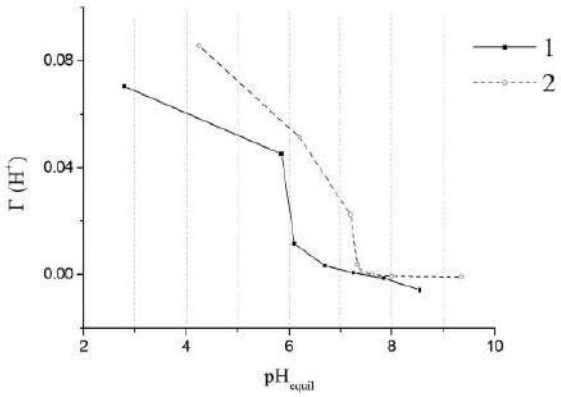

Figure 5 PbO_2 (0.5 g) potentiometric titration results; concentration of potassium perfluorobutanesulfonate 0 (1) and 0.003 mol L^{-1} (2).

$C_4F_9SO_3K$ in the deposition electrolyte changed from 0.0015 until 0.005 mol L^{-1}. A surfactant concentration of 0.003 mol L^{-1} was chosen as working solution. At this concentration, according to the adsorption isotherm (see Fig. 4), we are in the region of hundred-degree surface filling, which means that one molecule of a surfactant corresponds to each adsorption center on the surface; and the electrolyte will remain the true solution, when the surfactant is added.

The data obtained can be adequately explained on the basis of a number of hypotheses. On the one hand, using a classical electrodeposition scheme, when surfactant adsorption occurs on the surface of growing PbO_2, the phenomenon of changing the additive content in the coating can be caused by two factors: (i) heterogeneous (concentration on a growing surface due to adsorption) and (ii) migratory (flow from the solution bulk to the surface under the influence of an electric field). On the other, we cannot exclude that not only crystallization but also colloidal particle formation occurs in the supersaturated layer of the solution, and that some particles adhere to the surface of the growing crystals, as observed in the case of synthesis of PbO_2-TiO_2 composites.[29] It should be noted that it is possible that all of the described effects occur simultaneously with different contributions. None of these hypotheses contradict the obtained experimental data.

An increase in the anode current density allowed us to obtain composites containing ≤17.00 ± 0.05 wt% of organic substance (Table 1). The observed effect is probably due to an increase in the positive charge of the electrode, which contributes to an increase in the adsorption of anionic surfactants on the surface of the growing oxide. An increase of the deposition temperature to 60 °C facilitated coatings with surfactant contents ≤10.00 ± 0.05 wt%.

The inclusion of surfactants in a growing coating leads to a change in the texture and structure of the resulting film. It is widely recognized[8] that the surface of nonmodified PbO_2-sample is homogeneous and large-crystalline. With an increase of surfactants in the coating, a decrease in the size and shape of crystalline blocks of PbO_2 was observed. As can be seen from SEM images, the presence of surfactants in the coating prevented the formation of large crystalline blocks, and when the organic content was 14.00 ± 0.05 wt%, significant internal stresses were observed in the coating [Fig. 6(a) and (b)]. The crystals exhibit sharp angles on both images. SEM/EDAX experiments [Fig. 6(c)] were performed to evaluate the amount and distribution of elements in electrodeposited composite. Low peaks corresponding to O and F indicate a satisfactory distribution of modifying elements in the entire sample bulk, not only on the coating surface. In addition, it was not possible to detect the S peak because it is too near of the very intense Pb peak.

Table 1 The content of surfactant in PbO_2-$C_4F_9SO_3K$ composites depending on the anode current density[a]

j_a (mA cm^{-2})	$\omega \pm 0.05$ (wt%)
4	1.92
6	5.72
8	14.14
20	16.63

[a]Composites deposited from 0.1 mol L^{-1} HNO_3+ 0.1 mol L^{-1} $Pb(NO_3)_2$+ 0.003 mol L^{-1} $C_4F_9O_3SK$.

Because a change in the physicochemical properties of oxides should lead to a change in the degree of filling of oxygen-containing particles of various types,[27] it possible to assume that the electrocatalytic activity of the obtained electrode materials also should change.

The electrocatalytic activity of PbO_2 deposited from a solution containing a surfactant was studied both in the respect to the O_2 evolution reaction and the oxidation of 4-chlorophenol. As follows from the steady-state polarization curves shown in Fig. 7, the O_2 evolution reaction decelerated on a PbO_2-$C_4F_9SO_3K$ composite.

As has been found in many papers[13,16,21] the rate of the O_2 evolution process can change due to the nature and amount of additive. Such a change depends mainly on changes in chemical properties of the oxide surface that, in turn, change the bond strength of oxygen-containing particles chemisorbed on the electrode surface.

According to the mechanism proposed by Pavlov *et al.*,[33] O_2 evolution proceeds at active sites localized in the hydrated PbO_2 layer. The surface of lead dioxide has crystalline (PbO_2) and hydrated [$PbO(OH)_2$] zones, which are in equilibrium and, in the latter case, are capable of exchanging cations and anions. The process of O_2 evolution can be described by the following scheme:

$$PbO{\cdot}(OH)_2 + H_2O \rightarrow PbO{\cdot}(OH)_2 \ldots (OH^{\cdot}) + H^+ + e^- \quad (5)$$

$$PbO{\cdot}(OH)_2 \ldots (OH^{\cdot}) \rightarrow PbO{\cdot}(OH)_2 + O + H^+ + e^- \quad (6)$$

$$2\,O \rightarrow O_2 \quad (7)$$

Trassatti[34] has shown that if the oxygen evolution reaction is limited by the stage of transfer of the second electron (electrochemical desorption), an increase in the bond strength of chemisorbed oxygen will lead to an increase in the overvoltage of O_2 evolution. Under conditions when the transfer of the first electron (electrochemical adsorption) will be the limiting stage, the overvoltage of the O_2 evolution reaction will decrease. As is known, the process of O_2 evolution on PbO_2 is controlled by the stage of transfer of the second electron;[35] therefore, the growth in overvoltage in our case indicates an increase in the bond strength of oxygen-containing radicals with the electrode surface.

According to the obtained results, oxygen overpotential on modified electrodes is significantly higher than on the nonmodified PbO_2-electrode and depends on the surfactant content in deposit, as was observed in the case of bismuth.[16] The obtained values of the Tafel slopes are significantly higher than theoretical. The data obtained show that oxygen overpotential for undoped PbO_2 is 1.676 V; for 3×10^{-5} mol L^{-1} $C_4F_9SO_3K$ in the deposition electrolyte it is 1.727 V; for 3×10^{-4} mol L^{-1} it is 1.768 V; and for 3×10^{-3} mol L^{-1} it is 1.679 V, which indicates 100% filling of the surface of PbO_2 with a surfactant at such a concentration.

According to the literature,[36,37] at high anodic potentials, the electro-oxidation of most organic substances also proceeds with the participation of oxygen-containing particles chemisorbed on the electrode. 4-Chlorophenol was chosen as model compound in order to study the effect of $C_4F_9SO_3K$ on the catalytic activity of PbO_2-based composite electrodes with respect to organic substances. This is due to the fact that the process of electro-oxidation of phenolic compounds on unmodified PbO_2-electrodes is well studied and described in the literature.[38–41] Benzoquinone and maleic acid are recognized as the main

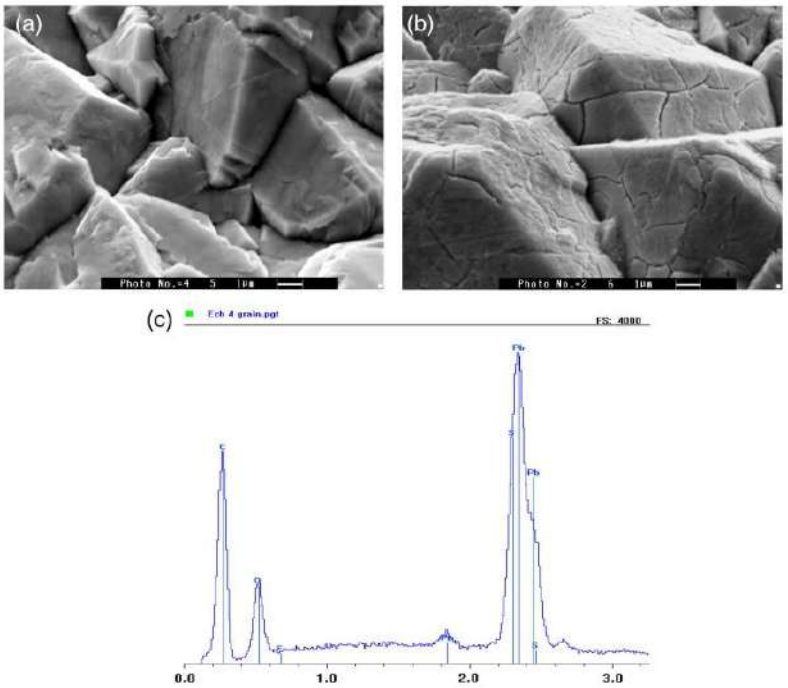

Figure 6 SEM micrographs of (a) PbO_2-1.92 wt% and (b) PbO_2-14.1 wt% $C_4F_9SO_3K$; (c) EDX spectrum of sample in (a). [Color figure can be viewed at wileyonlinelibrary.com]

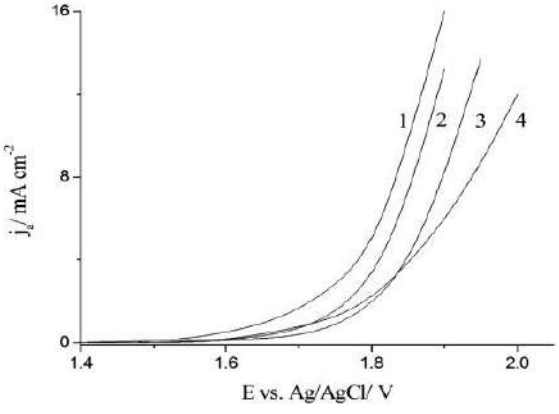

Figure 7 Steady-state polarization curves of oxygen evolution in 1 mol L^{-1} H_2SO_4 (Scan rate 1 mV s^{-1}, t = 25 °C) on PbO_2-electrodes, deposited from next solutions: 0.1 mol L^{-1} $Pb(NO_3)_2$ + 0.1 mol L^{-1} HNO_3 + X mol L^{-1} $C_4F_9SO_3K$, where X is 0 (1), 3 × 10^{-5} (2), 3 × 10^{-4} (3) and 3 × 10^{-3} (4). Coating electrodeposited on Ti/Pt sheet.

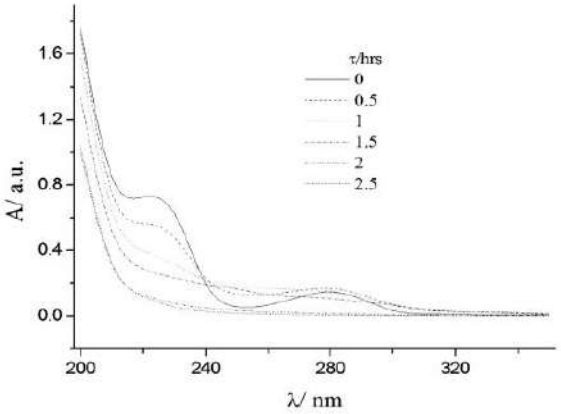

Figure 8 Electronic absorption spectra of solutions with 0.1 mmol L^{-1} initial concentration of 4-chlorophenol during electrolysis on PbO_2-1.92 wt% $C_4F_9SO_3K$ anode.

intermediate products in the anodic oxidation of 4-chlorophenol. In this regard, a convenient way to evaluate the conversion rate of 4-chlorophenol is the disappearance time of aromatic intermediates, which can be determined from the UV spectra of solutions at different electrolysis times.

The UV spectrum of the 4-chlorophenol initial solution is characterized by two peaks at wavelengths of 230 and 280 nm.[38] At the first time of electrolysis, there is a decrease in the peak at 230 nm, as well as a slight increase in the peak at 280 nm and the appearance of the plateau at 250–270 nm, which is due to a decrease in the concentration of 4-chlorophenol and the accumulation of benzoquinone in the solution. A further increase in electrolysis time leads to the disappearance of peaks at 230 and 280 nm, as well as a decrease of plateau at 250–270 nm due to a decrease in the concentrations of both 4-chlorophenol and benzoquinone (Fig. 8). HPLC data indicated that the aromatic compounds were completely destroyed with the formation of only aliphatic electrolysis products (in particular, maleic acid) after 4 h of electrolysis

Table 2 The rate of 4-chlorophenol oxidation on the composites involved

Anode	Heterogeneous rate constant (±0.01 h^{-1})
PbO_2	0.28
PbO_2-1.92 wt% $C_4F_9SO_3K$	0.82
PbO_2-14.1% wt$C_4F_9SO_3K$	0.83

on an unmodified PbO_2-anode. As follows from Table 2, the conversion rate of 4-chlorophenol increasef with increasing of surfactant content in the composite. The observed effect is due both to an increase in the direct electrochemical oxidation rate of 4-chlorophenol and inhibition of the oxygen evolution reaction on PbO_2–fluoropolymer composite. The simultaneous action of these two factors will increase the conversion rate of 4-chlorophenol.

CONCLUSION

The addition of $C_4F_9SO_3K$ into the PbO_2 deposition electrolyte has practically no effect on the kinetics of Pb^{2+} electro-oxidation; the mechanism of the process as a whole also does not change. In the region of low polarizations, the limiting stage is the second electron transfer, apparent from the slight decreased in heterogeneous rate constant with increasing surfactant concentration in the deposition electrolyte. It was shown that the observed effect is due to the adsorption of fluoropolymer and, as a consequence, the blocking of active centres on the surface of the growing oxide.

It was found that during electrodeposition of PbO_2 in the presence of $C_4F_9SO_3K$ in the electrolyte, the additive is included in the growing oxide with the formation of a composite oxide-surfactant coating. Depending on the composition of the deposition electrolyte and the electrolysis conditions, the surfactant content in the composite coating ranges from 2.00 ± 0.05 to 17.00 ± 0.05 wt%. The inclusion of surfactants in the growing coating with almost unchanged kinetic regularities of electrodeposition leads to a change in the texture and structure of the resulting films.

It was found that, the obtained PbO_2–fluoropolymer composite materials differ from unmodified PbO_2 in terms of their electrocatalytic activity. When using the composites involved as anodes, the inhibition of O_2 evolution and an almost three-fold increase in the rate of electrochemical conversion of 4-chlorophenol to aliphatic compounds were observed.

CONFLICT OF INTEREST

The authors declare that they have no conflict of interest.

FUNDING

This work was supported by Ministry of Education and Science of Ukraine.

REFERENCES

1 Walsh FC, Modern developments in electrodes for electrochemical technology and the role of surface finishing. *Int J Surf Eng Coat* **97**: 28–42 (2019). https://doi.org/10.1080/00202967.2019.1551277.
2 Yang Y, Luo M, Zhang W, Sun Y, Chen X and Guo S, Metal surface and interface energy electrocatalysis: fundamentals, performance, engineering and opportunities. *Chem* **4**:2054–2083 (2018). https://doi.org/10.1016/j.chempr.2018.05.019.
3 Velicky M and Toth PS, From two-dimensional materials to their heterostructures: an electrochemist's perspective. *Appl Mater Today* **8**: 68–103 (2017). https://doi.org/10.1016/j.apmt.2017.05.003.
4 Walsh FC, Arenas LF and Ponce de Leon C, Developments in electrode design: structure, decoration and applications of electrodes for electrochemical technology. *J Chem Technol Biotechnol* **93**:3073–3090 (2018). https://doi.org/10.1002/jctb.5706.
5 Vargas R, Borras C, Mendez D, Mostany J and Scharifker BR, Electrochemical oxygen transfer reactions: electrode materials, surface processes, kinetic models, linear free energy correlations, and perspectives. A review. *J Solid State Electrochem* **20**:875–893 (2016). https://doi.org/10.1007/s10008-015-2984-7.
6 Santos JEL, de Moura DC, da Silva DR, Panizza M and Martinez-Huitle CA, Application of TiO_2-nanotubes/PbO_2 as an anode for the electrochemical elimination of Acid Red 1 dye. *J Solid State Electrochem* **23**:351–360 (2019). https://doi.org/10.1007/s10008-018-4134-5.
7 Groult H and Tressaud A, Use of inorganic fluorinated materials in lithium batteries and in energy conversion systems. *Chem Commun* **54**: 11375–11382 (2018). https://doi.org/10.1039/C8CC05549A.
8 Li X, Pletcher D and Walsh FC, Electrodeposited lead dioxide coatings. *Chem Soc Rev* **40**:3879–3894 (2011). https://doi.org/10.1039/C0CS00213E.
9 Ponce de Leon C, Campbell SA, Smith JR and Walsh FC, Conducting polymer coatings in electrochemical technology part 2 - application areas. *Trans Inst Met Finish* **86**:34–40 (2008). https://doi.org/10.1179/174591908X264392.
10 Ghasemi S, Mousavi MF and Shamsipur M, Electrochemical deposition of lead dioxide in the presence of polyvinylpyrrolidone. A morphological study. *Electrochim Acta* **53**:459–467 (2007). https://doi.org/10.1016/j.electacta.2007.06.068.
11 Amadelli R, Armelao L, Velichenko AB, Nikolenko NV, Girenko DV, Kovalyov SV *et al.*, Oxygen and ozone evolution at fluoride modified lead dioxide electrodes. *Electrochim Acta* **45**:713–720 (1999). https://doi.org/10.1016/S0013-4686(99)00250-9.
12 Velichenko AB, Luk'yanenko TV, Nikolenko NV, Amadelli R and Danilov FI, Nafion effect on the lead dioxide electrodeposition kinetics. *Russ J Electrochem* **43**:118–120 (2007). https://doi.org/10.1134/S102319350701017X.
13 Velichenko A, Luk'yanenko T, Nikolenko N, Shmychkova O, Demchenko P and Gladyshevskii R, Composite electrodes PbO_2-Nafion®. *J Electrochem Soc* **167**:063501 (2020). https://doi.org/10.1149/1945-7111/ab805f.
14 Li X, Xu H and Yan W, Effects of twelve sodium dodecyl sulfate (SDS) on electro-catalytic performance and stability of PbO_2 electrode. *J Alloy Compd* **718**:386–395 (2017). https://doi.org/10.1016/j.jallcom.2017.05.147.
15 Shmychkova O, Luk'yanenko T, Amadelli R and Velichenko A, Electrodeposition of Ni^{2+}-doped PbO_2 and physicochemical properties of the coating. *J Electroanal Chem* **774**:88–94 (2016). https://doi.org/10.1016/j.jelechem.2016.05.017.
16 Shmychkova O, Luk'yanenko T, Velichenko A, Meda L and Amadelli R, Bi-doped PbO_2 anodes: electrodeposition and physico-chemical properties. *Electrochim Acta* **111**:332–338 (2013). https://doi.org/10.1016/j.electacta.2013.08.082.
17 Larew LA, Gordon JS, Hsiao Y-L, Johnson DC and Buttry DA, Electrocatalysis of anodic oxygen-transfer reactions: application of an electrochemical quartz crystal microbalance to a study of pure and bismuth-doped beta-lead dioxide film electrodes. *J Electrochem Soc* **137**:3071–3078 (1990). https://doi.org/10.1149/1.2086162.
18 Robinson JW, Skelly Frame EM and Frame II GM, in *Undergraduate Instrumental Analysis*, 7th edn. Marcel Dekker CRC Press, New York (2014).
19 Damaskin B, *Adsorption of Organic Compounds on Electrodes*. Plenum Press, New York (1971).
20 Adamson AW and Gast AP, *Physical Chemistry of Surfaces*, 6th edn. Wiley Interscience, New York (1997). ISBN: 978-0-471-14873-9
21 Shmychkova OB, Luk'yanenko TV, Amadelli R and Velichenko AB, PbO_2 anodes modified by cerium ions. *Prot Met Phys Chem Surf* **50**: 493–498 (2014). https://doi.org/10.1134/S2070205114040169.

22 Velichenko A, Knysh V, Luk'yanenko T, Devilliers D and Danilov F, Electrodeposition of PbO_2-ZrO_2 composite materials. *Russ J Electrochem* **44**:1251–1256 (2008). https://doi.org/10.1134/S1023193508110098.
23 Velichenko AB, Amadelli R, Gruzdeva EV, Luk'yanenko TV and Danilov FI, Electrodeposition of lead dioxide from methansulfonate solutions. *J Power Sources* **191**:103–110 (2009). https://doi.org/10.1016/j.jpowsour.2008.10.054.
24 Velichenko AB, Amadelli R, Knysh VA, Luk'yanenko TV and Danilov FI, Kinetics of lead dioxide electrodeposition from nitrate solutions containing colloidal TiO_2. *J Electroanal Chem* **632**:192–196 (2009). https://doi.org/10.1016/j.jelecem.2009.04.021.
25 Fleischmann M and Liler M, The anodic oxidation of solutions of plumbous salts. Part 1. The kinetics of deposition of α-lead dioxide from acetate solutions. *Trans Faraday Soc* **54**:1370–1381 (1958). https://doi.org/10.1039/TF9585401370.
26 Chang H and Johnson DC, Electrocatalysis of anodic oxygen-transfer reaction. Chronoamperometric and voltammetric studies of the nucleation and electrodeposition of β-lead dioxide at a rotated gold disk electrode in acidic media. *J Electrochem Soc* **136**:17–22 (1989). https://doi.org/10.1149/1.2096581.
27 Velichenko AB, Girenko DV and Danilov FI, Mechanism of lead dioxide electrodeposition. *J Electroanal Chem* **405**:127–132 (1996). https://doi.org/10.1016/0022-0728(95)04401-9.
28 Velichenko AB, Baranova EA, Girenko DV, Amadelli R, Kovalev SV and Danilov FI, Mechanism of electrodeposition of lead dioxide from nitrate solutions. *Russ J Electrochem* **39**:615–621 (2003). https://doi.org/10.1023/A:1024101210790.
29 Knysh V, Luk'yanenko T, Shmychkova O, Amadelli R and Velichenko A, Electrodeposition of composite PbO_2-TiO_2 materials from colloidal methanesulfonate electrolytes. *J Solid State Electrochem* **21**:537–544 (2017). https://doi.org/10.1007/s10008-016-3394-1.
30 Nikolenko NV, Surface properties of calcite: an adsorption model with the orbital control. *Adsorpt Sci Technol* **19**:237–244 (2001). https://doi.org/10.1260/0263617011494123.
31 Nikolenko NV and Esajenko EE, Surface properties of synthetic calcium hydroxyapatite. *Adsorpt Sci Technol* **23**:543–553 (2005). https://doi.org/10.1260/026361705775212466.
32 Campbell SA and Peter LM, Detection of soluble intermediates during deposition and reduction of lead dioxide. *J Electroanal Chem Interf Electrochem* **306**:185–194 (1991). https://doi.org/10.1016/0022-0728(91)85230-M.
33 Pavlov D, Monahov B and Petrov D, Influence of Ag as alloy additive on the oxygen evolution reaction on Pb/PbO_2 electrode. *J Power Sources* **85**:59–62 (2000). https://doi.org/10.1016/S0378-7753(99)00383-3.
34 Trassatti S, Electrocatalysis in the anodic evolution of oxygen and chlorine. *Electrochim Acta* **29**:1503–1512 (1984). https://doi.org/10.1016/0013-4686(84)85004-5.
35 Trassatti S, Lodi G and Trassatti S (ed.). *Electrodes of conductive Metallic Oxides. Part B*. Elsevier, Amsterdam (1981). ISBN: 0444419888
36 Shmychkova O, Luk'yanenko T, Dmitrikova L and Velichenko A, Modified lead dioxide for organic wastewater treatment: physico-chemical properties and electrocatalytic activity. *J Serb Chem Soc* **84**:187–198 (2019). https://doi.org/10.2298/JSC180712091S.
37 Shmychkova OB, Knysh VA, Luk'yanenko TV, Amadelli R and Velichenko AB, Electrocatalytic processes on PbO_2 electrodes at high anodic potentials. *Surf Eng Appl Electrochem* **54**:38–46 (2018). https://doi.org/10.3103/S1068375518010143.
38 Shmychkova O, Luk'yanenko T, Dmitrikova L and Velichenko A, Electrooxidation of 4-clorphenol on modified lead dioxide anodes. *Voprosy Khimii i Khimicheskoi Tekhnologii* **3**:50–57 (2018). https://doi.org/10.32434/0321-4095-2019-126-5-65-70.
39 Azzam MO, Al-Tarazi M and Tahboub Y, Anodic destruction of 4-chlorophenol solution. *J Hazard Mater* **75**:99–113 (2000). https://doi.org/10.1016/s0304-3894(00)00190-4.
40 Gherardini L, Michaud PA, Panizza M, Comninellis C and Vatistas N, Electrochemical oxidation of 4-chlorophenol for wastewater treatment. *J Electrochem Soc* **148**:D78–D82 (2001). https://doi.org/10.1149/1.1368105.
41 Iniesta J, Exposito E, Gonzalez-Garcia J, Montiel V and Aldaz A, Electrochemical treatment of industrial wastewater containing phenols. *J Electrochem Soc* **149**:D57–D62 (2002). https://doi.org/10.1149/1.1464136.

Таким чином, комплексні дослідження впливу аніонних ПАР на кінетику осадження PbO_2 *вказують на пригнічення процесу внаслідок адсорбції. За цього ефект залежить як від природи ПАР, так і довжини флуоркарбонового ланцюга. Так, за збільшення довжини флуоркарбонового ланцюга ефект інгібування проявляється більше.*

Введення в електроліт осадження ПАР впливає на кінетику електроосадження плюмбум(IV) оксиду, не змінюючи за цього механізму процесу в цілому. В області низьких поляризацій швидкістьвизначальною є кінетична стадія перенесення другого електрона, а високих – дифузійна стадія доставки іонів плюмбуму до поверхні електрода. Введення добавки приводить до інгібування процесу електроосадження PbO_2*, внаслідок зменшення числа активних центрів за рахунок адсорбції поверхнево-активних речовин на поверхні зростаючого осаду.*

За цих умов за застосування в якості добавок ПАР утворюються композити металоксид-ПАР, в яких добавка за рахунок адсорбції впроваджується у зростаючий осад оксиду металу.

Отримані дані можна адекватно пояснити на основі ряду гіпотез. З одного боку, всі отримані дані можна адекватно описати за допомогою класичної схеми електроосадження, коли на поверхні зростаючого PbO_2 *відбувається адсорбція ПАР, а явище зміни вмісту поліелектроліту в покритті може бути викликане двома факторами: і) гетерогенним та іі) міграційним. З іншого боку, ми не можемо виключити, що не тільки кристалізація відбувається з перенасиченого шару розчину, але й утворюються колоїдні частинки в тій чи іншій кількості, які прилипають до поверхні зростаючих кристалів. Механізм осадження* PbO_2 *це не виключає, оскільки проміжні продукти незакріплені, можуть перебувати і в об'ємі розчину і осідати на непровідні поверхні.*

Слід зазначити, що можливо, що всі описані ефекти можуть бути реалізовані одночасно з різними внесками, що не суперечить отриманим експериментальним даним.

РОЗДІЛ 5
КОМПОЗИТИ PbO_2-ПОЛІЕЛЕКТРОЛІТ

Введення поліелектролітів в електроліт осадження впливає на процес окиснення Pb^{2+}. За цього значну роль відіграє природа речовини. За додавання до електроліту осадження катіонного ПАГ відбувається гальмування процесу електроосадження плюмбум(IV) оксиду. За наявності в електроліті осадження аніонного полімера Nafion® на ЦВА можна бачити зростання піку катодного відновлення плюмбум(IV) оксиду (рис. 5.1), що вказує на збільшення швидкості утворення PbO_2.

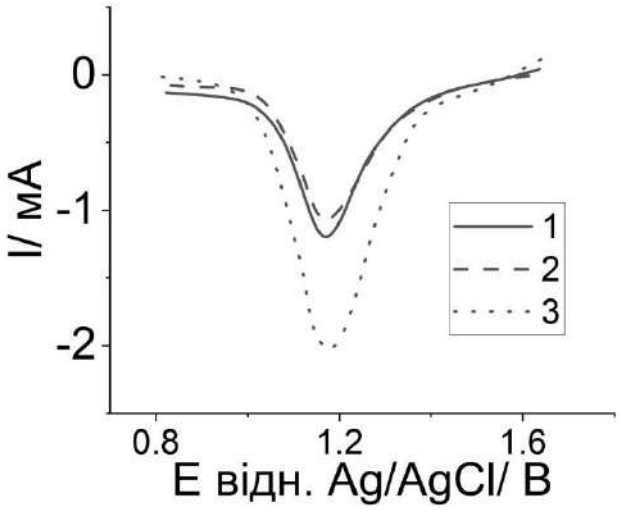

Рис. 5.1 Катодні гілки ЦВА осадження PbO_2 на платиновому електроді в розчинах 0,01 М $Pb(NO_3)_2$ + 0,1 М HNO_3 (1); 3×10^{-3} М $C_4F_6SO_3K$ (2); + 0,2% Nafion® (3)

За наявності в електроліті полімерної добавки відновлення починається дещо раніше. Також спостерігається більший пік струму порівняно зі стандартним електролітом (див. рис. 5.1). Отримані дані досліджень на золотому електроді додатково підтверджують збільшення швидкості осадження плюмбум(IV) оксиду за наявності Nafion® в електроліті (рис. 5.2). Зміна

потенціалу піка свідчить про відмінності в хімічному та фазовому складі отриманих покриттів.

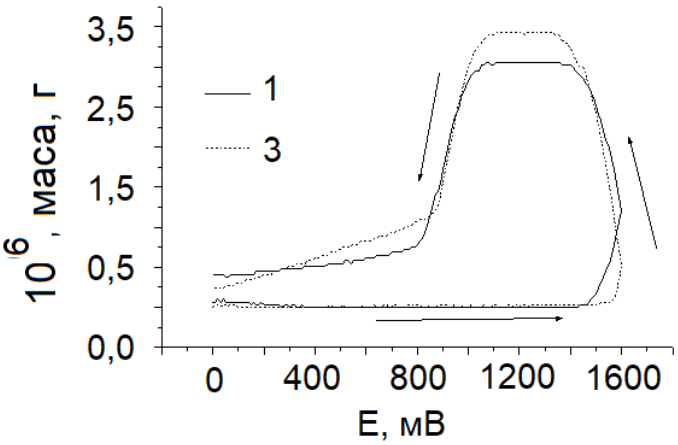

Рис. 5.2 Зміна маси золотого електрода впродовж ЦВА (рис. 5.1. 1 – 0,1 М HNO_3 + 0,1 М $Pb(NO_3)_2$; 2 – 0,1 М HNO_3 + 0,1 М $Pb(NO_3)_2$ + 0.05 мас.% Nafion®

Залежність константи швидкості стадії перенесення другого електрону від концентрації полімерної добавки Nafion® в електроліті має екстремальний характер (рис. 5.3).

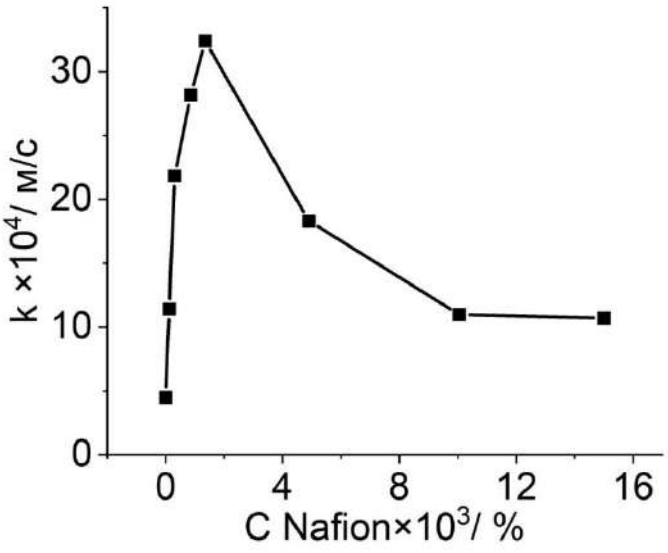

Рис. 5.3 Залежність константи швидкості гетерогенної реакції електрокиснення Pb^{2+} від концентрації Nafion® в електроліті осадження

За концентрації поліелектроліту $3{,}0\times10^{-3}$% константа швидкості збільшується майже на порядок порівняно з електролітом, який не має у своєму складі добавок. Отримані дані є непрямим доказом впливу адсорбції на осадження PbO_2.

Нами були проведені адсорбційні вимірювання на порошку PbO_2 за відсутності поляризації. Встановлено, що адсорбція Nafion® на поверхні плюмбум оксиду описується ізотермою, аналогічною за формою ізотермі Ленгмюра (рис. 5.4).

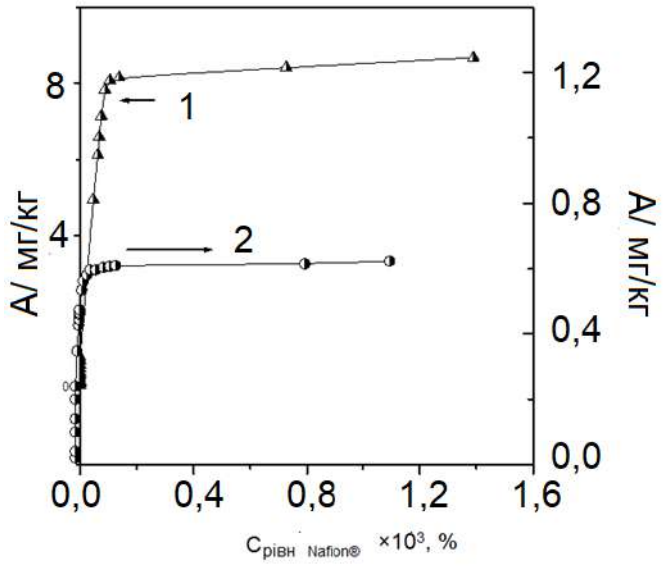

Рис. 5.4 Адсорбція аніонного поліелектроліту Nafion® на плюмбум(IV) оксиді в 0,1 М HCl (1), в H_2O (2)

Характер ізотерми адсорбції відображає високу спорідненість адсорбата до поверхні. Величина адсорбції вже за малих концентрацій різко зростає і швидко досягає практично постійного значення. В результаті потенціометричних вимірювань встановлено, що адсорбція Nafion® на PbO_2 супроводжується зміщенням pH нульового заряду оксиду в область більш високих pH. Це свідчить про те, що адсорбція поліелектролітів за pH < pHo здійснюється не тільки внаслідок електростатичного притягання поліаніону до позитивно зарядженої поверхні PbO_2, а й, мабуть, в результаті деякої

специфічної взаємодії. Це припущення добре підтверджується даними складання матеріального балансу адсорбції. Встановлено, що адсорбція полімерів супроводжується виділенням іонів OH^-. Якщо припустити, що адсорбція здійснюється за участю SO_3^--груп полімеру, то виділення гідроксид-іонів можна пояснити координаційною взаємодією поліаніона з катіонами плюмбуму на поверхні PbO_2:

$$\equiv PbOH + R_n(SO_3^-)_m \rightarrow \equiv Pb(SO_3^-)R_n(SO_3^-)_{m-1} + OH^- \quad (5.1)$$

За зменшення pH розчину адсорбція Nafion® на PbO_2 значно збільшується (див. рис. 5.4), що може бути пов'язано, як зі збільшенням ролі електростатичного фактора за рахунок збільшення позитивного заряду оксиду, так і з переходом полімеру в протоновану форму [40].

Зовсім інша картина спостерігається для ПАР. Їх молекули, порівняно із молекулою полімеру невеликі, і адсорбція їх на PbO_2 оборотна, то найповніше таку адсорбцію описує ізотерма Фрумкіна. Як ілюстративний приклад наведено ізотерму адсорбції $C_4F_9SO_3K$ на порошку PbO_2.

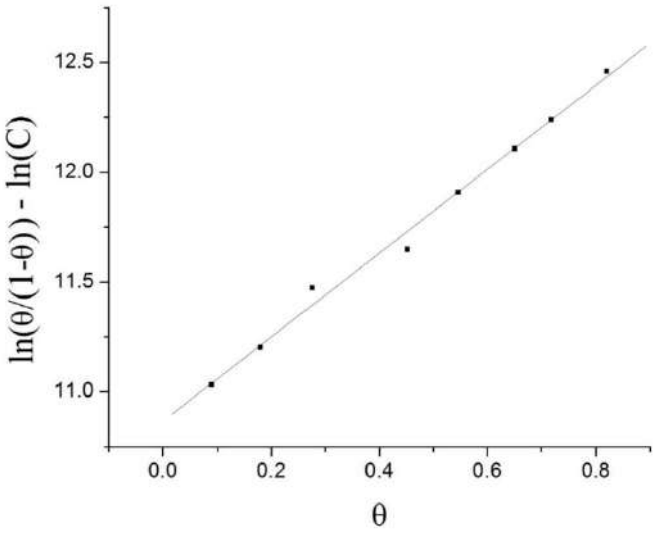

Рис. 5.5 Ізотерма адсорбції Фрумкіна $C_4F_9SO_3K$ на PbO_2. θ та C означають заповнення поверхні та рівноважну концентрацію відповідно

Всі спостережувані закономірності можна пояснити в рамках чотиристадійної схеми утворення PbO_2 [36]. Механізм був модифікований з першої версії [41], де були запропоновані нерозчинні кисеньвмісні проміжні продукти Pb(IV), через утворення кисеньвмісних частинкок Pb(IV), запропонованих Chang і Johnson [42], і кисеньвмісного проміжного продукту Pb(III), запропонованого Веліченком із співавт. [43], який згодом довів існування як кисень-Pb(III), так і кисень-Pb(IV) розчинних проміжних продуктів [44]:

$$H_2O \rightarrow OH^{\cdot}_{ads} + H^+ + e^- \quad (5.2)$$

$$Pb^{2+} + OH^{\cdot}_{ads} \rightarrow Pb(OH)^{2+} \quad (5.3)$$

$$Pb(OH)^{2+} + H_2O \rightarrow Pb(OH)_2{}^{2+} + H^+ + e^- \quad (5.4)$$

$$Pb(OH)_2{}^{2+} \rightarrow PbO_2 + 2H^+ \quad (5.5).$$

Згідно із цією схемою спочатку відбувається перенесення першого електрона з утворенням на поверхні електрода кисеньвмісних частинок типу $OH^{\bullet}_{ads}$ шляхом анодної іонізації води (5.2). Потім у наступній хімічній стадії (5.3) ці частинки реагують із іонами плюмбуму, утворюючи незакріплений на поверхні електрода кисеньвмісний проміжний продукт Pb(III), який надалі (5.4) окиснюється з перенесенням другого електрона. У результаті цієї реакції накопичуються проміжні сполуки чотиривалентного плюмбуму, що розпадаються в останній стадії (5.5) з утворенням плюмбум(IV) оксиду.

За низьких анодних поляризацій (E ≤ 1,6 В) зазвичай реалізується кінетичний контроль процесу. За переходу в область високих анодних поляризацій (E ≥ 1,6 В) швидкість електроосадження лімітується стадією доставки Pb(II) до поверхні електрода.

Вплив адсорбції на швидкість процесу можна описати наступним рівнянням:

$$\frac{i_\theta}{i_{\theta=0}} = (1-\theta)\, exp(-S\theta)\, exp[-\frac{(z+\beta n)F\Delta\psi'(\theta)}{RT}] \quad (5.6)$$

Оскільки величина z позитивна, зменшення значення потенціалу в площині локалізації активного комплексу ψ’ приведе збільшення швидкості стадії переносу заряду, що і спостерігається в реальності за невисоких концентрацій полімерної добавки в електроліті. Під час адсорбції аніонного поліелектроліту на поверхні електроду значення ψ’ може не тільки значно зменшитись, але навіть стати від’ємним за рахунок перезарядки подвійного електричного шару. На це вказує зміна електрокінетичного потенціалу PbO_2 з позитивного на негативний за додавання Nafion® до електроліту. Слід зазначити, що збільшення константи швидкості не є типовим ефектом і спостерігається тільки для аніонного поліелектроліту за рахунок значного негативного заряду на молекулі поліелектроліту. Зворотний ефект викличе адсорбція катіонного ПЕ на поверхні оксиду, яка веде до збільшення значення ψ' і, відповідно, зниження швидкості стадії перенесення заряду.

Параметр інгібування S відображає як електростатичну, так і хімічну взаємодію активованого комплекса з адсорбційним шаром. Подальше збільшення об’ємної концентрації добавки в електроліті приводить до збільшення ступеня заповнення поверхні електроду θ адсорбованим Nafion®, що викличе зменшення швидкості стадії перенесення заряду за рахунок блокування активних центрів.

У разі аніонних ПАР і ПЕ параметри ψ' і S діятимуть в протилежних напрямках, а спостережуваний ефект визначатиметься природою адсорбованих речовин. Так, для Nafion® в залежності від концентрації добавки проявляється як ефект прискорення так і ефект інгібування. У разі аніонних ПАР ефект блокування переважає, проте зменшення швидкості процесу не є значним, оскільки інгібування частково компенсується зниженням величини ψ'. Для катіонного ПЕ параметри ψ' і S будуть діяти в одному напрямку (в бік пригнічення процесу).

Таким чином, за характером впливу на кінетику осадження плюмбум оксиду досліджені добавки ПАР і ПЕ можна розбити на кілька груп:

– приводять до прискорення процесу електроосадження PbO_2. До них відносяться аніонні ПЕ, наприклад Nafion®;

– приводять до незначного пригнічення процесу осадження PbO_2. До цієї групи належать аніонні ПАР;

– приводять до значного пригнічення процесу електроосадження PbO_2. Наприклад, катіонний ПЕ.

За застосування в якості добавок до електролітів осадження PbO_2 ПАР та поліелектролітів утворюються композити металоксид-ПАР та металоксид-полімер.

За збільшення анодної густини струму вміст аніонних ПАР в осаді, як правило, зростає (рис. 5.6 – 5.8). Це пояснюється збільшенням сил кулонівського притягання між позитивно зарядженою поверхнею електрода і негативно зарядженими аніонними ПАР, що в свою чергу веде до збільшення адсорбції і, як результат, до зростання кількості добавки в оксиді.

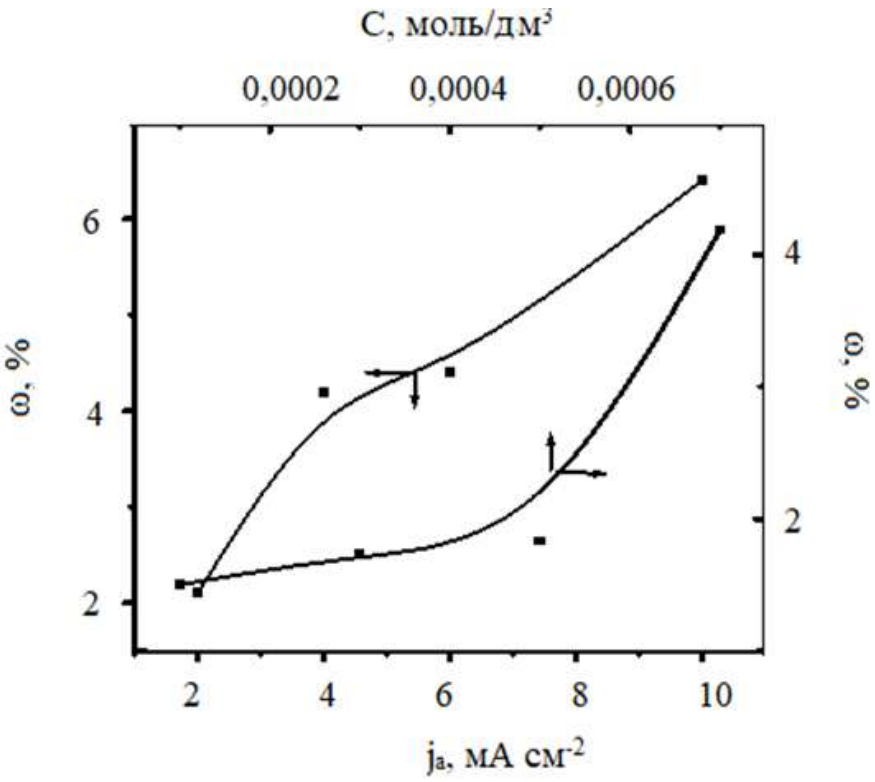

Рис. 5.6 Вміст натрію додецилсульфату в PbO_2 в залежності від концентрації в електроліті та від густини осадження

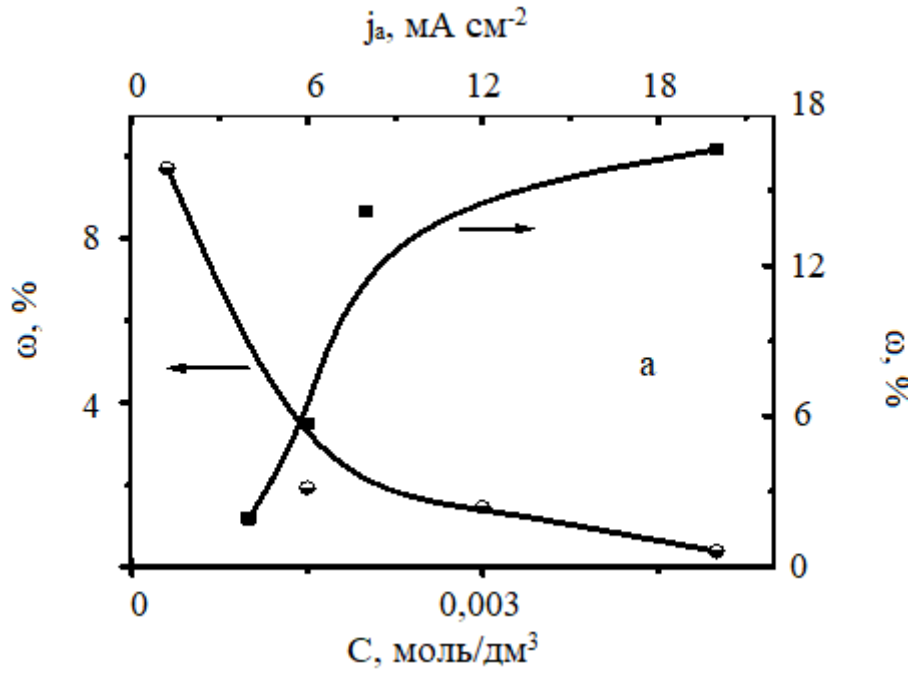

Рис. 5.7 Вміст калію перфлуоробутансульфонату в PbO_2 в залежності від концентрації в електроліті та від густини осадження

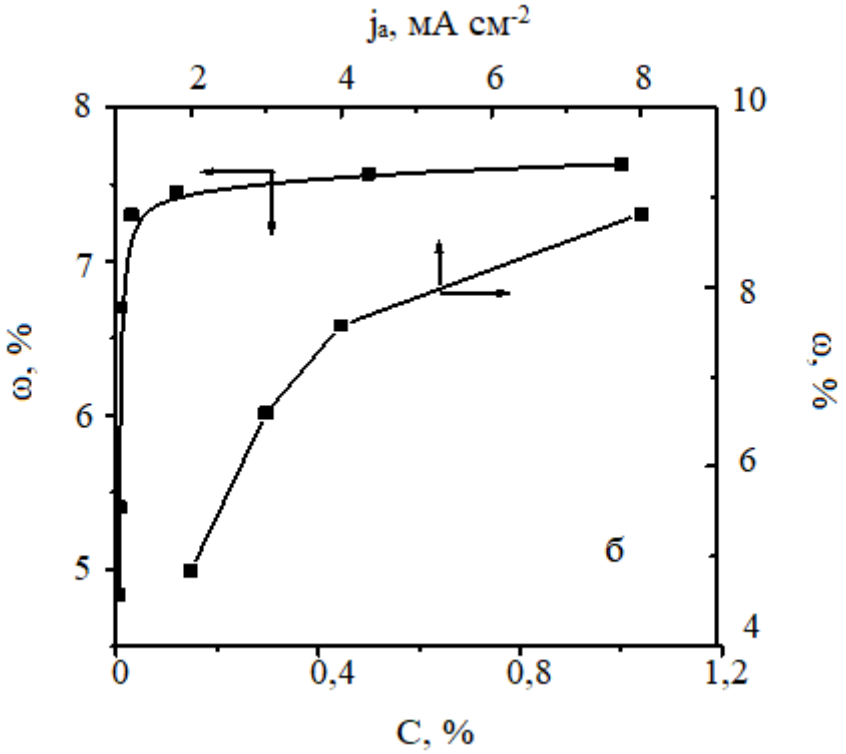

Рис. 5.8 Вміст поліелектроліту Nafion® в PbO_2 в залежності від концентрації в електроліті та від густини осадження

Винятком є лауретсульфат натрію, вміст якого в осаді знижується зі ростом анодної густини струму (рис. 5.9).

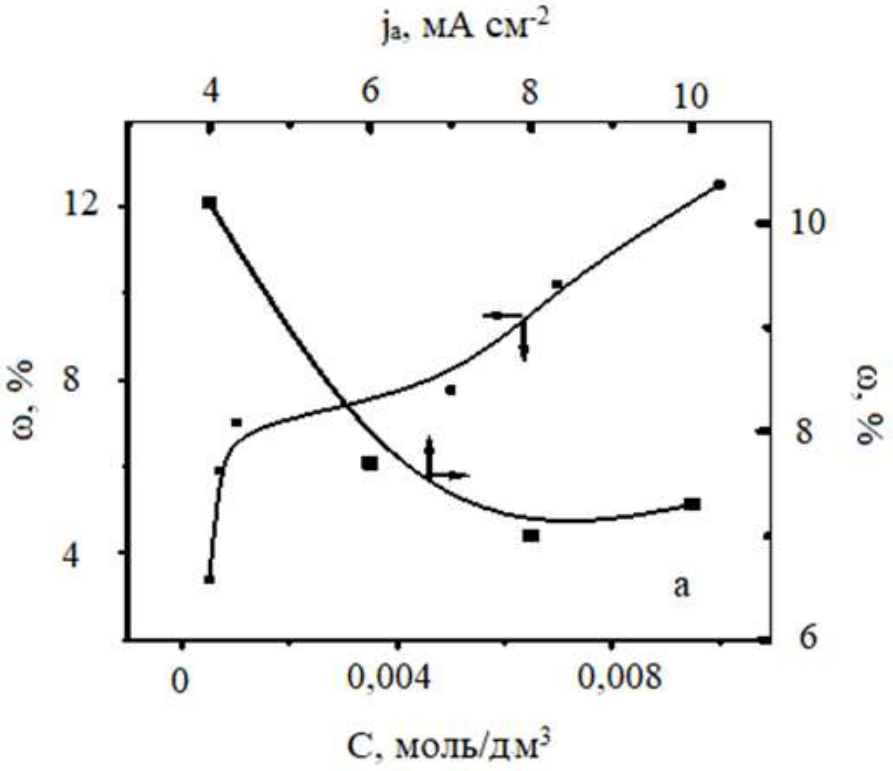

Рис. 5.9 Вміст натрію лауретсульфату в PbO_2 в залежності від концентрації в електроліті та від густини осадження

У цьому випадку на міжфазній межі розчин-повітря візуально спостерігається утворенням піни, кількість якої пропорційна інтенсивності виділення кисню. Таким чином, через високу поверхневу активність натрію лауретсульфата спостерігається явище газової флотації, що, в свою чергу, веде до зменшення концентрації добавки на поверхні електрода, і як наслідок до падіння її вмісту в покритті.

Оскільки паралельно з утворенням плюмбум оксиду на електроді виділяється газоподібний кисень, це може привести до зменшення рівноважної концентрації ПАР в розчині за рахунок його адсорбції на міжфазній межі рідина-газ. Для оцінки останньої з кривих σ = f(c) був розрахований

поверхневий надлишок ПАР за рівнянням Гіббса (рис. 5.10). Ізотерми адсорбції ПАР на міжфазній межі рідина-газ наведені на рисунку 5.11.

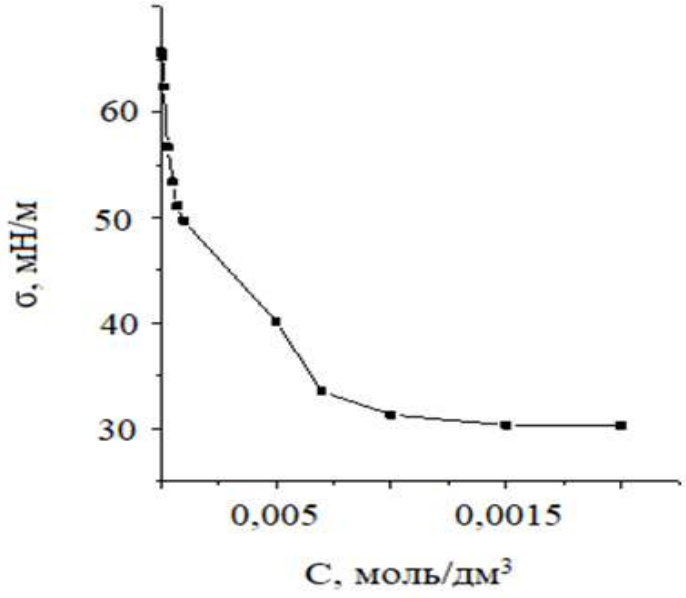

Рис. 5.10 Залежність поверхневого натягу розчинів, що містять натрію лауретсульфат, від концентрації розчиненої речовини

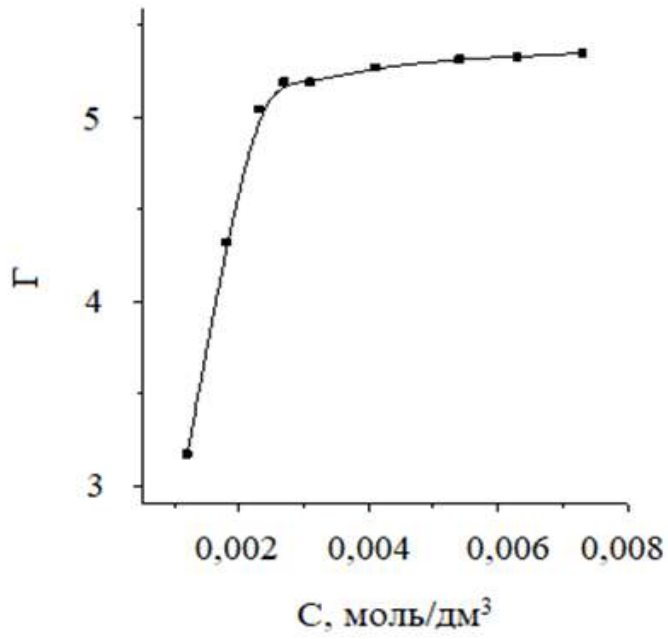

Рис. 5.11 Адсорбція натрію лауретсульфату на межі розчин-повітря

Як показали результати, адсорбція натрію лауретсульфату в два рази перевищує адсорбцію інших ПАР [36].

Необхідно відзначити, що вміст катіонного полімеру поліаміногуанідину також знижується з ростом анодної густини струму, що обумовлено збільшенням сил електростатичного відштовхування між позитивно зарядженими плюмбум оксидом і полімером, що приведе до зниження адсорбції [45].

Додатковим фактором впливу на склад композиту може бути використання суспензійних електролітів, в яких в якості частинок дисперсної фази використовують оксиди, на яких відбувається адсорбція ПАР. Без поверхнево-активних речовин вони відомі, наприклад, системи із TiO_2 [32]. Ми збільшили вміст ПАР, та доповнили композит TiO_2. Отримання композитів в таких спосіб дозволяє синтезувати потрійні системи PbO_2-TiO_2-ПАР (рис. 5.12).

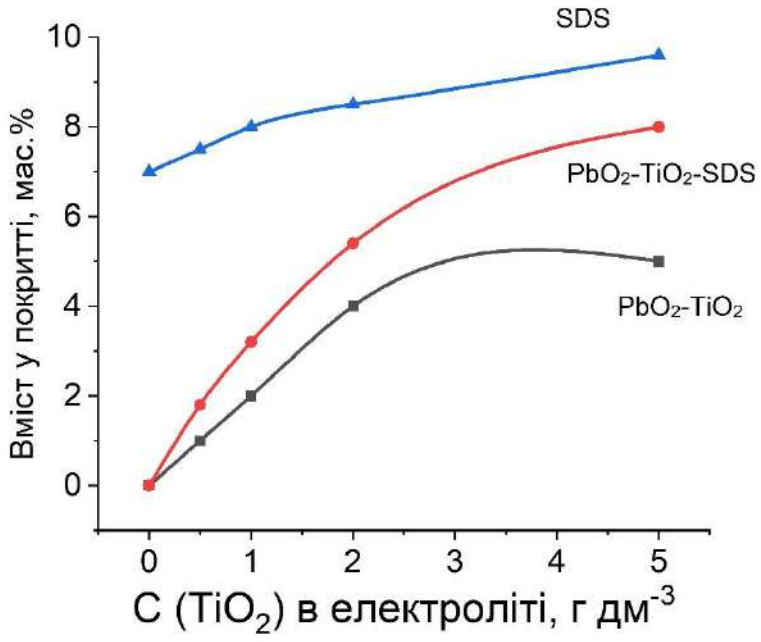

Рис. 5.12 Вміст TiO_2 у композитах PbO_2-TiO_2 та потрійних системах PbO_2-TiO_2-ПАР

До того ж доволі цікаво, коли матеріал проявляє не тільки електрохімічну активність, але і фотоактивність. Хоча, необхідно відмітити невисоку

агрегативну стійкість цих розчинів. Як спостерігалося за додавання стануму в електроліт осадження PbO_2 [46]. Тут можна рекомендувати використання свіжоприготованих розчинів. Фотоактивність матеріалів було досліджено за використання зондової реакції відновлення нітроаренів на CdS електродах та у сузпензії. Результати досліджень показали, що фотокаталітичний процес можна передбачити за допомогою електрохімічних вимірювань [47].

Отримані дані можна адекватно пояснити на основі ряду гіпотез. З одного боку, всі отримані дані можна адекватно описати за допомогою класичної схеми електроосадження, коли на поверхні зростаючого PbO_2 відбувається адсорбція ПАР, а явище зміни вмісту поліелектроліту в покритті може бути викликане двома факторами: і) гетерогенним та іі) міграційним. З іншого боку, ми не можемо виключити, що не тільки кристалізація відбувається з перенасиченого шару розчину, але й утворюються колоїдні частинки в тій чи іншій кількості, які прилипають до поверхні зростаючих кристалів. Механізм осадження PbO_2 це не виключає, оскільки проміжні продукти незакріплені, можуть перебувати і в об’ємі розчину та осідати на непровідні поверхні.

Слід зазначити, що можливо, що всі описані ефекти можуть бути реалізовані одночасно з різними внесками, що не суперечить отриманим експериментальним даним.

Використання різних ПАР приводить до зміни морфології і текстури осадів, але практично не впливає на фазовий склад PbO_2 (рис. 5.13). В композитах зменшується розмір кристалів та ступінь кристалічності, що підтверджується також даними рентгенівської дифракції (рис. 5.14).

Як результат бачимо, що за рахунок варіювання природи ПАР і його концентрації та режимів електролізу можна керувати складом композиту.

Основні результати розділу опубліковано в роботах автора [40, 45, 47].

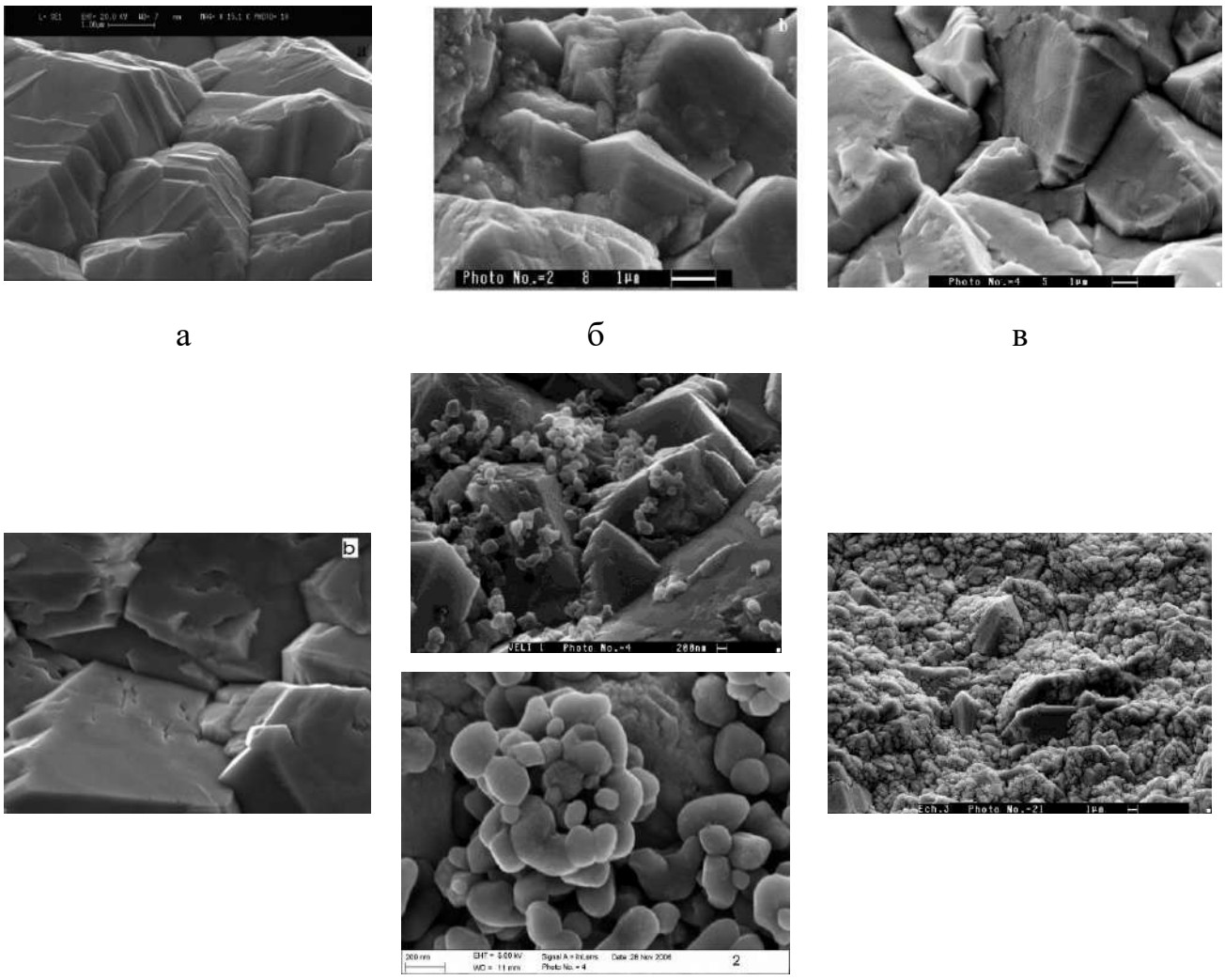

а б в

г д е

Рис. 5.13 СЕМ-зображення поверхні досліджуваних композитів. а – PbO_2; б – PbO_2-2% SLES; в – PbO_2-2% $C_4F_9SO_3K$; г – PbO_2-2% $C_6F_{13}SO_3K$; д – PbO_2-4% TiO_2 (згори), PbO_2-4% TiO_2 + 8,5% SDS (знизу); е – PbO_2-17% Nafion®

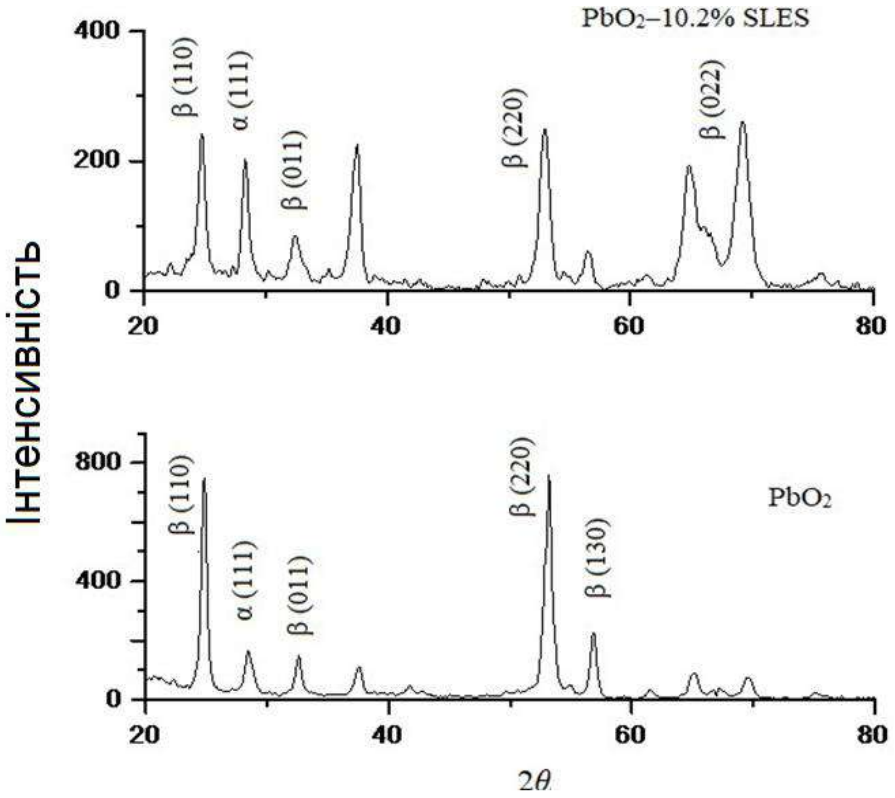

а

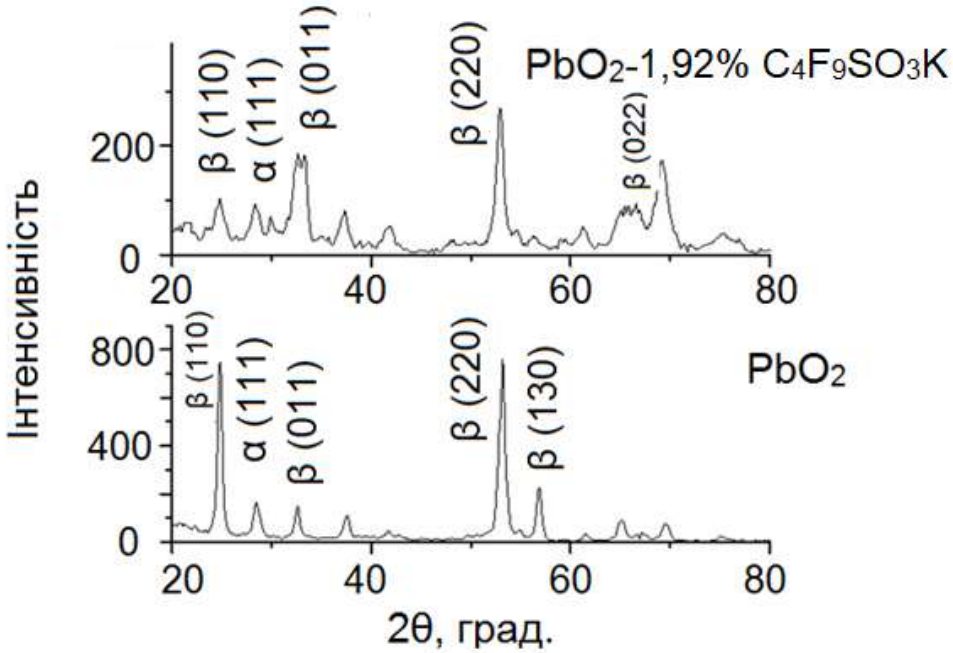

б

Рис. 5.14 Дифрактограми досліджуваних композитів. Склад покриттів зазначено на рисунку.

Journal of Chemistry and Technologies, 2019, *27*(1), 92-100

Journal of Chemistry and Technologies

pISSN 2663-2934 (Print), ISSN 2663-2942 (Online).

journal homepage: http://chemistry.dnu.dp.ua

UDC 544. 653.2

THE SYNTHESIS AND ELECTROCATALYTIC ACTIVITY OF PbO_2-POLYELECTROLYTE AND PbO_2-SURFACTANT COMPOSITE COATINGS

Tatiana V. Luk'yanenko, Olesia B. Shmychkova, Carolina V. Yanova, Natalia I. Krivonosova, Alexander B. Velichenko*

Ukrainian State University of Chemical Technology, 8, Gagarina Ave., 49005 Dnipro, Ukraine

Received 17 May 2019; accepted 14 June 2019, Available online 16 August 2019

Abstract

The regularities of the PbO_2-polyelectrolyte and PbO_2-surfactant composite coatings deposition have been investigated. On a cyclic voltammogram (CV) several characteristic areas can be distinguished: at the anode region of the CV at potentials higher than 1.4 V, the anode current is growing exponentially due to the simultaneous reactions of Pb(II) oxidation and the evolution of oxygen. At the cathodic branch of a CV, a current maximum is observed at potentials of 1.0–1.2 V, corresponding to the reaction of the reduction of lead dioxide. If the polyaminoguanidine hydrochloride is present in the electrolyte, the electrodeposition of lead dioxide is inhibited. If the anionic polymer additive Nafion® is in the electrolyte, one can see an increase in the peak of cathodic reduction of lead dioxide, which indicates an increase in the formation rate of PbO_2. The addition to the electrolyte of anionic surfactants leads to a slight inhibition of the process of deposition of PbO_2. As one can see from the experimental data, the adsorption of anionic surfactants is described satisfactorily by the Langmuir isotherm. Values of the limiting adsorption and the adsorption equilibrium constant were calculated. According to the results obtained, the anionic surfactants, cationic polyelectrolyte polyaminoguanidine hydrochloride and anionic polyelectrolyte Nafion® can be used as additives to the electrolyte during the deposition of the lead dioxide. It has been established, that they are being included into the growing deposit by forming the composite coatings with different composition and various electrocatalytic activity in the reaction of the evolution of oxygen. The content of organic compound in the oxide can vary from 2 to 16 w.%, a surfactant–oxide and polyelectrolyte–oxide composite coating is formed. The overpotential of the oxygen evolution decreases in the line $C_4F_9SO_3K$> $C_{12}H_{25}O_4SNa$> $C_{16}H_{29}O_6SNa$. It should be noted that the energy of adsorption on PbO_2 increases in the same line.

Keywords: polyelectrolyte; surfactant; lead dioxide; nitrate electrolyte; oxygen evolution reaction.

СИНТЕЗ ТА ЕЛЕКТРОКАТАЛІТИЧНА АКТИВНІСТЬ PbO_2-ПОЛІЕЛЕКТРОЛІТ ТА PbO_2-ПОВЕРХНЕВО-АКТИВНА РЕЧОВИНА КОМПОЗИЦИЙНИХ ПОКРИТТІВ

Тетяна В. Лук'яненко, Олександр Б. Величенко* Олеся Б. Шмичкова, Кароліна В. Янова, Наталія І. Кривоносова

ДВНЗ «Український державний хіміко-технологічний університет», просп. Гагаріна 8, м. Дніпро, 49005 Україна

Анотація

Досліджено закономірності електроосадження композиційних покриттів PbO_2-поліелектроліт і PbO_2-поверхнево-активна речовина. На циклічній вольтамперограмі можна виділити кілька характерних областей: на анодній гілці за потенціалів вище 1,4 В струм зростає експоненціально через одночасний перебіг реакцій окиснення Pb(II) та виділення кисню. На катодній гілці вольтамперограми спостерігається максимум струму за потенціалів 1,0-1,2 В, відповідно до реакції відновлення плюмбум(IV) оксиду. За наявності гідрохлориду поліаміногуанідіну в розчині, електроосадження плюмбум(IV) оксиду інгібується, тоді як наявність аніонної полімерної добавки Nafion® приводить до збільшення піку катодного відновлення плюмбум(IV) оксиду, що вказує на збільшення швидкості утворення PbO_2. Додавання в електроліт аніонних поверхнево-активних речовин приводить до незначного пригнічення процесу осадження PbO_2. Як видно з експериментальних даних, адсорбція аніонних ПАР задовільно описується ізотермою Ленгмюра. Були розраховані значення граничної адсорбції та константи адсорбційної рівноваги. Згідно з отриманими результатами, аніонні поверхнево-активні речовини, катіонний поліелектроліт поліаміногуанідін гідрохлорид і аніонний поліелектроліт Nafion® можуть використовуватися в якості добавок до електроліту осадження плюмбум(IV) оксиду. Встановлено, що вони включаються в оксид, утворюючи композиційні покриття з різним складом і електрокаталітичною активністю в реакції виділення кисню. Вміст органічної сполуки в оксиді може варіюватися від 2 до 16 мас.%, утворюючи композиційне покриття ПАР-оксид і поліелектроліт-оксид. Перенапруга виділення кисню зменшується в ряду $C_4F_9SO_3K$> $C_{12}H_{25}O_4SNa$> $C_{16}H_{29}O_6SNa$. Слід зазначити, що енергія адсорбційної взаємодії з PbO_2 збільшується в тому ж ряду.

Ключові слова: поліелектроліт; поверхнево-активна речовина; плюмбум діоксид; нітратний електроліт.

**Corresponding author: Tel.: +380562473627; fax: +380562473627; e-mail address: velichenko@ukr.net*

 doi: 10.15421/081910

Journal of Chemistry and Technologies, 2019, *27*(1), 92-100

СИНТЕЗ И ЭЛЕКТРОКАТАЛИТИЧЕСКАЯ АКТИВНОСТЬ PbO_2-ПОЛИЭЛЕКТРОЛИТ И PbO_2-ПОВЕРХНОСТНО-АКТИВНОЕ ВЕЩЕСТВО КОМПОЗИЦИОННЫХ ПОКРЫТИЙ

Татьяна В. Лукьяненко, Александр Б. Величенко*, Олеся Б. Шмычкова, Каролина В. Янова, Наталья И. Кривоносова

ГВУЗ «Украинский государственный химико-технологический университет», просп. Гагарина 8, г. Днипро, 49005, Украина

Аннотация

Исследованы закономерности электроосаждения композиционных покрытий PbO_2-полиэлектролит и PbO_2-поверхностно-активное вещество. На циклической вольтамперограмме можно выделить несколько характерных областей: на анодной ветви при потенциалах выше 1,4 В ток растет экспоненциально из-за одновременных реакций окисления Pb(II) и выделения кислорода. На катодной ветви вольтамперограммы наблюдается максимум тока при потенциалах 1,0–1,2 В, соответствующий реакции восстановления диоксида свинца. При наличии гидрохлорида полиаминогуанидина в растворе, электроосаждение диоксида свинца ингибируется, тогда как наличие анионной полимерной добавки Nafion® приводит к увеличению пика катодного восстановления диоксида свинца, что указывает на увеличение скорости образования PbO_2. Добавление в электролит анионных поверхностно-активных веществ приводит к незначительному ингибированию процесса осаждения PbO_2. Как видно из экспериментальных данных, адсорбция анионных ПАВ удовлетворительно описывается изотермой Ленгмюра. Были рассчитаны значения предельной адсорбции и константы адсорбционного равновесия. Согласно полученным результатам, анионные поверхностно-активные вещества, катионный полиэлектролит полиаминогуанидин гидрохлорид и анионный полиэлектролит Nafion® могут использоваться в качестве добавок к электролиту осаждения диоксида свинца. Установлено, что они включаются в растущий осадок, образуя композиционные покрытия с различным составом и электрокаталитической активностью в реакции выделения кислорода. Содержание органического соединения в оксиде может варьироваться от 2 до 16 мас.%, образуя композиционное покрытие ПАВ-оксид и полиэлектролит-оксид. Перенапряжение выделения кислорода уменьшается в ряду $C_4F_9SO_3K$> $C_{12}H_{25}O_4SNa$> $C_{16}H_{29}O_6SNa$. Следует отметить, что энергия адсорбционного взаимодействия с PbO_2 увеличивается в том же ряду.

Ключевые слова: полиэлектролит; поверхностно-активное вещество; диоксид свинца; нитратный электролит.

Introduction

Lead dioxide electrodes are of considerable interest in their use at high anodic polarizations [1–3]. They can be obtained by electrodeposition from aqueous solutions and are characterized by high electrical conductivity, low cost, suitable corrosion resistance and high electrocatalytic activity in reactions proceeding at high anodic potentials with the participation of oxygen-containing radicals [1; 4; 5]. At the same time, lead dioxide-based materials have not yet had wide practical application, because of unsuitable mechanical properties, which are manifested when the composite metal-based dimensionally-stable anodes are being created, such as the bad adhesion of the active layer to the substrate, in particular. In this case, the rate of mechanical destruction of the oxide layer of a dimensionally-stable anode is proportional to the intensity of the evolution of oxygen. One of the ways to solve this problem is the surface treatment, the creation of a transition layer, the deposition of a catalyst on the another type of substrate, for example Ebonex® [6]. Another way is to create a composite material that would not be inferior in its properties to the base oxide, but at the same time will have lower internal stresses [7–11].

It is widely recognized, that the presence in the solutions for the deposition of various additives of ions and oxides of other metals has a significant effect on the composition, physico-chemical properties and electrocatalytic activity of the obtained lead dioxide based materials [7; 12–15]. At the same time, in contrast to metal coatings, the effect of organic additives on the regularities of PbO_2 electrodeposition and the properties of resulting materials remains virtually uninvestigated. Since the electrodeposition of lead dioxide is carried out at high anodic potentials, at which most organic compounds oxidize at a sufficiently high rate, the choice of additives is a significant problem. Based on the general considerations, water-soluble polymers (polyelectrolytes) may have value for its usage as an additive to the deposition electrolyte. The long polymer chain and high molecular weight of the polyelectrolytes would ensure the stability of this class of compounds in the range of PbO_2 electrodeposition potentials. In this paper, we investigated the effect of a polymer additive on the electrodeposition of lead dioxide, the composition and the properties of the materials obtained.

Experimental and Methods

All chemicals were of the class of reagents. Lead dioxide was electrodeposited from the nitrate electrolytes which contained 0.1 M HNO_3, 0.1 M $Pb(NO_3)_2$.

Platinized titanium was used as a sheet. It was treated as described in [7] before the platinum

Journal of Chemistry and Technologies, 2018, *27*(1), 92-100

layer was deposited. The content of organic compounds varied within: $1 \cdot 10^{-6}$ to 0.01 M, depending on the purposes of the experiment. Electrolyte compositions and conditions of the deposition of composite coatings were selected in such a way that in all cases the current efficiency of lead dioxide deposition was about 100%.

Electrodeposition regularities of doped lead dioxide were studied on a Pt rotating disk electrode (Pt-RDE, 0.19 cm^2) by steady-state voltammetry, chronoamperometry. For the RDE experiments the voltammetry system SVA-1BM was used. The rate of the scanning potential was varied within 1÷100 mV/s depending on purposes of the experiments. Before an each experiment, the electrode surface was treated with freshly prepared mixture (1:1) of concentrated H_2SO_4 and H_2O_2 [7]. This preliminary treatment technique permits to stabilize the electrode surface, which is oxidized to a certain state under the action of strong oxidizing medium (the phase and chemical composition of the oxides on the surface is defined), which determines the favourable reproducibility in obtaining the cyclic voltammograms in the background electrolyte (0.1 M HNO_3). Voltammetry measurements were carried out in a standard temperature-controlled three-electrode cell.

The reaction of the evolution of oxygen was investigated by steady-state polarization on a computer controlled EG & G Princeton Applied Research potentiostat model 273A in 1M H_2SO_4. All potentials were recorded and reported vs. Ag / AgCl / KCl $_{(sat.)}$.

Adsorption measurements were carried out in 0.5 g of PbO_2 powder in 0.1 M HCl solutions containing various amounts of additive. It should be noted that the measurements were carried out with the presence of the indifferent electrolyte (0.1 M KCl), which shielded the electrostatic field of the oxide surface. The time for establishing the adsorption equilibrium was 24 hours. The content of organic substance was determined by the photocolorimetrical measurements after the extraction of ionic associate with chloroform.

Results and Discussion

The development of a technology sets the task of creating new composite polymer coatings or films that combine both metal and / or oxide properties and polymer properties (high elasticity and strength). The electrodeposition method has been well studied for the preparation of polymer films [16–19]. Electrodeposition is also an effective method in the manufacture of ceramic materials, as well as organoceramic films [20–22]. Electrodeposition of ceramic materials can be performed both in cathodic and anodic ways. At the same time the nanostructured ceramic films are formed. The main component of the formation of films is one that is used for the electrophoresis – a process in which the charged ceramic particles, which are dispersed in a solution, migrate in an electric field to the electrode. The formation of the composite occurs by coagulation of particles on the surface of the electrode. For a more successful deposition of ceramic films the electrolytes include various additives, such as polymers, which influence the formation of colloidal particles [23].

It should be noted that there are no data in the literature discribing the effect of polyelectrolytes on the regularities of electrodeposition and the physico-chemical properties of oxide materials, lead dioxide in particular.

In some cases, small amounts of ionic additives are included in the growing oxide, forming the micromodified materials based on lead dioxide [7; 12]. On this basis, it should be assumed that the addition of organic substances will also affect the electrodeposition, composition and the properties of the oxide materials.

At the beginning of investigation, polyelectrolytes and surfactants of various classes were selected.

Polyelectrolytes:

i) cationic

polyaminoguanidine hydrochloride;

acrylamide based polymer Magnafloc (Ciba);

ii) anionic

perfluorinated ionite Nafion® (Du pont).

Surfactants:

i) cationic

aethonium (1,2-ethylene-bis-(N-decyloxycarbonylmethyl-N, N-dimethylammonium) dichloride);

ii) anionic

potassium nonafluoro-1-butanesulfonate ($C_4F_9SO_3K$);

sodium dodecyl sulfate (SDS, $C_{12}H_{25}SO_4Na$);

sodium laureth sulfate (SLES, $C_{16}H_{29}SO_6Na$);

iii) non-ionic

nonoxynol-3 (monoalkyl ether of polyethylene glycol based on primary fatty alcohols).

Since the organic additives must be adsorbed on the surface of the oxide, the adsorprion of the compounds included in the PbO_2 has been investigated.

It was established that the adsorption of Nafion® (Fig. 1) and polyaminoguanidine hydrochloride (Fig. 2) on the surface of lead dioxide is described by an isotherm, similar to the Langmuir isotherm. The nature of the adsorption isotherm shows the high affinity of the adsorbate

to the surface. Even at low concentrations, the magnitude of adsorption increases sharply and quickly reaches an almost constant value. As a result of potentiometric measurements, it was established that the adsorption of Nafion® on PbO_2 is accompanied by a shift of the zero charge point of the oxide to a region of higher pH. This suggests that the adsorption of polyelectrolyte at $pH < pH_0$ is caused by not only the electrostatic attraction of the polyanion to the positively charged surface of lead dioxide, but also, apparently, as a result of some specific interaction. This assumption is well-supported by the data on the adsorption material balance [24]. It was established that the adsorption of the polymer is accompanied by the release of OH^- ions. If we assume that the adsorption is carried out with the participation of the SO_3^- groups of the polymer, the release of hydroxide ions can be explained by the coordinating interaction of the polyanion with the lead surface cations on the surface of PbO_2:

$$\equiv PbOH + R_n(SO_3^-)_m \rightarrow \equiv Pb(SO_3^-)R_n(SO_3^-)_{m-1} + OH^- \quad (1).$$

With a decrease of the pH of the solution, the adsorption of Nafion® on PbO_2 increases significantly (see Fig. 1), which can be associated with both the increasing role of the electrostatic factor, caused by the increase in the positive charge of the oxide, and the transition of the polymer to the protonated form.

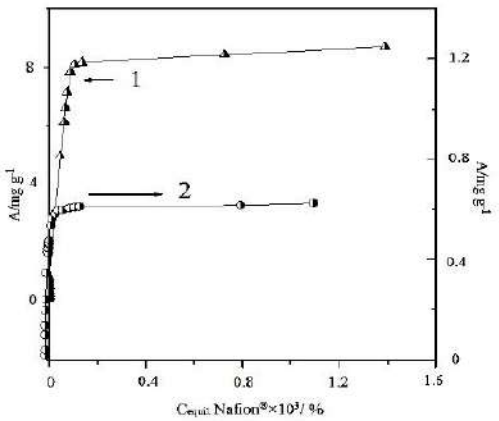

Fig. 1. The adsorption of anionic polyelectrolyte Nafion® on the lead dioxide in 0.1 M HCl (1) and H_2O (2)

The adsorption of Magnafloc is also specific, and its basic regularities are similar to those previously described for Nafion®.

As one can see from the experimental data, the adsorption of anionic surfactants is described satisfactorily by the Langmuir isotherm (Fig. 3).

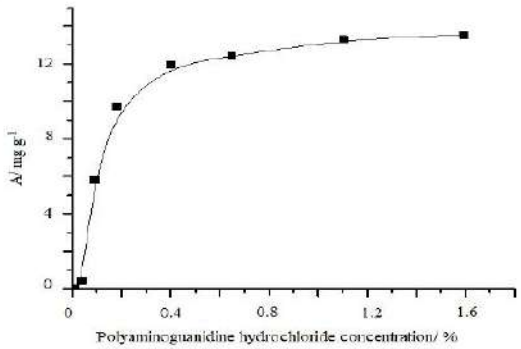

Fig. 2. The adsorption of cationic polyelectrolyte polyaminoguanidine hydrochloride on the lead dioxide in H_2O

In coordinates $A^{-1}=f(C^{-1})$, a linear dependence is observed (correlation factor 0.998), from which the values of the limiting adsorption and the adsorption equilibrium constant were calculated (Table 1).

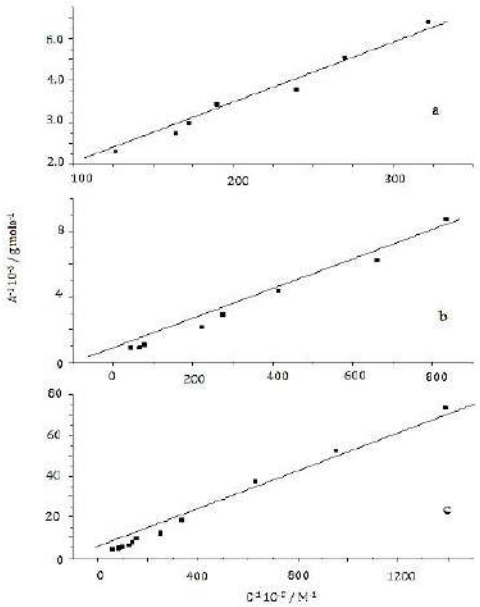

Fig. 3. The Langmuir isotherm of SDS (a), SLES (b) and potassium nonafluoro-1-butanesulfonate (c) on PbO_2 in linear coordinates

The values of the energy of adsorption interaction ($-\Delta G$) are changed in line $C_{16}H_{29}O_6SNa > C_{12}H_{25}O_4SNa > C_4F_9O_3SK$ and are 35.0; 34.1 and 31.5 kJ mol^{-1}, respectively. The obtained values indicate the electrostatic adsorption of anionic surfactants on the lead dioxide. This is also confirmed by a slight shift of the pH_0 of the oxide, which is 0.71±0.1 V in 0.1 M HNO_3 [7; 24].

Journal of Chemistry and Technologies, 2018, *27*(1), 92-100

Table 1

Adsorption parameters of anionic surfactants

Surfactant	Limiting adsorption $A_\infty 10^3$, mole g^{-1}	Adsorption equilibrium constant
$C_4F_9SO_3K$	3.07	6022.1
$C_{12}H_{25}SO_4Na$	3.72	17162.4
$C_{16}H_{29}SO_6Na$	4.15	24638.4

Non-ionic and cationic surfactants are not adsorbed on the positively charged PbO_2 surface.

The next step was to investigate the electrochemical stability of the organic additives which have an impact on the PbO_2 deposition potentials.

Cyclic voltammograms (CV) were taken on a Pt-electrode in a 0.1 M HNO_3 background electrolyte with the included additives (potential scan range 0–1.8 V). It was found that the cationic polyelectrolyte Magnafloc shows an electrochemical activity, forming a phase film on the electrode. In this regard, this polyelectrolyte is not of our interest in further research. The remaining additives, selected by the adsorption, did not show an electrochemical activity in the potential range under study. Thus, anionic polyelectrolyte Nafion®, cationic polyelectrolyte polyaminoguanidine hydrochloride and anionic surfactants can be used as additives to the lead dioxide deposition electrolyte.

To determine the effect of organic additives on electrodeposition of lead dioxide qualitatively, the cyclic voltammograms were obtained on a platinum electrode. On the CV (potential scan range 0.8–1.6 V) several characteristic areas can be distinguished [7, 25] (Fig. 4). At the anode region of the CV at potentials higher than 1.4 V, an anode current is growing exponentially due to the simultaneous reactions of Pb(II) oxidation and oxygen evolution. At the cathodic branch of the CV, a current maximum is observed at the potentials of 1.0–1.2 V, corresponding to the reaction of the reduction of lead dioxide:

$$PbO_2 + 4H^+ \rightarrow Pb^{2+} + 2H_2O + 2e^- \quad (2)$$

As it was established earlier [7; 25], the area and size of the cathode peak characterizes the amount of oxide formed on the electrode surface, that allows one to use these parameters for a qualitative assessment of the PbO_2 electrodeposition rate.

The addition of polyelectrolytes into the deposition electrolyte affects the oxidation process of Pb^{2+} (Fig. 4). At the same time, the nature of the substance plays a significant role. When polyaminoguanidine hydrochloride is present in the electrolyte, the electrodeposition of lead dioxide is inhibited. With the presence of anionic polymer additive Nafion® in the electrolyte, one can see an increase in the peak of cathodic reduction of lead dioxide on the CV (see Fig. 4), which indicates an increase in the formation rate of PbO_2.

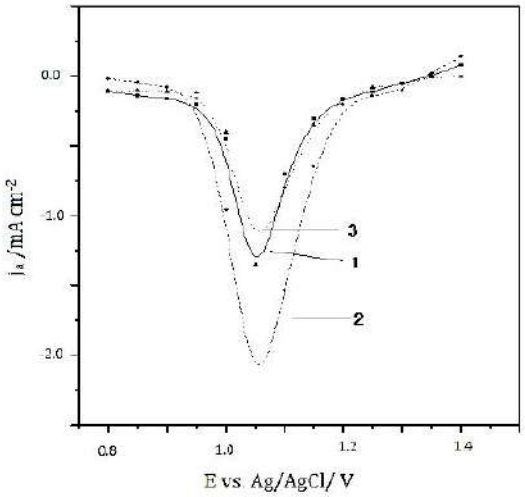

Fig. 4. Cyclic voltammograms cathodic branches (scan range 0.8 to 1.6 V) on Pt-DE in solutions containing 0.01 M $Pb(NO_3)_2$+0.1 M HNO_3 (1) + 0.2% Nafion® (2) or 0.2% of polyaminoguanidine hydrochloride. v=100 mV/s.

The addition to the deposition electrolyte of anionic surfactants leads to a slight inhibition of the process of deposition of PbO_2 (Fig. 5).

It was established that the additives chosen for further studies (anionic surfactants, polyaminoguanidine hydrochloride and Nafion®) are being included in the growing lead dioxide. The content of organic compound in the oxide can vary from 2 to 16 w.%, the surfactant–oxide and polyelectrolyte–oxide composite coating is formed (Table 2).

Journal of Chemistry and Technologies, 2019, *27*(1), 92-100

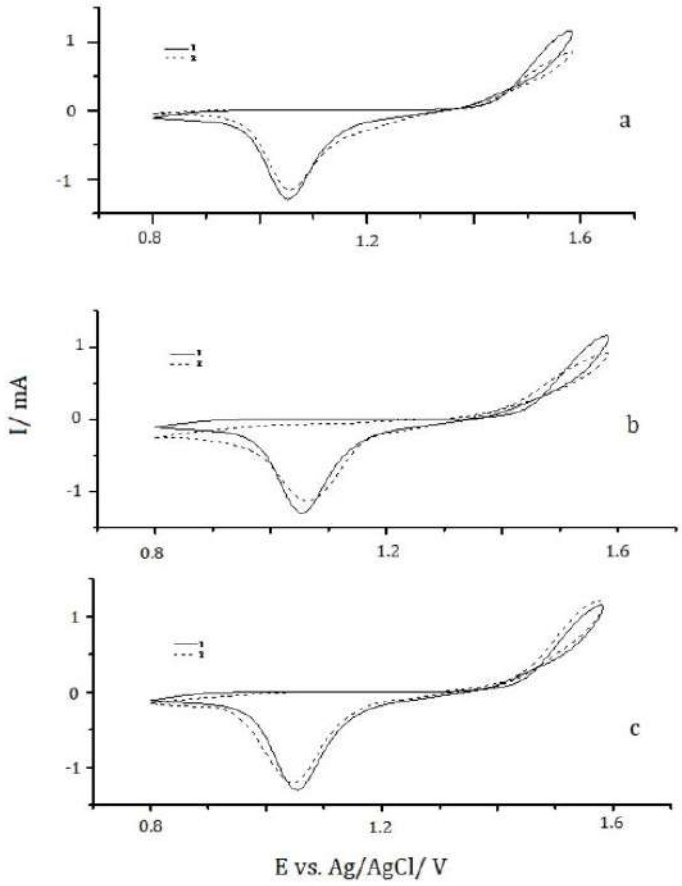

Fig. 5. Cyclic voltammograms (scan range 0.8 to 1.6 V) on Pt-DE in solutions containing 0.01 M $Pb(NO_3)_2$ + 0.1 M HNO_3 + 0.0003 M SDS (a); SLES (b); $C_4F_9SO_3K$ (c). v=100 mV/s.

Table 2

The content of polyelectrolytes anf surfactants in PbO_2-anodes due to deposition conditions

Solution, j_a= 4 mA cm^{-2}	w.%
0.1M HNO_3 + 0.1M $Pb(NO_3)_2$ + 0.02% polyaminoguanidine hydrochloride	1.9
0.1M HNO_3+ 0.1 M $Pb(NO_3)_2$+0.05% Nafion®	7.6
1M HNO_3+ 0.1 M $Pb(NO_3)_2$+ 0.005 M $C_4F_9O_3SI$	16.2
0.1M HNO_3+ 0.1 M $Pb(NO_3)_2$+ 0.0007 M $C_{12}H_2$	4.2
0.5M HNO_3+ 0.1 M $Pb(NO_3)_2$+ 0.007 M $C_{16}H_{29}$	4.8

The inclusion of organic additives into the coating (like the ionic additives [12, 25]) can have a significant impact on physico-chemical properties of obtained materials, for example, on their morphology and structure.

It should also be assumed that the composite oxide-surfactant and oxide-polyelectrolyte materials will differ significantly in their electrocatalytic activity from lead dioxide. Since the vast majority of electrochemical processes at high anodic potentials occur with the participation of oxygen-containing particles which are adsorbed on the electrode (so-called oxygen transfer reactions), it is convenient to evaluate the nature of effects by changing the reaction rate of the evolution of the oxygen.

The rate of the process of the evolution of oxygen on composite materials depends on both the nature and the content of the additive in the oxide (Fig. 6). Thus, the overpotential for the evolution of oxygen decreases in the line $C_4F_9SO_3K$> $C_{12}H_{25}O_4SNa$> $C_{16}H_{29}O_6SNa$. It should be noted that the adsorption energy on PbO_2 increases in the same row. The nature and content of polyelectrolytes in lead dioxide also have a significant effect on the reaction of the evolution of oxygen (Fig. 7).

Journal of Chemistry and Technologies, 2018, *27*(1), 92-100

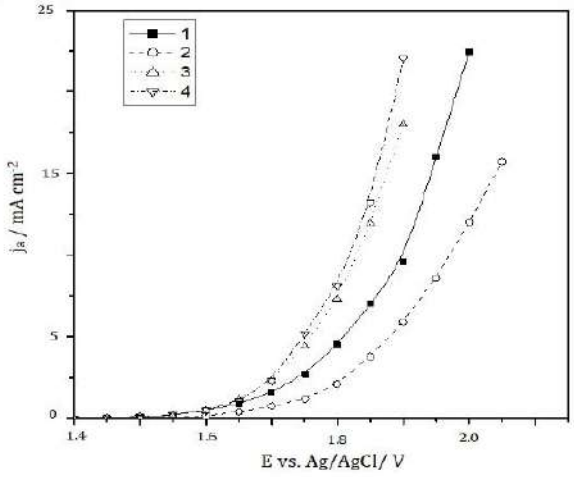

Fig. 6. Steady-state polarization curves of the evolution of oxygen in 1 M H_2SO_4 on the next electrodes: PbO_2 (1); PbO_2-2% $C_4F_9SO_3K$ (2); PbO_2-2.2 % $C_{12}H_{25}O_4SNa$ (3); PbO_2-2.4 % $C_{16}H_{29}O_6SNa$ (4).

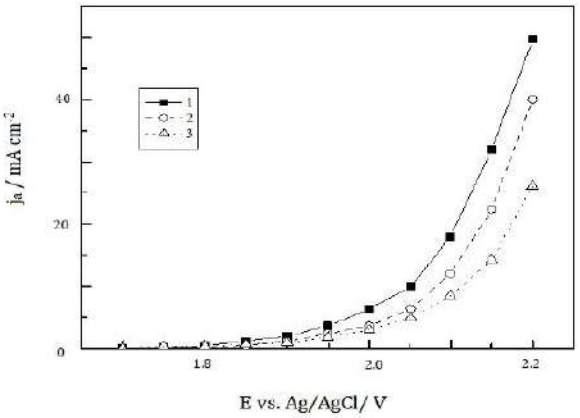

Fig. 7. Steady-state polarization curves of the evolution of oxygen in 1 M H_2SO_4 on the next electrodes: PbO_2 (1); PbO_2-2% polyaminoguanidine hydrochloride (2); PbO_2-6.6 % Nafion® (3)

Conclusions

Thus, according to the results obtained, anionic surfactants, cationic polyelectrolyte polyaminoguanidine hydrochloride and anionic polyelectrolyte Nafion® can be used as additives to the electrolyte during the deposition of the lead dioxide. It has been established, that they are included into the growing deposit and form the composite coatings with different composition and various electrocatalytic activity in the reaction of the evolution of oxygen. The content of organic compound in the oxide can vary from 2 to 16 w.% and the composite surfactant–oxide and polyelectrolyte–oxide coating is formed. The overpotential for the evolution of oxygen decreases in the line $C_4F_9SO_3K$> $C_{12}H_{25}O_4SNa$> $C_{16}H_{29}O_6SNa$. It should be noted that the adsorption energy on PbO_2 increases in the same line.

Бібліографічні посилання

[1] Electrochemical oxygen transfer reactions: electrode materials, surface processes, kinetic models, linear free energy correlations, and perspectives. A review / R. Vargas, C. Borras, D. Mendez [et al.] // J. Solid State Electrochem. – 2016. – Vol. 20. – P. 875–893.

[2] evelopments in soluble lead flow batteries and remaining challenges: An illustrated review / M. Krishna, E. J. Fraser, R. G. A. Wills [et al.] // J. Energy Storage. – 2018. – Vol. 15. – P. 69–90.

[3] Electrocatalytic processes on PbO_2 electrodes at high anodic potentials / O. B. Shmychkova, V. A. Knysh, T. V. Luk'yanenko [et al.] // Surf. Engin. Appl. Electrochem. – 2018. – Vol. 54(1). – P. 38–46.

[4] Wu W. Recent development of mixed metal oxide anodes for electrochemical oxidation of organic

pollutants in water / W. Wu, Z.-H. Huang, T.-T. Lim // Appl. Catal., A. – 2014. –Vol. 480. – P. 58–78.

[5] Application of TiO2-nanotubes/PbO_2 as an anode for the electrochemical elimination of Acid Red 1 dye / J. E. L. Santos, D. C. de Moura, D. R. da Silva [et al.] // J. Solid State Electrochem. – 2019. – Vol. 23. – P. 351–360.

[6] Electrochemical properties of thermally treated platinized Ebonex® with low content of Pt / O. I. Kasian, T. V. Luk'yanenko, P. Yu. Demchenko [et al.] // Electrochim. Acta. – 2013. – Vol. 109. – P. 630–637.

[7] Electrodeposition of composite PbO_2-TiO_2 materials from colloidal methanesulfonate electrolytes / V. Knysh, T. Luk'yanenko, O. Shmychkova [et al.] // J. Solid State Electrochem. – 2017. – Vol. 21. – P. 537–544.

[8] Study of the mechanisms underlying the effects of composite intermediate layers on the performance of Ti/SnO_2 -Sb-La electrodes / Q. Bi, W. Guan, Y. Gao [et al.] // Electrochim. Acta. – 2019. – Vol. 306. – P. 667–679.

[9] Fabrication of Ga_2O_3 –PbO_2 electrode and its performance in electrochemical advanced oxidation processes / H. Du, G. Duan, N. Vang [et al.] // J. Solid State Electrochem. – 2018. – Vol. 22(12). – P. 3799–3806.

[10] Hydrogel-graphene oxide nanocomposites as electrochemical platform to simultaneously determine dopamine in presence of ascorbic acid using an unmodified glassy carbon electrode / J. Pereyra, M. V. Martinez, C. Barbero [et al.] // J. Compos. Sci. – 2019. – Vol. 3. –P. 1–14.

[11] Pouladvand I. Characterization and electrochemical behavior of Ti/TiO_2–RuO_2–IrO_2–SnO_2 anodes prepared by sol–gel process / I. Pouladvand, S. K. Asl, M. G. Hoseini, M. Rezvani // J. Sol-Gel Sci. Technol. – 2019. – Vol. 89. – P. 553–561.

[12] Shmychkova O. Physico-chemical properties of PbO_2-anodes doped with Sn^{4+} and complex ions / O. Shmychkova, T. Luk'yanenko, R. Amadelli, A. Velichenko // J. Electroanal. Chem. – 2014. – Vol. 717–718. – P. 196–201.

[13] Li X. Effects of twelve sodium dodecyl sulfate (SDS) on electro-catalytic performance and stability of PbO2electrode / X. Li, H. Xu, W. Yan // J. Alloy Compd. – 2017. – Vol. 718. – P. 386–395.

[14] Shmychkova O. Electrodeposition of Ni^{2+}-doped PbO_2 and physicochemical properties of the coating / O. Shmychkova, T. Luk'yanenko, R. Amadelli, A. Velichenko // J. Electroanal. Chem. – 2016. – Vol. 774. – P. 88–94.

[15] The electrochemical oxidation of salicylic acid and its derivatives on modified PbO_2-electrodes / O. Shmychkova, T. Luk'yanenko, R. Amadelli [et al.] // Bull. Dnipr. Univ. Ser. Chem. – 2017. – Vol. 25 (2). – P. 57–61.

[16] Walsh F. C. Developments in electrode design: structure, decoration and applications of electrodes for electrochemical technology / F. C. Walsh, L. F. Arenas, C. Ponce de Leon // J. Chem. Tech. Biotechnol. – 2018. – Vol. 93(11). – P. 3073–3090.

[17] Ratcliff E. R. Directed electrodeposition of polymer films using spatially controllable electric field gradients / E. R. Ratcliff, A. C. Hillier // Langmuir. – 2007. – Vol. 23. – P. 9905–9910.

[18] Darmanin T. Electrodeposited polymer films with both superhydrophobicity and superoleophilicity / T. Darmanin, M. Nicolas, F. Guittard // Phys. Chem. Chem. Phys. – 2008. – Vol. 10. – P. 4322–4326.

[19] Electrodeposition of insulating poly(phenylene oxide) films with variable thickness / M. Y. Timmermans, F. Mattelaer, S. Moitzheim [et al.] J. Appl. Polym. Sci. – 2917. – Vol. 134. – P. 44533–44540.

[20] Zhitomirsky I. The electrodeposition of ceramic and organoceramic films for fuel cells I. Zhitomirsky, A. Petric // JOM. – 2001. – Vol. 53. – P. 48–50.

[21] Recent advances in complex functional materials: from design to application L. E. La Porta, F. de Almeida (Eds.) Springer Int. Publ., 2017.

[22] Tian Q. Electrophoretic deposition and characterization of nanocomposites and nanoparticles on magnesium substrates / Q. Tian, H. Liu // Nanotechnology. – 2015. – Vol. 26. – P. 175102–175108.

[23] Electrodeposited Ni-based magnetic mesoporous films as smart surfaces for atomic layer deposition: an "all-chemical" deposition approach toward 3D nanoengineered composite layers / J. Zhang, A. Quintana, E. Menendez [et al.] // ACS Appl. Mater. Interfaces. – 2018. – Vol. 10(17). – P. 14877–14885.

[24] Nafion effect on the lead dioxide electrodeposition kinetics / A. B. Velichenko, T. V. Luk'yanenko, N. V. Nikolenko [et al.] // Russ. J. Electrochem. – 2007. – Vol. 43. – P. 118–120.

[25] Bi-doped PbO_2 anodes: electrodeposition and physico-chemical properties / O. Shmychkova, T. Luk'yanenko, A. Velichenko [et. al.] // Electrochim. Acta. – 2013. – Vol. 111. – P. 332–338.

References

[1] Vargas, R., Borras, C., Mendez, D., Mostany, J., Scharifker, B.R. (2016). Electrochemical oxygen transfer reactions: electrode materials, surface processes, kinetic models, linear free energy correlations, and perspectives. A review. *J. Solid State Electrochem., 20,* 875–893. doi:10.1007/s10008-015-2984-7.

[2] Krishna, M., Fraser, E. J., Wills, R. G. A., Walsh, F. C. (2018). Developments in soluble lead flow batteries and remaining challenges: An illustrated review. *J. Energy Storage*, 15, 69-90. doi: 10.1016/j.est.2017.10.020.

[3] Shmychkova, O. B., Knysh, V. A., Luk'yanenko, T. V., Amadelli, R., Velichenko, A. B. (2018). Electrocatalytic processes on PbO_2 electrodes at high anodic potentials. *Surf. Engin. Applied Electrochem.*, 54(1), 38-46. doi: 10.3103/S1068375518010143.

[4] Wu, W., Huang, Z.-H., Lim, T.-T. (2014). Recent development of mixed metal oxide anodes for electrochemical oxidation of organic pollutants in water. *Appl. Catal., A,* 480, 58-78. doi: 10.1016/j.apcata.2014.04.035.

[5] Santos, J. E. L., de Moura, D. C., da Silva, D. R., Panizza, M., Martinez-Huitle, C. A. (2019). Application of TiO_2-nanotubes/PbO_2 as an anode for the electrochemical elimination of Acid Red 1 dye. *J. Solid State Electrochem.,* 23, 351–360. doi: 10.1007/s10008-018-4134-5.

[6] Kasian, O. I., Luk'yanenko, T. V., Demchenko, P. Yu., Gladyshevskii, R. E., Amadelli, R., Velichenko, A. B. (2013). Electrochemical properties of thermally treated platinized Ebonex® with low content of Pt *Electrochim. Acta*, 109, 630–637. doi: 10.1016/j.electacta.2013.07.162.

[7] Knysh, V., Luk'yanenko, T., Shmychkova, O., Amadelli, R., Velichenko, A. (2017). Electrodeposition of composite PbO_2-TiO_2 materials from colloidal methanesulfonate electrolytes, *J. Solid State*

Electrochem., 21, 537-544. doi: 10.1007/s10008-016-3394-1.

[8] Bi, Q., Guan, W., Gao, Y., Cui, Y., Ma, S., Xue, J. (2019). Study of the mechanisms underlying the effects of composite intermediate layers on the performance of Ti/SnO_2-Sb-La electrodes, *Electrochim. Acta*, 306, 667-679. doi: 10.1016/j.electacta.2019.03.122.

[9] Du, H., Duan, G., Vang, N., Liu, J., Tang, Y., Pang, R., Chen, Y., Wan, P. (2018). Fabrication of Ga_2O_3 – PbO_2 electrode and its performance in electrochemical advanced oxidation processes, *J. Solid State Electrochem.*, 22(12), 3799-3806. doi: 10.1007/s10008-018-4082-0.

[10] Pereyra, J., Martinez, M. V., Barbero, C., Bruno, M., Acevedo, D. (2019). Hydrogel-graphene oxide nanocomposites as electrochemical platform to simultaneously determine dopamine in presence of ascorbic acid using an unmodified glassy carbon electrode, *J. Compos. Sci.*, 3, 1-14. doi: 10.3390/jcs3010014.

[11] Pouladvand, I., Asl, S. K., Hoseini, M. G., Rezvani, M. (2019). Characterization and electrochemical behavior of Ti/TiO_2–RuO_2–IrO_2–SnO_2 anodes prepared by sol–gel process, *J. Sol-Gel Sci. Technol.*, 89, 553–561. doi: 10.1007/s10971-018-4887-4.

[12] Shmychkova, O., Luk'yanenko, T., Amadelli, R., Velichenko, A. (2014). Physico-chemical properties of PbO_2-anodes doped with Sn^{4+} and complex ions. *J. Electroanal. Chem., 717-718*, 196-201. http://www.sciencedirect.com/science/article/pii/S1572665714000502.

[13] Li, X., Xu, H., Yan, W. (2016). Effects of twelve sodium dodecyl sulfate (SDS) on electro-catalytic performance and stability of PbO_2 electrode, *J. Alloy Compd.*, 718, 386–395. doi: 10.1016/j.jallcom.2017.05.147.

[14] Shmychkova, O., Luk'yanenko, T., Amadelli, R., Velichenko, A. (2016). Electrodeposition of Ni^{2+}-doped PbO_2 and physicochemical properties of the coating, *J. Electroanal. Chem.*, 774, 88–94. doi: 10.1016/j.jelechem.2016.05.017.

[15] Shmychkova, O., Luk'yanenko, T., Amadelli, R., Dmitrikova, L., Velichenko, A. (2017). The electrochemical oxidation of salicylic acid and its derivatives on modified PbO_2-electrodes, *Bull. Dnipr. Univ. Ser. Chem.*, 25 (2), 57–61. doi:10.15421/081706.

[16] Walsh, F. C., Arenas, L. F., Ponce de Leon, C. (2018). Developments in electrode design: structure, decoration and applications of electrodes for electrochemical technology, *J. Chem. Tech. Biotechnol.*, 93(11), 3073-3090. doi: 10.1002/jctb.5706.

[17] Ratcliff, E. R., Hillier, A. C. (2007). Directed electrodeposition of polymer films using spatially controllable electric field gradients, *Langmuir*, **23**, 9905–9910. doi: 10.1021/la700827w.

[18] Darmanin, T., Nicolas, M., Guittard, F. (2008). Electrodeposited polymer films with both superhydrophobicity and superoleophilicity, *Phys. Chem. Chem. Phys.*, 10, 4322-4326. doi: 10.1039/B804617D.

[19] Timmermans, M. Y., Mattelaer, F., Moitzheim, S., Clerckx, N., Sepulveda, A., Deheryan, S., Detavernier, Ch., Vereecken, P. M. (2017), Electrodeposition of insulating poly(phenylene oxide) films with variable thickness, *J. Appl. Polym. Sci.*, 134, 44533-44540. doi: 10.1002/app.44533.

[20] Zhitomirsky, I. Petric, A. (2001). The electrodeposition of ceramic and organoceramic films for fuel cells, *JOM*, 53, 48-50. doi: 10.1007/s11837-001-0071-2.

[21] *Recent advances in complex functional materials: from design to application*, L. E. La Porta, F. de Almeida (Eds.), 2017, Springer Int. Publ. doi: 10.1007/978-3-319-53898-3_9.

[22] Tian, Q., Liu, H. (2015). Electrophoretic deposition and characterization of nanocomposites and nanoparticles on magnesium substrates, *Nanotechnology*, 26, 175102–175108. doi: 10.1088/0957-4484/26/17/175102.

[23] Zhang, J., Quintana, A., Menendez, E.,Coll, M., Pellicer, E, Sort, J. (2018). Electrodeposited Ni-based magnetic mesoporous films as smart surfaces for atomic layer deposition: an "all-chemical" deposition approach toward 3D nanoengineered composite layers, *ACS Appl. Mater. Interfaces*, 10(17), 14877–14885. doi: 10.1021/acsami.8b01626.

[24] Velichenko, A. B., Luk'yanenko, T. V., Nikolenko, N.V., Amadelli, R., Danilov, F. I. (2007). Nafion effect on the lead dioxide electrodeposition kinetics, *Russ. J. Electrochem.*, 43, 118–120. doi: 10.1134/S102319350701017X.

[25] Shmychkova, O., Luk'yanenko, T., Velichenko, A., Meda, L., Amadelli, R. (2013). Bi-doped PbO_2 anodes: electrodeposition and physico-chemical properties. *Electrochim. Acta, 111*, 332–338. http://www.sciencedirect.com/science/article/pii/S0013468613016125.

Journal of The Electrochemical Society, 2020 **167** 063501
1945-7111/2020/167(6)/063501/9/$40.00 © 2020 The Electrochemical Society ("ECS"). Published on behalf of ECS by IOP Publishing Limited

Composite Electrodes PbO_2-Nafion®

A. Velichenko,[1,z] T. Luk'yanenko,[1] N. Nikolenko,[1] O. Shmychkova,[1] P. Demchenko,[2] and R. Gladyshevskii[2]

[1]*Ukrainian State University of Chemical Technology, Dnipro, Ukraine*
[2]*Ivan Franko National University of Lviv, Lviv, Ukraine*

PbO_2-polyelectrolyte composite materials with a content of polyelectrolyte up to 13 wt% are formed by electrochemical deposition of PbO_2, depending on the solution composition and the deposition conditions. Several assumptions concerning the mechanism of the formation of composites that taking into account the oxygen-containing species of lead non-fixed on the surface, located in the near-electrode zone have been proposed. The shape and size of the PbO_2 crystals is altered by the presence of polyelectrolyte. The surface is more uniform and the crystals are smaller, there is not a pronounced crystallographic orientation, however the phase content remains practically the same as in the undoped sample. When using composite materials based on lead dioxide containing polyelectrolyte, selective changes in the overvoltage of oxygen evolution and electrochemical conversion of organic substances into aliphatic non-toxic compounds are observed. In this case, the electrocatalytic activity of composite materials depends on the nature and content of the polyelectrolyte additive in the oxide.
 [DOI: 10.1149/1945-7111/ab805f]

Manuscript submitted October 22, 2019; revised manuscript received March 16, 2020. Published March 30, 2020.

Lead dioxide electrodes are known to be of considerable interest in their application at high anodic polarizations.[1–3] They can be fabricated by electrodeposition from aqueous solutions, have high electrical conductivity, low cost, satisfactory corrosion resistance and high electrocatalytic activity in reactions proceeding at high anode potentials with oxygen-containing radicals participation.[4–6] At the same time, materials based on lead dioxide have still not found wide practical application, which is caused by unsatisfactory mechanical properties namely, inadequate adhesion of the active layer to the substrate.[7] The rate of mechanical destruction of the oxide layer of dimensionally stable anode is proportional to the intensity of oxygen evolution. One way to solve this problem is surface treatment, the creation of a transition layer, deposition of the catalyst on substrates of a different type, for example Ebonex®.[8,9] Another way is to create a composite material that by its properties would not be inferior to the base oxide, but would have lower internal stresses.[10,11]

It is well recognized,[12–14] that the presence of various ionic dopants and oxides of other metals in deposition electrolytes has a significant effect on the composition, physico-chemical properties and electrocatalytic activity of the resulting materials based on lead dioxide. At the same time, unlike metal coatings, the effect of organic additives on the regularities of PbO_2 electrodeposition and the properties of the resulting materials remains practically unexplored. Since the electrodeposition of lead dioxide is carried out at high anode potentials, at which most organic compounds are oxidized at a sufficiently high rate, the choice of dopant is a significant problem. Based on general considerations, water-soluble polymers (polyelectrolytes) may be of considerable interest as an additive to the deposition electrolyte.[15–17] A long polymer chain and a high molecular weight of polyelectrolytes will be able to ensure the stability of this class of compounds at the electrodeposition potentials of PbO_2. In this paper, the effect of a polymer additive on the electrodeposition of lead dioxide, the composition and properties of the resulting materials were investigated.

Experimental

All chemicals were reagent grade. Electrodeposition regularities of doped lead dioxide were studied on an Au disk electrode (Au-DE, 1 cm^2) by steady-state voltammetry, chronoamperometry. The voltammetry system SVA-1BM was used. The potential scan rate was varied within 1–100 mV s^{-1} depending on purposes of the experiments. Before each experiment, the electrode surface was treated with a freshly prepared mixture (1:1) of concentrated H_2SO_4 and H_2O_2.[12] This preliminary treatment technique permits to stabilize the electrode surface, which under the action of strong oxidizing medium is oxidized to a certain state (defined phase and chemical composition of the surface oxides), which determines the satisfactory reproducibility of cyclic voltammograms in the background electrolyte (0.1 M HNO_3). Voltammetry measurements were carried out in a standard temperature-controlled three-electrode cell. Change in the mass of the gold electrode under galvanostatic conditions was carried out gravimetrically with quartz microbalances.

The determination of current efficiency and partial current of lead dioxide deposition was done according the method described in details in previous publications.[18] Lead dioxide was electrodeposited from nitrate electrolytes that contained 0.1 M HNO_3, 0.1 M $Pb(NO_3)_2$ and 0.05 wt% of Nafion®. The polymeric additive was introduced into the deposition electrolyte from a 5% aqueous alcohol solution (a mixture of low molecular weight aliphatic alcohols containing 15%–20% water) prepared from the powder of the ion exchange membrane Nafion® 117 (Aldrich). Nafion® is a perfluorinated ion exchanger produced by Du Pont and characterized by general formula:

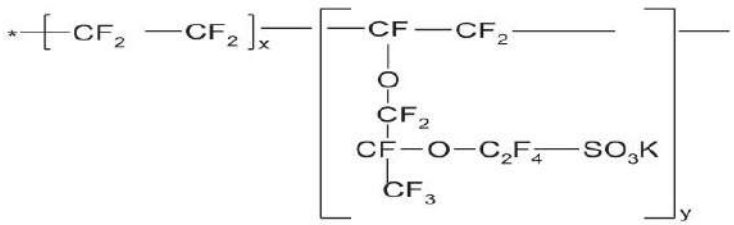

All the studies hereafter have been performed by scanning electron microscopy (SEM) with SEM-106I microscope or

[z]E-mail: velichenko@ukr.net

Stereoscan 440 apparatus. X-Ray powder diffraction (XRPD) data were collected in the transmission mode on a STOE STADI P diffractometer with Cu $K\alpha_1$-radiation, curved Ge (1 1 1) monochromator on primary beam, $2\theta/\omega$-scan, angular range for data collection 20.000–110.225 °2θ with increment 0.015, linear position sensitive detector with step of recording 0.480 °2θ and times per step 75–300 s, U = 40 kV, I = 35 mA, T = 298 K. A calibration procedure was performed utilizing SRM 640b (Si) and SRM 676 (Al_2O_3) NIST standards. Preliminary data processing and X-ray qualitative phase analysis were performed using STOE WinXPOW and PowderCell program packages. Crystal structures of the phases were refined by the Rietveld method with the program FullProf.2k, applying a pseudo-Voigt profile function and isotropic approximation for the atomic displacement parameters, together with quantitative phase analysis. Microstructural parameters (i.e., size of coherently diffracting domains accepted as average apparent crystallite size D, and average maximum strain ε) were identified by isotropic line broadening analysis using simplified integral breadth methods for reflections with maximal intensities: (110) for α-PbO_2 and (111) for β-PbO_2.

Adsorption measurements were carried out at a fixed pH value, the same as in the deposition electrolyte.

Oxygen evolution reaction was investigated by steady-state polarization on computer controlled EG & G Princeton Applied Research potentiostat model 273 A in phosphate buffer (0.25 M Na_2HPO_4 + 0.1 M KH_2PO_4). Traditionally, researchers pay attention to the study of the oxygen evolution reaction (OER) on lead dioxide coatings in sulfuric acid, since this type of coating is of potential interest for use in lead-acid batteries. The study of OER allows one to identify the passivation of coatings in sulfuric acid, since these systems are quite specific and are characterized by adsorption of SO_4^{2-} ions.[19] Having in mind the potential applications of obtained materials, we investigated the dependence of the overvoltage of the oxygen evolution reaction on the electrodes involved also in 1 M H_2SO_4. All potentials were recorded and reported vs $Ag/AgCl/KCl_{(sat.)}$.

The electrooxidation of organic compounds was carried out in divided cell at j_a = 50 mA cm^{-2}. Nafion® 117 perfluorinated membrane was used to separate the two compartments. The volume of anolyte was 130 cm^3. Solution, containing phosphate buffer (0.25 M Na_2HPO_4 + 0.1 M KH_2PO_4) + 0.1 mM organic compound, (pH = 7.0) was used as anolyte; phosphate buffer as catholyte. Stainless steel was used as cathode. Composite PbO_2-Nafion® electrodes were used as anodes. Composite coating was deposited on Ti/Pt that was treated as described in[11,17] before platinum layer depositing. Electrode surface area was 3 cm^2.

The changing of the concentration of the organic substance during the electrolysis was measured by sampling (volume of 5 cm^3) at regular intervals and measuring the optical density of the solution in the ultraviolet and visible region (wavelength range 200–570 nm) using a Kontron Uvikon 940 spectrometer. Since Beer–Lambert law maintains a linear relationship between absorbance (A) and concentration (c) of 4-chlorophenol (A = 1375.6c + 0.06097; r = 0,994), it was possible to establish the electrocatalytic activity of the composites involved. Analyses of the reaction products were conducted by HPLC using a Shimadzu RF-10A xL instrument equipped with Ultraviolet SPD-20AV detector and a 30 cm Discovery® C18 column.

Results and Discussion

As it is known,[20,21] the adsorption of Nafion® on lead dioxide surface is described by an isotherm similar to the Langmuir isotherm. The nature of the adsorption isotherm reflects the high affinity of the adsorbate to the surface. The value of adsorption already increases at small concentrations and rapidly reaches a practically constant value. Investigations of the relationship between the effectiveness of the action of organic dopants and the composition and structure of their molecules require the determination of the mechanism of their adsorption. In our opinion, clarification of the mechanisms of adsorption is possible on the basis of studying the material balance of adsorption-desorption processes.

According to the literature, adsorption of polar organic molecules on oxides is described, as a rule, from two different points of view. Under the first of them, the adsorption of a polar organic molecule on the oxide surface is usually described as the process of formation of hydrogen bonds with surface OH-groups of the oxide[20–22]:

$$\equiv MeOH + R \rightarrow \equiv MeOH \cdots R, \quad [1]$$

Other researchers[21,23] reported that adsorbed organic molecules or ions can enter into a donor-acceptor interaction with surface metal cations, displacing water molecules or OH^- ions from their coordination sphere:

$$\equiv MeOH + R \rightarrow \equiv Me^+OH \cdots R \quad [2]$$

From a comparison of these two equations, the basic idea of using a material balance to analyze the adsorption mechanism is obvious. In fact, based on a comparison of the amounts of adsorbed particles R and the released OH^- ions, it is possible to evaluate the contribution of one or another mechanism of adsorption interaction.

Examples of using data on the composition of solutions after reaching adsorption equilibrium to determine the shape of adsorbed ions are known in the literature.[24] However, this method is not widespread. This is apparently due to the complexity of describing the totality of data on hydrolytic, ion-exchange, dissociative, and adsorption equilibria that occur during adsorption in aqueous solutions. Examples of solving this problem can be found in publications.[25,26]

One can determine the nature of the surface bond, and also determine the composition of the adsorption complex by comparison the number of adsorbed R particles and originated OH^- ions. As it is known, the surface of oxides in aqueous solutions becomes charged due to the dissociation of surface groups ≡MeOH or adsorption of H^+ and OH^- (both models are thermodynamically indistinguishable):

$$\equiv MeOH + H^+ \rightarrow \equiv MeOH_2^+ \quad [3]$$

$$\equiv MeOH + OH^- \rightarrow \equiv MeO^- + H_2O. \quad [4]$$

Therefore, the hydroxylated surface of the oxides should generally be described by ≡MeOH, $\equiv MeO^-$ и $\equiv MeOH^+{}_2$ groups. Adsorption of organic molecules (R) on groups ≡MeOH can be described by the following equations:

i) adsorption without ion displacement H^+ and OH^-:

$$\equiv MeOH + R \rightarrow \equiv MeOH \cdots R, \quad [5]$$

$$\equiv MeOH + R \rightarrow \equiv MeO(H) \cdots R, \quad [6]$$

ii) adsorption with H^+ and OH^- ion displacement:

$$\equiv MeOH + R \rightarrow \equiv MeOR + H^+, \quad [7]$$

$$\equiv MeOH + R \rightarrow \equiv MeR + OH^-. \quad [8]$$

Similar equations can also be compiled for the surface groups $\equiv MeO^-$ and $\equiv MeOH_2^+$. It should be noted that the ratio of H^+ and OH^- ions in solution is determined by the equilibrium:

$$H^+ + OH^- \rightarrow H_2O, \quad [9]$$

and therefore possible changes in acidity of solutions during adsorption, for example, according to Eqs. 7 and 8, do not reflect the absolute amounts of released H^+ and OH^- ions, but only their relative excesses.

Let's formulate the equations of material balance for the case $pH_{init.} < pH_{equil.} \leqslant pH_0$ (where pH_0 is a zero charge point) on the basis of Eqs. 3–9. Assuming that the adsorption occurs according to Eq. 8 with exchange of OH^- ions, the initial and equilibrium amounts of H^+ и OH^- ions will be related by equations

$$n(H^+)_{init.} - n(H^+)_1 - n(H^+)_7 = n(H^+)_{equil.} \quad [10]$$

$$n(OH^-)_{init.} + n(OH^-)_6 - n(OH^-)_7 = n(OH^-)_{equil.} \quad [11]$$

where $n(H^+)$ and $n(OH^-)$ indexes correspond to the numbers of equations.

The number of OH^- ions adsorbed by Eq. 4 is neglected in this case, since for $pH < pH_0$ the fraction of $\equiv MeO^-$ is much less than fractions of $\equiv MeOH_2^+$ and $\equiv MeOH$. According to the Eq. 9, $n(H^+)_9 = n(OH^-)_9$. Combining Eqs. 10 and 11, one will obtain:

$$n(OH^-) = \Delta n(OH^-) + \Delta n(H^+) - \Gamma_{H^+}, \quad [12]$$

where $n(OH^-) \equiv n(OH^-)_8$ – the number of OH^- ions, released in Eq. 8; $\Delta n(H^+) = n(H^+)_{init.} - n(H^+)_{equil.}$; $\Delta n(OH^-) = n(OH^-)_{equil.} - n(OH^-)_{init.}$; $\Gamma_{H^+} \equiv n(H^+)_3$ – the number of H^+ ions adsorbed by oxide in Eq. 3.

Thus, knowing pH_{init} and $pH_{equil.}$ and calculating Γ_{H+} (from the potentiometric titration of the oxide), it is possible to calculate the amount of OH^- liberated by adsorption according to Eq. 8.

It was established that the adsorption of Nafion® on PbO_2 is accompanied by a shift of the zero charge point of the oxide to the alkaline region as a result of potentiometric measurements. This indicates that the adsorption of polyelectrolyte at $pH < pH_0$ carried out not only by electrostatic attraction of polyanion to the positively-charged lead dioxide surface, but also due to a specific interaction. It should be noted that the adsorption of polyelectrolyte occurs against the background of a large excess of indifferent electrolyte 0.1 M KCl, which shields the electrostatic field of the oxide surface. The specific character of Nafion® adsorption is confirmed by the data on the material balance of adsorption. It has been established that the adsorption of this polyelectrolyte is accompanied by the release of OH^- (Table I).

If it is assumed that the adsorption is carried out with the participation of the $-SO_3^-$ groups, then the hydroxide ion can be attributed to the coordination interaction of the polyanion with lead cations on the surface:

$$\equiv PbOH + R(F)_n(SO_3^-)_m \rightarrow \equiv Pb(SO_3^-)R(F)_n(SO_3^-)_{m-1} + OH^-, \quad [13]$$

$$\equiv PbOH_2^+ + R(F)_n(SO_3^-)_m \rightarrow \equiv Pb(SO_3^-)R(F)_n(SO_3^-)_{m-1} + H_2O \quad [14]$$

Here we are talking about chemical interaction, indirect evidence of which is a shift of pH_0.

According to these equilibria, the adsorption of polyelectrolyte on protonated $\equiv PbOH_2^+$ groups of oxide should not be accompanied by the release of additional hydroxide ions in the solution. Therefore, it should be concluded that Nafion® is adsorbed not only on charged surface centers, but also on neutral $\equiv PbOH$ groups. With increasing pH, the fraction of the surface $\equiv PbOH$ groups decreases, since the equilibrium of their dissociation process shifts to the right (see Eq. 4). Apparently, a decrease in the number of $\equiv PbOH$ groups causes a decrease in the amount of released OH^- ions during the adsorption of polyelectrolyte in alkaline solutions.

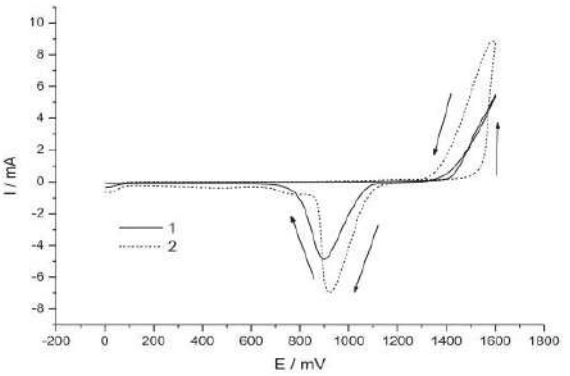

Figure 1. Cyclic voltammogram on Au-electrode in solutions: 1 – 0.1 M HNO_3 + 0.1 M $Pb(NO_3)_2$; 2 – 0.1 M HNO_3 + 0.1 M $Pb(NO_3)_2$ + 0.05 wt% Nafion®. Scaning rate is 0.1 V s^{-1}.

Since the electrodeposition of lead dioxide occurs through the formation of chemisorbed oxygen-containing species, the presence in the electrolyte of additives that capable to adsorb or forming oxygen-containing compounds with these species on the electrode surface can lead to a change in the kinetic regularities of PbO_2 formation. In this connection, we conducted combined electrochemical (cyclic voltammetry) and gravimetric (using quartz microbalances) measurements on a gold electrode in the presence of a polymer additive Nafion®.

There are two characteristic areas on the cyclic voltammogram (CV) on the gold electrode (Fig. 1). One can see an exponential current increasing at the anodic branch of the CV. At the same time, processes of oxygen evolution and deposition of lead dioxide with the predominance of the latter take place simultaneously in this area. On the reverse course of the curve, there is a hysteresis associated with an increase in the deposition rate of PbO_2 due to the accumulation of intermediate products on the electrode surface and in the near-electrode zone, as well as an increase in the overvoltage of oxygen evolution on the deposited lead dioxide. It should also be noted that in the presence of a polymer additive in the electrolyte, this effect is emerged much more strongly than in the standard electrolyte. As it has been shown previously on the platinum electrode,[27] at relatively low concentrations of the polymer additive, the deposition rate of lead dioxide increases, which is due to the adsorption of the polymer additive on the electrode and the ψ'-potential phenomenon.

At the cathodic branch of the CV, a peak current is observed (see Fig. 1), due to the reduction of the PbO_2 formed in the first region. In the presence of a polymer additive in the electrolyte, the reduction begins somewhat earlier, and the magnitude of the peak is observed at a higher potential. A larger peak current is also observed compared with the standard electrolyte (see Fig. 1). The data obtained further confirm the increase in the deposition rate of lead

Table I. Potentiometric titration data.

$pH_{init.}$	$pH_{equil.}$	$\Delta(H^+)$ 10^9, mole g^{-1}	$\Delta(OH^-)$, mole g^{-1}	$\Gamma(H^+)$ 10^6, mole g^{-1}	$n(OH^-)$ 10^9, mole g^{-1}
3.10	5.95	23796.20	0	1	22796.20
4.10	7.25	2381.30	0	0	2381.30
5.25	7.30	167.30	0	0	167.30
6.40	7.45	10.88	0	0	10.88
7.20	7.75	1.36	0	0	1.34

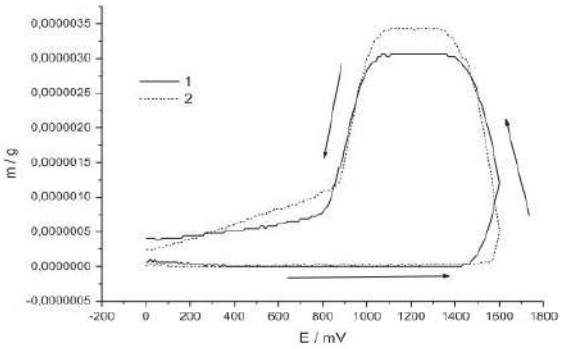

Figure 2. Change in the mass of the gold electrode during CVA (Fig. 1). 1 – 0.1 M HNO_3 + 0.1 M $Pb(NO_3)_2$; 2 – 0.1 M HNO_3 + 0.1 M $Pb(NO_3)_2$ + 0.05 wt% Nafion®.

dioxide in the presence of Nafion® in the electrolyte. The change in the peak potential indicates differences in the chemical and phase composition of the coatings obtained.

As one can see from Fig. 2, the mass of the gold electrode increases on the anodic branch of the CV because of lead dioxide deposition. At the same time, the deposition of PbO_2 in the presence of the polymer additive begins at a higher potential; however, due to the higher deposition rate, the oxide mass subsequently increases faster. The large mass of the coating obtained in the presence of polyelectrolyte in solution confirms the acceleration of the PbO_2 electrodeposition because of Nafion® polymer additive, which is in good agreement with the previously obtained data for the platinum electrode.[27]

The mechanism of lead dioxide formation is presented by a four stages kinetic scheme, described elsewhere.[12,18,28] The mechanism has been modified from the first version, proposed by Fleischmann and Liler,[29] where insoluble oxygen-containing Pb(IV) intermediates were proposed, through ones involving the presence of several soluble intermediates such as the oxygen-containing Pb(IV) species proposed by Chang and Johnson,[30] and the oxygen-containing Pb (III) intermediate suggested by Velichenko et al.,[31] who afterwards proved the existence of both oxygen-Pb(III) and oxygen-Pb(IV) soluble intermediates[32]:

$$H_2O \rightarrow OH^{\cdot}_{ads} + H^+ + e^- \quad [15]$$

$$Pb^{2+} + OH^{\cdot}_{ads} \rightarrow Pb(OH)^{2+} \quad [16]$$

$$Pb(OH)^{2+} + H_2O \rightarrow Pb(OH)_2{}^{2+} + H^+ + e^- \quad [17]$$

$$Pb(OH)_2{}^{2+} \rightarrow PbO_2 + 2H^+ \quad [18]$$

According to this mechanism, the first stage is the transfer of the first electron with the formation of oxygen-containing species $OH^{\bullet}_{ads}$, adsorbed on the electrode surface, which are formed by the anodic ionization of water (15). Then, in the subsequent chemical stage (16), these species react with lead ions to form an oxygen-containing intermediate Pb(III) of the $Pb(OH)^{2+}$ type, which is oxidized with the transfer of the second electron. As a result of this reaction, soluble intermediate compounds of tetravalent lead (such as $Pb(OH)_2{}^{2+}$) are formed, which decompose in the last stage (18) with formation of lead dioxide:

The limiting stage of PbO_2 electrodeposition process will be determined by several factors: i) the potential and surface state of the electrode; ii) the concentration of Pb^{2+} ions in the solution and iii) the hydrodynamic conditions of the process. At low anodic polarizations ($E < 1.6$ V), kinetic control of the process is realized. At high anodic polarizations ($E > 1.6$ V), the rate of electrodeposition is limited by the stage of Pb(II) delivery to the electrode surface.

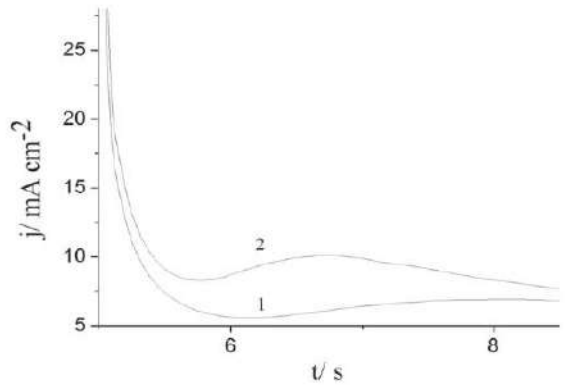

Figure 3. Chronoamperogramms on Au-electrode at E = 1.5 V, obtained during PbO_2 deposition from solutions containing 0.01 M $Pb(NO_3)_2$ + 0.1 M HNO_3 (1) + 0.05 wt% Nafion® (2).

Chronoamperograms were obtained on Au electrode in order to investigate the initial stages of deposition of lead dioxide in the presence of polyelectrolyte in solution. A typical j-t curve of PbO_2 deposition (Fig. 3) can be characterized by several features and fully consistent with the transients obtained and described in detail by Saez et al.[33] In this work lead dioxide was deposited on glassy carbon from nitrate bath and limiting step was under the kinetic control.

Since the formation of lead dioxide proceeds simultaneously with the oxygen evolution reaction, the current efficiency of PbO_2 is determined by the ratio of the two electrode processes. One can observe an increase in the current efficiency of lead dioxide (Fig. 4) at the area I in the low polarizations region. In this range of potentials, both processes are controlled by kinetic stages. With a further increase in the potential, the growth rate of the lead dioxide formation current decreases somewhat, deviating from the exponential dependence. The process occurs with mixed diffusion-kinetic control at average polarizations (area II). The evolution of oxygen still obeys the exponential dependence, which leads to a slight decrease in the current efficiency of PbO_2 (see Fig. 4, area II). At high polarizations (see Fig. 4, area III), the depositin of lead dioxide proceeds at the limiting current (diffusion control), and the oxygen evolution current increases with exponential growth of the potential, which leads to a sharp decrease in the current efficiency of PbO_2. The shape of the current efficiency vs potential dependence practically does not change when polyelectrolyte is added to the

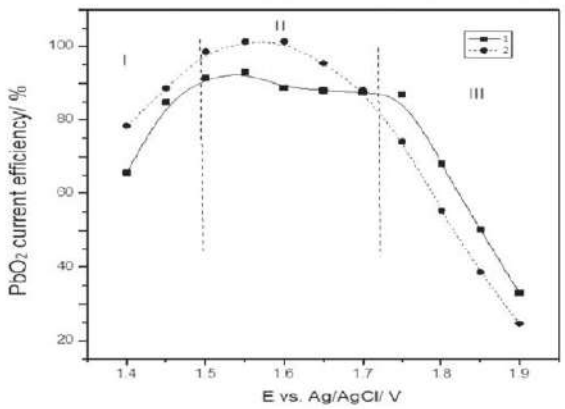

Figure 4. PbO_2 current efficiency vs electrodeposition potential obtained on Au electrode from solutions: 0.1 M HNO_3 + 0.1 M $Pb(NO_3)_2$ (1) + 0.05 wt% Nafion® (2).

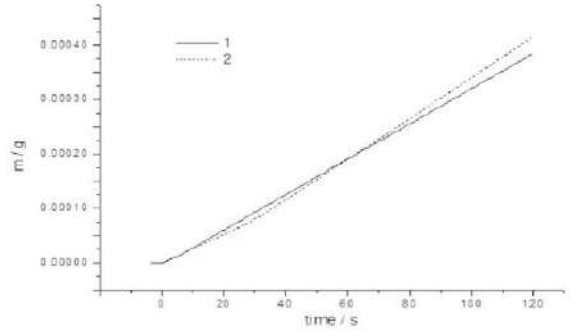

Figure 5. The change in the mass of the gold electrode under galvanostatic conditions ($j_a = 5$ mA cm^{-2}) during the electrodeposition of lead dioxide from various electrolytes: 1 – 0.1 M HNO_3 + 0.1 M $Pb(NO_3)_2$; 2 – 0.1 M HNO_3 + 0.1 M $Pb(NO_3)_2$ + 0.05 wt% Nafion®.

depiosition electrolyte. However, the use of Nafion® leads to an increase in the rate of PbO_2 formation, i.e. to the current efficiency growth at I and II areas (see Fig. 4).

As follows from the data on the change in the mass of the gold electrode under conditions of galvanostatic polarization (Fig. 5), at which electrodeposition of lead dioxide usually takes place (the first 60 s), at the initial stages of coating formation, the deposition rates do not practically differ, then the mass increases with acceleration in the presence of polyelectrolyte in the deposition electrolyte.

As it was indicated previously,[27] in the presence of Nafion® in the deposition electrolyte, PbO_2-Nafion® composite coatings with a content of polyelectrolyte up to 13 wt% are formed, depending on the solution composition and the deposition conditions.

The data obtained can be adequately explained on the basis of a number of assumptions. On the one hand, lead dioxide deposition is possible via colloid-electrochemical mechanism of the formation of composites, which was proposed for PbO_2-TiO_2 composites.[11] This mechanism is based on the formation in the near-electrode zone of Pb(IV) oxide species non-fixed on the surface. The adsorption of anionic surfactants and polyelectrolytes on the oxides in the solution bulk leads to a charge exchange of the double electric layer, as a result of which the electrokinetic potential of the oxide species of Pb (IV) becomes negative. Such particles under the action of electrophoretic forces move to a positively charged anode, where they are flocculated and crystallized on the surface of the electrode. The process of flocculation is facilitated by a local decrease in pH on the surface of the electrode and in the near-electrode zone as a result of electrochemical reactions:

$$Pb^{2+} + 2H_2O - 2e \rightarrow PbO_2 + 4H^+ \quad [19]$$

$$2H_2O - 4e \rightarrow O_2 + 4H^+ \quad [20]$$

At the same time, unfortunately, existing methods do not allow us to establish the nature of these non fixed oxygen-containing intermediates, i.e. we cannot determine whether they are chemical compounds or colloidal particles.

On the other hand, all the obtained data can also be adequately described using classical electrodeposition schemes,[29–32] when Nafion® adsorption occurs on the surface of growing PbO_2, and the phenomenon of changing in the polyelectrolyte content in the coating can be caused by two factors: i) heterogeneous (due to an increase in nonequilibrium adsorption and capture of polymer by growing deposit). In this case, the higher the growth rates of the oxide phase, the higher the probability of the inclusion of a large amount of polymer in the coating due to adsorption. And ii) migratory due to an increase in the rate of polymer delivery to the electrode surface. Since Nafion® is an anionic polyelectrolyte, and the electrode surface is positively charged, a change in conditions

Figure 6. SEM micrographs of nondoped PbO_2 (a) PbO_{2}-3.5% Nafion® (b).

such as acidity and current density will lead to an increase in the positive surface charge and an increase in the contribution of the migration component. So, for example, the migration effect has been described even for small molecules during electrodeposition of metals from solutions containing complex compounds.[34] It should be noted that it is possible that all the described effects can be realized simultaneously with different contributions. All the above assumptions do not contradict the obtained experimental data.

According to scanning electron microscopy (SEM) micrographs, a lead dioxide deposit is a set of large polycrystalline blocks with a highly pronounced preferred orientation, as evidenced by rather large number of publications (Fig. 6a). One can see the rough and crystallized deposit with very sharp angles. The morphology of composite electrodeposited in the presence of Nafion® is shown in Fig. 6b. It seems that the shape and size of the PbO_2 crystals is altered by the presence of polyelectrolyte. The surface is more uniform and the crystals are smaller, there is not a pronounced crystallographic orientation. With increasing of the polyelectrolyte content in the deposit, the size of crystals decreases. SEM/EDAX experiments (Fig. 7) were performed to evaluate the amount and distribution of elements in electrodeposited composite. The EDX spectra do not exhibit the peak corresponding to fluorine. In addition, it was not possible to detect the sulphur peak because it is too near of the very intense lead peak.

The XRPD data detected that all investigated samples contain two phases: α-PbO_2 (structure type $Fe_2N_{0.94}$, space group *Pbcn*) and β-PbO_2 (structure type TiO_2 rutile, space group $P4_2/mnm$). The difference is observed only in the ratio of these two phases and also

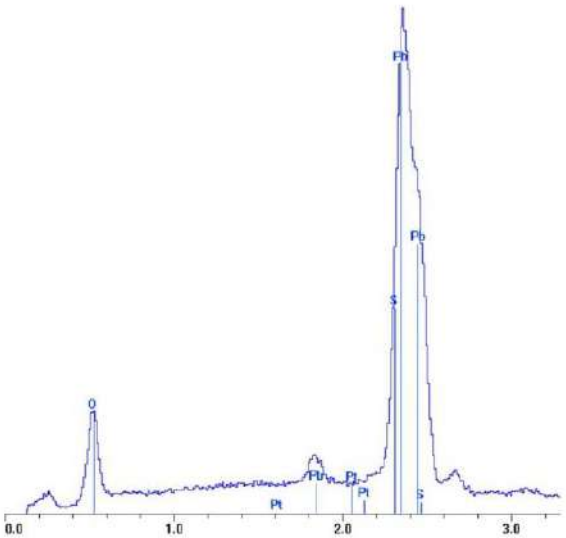

Figure 7. EDX spectrum of coating surface, obtained electrochemically from 0.1 M HNO_3 + 0.1 M $Pb(NO_3)_2$ + 0.05 wt% Nafion®.

in the degree of crystallinity (Table II). Typical powder pattern of modified sample is shown in Fig. 8. The data according nondoped sample were discussed in detail in our previous publication.[35]

Nevertheless, the electrochemical behavior of such materials is still virtually unknown. Electrodes of this type are in particular interest for the realization of processes occurring at high anode potentials with the oxygen-containing radicals' participation, primarily, the reactions of oxygen evolution and advanced oxidation of organic substances.

As follows from the obtained results (Fig. 9), the dependence of the overvoltage of oxygen evolution on the content of polyelectrolyte in the coating is of an extreme nature, which is a rather unusual effect. Based on the previously developed ideas,[36,37] if the oxygen evolution reaction is limited by second electron transfer (electrochemical desorption) stage, an increase in the bond strength of the chemisorbed oxygen will lead to an increase in oxygen evolution overvoltage. Under conditions when the transfer of the first electron (electrochemical adsorption) is the limiting stage, the overvoltage of the oxygen evolution reaction will decrease. As it is known, the process of oxygen evolution on nonmodified lead dioxide is controlled by the second electron transfer stage. It is

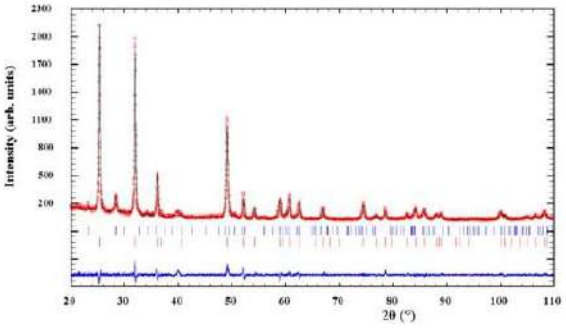

Figure 8. Observed and calculated X-ray powder profiles for the sample obtained from 0.1 M HNO_3 + 0.1 M $Pb(NO_3)_2$ + 0.05 wt% Nafion®. Experimental data (circles) and calculated profile (solid line through the circles) are presented together with the calculated Bragg positions (vertical ticks) and difference curve (bottom solid line). Upper ticks: α-PbO_2, bottom ticks: β-PbO_2.

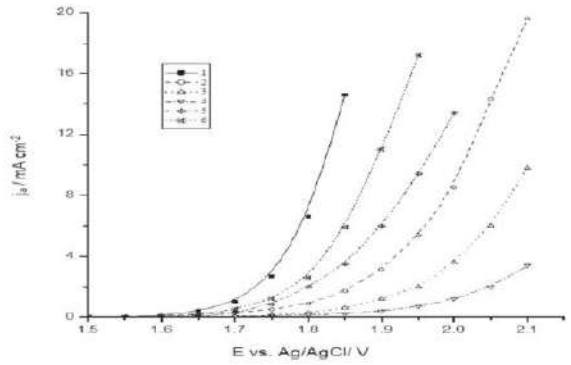

Figure 9. Steady state polarization curves of oxygen evolution in 1 M H_2SO_4 (Scan rate 1 mV s^{-1}, t = 25 °C) on PbO_2-electrodes, containing Nafion®, wt%: 0 (1), 2 (2), 4.8 (3), 6.8 (4), 10 (5), 13 (6). Coating electrodeposited on Ti/Pt sheet.

likely that with a low Nafion® content in the oxide, the oxygen evolution reaction is controlled by the stage of transfer of the first electron, while the increase in the polyelectrolyte concentration probably leads to a change in the rate-determining stage to electrochemical desorption.

Figure 10 presents the steady state polarization curves of oxygen evolution at the PbO_2-Nafion® anodes with the same polyelectrolyte content obtained by different methods. Electrodes 1, 2 were obtained at different anodic current densities from electrolytes, containing different concentration of polyelectrolyte additive, and 3, 4 were obtained at different anodic current densities and pH. As one can see from obtained results, with the same content of polyelectrolyte, the dependencies are identical. This indicates that the chemical factor is the determining factor for estimation of catalytic properties of composite electrocatalysts.

Figure 11 presents the steady state polarization curves of oxygen evolution at the PbO_2-Nafion® anodes in phosphate buffer. As it is known, lead dioxide tends to passivation by phosphates with the formation of insoluble mixed compounds.[1] As follows from the results obtained, the presence of Nafion® in the composite coating prevents electrode passivation, blocking the formation of insoluble compounds and increasing the rate of oxygen evolution and, therefore, the partial rate of oxidation of organic compounds.

Phenolic compounds, particularly, 4-chlorophenol and anodic materials based on lead dioxide were chosen to determine the nature of the electrocatalytic activity of materials in the oxidation of organic compounds. This choice was due to the fact that the electrooxidation processes of phenolic compounds at various

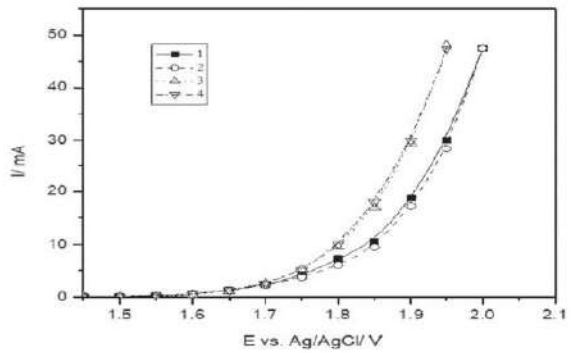

Figure 10. Steady state polarization curves of oxygen evolution in 1 M H_2SO_4 (Scan rate 1 mV s^{-1}, t = 25 °C) on PbO_2-electrodes, containing Nafion®, wt%: 6.6 (1,2); 8.8 (3,4). Coatings electrodeposited on Ti/Pt sheet.

Table II. Phase composition, crystallographic data and microstructural parameters[a] of coating synthesized from 0.1 M $Pb(NO_3)_2$ + 0.1 M HNO_3 + 0.05% Nafion®.

Phases	Content (mass %) α-PbO_2/β-PbO_2	Lattice parameters, Å			Unit cell volume, Å^3	Reliability factors	
		a	b	c	V	R_I/R_P, R_{WP}, R_{EXP}, χ^2	D, Å/ε
α-PbO_2	12.0(3)/	4.9908 (17)	5.951 (2)	5.4608(17)	162.20(10)	0.109	178/ 0.0088
β-PbO_2	88.0(7)	4.9529(2)		3.38385 (18)	83.008(7)	0.0350/0.0925, 0.122, 0.110, 1.24	340/ 0.0051

a) The meaning of parameters see in Experimental section.

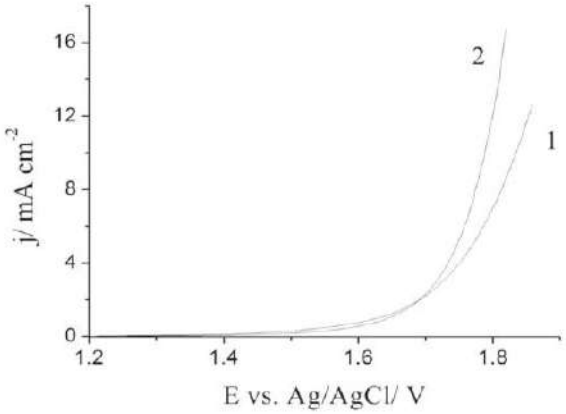

Figure 11. Steady state polarization curves of oxygen evolution in phosphate buffer (0.25 M Na_2HPO_4 + 0.1 M KH_2PO_4), (Scan rate 5 mV s^{-1}, t = 25 °C) on PbO_2 (1) and PbO_2–6.6 wt% Nafion® (2) electrodes. Coating electrodeposited on Ti/Pt sheet.

electrodes have been fairly well studied,[38] so the main focus can only be on clarifying the role of the anode material.

In particular, a significant number of publications have been devoted to the electrooxidation of chlorophenol,[38] where IrO_2 and other noble metal oxides, PbO_2 and SnO_2 were used as anode materials. It should be noted that, despite the rather large number of different oxide materials, most of them are chemically and electrochemically resistant only in alkaline solutions. In acidic and neutral solutions, only noble metal oxides, as well as lead, tin and manganese dioxide are stable. The electrocatalytic activity of noble metal oxides to direct anodic oxidation of chlorophenol is rather low, while lead dioxide exhibits the maximum activity.

According to the literature data,[39] the anodic oxidation of 4-chlorophenol produces a rather large number of intermediate products. The main intermediates include benozquinone and maleic acid. A rather simple and convenient way of estimating the electrocatalytic activity of an electrode material is the time of disappearance of aromatic intermediates, which can be determined from the UV spectra of solutions at different electrolysis times.

Figure 12 shows the absorption spectra of solutions obtained at different times of conversion of chlorophenol in phosphate buffer on PbO_2 at 50 mA cm^{-2} (the initial concentration of 4-chlorophenol is 1 mM). The initial solution of chlorphenol is characterized by two peaks at wavelengths of 230 and 280 nm. At first, the peak is reduced at 230 nm, as well as a slight increase in the peak at 280 nm and the appearance of the plateau at 250–270 nm, due to a decrease in the concentration of 4-chlorophenol and the accumulation of

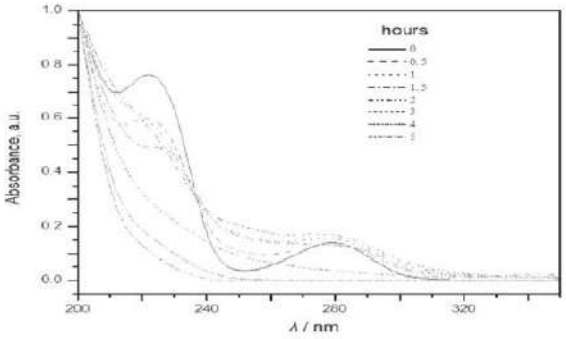

Figure 12. Electronic absorption spectra of solutions (0.5 M Na_2SO_4 + phosphate buffer, pH = 7.0) with 0.1 mM initial concentration of 4-chlorophenol at different electrolysis time on PbO_2 anode.

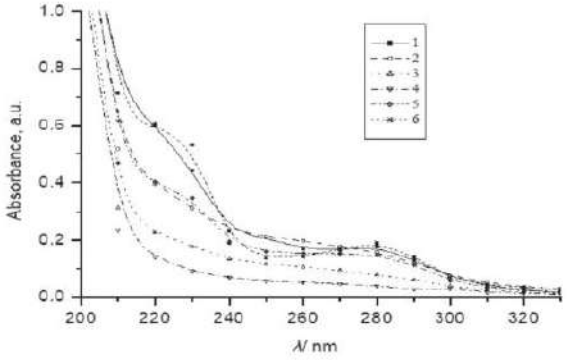

Figure 13. Electronic absorption spectra of solutions (0.5 M Na_2SO_4 + phosphate buffer, pH = 7.0) with 0.1 mM initial concentration of 4-chlorophenol after 90 min of electrolysis on PbO_2-anodes, containing Nafion®, wt%: 0 (1); 1.9 (2); 4.8 (3); 6.8 (4); 10.2 (5); 13 (6).

benzoquinone in the solution. A further increase in the electrolysis time leads to the disappearance of peaks at 230 and 280 nm, as well as the reduction of the plateau at 250–270 nm due to a decrease in the concentrations of both 4-chlorophenol and benzoquinone. Already after 4 h of electrolysis, complete destruction of aromatic compounds occurs with the formation of only aliphatic products of electrolysis (mainly maleic acid).

Thus, lead dioxide is characterized by a rather high electrocatalytic activity in the oxidation of 4-chlorophenol. As was shown earlier,[11,12,18] the modification of lead dioxide can lead to a significant increase in its electrocatalytic activity with respect to reactions occurring with the participation of oxygen-containing particles adsorbed on the electrode surface. In this connection, we investigated the electrochemical oxidation of 4-chlorophenol on composite anodes based on lead dioxide containing polyelectrolyte.

As one can see from Fig. 13, for the composite materials PbO_2-polyelectrolyte the conversion rate of 4-chlorophenol increases. In accordance with the oxygen evolution process in Fig. 9, the rate of conversion of 4-chlorophenol with an increase in the Nafion® content in the coating is extremal.

Conclusions

Thus, the use of composite materials based on lead dioxide leads to a significant increase in the conversion rate of 4-chlorophenol to non-toxic compounds.

The addition of polyelectrolyte has a significant effect on the kinetics of electrodeposition of lead dioxide without changing the mechanism of the process.

The presence of the Nafion® in the deposition electrolyte results in the formation of nanocomposite oxide-polyelectrolyte materials. The content of the additive in lead dioxide is mainly determined by its adsorption on the oxide. The data obtained can be adequately explained on the basis of a number of assumptions. On the one hand, lead dioxide deposition is possible via colloid-electrochemical mechanism of the formation of composites. On the other hand, all the obtained data can also be adequately described using classical electrodeposition schemes, when Nafion® adsorption occurs on the surface of growing PbO_2, and the phenomenon of changing in the polyelectrolyte content in the coating can be caused by two factors: i) heterogeneous and ii) migratory. It should be noted that it is possible that all the described effects can be realized simultaneously with different contributions. All the above assumptions do not contradict the obtained experimental data. When using composite materials based on lead dioxide containing polyelectrolyte, selective changes in the overvoltage of oxygen evolution and electrochemical conversion of organic substances into aliphatic non-toxic compounds are observed. In this case, the electrocatalytic activity of composite materials depends on the nature and content of the

polyelectrolyte additive in the oxide. An additional benefit of a coating containing a polyelectrolyte is the decrease of overvoltage of oxygen evolution, occurring together with the oxidation of organic substances, which, in turn, reduces energy consumption during prolonged electrolysis.

ORCID

A. Velichenko https://orcid.org/0000-0003-1076-9991

References

1. X. Li, D. Pletcher, and F. C. Walsh, *Chem. Soc. Rev.*, **40**, 3879 (2011).
2. J. F. Pereira, R. S. Figueiredo, C. Ponce-de-Leon, and R. Bertazzoli, *J. Solid State Electrochem.*, **20**, 1167 (2016).
3. M. A. Quiroz, C. A. Martinez-Huitle, Y. Meas-Vong, E. Bustos, and M. Cerro-Lopez, *J. Electroanal. Chem.*, **807**, 261 (2017).
4. F. C. Walsh and C. Ponce de Leon, *Surf. Coat. Technol.*, **259**, 676 (2014).
5. G. V. Kornienko, T. A. Kenova, V. L. Kornienko, O. A. Golubtsova, and N. G. Maksimov, *Russ. J. Appl. Chem.*, **90**, 1234 (2017).
6. Z. He, M. D. Hayat, S. Huang, X. Wang, and P. Cao, *J. Electroanal. Chem.*, **812**, 74 (2018).
7. A. B. Velichenko, R. Amadelli, E. V. Gruzdeva, T. V. Luk'yanenko, and F. I. Danilov, *J. Power Sources*, **191**, 103 (2009).
8. O. I. Kasian, T. V. Luk'yanenko, P. Demchenko, R. E. Gladyshevskii, R. Amadelli, and A. B. Velichenko, *Electrochim. Acta*, **109**, 630 (2013).
9. O. Kasian, T. Luk'yanenko, A. Velichenko, and R. Amadelli, *Int. J. Electrochem. Sci.*, **7**, 7915 (2012).
10. R. Vargas, C. Borras, D. Mendez, J. Mostany, and B. R. Scharifker, *J. Solid State Electrochem.*, **20**, 875 (2016).
11. V. Knysh, T. Luk'yanenko, O. Shmychkova, R. Amadelli, and A. Velichenko, *J. Solid State Electrochem.*, **21**, 537 (2017).
12. O. Shmychkova, T. Luk'yanenko, R. Amadelli, and A. Velichenko, *J. Electroanal. Chem.*, **717–718**, 196 (2014).
13. X. Hu, Y. Yu, and L. Yang, *J. Solid State Electrochem.*, **19**, 1599 (2015).
14. Y. Yao, L. Cui, C. Zhao, and L. Jiao, *J. Electrochem. Soc.*, **161**, D528 (2014).
15. S. Burazer, S. Sopcic, and Z. Mandic, *J. Solid State Electrochem.*, **20**, 3053 (2016).
16. X. Li, H. Xu, and W. Yan, *J. Alloys Compd.*, **718**, 386 (2017).
17. X. Li, H. Xu, and W. Yan, *Appl. Surf. Sci.*, **389**, 278 (2016).
18. O. Shmychkova, T. Luk'yanenko, A. Velichenko, L. Meda, and R. Amadelli, *Electrochim. Acta*, **111**, 332 (2013).
19. R. Amadelli, A. Maldotti, A. Molinari, F. I. Danilov, and A. B. Velichenko, *J. Electroanal. Chem.*, **534**, 1 (2002).
20. G. S. Parkinson and U. Diebold, *Surface and Interface Science*, ed. K. Wandelt (Wiley, New York) p.793 (2016).
21. G. E. Brown Jr et al., *Chem. Rev.*, **99**, 77 (1999).
22. L. R. Merte et al., *Nat. Commun.*, **5**, 4193 (2014).
23. S. Trasatti, *Electrochim. Acta*, **29**, 1503 (1984).
24. A. Breeuwsma and J. Lyklema, *J. Colloid Interface Sci.*, **43**, 437 (1973).
25. N. V. Nikolenko, *Colloid J.*, **63**, 441 (2001).
26. N. V. Nikolenko et al., *Voprosy khimii i khimicheskoi tekhnologii*, **3**, 35 (2019).
27. A. B. Velichenko, T. V. Luk'yanenko, N. V. Nikolenko, R. Amadelli, and F. I. Danilov, *Russ. J. Electrochem.*, **43**, 118 (2007).
28. O. Shmychkova, T. Luk'yanenko, R. Amadelli, and A. Velichenko, *J. Electroanal. Chem.*, **774**, 88 (2016).
29. M. Fleischmann and M. Liler, *Trans. Faraday Soc.*, **54**, 1370 (1958).
30. H. Chang and D. C. Johnson, *J. Electrochem. Soc.*, **136**, 17 (1989).
31. A. B. Velicheko, D. V. Girenko, and F. I. Danilov, *J. Electroanal. Chem.*, **425**, 127 (1996).
32. A. B. Velichenko, E. A. Baranova, D. V. Girenko, R. Amadelli, S. V. Kovalev, and F. I. Danilov, *Russ. J. Electrochem.*, **39**, 615 (2003).
33. V. Saez, E. Marchante, M. I. Diez, M. D. Esclapez, P. Bonete, T. Lana-Villarreal, J. Gonzalez Garcia, and J. Mostany, *Mat. Chem. Phys.*, **125**, 46 (2011).
34. R. Yu. Bek, T. E. Tsupak, L. I. Shuraeva, and G. V. Kosolanov, *Elektrokhimiya*, **23**, 1618 (1987).
35. O. Shmychkova, T. Luk'yanenko, A. Piletska, A. Velichenko, R. Gladyshevskii, P. Demchenko, and R. Amadelli, *J. Electroanal. Chem.*, **746**, 57 (2015).
36. S. Trassatti and G. Lodi, *Electrodes of Conductive Metallic Oxides*. (Elsevier) Part B(Amsterdam, Holland) (1981).
37. D. Pavlov and B. Monahov, *J. Electrochem. Soc.*, **143**, 3616 (1996).
38. Y. Chen, H. Li, W. Liu, Y. Tu, Y. Zhang, W. Han, and L. Wang, *Chemosphere*, **113**, 48 (2014).
39. L. Wang, Q. Zhang, D. Wang, and J. Wei, *Chemosphere*, **10**, 1664 (2016).
40. M. Pera-Titus, V. Garcia-Molina, M. A. Bacos, J. Gimenez, and S. Esplugas, *Appl. Catal., B*, **47**, 219 (2004).

Journal of Solid State Electrochemistry
https://doi.org/10.1007/s10008-020-04787-9

ORIGINAL PAPER

Reduction of nitroaromatics on cadmium sulfide: further probing the electrochemical model of semiconductor photocatalysis

Alexander B. Velichenko[1] · Olesia Shmychkova[1] · Luca Samiolo[2] · Rossano Amadelli[2]

Received: 29 April 2020 / Revised: 23 July 2020 / Accepted: 24 July 2020

Abstract
The photoreduction of nitroarene compounds is a typical multielectron process that is examined here at cadmium sulfide electrodes and particle suspensions. Electrochemistry in the dark and photoluminescence indicate that reduction is mediated by surface states (sulfur vacancies) approximately located at 0.55 eV below the conduction band. In keeping with the known reduction mechanism, phenylhydroxylamine intermediates are detected at both electrodes and in suspensions. A focus of the present work was to use the nitroarenes reduction as a probe reaction to confirm the common bases of photoelectrochemistry and photocatalysis. Superimposition photocurrents (due to oxidation of hole scavengers) and dark currents identifies one potential at which the net observed current is zero and then establishes the operative photocatalytic condition. Rates of reduction on electrodes at open circuit compare very well with currents calculated from the intersection of photocurrent and dark current confirming that the photocatalytic process can be predicted from electrochemical measurements. Analysis of reaction rates in CdS suspensions suggests that a significant portion of reduction occurs on dark sites of the particles.

Keywords Nitroaromatics · CdS · Suspensions · Photoelectrochemistry

Introduction

The reduction of nitroaromatics is a much investigated field of research due to considerable applied and academic importance [1, 2]. Despite a lot of literature, there are still open questions on mechanistic details that are presently under scrutiny. The search for process selectivity is understandably an important part of the studies in this field [3–7]. Additionally, the multielectron reduction of the nitro group can be a suitable case study that could highlight properties underlying the semiconductor-electrolyte interface [6, 7]. In the latter context, herein we examine the processes on CdS using electrodes and powder suspensions in parallel investigations.

It is now well known that irradiation of semiconductor powder suspensions creates electron-hole pairs and the particles behave in the same way as short-circuited photoelectrochemical cells where both cathodic and anodic reactions occur on the same particle. Adding to the suspension compounds which irreversibly react with photogenerated holes noticeably increases the lifetime of electrons. The accumulated negative charge on the particles could be collected at an inert metallic electrode immersed in the suspension and held at an appropriate positive potential [8, 9]. Alternatively, some electron relay such as methylviologen (MV^{2+}) can be reduced at CdS and re-oxidized at the collector electrode as described long ago [10, 11]; more recently, this setup was also used to determine the flat band potential of suspensions [12] and in studies with more complex electron relays than MV^{2+} [13, 14]. We discuss how this method can be unusually exploited to highlight the

Dedicated to Prof. José Zagal in the occasion of his 70th birthday and in recognition of his contribution to Electrochemistry

Electronic supplementary material The online version of this article (https://doi.org/10.1007/s10008-020-04787-9) contains supplementary material, which is available to authorized users.

✉ Alexander B. Velichenko
velichenko@ukr.net

✉ Rossano Amadelli
amr@unife.it

[1] Physical Chemistry Department, Ukrainian State University of Chemical Technology, Dnipro, Ukraine

[2] ISOF-CNR, c/o Department of Chemistry, University of Ferrara, via L. Borsari 46, 44121 Ferrara, Italy

Published online: 31 July 2020

formation of reduction intermediates in CdS particle suspensions which is a significant aspect of the mechanism.

In the context of basic research, in this work we present a reexamination (and revalidation) of the link between photoelectrochemistry and photocatalysis using the reduction of nitroaromatics as a typical multielectron transfer process instead of the simple monoelectronic redox species tested earlier. We think that it can be of interest since presently photoelectrochemistry is gaining increasing popularity [15, 16].

We followed a method of investigation that has been referred to in various ways such as polylectrodes, mixed potential theory, or local cells approach. This finds application in various fields of electrochemistry (e.g. in electroless deposition and corrosion) as well as in heterogeneous redox catalysis [17, 18]. Previously, it had been underlined that for open circuit photoelectrodes and suspensions at equilibrium, the interfacial charge-transfer flux of holes to electron donors must match that of electrons to acceptors [19–21]. Studies are seemingly discontinuous, and a major portion of the existing literature focuses again on monoelectronic processes involving species such as MV^{2+}.

Within the framework of the studies herein described, the results underline the important role of dark reduction for suspensions compared to open circuit electrodes of the same material.

Experimental

Reactants and equipment

Cadmium sulfide as powders and sintered form (used to prepare electrodes) were obtained from Strem Chemicals. Nitroaromatic compounds (4-nitrobenzaldehyde $CHOC_6H_4NO_2$; 4-chloronitrobenzene $ClC_6H_4NO_2$; 4-methylnitrobenzene $CH_3C_6H_4NO_2$), alcohols, Na_2SO_3, $NaClO_4$, HCOONa, HCOOH, and ultrapure CH_3CN were Fluka products. Millipore distilled water was used in all experiments. Metals were supplied by Johnson Matthey.

An EG&G potentiostat with EG&G software was used for electrochemical measurements. All measurements were made in argon deaerated H_2O/CH_3CN (80:20 v/v) using sodium perchlorate (0.2 mol dm^{-3}) as supporting electrolyte.

UV-visible spectra of solutions were obtained on a Kontron spectrophotometer (Uvikon 943), using a 2-mm quartz cell.

Photoluminescence spectra were recorded with a Jobin Yvon Spex Fluoromax II spectrofluorimeter (photomultiplier Hamamatsu R3896) using CdS film samples cast on quartz supports.

Experiments under irradiation (10 mW cm^{-2}) were performed with a Helios Q400 Ital quartz medium-pressure Hg lamp using a cutoff filter ($\lambda > 400$ nm).

Methods

A conventional three-compartment glass cell was employed for electrochemical measurements, where the working compartment had a flat quartz window for illumination. The CdS samples for the use as electrodes were polished using diamond pastes and finally etched in HCl [11]. Electric contact was obtained by spreading a In-Ga eutectic on the back of the CdS sheets and then fixing onto these a copper wire by means of a silver paste. The sample thus prepared was insulated on the back by a chemically inert silicone resin. The exposed area was 0.8 cm^2. All potentials are given vs. the saturated calomel electrode (SCE).

Photocatalytic experiments with suspensions were conducted in Pyrex semi-cylindrical reactors with a flat window, containing the test solution and the photocatalyst in an amount of 4 g dm^{-3}. In a typical experiment, CdS was suspended in a mixture of water and acetonitrile (80:20 v/v) containing the nitroarenes ($RC_6H_4NO_2$).Then, the suspension was purged with argon for 20 min and subsequently irradiated under stirring at wavelengths above 400 nm (10 mW cm^{-2}). The reaction course was followed by recording UV spectra of the irradiated solutions and comparing them with UV spectra of pure substances. The disappearance of $RC_6H_4NO_2$ was evaluated on the basis of the absorbance decrease of the peak at 260–280 nm, and the formation of the corresponding amines $RC_6H_4NH_2$ from the absorbance increases at 280–300 nm. Quantitative analyses were performed with calibration curves obtained with authentic samples.

Results and discussion

CdS electrodes in the dark

The flatband potential (E_{fb}) is an important parameter as it is related to the bands behavior of the seminconductor/electrolyte interface. The E_{fb} values were derived from Mott-Schottky plots (C^{-2} vs. E), with capacities obtained from cyclic voltammetry measurements at different scan rates (ν) using the relationship $C = I/\nu$. Experiments were performed in the potential range 0.0 to 1.0 V, in which pure capacitive behavior is observed. The values of E_{fb} obtained at pH 2 and 6.5 were −0.9 V and −1.035 V, respectively (Fig. S1, ESI).

In a following step, we examined the reduction of $CHOC_6H_4NO_2$, $ClC_6H_4NO_2$, and $CH_3C_6H_4NO_2$ at pH 2 and pH 6.5 (Fig. 1). The salient fact in this figure is that the reduction occurs as a single wave for the three compounds at potentials below E_{fb}. Conversely, on a metallic electrode, they are clearly reduced at appreciably different potentials; according to calculated one-electron reduction potentials [22],

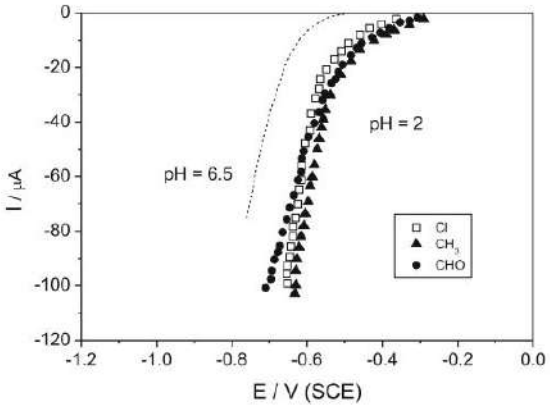

Fig. 1 Steady-state current-potential curves for the reduction of para-substituted nitrobenzene on a CdS electrode in the dark. Solvent: deaerated H_2O/CH_3CN (80/20%) containing 0.2 mol dm^{-3} $NaClO_4$ at pH 2 and 6.5. Concentration of the nitroaromatics: 1×10^{-3} mol dm^{-3}. The dashed line is the average of curves obtained for the three compounds at pH 6.5

$CH_3C_6H_4NO_2$ is reduced with greater difficulty and $CHOC_6H_4NO_2$ is the most easily reduced one (Fig. S2, ESI).

$$R{-}NO_2 + e^- \rightarrow R{-}NO_2^- \quad (1)$$

It will be recalled that protonation and further electron transfer then leads to formation of nitrosobenzene; however, we did not detect it and it is not generally observed since it is rapidly converted, via a second 2-electron reduction, to the phenylhydroxylamine (RC_6H_4NHOH) derivative as the isolatable product (see the next section).

The slopes of linear portions of the E vs. log I plots (Tafel slopes) often provide diagnostic criteria for establishing the mechanism of electrochemical reactions [23]. Using the data of Fig. 1, Tafel slopes ranged from 100 to 115 mV $decade^{-1}$. From a general point of view, for semiconductor electrodes, this may be due to a number of causes but often to the presence of consistent amount of surface states (ss) causing the applied potential to drop in the Helmholtz layer and not in the space charge [24].

Notably too, reduction currents saturate as a function of concentration, and the saturation current does not depend on the nature of the nitro-compound. This behavior was discussed in the literature as a two-step mechanism in which reduction is mediated by ss [25]. According to those authors' model, there are conditions, for reactant concentrations less that the saturation value, that can lead to Tafel slopes higher than the 60 mV $decade^{-1}$ that is predicted for semiconductors in the absence of intragap defects.

To further confirm the presence of ss, we performed luminescence measurements on CdS films that revealed an emission band at 660–670 nm. Extensive investigations report that emission in this wavelength range is due to recombination of photogenerated holes with electrons trapped in ss which have been associated to sulfur vacancies [26]. From our experimental data, these states are located at about 0.50–0.55 eV below the conduction band, in agreement with the other literature result [27]. The nitroaromatics examined here can quench emission (Fig. S3, ESI) by intercepting trapped electrons as schematically depicted in Fig. 2, which confirms that electron transfer is mediated by intragap states.

We finally remark that a number of papers give evidence of the important role of sulfur vacancies in the thermal, heterogeneous catalysis of nitroarene reduction on metal sulfides [28].

Illuminated CdS bulk and slurry electrodes

A typical linear sweep voltammetry curve for a CdS electrode irradiated at $\lambda > 400$ nm is displayed in Fig. 3. As the potential is scanned from negative values in the positive direction, a small anodic peak (a) appears; then, as the potential increases slightly in the positive direction, current interruption defines a small cathodic peak (b) that is observed only in the presence of nitroarenes. The behavior is observed at relatively high scan rates (> 20 mV s^{-1}) and can be explained by the known reduction mechanism of the nitro group that leads to hydroxylamine intermediate via a 4-electron reduction (reaction 2) followed by a slower reduction to aniline (reaction 3).

$$RC_6H_4NO_2 + 4e^- + 4H^+ \rightarrow RC_6H_4NHOH + H_2O \quad (2)$$

$$RC_6H_4NHOH + 2e^- + 2\,H^+ \rightarrow RC_6H_4NH_2 + H_2O \quad (3)$$

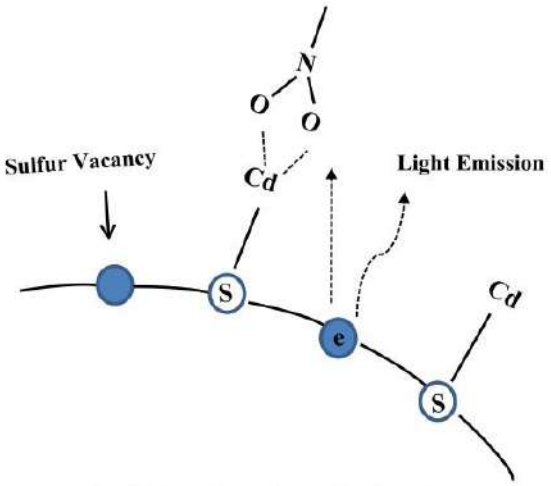

Fig. 2 A pictorial illustration of the possible interaction of a nitro-compound with sulfur vacancy surface. In this schematic description, the dotted lines represent an adsorption of species on the surface, while the full lines represent the lattice bonds independent of their covalent or ionic nature and length

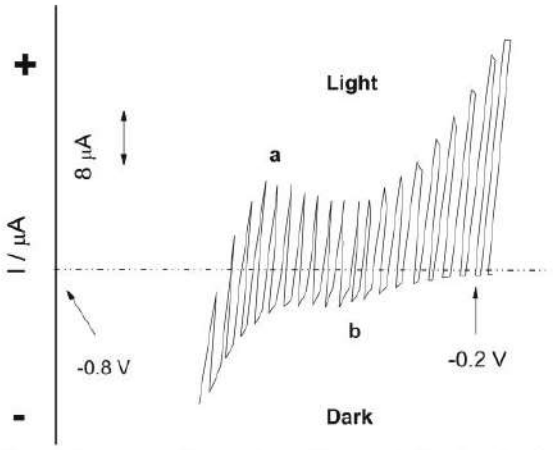

Fig. 3 Current-potential curve for a CdS electrode illuminated with manually chopped light (λ > 400 nm). Solvent: deaerated H_2O/CH_3CN (80/20%) containing 0.2 mol dm^{-3} $NaClO_4$. Results obtained in the presence of $CHOC_6H_4NO_2$ (1×10^{-3} mol dm^{-3}) and HCOOH (0.2 mol dm^{-3}, pH 2) as a representative example. Scan rate, 20 mV s^{-1}

Thus in Fig. 3 the oxidation peak (a) can be assigned to capture of holes (h^+) by RC_6H_4NHOH to give the corresponding nitroso species (reaction 4).

$$RC_6H_4NHOH + 2\,h^+ \rightarrow RC_6H_4NO + 2H^+ \quad (4)$$

As light is switched off, holes accumulated at the surface are consumed and reaction (4) takes place in the opposite direction since RC_6H_4NO reacts with excess electrons. At still more positive potentials, the photocurrent increases rapidly due to oxidation of hole scavengers (HCOOH, in this case) that are added in order to inhibit anodic photocorrosion. For comparison, at a metallic electrode one observes analogous oxidation/reduction peaks following pre-polarization in the range of nitro group reduction (Fig. S4, ESI).

The question was whether formation of intermediates of this multielectron process could also be observed in irradiated CdS suspensions. In this case, electron/hole (e^-/h^+) pairs generated by light (reaction 5) are sites of reduction and oxidation processes on the surface of each particle, i.e. they behave like a set of open circuit microelectrodes. So, following charge separation, reactions (2, 3) can occur and charge balance is ensured by oxidation of a hole scavenger as, for example HCOOH (reaction 6)

$$CdS + h\nu \rightarrow CdS\,(h^+ + e^-) \quad (5)$$

$$3HCOOH \rightarrow 3CO_2 + 6e^- + 6H^+ \quad (6)$$

The reaction course can be monitored by taking samples to be analyzed by conventional methods, but in the present work, we resorted to the relatively simple suspension (or slurry) electrode method [8–14] in order to detect the presence of reaction intermediates.

A Pt electrode was immersed in a stirred suspension of CdS particles in H_2O/CH_3CN (80/20%) containing a reducing species (hole scavenger) in the presence or absence of nitro-compounds. In the first case, under irradiation, a current is recorded at the Pt collector electrode polarized at a positive potential where oxidation of RC_6H_4NHOH is known to take place (Scheme S1, ESI). The current grows with time and declines to zero as light is switched off. The intensity of this current depends on potential as illustrated by the example of Fig. 4; at a fixed irradiation time, it reaches a maximum at a potential that depends on pH, and this maximum also depends on light intensity and on the nature of the added hole scavenger as discussed in the following section. Importantly, in blank experiments in the absence of nitroaromatics, the measured currents at Pt were less than a few μA; likewise, no appreciable current was recorded at the monitor Pt electrode when aniline derivatives were added instead of the parent nitro-compounds. These low currents are likely attributed to direct transfer of electrons accumulated on irradiated CdS to the collector Pt electrode [8, 9].

The currents at Pt were somewhat higher for a suspension at pH 2 which may well be due to an easier desorption from CdS [2] of protonated RC_6H_4NHOH (pK_a 3.2 for C_6H_5NHOH). There is much uncertainty about literature data on the point of zero surface charge (pzc) of CdS; the more recently reported values range from 1.5 to 3. At pH 2, one can then expect a competition between H^+ and $RC_6H_4NH_2OH^+$ for adsorption.

On the other hand, full reduction of an adsorbed nitroarene can very likely lead to an amine bound to the

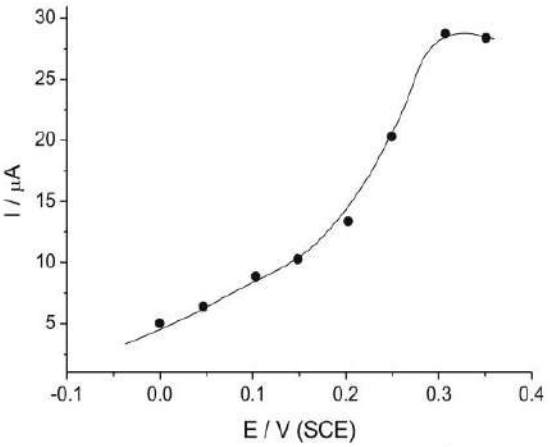

Fig. 4 Steady-state polarization for a Pt electrode (10 cm^2) at different potentials in an illuminated (λ > 400 nm) CdS suspension (4 g dm^{-3}). Solvent: deaerated H_2O/CH_3CN (80/20%) containing 0.2 mol dm^{-3} $NaClO_4$. Results obtained in the presence of $CHOC_6H_4NO_2$ (3×10^{-3} mol dm^{-3}) and HCOOH (pH 2) are shown as a representative example

same reactive site; strong coordination of amines to chalcogenides surfaces is, in fact, well documented and can cause a major perturbation of ss [29]. In the neutral pH interval and at higher concentrations than encountered in the present work can probably cause blocking of active sites for adsorption of the nitro-compounds.

In sum, adsorption of reduction products is an interesting, non-trivial question as underlined in a recent, interesting publication [30]. Further developments will need to address not only a quantitative analysis of the amount of intermediates, but also how ss can be modified.

Bridging photoelectrochemistry and phocatalysis

In principle, semiconductor slurries behave in the same way as photoelectrodes at open circuit [15]. So, using electrochemical data, it is interesting to assess whether it is possible to predict the feasibility of the photocatalytic reduction process examined herein, which is more complicated than those investigated in the past in similar studies.

Analysis can be first carried out electrochemically, using the local cell approach (see the "Introduction" section), separately measuring the quasi-steady state anodic photocurrents (I_{ph}) and cathodic dark currents (I_d) [19–21]. If the currents are superimposable, there is a point where

$$I_{ph} = I_d = I_m \tag{7}$$

at a potential E_m. These points define the working conditions of an electrode at open circuit that are relevant to those found in suspensions of particles of the same material as the electrodes.

The current vs. potential plots shown in Fig. 5 were constructed from the experimental results for the reduction of $CHOC_6H_4NO_2$ at a neutral and acid pH and photocurrents that, in this particular case, are due to the oxidation of $HCOO^-$ and HCOOH, respectively. The figure is an illustrative example of general behavior given that dark reduction of the other nitro-compounds occurs at the same potential (Fig. 1).

The values of the mixed currents I_m (Eq. 7) reached a limiting value as a function of the concentration of the nitro-compounds. This is expected since, as we mentioned above, the dark reduction currents do not grow linearly with concentration indicating that the process is mediated by ss.

From I_m values, we calculated a reduction rate r_e [17].

$$r_e = \frac{I_m}{nF} \tag{8}$$

where the number of electrons n required for reduction of the nitro group to yield the corresponding amino compound is equal to six (reactions 2 and 3). In order to verify that these

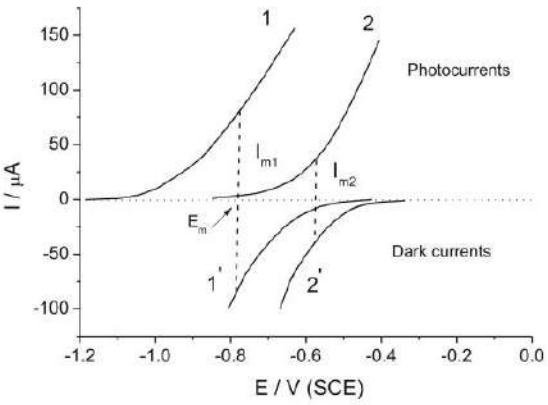

Fig. 5 Plots of the photocurrents and dark currents recorded on a CdS electrode in the presence of 0.2 mol dm^{-3} of HCOONa or HCOOH, and $CHOC_6H_4NO_2$ (1×10^{-3} mol dm^{-3}) as a representative nitroaromatic example. Solvent: deaerated H_2O/CH_3CN (80/20%); inert electrolyte: 0.2 mol dm^{-3} $NaClO_4$. Curves 1–1′, pH 6.5; Curves 2–2′, pH 2

values bear a close relationship to results obtained in photocatalytic condition, we used the irradiated electrode at open circuit to make the reaction take place.

Following the concentration decrease of the nitro-compound with time by analytical means, we obtained reaction rates at open circuit r_{oc}. Both I_m values (Fig. 5) and reaction rates r_{oc} increase with nitroaromatic concentration until a plateau is reached above $\sim 1 \times 10^{-3}$ mol dm^{-3} where the kinetics become zero order with respect to the reacting species. This behavior is the same for all nitro-compounds examined in this work. For comparison, with 2-propanol or methanol as hole acceptors at, for example, a neutral pH the magnitude of I_m followed the order $HCOO^- > (CH_3)_2CH_2OH > CH_3OH$.

Plots of r_{oc} vs. r_e for different concentrations of the reducible species should give a straight line with a slope of 1. Indeed, Fig. 6 shows a linear relationship and a slope of 0.98 in quite good agreement with that required, and hence, the approach can predict the photocatalytic behavior from electrochemical data.

The first step in the overall reduction process is adsorption of the nitroaromatic as shown by recent literature [2]. Assuming Langmuir conditions

$$r_{oc} = -\frac{dc_{ox}}{dt} = kn_s \frac{KC_{ox}}{1 - KC_{ox}} \tag{9}$$

For a constant number of surface electrons (n_s) and concentration of the nitro-compound (c_{ox}) at saturation conditions, the reaction order is zero as stated above. On the other hand, at constant light intensity and $Kc_{ox} \ll 1$, a pseudo first order reaction should be observed. This is verified experimentally at c_{ox} lower than the saturation value and the pseudo first order constants are reported in Table 1 for different hole

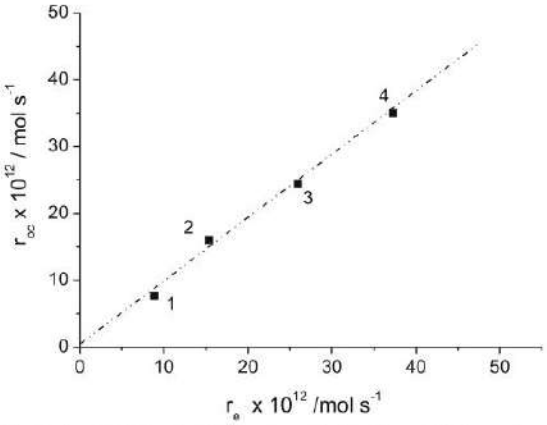

Fig. 6 A typical plot of reduction rates calculated for a CdS electrode at open circuit (r_{oc}) or using the electrochemical model as in Fig. 5 (r_e). Solvent: deaerated H_2O/CH_3CN (80/20%) containing HCOONa (0.2 mol dm^{-3}) and $CHOC_6H_4NO_2$ as a representative example of a nitroaromatic species

acceptors, using again the data for $CHOC_6H_4NO_2$ reduction as an illustrative example.

The higher reduction rate is observed when $HCOO^-$ and HCOOH are used. On the other hand, literature data, however fragmentary, clearly indicate that SO_3^{2-} is the species showing the highest reactivity with holes [24, 31]; therefore, the experimental results need an explanation. In all probability, the answer is the formation of active radical intermediates upon hole capture

$$R{-}H + h^+ \rightarrow R^{\bullet} + H^+ \quad (10)$$

where $R^{\bullet}$ is $COO^{\bullet-}/HCOO^{\bullet}$, $(CH_3)_2C^{\bullet}OH$ or $^{\bullet}CH_2OH$.

When the energy level of the radical specie $R^{\bullet}$ lies above the conduction band (CB) edge, electron injection can occur into it and/or into ss [24], increasing the number of surface electron and hence the reduction rate

$$R^{\bullet} \rightarrow R^+ + e^- \quad (11)$$

Table 1 Effect of the nature of the hole scavenger on the reduction rate of $CHOC_6H_4NO_2$ (3×10^{-4} mol dm^{-3}) in a CdS suspension in H_2O/CH_3CN (80/20%)

Hole scavenger	k_1 (s^{-1}) (pH 6.5)	k_2 (s^{-1}) (pH 2)
$HCOO^-$	0.300	*
HCOOH	*	0.07
2-propanol	0.040	0.04
Methanol	0.005	0.01
Sulfite	0.010	*

*Not tested

This phenomenon is known as current multiplication (or current doubling) as consumption of one hole yields two electrons (reactions 5, 10, 11) [24].

The reducing power of the above radicals [32] follows the order $HCOO^{\bullet}/COO^{\bullet-} > (CH_3)_2C^{\bullet}OH > {}^{\bullet}CH_2OH$, which seemingly reflects the reactivity (Table 1). Significantly, SO_3^{2-} is not known to give current multiplication despite its high hole-capture cross section.

A closer inspection of the data in Table 1 reveals that there is more to comment; for example, the low rate at pH 2 where HCOOH is expected to be oxidized to $HCOO^{\bullet}$. Rate constants are reported for the same concentration of HCOONa and HCOOH (0.2 mol dm^{-3}), but in the latter case ($pK_a = 3.75$), the concentration of formate is 3.5×10^{-3} mol dm^{-3} and one can suspect that its contribution is significant. Indeed, for a constant concentration of added HCOOH, it turns out that the rate increases at pH of 2.2 and decreases at pH 1.8, i.e., depending on the amount of formate. Thus, a possible reason for the observed behavior is the known difficulty for formic acid to dissociate even on active surfaces [33]; 2-propanol shows a similar slow equilibration with surfaces.

To complement the results discussed just above, we examined Hammett reactivity by evaluating the effect of the para substituents on first order reduction reaction rates at pH 2 where protonation of the resulting aniline favors desorption.

We found that the Hammett plot of the rate constants ($\log k = \rho\sigma_p$) gives a straight line with a positive slope ~ 1 (Fig. S5, ESI). According to the common interpretation, this indicates a building up of negative charge in the rate-determining step, and as expected, electron withdrawing groups favor the reduction process. Further studies will need to verify whether experimental Hammett slopes correlate with a charge transfer in adsorption in the dark.

Photocatalytic reactions are commonly conducted in semiconductor suspensions and should be an obvious extension of analogous processes obtained with open circuit electrodes. A conspicuous advantage is that the higher area increases the number of surface active sites [30]; a major limitation is recombination of photogenerated electron/hole pairs (reaction 5).

We carried out experiments with CdS suspension in small reactors that were covered to reflect light except for a window of geometric area 0.8 cm^2, i.e., the same as that of open circuit electrodes whose behavior is described above; then, the incident photon flux density is the same and the amount of dispersed CdS ensures its complete absorption.

Rates were 4.8 higher than for electrodes at open circuit, which confirms analogous results obtained for the reduction of MV^{2+} and Fe^{3+} at TiO_2. A model was proposed that considered that particles furthest from the optical window are at best partially shielded by the closest ones and, therefore, provide fewer electron-hole pairs [19 and refs therein]. Yet, if holes are efficiently consumed at the illuminated surface,

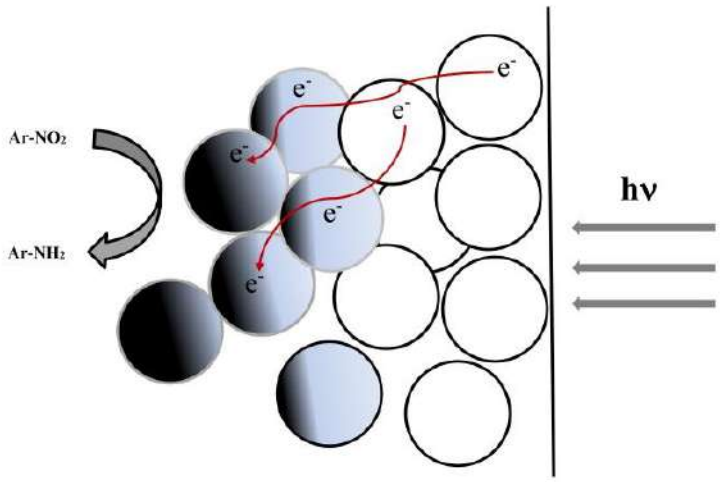

Fig. 7 An illustration of a possible reduction mechanism of nitroaromatics at dark sites of particles or aggregates in a CdS suspension

avoiding recombination, a large area will be available for dark reduction. As a matter of fact, earlier studies reported that reduction of Cu^{2+} occurs mainly at dark sites of particles [34].

A large number of parameters need to be optimized for suspension photocatalysis, among which is the formation of aggregates and agglomerates of particles [35]. In our case, a well-sonicated CdS powder showed primary particles with an average dimension of 1.0–1.5 μm that give 8-μm large aggregates. We have estimated that 400 nm light can penetrate inside an aggregate for about 50%. Assuming a good connection among particles, the reported antenna mechanism [36] might ensure electron transport from illuminated areas to remote dark sites where reduction can take place (see above) as schematically depicted in Fig. 7. Ongoing research in different laboratories can provide more valuable insights.

Conclusion

The photoreduction of nitroarene compounds, a typical multielectron process, is examined here at CdS electrodes and in parallel on particle suspensions of the same material.

Electrochemistry in the dark and photoluminescence indicate that reduction is mediated by surface states (sulfur vacancies) approximately located at 0.55 eV below the conduction band. In keeping with the known reduction mechanism, phenylhydroxylamine intermediates are detected at both electrodes and in suspensions. In the latter case, we employed a collector metallic electrode immersed in illuminated suspensions. Electron transfer between the collector and the particles can be direct or mediated by shuttle species such as methylviologen. In our particular case, hydroxylamine derivatives, resulting from partial reduction of the nitro group at CdS, were re-oxidized at the collector giving rise to a current, and thus, their presence was revealed.

The reduction of nitroarenes was used as a probe reaction to confirm the common bases of photoelectrochemistry and photocatalysis. Electrochemical measurements were shown to be useful for this purpose. We found that the net anodic photocurrent ($+I_{ph}$) due to oxidation of a sacrificial hole scavenger and the net cathodic dark current due to reduction of the nitro-compounds ($-I_d$) exactly balance at a potential E_m. The zero net current defines the operative photocatalytic condition, and each of these currents also represents the reduction rate. Based on these premises, we verified that the catalytic rate r_{oc} of the reduction at open circuit is the same as the value r_c predicted from current-potential curves confirming that the photocatalytic reduction process can be predicted from electrochemical measurements.

Finally and importantly, analysis of reaction rates in CdS suspensions indicates that a significant portion of reduction occurs on dark sites of the particles.

References

1. Song J, Huang ZF, Pan L, Li K, Zhang X, Wang L, Zou JJ (2018) Review on selective hydrogenation of nitroarene by catalytic, photocatalytic and electrocatalytic reactions. Appl Catal B 227:386–408
2. Jensen SC, Bettis Homan S, Weiss EA (2016) Photocatalytic conversion of nitrobenzene to aniline through sequential proton-coupled one-electron transfers from a cadmium sulfide quantum dot. J Am Chem Soc 138(5):1591–1600
3. Molinari A, Mazzanti M, Fogagnolo M (2019) Photocatalytic selective reduction by TiO_2 of 5-nitrosalicylic acid ethyl ester: a mild route to mesalazine. Catal Lett 150:1072–1080
4. Shiraishi Y, Togawa Y, Tsukamoto D, Tanaka S, Hirai T (2012) Highly efficient and selective hydrogenation of nitroaromatics on photoactivated rutile titanium dioxide. ACS Catal 12:2475–2481

5. El-Hosainy HM, El-Sheikh SM, Ismail AA, Hakki A, Dillert R, Killa HM, Ibrahim IA, Bahnemann DW (2018) Highly selective photocatalytic reduction of o-dinitrobenzene to o-phenylenediamine over non-metal-doped TiO_2 under simulated solar light irradiation. Catalysts 8(12):641–652
6. Molinari A, Maldotti A, Amadelli R (2014) Probing the role of surface energetics of electrons and their accumulation in photoreduction processes on TiO_2. Chem Eur J 20(25):7759–7765
7. Molinari A, Maldotti A, Amadelli R (2015) A photo(electro)-catalytic system illustrating the effect of lithium ions on titania surface energetics and charge transfer. J Electroanal Chem 755:143–150
8. Albery JW, Bartlett PN, Porter JD (1984) The electrochemistry of semiconductor particles. J Electrochem Soc 131(12):2892–2896
9. Albery JW, Bartlett PN, Porter JD (1984) The electrochemistry of semiconductor particles. J Electrochem Soc 131(12):2896–2900
10. Ward MD, Bard AJ (1983) Photocurrent enhancement via trapping of photogenerated electron of TiO_2 particles. J Phys Chem 86: 3599–3605
11. Finlayson MF, Wheeler BL, Narrioyshi K, Park KH, Bard AJ, Campion A, Fox MA, Webber SE, White JM (1985) Determination of flat-band position of CdS crystals, films and powders by photocurrent and impedance techniques. Photoredox reaction mediated by intragap States J Phys Chem 89:5676–5568
12. Beranek R (2011) (Photo)electrochemical methods for the determination of the band edge positions of TiO_2-based nanomaterials. Adv Phys Chem Article ID 786759, 20 pages
13. Cai R, Baba R, Hashimoto K, Kubota Y, Fujishima A (1993) Photoelectrochemistry of TiO_2 particles: efficient electron transfer from the TiO_2 particles to a redox enzyme. J Electroanal Chem 360(1-2):237–245
14. Park H, Choi W (2003) Photoelectrochemical investigation on electron transfer mediating behaviors of polyoxometalate in UV-illuminated suspensions of TiO_2 and Pt/TiO_2. J Phys Chem B 107(16):3885–3890
15. Amadelli R, Samiolo L (2013) In: Pichat P (ed) Photocatalysis for water purification. Wiley, Weinheim
16. Beranek R (2019) Selectivity of chemical conversions: do light-driven photoelectrocatalytic processes hold special promise? Angew Chem Int Ed 58:2–8
17. Spiro M (1986) Polyelectrodes: the behavior and applications of mixed redox systems. Chem Soc Rev 15(2):141–165
18. Spiro M (2002) In: Bockris, J O'M, Conway BE, White RE Modern Aspects Electrochem Vol 34, Kluwer, New York, Boston
19. Neumann-Spallart M (2007) Aspects of photocatalysis on semiconductors: photoelectrocatalysis. Chimia 61: 806–809 and refs. Therein
20. Amadelli R, Maldotti A, Sostero S, Carassiti V (1991) Photodeposition of uranium oxides onto TiO_2, from aqueous uranyl solutions. J Chem Soc Faraday Trans 87(19):3267–3273
21. Kesselman JM, Shreve GA, Hoffmann MR, Lewis NS (1994) Flux-matching conditions at TiO_2 photoelectrodes: is interfacial electron transfer to O_2 rate-limiting in the TiO_2-catalyzed photochemical degradation of organics? J Phys Chem 98(50):13385–13395
22. Salter-Blanc AJ, Bylaska EJ, Johnston HJ, Tratnyek GP (2015) Predicting reduction rates of energetic nitroaromatic compounds using calculated one-electron reduction potentials. Environ Sci Technol 49(6):3778–3786
23. Appleby AJ, Zagal JH (2011) Free energy relationships in electrochemistry: a history that started in 1935. J Solid State Electrochem 15(7-8):1811–1832
24. Morrison SR (1980) Electrochemistry at semiconductors and oxidized metal electrodes. Plenum Publishing Corporation, New York
25. Vandermolen J, Gomes WP, Cardon F (1980) Investigation of the kinetics of electroreduction processes at dark TiO_2 and $SrTiO_3$ single crystal semiconductor electrodes. J Electrochem Soc 127(2): 324–328
26. Grätzel M (1989) Heterogenous photochemical electron transfer. CRC Press, Boca Raton
27. Herrasti P, Peter L (1991) Photocurrent doubling during the oxidation of formic acid at n-CdS: an investigation by intensity modulated photocurrent spectroscopy. J Electroanal Chem 305(2):241–258
28. Sun T, Darling AJ, Li Y, Fujisawa K, Holder CF, Liu H, Janik MJ, Terrones M, Schaak RE (2019) Defect-mediated selective hydrogenation of nitroarenes on nanostructured WS_2. Chem Sci 10(44): 10310–10317
29. Murphy KC, Lisensky GC, Leung LK, Kowach GL, Ellis AB (1990) Photoluminescence-based correlation of semiconductor electric field thickness with adsorbate Hammett substituent constants. Adsorption of aniline derivatives onto cadmium selenide. J Am Chem Soc 112:8344–8348
30. Parrino F, De Pasquale C, Palmisano L (2019) The influence of some surface related phenomena on mechanism, selectivity and conversion of TiO_2 induced photocatalytic reactions. ChemSusChem 12(3):589–602
31. Pradhananga RR, Jüttner K (1987) Hole capture cross section on CdS photoelectrodes. Electrochim Acta 32(4):557–562
32. Lilie J, Beck G, Henglein A (1971) Pulsradiolyse und polarographie: halbstufenpotentiale für die oxydation und reduktion von kurzlebigen organischen radikale an der Hg-elektrode. Ber der Bunsegesellschaft Phys Chem 75(5):458–465
33. Bowker M (2016) The role of precursor states in adsorption, surface reactions and catalysis. Top Catal 59(8-9):663–670
34. Ward MD, Bard AJ (1982) Photocurrent enhancement via trapping of photogenerated electrons of TiO_2 particles. J Phys Chem 86(18): 3599–3605
35. Pellegrino F, Pellutiè L, Sordello F, Minero C, Ortel E, Hodoroaba VD, Maurino V (2017) Influence of agglomeration and aggregation on the photocatalytic activity of TiO_2 nanoparticles. Appl Catal B 216:80–87
36. Wang C, Pagel R, Dohrmann JK, Bahnemann DW (2006) Antenna mechanism and de-aggregation concept: novel mechanistic principles for photocatalysis. C R Chimie 9(5-6):761–773

Таким чином, встановлено вплив полімерів різної природи на кінетику електроосадження PbO_2. *Показано, що на відміну від поверхнево-активних речовин, за наявності в електроліті полімера* Nafon® *спостерігається екстремальна залежність гетерогенної константи швидкості осадження від концентрації добавки, що обумовлено одночасним впливом на кінетику електроосадження ψ` потенціалу та параметру інгібування* S.

За характером впливу на кінетику осадження плюмбум оксиду досліджені добавки ПАР і ПЕ можна розбити на кілька груп:

– *приводять до прискорення процесу електроосадження* PbO_2. *До них відносяться аніонні ПЕ, наприклад* Nafion®;

– *приводять до незначного пригнічення процесу осадження* PbO_2. *До цієї групи належать аніонні ПАР;*

– *приводять до значного пригнічення процесу електроосадження* PbO_2. *Наприклад, катіонний ПЕ.*

За наявності в електроліті добавок ПАР та полімерів утворюються композитні покриття PbO_2-*ПАР та* PbO_2-*полімер. Збільшення концентрації ПАР і полімерів в електроліті осадження приводить до росту їх вмісту композиті, що обумовлене збільшенням адсорбції. За однакових умов осадження кількість ПАР в композиті залежить від їх природи і зростає зі збільшенням довжини карбонового ланцюга. В цьому ж ряду зростає їх адсорбція на оксиді. За збільшення анодної густини струму кількість аніонних ПАР і поліелеткролітів, як правило, зростає. Виключенням є лауретсульфат натрію, який за збільшення густини струму (інтенсивності виділення кисню) за рахунок високої поверхневої активності частково перерозподіляється на межу розчин-повітря через газову флотацію. Збільшення температури та концентрації кислоти в електроліті приводить до збільшення вмісту добавок у композиті.*

Для одержання композитів складу PbO_2-TiO_2-*ПАР запропоновано використовувати суспензійні електроліти, де в якості частинок дисперсної фази виступає* TiO_2, *а в якості добавки – ПАР. Використання таких розчинів*

створює можливість одержання композиту зі збільшеною кількістю TiO_2 *та ПАР, порівняно з подвійними системами.*

Тобто, за використання у якості добавок ПАР і поліелектролітів, а також застосування агрегативно стабільних суспензійних електролітів із нанорозмірними частинками дисперсної фази та ПАР, можна отримувати новітні композитні матеріали (металоксид-ПАР, металоксид-полімер та потрійні системи PbO_2-TiO_2-*ПАР), що суттєво відрізняються за своїм складом. Варіювання складу електроліту осадження, густини струму і температури дозволяє змінювати вміст добавок у композитах від 1 до 18 мас.%, що дає змогу керовано впливати на морфологію, текстуру, фазовий склад, фізико-хімічні властивості, електрокаталітичну активність і селективність електрокаталізаторів на основі* PbO_2 *у цільових процесах*.

РОЗДІЛ 6
КАТАЛІТИЧНЕ РУЙНУВАННЯ ФАРМАЦЕВТИЧНИХ ПРЕПАРАТІВ ІЗ ВИКОРИСТАННЯМ РІЗНИХ ЕЛЕКТРОКАТАЛІЗАТОРІВ

Логічно припустити, що відмінності в електроосадженні, морфології та фазовому складі досліджуваних композитів порівняно з немодифікованим PbO_2 впливатимуть на електрокаталітичну активність і селективність матеріалів металоксид-ПАР та металоксид-полімер у процесах, що проходять за високих анодних потенціалів (виділення кисню, окиснення органічних сполук). І це дійсно підтверджується на практиці.

Характер ефектів зручно оцінювати за зміною швидкості реакції виділення кисню. Закономірності проходження реакції виділення кисню на PbO_2 можуть бути задовільно пояснені в рамках механізму, запропонованого Павловим і Монаховим [48]. Відповідно до цього механізму, виділення кисню проходить на активних місцях, локалізованих в гідратованому шарі PbO_2.

Відомо, що виділення кисню на PbO_2 лімітується стадією переносу другого електрона, тобто електрохімічною десорбцією [49]. Враховуючи це за збільшення енергії зв’язку кисеньвмісних радикалів із поверхнею електрода перенапруга виділення кисню зростатиме. Як видно з поляризаційних кривих перенапруга виділення кисню на покритті, що складається переважно з α-фази менше, ніж на покритті, що збагачене β-фазою, що узгоджується з даними про будову осадів (рис. 6.1). Зменшення перенапруги виділення кисню являється результатом гідратованості поверхні. Невеликі відмінності в перенапрузі виділення кисню на матеріалах, отриманих із базових електролітів пов’язані із незначними відмінностями в кристалографічних орієнтаціях. Коли ми говоримо про структурний фактор для PbO_2, кристалографічні орієнтації практично не впливають на перенапругу виділення кисню та інші процеси, що проходять за участі кисеньвмісних частинок. З точки зору окиснення органіки, де потрібні

електроди із високою перенапругою виділення кисню, таким матеріалам надається перевага.

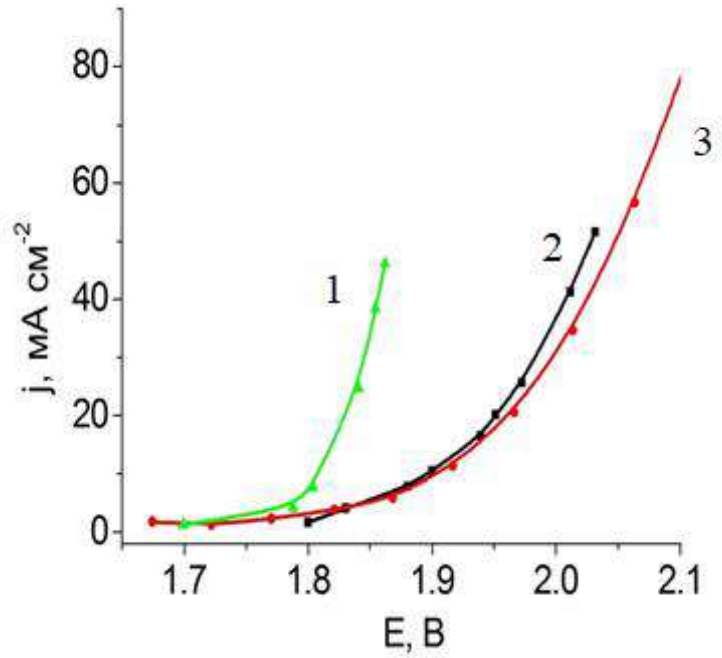

Рис. 6.1 Квазістаціонарні поляризаційні криві виділення кисню на PbO_2, осадженому з наступних електролітів: 1 – 0,1 М $Pb(CH_3SO_3)_2$ + 1 М CH_3SO_3H; 2 – 0,1 М $Pb(NO_3)_2$ + 0.1 М HNO_3; 3 – 0,1 М $Pb(CH_3SO_3)_2$ + 0,1 М CH_3SO_3H

Практичний інтерес представляє створення матеріалів із великою кількістю міцно зв’язаних кисеньвмісних частинок, на таких матеріалах спостерігається інгібування виділення кисню та збільшення парціальної швидкості окиснення органічних сполук. За використання ніколу в якості добавки також спостерігаємо зменшення перенапруги виділення кисню, що також корелює з даними, отриманими за проведення радіохімічних вимірювань та рентген фотоелектронної спектроскопії (рис. 6.2).

Що стосується ПАР, вони можуть змінювати енергію зв’язку через зменшення ступеня заповнення поверхні електрода електроактивними частинками. Тобто ПАР повинні збільшувати перенапругу виділення кисню, якщо специфічно не впливають на енергію зв’язку частинок. Так, наприклад

для SDS та SLES спостерігається зменшення перенапруги виділення кисню (рис. 6.3).

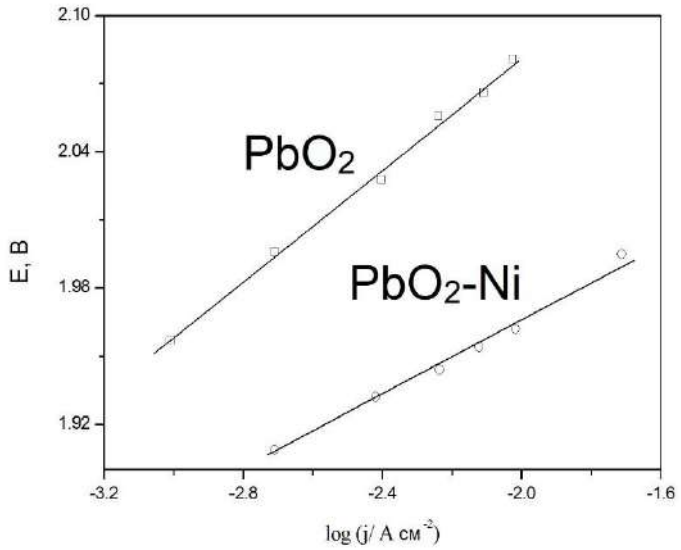

Рис. 6.2 Квазістаціонарні поляризаційні криві в 1,6 М $(NH_4)_2SO_4$

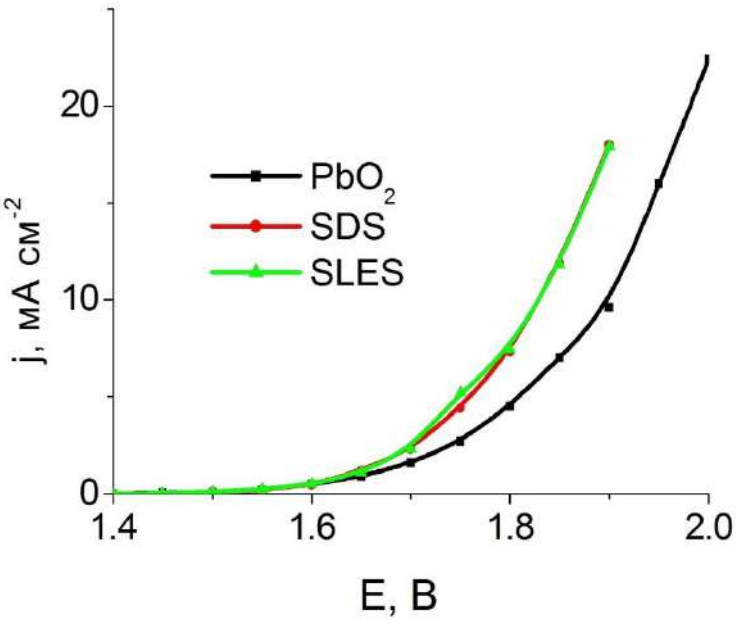

Рис. 6.3 Квазістаціонарні поляризаційні криві виділення кисню на композитах PbO_2

Флуоровмісні ПАР за рахунок гідрофобізації збільшують міцність зв’язку, що приводить до збільшення перенапруги виділення кисню (рис. 6.4).

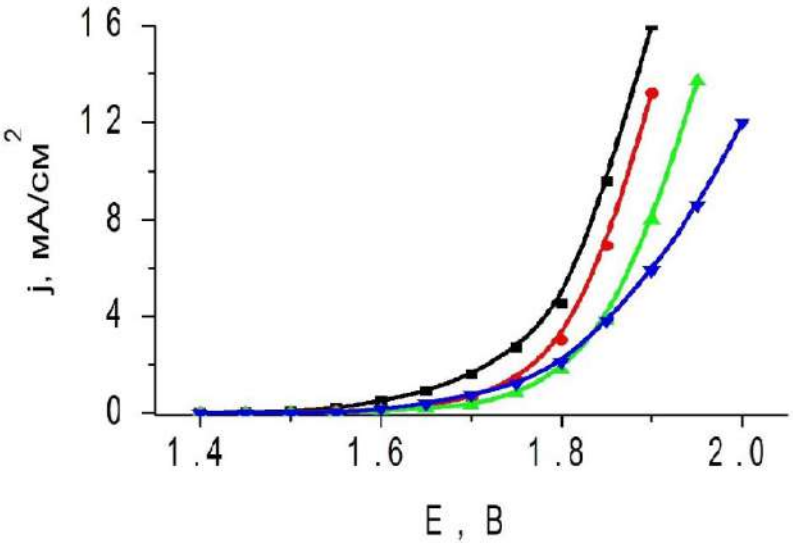

Рис. 6.4 Квазістаціонарні поляризаційні криві виділення кисню на композитах PbO_2-флуоровмісний ПАР. Зі збільшенням вмісту ПАР перенапруга РВК збільшується

Такі дані підтверджуються даними РФС, де ми бачимо збільшення частки інертних кисеньвмісних радикалів, що також спостерігалося в випадку використання флуору, як добавки до електроліту осадження PbO_2 [50].

Незважаючи на те, що цільовим процесом являється процес окиснення органічних сполук у розчині, у водних розчинах ми не можемо суттєво побороти виділення кисню, і воно вносить найбільший вклад у вихід за струмом. Ми намагаємося підвищити внесок цільового процесу.

І, повертаючись до питання про селективність матеріалу, на жаль, збільшення перенапруги виділення кисню не вказує на збільшення швидкості окиснення органічних сполук, оскільки остання може змінюватися незалежно від значення потенціалу виділення кисню, що свідчить про те, що в цих процесах беруть участь різні за енергією зв’язку кисеньвмісні частинки.

З огляду на селективність матеріалу, оскільки концентрація токсичних ароматичних сполук невелика, та досліджувані процеси проходять у водному середовищі, де основним процесом являється виділення кисню, а окиснення органічних речовин – вторинний процес. У таких процесах необхідно використовувати стабільні за високих анодних потенціалів електрокаталізатори. Вибрані нами електроди задовольняють цим вимогам. Нами вивчені процеси електрокаталітичного руйнування вибраних органічних сполук. Наприклад, нітрофуразон [51], хлорамфенікол [52], 4-нітроанілін. Моделлю галогенованих органічних сполук було обрано 4-хлорфенол, а бензохінон – як представника негалогенованих ароматичних органічних сполук. Більшість досліджуваних сполук окиснюється із утворенням проміжних продуктів хіноїдної структури.

Аналіз отриманих даних показує, що виділення кисню та окиснення органічних сполук (зокрема нітрофуразону) відбуваються через один і той же тип проміжних оксигеновмісних частинок. Спостерігається явне пригнічення виділення кисню на SnO_2 за наявності як органічної сполуки, так і іонів Cl^- в розчині. Нітрофуразон руйнується ефективніше на PbO_2, завдяки великій кількості оксигеновмісних частинок, міцно зв’язаних із поверхнею оксиду, що характерно для плюмбум(IV) оксиду [27].

Слід зазначити, що за наявності 3 г $дм^{-3}$ хлориду в електроліті найбільша кількість OCl^-, що бере участь у вторинних окисних процесах, виробляється на легованому SnO_2, що дозволяє досягти загальної швидкості процесу, зіставлюваної з PbO_2-анодами, що може бути цікавим з точки зору використання таких матеріалів для знезараження лікарняних стоків.

Досліджено властивості електрокаталізатора з активним шаром на основі SnO_2, допованого металами платинової групи, селективного до утворення гіпохлоритної кислоти з низькоконцентрованих хлоридних розчинів. Показано, що такий анод не є ефективним електрокаталізатором прямого електрохімічного окиснення забруднювачів, однак його застосування дозволяє на аноді одержати велику кількість гіпохлориту, а також певну кількість кисню,

що за відновлення на катоді приводить до синтезу гідроген пероксиду та утворення додаткової пероксенової системи.

Основні результати розділу опубліковано в роботах автора [27, 36-40, 51–53].

Received: 31 May 2021 | Revised: 28 July 2021 | Accepted: 12 August 2021

DOI: 10.1002/wer.1628

RESEARCH ARTICLE

water
ENVIRONMENT RESEARCH

Electrochemical oxidation of chloramphenicol with lead dioxide–surfactant composites

Olesia Shmychkova | **Svitlana Zahorulko** | **Tatiana Luk'yanenko** | **Alexander Velichenko**

Physical Chemistry Department, Ukrainian State University of Chemical Technology, Dnipro, Ukraine

Correspondence
Olesia Shmychkova, Physical Chemistry Department, Ukrainian State University of Chemical Technology, 8, Gagarina Ave, 49005 Dnipro, Ukraine.
Email: lesiandra08@gmail.com

Funding information
Ministry of Education and Science of Ukraine, Grant/Award Number: 0121U109529

Abstract

The PbO_2–2 wt.% sodium dodecyl sulfate composite formed from methanesulfonate electrolyte consists of 93.1% of α-phase PbO_2 in contrast to the similar one synthesized from nitrate electrolyte, which contains 73.3% of β phase. The electrocatalytic activity of the obtained composites in the oxygen evolution reaction and oxidation of chloramphenicol was investigated. It was found that the Tafel slope significantly exceeds the theoretical value, which indicates a decrease in the degree of filling of the electrode surface with oxygen-containing particles. In the presence of organic compound and chloride ions in the solution, irreversible adsorption of the intermediate is observed, which leads to additional blocking of active centers on the oxide surface, which are involved in the oxidation of organic substance. It was established that the maximum rate of chloramphenicol conversion is 83.5% and 85% at 50 and 80 mA cm^{-2}, respectively, under kinetic control. The heterogeneous oxidation rate constant of chloramphenicol is 0.0035 min^{-1}. Oxidation of chloramphenicol occurs through the formation of 4-(-2-amino-1,-3-dihydroxy-propanyl)-nitrobenzene with cleavage of dichloroacetic acid. Next, the amino group is oxidized to the nitro group to form 4-(2-nitro-1,-3-dihydroxy-propanyl)-nitrobenzene. Subsequent electrolysis produces nitrobenzoic acid, which is oxidized to benzoic acid, later hydroquinone, then benzoquinone and a set of aliphatic compounds.

Practitioner Points

- The PbO_2–2 wt.% SDS composite consists of 93.1% of α phase of PbO_2 in contrast to those synthesized from nitrate electrolyte.
- The Tafel slope indicates a decrease of surface filling with oxygen-containing particles.
- Irreversible adsorption of the intermediate is observed in the presence of chloride ions.

KEYWORDS

chloramphenicol, electrooxidation, lead dioxide–surfactant composites, oxygen evolution reaction, wastewater treatment

INTRODUCTION

Simultaneous chemical and biological pollution of the water environment is very dangerous in their combination, as it creates, first of all, the problem of direct toxic effects of chemicals on human health (Brillas, 2020; Ganiyu et al., 2020). Additionally, which is an even more dangerous, chemical factor stimulates the further evolution of pathogenic bacteria and viruses because of their numerous mutations. An example of this is the emergence of superbugs that are resistant to modern pharmaceuticals, as well as new strains of viruses (Zhang et al., 2016).

The main focus of researchers is on the development of promising reagent methods for the destruction of pharmaceutical residues. The proposed methods should be divided into several groups: reagents for the addition to the system of hydrogen peroxide and/or other oxidants, such as ozone, sodium hypochlorite, together with catalysts, photocatalytic and electrocatalytic (Hu et al., 2021; Salazar-Banda et al., 2021; Sanchez-Montes et al., 2018; Zhou et al., 2018, 2020).

Electrochemical methods of destruction of pharmaceutical residues are quite promising (Zhou et al., 2020). These methods may occur via two different mechanisms: (i) direct, where the oxidative destruction of pollutants occurs directly in the electrochemical process at the anode (Zhou et al., 2020; Sanchez-Montes et al., 2018), and (ii) indirect, in which due to electrochemical reactions strong oxidants are formed (Zhou et al., 2018). All electrochemical methods are relatively reagent free, as they do not require the addition of oxidants to the system, which is a significant advantage over reagents, and also have significant advantages over photocatalytic due to much higher rates of target processes. However, electrochemical processes strongly depend on the electrode material and the operating conditions such as current density and applied electric charge. According to previous studies (Hu et al., 2021; Sanchez-Montes et al., 2018), the most effective anodes are modified materials based on PbO_2. A number of our recent publications have demonstrated the high electrocatalytic activity and stability of PbO_2–surfactant composites deposited from nitrate electrolyte (Velichenko, Luk'yanenko, & Shmychkova, 2020; Velichenko, Luk'yanenko, Shmychkova, & Dmitrikova, 2020). However, it is impossible to synthesize mechanically stable coatings thicker than 100 μm from nitrate electrolytes. Based on this, the possibility of synthesis of PbO_2–surfactant composites from methanesulfonate solutions was considered in this work. It was previously shown (Velichenko et al., 2012) that from such electrolytes, it is possible to obtain a coating up to 2 mm thick with satisfactory mechanical properties. However, systematic studies that would allow the creation of such materials for the effective destruction of pharmaceuticals of various chemical natures, unfortunately, are missing.

It should be noted that indirect methods focus on the electrochemical synthesis of only one oxidant, and their efficiency is far from 100%. The presence of water as a solvent, as well as chloride and sulfate ions using appropriate catalysts, can serve as a source of strong oxidants, such as ozone, hypochlorous acid, and persulfate ion, which are environmentally friendly oxidants for the destruction of toxicants (Brillas, 2020; Ganiyu et al., 2020). In our previous work, we proposed the idea of integrated use of substances formed in the electrolysis process, both at the anode (ozone) and at the cathode (hydrogen peroxide) for the destruction of aromatic substances of the phenolic type (Amadelli et al., 2000).

The problem of environmental pollution by pharmaceuticals has become acute in recent decades in both developed and developing countries (Feng et al., 2013). The most common pharmaceuticals that enter the environment include analgesics and anti-inflammatory drugs, antibiotics, cardiovascular drugs (β-blockers and diuretics), hormonal drugs (estrogens), and antiepileptics (carbamazepine) (Feng et al., 2013). It should also be added that hospital wastewater, in addition to toxic and dangerous chemical components, usually contains pathogenic microflora (pathogens of various diseases).

Various pharmaceutical substances and medicines and veterinary drugs, getting and accumulating in natural reservoirs, sediments, soils, and living organisms, cause a very negative impact on the state of ecological systems, endanger human health, and significantly impair environmental safety.

Chloramphenicol is a commonly used broad-spectrum antibiotic belonging to *n*-substituted nitrobenzenes, effective against Gram-negative and Gram-positive bacteria, in particular active against pathogens of dysentery and typhoid fever, rickettsiae, and some major viruses. Its presence in hospital effluents reaches several mg L^{-1} (Sun et al., 2017), which is a potential danger from an environmental point of view. In this study, the regularities of oxidation of chloramphenicol on PbO_2 anodes modified with sodium dodecyl sulfate were investigated. Despite the existing publications concerning electrochemical oxidation of chloramphenicol (Chen et al., 2015; Cotillas et al., 2018; Herraiz-Carbone et al., 2020; Romero-Soto et al., 2018; Wu et al., 2020), some issues remain unclear, in particular the possibility of combined use of direct and indirect oxidation in order to create a compatible heterogeneous catalytic system to increase the efficiency of pollutant destruction.

It should be noted that a detailed study of the properties and electrocatalytic activity of lead dioxide–sodium dodecyl sulfate electrodes has so far been carried out in only three publications (Chen et al., 2020; Li et al., 2017; Velichenko, Luk'yanenko, Shmychkova, & Dmitrikova, 2020), and in all three coatings were deposited from nitrate electrolytes. There are no data in the literature on the coatings synthesized from methanesulfonate solutions. As it is known (Velichenko et al., 2009), the composition, structure, texture, and other properties of coatings obtained from methanesulfonate electrolytes differ significantly from others obtained from nitrate, plumbate, and sulfate baths. In this regard, in this work, we paid attention specifically to coatings obtained from methanesulfonate solutions, because the electrocatalytic processes occurring on the surface of lead dioxide are largely determined by their chemical, phase composition, and physicochemical properties.

METHODOLOGY

All chemicals were purchased from Sigma-Aldrich (ALSI, Ukraine). Bidistilled water with an electrolytic conductivity of 1.6 μS cm^{-1} was used for the preparation of solutions.

Lead dioxide was electrodeposited from methanesulfonate electrolytes of the next composition: 1.0-M CH_3SO_3H + 0.1-M $Pb(CH_3SO_3)_2$. The surfactant ($C_{12}H_{25}SO_4Na$, sodium dodecyl sulfate [SDS]) was added to the deposition electrolyte as aqueous solution with 7×10^{-5}-M concentration. The coatings were deposited at an anode current density of 5 mA cm^{-2} and a temperature of 298 K. Electrode surface area was 2.5 cm^2. The thickness of the coatings was ~50 μm. Platinized titanium was used as a substrate for the synthesis of PbO_2-based anodes. Before the platinum coating was applied, the titanium substrate was prepared according to the following procedure (Shmychkova et al., 2014). The surface was cleaned with sandpaper. Then it was degreased in 5-M KOH for several hours. Later, it was rinse thoroughly with bidistilled water. Then it was etched in a 6-M HCl solution for 20 min at a temperature of 333 K. Next, it was rinsed thoroughly with bidistilled water again. The deposition of platinum on previously prepared titanium substrates was carried out at a cathode current density of 12 mA cm^{-2} and a temperature of 353 K from an electrolyte of the following composition: K_2PtCl_6—0.25 g dm^{-3}; $NaNO_2$—1 g dm^{-3}; and NH_3 solution ($\rho = 0.915$ g cm^{-3})—0.2 cm^3. Under these conditions, the current efficiency of platinum was about 30%. The amount of platinum on the titanium substrate was 2 mg cm^{-2} of the visible electrode surface. Because the thickness of the coatings is about 50 μm, and they do not have through porosity, we exclude the influence of the substrate on the properties of the active layer. In fact, earlier, in one of our publications (Shmychkova et al., 2015), it was shown that the effect of the substrate occurs only at the initial stages of electrocrystallization, and in the case of thick coatings, these signs are absent. In addition, the obtained diffractograms do not show reflections of titanium, its oxides, or platinum.

The surface morphology of lead dioxide anodes was studied by scanning electron microscopy (SEM) using a Stereoscan 440 LEO microscope. X-ray powder diffraction (XRPD) data were collected in the transmission mode on a STOE STADI P diffractometer with Cu $K\alpha_1$ radiation, curved Ge (111) monochromator on primary beam, $2\theta/\omega$ scan, angular range for data collection 20.000–110.225°2θ with increment 0.015, linear position sensitive detector with step of recording 0.480°2θ and times per step 75–300 s, $U = 40$ kV, $I = 35$ mA, and $T = 298$ K. A calibration procedure was performed utilizing SRM 640b (Si) and SRM 676 (Al_2O_3) NIST standards. Preliminary data processing and X-ray qualitative phase analysis were performed using STOE WinXPOW and PowderCell program packages. Crystal structures of the phases were refined by the Rietveld method with the program FullProf.2k, applying a pseudo-Voigt profile function and isotropic approximation for the atomic displacement parameters, together with quantitative phase analysis.

The surface of the coatings was also examined by X-ray photoelectron spectroscopy on a PHI 5000 spectrometer using monochromatic Al Kα radiation. The C 1s binding energy was 284.8 (±0.3) eV and was used to normalize the spectra.

The oxygen evolution reaction (OER) was investigated by stationary polarization on a computer-controlled EG&G Princeton Applied Research potentiostat model 273A in 1-M $HClO_4$ and sulfate solution, depending on the requirements of the experiment.

Electrooxidation of a 0.2-mM aqueous solution of chloramphenicol was performed in a sulfate solution (0.5-M Na_2SO_4) in a space-separated cell at a current density of 50 and 80 mA cm^{-2}. With regard to direct electrochemical oxidation, the main parameter of influence here is the current density. It makes no sense to work at high current densities, because oxidation already occurs at the limiting current due to the low concentration of the initial material. And when using lower current densities, one cannot reach the oxidation potential, so the choice of the operating current density is justified. As for the pH, we do not vary it, because in real wastewater samples, this indicator is close to neutral. Research is carried out at room temperature in order to simulate real conditions as much as possible. We do not vary the

organic substance, because we oxidize the model compound. The rate of oxidation of an organic compound is proportional to the amount of electricity passed through the solution, which, in turn, is determined by the current density, the electrode area, and process duration, which can be easily calculated using the data given in the article. Oxidants (hypochlorite, persulfate, percarbonate, peroxodiphosphate, ozone, and hydrogen peroxide) were determined iodometrically according to Kolthoff and Carr (1953).

Unfortunately, we did not carry out yet long-term life tests of the electrodes, but the materials involved did not change their characteristics and did not display the weight loss during 700 h of electrolysis under the described conditions. Lead ions were not detected in the solution during electrolysis using the ICP spectroscopy method at operating current densities.

The change in chloramphenicol concentration and aromatic intermediates of its oxidation during electrolysis was determined by sampling (4 cm^3) and measuring the optical density of the solution in UV and visible areas using a Kontron Uvikon 940 spectrometer.

The oxidation products were analyzed by high-performance liquid chromatography using a Shimadzu RF-10A xL instrument equipped with an ultraviolet SPD-20AV detector and a 30-cm Discovery® C18 column.

The classical Fenton reaction was used in order to establish the basic regularities of chemical destruction of hazardous components of hospital effluents in heterogeneous catalytic systems. The conditions used were as follows: concentration of organic substance:H_2O_2:Fe(II) = 1:4:0.1.

RESULTS AND DISCUSSION

Characteristic of materials

Anode materials based on lead dioxide are widely used in industry (Li et al., 2011). PbO_2 exists in both amorphous and crystalline forms (Li et al., 2011). Two of its allotropic forms are known: α-PbO_2, which is characterized by an elementary rhombic lattice, and β-PbO_2, a tetragonal lattice of the rutile type. These forms differ greatly in crystal size and mechanical properties (Velichenko & Devilliers, 2007). It is known that α-PbO_2 has a more compact structure compared with β-PbO_2 (Casellato et al., 2003). Usually, electrodeposited coating often consists of different phase structures of α-PbO_2/β-PbO_2 (Velichenko, Luk'yanenko, Shmychkova, & Dmitrikova, 2020).

We used the XRPD method to investigate the effect of sodium dodecyl sulfate on the phase composition of electrodeposited PbO_2 and its texture. XRPD data revealed that all investigated samples contained two phases: α-PbO_2 (structure-type $Fe_2N_{0.94}$, Pbcn space group) and β-PbO_2 (structure-type TiO_2 rutile, space group P42/mnm). The difference is observed only in the ratio of these two phases, as well as in the degree of crystallinity (Table 1).

As can be seen from the obtained data, the formed coating consists of 93.1% of α-phase PbO_2 in contrast to the similar one synthesized from nitrate electrolyte, which contains 73.3% of β phase (Velichenko, Luk'yanenko, Shmychkova, & Dmitrikova, 2020). However, the main effect on the phase composition in this case has the content of methanesulfonic acid in the electrolyte deposition, against which the effect of surfactant is not noticeable.

A typical morphology of the obtained coatings is shown in Figure 1.

As in the case of coatings synthesized from nitrate solution (Velichenko, Luk'yanenko, Shmychkova, & Dmitrikova, 2020), the presence of surfactant in the deposition electrolyte leads to the loss of a clear direction of the individual faces of the crystals and an obvious reduction in their size (see Figure 1).

Direct electrochemical oxidation

On the electronic absorption spectrum, the initial solution of chloramphenicol is characterized by the main absorption maximum at 275 nm (Figure 2, inset).

A decrease in the optical density of the absorption maximum and the formation of intermediate oxidation products was observed first at 270 nm and over time at 265 nm during the electrolysis. The nature of the dependence of concentration logarithm on time indicates the pseudo-first order of the reaction or the initial compound.

Figure 2 can be divided into two areas. In I (the first 150 min of electrolysis), the process occurs with kinetic control, and the increase in current density leads to an increase in the reaction rate constant by almost 1.4 times.

Then, due to a significant decrease in the concentration of the initial compound, the limiting stage changes and the process enters the region with diffusion control (Area II; see Figure 2) and occurs at the limit current; at this time, the increase in current density does not affect the rate of the whole process, as the latter depends on the diffusion of reagents from the solution bulk to the surface of the electrocatalyst. This is also confirmed by the fact that as the stirring rate of the solution increases, the heterogeneous rate constant of the reaction increases. In this

TABLE 1 Phase composition of the samples involved

Deposition electrolyte	Content (wt.%) α-PbO_2/β-PbO_2	Phase	Lattice parameters (Å) a	b	c	Reliability factors R_I/R_P, R_{WP}, R_{EXP}
0.1-M $Pb(NO_3)_2$ + 1-M HNO_3 + 7 × 10^{-5}-M SDS[a]	26.7(2)/73.3(6)	α-PbO_2	4.9921(6)	5.9483(7)	5.4625(6)	0.0350
		β-PbO_2	4.9562(3)	—	3.3838(2)	0.0219/0.0699, 0.0940, 0.0712
0.1-M $Pb(MS)_2$ + 1-M MSA + 7 × 10^{-5}-M SDS	93.1(6)/6.9(2)	α-PbO_2	4.9925(1)	5.9428(4)	5.4577(4)	0.0460
		β-PbO_2	4.9596(14)	—	3.3640(13)	0.0631/0.0863, 0.115, 0.0844

[a]SDS—sodium dodecyl sulfate, $CH_3(CH_2)_{11}OSO_3Na$.

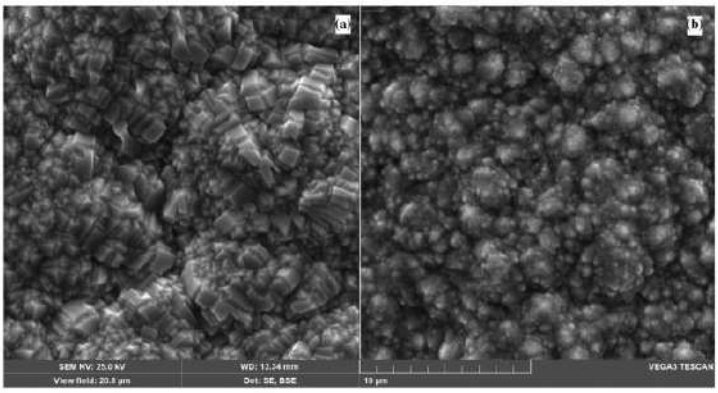

FIGURE 1 Scanning electron microscopy (SEM) images of coatings surface: (a) unmodified PbO_2 and (b) PbO_2–2 wt.% sodium dodecyl sulfate

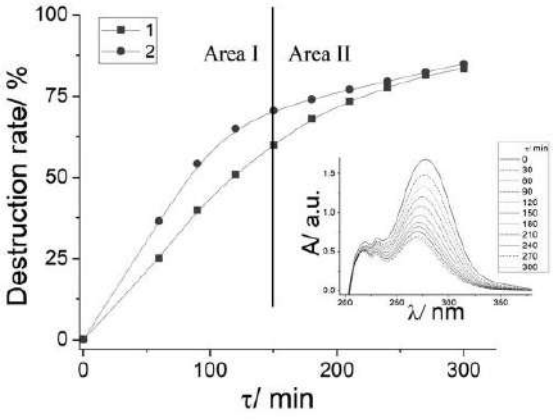

FIGURE 2 The degree of conversion of chloramphenicol during electrolysis at the PbO_2 anode. Solution: 0.5-M Na_2SO_4 + 0.2-mM chloramphenicol. Anode current density: 1–50, 2–80 mA cm^{-2}. Inset: electronic absorption spectra of 0.2-mM chloramphenicol solution at the PbO_2 anode

section, the rate constant for both studied current densities is 0.006 min^{-1}.

The maximum rate of chloramphenicol conversion is 83.5% and 85% at 50 and 80 mA cm^{-2}, respectively, under kinetic control. The heterogeneous oxidation rate constant of chloramphenicol is 0.0035 min^{-1}.

Oxidation of chloramphenicol occurs through the formation of 4-(-2-amino-1,3-dihydroxy-propanyl)-nitrobenzene with cleavage of dichloroacetic acid. Next, the amino group is oxidized to the nitro group to form 4-(2-nitro-1,3-dihydroxy-propanyl)-nitrobenzene. Subsequent electrolysis produces nitrobenzoic acid, which is oxidized to benzoic acid, later hydroquinone, then benzoquinone and a set of aliphatic compounds (Figure 3). *R*-substituted nitrobenzene, hydroquinone, benzoquinone, and aliphatic acids can be detected by high-performance liquid chromatography. Further details are described in Figure S1. The obtained data are in satisfactory agreement with the mechanisms proposed in works (Dong et al., 2017; Jin et al., 2018; Wu et al., 2020), where the

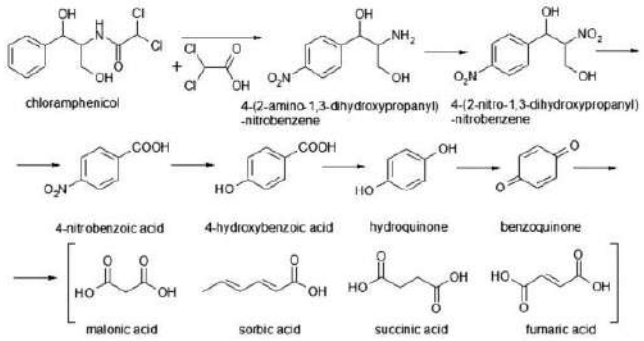

FIGURE 3 Probable scheme of chloramphenicol oxidation

photocatalytic decomposition of chloramphenicol was studied; and the work (Chen et al., 2015) devoted to the electrochemical oxidation of the compound involved on PbO_2 modified with aluminum.

Chemical destruction by oxidants of different nature in homogeneous and heterogeneous catalytic systems

We used the classical Fenton reaction to establish the basic regularities of chemical destruction of hazardous components of hospital effluents in heterogeneous catalytic systems. Iron ions were deliberately added into the solution in order to create a heterogeneous catalyst, because at neutral pH, iron hydroxide is formed in the solution.

A typical kinetic curve of the chemical interaction of selected compounds with Fenton's reagent is presented in Figure 4.

The obtained data showed that a relatively high oxidation rate (calculated rate constant was 0.1 min^{-1}), as in the case of a homogeneous system using hypochlorous acid, is observed for benzoquinone, that is, for simple organic compounds preoxidized to the prealiphatic stage, and in the reaction with more complex substances, especially halogenated, there is no drop in the concentration of organic compounds (4-chlorophenol). In some cases, there was a low process rate (chloramphenicol). In this case, the rate constant was 1.94×10^{-3} min^{-1}.

However, the main disadvantages of the used Fenton process were the formation of a large number of iron-containing sludge and very limited intervals of working pH values, as well as high sensitivity to the catalyst composition and low process rate due to problems with delivery of pollutants to the interfacial boundary.

Unlike hydrogen peroxide, the decomposition products of which are effective oxidants only in the presence of catalysts, the main advantage of using hypochlorous

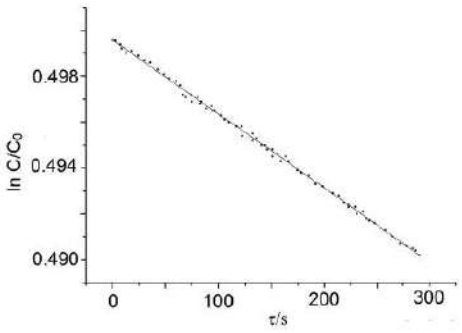

FIGURE 4 Logarithm of concentration versus time in heterogeneous catalytic chemical reaction between chloramphenicol and Fenton's reagent

acid is its own oxidative activity and combined action. On the one hand, as a strong oxidant, it can interact with hazardous chemicals, leading to their partial or complete destruction. On the other hand, hypochlorite show bactericidal, virulent, and fungicidal activity and are widely used for disinfection, which is an additional advantage for the treatment of hospital effluents (Yu et al., 2019). Additionally, the destruction of hypochlorous acid in the photocatalytic system under the action of light leads to the formation of oxygen-containing radicals (one of the options for the implementation of peroxene systems), which will contribute to the destruction of resistance genes in bacteria. In our studies, we synthesized hypochlorous acid electrochemically. The general regularities of chemical processes that take place in hypochlorous acid solutions are well studied (Yu et al., 2019), however, still has specificity depending on the structure of the substance with which the oxidant interacts.

The chemical reaction of chloramphenicol with hypochlorous acid synthesized during electrolysis was investigated. We selected several model compounds

TABLE 2 Interaction of model compounds (0.2 mM) with hypochlorous acid

Compound	Apparent heterogeneous rate constant k (10^2 min^{-1})
Chloramphenicol	1.38×10^{-2}
4-Chlorphenol	2.81
Benzoquinone	2.55

based on possible intermediates of oxidation of chloramphenicol. The obtained data are presented in Table 2.

Obviously, in this case, the process is realized in the solution bulk and is classified as a homogeneous chemical reaction. Because the process was carried out with an excess of oxidant, this reaction was satisfactorily described by a first-order kinetic equation for organic substance. In fact, the concentration of oxidant (hypochlorous acid) is part of the reaction constant of the pseudo-first order. As can be seen from the results obtained, the rate constant of a homogeneous chemical reaction depends on the nature of the substance, in particular on the number of groups and types of bonds, their ease of oxidation, and the concentration of the oxidant. In reactions of this type, it is customary to use a fixed amount of oxidant (stationary concentration) (Castagna et al., 2008). This is quite difficult to implement in classical reagent systems, such as the Fenton process, because one needs to constantly add reagents to the system, even with their initial excess. All this significantly complicates the practical implementation. In our case, the oxidant is constantly formed during electrolysis, so maintaining its steady-state concentration is not an obstacle. The obtained results showed a satisfactory reaction for benzoquinone and phenol derivatives, but the increase in the number of halogen atoms in the contaminant molecule led to a significant decrease in the process rate. That is, before carrying out a homogeneous chemical reaction, the dehalogenation of such compounds is desirable; this can be realized by a combination of direct electrochemical and secondary chemical destruction of hazardous components of hospital effluents. Despite the relatively low rates of chemical destruction, which is a disadvantage, the main advantage of such systems is the prolonged action of the oxidant even in the absence of electrolysis. Thus, even outside the equipment, the processes of neutralization of hazardous substances and disinfection of hospital effluents will be prolonged for some time.

We also studied the synthesis of hypochlorous acid from low concentrated chloride-containing electrolytes on various oxide materials at an anode current density of 50 mA cm^{-2}. The results are presented in Table 3.

TABLE 3 The effect of anode material on the synthesis of hypochlorous acid from sulfate solution (0.5-M Na_2SO_4), which additionally contained 0.05-M NaCl

	ClO^- concentration (10^3 M)				
	Electrolysis duration (min)				
Material	60	120	180	240	300
PbO_2	1.0	1.6	1.7	1.5	1.3
PbO_2–2 wt.% SDS	1.2	1.6	1.6	1.5	1.0

However, when trying to combine direct electrochemical and secondary chemical processes in one cell, we encountered several problems, which will be discussed below. For example, in the presence of chloride ions and an organic compound in the sulfate solution, the reaction on the electrode modified with surfactants does not occur.

Oxygen evolution reaction

It is believed that there are some deviations from the ideal stoichiometry of PbO_2, which is associated with the occurrence of a cationic disorder in the crystallographic structure, with vacancies of cations form the inner surfaces between the crystallographically ordered areas (Ruetschi & Giovanoli, 1991). Each missing Pb^{4+} ion will be compensated by Pb^{2+} and OH^- ions, and the chemical composition is described by the formula $Pb^{4+}_{(1-x-y)}Pb^{2+}_{y}O^{2-}_{(2-4x-2y)}OH^{-}_{(4x+2y)}$. Especially in the case of electrochemically deposited films, the coefficients x and y can have high values (Ruetschi, 1992).

Modification of lead(IV) oxide has a very strong effect on the properties of the material and depends on the places where these additives enter the oxide cell, as shown in our previous work (Shmychkova et al., 2016).

The rate of oxygen evolution can vary depending on the nature and amount of additive (Shmychkova et al., 2013). This change mainly depends on the chemical properties of the oxide surface, which in turn leads to a change in the bond strength of oxygen-containing particles chemisorbed on the electrode surface.

Pavlov et al. (2000) proposed a mechanism according to which the oxygen evolution occurs in the active centers located in the hydrated zone of PbO_2. It is believed that the OER is limited by the transfer of the second electron (electrochemical desorption) (Trasatti & Lodi, 1981) and depends on the bond strength of oxygen-containing particles chemisorbed on the surface. Thus, increasing the bond strength of chemisorbed oxygen will increase the OER overvoltage (Shmychkova et al., 2013).

According to the obtained results (Figure 5), the overvoltage of oxygen evolution on PbO_2–surfactant coatings deposited from methanesulfonate electrolytes decreases, as was observed in the case of bismuth (Shmychkova et al., 2013).

As can be concluded from the calculated results, the Tafel slope significantly exceeds the theoretical value, which indicates a decrease in the degree of filling of the electrode surface with oxygen-containing particles, probably due to blockage by sulfate ions when the investigation is performed in sulfate solution. In the presence of an organic compound and chloride ions in the solution, irreversible adsorption of an intermediate compound is observed, which leads to additional blocking of active centers on the oxide surface involved in the oxidation of organic substance and those involved in oxygen evolution. It is possible that these may be the same active centers.

It should be noted that the adsorption depends on the allotropic modification of the oxide, because the α and β phases of PbO_2 due to different configurations contain different amounts of adsorbed water. Thus, the α phase of PbO_2 contains a larger amount of adsorbed water (Amadelli et al., 1998). The high content of adsorbed water and hydroxyl groups in PbO_2–SDS was confirmed by X-ray photoelectron spectroscopy of the surface layer of the samples (Figure 6). The X-ray photoelectron spectrum of the unmodified sample was discussed in our previous (Shmychkova et al., 2016). It is necessary to investigate in more detail the O 1s region of lead dioxide-surfactant composite, as this will provide information on surface hydration (Amadelli et al., 1999).

In particular, modification of PbO_2 by bismuth leads to the accumulation of a large number of weakly bound to the surface oxygen-containing particles (adsorbed OH and water) (Shmychkova et al., 2013), whereas Ni leads to a strong accumulation of oxygen relative to the stoichiometry of PbO_2 (Shmychkova et al., 2016).

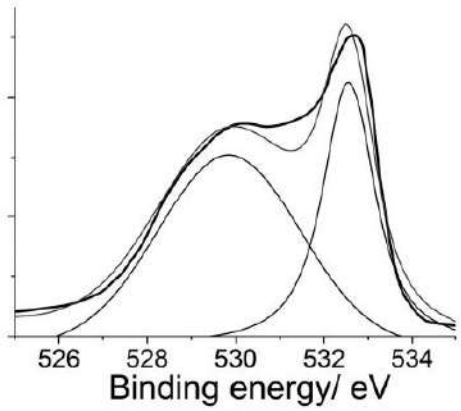

FIGURE 6 The simulated O 1s level of the X-ray photoelectron spectrum of the PbO_2–2 wt.% sodium dodecyl sulfate surface

Analysis of the O 1s region (see Figure 6) revealed peaks at 528.0 and 530.7 eV, which corresponds to the oxygen of the crystal lattice and hydroxylated particles, respectively. The intensity of the last peak is 1.4 times higher, but we cannot take into account the contamination of the surface with carbonates. This indicated the hydroxylation of the composite surface.

The obtained data are an indirect confirmation of the assumption that most of the active centers of the surface are blocked due to chemisorption of intermediates, as a result of which organic molecules are pushed out of the surface due to hydrophobic hydration in the presence of chloride ions in solution. In fact, it is a chemical reaction on the surface of the oxide.

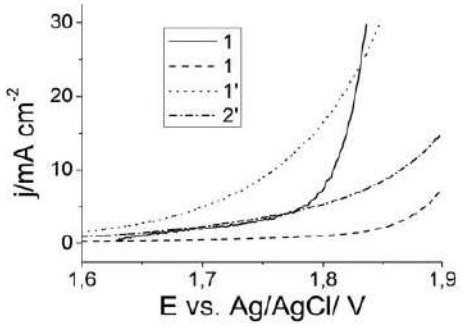

FIGURE 5 Steady-state polarization curves of oxygen evolution in 1-M $HClO_4$ (1 and 2) and sulfate solution, additionally containing 0.2-mM chloramphenicol and 3-g L^{-1} sodium chloride (1′ and 2′), where 1 is PbO_2 and 2 is PbO_2–2 wt.% SDS

CONCLUSIONS

Thus, it has been found that the process of electrochemical oxidation of chloramphenicol passes through the stage of formation of oxygen-containing radicals, which further in the electrochemical or chemical stage destroy individual functional groups or conjugated bonds of organic substances.

The properties of PbO_2–surfactant composites synthesized from methanesulfonate solutions were studied. It was found that the formed coating by 93.1% consists of α-phase PbO_2 in contrast to the similar one synthesized from nitrate electrolyte, which contains 73.3% β phase. However, the main effect on the phase composition in this case has the content of methanesulfonic acid in the

electrolyte of deposition, against which the effect of surfactant is not noticeable.

It is shown that the rate of chemical processes depends on the nature of the pollutant and in the case of nonhalogenated chemical compounds is practically not inferior to electrochemical destruction.

The electrocatalytic activity of the obtained composites in the OER was investigated. It was found that the Tafel slope significantly exceeds the theoretical value, which indicates a decrease in the degree of filling of the electrode surface with oxygen-containing particles, probably due to blockage by sulfate ions, when the investigation is performed in sulfate solution. In the presence of organic compound and chloride ions in the solution, irreversible adsorption of the intermediate is observed, which leads to additional blocking of active centers on the oxide surface, which are involved in the oxidation of organic substance and those involved in oxygen evolution.

ACKNOWLEDGMENT

This work was funded by the Ministry of Education and Science of Ukraine (Grant Number 0121U109529, 2021).

AUTHOR CONTRIBUTIONS

Olesia Shmychkova: Investigation; methodology; validation. **Svitlana Zahorulko:** Investigation. **Tatiana Luk'yanenko:** Conceptualization; data curation. **Alexander Velichenko:** Funding acquisition; project administration; resources; supervision.

CONFLICT OF INTERESTS

There are no conflicts of interest to declare.

ORCID

Olesia Shmychkova https://orcid.org/0000-0001-9490-9706

REFERENCES

Amadelli, R., Armelao, L., Tondello, E., Daolio, S., Fabrizio, M., Pagura, C., & Velichenko, A. (1999). A SIMS and XPS study about ions influence on electrodeposited PbO_2 films. *Applied Surface Science, 142*, 200–203. https://doi.org/10.1016/S0169-4332(98)00707-7

Amadelli, R., De Battisti, A., Girenko, D. V., Kovalyov, S. V., & Velichenko, A. B. (2000). Electrochemical oxidation of trans-3,-4-dihydroxycinnamic acid at PbO_2 electrodes: Direct electrolysis and ozone mediated reactions compared. *Electrochimica Acta, 46*(2–3), 341–347. https://doi.org/10.1016/S0013-4686(00)00590-9

Amadelli, R., Velichenko, A. B., Tondello, E., Armelao, L., Daolio, S., & Fabrizio, M. (1998). Ion bombardment of PbO_2 films: Water influence of cluster production. *International Journal of Mass Spectrometry, 179–180*, 309–317. https://doi.org/10.1016/S1387-3806(98)14142-8

Brillas, E. (2020). A review on the photoelectro-Fenton process as efficient electrochemical advanced oxidation for wastewater remediation. Treatment with UV light, sunlight, and coupling with conventional and other photo-assisted advanced technologies. *Chemosphere, 250*, 126198. https://doi.org/10.1016/j.chemosphere.2020.126198

Casellato, U., Cattarin, S., & Musiani, M. (2003). Preparation of porous PbO_2 electrodes by electrochemical deposition of composites. *Electrochimica Acta, 48*, 3991–3998. https://doi.org/10.1016/S0013-4686(03)00527-9

Castagna, R., Eiserich, J. P., Budamagunta, M. S., Stipa, P., Cross, C. E., Proietti, E., Voss, J. C., & Greci, L. (2008). Hydroxyl radical from the reaction between hypochlorite and hydrogen peroxide. *Atmospheric Environment, 42*, 6551–6554. https://doi.org/10.1016/j.atmosenv.2008.04.029

Chen, D., Xiong, F., Zhang, H., Ma, C., Cao, L., & Yang, J. (2020). Dimensional stable lead electrode modified by SDS for efficient degradation of bisphenol A. *ACS Omega, 5*(2), 1198–1205. https://doi.org/10.1021/acsomega.9b03571

Chen, J., Xia, Y., & Dai, Q. (2015). Electrochemical degradation of chloramphenicol with a novel Al doped PbO_2 electrode: Performance, kinetics and degradation mechanism. *Electrochimica Acta, 165*, 277–287. https://doi.org/10.1016/j.electacta.2015.02.029

Cotillas, S., Lacasa, E., Saez, C., Canizares, P., & Rodrigo, M. A. (2018). Electrolytic and electro-irradiated technologies for the removal of chloramphenicol in synthetic urine with diamond anodes. *Water Research, 128*, 383–392. https://doi.org/10.1016/j.watres.2017.10.072

Dong, H., Qiang, Z., Hu, J., & Qu, J. (2017). Degradation of chloramphenicol by UV/chlorine treatment: Kinetics, mechanism and enhanced formation of halonitromethanes. *Water Research, 121*, 178–185. https://doi.org/10.1016/j.watres.2017.05.030

Feng, L., van Hullebusch, E. D., Rodrigo, M. A., Esposito, G., & Oturan, M. A. (2013). Removal of residual anti-inflammatory and analgesic pharmaceuticals from aqueous systems by electrochemical advanced oxidation processes. A review. *Chemical Engineering Journal, 228*, 944–964. https://doi.org/10.1016/j.cej.2013.05.061

Ganiyu, S. O., Martinez-Huitle, C. A., & Rodrigo, M. A. (2020). Renewable energies driven electrochemical wastewater/soil decontamination technologies: A critical review of fundamental concepts and applications. *Applied Catalysis B: Environmental, 270*, 118857. https://doi.org/10.1016/j.apcatb.2020.118857

Herraiz-Carbone, M., Cotillas, S., Lacasa, E., Moratalla, A., Canizares, P., Rodrigo, M. A., & Saez, C. (2020). Improving the biodegradability of hospital urines polluted with chloramphenicol by the application of electrochemical oxidation. *Science of the Total Environment, 10*, 138430. https://doi.org/10.1016/j.scitotenv.2020.138430

Hu, Z., Cai, J., Song, G., Tian, Y., & Zhou, M. (2021). Anodic oxidation of organic pollutants: Anode fabrication, process hybrid and environmental applications. *Current Opinion in Electrochemistry, 26*, 100659. https://doi.org/10.1016/j.coelec.2020.100659

Jin, Q., Wang, H., Hu, C., Chen, Z., & Wang, X. (2018). Effects of NOM on the degradation of chloramphenicol by UV/H_2O_2 and the characteristics of degradation products. *Separation and Purification Technology*, *191*, 108–115. https://doi.org/10.1016/j.seppur.2017.09.014

Kolthoff, I. M., & Carr, E. M. (1953). Volumetric determination of persulfate in presence of organic substances. *Analytical Chemistry*, *25*(2), 298–301. https://doi.org/10.1021/AC60074A024

Li, X., Pletcher, D., & Walsh, F. C. (2011). Electrodeposited lead dioxide coatings. *Chemical Society Reviews*, *40*, 3879–3894. https://doi.org/10.1039/C0CS00213E

Li, X., Xu, H., & Yan, W. (2017). Effects of twelve sodium dodecyl sulfate (SDS) on electro-catalytic performance and stability of PbO_2 electrode. *Journal of Alloys and Compounds*, *718*, 386–395. https://doi.org/10.1016/j.jallcom.2017.05.147

Pavlov, D., Monahov, B., & Petrov, D. (2000). Influence of Ag as alloy additive on the oxygen evolution reaction on Pb/PbO_2 electrode. *Journal of Power Sources*, *85*, 59–62. https://doi.org/10.1016/S0378-7753(99)00383-3

Romero-Soto, I. C., Dia, O., Leyva-Soto, L. A., Drogui, P., Buelna, G., Diaz-Tenorio, L. M., Ulloa-Mercado, R. G., & Gortares-Moroyoqui, P. (2018). Degradation of chloramphenicol in synthetic and aquaculture wastewater using electrooxidation. *Journal of Environmental Quality*, *47*, 805–811. https://doi.org/10.2134/jeq2017.12.0475

Ruetschi, P. (1992). Influence of crystal structure and interparticle contact on the capacity of PbO_2 electrodes. *Journal of Electrochemical Society*, *139*, 1347–1351. https://doi.org/10.1149/1.2069410

Ruetschi, P., & Giovanoli, R. (1991). On the presence of OH^- ions, Pb^{2+} ions and cation vacancies in PbO_2. *Power Sources*, *13*, 81–97.

Salazar-Banda, G. R., Santos, G. O. S., Gonzaga, I. M. D., Doria, A. R., & Eguiluz, K. I. B. (2021). Developments in electrode materials for wastewater treatment. *Current Opinion in Electrochemistry*, *26*, 100663. https://doi.org/10.1016/j.coelec.2020.100663

Sanchez-Montes, I., Fuser, J. R., Neto, B., Silva, B. R., Silva, A. J., Aquino, J. M., & Rocha-Filho, R. C. (2018). Evolution of the antibacterial activity and oxidation intermediates during the electrochemical degradation of norfloxacin in a flow cell with a PTFE-doped β-PbO_2 anode: Critical comparison to a BDD anode. *Electrochimica Acta*, *284*, 260–270. https://doi.org/10.1016/j.electacta.2018.07.122

Shmychkova, O., Luk'yanenko, T., Amadelli, R., & Velichenko, A. (2016). Electrodeposition of Ni^{2+}-doped PbO_2 and physicochemical properties of the coating. *Journal of Electroanalytical Chemistry*, *774*, 88–94. https://doi.org/10.1016/j.jelechem.2016.05.017

Shmychkova, O., Luk'yanenko, T., Piletska, A., Velichenko, A., Gladyshevskii, R., Demchenko, P., & Amadelli, R. (2015). Electrocrystallization of lead dioxide: Influence of early stages of nucleation on phase composition. *Journal of Electroanalytical Chemistry*, *746*, 57–61. https://doi.org/10.1016/j.jelechem.2015.03.031

Shmychkova, O., Luk'yanenko, T., Velichenko, A., Meda, L., & Amadelli, R. (2013). Bi-doped PbO_2 anodes: Electrodeposition and physico-chemical properties. *Electrochimica Acta*, *111*, 332–338. https://doi.org/10.1016/j.electacta.2013.08.082

Shmychkova, O. B., Luk'yanenko, T. V., Amadelli, R., & Velichenko, A. B. (2014). PbO_2 anodes modified by cerium ions. *Protection of Metals and Physical Chemistry of Surfaces*, *50*(4), 493–499. https://doi.org/10.1134/S2070205114040169

Sun, Y., Li, P., Zheng, H., Zhao, C., Xiao, X., Xu, Y., Sun, W., Wu, H., & Ren, M. (2017). Electrochemical treatment of chloramphenicol using Ti-Sn/γ-Al_2O_3 particle electrodes with a three-dimensional reactor. *Chemical Engineering Journal*, *308*, 1233–1242. https://doi.org/10.1016/j.cej.2016.10.072

Trasatti, S., & Lodi, G. (1981). *Electrodes of conductive metallic oxides. Part B*. Amsterdam, The Netherlands: Elsevier.

Velichenko, A., Luk'yanenko, T., & Shmychkova, O. (2020). Lead dioxide-SDS composites: Design and properties. *Journal of Electroanalytical Chemistry*, *873*, 114412. https://doi.org/10.1016/j.jelechem.2020.114412

Velichenko, A., Luk'yanenko, T., Shmychkova, O., & Dmitrikova, L. (2020). Electrosynthesis and catalytic activity of PbO_2-fluorinated surfactant composites. *Journal of Chemical Technology and Biotechnology*, *95*(12), 3085–3092. https://doi.org/10.1002/jctb.6483

Velichenko, A. B., Amadelli, R., Gruzdeva, E. V., Luk'yanenko, T. V., & Danilov, F. I. (2009). Electrodeposition of lead dioxide from methanesulfonate solutions. *Journal of Power Sources*, *191*(1), 103–110. https://doi.org/10.1016/j.jpowsour.2008.10.054

Velichenko, A. B., & Devilliers, D. (2007). Electrodeposition of fluorine-doped lead dioxide. *Journal of Fluorine Chemistry*, *128*, 269–276. https://doi.org/10.1016/j.jfluchem.2006.11.010

Velichenko, A. B., Knysh, V. A., Luk'yanenko, T. V., Velichenko, Y. A., & Devilliers, D. (2012). Electrodeposition PbO_2–TiO_2 and PbO_2–ZrO_2 and its physicochemical properties. *Materials Chemistry and Physics*, *131*, 686–693. https://doi.org/10.1016/j.matchemphys.2011.10.035

Wu, M., Tang, Y., Liu, Q., Tan, Z., Wang, M., Xu, B., Xia, S., Mao, S., & Gao, N. (2020). Highly efficient chloramphenicol degradation by UV and UV/H_2O_2 processes based on LED light source. *Water Environment Research*, *92*(12), 2049–2059. https://doi.org/10.1002/wer.1365

Yu, W., Wen, Q., Yang, J., Xiao, K., Zhu, Y., Tao, S., Lv, Y., Liang, S., Fan, W., Zhu, S., Liu, B., Hou, H., & Hu, J. (2019). Unraveling oxidation behaviors for intracellular and extracellular from different oxidants (HOCl vs. H_2O_2) catalyzed by ferrous iron in waste activated sludge dewatering. *Water Research*, *148*, 60–69. https://doi.org/10.1016/j.watres.2018.10.033

Zhang, Y., Zhuang, Y., Geng, J., Ren, H., Xu, D., & Ding, L. (2016). Reduction of antibiotic resistance genes in municipal wastewater effluent by advanced oxidation processes. *Science of the Total Environment*, *550*, 184–191. https://doi.org/10.1016/j.scitotenv.2016.01.078

Zhou, J., Ma, F., Guo, H., & Su, D. (2020). Activate hydrogen peroxide for efficient tetracycline degradation via a facile assembled carbon-based composite: Synergism of powdered activated carbon and ferroferric oxide nanocatalyst. *Applied Catalisys B: Environmental*, *269*, 118784. https://doi.org/10.1016/j.apcatb.2020.118784

Zhou, X., Liu, S., Yu, H., Zhou, X., Liu, S., Yu, H., Xu, A., Li, J., Sun, X., Shen, J., Han, W., & Wang, L. (2018). Electrochemical

oxidation of pyrrole, pyrazole and tetrazole using a TiO_2 nanotubes based SnO_2-Sb/3D highly ordered macro-porous PbO_2 electrode. *Journal of Electroanalytical Chemistry*, *826*, 181–190. https://doi.org/10.1016/j.jelechem.2018.08.039

SUPPORTING INFORMATION

Additional supporting information may be found in the online version of the article at the publisher's website.

How to cite this article: Shmychkova, O., Zahorulko, S., Luk'yanenko, T., & Velichenko, A. (2021). Electrochemical oxidation of chloramphenicol with lead dioxide–surfactant composites. *Water Environment Research*, 1–11. https://doi.org/10.1002/wer.1628

Journal of The Electrochemical Society, 2021 **168** 086507
1945-7111/2021/168(8)/086507/8/$40.00 © 2021 The Electrochemical Society ("ECS"). Published on behalf of ECS by IOP Publishing Limited

Material Selection And Optimization Of Conditions For Electrooxidation Of Nitrofurazone: A Comparative Study Of Tin And Lead Dioxides

O. Shmychkova,[1,z] S. Zahorulko,[1] D. Girenko,[1] T. Luk'yanenko,[1] L. Dmitrikova,[2] and A. Velichenko[1]

[1]*Ukrainian State University of Chemical Technology, Dnipro, Ukraine*
[2]*Dnipro State Medical University, Dnipro, Ukraine*

The electrochemical oxidation of nitrofurazone with SnO_2, doped by platinum group metals, and pure PbO_2 has been investigated. The oxidation rate of nitrofurazone with PbO_2-anode is 5.3 times higher compared to doped SnO_2 anodes. It was found that the presence of 1; 2 and 3 g l^{-1} NaCl in electrolyte affects the efficiency of the electrooxidation process in the case of doped SnO_2 anodes, the oxidation rate of nitrofurazone increases by 2.3; 3.7; 5.8 times, respectively. Using of doped SnO_2 in chloride-containing media allows one to achieve the same rate of destruction of nitrofurazone as when using lead dioxide. Moreover, SnO_2 doped electrodes are characterized by the production of a large number of hypochlorous acid and have a higher service life compared to PbO_2 in such harsh conditions.
 [DOI: 10.1149/1945-7111/ac1e58]

Manuscript submitted February 25, 2021; revised manuscript received July 31, 2021. Published August 26, 2021.

Supplementary material for this article is available online

The problem of environmental pollution by pharmaceuticals has become acute in recent decades in both developed and developing countries.[1–5] Many different methods have been proposed for wastewater treatment containing drugs, pharmaceuticals and veterinary drugs, which can be classified into destructive (accompanied by the decomposition of pollutants) and non-destructive (without chemical conversion of pollutant). Among them there are traditional treatment methods: biological treatment, filtration and coagulation / flocculation / sedimentation processes, which are one of the most common in practice wastewater disinfection technologies, as well as more modern and advanced methods.[6] Various types of advanced oxidation processes (AOPs) are very effective for disposal and disinfection, although they are not able to provide complete cleaning and must be combined with other treatment methods.[7] In recent years, special attention has been paid to electrochemical methods of disinfection and disinfection of wastewater contaminated with pharmaceuticals.[8,9] Such processes are considered as an attractive alternative to other traditional methods due to the development of new and highly efficient electrode materials and the possibility of their flexible combination with relatively cheap renewable energy sources.[10–13] The last two factors are the main trends in the improvement of existing electrochemical methods of wastewater treatment containing pharmaceutical residues. In this context, the development of conditionally reagent-free electrochemical wastewater treatment methods containing pharmaceutical residues can be extremely effective and attractive.

It is recognized that the efficiency of electrooxidation of organic pollutants depends primarily on the anode material, the nature of the electrolyte, as well as the structure and composition of the toxicant.[14] It is believed[15] that the process of electrooxidation of organic compounds occurs via the mechanism where the secondary transfer of oxygen and adsorbed on the surface of the electrode or free hydroxyl radicals is preferred, rather than direct electron transfer from the compound to the anode. When choosing an electrode material for aqueous solutions, first of all, it is necessary to pay attention to their high mechanical and chemical stability, as well as satisfactory electrical conductivity. In most cases, the anode material must have a high oxygen evolution overvoltage in order to achieve the high selectivity to the target process. Unfortunately, the number of such materials is very limited. Materials based on lead dioxide are recognized as one of the most promising. Their advantage is low cost, manufacturability of creating an active layer, high electrical conductivity and corrosion resistance, especially when polarized at low and medium current densities. Lead dioxide can be relatively easily modified during its electrodeposition in order to improve the electrocatalytic activity and selectivity. Lead dioxide anodes are widely recognized material for electrooxidation of vast organic pollutants.[15,16] However, these electrodes are undergone to significant deterioration in chloride-containing media. In this work we tried to find an alternative material that would not be inferior to lead dioxide in terms of integral activity. Under these conditions, DSA® cannot be used, since in low-concentration chloride media they quickly reach the critical potential of destruction.[17] And materials containing metals of the platinum group or their oxides behave similarly and, as a rule, do not possess their own electrochemical activity in the oxidation of toxic organic substances.[18] The use of BDD results in high cell voltage.[5] In this regard, it is important to the material to have satisfactory stability, electrical conductivity, low cell voltage as well as high selectivity for the electrochemical generation of oxidants capable of effectively destroying contaminants in indirect oxidation. From this point of view, tin and lead dioxides are promising materials. Most of researchers avoid using materials with low oxygen evolution overvoltage in advanced oxidation processes. Nevertheless, there is a practical interest in anodic materials based on SnO_2, which is due to their high chemical resistance in both acidic and alkaline solutions and a fairly high electrocatalytic activity in oxygen transfer reactions.[19–21] An additional advantage is that in the presence of chloride ions in solution, such materials are able to create oxidizing agents that take part in secondary oxidation processes. Naked SnO_2 is a n-type semiconductor with a band gap of 3.6 eV. It is modified with various electron donors (antimony, fluorine, etc) in order to increase the electrical conductivity.[22–24] However, Sb doped SnO_2 undergoes passivation in sulfate and phosphate solutions and has high cell voltage. It is also promising to create composite coatings based on SnO_2 and platinum group metal oxides, which are semiconductors with large number of charge carriers.[25] Nevertheless, in terms of their own electrocatalytic activity in the processes of direct electrochemical oxidation, composites based on SnO_2 and Pt group metals are significantly inferior to lead dioxide and exhibit high electrocatalytic activity only in chloride-containing media. Yet, tin oxide-based materials, doped with Pd are interesting due to production of high hypochlorous acid amount.

Nitrofurazone was chosen as a model compound; this choice was convenient for us, since the main intermediate products of its

[z]E-mail: lesiandra08@gmail.com

destruction are known.[26] Some nitrofuran derivatives are synthetic chemotherapeutic agents with a broad antimicrobial spectrum. They are active against both Gram-positive and Gram-negative bacteria.[27] The drug is low-toxic; however, high concentrations can cause dyspeptic and neurotoxic effects. Accumulating in natural objects, it has a mutagenic and carcinogenic effect on the human body, which has been confirmed by animal studies.[28] Since the European Union has forbidden the administration of these compounds to food-producing animals[29] with the aim of avoiding harmful effects on human health due to their toxicity, mutagenic and carcinogenic ability, the main focus of researchers was to develop the appropriate technique for the quantification of trace levels of nitrofuran residues.[30] On the one hand, there are a lot of reports concerning the determination of nitrofurazone in different matrices by luminescence, fluorescence, Raman spectroscopy, high-performance liquid chromatography etc.[31] On the other hand, despite a large number of publications, several issues remain to be explained, since there are no reports on the electrooxidation of nitrofurazone, although the collection of electrochemical oxidation signal is more convenient. In addition, the organization of the oxidation process also remains unreported.

Experimental

All chemicals were reagent grade and were purchased from Sigma-Aldrich. Bidistilled tap water with electrolytic conductivity 1.6 μS cm^{-1} was used to prepare solutions.

Lead dioxide anodes were prepared according to the standard method described in a number of our publications[32–34] by electrodeposition of PbO_2 on a Ti/Pt current collector. Ti sheet was pre-machined, and then degreased in 5 M NaOH at room temperature; and then it was etched in 6 M HCl at 80 °C during 20 min.[32] Platinum layer was deposited catodically at 20 mA cm^{-2} and a temperature of 70 °C from the following electrolyte: 25 g l^{-1} K_2PtCl_6; 100 g l^{-1} $NaNO_2$; 10 cm^3 of ammonia solution.[35] Under these conditions, the current efficiency of platinum was about 30%. The surface platinum content was 2 mg cm^{-2}. The content of deposited platinum was monitored gravimetrically. A solution of the following composition, M: Pb $(CH_3SO_3)_2$–0.1; CH_3SO_3H–0.11 was used as the deposition electrolyte. In most cases, the coating was deposited at 4 mA cm^{-2} and 25 °C during 60 min.

SnO_2 coatings doped with Pt group metals were pyrolytically applied directly to the titanium surface. It should be noted, that there is a significant oxidation of the titanium surface in the process of forming the first oxide layers. Such process is especially active if the pyrolysis temperature is higher than 450 °C–500 °C. This reduces the adhesion to the surface and increases the transient resistance, which is due to the formation of an oxide layer on the surface of titanium. In this regard, before applying the base coat, 2 layers of TiO_2-PtO_x were applied. The intermediate coating solution was prepared by $TiCl_4$ and n-C_4H_9OH mixing in a ratio of 1:4. A solution of $H_2PtCl_6 \times 6H_2O$ in HCl was introduced into the obtained alcoholate. Heat treatment of the first layer was performed for 5 min, and the second for 10 min at a temperature of 400 °C–420 °C. As a base coat, a solution obtained by dissolving an equivalent amount of $SnCl_4$ in n-butanol (5 cm^3 of $SnCl_4$ under cooling in 15 cm^3 of n-C_4H_9OH) was used. Dopants (0.12 g of metallic Pt as $H_2PtCl_6 \times 6H_2O$, and 0.015 g of metallic Pd as $PdCl_2$) were pre-dissolved in HCl before adding to the electrolyte.

The precursor layers were applied with a brush, followed by drying at a temperature of 80 °C–90 °C for 10 min. This was followed by heat treatment in a muffle furnace for 5 min at a temperature of 400 °C–420 °C. After applying 7 layers, heat treatment was performed for 60 min at 500 °C–520 °C. Next, the anode was washed with bidistilled water in an ultrasonic washer, dried at a temperature of 80 °C–90 °C and was polarized in 0.3 M NaCl for 30 min at $j_a = 50$ mA cm^{-2} in order to remove the residues of precursors. The proposed original technique allows one to deposit the compact, homogeneous coatings with high adhesion to the titanium surface. Materials modified with platinum were dark gray, and with palladium they were black.

Anodes surface morphology was studied by scanning electron microscopy (SEM) with Tescan Vega 3 LMU with energy-dispersive X-ray microanalyzer Oxford Instruments Aztec ONE with X-Max^{N}20 detector. X-Ray powder diffraction (XRPD) data were collected in the transmission mode on a STOE STADI P diffractometer with Cu $K\alpha_1$-radiation, curved Ge (1 1 1) monochromator on primary beam, $2\theta/\omega$-scan, angular range for data collection 20.000–110.225 °2θ with increment 0.015, linear position sensitive detector with step of recording 0.480 °2θ and times per step 75–300 s, U = 40 kV, I = 35 mA, T = 298 K. A calibration procedure was performed utilizing SRM 640b (Si) and SRM 676 (Al_2O_3) NIST standards. Preliminary data processing and X-ray qualitative phase analysis were performed using STOE WinXPOW and PowderCell program packages. Crystal structures of the phases were refined by the Rietveld method with the program FullProf.2k, applying a pseudo-Voigt profile function and isotropic approximation for the atomic displacement parameters, together with quantitative phase analysis.

XPS studies were carried out on a PHI 5000 spectrometer using monochromatic AlKα radiation for excitation. The BE value of C (1s), due to adventitious carbon and residual solvent, is 284.8 (±0.3) eV.

Oxygen evolution reaction was investigated by steady-state polarization and impedance spectroscopy on computer controlled EG & G Princeton Applied Research potentiostat model 273 A and lock-in Amplifier model 5210 in different media (see in Results and Discussion).

Since in the case of using a sulfate solution at high anodic potentials on the surface of electrodes modified with platinum group ions, the formation of persulfates is possible,[36] a phosphate buffer was used as a supporting electrolyte. The electrooxidation of organic compounds was carried out in divided cell at $j_a = 50$ mA cm^{-2}. The volume of anolyte was 130 cm^3. Solution, containing phosphate buffer (0.25 M Na_2HPO_4 + 0.1 M KH_2PO_4) + 10^{-4} M organic compound, (pH = 6.55) was used as anolyte; phosphate buffer as catholyte. Stainless steel was used as cathode. Doped SnO_2 or PbO_2 electrodes were used as anodes. Electrode surface area was 2.5 cm^2.

The changing of the concentration of the organic substance during the electrolysis was measured by sampling (volume of 5 cm^3) at regular intervals and measuring the optical density of the solution in the ultraviolet and visible region (wavelength range 200–350 nm) using a Kontron Uvikon 940 spectrometer.

Analyses of the reaction products were conducted by high performance liquid chromatography (HPLC) using a Shimadzu RF-10A xL instrument equipped with an Ultraviolet SPD-20AV detector and a 30 cm Discovery® C18 column.

Results and Discussion

Morphology and physico-chemical properties of materials.— The morphology and physico-chemical properties of lead dioxide are described in our previous publications in detail.[14,34,35] SEM/EDAX experiments were performed to evaluate the amount and distribution of dopants in SnO_2 (see Fig. 1). As one can see, doped SnO_2 anode has a slightly porous developed surface. In the porous matrix, probably Pt, there are large well visible inclusions with a size of 20–40 μm. Palladium is distributed less evenly on the surface: the maximum concentration of palladium is observed in the protruding parts of the surface, and the minimum—in the depressions. Probably these inclusions are the PdO phase, the presence of which in the coating was proved by the X-ray diffraction method (Fig. 2). The parameter of the elementary cubic lattice of Pt is a = 3.9236 Å, the volume V = 60.402 Å^3.[37] The parameter of the elementary cubic lattice of Pd is a = 3.8903 Å, the volume V = 58.877 Å^3.[38] Since Pt and Pd are isostructural and have similar parameters, their reflexes are superimposed (merged). The closer the lattice parameters (a) are, the less noticeable the XRD reflexes become, which does not allow

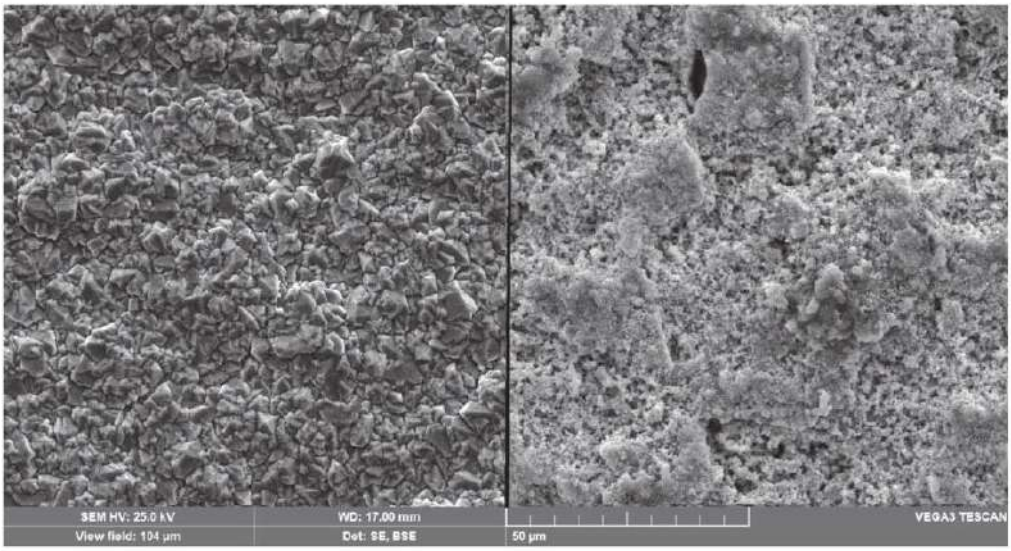

Figure 1. SEM micrographs of PbO_2 (left); SnO_2–8 at.% Pt-12 at.% Pd.

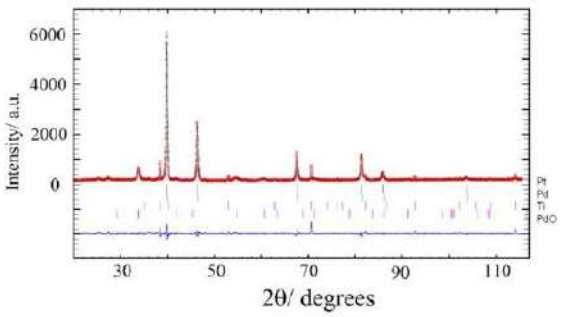

Figure 2. Observed and calculated X-ray powder profiles for doped SnO_2-electrode. Experimental data (circles) and calculated profile (solid line through the circles) are presented together with the calculated Bragg positions (vertical ticks) and difference curve (bottom solid line).

one to conclude that there are different phases. In our case, the surface content of palladium and platinum is sufficient to separate the reflexes, which allows one to identify the individual phases of platinum and palladium.[39]

According to EDAX analysis (Fig. S1 (available online at stacks.iop.org/JES/168/086507/mmedia)), platinum is evenly distributed on the surface. The distribution of Pd, Sn and Ti coincide with the distribution of oxygen, which indirectly confirms the presence on the surface of the oxides of these elements. This method also identified impurities of TiO_2 of rutile and anatase modifications.[40–42]

To get further insight into the effects of doping, we investigated the surface layers by X-ray photoelectron spectroscopy. The XPS spectra of PbO_2 have been discussed in detail in our previous publications.[43–45] Works on the XPS characterization of PbO_2[46] pointed out the importance of the examination of O1s region as it provides information on the hydration state of the surface. In particular Bi causes a very high hydroxylation with respect to PbO_2 stoichiometry.[46]

As one can see from the obtained photoelectron spectra of doped SnO_2 sample (Fig. 3), there is titanium on the surface, most likely in the form of oxide. Titanium appears on the surface as a result of thermal diffusion from the surface of titanium during heat treatment of the anode.

Some tin content is recorded in the surface layer. Tin alcoholate, which is used as the main precursor, is able to partially sublimate from the surface to thermal decomposition, without participating in the formation of the SnO_2 matrix. This is the main problem of obtaining reproducible coatings based on SnO_2.

The content of elements in the surface layer 4–5 nm thick was calculated for the obtained anodes. The surface ratio of Pt, Pd with the ratio of elements in precursors is quite close. Tin in the coating is present in a concentration of 6.7 at.%, and Ti in small quantities (3.8 at.%). The collected spectra show three peaks in the O 1 s region: the one at the lower binding energy was assigned to strongly bounded lattice oxygen of $PdO_x/PtO_x/SnO_x$, while the broader one at higher binding energy was attributed to weakly bound oxygen species: adsorbed OH^- at 531.2 eV and water at 533.8 eV,[45,46] that means interaction with water in outer regions (see Fig. 3, O 1s core level), since such binding energy is too high for the oxide-hydroxide compounds of metals.[47] The integrated area of O1s peaks assigned to labile oxygen-containing particles are significantly higher in this spectrum compared to peak of inert particles, which indicates a high surface content of water adsorbed on the active clusters in the amorphous zone of the oxide surface.[48] We assumed that palladium oxides are the main centers of water adsorption, and their presence in the coating contributes to the hydroxylation of the anode surface. Most likely, this property of palladium compounds provides its high electrocatalytic activity in the reaction of formation of hypochlorite, which involves oxygen-containing particles with low bond strength.

Electrocatalytic properties of materials.— *The oxygen evolution reaction.*—The next step of our work was to evaluate the electrocatalytic activity of materials in oxygen transfer reactions. It is now well recognized[49] that, in the direct electrolysis process, the oxidation of a large number of organic and inorganic compounds on different electrode materials, including PbO_2 and SnO_2, proceeds simultaneously with the evolution of oxygen. Highly oxidizing oxygen species, such as OH radicals, formed during the anodic oxidation of water are able, in turn, to oxidize most of organic compounds.

The rate of the oxygen evolution reaction can vary depending on the nature and amount of the dopant.[42,44,50] The change in the

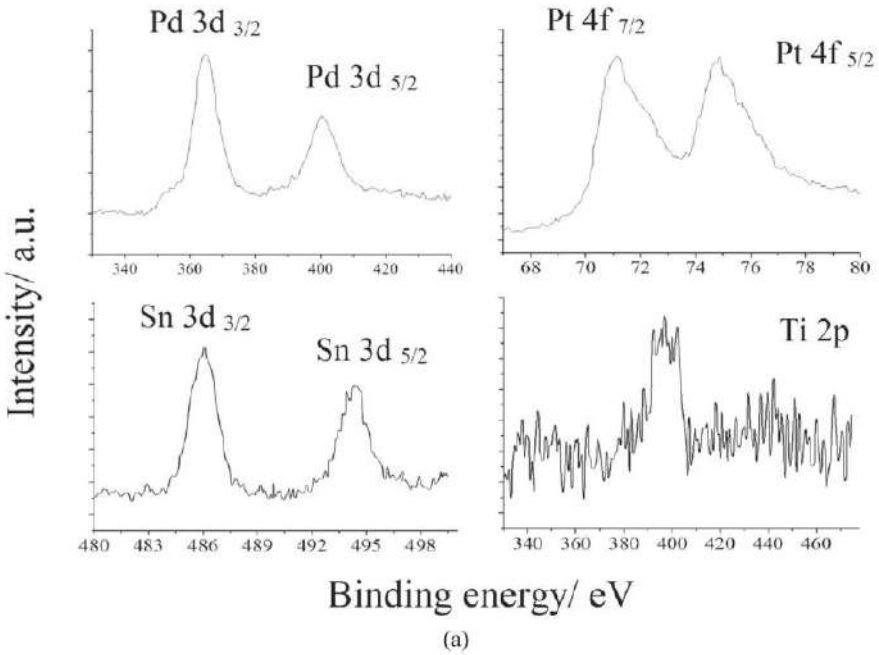

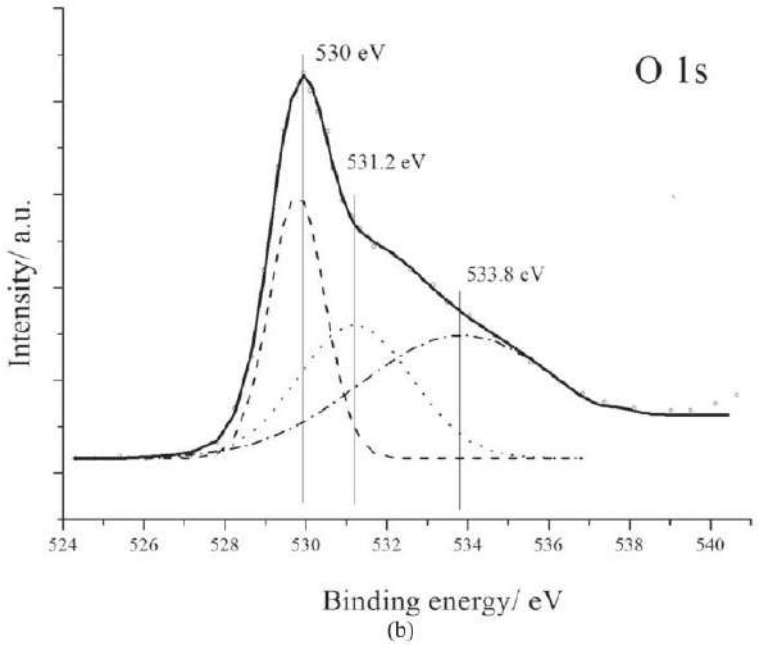

Figure 3. Pd 3d, Sn 3d, Pt 4f, Ti 2p core levels (a) and modeled O 1s level (b) structures in SnO_2–8 at.% Pt-12 at.% Pd.

properties of modified coatings in the oxygen evolution reaction mainly depends on the change in the chemical properties of the oxide surface, which in turn leads to a change in the bond strength of oxygen-containing particles chemisorbed on the electrode surface.

The regularities of the reaction of oxygen evolution on PbO_2 can be satisfactorily explained within the framework of the mechanism proposed by Pavlov et al.[51]

$$PbO\cdot(OH)_2 + H_2O \rightarrow PbO\cdot(OH)_2\ldots(OH^{\cdot}) + H^+ + e^- \quad [1]$$

$$PbO\cdot(OH)_2\ldots(OH^{\cdot}) \rightarrow PbO\cdot(OH)_2 + O + H^+ + e^- \quad [2]$$

$$2\,O \rightarrow O_2 \quad [3]$$

According to,[51] if the oxygen evolution reaction is limited by the second electron transfer stage (electrochemical desorption), an increase in the bond strength of chemisorbed oxygen will lead to an increase in the oxygen evolution overvoltage. Under conditions when the transfer of the first electron (electrochemical adsorption) is the limiting stage, the overvoltage of the oxygen evolution reaction will decrease.

Oxygen evolution was studied in buffer instead of perchloric acid in order to get further insight in simultaneous processes of oxygen evolution and oxidation of organic compound in the same media.

As one can see from obtained results (Fig. 4), the oxygen evolution potential on doped SnO_2 is significantly lower than on PbO_2. The value is 1.1 and 1.7 V for SnO_2 and PbO_2, respectively. All polarization curves are linear in semi-logarithmic coordinates, and have a tafel slope 110 mV for SnO_2 and 190 mV (in phosphate buffer) for PbO_2, respectively. Such a small slope for doped SnO_2 indicates a drop in transfer of the first electron in the formation of adsorbed oxygen-containing OH_{ads} particles. Obtained data are satisfactorily agreed with the results of photoelectron spectroscopy for the O 1 s region, where the strongly bounded lattice oxygen is high for tin dioxide-based materials.

Oxidation of nitrofurazone.—The initial spectrum of the nitrofurazone solution is characterized by two absorption maxima at 260 and 380 nm (Fig. 5).

Nitrofurazone shows rapid isomerization by the C-N double bond to the syn-form, with a shift of the main peak from 380 to 370 nm during electrooxidation. This phenomenon is consistent with the data of De Luca et al.,[52] which showed the presence of the syn-isomer in solution during the photolysis of nitrofurazone. Afterwards one can see a decrease in the optical density of absorption maxima, and the sequential formation of 5-nitro-2-furaldehyde 5-nitro-2-furoic acid as intermediate oxidation products at 310–320 nm after 5 h of electrolysis, which formation were detected by high performance liquid chromatography method (Fig. S2). These results coincide with the data obtained by Nakamura et al.[53] during aqueous chlorination of initial compound. It is interesting to note that the rate of destruction of 5-nitro-furaldehyde is significantly lower than the rate of destruction of 5-nitro-furoic acid. Further oxidation leads to the disappearance of peaks at 260 and 380 nm and the lack of absorption in the range of 310–320 nm, which indicates the complete conversion of nirtofurazone and aromatic products of its oxidation to aliphatic acids after 9 h of electrolysis.

Plot of concentration of the initial compound versus electrolysis time indicates the zero-order reaction (Fig. 5, inset) and considering the catalytic nature of the destruction of nitrofurazone. A heterogeneous rate constant of nitrofurazone destruction was calculated, the value of which is 1.92×10^{-7} mol l^{-1} min^{-1}.

On the opposite, spectral data showed that the complete conversion of nitrofurazone to aliphatic products at lead dioxide anodes occurs in approximately 2 h (Fig. 6).

The spectrum of initial solution is characterized by absorption maxima at 260 and 380 nm. A decrease in the optical density of the absorption and decolorization maxima was observed during electrolysis. In this case, the intermediate oxidation product 5-nitro-2-furoic acid does not accumulate, but is immediately oxidized.

The oxidation of nitrofurazone on PbO_2 anode can also be described by the kinetic equation of zero-order reaction, which indicates a significant role of the adsorption stage of the heterogeneous catalytic process. A heterogeneous rate constant of nitrofurazone destruction was calculated, the value of which is 1.02×10^{-6} mol l^{-1} min^{-1}.

As one can see, the rate oxidation of nitrofurazone on lead dioxide is 5.3 times higher than on Pt, Pd-doped SnO_2. It is obvious that the slow oxidation of the pollutant on SnO_2 anodes is associated with the accumulation of 5-nitro-2-furaldehyde, the destruction of which requires much more electrolysis time, in contrast to PbO_2 anodes, in which case the intermediate product is immediately oxidized.

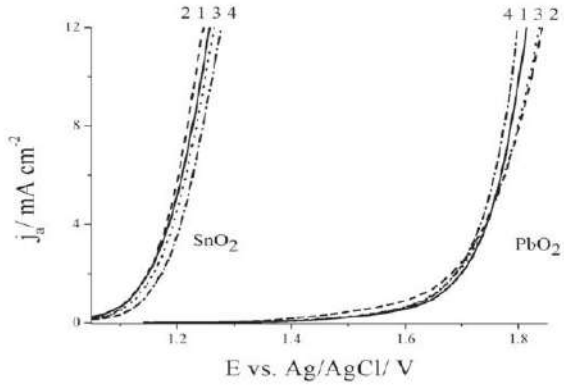

Figure 4. Steady state polarization curves of oxygen evolution in different media (Scan rate 1 mV s^{-1}, t = 25 °C) on doped SnO_2 and PbO_2-electrodes, where 1 was recorded in buffer solution; 2–in buffer with 3 g l^{-1} NaCl; 3–in buffer solution with 0.1 mM nitrofurazone; 4–in buffer solution with 0.1 mM nitrofurazone and 3 g l^{-1} NaCl. Coatings were deposited on Ti/Pt sheet.

According to results, obtained by UV-spectroscopy and high-performance liquid chromatography, we propose the probable mechanism of nitrofurazone electrooxidation (Fig. 7).

Oxidation of nitrofurazone in the presence of chloride-ions.—The presence of sodium chloride in hospital effluents is a positive aspect because it improves electrical conductivity and is involved in the generation of oxygen-containing chlorine compounds, such as ClO^-, HClO, formed during electrolysis and involved in chemical reactions of indirect oxidative destruction of nitrofurazone.

Initial spectra of nitrofurazone solutions with 1–3 g l^{-1} NaCl are characterized by absorption maxima at 260 and 380 nm (not shown). There is a decrease in the optical density of the absorption maxima, and the formation of 5-nitro-2-furaldehyde, as evidenced by the appearance of a peak at 320 nm. 3, 2 and 1.33 h are needed for maximum accumulation of 5-nitro-2-furaldehyde; 4, 2.5 and 1.67 h are needed for the disappearance of the peak at 380 nm, when 1; 2; and 3 g l^{-1} Cl^- are added to the initial solution, respectively. The disappearance of absorption maxima at 260, 320 nm after 7; 5 and 2.5 h, respectively, indicates the complete degradation of nitrofurazone.

The nature of the concentration versus time plot indicates the zero order of the reaction (Fig. 8).

Heterogeneous rate constants of nitrofurazone degradation in solutions with different concentrations of chloride ions were calculated, the data are shown in the Table I.

The SnO_2-based coating doped with both palladium (12 at.%) and platinum (8 at.%) is the optimal electrocatalyst for the synthesis of sodium hypochlorite.[54] Therefore, there is an acceleration of the rate of nitrofurazone destruction, due to the formation of hypochlorite and hypochlorous acid with increasing concentration of chloride ions in the solution.

The obtained results showed that the destruction time of nitrofurazone is 1.3 h on PbO_2 anodes, regardless of the amount of sodium chloride in the solution. The nature of the concentration versus time plot indicates the zero order of the reaction; the value of the heterogeneous rate constant in the presence of NaCl is 1.14×10^{-6} mol l^{-1} min^{-1}.

The processes of electrooxidation of nitrofurazone on lead dioxide anodes without and in the presence of 1–3 g l^{-1} NaCl are qualitatively the same. The oxidation rate of initial compound in the presence of NaCl is 1.12 times higher compared to pure buffer without chloride-ions. In addition, the rate of OCl^- generation remained constant under the experimental conditions. Most likely, hypochlorite is developed very slowly and does not significantly affect the rate of this reaction. Therefore, one can assume that the

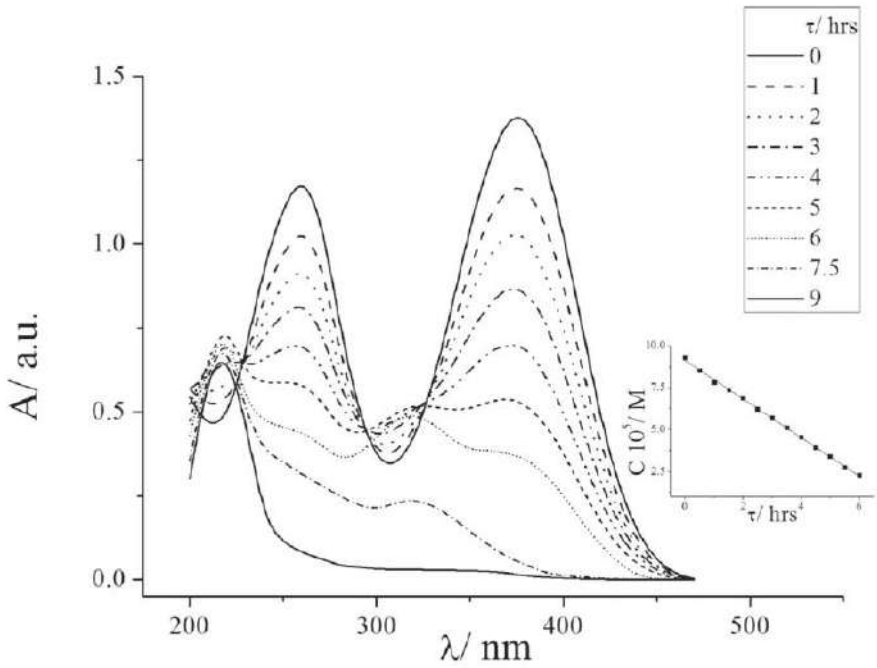

Figure 5. Electronic absorption spectra of solutions with 0.1 mM initial concentration of nitrofurazone during electrolysis on Pt, Pd-doped SnO_2 anode at 50 mA cm^{-2}. Inset: concentration of nitrofurazone versus electrolysis time.

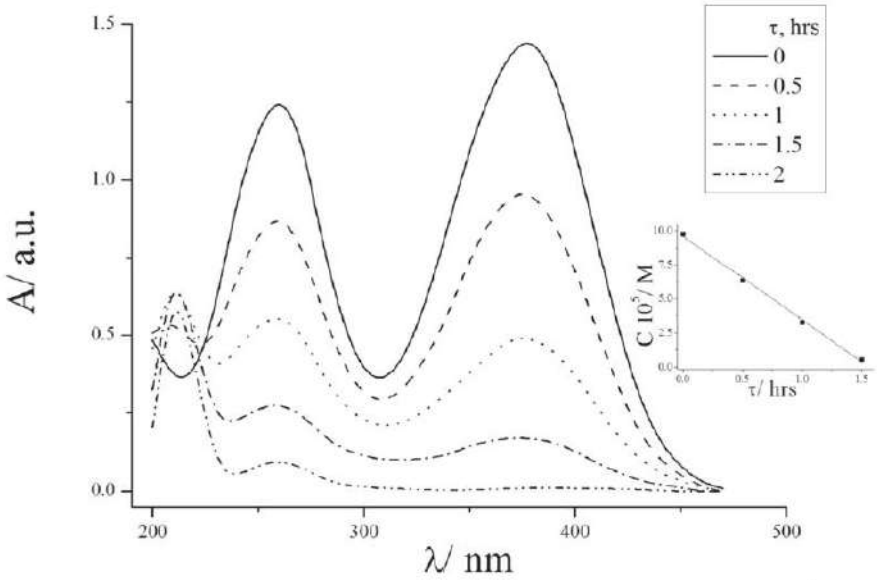

Figure 6. Electronic absorption spectra of 0.1 mM solutions of nitrofurazone during electrolysis on PbO_2 anode at 50 mA cm^{-2}.

presence of chloride ions in the solution does not significantly affect the rate of oxidation of nitrofurazone during the electrolysis on lead dioxide.

Analysis of the data obtained (see Fig. 4) shows that the oxygen evolution and the oxidation of organic compounds (in particular nitrofurazone) occur through the same type of intermediate oxygen-containing particles. There is a clear inhibition of oxygen evolution on SnO_2 in the presence of both organic compound and Cl^- ions in the solution. No one sees contribution from direct organic oxidation. Nitrofurazone is removed more efficiently on PbO_2 due to high number of oxygen-containing particles, strongly bounded to the oxide surface, which is typical for lead dioxide.[46,55]

It should be noted, that in the presence of 3 $g\,l^{-1}$ of chloride in the electrolyte, the largest amount of OCl^- involved in secondary oxidative processes is produced on doped SnO_2, which allows one to achieve the total rate of the process, the same as when using a PbO_2

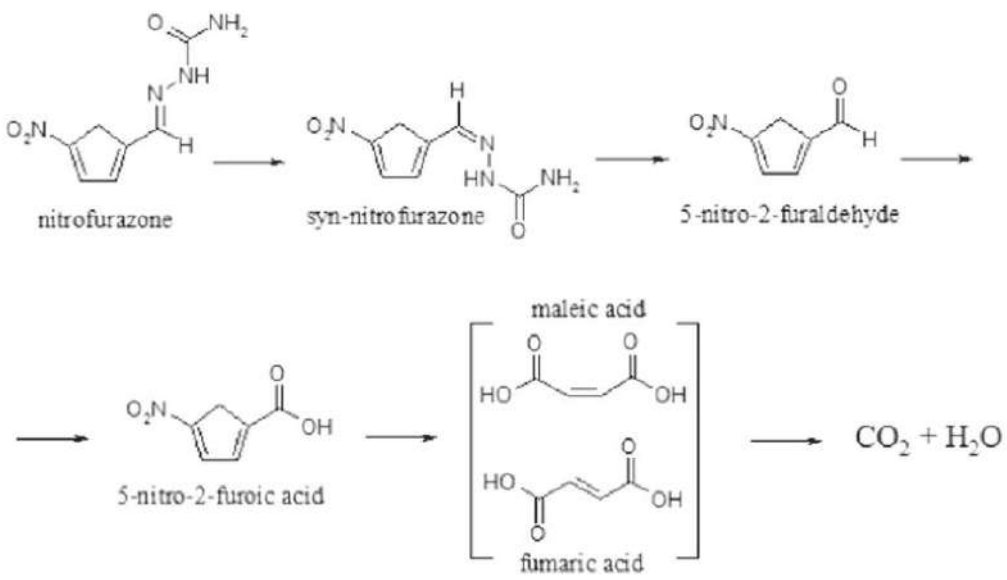

Figure 7. Scheme of electrooxidation pathway of nitrofurazone.

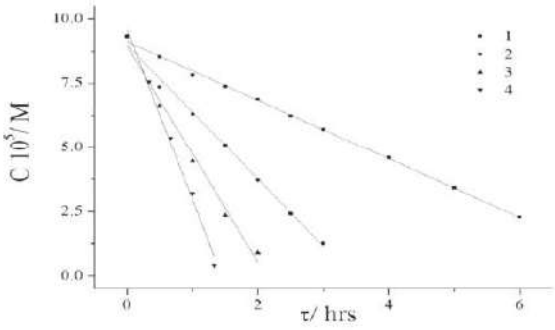

Figure 8. Concentration of nitrofurazone versus time of electrolysis in phosphate buffer in the presence of X g l^{-1} NaCl, where 1 is 0; 2–1; 3–2; 3–3.

Table I. Heterogeneous rate constants of nitrofurazone oxidation in the presence of chloride-ions in the solution.

C_{NaCl}, g l^{-1}	k × 10^7, mol l^{-1} min^{-1}
0	1.92
1	4.36
2	7.04
3	11.1

anode, which can be interesting in terms of using such materials for wastewater disinfection.

Conclusions

It was revealed that the oxidation rate of nitrofurazone with PbO_2-anode is 5.3 times higher compared to SnO_2 anodes doped with platinum group metals. In terms of their own electrocatalytic activity in the processes of direct electrochemical oxidation, composites based on SnO_2 and Pt group metals are significantly inferior to lead dioxide and exhibit high electrocatalytic activity only in chloride-containing media. It was found that the presence of 1; 2 and 3 g l^{-1} NaCl in electrolyte affects the efficiency of the electrooxidation process in the case of using doped SnO_2 anodes, the oxidation rate of nitrofurazone increases by 2.3; 3.7; 5.8 times, respectively. Whereas in the case lead dioxide anodes, the rate of destruction is almost unchanged, regardless of the number of chloride ions in solution.

According to the X-ray diffraction analysis results, palladium in the heat-treated electrocatalytic tin dioxide-based coating Ti/SnO_2-Pt-Pd is in the form of a PdO_x phase. X-ray photoelectron spectroscopy has shown that the surface of PdO_x has a high affinity for hydroxylation—adsorption of H_2O and OH^-, and their surface content is proportional to the concentration of palladium in the coating.

It has been shown that SnO_2 electrodes modified with platinum group metals in media containing chloride ions are characterized by the production of a large number of chloro- and oxygen-containing oxidants (hypochlorous acid) and have a higher service life compared to PbO_2, so the use of such materials in chlorine-containing wastewaters will allow not only direct electrooxidation of organic pollutants, but also disinfection simultaneously.

Funding

This work was supported by National Research Foundation of Ukraine [grant number 2020.01/0015, 2020].

ORCID

O. Shmychkova https://orcid.org/0000-0001-9490-9706
A. Velichenko https://orcid.org/0000-0003-1076-9991

References

1. L. Feng, E. D. van Hullebusch, M. A. Rodrigo, G. Esposito, and M. A. Oturan, *Chem. Eng. J.*, **228**, 944 (2013).
2. M. A. Oturan, *Curr. Opin. Solid State Mater. Sci.*, **25**, 100925 (2021).
3. C. A. Martinez-Huitle and M. Panizza, *Curr. Opin. Electrochem.*, **11**, 62 (2018).
4. C. A. Martinez-Huitle and E. Brillas, *Appl. Catal. B*, **87**, 105 (2009).
5. E. Brillas and C. A. Martinez-Huitle, *Appl. Catal. B*, **166–167**, 603 (2015).
6. S. O. Ganiyu, C. A. Martinez-Huitle, and M. A. Oturan, *Curr. Opin. Electrochem.*, **27**, 100678 (2021).
7. E. T. Anthony, M. O. Ojemaye, O. O. Okoh, and A. I. Okoh, *Environ. Pollut.*, **263**, 113791 (2020).
8. I. Sires and E. Brillas, *Curr. Opin. Electrochem.*, **40**, 212 (2021).

9. C. A. Martinez-Huitle and S. Ferro, *Chem. Soc. Rev.*, **35**, 1324 (2006).
10. S. O. Ganiyu, C. A. Martinez-Huitle, and M. A. Rodrigo, *Appl. Catal. B*, **270**, 118857 (2020).
11. Z. Hu, J. Cai, G. Song, Y. Tian, and M. Zhou, *Curr. Opin. Electrochem.*, **26**, 100659 (2021).
12. G. R. Salazar-Banda, G. O. S. Santos, I. M. D. Gonzaga, A. R. Doria, and K. I. B. Eguiluz, *Curr. Opin. Electrochem.*, **26**, 100663 (2021).
13. S. O. Ganiyu and C. A. Martinez-Huitle, *Curr. Opin. Electrochem.*, **22**, 211 (2021).
14. O. Shmychkova, T. Luk'yanenko, L. Dmirtikova, and A. Velichenko, *J. Serbian Chem. Soc.*, **84**, 187 (2019).
15. R. Vargas, C. Borras, D. Mendez, J. Mostany, and B. R. Scharifker, *J. Solid State Electrochem.*, **20**, 875 (2016).
16. X. Li, D. Pletcher, and F. C. Walsh, *Chem. Soc. Rev.*, **40**, 3879 (2011).
17. C. R. Costa, F. Montilla, E. Morallon, and P. Olivi, *J. Hazard. Mater.*, **180**, 429 (2010).
18. G. V. Fortunato, E. S. F. Cardoso, B. K. Martini, and G. Maia, *Chem. Electro. Chem.*, **7**, 1610 (2020).
19. P. Yao, X. Chen, H. Wu, and D. Wang, *Surf. Coat. Tech.*, **202**, 3850 (2008).
20. R. J. Watts, D. D. Finn, M. S. Wyeth, and A. L. Teel, *Water Environ. Res.*, **80**, 490 (2008).
21. F. Li, Q. Liu, J. Hu, J. Yang, and J. Ma, *J. Phys. D*, **53**, 353001 (2020).
22. J. E. L. Santos, D. C. de Moura, M. Cerro-Lopez, M. A. Quiroz, and C. A. Martinez-Huitle, *J. Electroanal. Chem.*, **873**, 114438 (2020).
23. N. Bravo-Yumi, P. Espinoza-Montero, A. Picos-Benitez, R. Navarro-Mendoza, E. Brillas, and J. M. Peralta-Hernandez, *Electrochim. Acta*, **358**, 136904 (2020).
24. G. O. S. Santos, A. R. Doria, V. M. Vasconcelos, C. Saez, M. A. Rodrigo, K. I. B. Eguiluz, and G. R. Salazar-Banda, *Chemosphere*, **259**, 127475 (2020).
25. M. G. Fernandez-Aguirre, R. Berenguer, S. Beaumont, M. Nuez, A. La Rosa-Toro, J. M. Peralta-Hernandez, and E. Morallon, *Electrochim. Acta*, **354**, 136686 (2020).
26. Y. Hou, G. Huan, S. Wang, Z. Yu, S. Qin, L. Tu, Y. Yan, X. Chen, H. Zhu, and Y. Tan, *J. Hazard. Mater.*, **384**, 121438 (2020).
27. T. Delatour, E. Gremaud, P. Mottier, J. Richoz, F. A. Vera, and R. H. Stadler, *J. Agric. Food Chem.*, **51**, 6371 (2003).
28. L. Charnaud, E. Jarde, A. Jaffrezic, M.-F. Thomas, and B. Le Bot, *J. Hazard. Mater.*, **361**, 169 (2019).
29. A. Guzman, L. Agui, M. Pedrero, P. Yanez-Sedeno, and J. M. Pingarron, *Electroanalysis*, **16**, 1763 (2004).
30. M. S. da Silva Juliao, E. C. Almeida, M. A. La Scalea, N. G. Ferreira, R. G. Compton, and S. H. P. Serrano, *Electroanalysis*, **17**, 269 (2005).
31. T. Gan, J. Li, L. Xu, Y. Yao, and Y. Liu, *J. Electroanal. Chem.*, **848**, 113287 (2019).
32. A. Velichenko, T. Luk'yanenko, and O. Shmychkova, *J. Energy Storage*, **30**, 101581 (2020).
33. V. Knysh, T. Luk'yanenko, O. Shmychkova, R. Amadelli, and A. Velichenko, *J. Solid State Electrochem.*, **21**, 537 (2017).
34. O. Shmychkova, T. Luk'yanenko, A. Piletska, A. Velichenko, R. Gladyshevskii, P. Demchenko, and R. Amadelli, *J. Electroanal. Chem.*, **746**, 57 (2015).
35. O. Shmychkova, T. Luk'yanenko, A. Yakubenko, R. Amadelli, and A. Velichenko, *Appl. Catal. B*, **162**, 346 (2015).
36. L. W. Matzek and K. E. Carter, *Chemosphere*, **151**, 178 (2016).
37. J. W. Arblaster, *Platinum Metals Rev.*, **41**, 12 (1997).
38. J. W. Arblaster, *Platinum Metals Rev.*, **56**, 181 (2012).
39. K. Sakurai and M. Mizusawa, *Anal. Chem.*, **82**, 3519 (2010).
40. D. A. H. Hanaor and C. C. Sorrell, *J. Mater. Sci.*, **46**, 855 (2011).
41. A. R. Khataee, H. Aleboyeh, and A. Aleboyeh, *J. Exp. Nanosci.*, **4**, 121 (2009).
42. E. J. Mittemeijer and P. Scardi, *Diffraction analysis of the microstructure of materials* 549(Springer, Berlin) (2004).
43. O. Shmychkova, T. Luk'yanenko, A. Velichenko, L. Meda, and R. Amadelli, *Electrochim. Acta*, **111**, 332 (2013).
44. O. Shmychkova, T. Luk'yanenko, A. Velichenko, and R. Amadelli, *J. Electroanal. Chem.*, **706**, 86 (2013).
45. O. Shmychkova, T. Luk'yanenko, R. Amadelli, and A. Velichenko, *J. Electroanal. Chem.*, **717–718**, 196 (2014).
46. R. Amadelli, L. Armelao, E. Tondello, S. Daolio, M. Fabrizio, C. Pagura, and A. Velichenko, *Appl. Surf. Sci.*, **142**, 200 (1999).
47. J. F. Moulder, W. F. Stickle, P. E. Sobol, and K. D. Bomben, *Handbook of X-ray Photoelectron Spectroscopy, Physical Electronics* (Perkin-Elmer Corporation) (Eden Prairie, Minnesota, USA) (1995).
48. P. Ruetschi and R. Giovanoli, *Power Sources*, **13**, 81 (1991).
49. S. Trasatti, *Electrochim. Acta*, **45**, 2377 (2000).
50. A. Velichenko, T. Luk'yanenko, N. Nikolenko, O. Shmychkova, P. Demchenko, and R. Gladyshevskii, *J. Electrochem. Soc.*, **167**, 063501 (2020).
51. D. Pavlov, B. Monahov, and D. Petrov, *J. Power Sources*, **85**, 59 (2000).
52. M. De Luca, S. Mas, G. Ioele, F. Oliverio, G. Ragno, and R. Tauler, *Int. J. Pharm.*, **386**, 99 (2010).
53. H. Nakamura, T. Kawakami, T. Niino, Y. Takahashi, and S. Onodera, *J. Toxicol. Sci.*, **33**, 621 (2008).
54. D. V. Girenko and A. B. Velichenko, *Surf. Eng. Appl. Electrochem.*, **54**, 88 (2018).
55. O. Shmychkova, T. Luk'yanenko, R. Amadelli, and A. Velichenko, *J. Electroanal. Chem.*, **774**, 88 (2016).

Research Article

Received: 4 August 2021 Revised: 13 October 2021 Accepted article published: 4 November 2021 Published online in Wiley Online Library:

(wileyonlinelibrary.com) DOI 10.1002/jctb.6973

Noble metals doped tin dioxide for sodium hypochlorite synthesis from low concentrated NaCl solutions

Olesia Shmychkova, Dmitry Girenko and Alexander Velichenko*

Abstract

BACKGROUND: Creation of anode materials with high selectivity to the target process is the main problem in low concentration sodium chloride (NaCl) solutions. A specificity of such solutions is the achievement of high potentials at which the anodes traditionally used for the synthesis of chlorine [rutile oxide/titania (RuO_2-TiO_2)] are destroyed. The main aim of the work concerns the eveluation of the effect of platinum (Pt) group metals in a tin oxide (SnO_2) matrix on the electrocatalytic activity and selectivity in reactions of the synthesis of sodium hypochlorite and chlorate (NaClO and $NaClO_3$) and oxygen (O_2) evolution.

RESULTS: It was revealed that palladium (Pd) in oxide Ti/SnO_2-Pd and Ti/SnO_2-Pt-Pd coatings existed in the PdO form, which has a high affinity for hydroxylation. Electrocatalytic activity of coatings in anode processes in low concentrated chloride-containing solutions would be determined by the bond strength of chemisorbed with the surface O-containing particles. Participation in the process of Cl^- oxidation of labile O-containing particles increased the rate of formation of NaClO and led to inhibition of adverse reactions of O_2 evolution and synthesis of chlorates and chlorites.

CONCLUSION: A correlation between the selectivity of formation of NaClO and $NaClO_3$, and the activity of the catalyst in the O_2 evolution reaction is proposed. Significant formation of chlorates occurred only at the anodes, where in 1 mol L^{-1} $HClO_4$ the O_2 evolution potential was >1.58 V. Parameters influencing the electrocatalytic activity and selectivity of electrode materials in the target process were proposed based on this dependence.

Keywords: tin dioxide; platinum group metals; sodium hypochlorite; oxygen-containing particles; binding energy

INTRODUCTION

Sodium hypochlorite (NaClO) solutions are known to exhibit high biocidal activity against many bacteria, most pathogenic fungi, viruses and protozoa.[1] Owing to these properties, NaClO solutions are used widely as antiseptic agents for external and local use, as well as for direct detoxification of the body when administered intravenously.[2] The use of NaClO solutions in medicine and veterinary medicine is possible only if a number of stringent requirements are met: (i) solutions must not contain dissolved chlorites, chlorates and perchlorates; (ii) solutions must have a pH in the range of 7.5–8.5; and (iii) solutions must have long stability without significant changes in composition and biological activity.

Solutions of NaClO used today, in the vast majority of cases, do not meet these requirements. For example, alkalis contained in a technical product obtained by classical technology, lead to the destruction of proteins, and chlorates and chlorites are highly toxic compounds for humans and animals. As a result, in recent years there has been a significant increase in attention to new electrochemical methods for the synthesis of high-purity NaClO solutions. The interest in hypochlorite obtained by this method is a result of the prospects of its use as an antiseptic and drug in medicine and veterinary medicine.

The main attention of researchers is focused on the development of oxide-metal and carbon (C) materials for electrochemical synthesis of NaClO solutions in stationary cells.[3] However, the proposed anodes, as well as DSA® are not suitable for use in low concentration sodium chloride (NaCl) solutions, where the current efficiency of the target process of NaClO formation is <100%. In neutral solutions, this leads to the rapid destruction of the anodes. In addition, the synthesis produces alkaline NaOCl solutions, which contain a significant number of impurities of chlorites and chlorates, so they are unsuitable for use in medicine and veterinary medicine. Materials such as oxides of cobalt (Co) and platinum (Pt),[4] obtained by classical sol–gel technology, do not have a high selectivity to the target product, so the resulting solutions are significantly contaminated with chlorates and chlorites. A similar problem is observed for lead oxide (PbO_2),[5] as well as different types of C anodes.[6–8] The current efficiency of NaClO in such systems in the electrolysis of low concentration solutions is relatively small. Anodes based on iridium oxide (IrO_2)[9,10] do not have the disadvantages outlined above, but their high cost, the imperfect sol–gel anode fabrication technology, and increasing chlorate content in the target product with increasing current density are significant barriers for application.

* Correspondence to: A Velichenko, 8, Gagarina Ave., Dnipro, Ukraine, 49005. E-mail: velichenko@ukr.net

Ukrainian State University of Chemical Technology, Dnipro, Ukraine

Researchers also are focusing on the development of promising anode materials for the electrolysis of low concentration NaCl solutions using IrO_2 and PbO_2 as electrocatalysts,[3,5,9,10] as well as on establishing the effect of current density on the current efficiency of the target product.

Anodic materials based on SnO_2 are known to have high chemical resistance in both acidic and alkaline solutions as well as high electrocatalytic activity in O transfer reactions.[11,12] Pure SnO_2 is a *n*-type semiconductor with a band gap of 3.6 eV that can be modified with various dopants (e.g. antimony, fluorine), which are electron donors, in order to increase its electrical conductivity.[13] It also is promising to create composite coatings based on SnO_2 and noble metal oxides.[14]

It is known[15] that doped SnO_2 has a high catalytic activity in O transfer reactions. The mechanism of O transfer reactions was proposed by Johnson *et al.*[16] In accordance with this mechanism, labile surface-bound O, which probably exists in the form of adsorbed hydroxyl radicals, takes part in electrocatalytic anodic reactions. Thus, it is possible to influence the electrocatalytic properties of anode materials in O transfer reactions by changing the surface concentration of active centers and the bond strength of adsorbed O-containing particles. Based on the aforementioned, it is necessary to have information about the Pt group metals into the matrix of SnO_2-TiO_2 on the electrocatalytic activity and selectivity in the reactions of the synthesis of hypochlorite, chlorate and O_2 evolution.

Usually, for different systems of this type, the selection of material occurs empirically and, therefore, when a number of parameters are changed, it is very difficult to foresee which material to choose. This paper presents comprehensive studies aimed at investigating the processes occurring in low concentration solutions, in order to make it possible to propose a correlation dependence for the directed production of anode materials with specified properties.

MATERIALS AND MTHODS

All chemicals were purchased from Sigma-Aldrich (ALSI, Kiev, Ukraine). Bidistilled water (H_2O) with an electrolytic conductivity of 1.6 μS cm^{-1} was used for the preparation of solutions.

Multilayer SnO_2 coatings modified with ruthenium (Ru), Pt and palladium (Pd) were pyrolytically applied directly to the Ti surface. In should be noted that there is a significant oxidation of the Ti surface in the process of forming the first oxide layers. This process is especially active if the pyrolysis temperature is >450–500 °C. This reduces the adhesion to the surface and increases the transient resistance, which is due to the formation of an oxide layer on the Ti surface.[17] In this regard, before applying the base coat two layers of TiO_2-PtO_x were applied. The intermediate coating solution was prepared by $TiCl_4$ and *n*-butyl alcohol (*n*-C_4H_9OH) mixing in a ratio of 1:4. A solution of chloroplatinic acid ($H_2PtCl_6 \times 6H_2O$) in HCl was introduced into the obtained alcoholate. Heat treatment of the first layer was performed for 5 min, and the second for 10 min at a temperature of 400–420 °C. Accuracy of the temperature setting is ±2 °C.

As a base coat, a solution obtained by dissolving an equivalent amount of $SnCl_4$ in *n*-butanol (5 cm^3 $SnCl_4$ under cooling in 15 cm^3 *n*-C_4H_9OH) was used. Dopants (0.12 g metallic Pt as $H_2PtCl_6 \times 6H_2O$, and 0.015 g metallic Pd as $PdCl_2$) were predissolved in HCl before being added to the electrolyte.

The precursor layers were applied with a brush, followed by drying at a temperature of 80–90 °C for 10 min. This was followed by heat treatment in a tube furnace for 5 min at 400–420 °C. After applying seven layers, heat treatment was performed for 60 min at 500–520 °C. Next, the anode was washed with bidistilled H_2O in an ultrasonic washer, dried at a temperature of 80–90 °C and polarized in 0.3 mol l^{-1} NaCl for 30 min at j_a = 50 mA cm^{-2} in order to remove the residues of the initial reagents. The proposed original technique allows one to deposit compact, homogeneous coatings with high adhesion to the Ti surface. Materials modified with Pt were dark gray and those with Pd were black.

All potentials were recorded and reported *versus* silver/potassium chloride [Ag/AgCl/KCl $_{(sat.)}$]. Each SnO_2-based anode modified simultaneously with Pt and Pd operated at 80 mA cm^{-2} for >1000 h without changing the catalytic activity or signs of corrosion failure.

The electrocatalytic activity of the obtained anodes in the hypochlorite synthesis reaction was evaluated under the following electrolysis conditions: 300 cm^3 of 0.15 mol L^{-1} NaCl solution in a cell without a diaphragm with a Ti cathode; the area of the cathode was varied so that the cathode current density was 40 mA cm^{-2}; stirring was performed with a compact electric stirrer; and the pH of the solutions was controlled. The pH was maintained in the range 7.5–8.5 during the electrolysis in a diaphragmless flow electrochemical system. In this case, the formation of hydrogen ions (H^+) in the anode processes was largely compensated by the formation of hydroxide ions (OH^-) at the cathode. At operating pH the resulting solution consists of a mixture of hypochlorous acid (HOCl) and hypochlorite ions (ClO–).

The current efficiencies (%) of ClO and chlorate were calculated according to the following Eqns (1) and (2):

$$CE(ClO^-) = \frac{2 \cdot 60 \cdot F \cdot V \cdot C(NaClO)}{M(NaClO) \cdot I \cdot t} 100\%, \quad (1)$$

where $C(ClO^-)$ is the concentration of NaClO in solution (g L^{-1}), *t* is the duration of electrolysis (min), V is the electrolyte volume (L), $F = 26.8$ A h, $M(ClO) = 74.5$ g mol^{-1} and *I* is the electrolysis current (A).

$$CE(NaClO3) = \frac{6 \cdot 60 \cdot F \cdot V \cdot C(NaClO_3)}{M(NaClO_3) \cdot I \cdot t} 100\%, \quad (2)$$

where $C(NaClO_3)$ is the concentration of $NaClO_3$ in solution (g L^{-1}) and $M(NaClO_3)$ = 106.5 g mol^{-1}. A proper experimental error is ±0.15%; the error at the current setting was ±1 mA cm^{-2}.

Determination of hypochlorite content was performed according to the following method: 10 cm^3 of 1 mol L^{-1} acetic acid solution, 2 cm^3 test solution and 5 cm^3 of 10% potassium iodide (KI) solution were added sequentially to a 250-cm^3 titration flask. The solution was stirred, covered with a watch glass and kept in a dark place for 5 min. The iodine released as a result of the reaction was rapidly titrated with 0.002 mol L^{-1} sodium thiosulfate solution to a straw color, 1 cm^3 of 0.5% starch solution as an indicator was added and the titration continued until the blue color of the iodine–starch complex disappeared and the solution discolored. The measurements were repeated at least three times. The content of NaClO in mg L^{-1}, was calculated using Eqn (3):

$$C(ClO^-) = \frac{[V_1 \cdot K \cdot C(Na_2S_2O_3)] \cdot M(1/2NaClO) \cdot 10^3}{V_{sample}}, \quad (3)$$

where V_1 is the volume of sodium thiosulfate ($Na_2S_2O_3$) solution spent on titration of NaClO (cm^3), M (1/2 NaClO) = 37.25 g mol^{-1}, C

($Na_2S_2O_3$) is the concentration of sodium thiosulfate, K is the correction factor for the concentration of sodium thiosulfate and V_{sample} is the volume of the sample used for analysis (2 cm^3).Determination of the $NaClO_3$ content was performed according to a method described previously.[18] It should be noted that chlorites were not detected in NaClO solutions due to the rapid reaction of chlorite oxidation to chlorate in the presence of excess hypochlorite.

The anode surface morphology was studied by scanning electron microscopy (SEM) with a Vega 3 LMU (Tescan, Brno, Czech Republic) with the energy-dispersive X-ray spectroscopy (EDAX) microanalyzer Aztec ONE (Oxford Instruments, Abingdon, UK) with X-Max^{N}20 detector. X-ray powder diffraction (XRPD) data were collected in the transmission mode on a STADI P diffractometer (STOE, Darmstadt, Germany) with Cu $K\alpha_1$-radiation, using a curved Ge (1 1 1) monochromator on primary beam, $2\theta/\omega$-scan, with angular range for data collection 20.000–110.225 °2θ with increment 0.015, linear position sensitive detector with step of recording 0.480 °2θ and times per step 75–300 s; U = 40 kV, I = 35 mA, T = 298 K. A calibration procedure was performed utilizing SRM 640b (Si) and SRM 676 (Al_2O_3) NIST standards. Preliminary data processing and X-ray qualitative phase analysis were performed using STOE WinXPOW and PowderCell program packages. Crystal structures of the phases were refined by the Rietveld method with the program FullProf.2k, applying a pseudo-Voigt profile function and isotropic approximation for the atomic displacement parameters, together with quantitative phase analysis.

X-ray photon spectroscopy (XPS) studies were carried out on a PHI 5000 spectrometer (Ulvac-Phi, Inc., Kanagawa, Japan) using monochromatic AlKα radiation for excitation. The BE value of C(1s), due to adventitious C and residual solvent, was 284.8 (±0.3) eV.

The O_2 evolution reaction was investigated by steady-state polarization on a computer controlled EG & G potentiostat model 273A (Princeton Applied Research, Oak Ridge, TN, USA) in different electrolytes depending on the purposes of experiment.

All of the experiments were repeated at least twice in order to achieve satisfactory reproducibility. All instruments had normalized metrological characteristics and were calibrated. The data for the linearized plots were processed using the least squares method, which requires that the sum of the squared deviations of the experimental points from the curve be the smallest. For straight lines, equations were found from which constants were determined. Reliable data were considered for which the correlation factor was >0.99. Calibration plots were processed by a data processing program for calibration plots. The results were processed using methods of mathematical statistics in order to determine the required number of measurements and assess the reliability of the obtained experimental data. The reliability of the results and the validity of the conclusions were confirmed by the integrated use of a set of modern techniques and by reproducibility of experimental data.

The accuracy of the XPS method was ±0.5%, and that for XRD and EDAX was ±1%. The experimental error at the electrochemical parameters used was ±10%.

RESULTS AND DISCUSSION

Morphology and phase content of composites

The surfaces of Ti/SnO_2 anodes doped with Pt group metals were studied using XPS, XRD, EDAX and SEM. The content of doping elements on the surface of electrodes involved was determined by XPS and reported in at.%. (Table 1). Titanium, most likely in the form of oxide, was on the surface of all investigated samples, as a result of thermal diffusion from the surface of the Ti during heat treatment of the anode. In some samples, at least a minimum Sn content was recorded in the surface layer. Tin alcoholate, which is used as the main precursor, was able to partially sublimate from the surface before thermal decomposition, without participating in the formation of the SnO_2 matrix, a process that is recognized as the main problem of obtaining reproducible SnO_2-based coatings. The catalytic activity of SnO_2-based composites doped with Pt and Pd simultaneously does not depend on the concentration of doping elements in the range of 5–10 Pt and 5–15 Pd, which allows one to obtain anodes with reproducible properties by pyrolysis. It was established that the coating has good adhesion and corrosion resistance at an anode current density of ≤80 mA cm^{-2} with a total content of doping elements of ≤20–25 at.%/.

Based on the analysis of the obtained XPS spectra, the content of elements in the surface layer (4–5-nm-thick) was calculated for the anodes involved. The compositions of the coating solutions and the content of doping elements are in good agreement. The surface ratio of Pt, Pd and Ru with the ratio of elements in the precursors was quite close. However, the content of Sn in the form of SnO_2 in the obtained coatings varied from 0.2 to 32 at.%. These data are consistent with EDAX and XRD analysis data. As will be shown later only on the sample of the anode Ti/SnO_2–9 (at.%) Pt–4 (at.%)Ru, was a phase of SnO_2 detected, indicating its quite large content in the coating; according to XPS data the surface is 32 Sn (see Table 1).

The SEM images obtained at the Ti/SnO_2–19.5 Pd anode clearly show the layered structure of the oxide coating, which is a consequence of the layer-by-layer application of the precursor with intermediate short-term heat treatment [Fig. 1(a)]. The coating had a network of microcracks and the morphology of the surface had not changed after long-term anodic polarization in 0.15 mol L^{-1} NaCl at 40–60 mA cm^{-2}. EDAX data showed a close distribution of elements on the surface. Palladium was fairly evenly distributed on the surface of the anode. Since Pt and Pd are isostructural and have similar parameters, their reflexes are merged. The surface contents of Pd and Pt were sufficient to separate their reflexes in the coatings involved, which allows one to identify the individual phases of platinum and palladium.[19] XRD analysis data indicate the presence in the coating bulk of the PdO (28.6%) and Pd (14.3%) phases. EDAX analysis showed the presence of Ti on the surface, and XRD analysis indicates the presence of TiO_2 in the modification of rutile.

Figure 1(b) shows the SEM data for Ti/SnO_2–19 Pt. The sample had a porous developed surface; O on the surface was ≈33 at.%, but its distribution, as well as that of Ti (19 at.%) was not so uniform according to EDAX data. According to the XRD data, no PtO_x phase was detected in the coating, but a Pt metal phase was found.

The surface of Ti/SnO_2–4 Pt–9 Ru is covered with a network of microcracks, with a layered structure visible (Fig. 2(a)). On the surface are 12 (32%) Sn and 66 (55%, in the bulk) O. The distribution of the elements Sn, Ru and O on the surface was almost the same. This probably indicates the presence of phase oxides of SnO_x and RuO_x. As with the previous anode, the surface distribution of Pt was uniform and did not coincide with the distribution of O. This may indicate that Pt was present mainly in the form of metal particles coated with a layer of phase oxides, which were not registered owing to their small total amount. According to XRD data, SnO_2 phase and Pt metal were present in the coating (Fig. 3). The RuO_2 phase was not recorded owing to the low content in the coating.

Figure 2(b) shows the SEM image for anode doped simultaneously with Pt and Pd. The sample, as for SnO_2–19 Pt, has a

Table 1. Content (at.%) of elements in the active surface of the anodes

Material	O 1s	Ti 2p	Sn 3d5	Pt 4f	Pd 3d	Ru 3d	Layers applied
Ti/SnO_2–2 Ru	60.0	0.3	38.4			2	5
Ti/SnO_2–19 Pt	66.2	12.8	2.3	18.7			5
Ti/SnO_2–9 Pt–4 Ru	54,8	0.0	32.3	9.30		3.6	5
Ti/SnO_2–13 Pt–Ru	77.4	6.3	2.7	12.6		1.0	5
Ti/SnO_2–18 Pt–14 Ru	59.0	7.2	1.3	18.0		14.4	5
Ti/SnO_2–7 Pt–4 Pd	68.3	17.4	3. 6	7.2	3.6		5
Ti/SnO_2–7 Pt–11 Ru–3 Pd	59.7	8.0	2.4	15.8	3.2	10.9	5
Ti/SnO_2–9 Pt–5 Pd	71.2	14.9	0.4	8.8	4.8		6
Ti/SnO_2–4 Pt–10 Pd	71.4	11.8	2.2	4.8	9.8		6
Ti/SnO_2–8 Pt–12 Pd	69.7	3.8	6.7	7.9	12		7
Ti/SnO_2–2.5 Pt	74.0	22.3	1.2	2.5			7
Ti/SnO_2–1 Pt	76.6	22.2	0.4	0.9			10
Ti/SnO_2–5 Pt–10 Pd	71.6	12.9	1.1	5.0	9.59		10
Ti/SnO_2–4 Pt	72.9	23.2	0.2	3.7			10
Ti/SnO_2–3 Pt–5 Pd	72.1	17.1	2.7	2.9	5.2		10
Ti/SnO_2–19.5 Pd	73.1	0.00	7.3		19.5		10
Ti/SnO_2–5 Pt–7 Pd	71.4	13.9	3.1	4.9	6.6		10
Ti/SnO_2–3 Pt–4 Pd	74.6	14.9	3.2	3.3	4,0		5
Ti/SnO_2–8 Pt–9 Pd	67.6	5.9	9.7	7.9	9.0		10
Ti/SnO_2–3 Pt–13 Pd	66.3	0.5	17.3	3.2	12.7		5

porous developed surface. There are large inclusions with a size of 20–40 μm in the porous matrix, probably Pt. If Pt, according to the EDAX data, was distributed on a surface rather evenly, Pd was concentrated on the protruding sites. On a sample with a surface content of 10 Pd (not shown), these inclusions were well visible, and the porosity of such a coating was significantly less. Probably these inclusions were the PdO phase, the presence of which in the coating was proven by XRD analysis (Figs 4 and 5). The distribution of Pd, Sn and Ti were consistent with the distribution of O, which indirectly confirms the presence on the surface of the oxides of these elements. The XRD method in both samples also identified impurities of TiO_2 modification of rutile and anatase.[20-22] Thus, this series of anodes can more correctly conventionally be denoted as Ti/SnO_2-Pt-PdO.

XPS characterization of surface

In order to get further insight into the effects of doping, we investigated the surface layers by XPS. As has been shown previously,[23] the position of the O 1s XPS signal is a good indicator of the nature of chemisorbed O-containing particles on PbO_2. In the present case, the binding energy of oxygen in SnO_2 (530.3 eV) was slightly different from the binding energy of the inert (strongly bounded) adsorbed O-containing particles (530.6 eV[24]), whereas the binding energy of the labile O (530.2 eV[24]), as well as OH^- groups and H_2O molecules 531.0–533.0 eV[25] was much higher. Such large differences in binding energies allowed the experimental detection of labile chemisorbed O-containing particles on the SnO_2 surface. Herein, we paid special attention to the interpretation of the signal in the O 1s region, because O-containing particles adsorbed

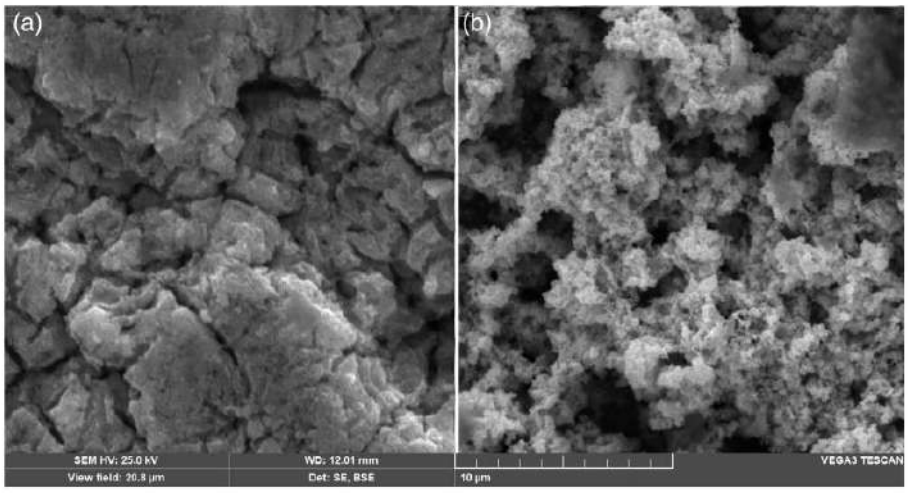

Figure 1. SEM micrographs of Ti/SnO_2–19.5 Pd (a) and Ti/SnO_2–19 Pt (b) electrodes after 100 min anodic polarization.

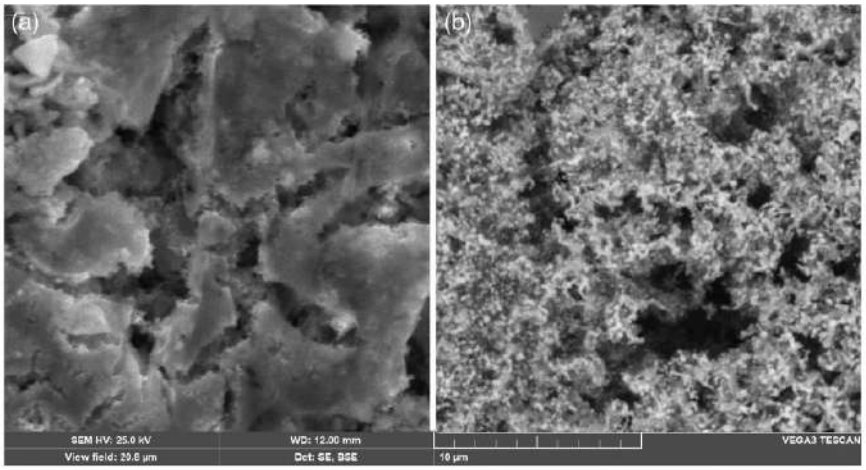

Figure 2. SEM micrographs of Ti/SnO_2–4 Pt–9 Ru (a) and Ti/SnO_2–10 Pt–6 Pd (b) electrodes as prepared.

on the electrode surface affect the electrocatalytic activity and selectivity of the coating to the target process. Figures 6 and 7 show some core levels of XPS spectra of Ti/SnO_2–8 Pt–12 Pd, Ti/SnO_2–3 Pt–13 Pd and Ti/SnO_2–10 Pt–6 Pd anode surfaces. The Sn 3d core level of XPS spectra [see Fig. 6(b) for example] show the reported Sn $3d_{3/2}$ and Sn $3d_{5/2}$ binding energies and peak separation of ~8 eV, which can be assigned to Sn(IV).[26,27] Tin in the coating is present in appreciable concentrations from 2.2 to 17.7 at.%, and Ti is present in small quantities. The binding energy of the Pd peak [336.8 eV, see Fig. 6(c)] corresponded to Pd in PdO.[25] The Pt core level [Fig. 6(d)] demonstrated Pt $4f_{7/2}$ at 71.2 eV and Pt $4f_{5/2}$ with $\Delta = 3.33$ eV peak separation, that can be assigned to metallic Pt.[25] The width of O 1S peak (531.0 eV) indicates the superposition of three signals: i) the high one with an energy of 530.3 eV; and low ones ii) with an energy of 531.3 and iii) 534.2 eV [see Fig. 6(a)]. The presence of maxima at 531.3 and 534.2 eV, which corresponds to the presence of adsorbed OH and H_2O on the surface, respectively, was not associated with the previous anodic polarization of the Ti/SnO_2-Pt-Pd anode in NaCl solution. For example, although the electrode Ti/SnO_2–3 Pt–13 Pd after finishing heat treatment at 500 °C did not come into contact with H_2O and aqueous solutions, it had the well-marked maximum of 534.2 eV O_2 adsorbed from the air. This indicates a high affinity of PdO for hydroxylation of the surface.

In the spectrum of Ti/SnO_2–3 Pt–13 Pd [see Fig. 7(a)] peak O1s (531.0 eV) also was a superposition of three signals with an energy of 530.6 eV (binding energy of oxygen in SnO_2[25]) and low ones with an energy of 531.9 and 534.2 eV. Maxima at 531.9 and 534.2 eV correspond to the presence of adsorbed OH and H_2O on the surface, respectively. A similar picture was observed in the case of Ti/SnO_2–10 Pt–6 Pd [see Fig. 7(b)]; however, the peak of inert O-containing particles (529.9 eV) was shifted towards lower binding energies, but it also can be assigned to O in the oxide crystal lattice (528–531 eV[25]).

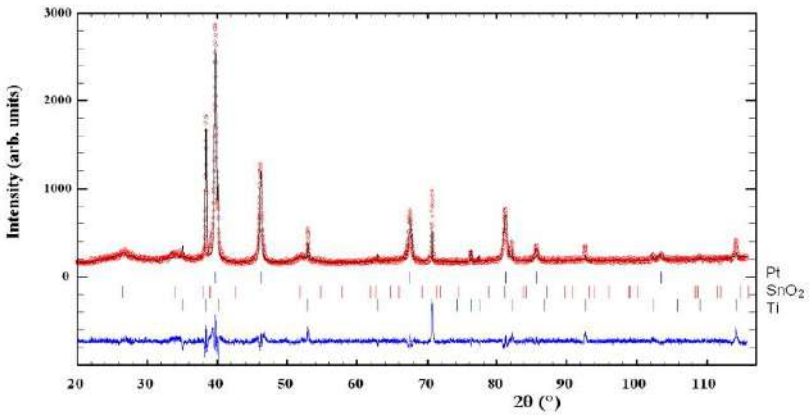

Figure 3. Observed and calculated XRD powder profiles for the Ti/SnO_2–4 Pt–9 Ru electrode. Experimental data (circles) and calculated profile (solid line through the circles) are presented together with the calculated Bragg positions (vertical ticks) and difference curve (bottom solid line).

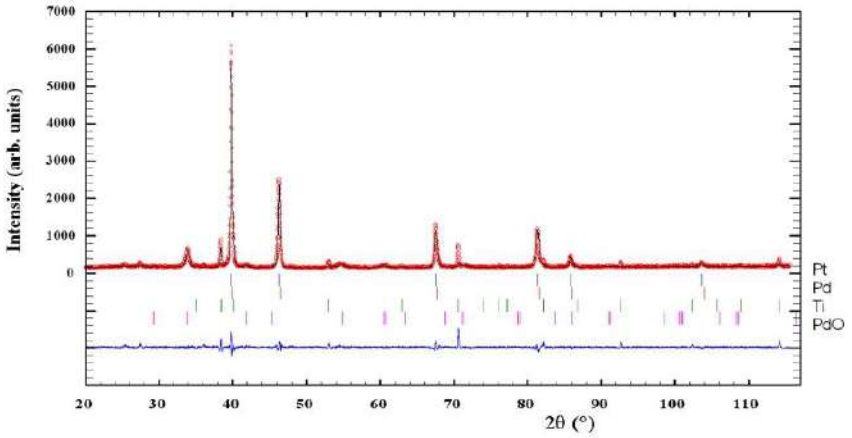

Figure 4. Observed and calculated XRD powder profiles for the Ti/SnO_2–9 Pt–5 Pd electrode. Experimental data (circles) and calculated profile (solid line through the circles) are presented together with the calculated Bragg positions (vertical ticks) and difference curve (bottom solid line).

In the XPS spectrum of Ti/SnO_2–4 Pt–9 Ru anode, the maximum at 530.7 eV corresponds to O in the structure of phase oxides, and the maxima at 531.9 and 533.1 correspond to adsorbed OH^- and H_2O, respectively [Fig. 7(c)]. A maximum corresponding to Ru (284.0 eV[25]) was slightly shifted toward higher binding energies (284.6 eV). In this coating, as in Ti/SnO_2-14 Ru, a high content of Sn was recorded (32 at.%) and Ti was present in small quantities. This series of coatings was a composite with SnO_x-Pt-RuO_x structure. The main anode processes are realized with high rate on the active centers of RuO_2 by a known mechanism, due to the implementation of the redox transition in the Ru(IV)–Ru(VI) pair.[28]

Figure 7(d) demonstrates the XPS spectra of the Ti/SnO_2-19.5 Pd surface. There are traces of Ti in the surface layer and the peaks of Sn $3d_5$ of sufficiently high intensity corresponded to 7.3 at.% in the coating. The peak O 1s (531 eV) is split into three maxima at 530.4, 531.1 and 534.2 eV. Most likely, the first peak corresponded to the O of PdO and the second to OH^- ions, which compensated for the excess charge of cationic vacancies.[24] Oxygen reflexes in Ti and Sn oxides also could be layered on this peak. The binding energy of the third peak is too high for oxide-hydroxide compounds of metals and instead is characteristic of the O atom in adsorbed H_2O molecules.[25,29,30] This assumption is confirmed by the fact that the O peak was observed at these high binding energies, with its value being proportional to the Pd content in the coating just when film-modified with Pd only. The proportionality of the O 1s peaks indicated a high surface content of H_2O adsorbed on the surface. Thus, Pd oxides were the main centers of H_2O adsorption, and their presence in the coating contributed to the hydroxylation of the anode surface. Most likely, this property of Pd compounds provides its high electrocatalytic activity in the reaction of formation of hypochlorite, which involves O-containing particles weakly bonded to the surface.

Catalytic activity and selectivity of the composites in hypochlorite and chlorate synthesis

One should consider several mechanisms of Cl_2 evolution involving adsorbed O-containing particles:

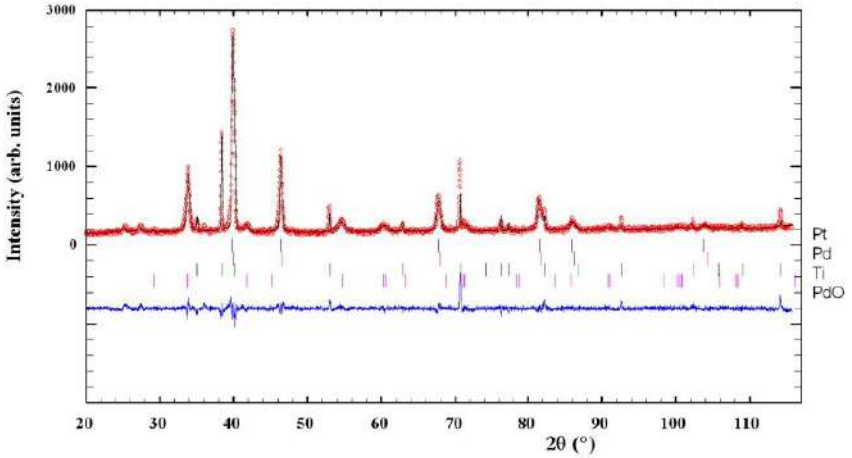

Figure 5. Observed and calculated XRD powder profiles for Ti/SnO_2–4 Pt–10 Pd electrode. Experimental data (circles) and calculated profile (solid line through the circles) are presented together with the calculated Bragg positions (vertical ticks) and difference curve (bottom solid line).

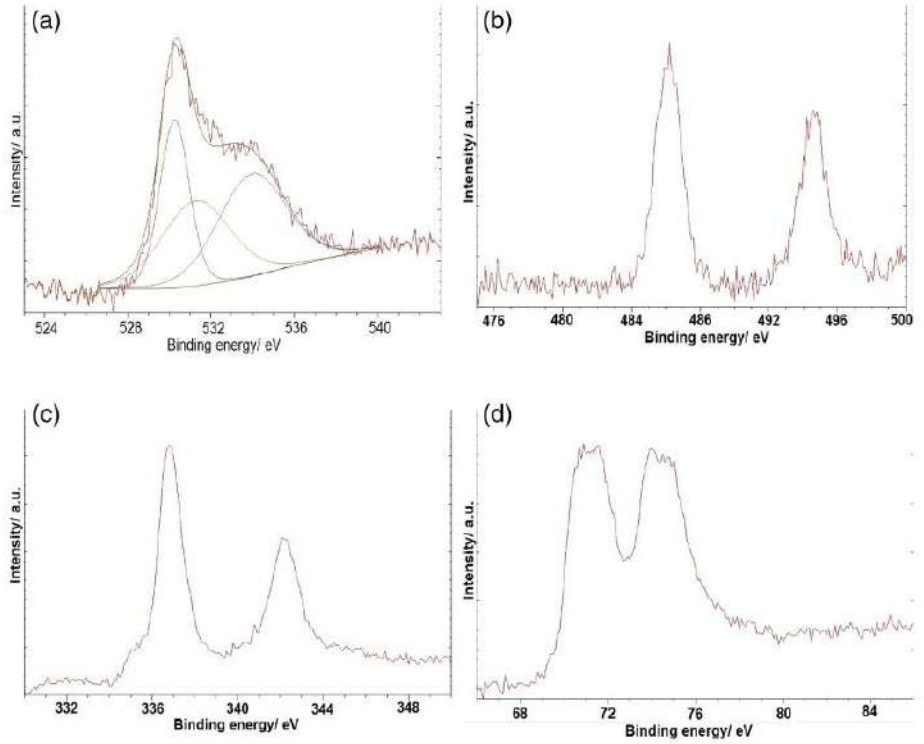

Figure 6. XPS spectra of Ti/SnO_2–8 Pt–12 Pd surface showing (a) simulated O 1s, (b) Sn 3d, (c) Pd 3d and (d) Pt 4f core levels.

(i) Denton and Harrison[31] suggest the possibility of electrochemical adsorption of Cl on the active site of the surface in close proximity to the adsorbed particle OH_{ads} and their subsequent recombination with the formation of HOCl:

$$Cl^- + \leftrightarrows Cl_{ads} + e \quad (4)$$

$$H_2O + \leftrightarrows OH_{ads} + H^+ + e^- \quad (5)$$

$$Cl_{ads} + OH_{ads} \rightarrow HOCl_{ads} \quad (6)$$

However, at high degrees of filling of the surface with O-containing particles, the probability of direct discharge of Cl^- [see Eqn (4)] is unlikely, which also is indicated by the results of studying the surface of RuO_2 by Raman spectroscopy.[32]

(ii) Burke and O'Neill[33] tried to describe the Cl_2 evolution reaction on the surface of oxides in the region of potentials, where the surface is filled with O_{ads} particles, which act as active centers and regenerate at the time of electrochemical desorption of the Cl_2 molecule with the formation of O_{ads}:

$$O_{ads} + Cl^- = OCl_{ads} + e^- \quad (7)$$

$$OCl_{ads} + Cl^- = Cl_2 + O_{ads} + e^- \quad (8)$$

(iii) Krishtalik and Erenburg[34] suggested two successive main stages: the discharge of the H_2O molecule adsorbed on the active center with the formation of OH_{ads} particles and the subsequent discharge of Cl^- ions with the formation of adsorbed molecule of HOCl, which in an acidic medium is converted into a Cl_2 molecule.

$$H_2O \leftrightarrows OH_{ads} + H^+ + e^- \quad (9)$$

$$OH_{ads} + Cl^- \rightarrow M(HO)Cl + e^- \quad (10)$$

$$HOCl + HCl \leftrightarrows Cl_2 + H_2O, \quad (11)$$

(iiii) Erenburg[35] expanded on the mechanism proposed by Burke and O'Neill[33] considering the possibility of Cl^- ion discharge at the active centers of two types M-OH and M-O with their subsequent regeneration without the stage of adsorption–desorption of O-containing particles, which is energetically advantageous for surfaces with high O affinity:

$$M{-}OH_2^+ \leftrightarrows M{-}OH + H^+ \quad (12)$$

$$M{-}OH \leftrightarrows M{-}O + H^+ + e \quad (13)$$

$$M{-}O + Cl^- \rightarrow M{-}OCl + e \quad (14)$$

$$M{-}OCl + Cl^- + H^+ \leftrightarrows M{-}OH + Cl_2 \quad (15)$$

$$M{-}OCl + Cl^- \leftrightarrows M{-}O + Cl_2 + e \quad (16)$$

The nature of Cl particles adsorbed on the anode surface remains under discussion: electrochemical adsorption occurs directly on the active center of the metal oxide M^{z+} [Eqn (17)] or on the active center with adsorbed O-containing particles M-OH or M-O [Eqn (18)].

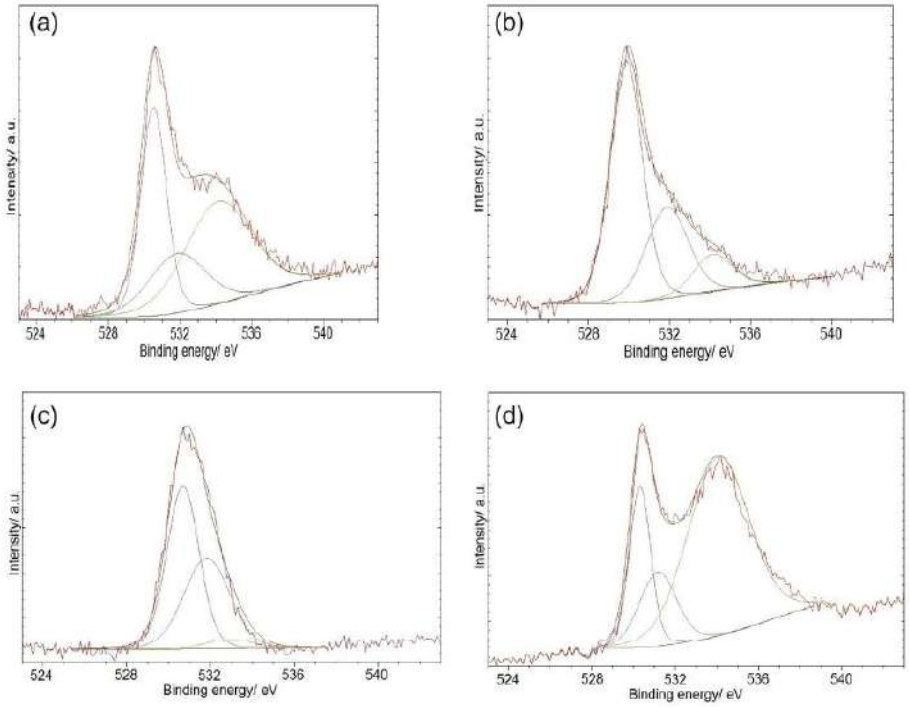

Figure 7. Modeled O 1s core level of XPS spectra of several composite surfaces: (a) Ti/SnO_2–3 Pt–13 Pd; (b) Ti/SnO_2–10 Pt–6 Pd; (c) Ti/SnO_2–4 Pt–9 Ru; (d) Ti/SnO_2–19.5 Pd.

$$(M^{z+1}) + Cl^- \rightarrow (M^{z+1})Cl + e \quad (17)$$

$$M{-}OH + Cl^- \rightarrow M(OH)Cl + e \quad (18)$$

Krishtalik and Erenburg[34-36] have shown that hydroxyl radicals ('OH) formed during the electrolysis of H_2O on the surface of the electrode have a significant effect on the kinetics of Cl_2 formation.

Based on the above mechanisms, we assume that the oxidation of Cl^- ions on the electrode surface occurs with the participation of particles such as OH_{ads} or O_{ads}, which comprise an active center on the surface, and that polarization at high anodic potentials simultaneously decreases the degree of surface filling with labile particles and increases the filling with inert particles, and hence that the formation of Cl_2 and hypochlorite should proceed with the participation of labile O-containing particles. The results obtained confirmed these assumptions.

We assume that in low-concentrated solutions HClO is formed not as a result of a secondary chemical reaction involving molecular Cl_2, but rather as a result of direct electrochemical oxidation of the Cl^- ion in accordance with the mechanism, where the first stage in the transfer of the first electron is the formation of O-containing radicals adsorbed on the electrode, as a result of anodic ionization of H_2O.

It was found that the decrease in the surface content of Ru and the increase in the surface content of Pt led to an increase in the proportion of the surface on which the reactions with O transfer occur with the participation of inert O-containing particles. The potential of the anode is shifted to positive values, increasing the current efficiency of hypochlorite formation (Table 2).

The highest catalytic activity and selectivity in NaClO synthesis was shown for the Ti/SnO_2–8 Pt–12 Pd, Ti/SnO_2–3 Pt–13 Pd and SnO_2–10 Pt–6 Pd electrodes.

It is possible to obtain an anode with a given electrocatalytic activity for O_2 evolution reaction in the range from 1.10 to 1.55 V by modifying the coating with varying contents of several metals simultaneously. Data presented as semi-logarithmic coordinates reveal that all polarization curves are linear and have a Tafel slope of 100–140 mV, and the charge transfer coefficient had an average value of 0.5, which indicates a deceleration in the transfer of the first electron during the formation of adsorbed O-containing particles such as OH_{ads}. Despite the simultaneous occurrence of the two processes of H_2O and Cl^- oxidation, in most cases, the prevailing one is the formation of HClO. Because the current efficiency of the main process at the proposed electrodes (Ti/SnO_2–8 Pt–12 Pd, Ti/SnO_2–3 Pt–13 Pd and SnO_2–10 Pt–6 Pd) was 91–95%, it is taken that in the range of operating potentials the contribution of O_2 evolution to the Tafel slope is insignificant and can thus be neglected by referring it to the main reaction. It is possible to directly influence the energy distribution of O-containing particles on the surface by changing the nature and amount of the modifying additive and their combination.

A correlation between the O_2 evolution overvoltage in the background electrolyte, and the catalytic activity and selectivity of the electrodes in hypochlorite and chlorate synthesis has been established (Fig. 8). The dependence of the current efficiency of NaClO formation in low concentration NaCl solutions *versus* the polarization of the O_2 evolution reaction in 1 mol L^{-1} $HClO_4$ is the volcano-shaped curve. It was found that the current efficiency of NaClO

Table 2. Current efficiencies of NaClO and $NaClO_3$ in 0.15 mol L^{-1} NaCl during 60 min of accumulative electrolysis at j_a = 40 mA cm^{-2}

Anode	Current efficiency (%) NaClO	$NaClO_3$
Ti/SnO_2–9 Pt–4 Ru	85	0.8
Ti/SnO_2–16 Pt–11 Ru–3 Pd	80	1.0
Ti/SnO_2–13 Pt–1 Ru	71	3.8
Ti/SnO_2–19 Pt	66	4.0
Ti/SnO_2–2.5 Pt	57	8.0
Ti/SnO_2–0.8 Pt	51	12.0
Ti/SnO_2–5 Pt–10 Pd	95	0.9
Ti/SnO_2–8 Pt–12 Pd	95	1.1
Ti/SnO_2–7 Pt–4 Pd	93	0.8
Ti/SnO_2–19.5 Pd	91	1.1

was >90% and that of $NaClO_3$ was <1%, when O_2 evolution overpotential in 1.0 mol L^{-1} $HClO_4$ was realized at potentials of 1.50–1.58 V.

It should be noted that the bulk formation of chlorates is a lengthy and not an instantaneous process, and our contact time with the electrode herein was limited. This process is electrochemical, because if it were chemical, a change in concentration would have been observed after the termination of electrolysis. This can occur during a photochemical or thermal reaction (>30 °C), but even though the storage conditions of the solution were met, we did not observe either a drop in the concentration of HClO or the accumulation of chlorates for a long time.[37,38] Chlorates are formed exclusively when electric current is applied, and the concentrations of the substances do not change after the termination of electrolysis, which suggests that the formation of chlorates occurs as a result of the electrochemical oxidation of HClO to chlorate. Thus, the accumulation of chlorates during electrolysis is determined solely by the electrode material and the electrolysis conditions.

Labile, inert O-containing particles of different energies which are strongly and weakly bound to the surface are recognized to take part in anodic O transfer reactions.[39–41] Different reactions require particles with a certain energy, for example, the oxidation of ClO^- to ClO_2^- and ClO_3^- requires O-containing particles with a higher energy. Because the average energy of O-containing particles is related to the potential of the electrode under current, this explains the aforementioned relationship between the polarization of the reaction of O_2 evolution in the background solution and the current efficiencies of hypochlorite and chlorate in solutions containing chlorides. Because minimal polarizations of O_2 evolution and Cl^- oxidation were observed on samples of Ti/SnO_2 doped with Ru, relatively low hypochlorite current efficiency and <1% chlorate current efficiency was realized on these electrodes. On Pt-doped coatings, high oxygen evolution overvoltage was observed, with low current efficiency of hypochlorite and high current efficiency of chlorate. As the polarization increases, the energy of O-containing particles increases, and the rate of ClO_3^- formation increases.[42,43]

Thus, significant formation of chlorates occurs only at the anodes, where in 1 mol L^{-1} $HClO_4$ the O_2 evolution potential was >1.58 V. On such surfaces, owing to the formation of particles with higher binding energies, the evolution of O_2, and synthesis of HClO and ClO^-, and their subsequent conversion into ClO_2^- and ClO_3^-, occur simultaneously.

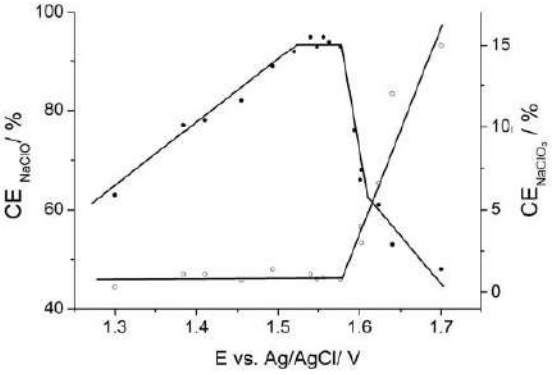

Figure 8. Current efficiencies of NaClO and $NaClO_3$ on Ti/SnO_2-anodes modified with Ru, Pd and Pt during electrolysis of 0.15 mol L^{-1} NaCl *versus* the oxygen evolution potential of 1.0 mol L^{-1} $HClO_4$ at 40 mA cm^{-2}.

CONCLUSION

Modification of anode materials with Pd was proposed in order to increase the catalytic activity and selectivity in the hypochlorite synthesis reaction from low concentrated NaCl solutions. According to XRD analysis, Pd in the thermally treated electrocatalytic coating based on oxide Ti/SnO_2-Pd and Ti/SnO_2-Pt-Pd exists in the form of PdO oxide. XPS showed that the PdO surface has a high affinity for hydroxylation (i.e. adsorption of H_2O and OH^-).

The electrocatalytic activity of electrodes in anode processes in low concentration Cl^- solutions depends on the bond strength of chemisorbed O-containing particles of different natures. Participation of labile O-containing particles in the oxidation of Cl^- increases the rate of hypochlorite formation and leads to inhibition of undesirable reactions of O_2 evolution and synthesis of chlorates and chlorites. This makes it possible to influence the electrocatalytic activity and selectivity for the target process due to the direct modification of the anodes, leading to a change in the bond strength of chemisorbed O-containing particles.

The maximum efficiency in the synthesis of NaClO in low concentration NaCl solutions was demonstrated by electrocatalysts based on SnO_2 doped simultaneously with Pd (5–15 at.%) and Pt (5–10 at.%).

ACKNOWLEDGEMENTS

The authors are indebted to Laboratory of Material Science and Intermetallic compounds (Ivan Franko Lviv National University) for help in the discussion of obtained results. This work was supported by the Ministry of Education and Science of Ukraine (grant no. 0121U109529, 2021).

CONFLICTS OF INTEREST

The authors declare that they have no conflict of interest.

REFERENCES

1 Block MS and Rowan BG, Hypochlorous acid: a review. *J Oral Maxillofac Surg* **78**:1461–1466 (2020). https://doi.org/10.1016/j.joms.2020.06.029.

2 Gold MH, Andriessen A, Bhatia AC, Bitter P Jr, Chilukuri S, Cohen JL *et al.*, Topical stabilized hypochlorous acid: the future gold standard for wound care and scar management in dermatologic and plastic surgery procedures. *J Cosmet Dermatol* **19**:270–277 (2020). https://doi.org/10.1111/jocd.13280.

3 Spasojevic M, Krstajic N, Spasojevic P and Ribic-Zelenovic L, Modelling current efficiency in an electrochemical hypochlorite reactor. *Chem Eng Res Des* **93**:591–601 (2015). https://doi.org/10.1016/j.cherd.2014.07.025.

4 Mijin DZ, Tomic VD and Grgur BN, Electrochemical decolorization of the Reactive Orange 16 dye using a dimensionaly stable Ti/PtO_x anode. *J Serb Chem Soc* **80**:903–915 (2015). https://doi.org/10.2298/JSC140917107M.

5 Ghalwa NA, Tamox H, El Askaln M and El Agha AR, Generation of sodium hypochlorite (NaOCl) from sodium chloride solution using C/PbO_2 and Pb/PbO_2 electrodes. *Int J Miner Metall Mater* **19**:561–566 (2013). https://doi.org/10.1007/s12613-012-0596-0.

6 Cotillas S, Lacasa E, Saez C, Canizares P and Rodrigo MA, Disinfection of urine by conductive-diamond electrochemical oxidation. *Appl Catal B* **229**:63–70 (2018). https://doi.org/10.1016/j.apcatb.2018.02.013.

7 Locker J, Fitzgerald P and Sharp D, Antibacterial validation of electrogenerated hypochlorite using carbon-based electrodes. *Lett Appl Microbiol* **59**:636–641 (2014). https://doi.org/10.1111/lam.12324.

8 Al-Qaim FF, Mussa ZH, Othman MR and Abdullah MP, Removal of caffeine from aqueous solution by indirect electrochemical oxidation using a graphite-PVC composite electrode: a role of hypochlorite ion as an oxidising agent. *J Hazard Mater* **300**:387–397 (2015). https://doi.org/10.1016/j.jhazmat.2015.07.007.

9 Rosestolato D, Fregon J, Ferro S and De Battisti A, Influence of the nature of the electrode material and process variables on the kinetics of the chlorine evolution reaction. The case of IrO_2-based electrocatalysts. *Electrochim Acta* **139**:180–189 (2014). https://doi.org/10.1016/j.electacta.2014.07.037.

10 Battaglin G, Rosestolato D, Ferro S and De Battisti A, Characterization of IrO_2-SnO_2 films prepared by physical vapor deposition at ambient temperature electrocatalysis. *Electrocatalysis* **4**:358–366 (2013). https://doi.org/10.1007/s12678-013-0137-2.

11 Watts RJ, Finn DD, Wyeth MS and Teel AL, Performance comparison of tin oxide anodes to commercially available dimensionally stable anodes. *Water Environ Res* **80**:490–496 (2008). https://doi.org/10.2175/106143008X266760.

12 Li F, Liu Q, Hu J, Yang J and Ma J, Recent progresses on SnO_2 anode materials for sodium storage (Review). *J Phys D Appl Phys* **53**:353001 (2020). https://doi.org/10.1088/1361-6463/ab8e79.

13 Santos GOS, Doria AR, Vasconcelos VM, Saez C, Rodrigo MA, Eguiluz KIB *et al.*, Enhancement of wastewater treatment using novel laser-made Ti/SnO_2–Sb anodes with improved electrocatalytic properties. *Chemosphere* **259**:127475 (2020). https://doi.org/10.1016/j.chemosphere.2020.127475.

14 Fernandez-Aguirre MG, Berenguer R, Beaumont S, Nuez M, La Rosa-Toro A, Peralta-Hernandez JM *et al.*, The generation of hydroxyl radicals and electro-oxidation of diclofenac on Pt-doped SnO_2-Sb electrodes. *Electrochim Acta* **354**:136686 (2020). https://doi.org/10.1016/j.electacta.2020.136686.

15 Bravo-Yumi N, Espinoza-Montero P, Picos-Benitez A, Navarro-Mendoza R, Brillas E and Peralta-Hernandez JM, Synthesis and characterization of Sb_2O_5-doped Ti/SnO_2-IrO_2 anodes toward efficient degradation tannery dyes by in situ generated oxidizing species. *Electrochim Acta* **358**:136904 (2020). https://doi.org/10.1016/j.electacta.2020.136904.

16 LaCourse WR, Hsiao Y-L and Johnson DC, Electrocatalytic oxidation at electrodeposited bismuth(III)-doped beta-lead dioxide film electrodes. *J Electrochem Soc* **136**:3714–3719 (1989). https://doi.org/10.1149/1.2096536.

17 Luk'yanenko TV, Velichenko AB, Kasian OI, Shmychkova OB, Demchenko PY and Gladyshevskii RE, Voltametric behavior of platinized titanium electrodes. *J Chem Technol* **27**:111–121 (2019). https://doi.org/10.15421/081912.

18 Girenko DV, Girenko AA and Nikolenko NV, Potentiometric determination of chlorate impurities in hypochlorite solutions. *Int J Anal Chem* **2019**:2360420 (2019). https://doi.org/10.1155/2019/2360420.

19 Sakurai K and Mizusawa M, X-ray diffraction imaging of anatase and rutile. *Anal Chem* **82**:3519–3522 (2010). https://doi.org/10.1021/ac9024126.

20 Hanaor DAH and Sorrell CC, Review of the anatase to rutile phase transformation. *J Mater Sci* **46**:855–874 (2011). https://doi.org/10.1007/s10853-010-5113-0.

21 Khataee AR, Aleboyeh H and Aleboyeh A, Crystallite phase-controlled preparation, characterisation and photocatalytic properties of titanium dioxide nanoparticles. *J Exp Nanosci* **4**:121–137 (2009). https://doi.org/10.1080/17458080902929945.

22 Mittemeijer EJ and Scardi P, *Diffraction Analysis of the Microstructure of Materials*. Springer, Berlin (2004).

23 Velichenko AB and Devilliers D, Electrodeposition of fluorine-doped PbO_2. *J Fluorine Chem* **128**:269–276 (2007). https://doi.org/10.1016/j.jfluchem.2006.11.010.

24 Amadelli R, Armelao L, Tondello E, Daolio S, Fabrizio M, Pagura C *et al.*, SIMS and XPS study about ions influence on electrodeposited PbO_2 films. *Appl Surf Sci* **142**:200–203 (1999). https://doi.org/10.1016/S0169-4332(98)00707-7.

25 Wanger CD, Riggs WM, Davis LE, Moulder JF and Muilenberg GE, *Handbook of X-Ray Photoelectron Spectroscopy*. Perkin-Elmer Corp, Eden Prairie, MN (1995).

26 Themlin J-M, Chtaib M, Henrard L, Lambin P, Darville J and Gilles J-M, Characterization of tin oxides by X-ray-photoemission spectroscopy. *Phys Rev B* **46**:2460–2466 (1992). https://doi.org/10.1103/physrevb.46.2460.

27 Batzill M and Diebold U, The surface and material science of tin oxide. *Prog Surf Sci* **79**:47–154 (2005). https://doi.org/10.1016/j.progsurf.2005.09.002.

28 Kim J, Kim C, Kim S and Yoon J, A review of chlorine evolution mechanism on dimensionally stable anode (DSA®). *Korean Chem Eng Res* **53**:531–539 (2015). https://doi.org/10.9713/kcer.2015.53.5.531.

29 Kim KS, O'Leary TJ and Winograd N, X ray photoelectron spectra of lead oxides. *Anal Chem* **45**:2214–2218 (1973). https://doi.org/10.1021/ac60335a009.

30 Briggs D and Seah MP, *Practical Surface Analysis*, Vol. **1**, Auger and X-Ray Photoelectron Spectroscopy, 2nd edn. John Wiley & Sons, Chichester, UK (1990).

31 Denton DA, Harrison JA and Knowles RI, Chlorine evolution and reduction on RuO_2/TiO_2 electrodes. *Electrochim Acta* **24**:521–527 (1979). https://doi.org/10.1016/0013-4686(79)85027-6.

32 Zeradjanin AR, Menzel N, Strasser P and Schuhmann W, Role of water in the chlorine evolution reaction at RuO_2-based electrodes – understanding electrocatalysis as a resonance phenomenon. *ChemSusChem* **5**:1897–1904 (2012). https://doi.org/10.1002/cssc.201200193.

33 Burke LD and O'Neill JF, Some aspects of the chlorine evolution reaction at ruthenium dioxide anodes. *J Electroanal Chem Interf Electrochem* **101**:341–349 (1979). https://doi.org/10.1016/S0022-0728(79)80045-5.

34 Krishtalik LI, Kinetics and mechanism of anodic chlorine and oxygen evolution reactions on transition metal oxide electrodes. *Electrochim Acta* **26**:329–337 (1981). https://doi.org/10.1016/0013-4686(81)85019-0.

35 Erenburg R, Mechanism of the chlorine reaction of ruthenium titanium oxide anodes. *Soviet Electrochem* **20**:1481–1486 (1984).

36 Hansen HA, Man IC, Studt F, Abid-Pedersen F, Bligaard T and Rossmeisl J, Electrochemical chlorine evolution at rutile oxide (110) surfaces. *Phys Chem Chem Phys* **12**:283–290 (2010). https://doi.org/10.1039/B917459A.

37 Girenko D, Smychkova O and Velichenko A, Low concentrated green NaClO: influence of cathode material on kinetic regularities of electrolysis. *Vopr Khim Khimichesk Tekhnol* **3**:73–82 (2021). https://doi.org/10.32434/0321-4095-2021-136-3-73-82.

38 Smychkova O, Borovik I, Girenko D, Davydenko P and Velichenko A, The effect of impurities on the stability of low concentrated eco-friendly solutions of NaOCl. *Vopr Khim Khimichesk Tekhnol* **4**:142–150 (2021). https://doi.org/10.32434/0321-4095-2021-137-4-142-150.

39 Burke LD and Roche MBC, Hydrous oxide formation on platinum. A useful route to controlled platinization. *J Electroanal Chem Interf Electrochem* **164**:315–334 (1984). https://doi.org/10.1016/S0022-0728(84)80215-6.

40 Tarasevich MR, Sadkowski A and Yeager E, Oxygen electrochemistry, in *Comprehensive Treatise of Electrochemistry*, ed. by Conway BE, Bockris JO, Yeager E, Khan SUM and White RE. Springer, Boston (1983).

41 Gilman S, Electrochemical surface oxidation of platinum. *Electrochim Acta* **9**:1025–1046 (1964). https://doi.org/10.1016/0013-4686(64)85049-0.
42 Jung YJ, Baek KW, Oh BS and Kang J-W, An investigation of the formation of chlorate and perchlorate during electrolysis using Pt/Ti electrodes: the effects of pH and reactive oxygen species and the results of kinetic studies. *Water Res* **44**:5345–5355 (2010). https://doi.org/10.1016/j.watres.2010.06.029.
43 Kodera F, Umeda M and Yamada A, Effect of platinum oxide on electro oxidation of trace amounts of sodium hypochlorite in aqueous medium. *J Electroanal Chem* **625**:92–96 (2009). https://doi.org/10.1016/j.jelechem.2008.10.010.

*Таким чином, встановлено, що на покритті, що складається практично із α-фази, перенапруга виділення кисню значно менше в результаті більшої гідратованості покриття порівняно з покриттям із більшим вмістом β-фази. Відмінності в кристалографічній орієнтації за фіксованого фазового складу плюмбум(*IV*) оксиду практично не впливають на кінетику виділення кисню. За характером впливу на реакцію виділення кисню, композитні матеріали з ПАР можна поділити на дві групи: такі, що зменшують перенапругу виділення кисню (з гідрогенкарбоновим ланцюгом) та такі, що збільшують перенапругу виділення кисню (з флуоркарбоновим ланцюгом). В останньому випадку це пов'язано, як і у випадку модифікування* PbO_2 *атомами Флуору, зі збільшенням міцності зв'язку кисеньвмісних радикалів із поверхнею електрода.*

На прикладі модельних сполук було зроблено порівняння електрокаталітичної активності оксидних анодів SnO_2 *та* PbO_2*. Так, було виявлено, що нітрофуразон руйнується ефективніше на* PbO_2*, завдяки великій кількості оксигеновмісних частинок, міцно зв'язаних із поверхнею оксиду, що характерно для плюмбум(*IV*) оксиду.*

Разом із тим, за наявності хлорид-іонів в електроліті найбільша кількість гіпохлоритної кислоти, що бере участь у вторинних окисних процесах, виробляється на легованому SnO_2*, що дозволяє досягти загальної швидкості процесу, зіставлюваної з* PbO_2*-анодами, та може бути цікавим з точки зору використання таких матеріалів для знезараження лікарняних стоків.*

Показано, що SnO_2*-електрод не є ефективним електрокаталізатором прямого електрохімічного окиснення забруднювачів, однак його застосування дозволяє на аноді одержати велику кількість гіпохлориту, а також певну кількість кисню, що за відновлення на катоді приводить до синтезу гідроген пероксиду та утворення додаткової пероксенової системи.*

Виявлено, що електрокаталітичну активність PbO_2 *можна підвищити за рахунок утворення композитів металоксид-ПАР. Так, наприклад, за*

використання PbO_2*-натрію додецилсульфату константа швидкості руйнування хлорамфеніколу збільшується в кілька разів.*

РОЗДІЛ 7
ЕЛЕКТРОХІМІЧНЕ ОКИСНЕННЯ АРОМАТИЧНИХ СПОЛУК – ПРОМІЖНИХ ПРОДУКТІВ ОКИСНЕННЯ ФАРМАЦЕВТИЧНИХ ПРЕПАРАТІВ

Розглянемо електрохімічну конверсію ароматичних сполук в аліфатичні на прикладі 4-нітроаніліну (табл. 7.1).

Таблиця 7.1

Електрохімічна конверсія 4-нітроаніліну в аліфатичні сполуки

Анодний матеріал	Константа швидкості деградації вихідної речовини, $k \cdot 10^2$, $хв^{-1}$	Досягнення ступеня конверсії 95 %, хв
PbO_2 (α-фаза)	1,68	178
PbO_2 (β-фаза)	1,84	162
PbO_2–0,042% Ni	2,66	113
PbO_2–4% TiO_2	3,02	99
PbO_2–2% SDS	3,20	94
PbO_2-Nafion®	4,2	71
PbO_2–TiO_2–SDS	4,5	67

Як і в процесі виділення кисню на покритті, що переважно складається із α-фази, спостерігається найнижча парціальна швидкість окиснення ароматичних сполук, що підкреслює, що для нас таки матеріали не цікаві. Покриття модифіковане нікелем, нестійке та має обмежений ефект. Найбільший практичний інтерес представляють досліджувані електрокаталізатори PbO_2-ПАР, PbO_2-полімер, PbO_2-TiO_2-ПАР. Їх каталітична активність збільшується майже в 2,5 рази. Ми припускаємо, що такий ефект, як і в процесі виділення кисню пов'язаний із утворенням частинок з більшою

міцністю зв’язку, які, виходячи з експериментальних даних, и беруть участь в окисненні органічних сполук.

Хоча такі значення дуже низькі для використання в очистці стічних вод. Ми пропонуємо для інтенсифікації процесу очистки стічних вод збільшити вихід вторинного окиснення органічних сполук. Зробити це можна за рахунок перемішування електроліту з використанням стаціонарної мішалки, що не досить доцільно під час очистки стічної води, або проведенням процесу в протоці води.

Однією з особливостей електролізу органічних сполук являється низька електропровідність електроліту. Тому для успішного електролізу відстань між електродами повинна бути дуже малою, а площа електродів за можливістю великою. Останнього можна досягти за використання щілинного електролізеру з плоскопаралельними електродами, які чергуються, або використовуючи систему з коаксіальним розташуванням електродів (рис. 7.1), в якій можна в широкому діапазоні змінювати співвідношення анодної та катодної густин струму.

Рис. 7.1 Електрохімічна комірка з коаксіальним розташуванням електродів

Проте навіть для таких систем не існує універсального анодного матеріалу. Для руйнування різної за природою органіки потрібні різні за складом електрокаталізатори.

Ми пропонуємо використовувати послідовну гідродинамічну схему, що представляє собою електролізер, побудований з кількох послідовно з’єднаних бездіафрагменних протокових електрохімічних комірок із коаксіальним розташуванням електродів (анод – стрижень із матеріалу на основі модифікованого плюмбум(IV) оксиду із високою каталітичною активністю та селективністю до електрохімічної конверсії в залежності від функціональної групи (галоген-, нітро- та аміногрупи); катод – титанова трубка) (рис. 7.2).

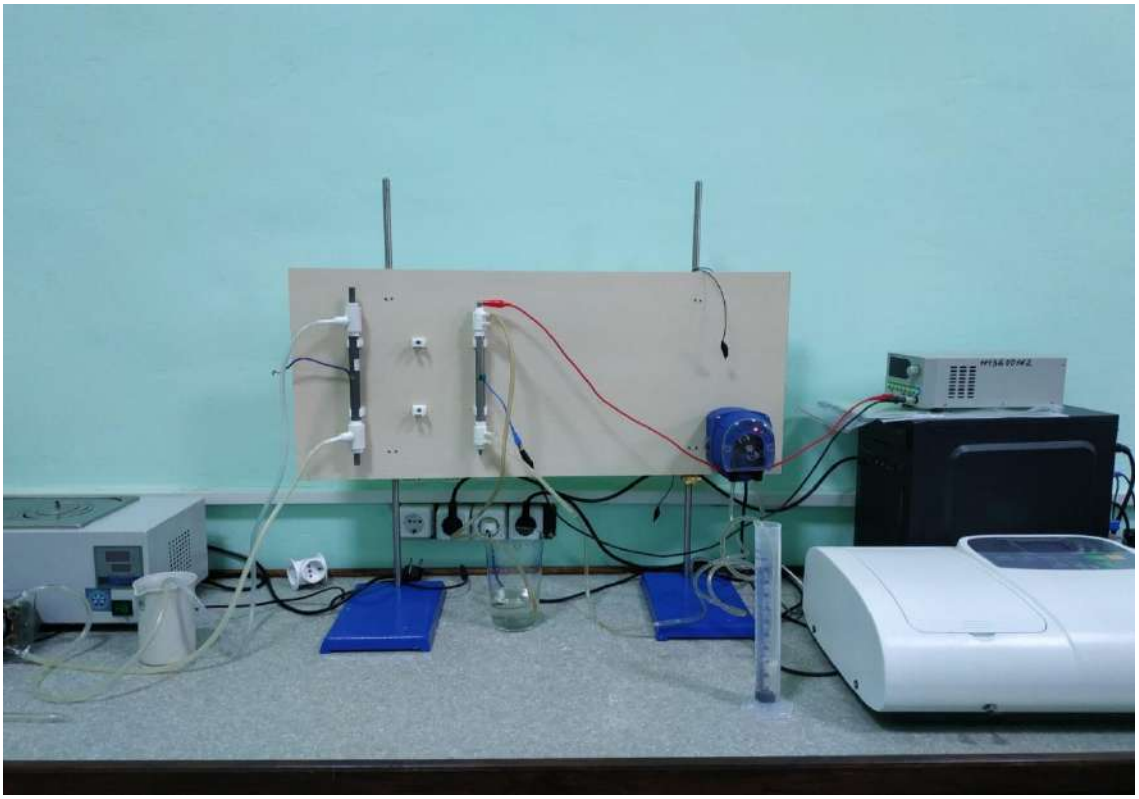

Рис. 7.2 Електролізер

Інтенсифікація процесу відбуватиметься шляхом використання різних матеріалів для різних призначень та комбінуванням комірок для збільшення парціальної швидкості проміжних процесів. Параметрами варіювання виступатимуть густина струму та швидкість протоку води.

Як бачимо, така система надає переваги (табл. 7.2). В таблиці наведено кінетичні розрахунки електроокиснення п-бензохінону в протоковій ситемі.

Таблиця 7.2

Константи швидкості електроокиснення п-бензохінону

j_a, мА см$^{-1}$ / $V_{прот.}$, л год$^{-1}$	20	30	50
4	0,01	0,03	0,06
6	0,01	0,03	0,08
10	0,01	0,03	0,13

В проточних електролізерах, на відміну від стаціонарних, час електролізу, необхідний для досягнення ступеня конверсії 95%, буде скорочений більше ніж в 10 разів за рахунок підвищення об’ємної густини струму і граничного струму, а також утворення хімічних окисників. Це і час перетворення скоротить в 10 разів.

Для створення ефективних модулів необхідно в одній системі поєднати різні процеси: електрохімічні та хімічні, наприклад, провести пряме електрохімічне окиснення забруднювачів до відсутності біологічної активності, а подальше руйнування та знезараження проводити у вторинній хімічній гомогенно- або гетерогенно-каталітичній системі.

Основні результати розділу опубліковано в роботах автора [54–58].

Bulletin of Dnipropetrovsk University. Series Chemistry, 2017, *25*(1), 27–35

Вісник Дніпропетровського університету. Серія Хімія
Bulletin of Dnipropetrovsk University. Series Chemistry

p-ISSN 2306-871X, e-ISSN 2313-4984
journal homepage: http://chemistry.dnu.dp.ua

UDC 544. 653.2

THE ELECTROCHEMICAL OXIDATION OF 4-NITROANILINE AND 4-NITROPHENOL ON MODIFIED PbO_2-ELECTRODES

Olesia B. Shmychkova,[1] Tatiana V. Luk'yanenko,[1] Rossano Amadelli,[2] Alexander B. Velichenko[1,*]
[1]*Ukrainian State University of Chemical Technology, 8, Gagarin Ave., 49005 Dnipro, Ukraine*
[2]*ISOF-CNR u.o.s Ferrara c/o Department of Chemical and Pharmaceutical Sciences, University of Ferrara, Via Luigi Borsari, 46–44121 Ferrara, Italy*
Received 03 January 2017; revised 14 February 2017; accepted 28 June 2017, available online 05 December 2017

Abstract

The electrochemical oxidation of *p*-nitroanilline and *p*-nitrophenol on lead dioxide anodes, modified by different ionic dopants has been investigated. The general mechanism of the oxidation of organic compounds of aromatic nature includes oxidizing of compounds to the intermediates with quinoid structure, reactions of aromatic ring opening and formation of aliphatic products (mainly acids) and in ideal case – the complete mineralization to CO_2 and H_2O. According to obtained results one can conclude that both reactions occur via formation of *p*-benzoquinon. Calculations, based on kinetic studies of the reaction, have shown that the rate constant of the degradation of the organics involved depends on the composition of the electrode material and varies due to the nature and the content of ionic additives in lead dioxide. The maximum interest for the electrochemical destruction of organic substances represents lead dioxide electrodes modified by bismuth to which a rate constant of p-nitroaniline oxidation increases in 1.6 times compared with nonmodified electrodes. Maximum electrocatalytic activity is achieved by increasing the proportion of α-phase, on the one hand, and increase the crystalline zone of oxide on the other, which leads to increased amounts of oxygen containing particles strongly bounded to the electrode surface that participate in the electrochemical oxidation of aromatic compounds.

Keywords: electrochemical oxidation, hydroxyl radicals, lead dioxide, methanesulfonate electrolyte.

ЕЛЕКТРОХІМІЧНЕ ОКИСНЕННЯ 4-НІТРОАНІЛІНУ ТА 4-НІТРОФЕНОЛУ НА МОДИФІКОВАНИХ PbO_2-ЕЛЕКТРОДАХ

Олеся Б. Шмичкова,[1] Тетяна В. Лук'яненко,[1] Россано Амаделлі,[2] Олександр Б. Величенко[1,*]
[1]*ДВНЗ «Український державний хіміко-технологічний університет», пр. Гагаріна 8, м. Дніпро, 49005 Україна*
[2]*ISOF-CNR відділення в Феррарі, департамент хімії та фармації, Університет Феррари, вул. Л. Борсарі, 46–44121 Феррара, Італія*

Анотація

Досліджено електрохімічне окиснення п-нітроаніліну та *п*-нітрофенолу на діоксидносвинцевих анодах, модифікованих різними іонними добавками. Загальний механізм окиснення органічних сполук ароматичної природи включає окиснення до проміжних сполук із хіноїдною будовою, реакції ароматичного розімкнення кільця та формування аліфатичних продуктів (головним чином, кислот) і в ідеальному випадку – повна мінералізація до CO_2 і H_2O. Результати досліджень показали, що обидві реакції проходять через утворення п-бензохінону. Розрахунки, засновані на кінетичних дослідженях, показали, що константи швидкості руйнації досліджуваних органічних сполук залежать від складу електроду та варіюються залежно від природи та кількості модифікуючих добавок у плюмбум діоксиді. Найбільший інтерес для електрохімічної руйнації органічних сполук представляють модифіковані Бісмутом діоксидносвинцеві аноди, для яких константа швидкості окиснення *п*-нітроаніліну збільшується в 1.6 разів порівняно з немодифікованим покриттям. Максимальна електроактивність каталізатора досягається за збільшення частки α-фази, з одного боку, та збільшення кількості лабільних оксигеновмісних часточок на поверхні електроду, які беруть участь в електрохімічному окисненні ароматичних сполук, з іншого боку.

Ключові слова: електрохімічне окиснення, гідроксил-радикали, плюмбум діоксид, метансульфонатний електроліт.

**Corresponding author: tel.: +380562473627; e-mail address: velichenko@ukr.net*

doi: 10.15421/081705

Bulletin of Dnipropetrovsk University. Series Chemistry, 2017, *25*(1), 27–35

ЭЛЕКТРОХИМИЧЕСКОЕ ОКИСЛЕНИЕ 4-НИТРОАНИЛИНА И 4-НИТРОФЕНОЛА НА МОДИФИЦИРОВАННЫХ PbO_2-ЭЛЕКТРОДАХ

Олеся Б. Шмычкова,[1] Татьяна В. Лукьяненко,[1] Россано Амаделли,[2] Александр Б. Величенко[1,*]
[1]*ГВУЗ «Украинский государственных химико-технологический университет», пр Гагарина 8, г. Днепр, 49005, Украина*
[2]*ISOF-CNR отделение в Ферраре, департамент химии и фармации, Университет Феррары, ул. Л. Борсари, 46–44121 Феррара, Италия*

Аннотация

Исследовано электрохимическое окисление п-нитроанилина и *п*-нитрофенола на диоксидносвинцовых анодах, модифицированных различными ионными добавками. Общий механизм окисления органических соединений ароматической природы включает окисление до промежуточных соединений с хиноидным строением, реакции ароматического размыкания кольца и формирования алифатических продуктов (главным образом, кислот) и в идеальном случае – полная минерализация до CO_2 и H_2O. Результаты исследований показали, что обе реакции протекают через образование *п*-бензохинона. Расчеты, основанные на кинетических исследованиях, показали, что константы скорости разрушения исследуемых органических соединений зависят от состава электрода и варьируются в зависимости от природы и количества модифицирующих добавок в диоксиде свинца. Наибольший интерес для электрохимического разрушения органических соединений представляют модифицированные висмутом диоксидносвинцовые аноды, для которых константа скорости окисления *п*-нитроанилина увеличивается в 1.6 раз по сравнению с немодифицированным покрытием. Максимальная электроактивность катализатора достигается при увеличении доли α-фазы, с одной стороны, и увеличении количества лабильных кислородсодержащих частиц на поверхности электрода, которые участвуют в электрохимическом окислении ароматических соединений, с другой стороны.

Ключевые слова: электрохимическое окисление, гидроксил-радикалы, диоксид свинца, метансульфонатный электролит.

Introduction

The line of research involved in the manuscript belongs to the world's key development priorities of modern chemistry and attracted considerable attention of researchers as indicated by the large number of publications. The results on the use of advanced catalytic oxidation method (advanced oxidation process – AOP) achieved over the last 5 years for the destruction of chemical and biological toxins and pollutants listed in review [1]. Based on the information provided in the publications [2–4], clearing of the aquatic environment from pollution by anthropogenic organic chemicals are known to be a very difficult problem even in industrial enterprises, which are widely used chemical reagent methods. Attempts to transfer this experience in agriculture in general has not been successful because the traditional methods and technologies are not adapted to the conditions of agriculture require huge capital costs for associated infrastructure and industrial engineering of the necessary reagents of shipping them over long distances to the place of use.

An alternative to traditional methods of water purification from toxic aromatics are electrochemical technologies that should be attributed to relatively reagent less, as latter are formed at the time of use. Other advantages include their efficiency, ease of use, ease of automation, modularity structures and the flexibility to scale based on the needs in use [5]. These techniques are promising for the treatment of water from a wide range of organic compounds of different types [6], for example, phenolic compounds [7; 8] and pesticides [9]. The electrochemical degradation of toxic pollutants is achieved both through direct transfer of electric charge between the electrode and the organic compounds and secondary chemical reactions, the oxidant in which are oxygen-containing radicals formed during electrolysis of water molecules. In both cases the optimal choice of anode material is critical, not only ratio, and direction of oxidation depends on it. For example, some electrodes in the oxidation of organic compounds may form polymers due to the nucleophilic attack of neutral molecules by radicals [10]. In recent years, a large number of materials have been used for the selective and non-selective anodic oxidation of resistant organic compounds, but the problem of choosing the optimal and chemically stable material still remains an open question requiring further study.

Experimental and Methods

All chemicals were reagent grade. Platinized titanium was used as substrate. Titanium sheet was treated as described in [11] before platinum layer depositing. Lead dioxide coatings were electrodeposited at anodic current density 10 $mA \cdot cm^{-2}$ from methanesulfonate electrolytes that contained 1M CH_3SO_3H, 0.1 M $Pb(CH_3SO_3)_2$ and 0.1 M $Bi(NO_3)_3$, $Ce(NO_3)_3$, $(CH_3COO)_4Sn$, $K_2(NiF_6)$, $K_2(SnF_6)$ as dopants. The determination of modifying additive in anodic materials was carried out with Graphite furnace atomic adsorption spectroscope [GF-AAS] model Analyst 800.

Bulletin of Dnipropetrovsk University. Series Chemistry, 2017, *25*(1), 27–35

Having in mind that the challenge in PbO_2 research is to obtain an electrochemically active and durable material, in this work we electrodeposited PbO_2 from $CH_3SO_3^-$-containing medium.

Since methanesulfonate is becoming the most popular electrolyte for PbO_2 electrosynthesis due to probability of the deposition of coatings up to 2 mm thick with low internal stresses [12], we chose these electrolytes because they are easy to prepare and work with; and PbO_2 obtained in this medium has satisfactory mechanical properties and significantly different electrocatalytical activity in respect to coatings, obtained in traditional nitrare baths.

X-ray powder diffraction data were collected on a STOE STADI P automatic diffractometer [13] equipped with linear PSD detector (transmission mode, $2\theta/\omega$-scan; Cu $K\alpha_1$ radiation, curved germanium (1 1 1) monochromator; 2θ-range $6.000 \le 2\theta \le 102.945$ 2θ with step 0.015 2θ; PSD step 0.480 °2θ, scan time 50 s/step).

Qualitative and quantitative phase analysis was performed using the PowderCell program [14]. For selected samples with relatively high degree of crystallinity the Rietveld refinement was carried out using FullProf.2k (version 5.40) program [15].

XPS studies were carried out on a PHI 5000 spectrometer using monochromatic AlKα radiation for excitation. The BE value of C(1s), due to adventtious carbon and residual solvent, is 284.8 [±0.3] eV.

The electrooxidation of organic compounds was carried out in undivided cell at $j_a = 50$mA cm^{-2}. The volume of anolyte was 50 cm^3. Solution, containing phosphate buffer (0.25 M Na_2HPO_4 + 0.1 M KH_2PO_4) + $2 \cdot 10^{-4}$ M organic compound, (pH = 6.55) was used as electrolyte. Stainless steel was used as cathode. Modified lead dioxide electrodes were used as anodes. Electrode surface area was 1 cm^2.

Analyses of the reaction products were conducted by HPLC using a Shimadzu RF-10A xL instrument equipped with a Ultraviolet SPD-20AV detector and a 30 cm Discovery® C18 column. Ozone analysis was carried out mostly by iodometric titration [16]. In some cases the results were checked by the spectrophotometric method. The formation of colored compounds during electrolysis was followed by UV-visible spectroscopy. The changing of the concentration of the organic substance during the electrolysis was measured by sampling (volume of 5 cm^3) at regular intervals and measuring the optical density of the solution in the ultraviolet and visible region (wavelength range 200–570 nm) using a Kontron Uvikon 940 spectrometer. Solution, containing phosphate buffer, was used as reference solution.

Results and Discussion

Electrochemical degradation of organics in the wastewater is known to be a very important task. The development of electrode materials used for wastewater treatment is recognized as the subject of many investigations. Synthetic diamond electrodes modified with boron (BDD), for example, commonly used as electrocatalysts [17], as well as anodes based on PbO_2 [18]. It should be noted that in the first case the basic problem is the high power consumption due to the low conductivity of modified synthetic diamond, which makes them unsuitable for use as anodes in industry. Thus, more promising are materials based on lead dioxide, the more so because of their electrocatalytic activity, which can be significantly increased by the modification.

The process of oxidation of organic substances is not necessarily a direct electrochemical process. Quite likely, it occurs via oxidants generated in the primary electrochemical reaction, for example, the formation of hydroxyl radicals and ozone. So this process is a secondary chemical process. It should also be noted, that it is not always taken into account the fact that the oxygen evolution reaction on the electrode can occur in conjunction with other reactions with the transfer of oxygen, such as oxidation of organic [17; 19] or inorganic compounds [18], which are not necessarily implemented independently of other.

The effectiveness of such processes depends on the ratio of the rates of reactions both of the formation and the disappearance of OH-radicals. The accumulation of a sufficient amount of radicals on the electrode surface and the near electrode layer facilitates their interaction with inorganic and organic compounds, causing partial or complete destruction of these compounds [12].

The synthesis of strong oxidants such as ozone can be assigned to another group of anodic reactions occurring at high anodic potentials with oxygen-containing particles participation. Since ozone formation occurs simultaneously with the oxidation processes of organic compounds [20; 21], its synthesis in the electrolysis process can contribute to the destruction of toxic organic substances. As one can conclude from the obtained results, the current efficiencies of ozone evolution on electrodes deposited from methanesulfonate electrolytes are approximately three times lower than on the materials obtained from

nitrate bath [22]. Modification by ionic additives increases the current efficiency of ozone, but the latter is characterized by the values in the range of a few percent [12].

An observed phenomenon is caused by differences in the chemical and phase composition of deposits obtained from nitrate and methanesulfonate electrolytes, namely, in the degree of surface hydroxylation. As the oxygen species strongly bounded with the electrode surface are involved in the process of ozone evolution [23], the decrease in their number would lead to a decrease in current efficiencies of ozone evolution, which is observed in the case of coatings obtained from the methanesulfonate electrolytes [22; 24; 25].

In order to determine the influence of deposition conditions and the composition of the anode materials, based on lead dioxide, on their electrocatalytic activity in respect to the oxidation of organic toxicants 4-nitroaniline and 4-nitrophenol were selected as model aromatics. This choice was due to the fact that the electrochemical incineration of phenolic compounds on the different electrodes is well studied process, so the attention can be focused only on the clarifying of the role of the anode material.

Thus, in particular, a considerable number of publications are devoted to aromatic compounds electrooxidation, in which PbO_2 and other oxides of noble metals are used as anode materials [2; 12; 26]. The anodic oxidation of phenols may occur in two pathways, depending on the acid-base properties of the system [27–31].

Oxidation of *p*-nitroaniline. As it is noted in [32], the general mechanism of the oxidation of organic compounds of aromatic nature will include oxidizing of compounds to the intermediates with quinoid structure, reactions of aromatic ring opening and formation of aliphatic products [mainly acids] and in ideal case – the complete mineralization to CO_2 and H_2O. According to [33], quite a number of intermediates are produced during anodic oxidation of *p*-nitroaniline. The primary intermediates include maleic acid and benzoquinone.

The mechanism of *p*-nitroaniline electrooxidation on modified lead dioxide electrodes was considered in detail in our previous publications [12]. The HPLC investigation has shown 1,4-benzoquinone as the major aromatic intermediate. Only aliphatic acids can be detected in a solution after long-term electrolysis.

Electronic absorption spectra of solutions at different electrolysis time were taken in order to determine the time of the disappearance of intermediate aromatic products and a change in the concentration of the initial compound.

Fig. 1 shows the absorption spectra in the visible and UV regions obtained at different times of electrolysis in a phosphate buffer on nonmodified lead dioxide anode.

It should be noted that electrocatalytic activity of lead dioxide anodes in respect to the oxidation of *p*-nitroaniline depends on the concentration of methanesulfonate ions in the deposition electrolyte.

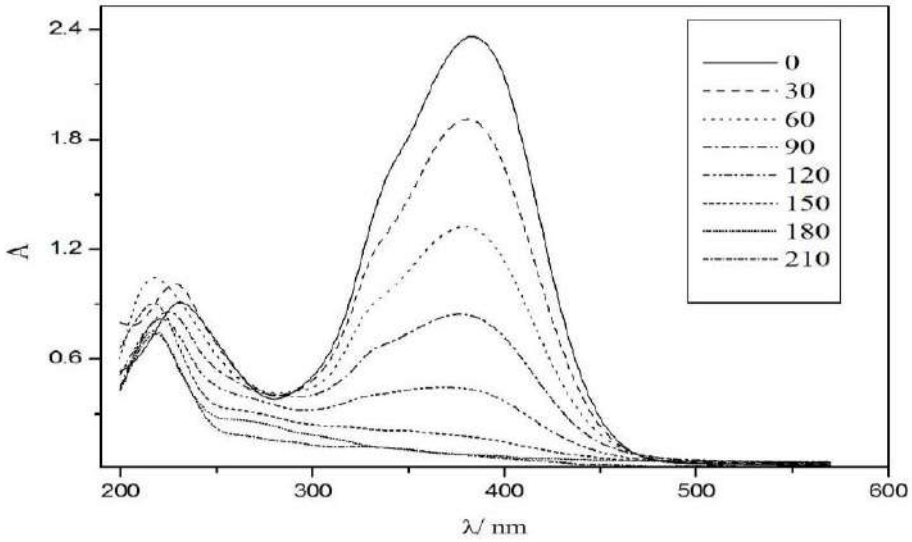

Fig. 1. The absorption spectra of *p*-nitroanilline solution (initial concentration $2 \cdot 10^{-4}$M) obtained at different time of electrolysis in a phosphate buffer on lead dioxide anode

Bulletin of Dnipropetrovsk University. Series Chemistry, 2017, *25*(1), 27–35

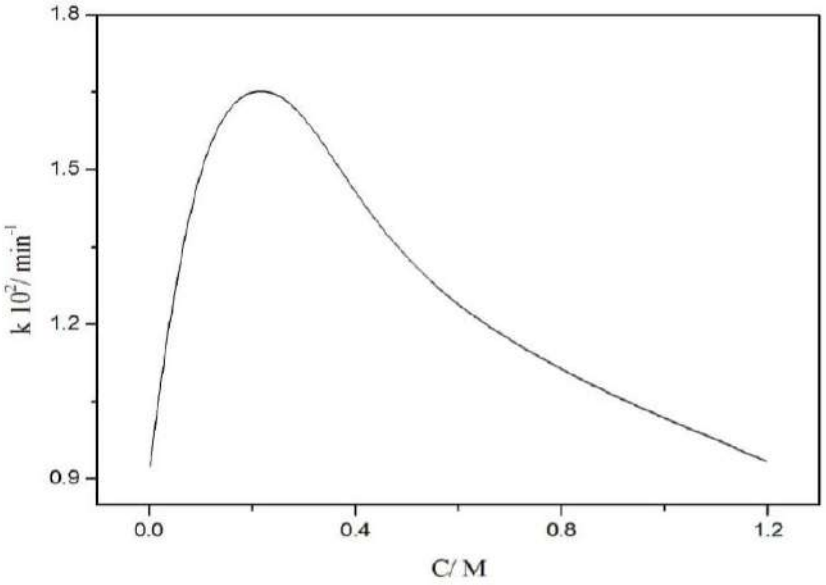

Fig. 2. The plot of apparent heterogeneous rate constant of *p*-nitroanilline oxidation on PbO_2-anodes versus the concentration of CH_3SO_3Na in the deposition solution

The dependence has extreme character with a maximum at 0.1–0.3 M concentrations of CH_3SO_3Na (Fig. 2). As follows from the obtained results (Table 1), the chemical composition of lead dioxide is practically no changed. In this case, structural factors play a significant role. Maximum electrocatalytic activity is achieved by increasing the proportion of α-phase, on the one hand, and increase the crystalline zone of oxide on the other, which leads to increased amounts of oxygen containing particles strongly bounded to the electrode surface that participate in the electrochemical oxidation of aromatic compounds [12].

Table 1

The phase composition of lead dioxide coatings depending on deposition conditions

Deposit	T/K	Content /wt.%/ α-PbO_2/β-PbO_2
PbO_2	282	59/41
PbO_2	298	90/10
PbO_2–1.81 wt.% Bi	282	5/95
PbO_2–0.019 wt.% Ce	298	83/17
PbO_2–1.81 wt.% Sn	298	44/56
PbO_2–0.042 wt.% Ni; 0.043 wt.% F	298	0/100
PbO_2–1.56 wt.% Sn; 0.04 wt.% F	298	38/62

Obtained results can be satisfactorily described in the framework of the mechanism [12], wherein the primary intermediate is benzoquinone. Since the electrochemical destruction of *p*-nitroaniline occurs via the formation of benzoquinone, electrochemical destruction of this compound was investigated further. Fig. 3 shows the absorption spectra of *p*-benzoquinone solution obtained at different time of electrolysis in a phosphate buffer on lead dioxide anode. Kinetic parameters of the electrochemical oxidation of *p*-benzoquinone were commented in [12].

The processes of *p*-nitroaniline electrochemical oxidation on unmodified and modified lead dioxide electrodes occur qualitatively the same and differ only in the rate. This suggests the invariability of the mechanism of *p*-nitroaniline oxidation on different materials that allows one for a correct comparison of their electrocatalytic activity.

According to calculations (Table 2), based on kinetic studies of the reaction rate constant of *p*-nitroaniline degradation depends on the composition of the electrode material and varies due to the nature and content of ionic additives in lead dioxide.

The maximum interest for the electrochemical destruction of organic substances represents lead dioxide electrodes modified by bismuth to which a rate constant of *p*-nitroaniline oxidation increases in 1.6 times compared with nonmodified electrodes (see Table 2). In other cases, the rate constants are comparable.

Oxidation of *p*-nitrophenol. Since mechanism of electrooxidation of *p*-nitrophenol was considered in detail previously, let's concentrate only of the effect of dopants on the reaction rate. Fig. 4 shows the absorption spectra of *p*-nitrophenol solution obtained at different time of electrolysis in a phosphate buffer on lead dioxide anode.

Bulletin of Dnipropetrovsk University. Series Chemistry, 2017, *25*(1), 27–35

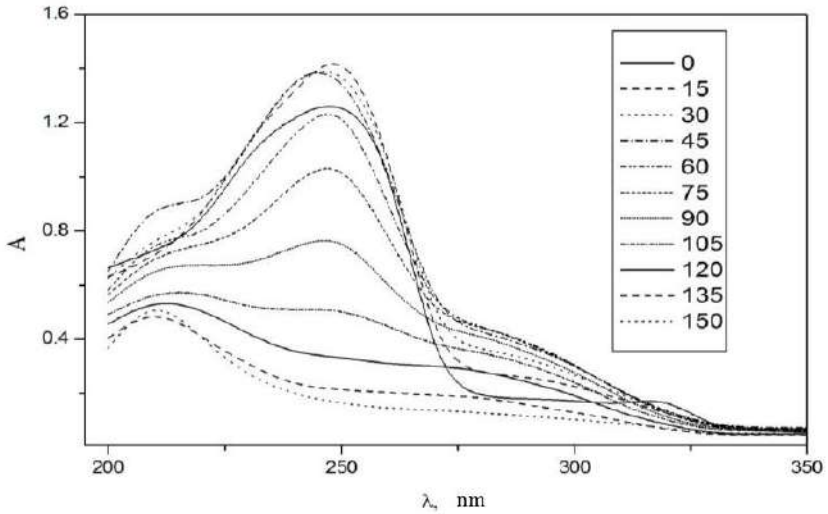

Fig. 3. The absorption spectra of *p*-benzoquinone solution (initial concentration 10^{-4}M) obtained at different time of electrolysis in a phosphate buffer on lead dioxide anode

As was suggested in [12], maleic acid and a stoichiometric amount of NO_3^- were detected as electrolysis products by high performance liquid chromatography. The primary aromatic intermediate in this case was also a 1,4-benzoquinone, but its concentration was an order of magnitude higher than in the oxidation of *p*-nitroaniline [12]. The latter indicates a more effective destruction of the aromatic ring in the case of *p*-nitroaniline.

As one can conclude from obtained results (Table 3) rate constants of *p*-nitrophenol oxidation on modified lead dioxide electrodes somewhat lower than those for *p*-nitroaniline [12].

Table 2

Kinetic parameters of the electrochemical oxidation of *p*-nitroaniline ($2 \cdot 10^{-4}$ M) on modified PbO_2-anodes

Anode	Apparent heterogeneous rate constant, $k \cdot 10^2$, min^{-1}
PbO_2	1.68
PbO_2–1.81 wt.% Bi	2.76
PbO_2–0.019 wt.% Ce	1.36
PbO_2–1.81 wt.% Sn	1.38
PbO_2–0.042 wt.% Ni; 0.043 wt.% F	1.66
PbO_2–1.56 wt.% Sn; 0.04 wt.% F	1.38

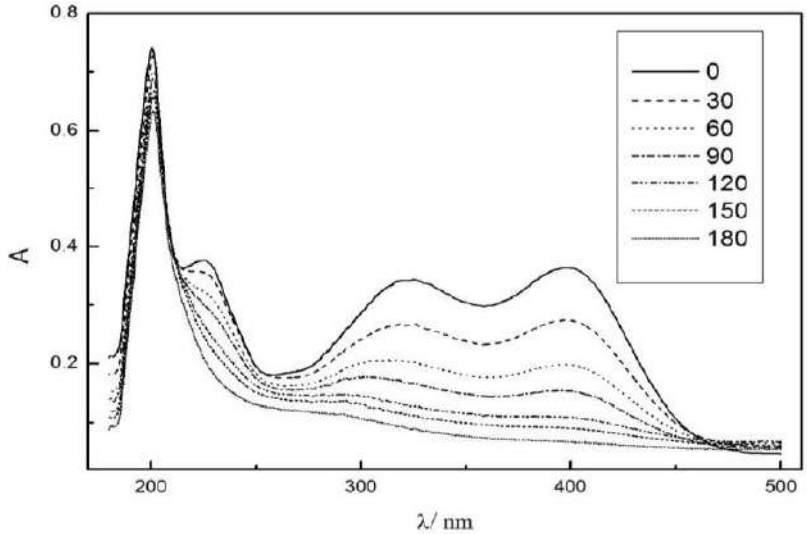

Fig. 4. The absorption spectra of *p*-nitrophenol solution (initial concentration $2 \cdot 10^{-4}$M) obtained at different time of electrolysis in a phosphate buffer on lead dioxide anode

Table 3

Kinetic parameters of the electrochemical oxidation of *p*-nitrophenol ($2 \cdot 10^{-4}$ M) on modified PbO_2-anodes

Anode	Apparent heterogeneous rate constant, $k \cdot 10^2$, min^{-1}
PbO_2	0.84
PbO_2–1.81 wt.% Bi	0.88
PbO_2–0.019 wt.% Ce	0.52
PbO_2–1.87 wt.% Sn	0.54
PbO_2–0.042 wt.% Ni; 0.043 wt.% F	0.82
PbO_2–1.56 wt.% Sn; 0.04 wt.% F	0.52

Conclusions

The processes of electrochemical oxidation of investigated organic compound on unmodified and modified lead dioxide electrodes occur qualitatively the same and differ only in the rate. This suggests the invariability of the mechanism of their oxidation on different materials that allows one for a correct comparison of their electrocatalytic activity.

According to calculations, based on kinetic studies of the reaction rate constant of organic compounds degradation depends on the composition of the electrode material and varies due to the nature and content of ionic additives in lead dioxide.

The maximum interest for the electrochemical destruction of organic substances represents lead dioxide electrodes modified by bismuth to which a rate constant of *p*-nitroaniline oxidation increases in 1.6 times compared with nonmodified electrodes. In other cases, the rate constants are comparable.

Bibliography

[1] Oturan M. A. Advanced oxidation processes in water/-wastewater treatment: principles and applications. A review / M. A. Oturan, J.-J. Aaron // Crit. Rev. Env. Sci. Tech. – 2014. – Vol. 44. – P. 2577–2641.

[2] Chaplin B. P. Critical review of electrochemical advanced oxidation processes for water treatment applications / B.P. Chaplin // Environ. Sci.: Processes Impacts. – 2014. – Vol. 16. – P. 1182–1203.

[3] Brillas E. Decontamination of wastewaters containing synthetic organic dyes by electrochemical methods. An updated review /E. Brillas, C. A. Martinez-Huitle // Appl Catal., B. – 2015. – Vol. 166–167. – P. 603–643.

[4] Martinez-Huitle C. A. Decontamination of wastewaters containing synthetic organic dyes by electrochemical methods: a general review / C. A. Martinez-Huitle, E. Brillas// Appl Catal., B. – 2009. – Vol. 87. – P. 105–145.

[5] Reaction sequence for the mineralization of the short-chain carboxylic acids usually formed upon cleavage of aromatics during electrochemical Fenton treatment /M. A. Oturan, M. Pimentel, N. Oturan, I. Sires // Electrochim. Acta. – 2008. – Vol. 54. – P. 173–182.

[6] Electrochemical oxygen transfer reactions: electrode materials, surface processes, kinetic models, linear free energy correlations, and perspectives. A review / R. Vargas, C. Borras, D. Mendez [et al.] // J. Solid State Electrochem. – 2016. – Vol. 20. – P. 875–893.

[7] Degradation of chlorophenols by means of advanced oxidation processes: a general review / M. Pera-Titus, V. Garcia-Molina, M. A. Bacos [et al.] // Appl. Catal., B. – 2004. – Vol. 47. – P. 219–256.

[8] Enache T. A. Phenol and para-substituted phenols electrochemical oxidation pathways / T. A. Enache, A. M. Oliveira-Brett // J. Electroanal. Chem. – 2011. – Vol. 655. – P. 9–16.

[9] Dhaouadi A. Degradation of paraquat herbicide by electrochemical advanced oxidation methods / A. Dhaouadi, N. Adhoum // J. Electroanal. Chem. – 2009. – Vol. 637. – P. 33–42.

[10] Antonopoulou M. A review on advanced oxidation processes for the removal of taste and odor compounds from aqueous media / M. Antonopoulou, E. Evgenidou, D. Lambropoulou, I. Konstantinou // Water Res. – 2014. – Vol. 53. – P. 215–234.

[11] Electrodeposition of Ni^{2+}-doped PbO_2 and physico-chemical properties of the coating / O. Shmychkova, T. Luk'yanenko, R. Amadelli, A. Velichenko // J. Electroanal. Chem. – 2016. – Vol. 774. – P. 88-94.

[12] Electrooxidation of some phenolic compounds at Bi-doped PbO_2 / O. Shmychkova, T. Luk'yanenko, A. Yakubenko [et al.] // Appl. Catal., B. – 2015. – Vol. 162. – P. 346–351.

[13] STOE WinXPOW, version 3.03. Darmstadt: Stoe & Cie GmbH, 2010.

[14] Kraus W. PowderCell for Windows (version 2.4) / W. Kraus, G. Nolze. – Berlin: Federal Institute for Materials Research and Testing, 2000.

[15] Rodriguez-Carvajal J. Recent developments of the program FULLPROF, commission on powder diffraction (IUCr) / J. Rodriguez-Carvajal // Newsletter. – 2001. – Vol. 26. – P. 12-19.

[16] Electrocatalytic dechlorination of atrazine using binuclear iron phthalocyanine as electrocatalysts / Y. M. Vera, R. J. de Carvalho, M. L. Torem, B. A. Calfa // Chem. Eng. J. – 2009. – Vol. 155. – P. 691-697.

[17] Comninellis C., Chen G. (Ed.). Electrochemistry for the environment. – New York: Springer, 2010. – 553 p.

[18] Li X. Electrodeposited lead dioxide coatings /X. Li, D. Pletcher, F. C. Walsh // Chem. Soc. Rev. – 2011. – Vol. 40. – P. 3879–3894.

[19] Panizza M. Direct and mediated anodic oxidation of organic pollutants/ M. Panizza, G. Cerisola // Chem. Rev. – 2009. – Vol. 109. – P. 6541–6569.

[20] Influence of anions on oxygen/ozone evolution on PbO_2/spe and PbO_2/Ti electrodes in neutral pH media/ A. A. Babak, R. Amadelli, A. De Battisti, V. N. Fateev // Electrochim. Acta. – 1994. – Vol. 39. – P. 1597–1602.

[21] Ozone electrosynthesis in an electrolyzer with solid polymer electrolyte/ A. A. Babak, V. N. Fateev, R. Amadelli, G. F. Potapova // Russ. J. Electrochem. – 1994. – Vol. 30. – P. 739–741.

[22] Physico-chemical properties of PbO_2-anodes doped with Sn^{4+} and complex ions / O. Shmychkova, T. Luk'yanenko, R. Amadelli, A. Velichenko // J. Electroanal. Chem. – 2014. – Vol. 717–718. – P. 196–201.

[23] Trassatti S. Electrodes of conductive metallic oxide. Part B / S. Trassatti, G. Lodi. – Amsterdam, Oxford, New York, 1981. – P. 521–626.

[24] Bi-doped PbO_2 anodes: electrodeposition and physico-chemical properties / O. Shmychkova, T. Luk'yanenko, A. Velichenko [et. al.] // Electrochim. Acta. 2013, 111, 332–338.

[25] Electrodeposition of Ce-doped PbO_2/ O. Shmychkova, T. Luk'yanenko, A. Velichenko, R. Amadelli // J. Electroanal. Chem. – 2013. – Vol. 706. – P. 86–92.
[26] Liu Y. Comparative studies on the electrocatalytic properties of modified PbO_2 anodes /Y. Liu, H. Liu // Electrochim. Acta. – 2008. – Vol. 53. – P. 5077–5476.
[27] Kim J. Comparative study of electrochemical degradation and ozonation of nonylphenol / J. Kim, G. V. Korshin, A. B. Velichenko // Water Res. – 2005. – Vol. 39. – P. 2527–2534.
[28] Electrocatalytic degradation of 4-chlorophenol on F-doped PbO_2 anodes/ J. Cao, H. Zhao, F. Cao [et al.] // Electrochim. Acta. – 2009. – Vol. 54. – P. 2595–2602.
[29] Electrocatalytic oxidation of *p*-nitrophenol from aqueous solutions at Pb/PbO_2 anodes / M. A. Quiroz, S. Reyna, C. A. Martinez-Huitle [et al.] // Appl. Catal., B. – 2005. – Vol. 59. – P. 259–266.
[30] Influence of chloride ion on electrochemical degradation of phenol in alkaline medium using bismuth doped and pure PbO_2 anodes / J. Iniesta, J. Gonzalez-Garsia, E. Exposito [et al.] // Water Res. – 2001. – Vol. 35. – P. 3291–3300.
[31] Kawagoe K. T. Electrosynthesis and physicochemical properties of PbO_2 films / K. T. Kawagoe, D. C. Johnson // J. Electrochem. Soc. – 1994. – Vol. 141. – P. 3404–3409.
[32] Study of the oxidation of solutions of *p*-chlorophenol and *p*-nitrophenol on Bi-doped PbO_2 electrodes by UV-vis and FTIR in situ spectroscopy / C. Borras, T. Laredo, J. Mostany, B. R. Scharifker // Electrochim. Acta. – 2004. – Vol. 49. – P. 641–648.
[33] Widera J. Electrochemical oxidation of aniline in a silica sol–gel matrix/ J. Widera, J. A. Cox // Electrochem. Commun. – 2002. – Vol. 4. – P. 118–122.

References

[1] Oturan, M. A., Aaron, J.-J. (2014). Advanced oxidation processes in water/wastewater treatment: principles and applications. A review. *Crit. Rev. Env. Sci. Tech., 44*, 2577–2641. doi: http://dx.doi.org/10.1080/10643389.2013.829765
[2] Chaplin, B. P. (2014). Critical review of electrochemical advanced oxidation processes for water treatment applications. *Environ. Sci.: Processes Impacts., 16*, 1182–1203. doi: http://dx.doi.org/10.1039/C3EM00679D
[3] Brillas, E., Martinez-Huitle, C. A. (2015). Decontamination of wastewaters containing synthetic organic dyes by electrochemical methods. An updated review. *Appl Catal., B, 166–167*, 603–643. doi: https://doi.org/10.1016/j.apcatb.2014.11.016
[4] Martinez-Huitle, C. A., Brillas, E. (2009). Decontamination of wastewaters containing synthetic organic dyes by electrochemical methods: a general review. *Appl. Catal., B, 87*, 105–145. doi: https://doi.org/10.1016/j.apcatb.2008.09.017
[5] Oturan, M. A., Pimentel, M., Oturan N., Sires, I. (2008). Reaction sequence for the mineralization of the short-chain carboxylic acids usually formed upon cleavage of aromatics during electrochemical Fenton treatment. *Electrochim. Acta, 54*, 173–182. doi: https://doi.org/10.1016/j.electacta.2008.08.012
[6] Vargas, R., Borras, C., Mendez, D., Mostany, J., Scharifker, B. R. (2016). Electrochemical oxygen transfer reactions: electrode materials, surface processes, kinetic models, linear free energy correlations, and perspectives. A review. *J. Solid State Electrochem., 20*, 875–893. doi: https://doi.org/10.1007/s10008-015-2984-7
[7] Pera-Titus, M., Garcia-Molina, V., Bacos, M. A., Gimenez, J., Esplugas, S. (2004). Degradation of chlorophenols by means of advanced oxidation processes: a general review. *Appl. Catal., B, 47*, 219–256. doi: https://doi.org/10.1016/j.apcatb.2003.09.010
[8] Enache, T. A., Oliveira-Brett, A. M. (2011). Phenol and para-substituted phenols electrochemical oxidation pathways. *J. Electroanal. Chem., 655*, 9–16. doi: https://doi.org/10.1016/j.jelechem.2011.02.022
[9] Dhaouadi, A., Adhoum, N. (2009). Degradation of paraquat herbicide by electrochemical advanced oxidation methods. *J. Electroanal. Chem., 637*, 33–42. doi: https://doi.org/10.1016/j.jelechem.2009.09.027
[10] Antonopoulou, M., Evgenidou, E., Lambropoulou, D., Konstantinou, I. (2014). A review on advanced oxidation processes for the removal of taste and odor compounds from aqueous media. *Water Res., 53*, 215–234. doi: https://doi.org/10.1016/j.watres.2014.01.028
[11] Shmychkova, O., Luk'yanenko, T., Amadelli, R., Velichenko, A. (2016). Electrodeposition of Ni^{2+}-doped PbO_2 and physico-chemical of the coating. *J. Electroanal. Chem., 774*, 88-94. doi: https://doi.org/10.1016/j.jelechem.2016.05.017
[12] Shmychkova, O., Luk'yanenko, T., Yakubenko, A., Amadelli, R., Velichenko, A. (2015). Electrooxidation of some phenolic compounds at Bi-doped PbO_2. *Appl. Catal., B, 162*, 346–351. doi: https://doi.org/10.1016/j.apcatb.2014.07.011
[13] STOE WinXPOW, version 3.03. (2010). Darmstadt: Stoe & Cie GmbH.
[14] Kraus, W., Nolze, G. (2000). PowderCell for Windows (version 2.4) Berlin: Federal Institute for Materials Research and Testing.
[15] Rodriguez-Carvajal, J. (2001). *Recent developments of the program FULLPROF, Commission on powder diffraction (IUCr)*. Newsletter, *26*, 12–19.
[16] Vera, Y. M., de Carvalho, R. J., Torem, M. L., Calfa, B. A. (2009). Atrazine degradation by in situ electrochemically generated ozone. *Chem. Eng. J., 155*, 691-697. doi: https://doi.org/10.1016/j.cej.2009.09.001
[17] Comninellis C., Chen Guohua. (Ed.). *Electrochemistry for the environment* (2010). New York, USA: Springer. doi: http://dx.doi.org/10.1007/978-0-387-68318-8
[18] Li, X., Pletcher, D., Walsh, F.C. (2011). Electrodeposited lead dioxide coatings. *Chem. Soc. Rev., 40*, 3879–3894. doi: http://dx.doi.org/10.1039/c0cs00213e
[19] Panizza, M., Cerisola, G. (2009). Direct and mediated anodic oxidation of organic pollutants. *Chem. Rev., 109*, 6541–6569. doi: http://dx.doi.org/10.1021/cr9001319
[20] Babak, A. A., Amadelli, R., De Battisti, A., Fateev, V. N. (1994). Influence of anions on oxygen/ozone evolution on PbO_2/*spe* and PbO_2/Ti electrodes in neutral pH media. *Electrochim. Acta, 39*, 1597–1602. doi: https://doi.org/10.1016/0013-4686(94)85141-7
[21] Babak, A. A., Fateev, V. N., Amadelli, R., Potapova, G. F. (1994). Ozone electrosynthesis in an electrolyzer with solid polymer electrolyte. *Russ. J. Electrochem., 30*, 739–741.
[22] Shmychkova, O., Luk'yanenko, T., Amadelli, R., Velichenko, A. (2014). Physico-chemical properties of PbO_2-anodes doped with Sn^{4+} and complex ions. *J. Electroanal. Chem., 717-718*, 196-201. doi: https://doi.org/10.1016/j.jelechem.2014.01.029
[23] Trassatti, S., Lodi, G. (1981). *Electrodes of conductive metallic oxide. Part B.* (pp. 521-626). Amsterdam, Oxford, New York.
[24] Shmychkova, O., Luk'yanenko, T., Velichenko, A., Meda, L., Amadelli, R. (2013). Bi-doped PbO_2 anodes: electrodeposition and physico-chemical properties. *Electrochim. Acta, 111*, 332–338. doi: https://doi.org/10.1016/j.electacta.2013.08.082

[25] Shmychkova, O., Luk'yanenko, T., Velichenko, A., Amadelli, R. (2013). Electrodeposition of Ce-doped PbO_2. *J. Electroanal. Chem.*, *706*, 86–92. doi: https://doi.org/10.1016/j.jelechem.2013.08.002

[26] Liu, Y., Liu, H. (2008). Comparative studies on the electrocatalytic properties of modified PbO_2 anodes. *Electrochim. Acta*, *53*, 5077–5476. doi: https://doi.org/10.1016/j.electacta.2008.02.103

[27] Kim, J., Korshin, G. V., Velichenko, A. B. (2005). Comparative study of electrochemical degradation and ozonation of nonylphenol. *Water Res.*, *39*, 2527–2534. doi: https://doi.org/10.1016/j.watres.2005.04.070

[28] Cao, J., Zhao, H., Cao, F., Zhang, J., Cao, C. (2009). Electrocatalytic degradation of 4-chlorophenol on F-doped PbO_2 anodes. *Electrochim. Acta*, *54*, 2595–2602. doi: https://doi.org/10.1016/j.electacta.2008.10.049

[29] Quiroz, M. A., Reyna, S., Martinez-Huitle, C. A., Ferro, S., De Battisti, A. (2005). Electrocatalytic oxidation of *p*-nitro-phenol from aqueous solutions at Pb/PbO_2 anodes. *Appl. Catal., B*, *59*, 259–266. doi: https://doi.org/10.1016/j.apcatb.2005.02.009

[30] Iniesta, J., Gonzalez-Garsia, J., Exposito, E., Montiel, V., Aldaz, A. (2001). Influence of chloride ion on electrochemical degradation of phenol in alkaline medium using bismuth doped and pure PbO_2 anodes. *Water Res.*, *35*, 3291–3300. doi: https://doi.org/10.1016/S0043-1354(01)00043-4

[31] Kawagoe, K. T., Johnson, D. C. (1994). Electrosynthesis and physicochemical properties of PbO_2 films. *J. Electrochem. Soc.*, *141*, 3404–3409. doi: https://doi.org/10.1149/1.2059345

[32] Borras, C., Laredo, T., Mostany, J., Scharifker, B. R. (2004). Study of the oxidation of solutions of *p*-chlorophenol and p-nitrophenol on Bi-doped PbO_2 electrodes by UV-vis and FTIR in situ spectroscopy. *Electrochim. Acta*, *49*, 641–648. doi: https://doi.org/10.1016/j.electacta.2003.09.019

[33] Widera, J., Cox, J. A. (2002). Electrochemical oxidation of aniline in a silica sol–gel matrix. *Electrochem. Commun.*, *4*, 118–122. doi: https://doi.org/10.1016/S1388-2481(01)00287-9

Bulletin of Dnipropetrovsk University. Series Chemistry, 2017, *25*(1), 36–44

Вісник Дніпропетровського університету. Серія Хімія
Bulletin of Dnipropetrovsk University. Series Chemistry

p-ISSN 2306-871X, e-ISSN 2313-4984
journal homepage: http://chemistry.dnu.dp.ua

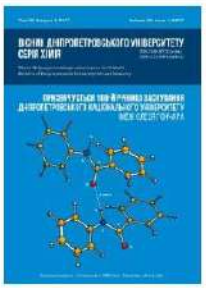

UDC 544.653.2

THE ELECTROCHEMICAL OXIDATION OF SALICYLIC ACID AND ITS DERIVATIVES ON MODIFIED PbO_2-ELECTRODES

Olesia B. Shmychkova[1], Tatiana V. Luk'yanenko[1], Rossano Amadelli[2], Larisa V. Dmitrikova[3], Alexander B. Velichenko[1*]

[1] *Ukrainian State University of Chemical Technology, 8, Gagarin Ave., 49005 Dnipro, Ukraine*
[2] *ISOF-CNR u.o.s Ferrara c/o Department of Chemical and Pharmaceutical Sciences, University of Ferrara, Via Luigi Borsari, 46-44121 Ferrara, Italy*
[3] *Oles Honchar Dnipropetrovsk National University, 72, Gagarin Ave., 49050 Dnipro, Ukraine*
Received 30 March 2017; revised 05 May 2017; accepted 26 June 2017, available online 05 December 2017

Abstract

The results of the study of electrochemical oxidation of salicylic acid on PbO_2-based anodes for effective wastewater treatment from organic pollutants have been summarized. Both the influence of various factors on the decomposition rate of organic substances and the influence of various modifying additives of lead dioxide anode on the process of mineralization of salicylic acid have been established. The total probable sequence of reactions to salicylic acid mineralization has been proposed. It is established that the destruction of salicylic acid in the first stage occurs through the accumulation of aromatic hydroxylation products, and during the total destruction - the destruction of the aromatic system with the formation of aliphatic compounds takes place. It is shown that the use of PbO_2, deposited from methanesulfonate electrolytes and modified electrodes significantly reduces the conversion time of salicylic acid in aliphatic products compared to lead dioxide anodes obtained by traditional technology from nitrate bath. The highest degradation rate occurs at the anodes modified by bismuth. It was found that the destruction of the 5-aminosalicylic acid occurs through an intermediate oxidation of amino-group to hydroxy.

Keywords: lead(IV) oxide, methanesulfonate electrolyte, electrochemical oxidation, salicylic acid.

ЕЛЕКТРОХІМІЧНЕ ОКИСНЕННЯ САЛІЦИЛОВОЇ КИСЛОТИ ТА ЇЇ ПОХІДНИХ НА МОДИФІКОВАНИХ PbO_2-ЕЛЕКТРОДАХ

Олеся Б. Шмичкова[1], Тетяна В. Лук'яненко[1], Росано Амаделлі[2], Лариса В. Дмітрікова[3], Олександр Б. Величенко[1,*]

[1] *ДВНЗ «Український державний хіміко-технологічний університет», пр. Гагаріна 8, м. Дніпро, 49005 Україна*
[2] *ISOF-CNR відділення в Феррарі, департамент хімії та фармації, Університет Феррари, вул. Л. Борсарі, 46–44121 Феррара, Італія*
[3] *Дніпропетровський національний університет імені Олеся Гончара, 72, пр. Гагаріна, Дніпро, 49050 Україна*

Анотація

У роботі наведено результати дослідження електрохімічного окиснення саліцилової кислоти на діоксидно-свинцевих анодах з метою ефективного очищення стічної води від органічних забрудників. Встановлено вплив різних факторів на швидкість процесів деструкції органічних речовин. Виявлено вплив різноманітних модифікуючих домішок діоксидносвинцевого електроду на процес окиснення саліцилової кислоти. Запропонована ймовірна загальна послідовність реакцій для мінералізації саліцилової кислоти. Показано, що під час руйнування саліцилової кислоти на першому етапі відбувається накопичення ароматичних продуктів гідроксилювання, а під час повної деструкції – руйнування ароматичної системи з утворенням аліфатичних сполук. Виявлено, що за використання PbO_2, осадженого з метансульфонатних розчинів, та PbO_2, модифікованого добавками іонів, суттєво зменшується час конверсії саліцилової кислоти в аліфатичні продукти порівняно із часом за використання плюмбум(IV) оксиду, осадженого за традиційною технологією з нітратних розчинів. Найбільша швидкість перетворення спостерігається за використання діоксидно-свинцевого аноду, модифікованого Бісмутом. Було виявлено, що руйнування 5-аміносаліцилової кислоти проходить через проміжне окиснення аміно-групи до гідрокси-групи.

Ключові слова: плюмбум(IV) оксид, метансульфонатний електроліт, електрохімічне окиснення, саліцилова кислота.

**Corresponding author: Tel.: +380562473627; e-mail address: velichenko@ukr.net*

doi: 10.15421/081706

Bulletin of Dnipropetrovsk University. Series Chemistry, 2017, *25*(1), 36–44

ЭЛЕКТРОХИМИЧЕСКОЕ ОКИСЛЕНИЕ САЛИЦИЛОВОЙ КИСЛОТЫ И ЕЕ ПРОИЗВОДНЫХ НА МОДИФИЦИРОВАННЫХ PbO_2-ЭЛЕКТРОДАХ

Олеся Б. Шмычкова[1], Татьяна В. Лукьяненко[1], Россано Амаделли[2], Лариса В. Дмитрикова[3], Александр Б. Величенко[1,*]

[1]*ГВУЗ «Украинский государственных химико-технологический университет», пр Гагарина 8, г. Днипро, 49005, Украина*

[2]*ISOF-CNR отделение в Ферраре, департамент химии и фармации, Университет Феррары, ул. Л. Борсари, 46–44121 Феррара, Италия*

[3] *Днепропетровский национальный университет имени Олеся Гончара, 72, пр. Гагарина, Днипро, 49050 Украина*

Аннотация

В работе приведены результаты исследования электрохимического окисления салициловой кислоты на диоксидносвинцовых анодах с целью эффективной очистки сточной воды от органических загрязнителей. Установлено влияние различных факторов на скорость процессов деструкции органических веществ. Показано влияние различных модифицирующих добавок диоксидносвинцового электрода на процесс окисления салициловой кислоты. Предложена вероятная общая последовательность реакций для минерализации салициловой кислоты. Установлено, что при разрушении салициловой кислоты на первом этапе происходит накопление ароматических продуктов гидроксилирования, а при полной деструкции – разрушение ароматической системы с образованием алифатических соединений. Показано, что при использовании PbO_2, осажденного из метансульфонатных электролитов, а также модифицированного PbO_2 существенно снижается время конверсии салициловой кислоты в алифатические продукты по сравнению со временем при использовании диоксидносвинцового анода, осажденного по традиционной технологии из нитратной ванны. Наибольшая скорость превращения наблюдается на диоксидносвинцовом аноде, модифицированном висмутом. Было установлено, что деструкция 5-аминосалициловой кислоты происходит через промежуточное окисление амино-группы до гидрокси-группы.

Ключевые слова: плюмбум(IV) оксид, метансульфонатный электролит, электрохимическое окисление, салициловая кислота.

Introduction

The development of new highly efficient methods to wastewater treatment is one of the most serious problems faced by researchers [1; 2]. Known purification methods have several disadvantages associated with significant energy consumption or imperfection of disinfection. Hence there is the need for new methods to rapidly and efficiently destruct organic pollutants to CO_2 and H_2O.

The choice of optimal technological schemes of water purification are quite a challenge because of the large amount of impurities that are in it, and because of the high demands placed on the quality of treated water. However, it should be noted that the electrochemical water treatment methods are now increasingly spreading in practice due to their high efficiency and functionality. Apparatus for implementing these methods is quite compact, high-performance, management and operation processes can be relatively easily automated. In addition, electrotreatment for its proper combination with other methods can successfully purify natural and wastewater from a number of different additives and dispersion. Very positive is the fact that for the electrochemical treatment is usually not increased salinity of water and ruled out the formation of more toxic pollutants. This method provides in some cases not only clean but also disinfected water. This provides significant advantages of electrochemical methods to traditional methods of water treatment [3–10].

Careful study of the mechanism of anodic reactions might help in the future to increase the selectivity and the using of preparative electrochemical organic chemistry processes [11].

Salicylic acid is one of the most common pollutants of wastewater. The latter is used in many pharmaceutical and cosmetic preparations. It is known to get by hydrolytic deacetylation of acetylsalicylic acid (aspirin), which is a major source of accumulation in wastewater. Thousands of tons of pharmaceuticals consumed annually worldwide man used in veterinary medicine and in agriculture. Due to inefficient destruction of pollutants sewage plants, quite a number of these substances was found in soil and even water. This necessitates the development of powerful methods for oxidation to effectively remove drugs and their metabolites from wastewater [12].

Water purification of salicylic acid is possible through oxidative destruction. There are different ways of salicylic acid oxidation of which the electrochemical oxidation is considered the most promising [13–15]. It is proved that the efficiency of oxidation depends on the material of the anode. The use of oxides as electrode materials in most cases is advantageous compared to metal electrodes, this allows a lower cost electrode and ensures to control occurred electrochemical processes due to change of the composition of oxide during its synthesis.

Bulletin of Dnipropetrovsk University. Series Chemistry, 2017, *25*(1), 36–44

The aim of our work was to study the electrochemical destruction of salicylic acid and its derivatives on lead(IV) oxide-based anode materials.

Experimental and Methods

All chemicals were reagent grade. Platinized titanium was used as substrate. Titanium sheet was treated as described in [16] before platinum layer depositing. Lead dioxide coatings were electrodeposited at anodic current density 10 mA · cm^{-2} from nitrate / methanesulfonate electrolytes that contained 0.1M HNO_3/CH_3SO_3H, 0.1 M $Pb(NO_3)_2$/$Pb(CH_3SO_3)_2$ and 0.1 M $Bi(NO_3)_3$, $Ce(NO_3)_3$ as dopants.

X-ray powder diffraction data were collected on a STOE STADI P automatic diffractometer [17] equipped with linear PSD detector (transmission mode, $2\theta/\omega$-scan; Cu $K\alpha_1$ radiation, curved germanium (1 1 1) monochromator; 2θ-range $6.000 \le 2\theta \le 102.945$ °2θ with step 0.015 °2θ; PSD step 0.480 °2θ, scan time 50 s/step).

Qualitative and quantitative phase analysis was performed using the PowderCell program [18]. For selected samples with relatively high degree of crystallinity the Rietveld refinement was carried out using FullProf.2k (version 5.40) program [19].

The electrooxidation of organic compounds was carried out in divided cell at j_a = 50 mA cm^{-2}. The volume of anolyte was 1300 cm^3. Solution, containing phosphate buffer (0.25 M Na_2HPO_4 + 0.1 M KH_2PO_4) + $2 \cdot 10^{-4}$ M organic compound, (pH = 6.55) was used as electrolyte. Stainless steel was used as cathode. Modified lead dioxide electrodes were used as anodes. Electrode surface area was 2.5 cm^2.

Analyses of the reaction products were conducted by HPLC using a Shimadzu RF-10A xL instrument equipped with a Ultraviolet SPD-20AV detector and a 30 cm Discovery® C18 column. The formation of colored compounds during electrolysis was followed by UV-visible spectroscopy using a UV mini 1240 Shimadzu spectrometer.

The composition and structure of intermediates was confirmed by HPLC using a Shimadzu RF-10A xL instrument equipped with a Ultraviolet SPD-20AV detector and a 30 cm Discovery® C18 column.

Since the action of iron(III) chloride to monohydric and polyhydric phenols in aqueous neutral or weakly acidic solutions having the characteristic color, which does not depend, however, on the structure of phenols [20], a qualitative analysis of diluting solution with 1% solution of iron(III) chloride was conducted.

It is known that salicylic acid gives violet, hydroquinone, 2,3-dihydroxybenzoic and 2,5-dihydroxybenzoic acids give blue color. If in the ortho position to the phenolic groups are complexing group, the color with iron(III) chloride appears both in water and alcohol medium, resulting in formation of complex iron salts. These complexing groups include mainly carbonyl (aldehyde and ketone), carboxyl, hydroxyl and alkoxyl, and sulpho-groups [20].

Results and Discussion

Since the electrodeposition of lead(IV) oxide occurs through the formation of chemisorbed oxygen-containing particles, the presence in the electrolyte of ionic dopants which can be adsorbed or form oxygen-containing compounds with these particles on the surface of the electrode, leads to changes in kinetic regularities of PbO_2 formation and physicochemical properties of coatings. The electrodeposition rate is affected by the composition of the electrolyte.

The typical morphology of lead(IV) oxide that was deposited from nitrate and methanesulfonate electrolytes, is shown on fig. 1. As one can see (fig. 1a), PbO_2 obtained from nitrate solutions is represented by a set of large polycrystalline blocks with no significant preferences in crystallographic orientation [15]. The using of methanesulfonate electrolytes leads to significant changes in the morphology of the coating (fig. 1b). In this case, polycrystalline blocks are not formed and the surface is a mixture of randomly oriented fine-grained crystals of nano and submicron size with a uniform surface. Specific electrode surface increases in several times. A similar phenomenon was observed when the polyelectrolyte and surfactant particles were included in the growing PbO_2 deposit [21].

In order to determine the influence of deposition conditions and the composition of the anode materials, based on lead dioxide, on their electrocatalytic activity in respect to the oxidation of organic toxicants salicylic acid and its derivatives were selected as model aromatics.

According to [14], quite a number of intermediates are produced during anodic oxidation of salicylic acid. The primary intermediates include dihydroxybenzoic acids.

Electronic absorption spectra of solutions at different electrolysis time were taken in order to determine the time of the disappearance of intermediate aromatic products and a change in the concentration of the initial compound.

Bulletin of Dnipropetrovsk University. Series Chemistry, 2017, *25*(1), 36–44

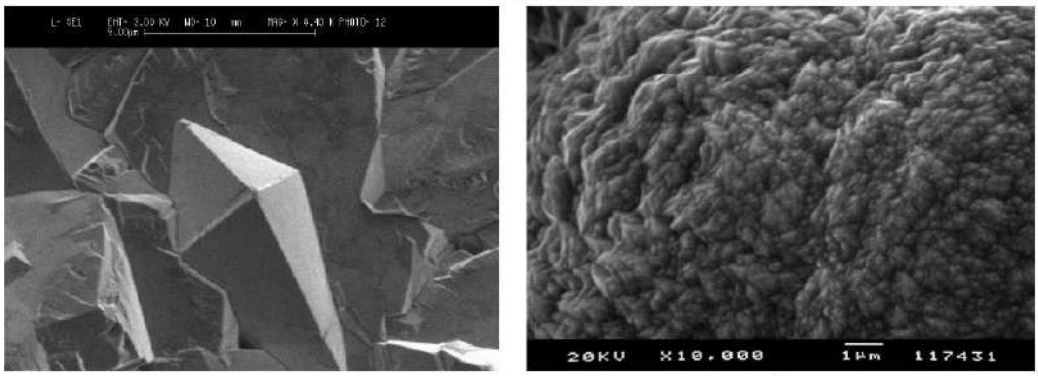

a *b*

Fig. 1. SEM micrographs of coatings, obtained from next solutions: *a* – 0.1 M $Pb(NO_3)_2$ +0.1 $MHNO_3$; *b* – 0.1M $Pb(CH_3SO_3)_2$ + 0.1M CH_3SO_3H

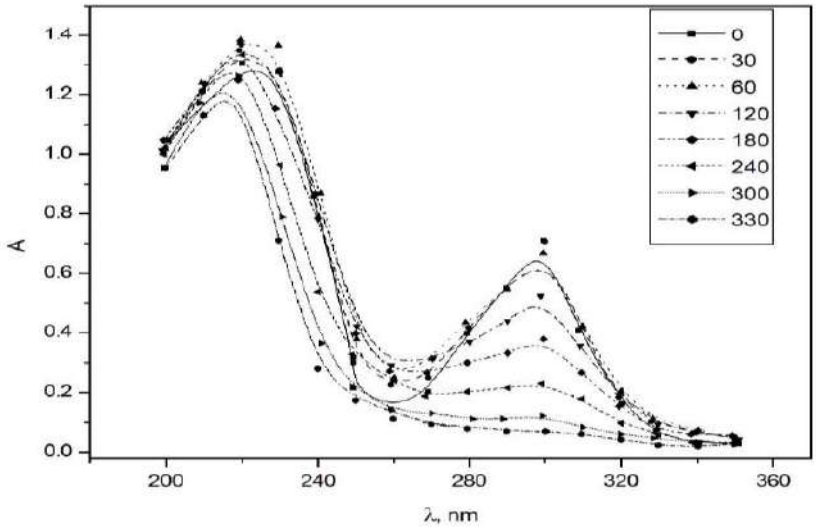

Fig. 2. The absorption spectra of salicylic acid solution (initial concentration $2 \cdot 10^{-4}$M) obtained at different time of electrolysis in a phosphate buffer on lead dioxide anode, pH = 6.55

Fig. 2 shows the absorption spectra in the visible and UV regions obtained at different times of electrolysis in a phosphate buffer on nonmodified lead dioxide anode.

The initial solution of salicylic acid is characterized by a peak in the 290–300 nm. After 30 minutes of electrolysis the intensity of the peak decreases and the plateau at 250–270 nm appears, due to the drop in the concentration of salicylic acid and the formation of intermediate aromatic products. Further increase in electrolysis time leads to the disappearance of peak at 290–300 nm, and reducing the plateau at 250–270 nm due to the complete destruction of salicylic acid and intermediates. After 5.5 hours of electrolysis the complete conversion of aromatic compounds with the formation of only aliphatic products takes place.

Phenolic compounds are known to form intensely colored complex compounds with aqueous solutions of $FeCl_3$. And with the accumulation of hydroxyl groups in the ring, as well as decarboxylation the color of complexes changes from blue to purple then to blue or green [19]. We used this feature of phenol derivatives in order to deal with products that are formed during oxidation. Salicylic acid with $FeCl_3$ forms violet colored complex. After 30 minutes of electrolysis the color of solution changed to blue-violet, indicating a partial destruction of salicylic acid and accumulation of 2,3-, 2,5-dihydroxybenzoic and trihydroxybenzoic acids. They give dark blue color with ferric chloride. After 2 hours the violet color completely disappeared and the solution became intensely blue, that in our opinion, demonstrates the complete destruction

Bulletin of Dnipropetrovsk University. Series Chemistry, 2017, *25*(1), 36–44

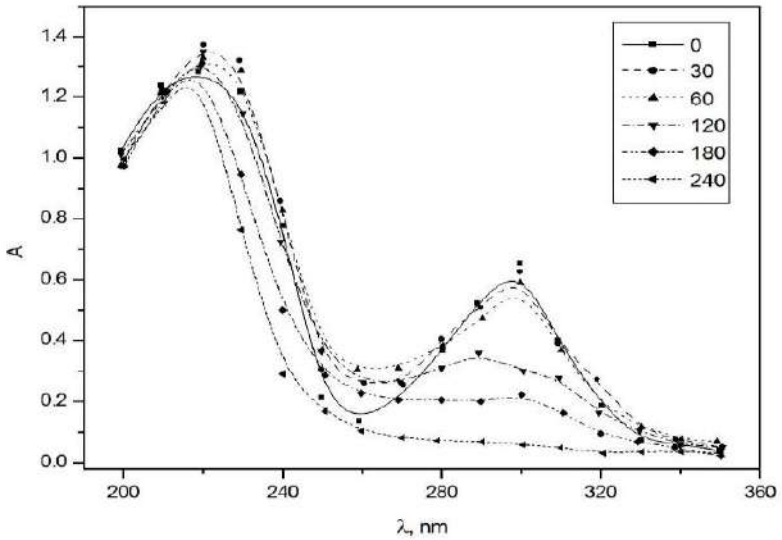

Fig. 3. The absorption spectra of salicylic acid solution (initial concentration $2 \cdot 10^{-4}$M) obtained at different time of electrolysis in a phosphate buffer on PbO_2-Bi anode, pH = 6.55

of salicylic acid and hydroquinone accumulation, which is rapidly oxidized to benzoquinone. Over time, the color of the solution becomes blue, light blue and colorless, indicating the gradual destruction of aromatic products.

The process of oxidation of salicylic acid on lead dioxide anodes, modified by bismuth results in 4 hours, which is 1.5 hours faster compared to nonmodified anodes, as evidenced by electronic absorption spectra (fig. 3). We have not seen the appearance of violet-blue color by using the qualitative reaction. After 30 minutes of electrolysis the solution was blue, after 60 minutes – saturated blue, and after 180 minutes the color was almost disappeared.

Table 1 represents the phase composition of lead dioxide. In this case, structural factors play a significant role. Maximum electrocatalytic activity is achieved by increasing the proportion of α-phase, on the one hand, and increase the crystalline zone of oxide on the other, which leads to increased amounts of oxygen containing particles strongly bounded to the electrode surface that participate in the electrochemical oxidation of aromatic compounds [22].

Table 1

The phase composition of lead dioxide coatings depending on deposition conditions

Deposit	T/K	Content /wt.%/ α-PbO_2/β-PbO_2
PbO_2	282	59/41
PbO_2	298	90/10
PbO_2–Bi	282	5/95
PbO_2–Ce	298	83/17

The degradation rate is lower on lead dioxide anodes, modified by cerium ions. The complete destruction of aromatics ended after 5 hours. Qualitative reaction to benzoic acid derivatives showed a similar color shift as in the case of anodes, modified by bismuth.

Obviously, these processes proceed through the same intermediates and qualitatively are not different. But one can see different catalytic activity of modified and nonnmodified lead dioxide anodes.

During the sulfosalicylic acid oxidation we observed no differences in the rate of destruction of the initial compound at various anodes. In all cases, the process ended after 4.5 hours (fig. 4).

Interesting results were obtained during the oxidation of 5-aminosalicylic acid. The presence of amino-group obviously increases the amount of formed intermediates. The gradual color change of the solution confirms the multistage process. It was colorless first, but after 30 minutes it became yellow, after 120 minutes the color was yellow-brown; after 150 minutes the color intensity was reduced to colorless. The absorption spectra also show preliminary oxidation of the amino group.

The initial acid solution is characterized by a peak in the 320–340 nm (fig. 5). After 120 minutes one can see peak shifting in the 290–310 nm region, indicating the complete destruction of amino-group; the plateau gradually appears in the 260–280 nm, indicating the formation of benzoquinones. Unlike salicylic acid (see fig. 2), the complete conversion of 5-aminosalicylic acid is slightly slower.

Bulletin of Dnipropetrovsk University. Series Chemistry, 2017, *25*(1), 36–44

The presence of donor functional group reduces the rate of the 5-aminosalicylic acid oxidation. The process is completed after 6.5 hours on lead dioxide anodes.

On electrodes modified by bismuth the process is much faster – about 4 hours. In our opinion bismuth ions accelerate the transition to benzoquinones due to the ease of oxidation of the amino-group to hydroxy-. It is known that in the phenolic compounds such destruction is always formed benzoquinones, which is hardly degraded. Obviously, the sooner the compound formed less time is needed for the decomposition of the initial compound. On electrodes modified by cerium the process is much slower and results in 5 hours.

As one can see from electronic absorption spectra of 5-aminosalicylic acid, in all cases after 120 minutes the appearance of new compounds in the reaction mixture can be witnessed, as evidenced by the shift of the absorption peak in the region of 290–300 nm. Thus the highest activity in respect to aminosalicylic acid oxidation exhibit lead dioxide anodes modified by bismuth. For other derivatives of salicylic acid difference in time of the destruction on modified and nonmodified lead dioxide anodes was less significant.

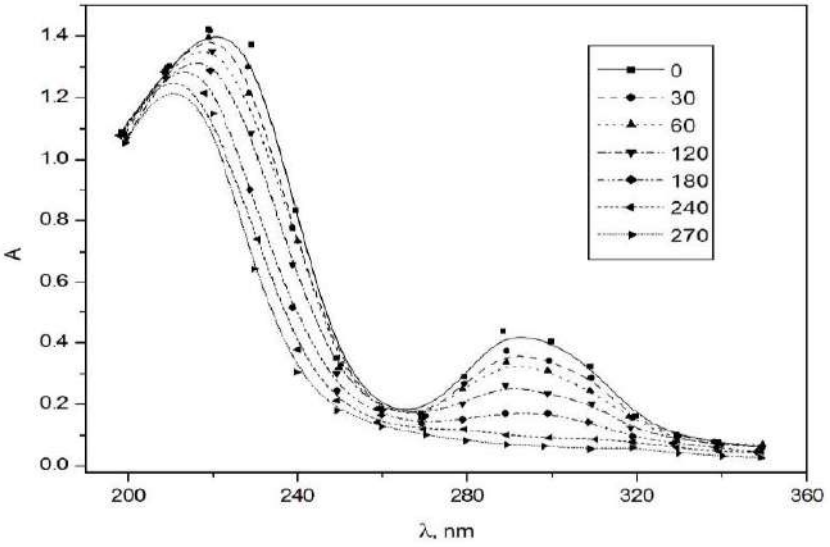

Fig. 4. The absorption spectra of sulfosalicylic acid solution (initial concentration 10^{-4}M) obtained at different time of electrolysis in a phosphate buffer on lead dioxide anode, pH = 6.55

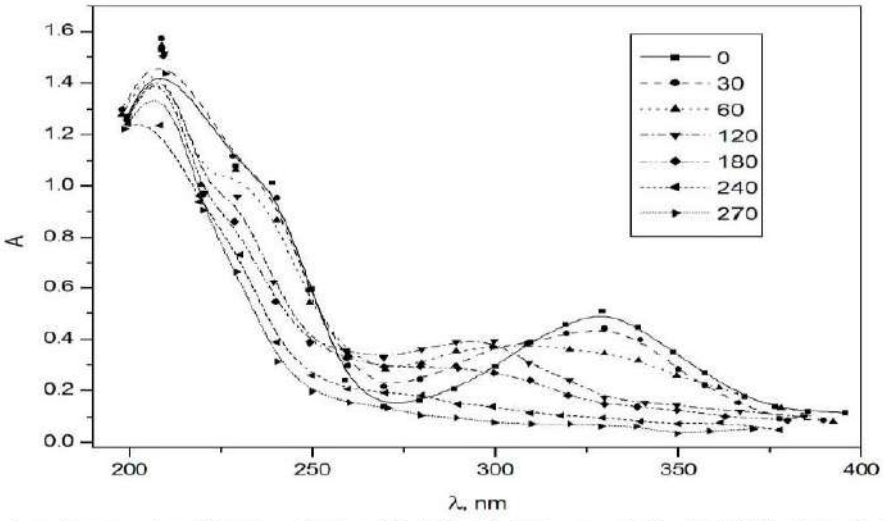

Fig. 5. The absorption spectra of 5-aminosalicylic acid solution (initial concentration $2 \cdot 10^{-4}$M) obtained at different time of electrolysis in a phosphate buffer on PbO_2-Bi anode, pH = 6.55

The processes of electrochemical oxidation of investigated organic compound on unmodified and modified lead dioxide electrodes occur qualitatively the same and differ only in the rate. This suggests the invariability of the mechanism of their oxidation on different materials that allows one for a correct comparison of their electrocatalytic activity.

According to calculations (table 2), based on kinetic studies of the reaction rate constant of salicylic acid degradation depends on the composition of the electrode material and varies due to the nature and content of ionic additives in lead dioxide.

Table 2

Kinetic parameters of the electrochemical oxidation of salicylic acid ($2 \cdot 10^{-4}$ M) on modified PbO_2-anodes

Anode	Apparent heterogeneous rate constant, $k \cdot 10^2$, min^{-1}
PbO_2	0.70
PbO_2–Bi	0.81
PbO_2–Ce	0.72

The maximum interest for the electrochemical destruction of organic substances represents lead dioxide electrodes modified by bismuth to which a rate constant of salicylic acid oxidation increases in 1.2 times compared with nonmodified electrodes. In other cases, the rate constants are comparable.

Intermediates formed during the oxidation of salicylic and sulfosalicylic acids depend on conditions of the oxidation. Often these intermediates are α-, β-resorcinol acid, gallic acid, pyrocatechol, hydroquinone [14]. All of these compounds oxidized to benzoquinones, which is further degraded into aliphatic acids – succinic, maleic, oxalic, etc. But the general stage of destruction of salicylic and sulfosalicylic acids are aromatic nucleus hydroxylation and decarboxylation.

Hydroxylation occurs in the *o*- and *p*-position to the carboxyl group with the formation of isomeric dihydroxybenzoic acids. Decarboxylation of salicylic acid occurs at heating and leads to the formation of phenols.

Further oxidation leads to the formation of diketones and their oxidation through di- and monocarboxylic acid to carbon dioxide (scheme 1).

Stages of sulfosalicylic acid oxidation coincide with salicylic acid oxidation. The multistage of this process confirmed by the colour change of ferrous sulfate aqueous solutions of hydroxy acids during the electrolysis: colorless → yellow → orange → brown → colorless, indicating that the reaction occurs through a series of intermediates.

The rate of conversion of organic compounds depends on the nature of organics on the one hand and the nature of the anode material on the other. Experimental data show that there is no universal anode material on which the conversion rate would be maximized. In each case the choice of material was individual.

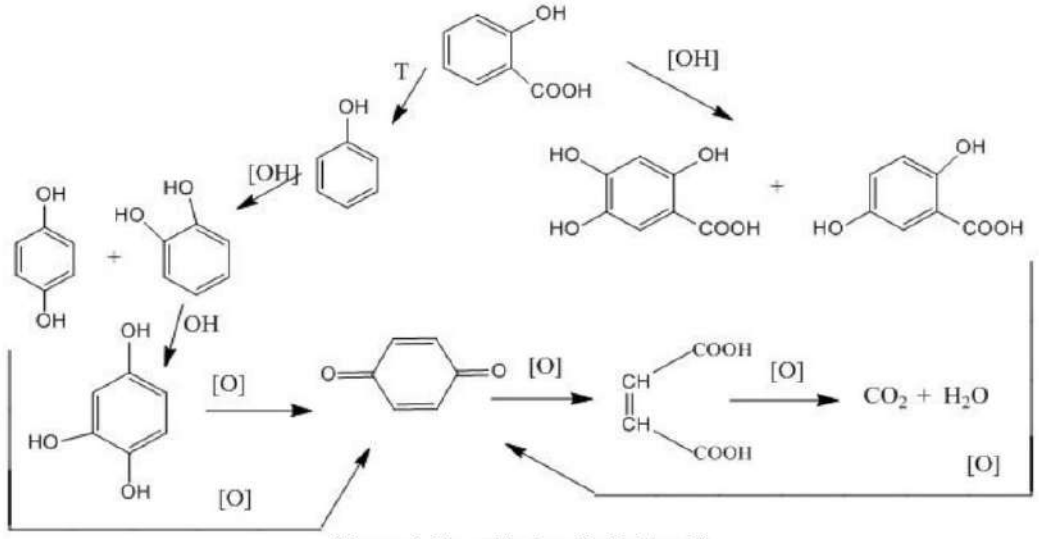

Scheme 1. The oxidation of salicylic acid

Conclusions

It has been found that the destruction of salicylic acid in the first stage occurs through the accumulation of aromatic hydroxylation products, and during the complete destruction – incineration to form aromatic aliphatic compounds.

It is shown that the use of PbO_2, deposited from methanesulfonate electrolytes and modified electrodes significantly reduces the conversion

time of salicylic acid in aliphatic products compared to lead dioxide anodes obtained by traditional technology from nitrate bath. The highest degradation rate occurs at the anodes modified by bismuth. It was found that the destruction of the 5-aminosalicylic acid occurs through an intermediate oxidation of amino-group to hydroxy.

Bibliography

[1] Oturan M. A. Advanced oxidation processes in water/ wastewater treatment: principles and applications. A review / M. A. Oturan, J.-J. Aaron // Crit. Rev. Env. Sci. Tech. – 2014. – Vol. 44. – P. 2577–2641.

[2] Chaplin B. P. Critical review of electrochemical advanced oxidation processes for water treatment applications / B.P. Chaplin // Environ. Sci.: Processes Impacts. – 2014. – Vol. 16. – P. 1182–1203.

[3] Electrochemical oxygen transfer reactions: electrode materials, surface processes, kinetic models, linear free energy correlations, and perspectives. A review / R. Vargas, C. Borras, D. Mendez [et al.] // J. Solid State Electrochem. – 2016. – Vol. 20. – P. 875–893.

[4] Brillas E. Decontamination of wastewaters containing synthetic organic dyes by electrochemical methods. An updated review / E. Brillas, C. A. Martinez-Huitle // Appl. Catal., B. – 2015. – Vol. 166–167. – P. 603–643.

[5] Martinez-Huitle C. A. Decontamination of wastewaters containing synthetic organic dyes by electrochemical methods: A general review / C. A. Martinez-Huitle, E. Brillas// Appl Catal., B. – 2009. – Vol. 87. – P. 105–145.

[6] Reaction sequence for the mineralization of the short-chain carboxylic acids usually formed upon cleavage of aromatics during electrochemical Fenton treatment / M. A. Oturan, M. Pimentel, N. Oturan, I. Sires // Electrochim. Acta. – 2008. – Vol. 54. – P. 173–182.

[7] Degradation of chlorophenols by means of advanced oxidation processes: a general review / M. Pera-Titus, V. Garcıa-Molina, M. A. Bacos [et al.] // Appl. Catal., B. – 2004. – Vol. 47. – P. 219–256.

[8] Enache T. A. Phenol and para-substituted phenols electrochemical oxidation pathways / T. A. Enache, A. M. Oliveira-Brett // J. Electroanal. Chem. – 2011. – Vol. 655. – P. 9–16.

[9] Dhaouadi A. Degradation of paraquat herbicide by electrochemical advanced oxidation methods / A. Dhaouadi, N. Adhoum // J. Electroanal. Chem. – 2009. – Vol. 637. – P. 33–42.

[10] A review on advanced oxidation processes for the removal of taste and odor compounds from aqueous media / M. Antonopoulou, E. Evgenidou, D. Lambropoulou, I. Konstantinou // Water Res. – 2014. – Vol. 53. – P. 215–234.

[11] Cattarin S. Electrosynthesis of nancomposite materials for electrocatalysis / S. Cattarin, M. Musiani // Electrochim. Acta. – 2007. –Vol. 52. – P. 1339–1348.

[12] Photoelectrochemical oxidation of salicylic acid and salicylaldehyde on titanium dioxide nanotube arrays / M. Tian, B. Adams, J. Wen [et al.] // Electrochim. Acta. – 2009. –Vol. 54. – P. 3799–3805.

[13] Study on production of free hydroxyl radical and its reaction with salicylic acid at lead dioxide electrode / S. Ai, Q. Wang, H. Li, L. Jin // J. Electroanal. Chem. – 2005. – Vol. 578. – P. 223–229.

[14] Electrogeneration of hydroxyl radicals on boron-doped diamond electrodes / B. Marselli, J. Garcia-Gomez, P.-A. Michaud [et al.] // J. Electrochem. Soc. – 2003. – Vol. 150. – P. D79-D83.

[15] Mineralization of salicylic acid in acidic aqueous medium by electrochemical advanced oxidation processes using platinum and boron-doped diamond as anode and cathodically generated hydrogen peroxide / E. Guinea, C. Arias, P. L. Cabot [et al.] // Wat. Res. – 2008. – 42. – P. 499-511.

[16] Electrodeposition of Ni^{2+}-doped PbO_2 and physico-chemical properties of the coating / O. Shmychkova, T. Luk'yanenko, R. Amadelli, A. Velichenko // J. Electroanal. Chem. – 2016. – Vol. 774. – P. 88-94.

[17] STOE WinXPOW, version 3.03. Darmstadt: Stoe & Cie GmbH, 2010.

[18] Kraus W. PowderCell for Windows (version 2.4) / W. Kraus, G. Nolze. – Berlin: Federal Institute for Materials Research and Testing, 2000.

[19] Rodriguez-Carvajal J. Recent developments of the program FULLPROF, Commission on Powder Diffraction (IUCr) / J. Rodriguez-Carvajal // Newsletter. – 2001. – Vol. 26. – P. 12-19.

[20] Shriner R. L. The systematic identification of organic compounds / R. L. Shriner, C. K. F. Hermann, T. C. Morrill [et al.]. – 8th Edition, Hoboken, NJ: John Wiley & Sons, Inc., 2004. – 736 p.

[21] Nafion effect on the lead dioxide electrodeposition kinetics / A. Velichenko, T. Luk'yanenko, N. Nikolenko [et al.] // Russ. J. Electrochem. – 2007. – 43. – P. 118-120.

[22] Electrooxidation of some phenolic compounds at Bi-doped PbO_2/ O. Shmychkova, T. Luk'yanenko, A. Yakubenko [et al.] // Appl. Catal., B. – 2015. – Vol. 162. – P. 346–351.

References

[1] Oturan, M. A., Aaron, J.-J. (2014). Advanced oxidation processes in water/wastewater treatment: principles and applications. A review. *Crit. Rev. Env. Sci. Tech., 44*, 2577–2641. doi: http://dx.doi.org/10.1080/10643389.2013.829765

[2] Chaplin, B.P. (2014). Critical review of electrochemical advanced oxidation processes for water treatment applications. *Environ. Sci.: Processes Impacts., 16*, 1182–1203. doi: http://dx.doi.org/10.1039/C4EM90018A

[3] Vargas, R., Borras, C., Mendez, D., Mostany, J., Scharifker, B. R. (2016). Electrochemical oxygen transfer reactions: electrode materials, surface processes, kinetic models, linear free energy correlations, and perspectives. A review. *J. Solid State Electrochem., 20*, 875–893. doi: https://doi.org/10.1007/s10008-015-2984-7

[4] Brillas, E., Martinez-Huitle, C. A. (2015). Decontamination of wastewaters containing synthetic organic dyes by electrochemical methods. An updated review. *Appl. Catal., B, 166–167*, 603–643. doi: https://doi.org/10.1016/j.apcatb.2014.11.016

[5] Martinez-Huitle, C. A., Brillas, E. (2009). Decontamination of wastewaters containing synthetic oranic dyes by electrochemical methods: a general review. *Appl. Catal., B, 87*, 105–145. doi: https://doi.org/10.1016/j.apcatb.2008.09.017

[6] Oturan, M. A., Pimentel, M., Oturan N., Sires, I. (2008). Reaction sequence for the mineralization of the short-chain carboxylic acids usually formed upon cleavage of aromatics during electrochemical fenton treatment. *Electrochim. Acta, 54*, 173–182. doi: https://doi.org/10.1016/j.electacta.2008.08.012

[7] Pera-Titus, M. Garcia-Molina, V., Bacos, M. A., Gimenez, J., Esplugas, S. (2011). Degradation of chlorophenols by means of advanced oxidation processes: a general review. *Appl. Catal.*, B, 47, 219–256. doi: https://doi.org/10.1016/j.apcatb.2003.09.010

[8] Enache, T. A., Oliveira-Brett, A. M. (2011). Phenol and para-substituted phenols electrochemical oxidation pathways. *J. Electroanal. Chem.*, *655*, 9–16. doi: https://doi.org/10.1016/j.jelechem.2011.02.022

[9] Dhaouadi, A., Adhoum, N. (2009). Degradation of paraquat herbicide by electrochemical advanced oxidation methods. *J. Electroanal. Chem.*, *637*, 33–42. doi: https://doi.org/10.1016/j.jelechem.2009.09.027

[10] Antonopoulou, M., Evgenidou, E., Lambropoulou, D., Konstantinou, I. (2014). A review on advanced oxidation processes for the removal of taste and odor compounds from aqueous media. *Water Res.*, *53*, 215–234. doi: https://doi.org/10.1016/j.watres.2014.01.028

[11] Cattarin, S., Musiani, M. (2007). Electrosynthesis of nancomposite materials for electrocatalysis. *Electrochim. Acta*, *52*, 2796–2805. doi: https://doi.org/10.1016/j.electacta.2006.07.035

[12] Tian, M., Adams, B., Wen, J., Asmussen, R. M., Chen, A. (2009). Photoelectrochemical oxidation of salicylic acid and salicylaldehyde on titanium dioxide nanotube arrays. *Electrochim. Acta*, *54*, 3799–3805. doi: https://doi.org/10.1016/j.electacta.2009.01.077

[13] Ai, S., Wang Q., Li, H., Jin, L. (2005). Study on production of free hydroxyl radical and its reaction with salicylic acid at lead dioxide electrode. *J. Electroanal. Chem.*, *578*, 223–229. doi: https://doi.org/10.1016/j.jelechem.2005.01.002

[14] Marselli, B., Garcia-Gomez, J., Michaud, P.-A., Rodrigo, M. A., Comninellis Ch. (2003). Electrogeneration of hydroxyl radicals on boron-doped diamond electrodes. *J. Electrochem. Soc.*, *150*, D79-D83. doi: http://dx.doi.org/10.1149/1.1553790

[15] Guinea, E., Arias, C., Cabot, P. L., Garrido, J. A., Rodriguez, R. M., Centellas, F., Brillas, E. (2008). Mineralization of salicylic acid in acidic aqueous medium by electrochemical advanced oxidation processes using platinum and boron-doped diamond as anode and cathodically generated hydrogen peroxide. *Wat. Res.*, *42*, 499-511. doi: https://doi.org/10.1016/j.watres.2007.07.046

[16] Shmychkova, O., Luk'yanenko, T., Amadelli, R., Velichenko, A. (2016). Electrodeposition of Ni^{2+}-doped PbO_2 and physicochemical properties of the coating. *J. Electroanal. Chem.*, *774*, 88-94. doi: https://doi.org/10.1016/j.jelechem.2016.05.017

[17] STOE WinXPOW, version 3.03. (2010). Darmstadt: Stoe & Cie GmbH.

[18] Kraus, W., Nolze, G. (2000). PowderCell for Windows (version 2.4) Berlin: Federal Institute for Materials Research and Testing.

[19] Rodriguez-Carvajal, J. (2001). Recent developments of the program FULLPROF, Commission on Powder Diffraction (IUCr). Newsletter, *26*, 12-19.

[20] Shriner, R. L., Hermann, C. K. F., Morrill, T. C., Curtin, D. Y., Fuson, R. C. (2004). *The systematic identification of organic compounds*. 8th Edition, Hoboken, NJ: John Wiley & Sons, Inc. doi: https://doi.org/10.1021/np058223w

[21] Velichenko, A., Luk'yanenko, T., Nikolenko, N., Amadelli, R., Danilov, F. (2007). Nafion effect on the lead dioxide electrodeposition kinetics. *Russ. J. Electrochem.*, *43*, 118-120. doi: https://doi.org/10.1134/S102319350701017X

[22] Shmychkova, O., Luk'yanenko, T., Yakubenko, A., Amadelli, R. Velichenko, A. (2015). Electrooxidation of some phenolic compounds at Bi-doped PbO_2. *Appl. Catal., B*, *162*, 346–351. doi: https://doi.org/10.1016/j.apcatb.2014.07.011

14 ISSN 0321-4095, Voprosy khimii i khimicheskoi tekhnologii, 2017, No. 4, pp. 14-20

UDC 544.653.2

A. Velichenko, V. Knysh, O. Shmychkova, T. Luk'yanenko

THE COMPOSITION AND PROPERTIES OF COMPOSITE PbO_2–TiO_2 MATERIALS ELECTRODEPOSITED FROM COLLOIDAL METHANESULFONATE ELECTROLYTES

Ukrainian State University of Chemical Technology, Dnipro, Ukraine

PbO_2–TiO_2 nanocomposite materials are formed by electrochemical deposition of PbO_2 from colloidal nitrate and methanesulfonate electrolytes through the inclusion of a TiO_2 dispersed phase in the growing PbO_2 coating. These particles are delivered from the electrolyte bulk to the electrode surface by diffusion and/or migration (as a result of the appearance of partial concentration gradient in a colloidal solution due to the depletion of particles, included in the growing coating, in near-electrode zone). Composites containing from 4 to 27 wt.%. TiO_2 can be synthesized by varying the electrolysis regimes and the composition of the electrolyte. The presence of TiO_2 particles in the electrolyte leads, as a rule, to the decrease of the crystal size and the growth of the content of β-phase of lead dioxide in the deposit. The inclusion of particles of valve metal oxides in a PbO_2 matrix typically results in an increase in oxygen evolution reaction overvoltage and promotes a high activity towards the oxidative degradation of organic substances likely due to an increase in the amount of strongly bound oxygen-containing species on the electrode surface.

Keywords: PbO_2–TiO_2 nanocomposites, methanesulfonate electrolyte, oxygen evolution, electrooxidation, phenolic compounds.

Introduction

It is recognized that electrodeposition of lead dioxide (PbO_2) from different oxide particle suspensions leads to composite materials that notably differ from pure PbO_2 composition in terms of physico-chemical properties and electrocatalytic activity [1]. Several reviews describe the preparation of composites based on lead dioxide additionally containing oxides particles of other metals, in particular TiO_2, RuO_2, Al_2O_3 [2].

It appears that the deposition and formation of composite materials are also influenced by the nature of the dispersed phase, the time stability of the resulting suspension and the use of additives in the electrolytes [3,4]. Stirring of the deposition electrolyte has a significant influence as it helps to maintain the particles in suspension and favors their transportation to the electrode surface. It has been shown that increasing the stirring rate results in an increase of the dispersed phase in the coating. However, the issue of the directed synthesis of these materials is still open since some details concerning the effect of various factors on the composition and physico-chemical properties of the coatings remain to be investigated.

There are significant difficulties in preparation of the suspension electrolyte with high aggregative stability. Sedimentation of the dispersed phase highly complicates the application of suspension electrolytes, because electrolysis can be carried out only under conditions of forced mixing. Even in this case, the deposition of coatings with the stable composition is problematic due to the turbulent flows of the solution in the near-electrode zone, which creates considerable fluctuations in the content of the dispersed phase; this phenomenon becomes more and more significant as the particle size of the dispersed oxide increases. Then, an alternative experimental approach is the use of nanoparticle TiO_2 suspensions that are obtained, for example, by the hydrolysis of titanium alkoxy-precursors in nitric acid. In this case, the primary particle size does not exceed 15 nm [5] and, due to the high stability of suspensions towards aggregation, forced mixing in the process of coating electrodeposition is not needed. However, due to limitations on the mechanical strength, in nitrate solutions it is not possible to obtain coatings with a thickness greater than 100 microns. In this regard, we proposed to use methanesulfonate electrolytes in which PbO_2 composite coatings up to

ISSN 0321-4095, Voprosy khimii i khimicheskoi tekhnologii, 2017, No. 4, pp. 14-20 15

2 mm thick with satisfactory mechanical properties can be prepared [4,5].

In a recent work by our group [3], we have investigated the chemical properties of these colloidal systems as well as the nucleation laws and kinetics of the electrodeposition of coatings. Herein, we report further important details on the effect of deposition conditions on the composition, physico-chemical properties and electrocatalytic activity of composite PbO_2–TiO_2 materials obtained from methanesulfonate electrolytes containing nanosized TiO_2 particles as a dispersed phase.

Material and methods

All chemicals were reagent grade. Lead dioxide was electrodeposited from methanesulfonate or nitrate electrolytes that contained 0.1 M CH_3SO_3H or HNO_3, and 0.1 M $Pb(CH_3SO_3)_2$ or $Pb(NO_3)_2$.

Platinized titanium was used as a sheet. It was treated as described in [6] before platinum layer depositing. Suspension electrolytes containing TiO_2 as dispersed phase were prepared by hydrolysis of Ti(IV) isopropylate [4]. Electrolyte compositions and conditions of the deposition of composite coatings were selected hereby that in all cases the current efficiency of lead dioxide deposition was about 100%.

The results of our previous investigations [4] showed that the aggregative stabled suspension electrolytes can be obtained based through the sols of titanium dioxide, which are formed by hydrolysis of titanium isopropylate. These electrolytes do not require mixing to maintain their stability. The amount of PbO_2 in the samples was determined after the coating dissolution by Pb^{2+} content, which was found after amperometric titration with sodium N,N-diethyldithiocarbamate [4].

X-ray powder diffraction data were collected on a STOE STADI P automatic diffractometer equipped with linear PSD detector (transmission mode, $2\theta/\omega$-scan; $CuK_{\alpha 1}$ radiation, curved germanium (1 1 1) monochromator; 2θ-range $6.000 \le 2\theta \le 102.945°2\theta$ with step $0.015°2\theta$; PSD step $0.480°2\theta$, scan time 50 s/step).

Qualitative and quantitative phase analysis was performed using the PowderCell program. For selected samples with relatively high degree of crystallinity the Rietveld refinement was carried out using FullProf.2k (version 5.40) program.

Oxygen evolution reaction was investigated by steady-state polarization on computer controlled EG&G Princeton Applied Research potentiostat model 273A in 1 M $HClO_4$. All potentials were recorded and reported vs. $Ag/AgCl/KCl_{(sat.)}$.

The electrooxidation of organic compounds was carried out in divided cell at j_a=50 mA cm^{-2}. The volume of anolyte was 130 cm^3. Solution containing phosphate buffer (0.25 M Na_2HPO_4+0.1 M KH_2PO_4)+2×10^{-4} M organic compound (pH 6.55) was used as anolyte; phosphate buffer as catholyte. Stainless steel was used as cathode. Composite PbO_2–TiO_2 electrodes were used as anodes. Electrode surface area was 3 cm^2.

The changing of the concentration of the organic substance during the electrolysis was measured by sampling (volume of 5 cm^3) at regular intervals and measuring the absorbance of the solution in the ultraviolet and visible region (wavelength range of 200–570 nm) using a Kontron Uvikon 940 spectrometer.

Accelerated life tests with the anode active layer of composite PbO_2–TiO_2 materials were carried out in 1 M H_2SO_4.

Results and Discussion

As one can conclude from recently obtained data [4], PbO_2–TiO_2 nanocomposite materials are formed by electrochemical deposition of PbO_2 from colloidal nitrate and methanesulfonate electrolytes through the inclusion of a TiO_2 dispersed phase in the growing PbO_2 coating. In the following, we present and discuss results on important aspects concerning the characteristics of composite electrodes, including their electrochemical activity.

The composition of PbO_2–TiO_2 composite materials

The content of the dispersed phase in the composite depends on current density as seen in the plots of Fig. 1, where two regions can be clearly identified. In region I, the PbO_2 deposition process is controlled by kinetics, which implies an increase in the deposition current of oxide with increasing potential [5–7]. This enhances the likelihood that colloidal TiO_2 particles are captured, and the content of an inert oxide in the composite increases (Fig. 1, region I). In region II, when the deposition rate reaches a limiting value and the process becomes diffusion-controlled [5–7], the TiO_2 content in the coating remains practically constant (Fig. 2, region II). Thus, the amount of the dispersed phase in the oxide coating is proportional to the formation rate of the oxide of the dispersion medium (PbO_2).

The content of colloidal TiO_2 in the composite can be affected by diffusion and/or migration delivery of the dispersed particles to the electrode as well as by their interaction with the surface. In the context of the latter phenomenon, it is noteworthy that the particles of the dispersed phase are included in the growing coating despite the fact that TiO_2 has a positive surface charge in the base electrolyte and the charge of the electrode surface will also be positive, at the typical deposition potentials (>1.5 V), since the value of the zero-charge potential of PbO_2

in the 0.1 M HNO_3 is 0.89±0.1 [8]. Interestingly, a significant increase of TiO_2 content occurs when deposition is carried out in methanesulfonate electrolytes (Fig. 1). The observed phenomenon is likely determined by a decrease of both the charge of discharging particles in the dispersion and that of the electrode surface due to complexation and adsorption of methanesulfonate ions, which leads to an increase in the rate of TiO_2 particle delivery to the electrode surface by increasing the contribution of migration component and reduce of electrostatic repulsion forces in the near-electrode area.

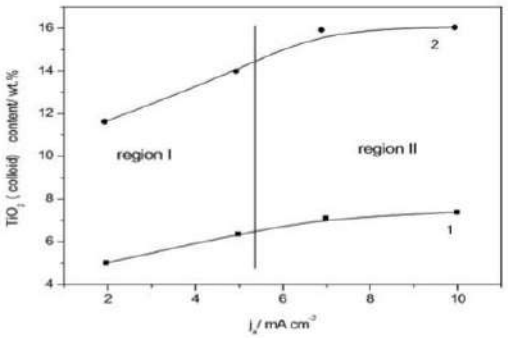

Fig. 1. The TiO_2 content in the composite versus anodic current density of deposition. The deposition solutions are as follows: (1) 0.1 M $Pb(NO_3)_2$+0.1 M HNO_3+5.0 g dm^{-3} $TiO_{2(colloidal)}$ and (2) 0.1 M $Pb(CH_3SO_3)_2$+0.1 M CH_3SO_3H+ +5.0 g dm^{-3} $TiO_{2(colloidal)}$

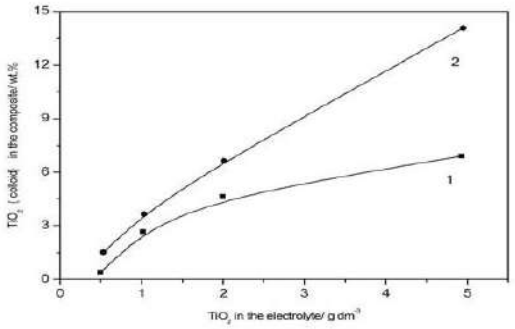

Fig. 2. The TiO_2 content in the composite versus TiO_2 content in deposition solutions: (1) 0.1 M $Pb(NO_3)_2$+0.1 M HNO_3+ +X g dm^{-3} $TiO_{2(colloidal)}$ and (2) 0.1 M $Pb(CH_3SO_3)_2$+ +0.1 M CH_3SO_3H+X g dm^{-3} $TiO_{2(colloidal)}$. j_a=10 mA cm^{-2}

One can conclude from the obtained results (Fig. 2) that an increase of the content of TiO_2 in the deposition electrolyte up to 5 g dm^{-3} determines an increase of the probability of particles capturing into the growing deposit, which leads to an increase of the TiO_2 content in the composite. The observed effect is probably due to an increase in the partial concentration gradient of the dispersed phase oxide with increasing its content in the electrolyte. As in the previous case, the TiO_2 content in the composite materials obtained from the methanesulfonate electrolytes is much higher than in analogous experiments in nitrate baths.

It is noteworthy that a significant increase in the occluded particles from the dispersed phase is observed when the deposition temperature is raised (Fig. 3). This effect is due to a decrease in the solution viscosity at higher temperatures, which, in turn, reduces diffusion limitations and accelerates the delivery of TiO_2 particles to the electrode surface. As mentioned earlier, the use of methanesulfonate electrolytes allows preparing composite coatings where the TiO_2 content is about 2-fold higher than that obtained in nitrate solutions.

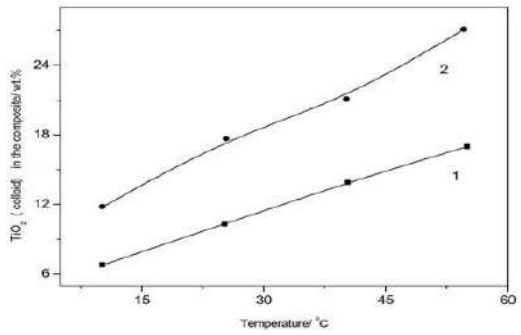

Fig. 3. The TiO_2 content in the composite versus temperature of deposition. The deposition solutions are as follows: (1) 0.1 M $Pb(NO_3)_2$+0.1 M HNO_3+5.0 g dm^{-3} $TiO_{2(colloidal)}$ and (2) 0.1 M $Pb(CH_3SO_3)_2$+0.1 M CH_3SO_3H+5.0 g dm^{-3} $TiO_{2(colloidal)}$. j_a=10 mA cm^{-2}

According to the obtained data, the use of colloidal methanesulfonate electrolytes allows varying the content of TiO_2 in the composite material in the range from 4 to 27 wt.% by changing the amount of TiO_2 particles in the solution, the temperature and the deposition current density. Thus, in contrast to the nitrate solution, the current efficiency for all proposed regimes of electrolysis and compositions of methanesulfonate solution is 100%, and the resulting coatings are characterized by a low mechanical stress and good adhesion to the substrate even for a thickness as large as 2 mm.

ISSN 0321-4095, Voprosy khimii i khimicheskoi tekhnologii, 2017, No. 4, pp. 14-20 17

The phase composition and the texture of PbO_2–TiO_2 composite materials

It follows from the above results that the systems based on nanoparticles dispersed in methanesulfonate electrolytes are of considerable practical interest and are worth of detailed studies. In this regard, we performed an investigation of the phase composition and texture of the obtained composites. As can be seen in Tables 1 and 2, the content of the PbO_2 β-phase depends on the TiO_2 concentration in the suspension electrolyte and has a maximum at 1.0 g dm^{-3} TiO_2.

Table 1

The phase composition of PbO_2–TiO_2 composites

Deposition electrolyte	The content of PbO_2 phase, %	
	α	β
(M)*	17.0	83.0
(M)+1 g dm^{-3} TiO_2	32.7	67.3
(M)+2 g dm^{-3} TiO_2	23.7	76.3
(M)+5 g dm^{-3} TiO_2	15.5	84.5

Note: * – (M) means 0.1 M $Pb(CH_3SO_3)_2$+0.1 M CH_3SO_3H. Coatings are deposited at j_a=5 mA cm^{-2}, T=298 K.

Table 2

The phase composition of PbO_2–TiO_2 composites

Deposition electrolyte	The content of PbO_2 phase, %	
	α	β
(M)*	17.0	83.0
(M)+0.5g dm^{-3} TiO_2	31.9	68.1
(M)+1 g dm^{-3} TiO_2	56.1	43.9
(M)+2 g dm^{-3} TiO_2	57.3	42.7
(M)+5 g dm^{-3} TiO_2	33.8	62.2

Note: * – (M) means 0.1 M $Pb(CH_3SO_3)_2$+0.1 M CH_3SO_3H. Coatings are deposited at j_a=10 mA cm^{-2}, T=298 K.

The texture differs substantially for deposits obtained from a true solution and for deposits prepared from electrolytes with a high content of disperse particles (Fig. 4). In the latter case, the degree of crystallinity of the coatings increases, as evidence by the increase of the peaks intensity and sharpness on diffractogramms.

The phase composition and texture of composite coatings as well as their TiO_2 content are markedly affected by raising the concentration of dispersed particles and the current density because this increases the number of nucleation sites by facilitating TiO_2 transport to the electrode surface by diffusion or migration. The data suggest that the presence of nucleation sites on the dispersed phase particles, both on the electrode surface and in the near-electrode area, facilitates the crystallization of PbO_2 β-phase. It should be pointed out that a significant increase in the number of particles leads to the surface shielding, causing polarization and accelerating of the β-phase. This explains the extreme dependence of the phase composition of lead dioxide on the content of the dispersed phase particles in the suspension electrolyte. The lack of TiO_2 peaks on X-ray diffraction patterns is likely due to nanoscale of dispersed phase particles in composite materials based on lead dioxide.

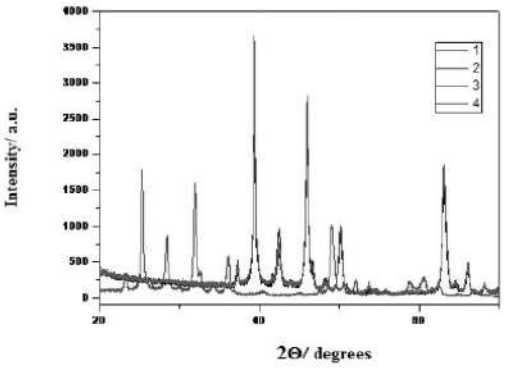

Fig. 4. X-ray diffractogramms of composite materials obtained at j_a=5 mA cm^{-2} and 298 K from the following solutions: 0.1 M $Pb(CH_3SO_3)_2$+0.1 M CH_3SO_3H+X g dm^{-3} $TiO_{2(colloidal)}$, where X is: (1) – 0; (2) – 1.0; (3) – 2.0; (4) – 5.0

The electrocatalytic activity of PbO_2–TiO_2 composites

Earlier it has been reported [7] that deposition conditions of PbO_2-based materials, their chemical and phase composition, as well as a number of structural factors such as the texture of the coating, are largely affected by the surface coverage by oxygen-containing radicals which also determine the electrocatalytic activity and selectivity of deposits in respect to oxygen transfer reactions.

According to the mechanism proposed by Pavlov et al. [9], oxygen evolution occurs at active sites located in a hydrous layer on PbO_2. The surface consists of crystal line (PbO_2) and hydrated [$PbO(OH)_2$] zones which are in equilibrium, and the latter can exchange cations and anions due to their open structure. Oxygen evolution proceeds through the following elementary steps:

$$PbO(OH)_2+H_2O \rightarrow PbO(OH)_2...(OH^{\cdot})+H^{+}+\bar{e}; \quad (1)$$

$$PbO(OH)_2...(OH^{\cdot}) \rightarrow PbO(OH)_2+O+H^{+}+\bar{e}; \quad (2)$$

$$2O \rightarrow O_2. \quad (3)$$

According to Trasatti and Lodi [10], if oxygen evolution reaction (OER) is limited by a second electron transfer (electrochemical desorption), an increase of bond strength of chemisorbed oxygen will lead to an increase of OER overvoltage.

According to the obtained results (Fig. 5), the OER overvoltage on PbO_2–TiO_2 electrodes increases with the content of TiO_2 in the composite. It should be noted that the addition of TiO_2 particles to the solution increases O_2 evolution on the metal substrate, similarly to data, obtained on lead dioxide doped by cobalt, nickel, and cerium ions [6,11,12]. Most likely, the observed phenomenon is due to a quite significant surface hydroxylation by oxygen-containing particles with low bond strength, which is indirectly confirmed by the phase composition and texture, significantly different from the other prepared coatings (Table 1, Fig. 4). In all other cases, the OER overvoltage on composite electrodes exceeds that which is typical of PbO_2. This is an advantage in cases where the anode works in aqueous solutions at high polarizations, and the oxygen evolution reaction is not the target process.

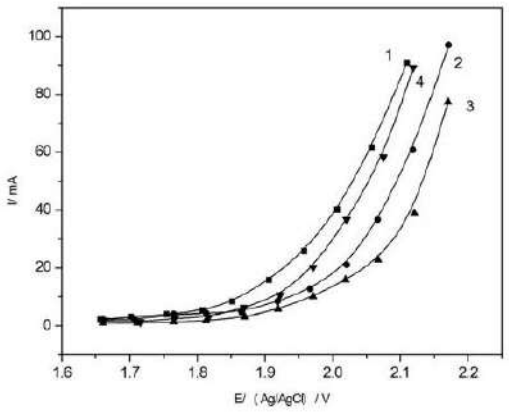

Fig. 5. Steady state polarization curves of oxygen evolution on PbO_2-based electrodes in the following solutions:

0.1 M $Pb(CH_3SO_3)_2$+0.1 M CH_3SO_3H+X g dm^{-3} $TiO_{2\ (colloidal)}$, where X is: (1) – 1.0; (2) – 2.0; (3) – 5.0; (4) – 0. j_a=5 mA cm^{-2}. Supporting electrolyte is 1 M $HClO_4$

The current efficiency of the electrodeposition reaction on composite anodes of such type is expected to increase due to inhibition of OER. It is noteworthy that increasing of the content of TiO_2 in the composite leads to the OER overvoltage growth, probably due to increasing the surface concentration of the valve metal oxide. Evidently, sites of this type have a higher affinity for oxygen, which leads to a change in the ratio of labile and inert forms of oxygen-containing particles in favor of the latter. Since the likely rate-limiting step of OER is the electrochemical desorption (transfer of the second electron) [13], it causes a natural increase of the oxygen evolution overvoltage.

We chose the degradation of an aromatic compound, namely 4-nitroaniline, for elucidating the electrocatalytic activity of PbO_2–TiO_2 anode materials. This compound was chosen as a model since it is an important pollutant and, additionally, the kinetics of its degradative oxidation can be easily studied by UV-vis spectroscopy.

As shown by Borras et al. [14], the overall mechanism for the electrochemical oxidation of aromatic organic compounds involves three following consecutive irreversible steps: (i) oxidation to a quinoid compound; (ii) ring opening reaction with formation of aliphatic acids; and (iii) mineralization to CO_2 and H_2O. According to literature data [15], a relatively large number of intermediates is formed during the anodic oxidation of p-nitroaniline. Main intermediates are benzoquinone and maleic acid. Only aliphatic acids are detected in the solution after prolonged electrolysis.

We followed the disappearance of intermediate aromatic products as a function of electrolysis time for different concentrations of the initial compound. The mechanism of electrochemical oxidation of the target compound is qualitatively the same for unmodified and modified PbO_2 electrodes; this allows a comparison of electrocatalytic activities in terms process rates which, instead depend appreciably on the electrode material.

Interesting data have been obtained for composite electrodes based on PbO_2 deposited from suspension methanesulfonate electrolytes containing nanosized TiO_2 particles as the dispersed phase. As shown in Table 3, the degradation rate of p-nitroaniline is higher PbO_2–TiO_2 than for pure PbO_2 electrodes and is enhanced by an increase in TiO_2 content in the composite. It is also seen in Table 3 that stirring of the suspension causes a further increase in the rate constants of p-nitroaniline degradation.

Increasing of the oxidation rate of p-nitroaniline on composite PbO_2–TiO_2 anodes is presumably due to the increasing of number of oxygen-containing species with high bond strength.

Table 3

Kinetic parameters of the electrochemical oxidation of p-nitroaniline (2×10^{-4} M) on modified PbO_2-anodes

Deposition electrolyte	Apparent heterogeneous rate constant, $k\cdot10^2$, min^{-1}
(M)*	1.68
(M)+1g dm^{-3} TiO_2	2.33
(M)+2 g dm^{-3} TiO_2	2.76
(M)+5 g dm^{-3} TiO_2	3.02

Note: * – (M) means 0.1 M $Pb(CH_3SO_3)_2$+0.1 M CH_3SO_3H. Coatings are deposited for 30 min at j_a=10 mA cm^{-2}, T=298 K. Electrode area is 3 cm^2.

Conclusions

Composites containing TiO_2 nanoparticle in PbO_2 matrics can be obtained by electrodeposition technique. These particles are delivered from the electrolyte bulk to the electrode surface by diffusion and/or migration (as a result of the appearance of partial concentration gradient in a colloidal solution due to the depletion of particles, included in the growing coating, in near-electrode zone). The content of the composite material depends on: (i) the electrolysis conditions; (ii) the surface charge of the dispersed phase particles and of the electrode; (iii) the PbO_2 deposition rate; and (iv) the concentration of components in the solution. By varying the electrolysis regimes and the composition of the electrolyte, composites containing of 4 to 27 wt.%. TiO_2 can be synthesized. The phase composition and texture of the resulting composites depend on the electrolysis conditions and the composition of the electrolyte. Thus, the presence of TiO_2 particles in the electrolyte leads, as a rule, to a decrease of the crystal size and growth of the content of α-phase of lead dioxide in the deposit.

The inclusion of particles of valve metal oxides into a PbO_2 matrix typically leads to an increase of OER overvoltage likely due to an increase of the amount of strongly bound oxygen-containing species on the electrode surface. Composite materials based on lead dioxide containing occluded TiO_2 nanoparticles exhibit a high activity towards the oxidative degradation of organic substances due to increasing of the number of oxygen-containing particles strongly bounded to the electrode surface.

Acknowledgements

The authors are indebted to Rossano Amadelli (University of Ferrara, Italy) for his help in the discussion of obtained results.

REFERENCES

1. *Electrochemical* oxygen transfer reactions: electrode materials, surface processes, kinetic models, linear free energy correlations, and perspectives. A review / R. Vargas, C. Borras, D. Mendez et al. // J. Solid State Electrochem. – 2016. – Vol.20. – P.875-893.

2. *Cattrin S., Musiani M.* Electrosynthesis of nancomposite materials for electrocatalysis / S. Cattarin // Electrochim. Acta. – 2007. – Vol.52. – P.2796-2805.

3. *Electrodeposition* of composite PbO_2–TiO_2 materials from colloidal methanesulfonate electrolytes / V. Knysh, T. Luk'yanenko, O. Shmychkova et al. // J. Solid State Electrochem. – 2017. – Vol.21. – P.537-544.

4. *Electrodeposition* of PbO_2–TiO_2 nanocomposite materials from suspension electrolytes / A.B. Velichenko, V.A. Knysh, T.V. Luk'yanenko et al. // Theor. Exp. Chem. – 2016. – Vol.52. – P.127-131.

5. *Electrodeposition* PbO_2–TiO_2 and PbO_2–ZrO_2 and its physicochemical properties / A.B. Velichenko, V.A. Knysh, T.V. Luk'yanenko et al. // Mater. Chem. Phys. – 2012. – Vol.131. – P.686-693.

6. *Electrodeposition* of Ni^{2+}-doped PbO_2 and physicochemical properties of the coating / O. Shmychkova, T. Luk'yanenko, R. Amadelli et al. // J. Electroanal. Chem. – 2016. – Vol.774. – P.88-94.

7. *Bi-doped* PbO_2 anodes: electrodeposition and physicochemical properties / O. Shmychkova, T. Luk'yanenko, A. Velichenko et al. // Electrochim. Acta. – 2013. – Vol.111. – P.332-338.

8. *Campbell M.A., Peter L.M.* Detection of soluble intermediates during deposition and reduction of lead dioxide // J. Electroanal. Chem. – 1996. – Vol.306. – P.185-194.

9. *Pavlov D., Monahov B.* Mechanism of the elementary electrochemical processes taking place during oxygen evolution on the lead dioxide electrode // J. Electrochem. Soc. –1996. – Vol.143. – P.3616-3629.

10. *Trasatti S., Lodi G.* Electrodes of conductive metallic oxides. Part B. – Elsevier: Amsterdam, 1981. – 521 p.

11. *Electrodeposition* of Co-doped lead dioxide and its physicochemical properties / A. B. Velichenko, R. Amadelli, E. A. Baranova et al. // J. Electroanal. Chem. – 2002. – Vol.527. – P.56-64.

12. *Electrodeposition* of Ce-doped PbO_2 / O. Shmychkova, T. Luk'yanenko, A. Velichenko et al. // J. Electroanal. Chem. – 2013. – Vol.706. – P.86-92.

13. *Influence* of the electrode history and effects of the electrolyte composition and temperature on O_2 evolution at β-PbO_2 anodes in acid media / R. Amadelli, A. Maldotti, A. Molinari et al. // J. Electroanal. Chem. – 2002. – Vol.534. – P.1-12.

14. *Study* of the oxidation of solutions of p-chlorophenol and p-nitrophenol on Bi-doped PbO_2 electrodes by UV-Vis and FTIR in situ spectroscopy / C. Borras, T. Laredo, J. Mostany et al. // Electrochim. Acta. – 2004. – Vol.49. – P.641-648.

15. *Jimenez Jado N.E., Fernandez Sanchez C., Ochoa Gomez J.R.* Electrochemical degradation of nitroaromatic wastes in sulfuric acid solutions: Part I // J. Appl. Electrochem. – 2004. – Vol.34. – P.551-556.

Received 8.06.2017

THE COMPOSITION AND PROPERTIES OF COMPOSITE PbO_2–TiO_2 MATERIALS ELECTRODEPOSITED FROM COLLOIDAL METHANESULFONATE ELECTROLYTES

A. Velichenko, V. Knysh, O. Shmychkova, T. Luk'yanenko

Ukrainian State University of Chemical Technology, Dnipro, Ukraine

PbO_2–TiO_2 nanocomposite materials are formed by electrochemical deposition of PbO_2 from colloidal nitrate and methanesulfonate electrolytes through the inclusion of a TiO_2 dispersed phase in the growing PbO_2 coating. These particles are delivered from the electrolyte bulk to the electrode surface by diffusion and/or migration (as a result of the appearance of partial concentration gradient in a colloidal solution due to the depletion of particles, included in the growing coating, in near-electrode zone). Composites containing from 4 to 27 wt.% TiO_2 can be synthesized by varying the electrolysis regimes and the composition of the electrolyte. The presence of TiO_2 particles in the electrolyte leads, as a rule, to the decrease of the crystal size and the growth of the content of α-phase of lead dioxide in the deposit. The inclusion of particles of valve metal oxides in a PbO_2 matrix typically results in an increase in oxygen evolution reaction overvoltage and promotes a high activity towards the oxidative degradation of organic substances likely due to an increase in the amount of strongly bound oxygen-containing species on the electrode surface.

Keywords: PbO_2–TiO_2 nanocomposites; methanesulfonate electrolyte; oxygen evolution; electrooxidation; phenolic compounds.

REFERENCES

1. Vargas R., Borras C., Méndez D., Mostany J., Scharifker B.R. Electrochemical oxygen transfer reactions: electrode materials, surface processes, kinetic models, linear free energy correlations, and perspectives. A review. *Journal of Solid State Electrochemistry*, 2016, vol. 20, pp. 875-893.

2. Cattarin S., Musiani M. Electrosynthesis of nancomposite materials for electrocatalysis. *Electrochimica Acta*, 2007, vol. 52, pp. 2796-2805.

3. Knysh V., Luk'yanenko T., Shmychkova O., Amadelli R., Velichenko A. Electrodeposition of composite PbO_2–TiO_2 materials from colloidal methanesulfonate electrolytes. *Journal of Solid State Electrochemistry*, 2017, vol. 21, pp. 537-544.

4. Velichenko A.B., Knysh V.A., Luk'yanenko T.V., Nikolenko N.V. Electrodeposition of PbO_2–TiO_2 nanocomposite materials from suspension electrolytes. *Theoretical and Experimental Chemistry*, 2016, vol. 52, pp. 127-131.

5. Velichenko A.B., Knysh V.A., Luk'yanenko T.V., Velichenko Yu.A., Devilliers D. Electrodeposition PbO_2–TiO_2 and PbO_2–ZrO_2 and its physicochemical properties. *Materials Chemistry and Physics*, 2012, vol. 131, pp. 686-693.

6. Shmychkova O., Luk'yanenko T., Amadelli R., Velichenko A. Electrodeposition of Ni^{2+}-doped PbO_2 and physicochemical properties of the coating. *Journal of Electroanalytical Chemistry*, 2016, vol. 774, pp. 88-94.

7. Shmychkova O., Luk'yanenko T., Velichenko A., Meda L., Amadelli R. Bi-doped PbO_2 anodes: electrodeposition and physico-chemical properties. *Electrochimica Acta*, 2013, vol. 111, pp. 332-338.

8. Campbell S.A., Peter L.M. Detection of soluble intermediates during deposition and reduction of lead dioxide. *Journal of Electroanalytical Chemistry and Interfacial Electrochemistry*, 1991, vol. 306, pp. 185-194.

9. Pavlov D., Monahov B. Mechanism of the elementary electrochemical processes taking place during oxygen evolution on the lead dioxide electrode. *Journal of the Electrochemistry Society*, 1996, vol. 143, pp. 3616-3629.

10. Trasatti S., Lodi G., *Electrodes of conductive metallic oxides. Part B.* Elsevier, Amsterdam, 1981. 521 p.

11. Velichenko A.B., Amadelli R., Baranova E.A., Girenko D.V., Danilov F.I. Electrodeposition of Co-doped lead dioxide and its physicochemical properties. *Journal of Electroanalytical Chemistry*, 2002, vol. 527, pp. 56-64.

12. Shmychkova O., Luk'yanenko T., Amadelli R., Velichenko A. Electrodeposition of Ce-doped PbO_2. *Journal of Electroanalytical Chemistry*, 2013, vol. 706, pp. 86-92.

13. Amadelli R., Maldotti A., Molinari A., Danilov F.I., Velichenko A.B. Influence of the electrode history and effects of the electrolyte composition and temperature on O_2 evolution at β-PbO_2 anodes in acid media. *Journal of Electroanalytical Chemistry*, 2002, vol. 534, pp. 1-12.

14. Borrás C., Laredo T., Mostany J., Sharifker B.R. Study of the oxidation of solutions of *p*-chlorophenol and *p*-nitrophenol on Bi-doped PbO_2 electrodes by UV-Vis and FTIR in situ spectroscopy. *Electrochimica Acta*, 2004, vol. 49, pp. 641-648.

15. Jiménez Jado N.E., Fernández Sánchez C., Ochoa Gómez J.R. Electrochemical degradation of nitroaromatic wastes in sulfuric acid solutions: Part I. *Journal of Applied Electrochemistry*, 2004, vol. 34, pp. 551-556.

ISSN 1068-3755, Surface Engineering and Applied Electrochemistry, 2018, Vol. 54, No. 1, pp. 38–46. © Allerton Press, Inc., 2018.
Original Russian Text © O.B. Shmychkova, V.A. Knysh, T.V. Luk'yanenko, R. Amadelli, A.B. Velichenko, 2017, published in Elektronnaya Obrabotka Materialov, 2017, No. 3, pp. 55–63.

Electrocatalytic Processes on PbO_2 Electrodes at High Anodic Potentials

O. B. Shmychkova[a], V. A. Knysh[a], T. V. Luk'yanenko[a], R. Amadelli[b], and A. B. Velichenko[a, *]

[a] *Ukrainian State University of Chemical Technology, Dnipro, 49005 Ukraine*

[b] *ISOF-CNR u.o.s Ferrara c/o Dipartimento di Scienze Chimiche e Farmaceutiche, Universita di Ferrara, via L. Borsari, Ferrara, 46—44121 Italy*

**e-mail: velichenko@ukr.net*

Received June 22, 2016; in final form, July 13, 2016

Abstract—The determination of the electrocatalytic activity and selectivity of electrodes with respect to the target process is considered to be of interest both in the theoretical aspect for the development of electrocatalysis theory and in application for efficient electrocatalysts which can be used in electrochemical systems for wastewater treatment. The purpose of the given work was to identify the relationship between the chemical and phase composition of materials based on lead dioxide, their physicochemical properties, and their electrocatalytic activity. The main research methods were quasi-stationary polarization and impedance spectroscopy, photocolorimetry, fluorescent and spectrophotometry in the UV and visible regions, atomic absorption spectroscopy, and high performance liquid chromatography (analysis of the solutions). It was shown that the modification of lead dioxide by ionic additives results in significant changes in the electrocatalytic activity of the system in respect to the oxygen evolution reaction and electrochemical oxidation reactions of organic compounds. It was found that, at low polarizations, the oxygen evolution reaction is limited by the electrochemical desorption step (the second electron transfer), and its overpotential at PbO_2-modified electrodes increases in the order that coincides with the number of oxygen-containing particles strongly bound to the electrode surface increases. It was found that the rate of oxidation of organic substances on the anode materials involved is directly proportional to the amount of oxygen-containing radicals formed on the electrode during the water oxidation.

Keywords: lead dioxide, methanesulfonate electrolyte, oxygen evolution, ozone generation, oxidation of organic compounds

DOI: 10.3103/S1068375518010143

INTRODUCTION

Almost all anodic processes in aqueous solutions at high anodic potentials (oxygen and ozone evolution, as well as oxidation of inorganic and organic compounds) are conditionally combined into a group of so-called oxygen transfer reactions owing to the similarity of mechanisms and participation of oxygen-containing radicals. In this case, the nature and energetics of oxygen-containing particles can significantly differ. Depending on the strength of binding to the electrode surface, oxygen-containing particles are divided into two large groups, which are inert (localized in the crystal zone of oxide) and labile (associated in the hydrated zone) [1]. Not only electrocatalytic activity of an electrode with respect to the chosen process but also its selectivity during several simultaneous reactions would depend on the distribution of these particles. In the latter case, the statement of the independent electrochemical processes does not seem to be correct, because particles of identical origin may participate; for this reason, interplay of these reactions may occur in several cases. One example is the inhibition of the oxygen evolution reaction in the presence of a series of organic substances, which are oxidized on the electrode with the consumption of oxygen-containing particles of radical type [2, 3].

As has been shown earlier [4—6], conditions of the synthesis of materials based on lead dioxide, their chemical and phase composition, as well as a number of structural factors (surface morphology and texture) substantially determine the surface coverage of the coating by one or another type of oxygen-containing radicals and, in turn, electrocatalytic activity and selectivity to the target process. Thus, the determination of the relationship between the chemical and phase compositions of the materials based on lead dioxide, their physicochemical properties, and their electrocatalytic activity is of a significant interest both in the theoretical aspect for the development of the theory of electrocatalysis and from a practical viewpoint for the design of effective electrocatalysts which can be employed in the systems of electrochemical

wastewater treatment. It should be noted that there are almost no such data on the materials based on lead dioxide, which were prepared from methanesulfonate electrolytes.

MATERIALS AND METHODS

Reagents of reagent grade and analytical grade and distilled water prepared through the double distillation of tap water using a glass bidistillate of BS type were employed in this work.

Electrolytes were prepared from solutions with known concentrations by sampling of an aliquot followed by the dilution with water to a required volume. To prepare the anodes with active coating based on lead dioxide, the solution of the following composition was used as a basic electrolyte, mol/dm^3: $Pb(CH_3SO_3)_2$, 0.1; CH_3SO_3H, 0.1. Depending on the purpose of the experiment, the concentrations of methanesulfonic acid and its salt were varied in the range of 0.1–1 mol/dm^3 (CH_3SO_3H) and 0.1–1 mol/dm^3 ($Pb(CH_3SO_3)_2$). To prepare micromodified electrodes, $Bi(NO_3)_3$, $Ce(NO_3)_3$, $(CH_3COO)_4Sn$, $K_2[NiF_6]$, $K_2[SnF_6]$, and suspensions of TiO_2 and ZrO_2 were added to the methanesulfonate electrolyte.

The oxygen evolution reactions on unmodified and modified lead dioxide were studied in the solutions of $HClO_4$ and H_2SO_4, as well as in nitrate electrolyte ($Pb(NO_3)_2$, 0.1; HNO_3, 0.1), containing various amounts of CH_3SO_3Na. Ozone evolution and oxidation of organic compounds were studied in phosphate buffer.

The coatings were deposited at the anodic current intensity of 5 mA/cm^2 and the temperature of 298 K. Platinated titanium was employed as a substrate during preparation of anodes based on PbO_2. Before depositing the platinum coating, the titanium substrate was prepared according to the procedure described in [7].

The content of additive in the coating was determined using atomic absorption with atomization in a graphite furnace, model Analyst 800.

Electrooxidation of organic substances was carried out in a cell with cathode and anode spaces separated by an ion-exchange membrane at $j_a = 50$ mA/cm^2. The anolyte volume was 130 cm^3. Aqueous solutions of the substance with the following composition: phosphate buffer (0.25 M Na_2HPO_4 + 0.1 M KH_2PO_4) + 2×10^{-4} M organic substance (pH 6.68) was used as anolyte, phosphate buffer was used as catholyte. As the cathode, a steel plate was used, modified lead dioxide electrodes were used as anodes. The electrode area was 3 cm^2.

The change in the concentration of organic substance during electrolysis was determined by sampling (5 cm^3 in volume) with a particular periodicity and measurement of absorbance of the solution in the ultraviolet and visible regions (the wavelength range of 200–570 nm). Absorption spectra of the solutions containing organic substances were recorded using SF-46 or UVIKON spectrophotometers.

The oxygen evolution reaction was studied via quasistationary polarization and impedance spectroscopy using a software-controlled EG & G Princeton Applied Research potentiostat, model 273A, and an Amplifier lock-in amplifier, model 5210. For these studies, PbO_2 was deposited onto Pt wire (0.13 cm^2). The experimental data were processed using Boucamp's equivalent circuit simulation program and the ZsimpWin 3.21 program. All potentials were recorded and reported vs. $Ag/AgCl/KCl_{(sat)}$.

The current efficiency of the ozone evolution were determined using phosphate buffer at 278 K. The temperature of the solution was maintained using a Julabo F 12 cryostat; carrier gas (argon) was blown through the electrochemical cell, which provided a significant increase in the rate of establishment of equilibrium, as well as filling of the cell and cuvette volumes of the measuring system with the gas mixture formed on anode. The flow rate of the carrier gas was 60–120 cm^3/min. The concentration of ozone was determined using iodometric titration [8].

RESULTS AND DISCUSSION

Oxygen evolution reaction. The results of the studies (Fig. 1) showed that, the addition of 0.1 M CH_3SO_3Na to the nitrate electrolyte results in the decreasing of the overvoltage of the oxygen evolution reaction (OER) towards to the basic nitrate electrolyte and, then, its increasing is observed with the growth of the concentration of CH_3SO_3Na to 0.5 M in the electrolyte. However, further growth of the content of sodium methanesulfonate to 1.2 M again leads to the decrease in the overvoltage of OER, though it does not amount to the values for the basic nitrate electrolyte even at the maximum concentration (Fig. 2).

The mechanism of oxygen evolution on PbO_2 electrodes was suggested in the works of Pavlov et al. [9–11]. According to the developed considerations, the electrode surface consists of crystal (PbO_2) and hydrated [$PbO(OH)_2$] zones, which exist in equilibrium, while the latter may exchange cations and anions with the solution. Oxygen evolution can be described via the following mechanism (1–3):

$$PbO \cdot (OH)_2 + H_2O \rightarrow PbO \cdot (OH)_2...(OH^{\bullet}) + H^+ + e^-, \quad (1)$$

$$PbO \cdot (OH)_2...(OH^{\bullet}) \rightarrow PbO \cdot (OH)_2 + O + H^+ + e^-, \quad (2)$$

$$2O \rightarrow O_2. \quad (3)$$

Since the second electron transfer (electrochemical desorption) is the limiting step, an increase in the binding strength of chemisorbed oxygen results in the growth of the overvoltage of oxygen evolution [1].

To rationalize this significantly complex effect, the principles of oxygen evolution and the composition and physicochemical properties of lead dioxide should be compared. Since methanesulfonate ions are not included in the lead dioxide coating with the formation of modified material, its chemical composition does not depend on the content of CH_3SO_3Na in the electrolyte [4]. At the same time, we determined that, the addition of 0.1 M sodium methanesulfonate to the nitrate solution, remarkably changes the phase composition of the coating. In this case, the content of the α phase increases by a factor of nearly three to 41%. This can be the main reason for the decrease in the overvoltage of OER, because there are favorable conditions for the formation of labile oxygen-containing particles [1]. With an increase in the concentration of CH_3SO_3Na in the deposition electrolyte, the phase composition of the electrodes hardly changes, as well as the crystallographic orientations of individual faces of the α and β phases of lead dioxide. On the contrary, as follows from intensities and half-height widths of the peaks of individual faces, the size of the crystals of lead dioxide first grows to the concentration of sodium methanesulfonate of 0.6 M, which indicates an increase in the crystal zone of oxide, which is characterized by the predomination of inert oxygen-containing particles, and, then, drops (growth of the hydrated zone with the predomination of labile oxygen-containing particles). This is the reason for such a complex dependence of oxygen overvoltage on the content of methanesulfonate ions in the deposition electrolyte.

The rate of the oxygen evolution reaction can also change depending on the nature and amount of ionic additive in solution during the formation of modified lead dioxide [4–6].

According to the obtained data (Fig. 3), the oxygen overvoltage on composition materials is significantly higher than that on PbO_2 electrode. This is an advantage when the anode operates in aqueous solutions at high polarizations and the oxygen evolution reaction is not the target process. When using composition anodes of this type, the efficiency of the target reaction may increase owing to the inhibition of OER.

It is noteworthy, that the increase in the content of titanium dioxide in the composite results in the growth of the overvoltage of OER presumably because of the increase in the surface concentration of valve metal oxide. In this case, these centers possess higher oxygen affinity, which shifts the ratio of labile to inert forms of oxygen-containing particles to the latter. Because the mechanism of OER and the nature of the limiting step of the process do not change, this leads to an evident increase in the overvoltage of oxygen evolution.

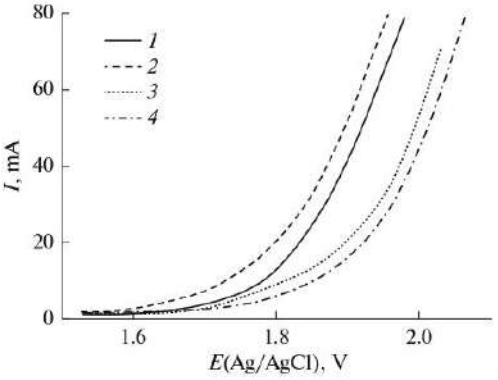

Fig. 1. Quasistationary polarization curves (5 mV/s) of lead dioxide electrodes in 1 M $HClO_4$ prepared at 5 mA/cm^2 from electrolytes of 0.1 M $Pb(NO_3)_2$ + 1.0 M HNO_3 (*1*) containing various amounts of CH_3SO_3Na (M): (*2*) 0.1, (*3*) 0.3, and (*4*) 0.5. $S_{electrode}$ = 3 cm^2.

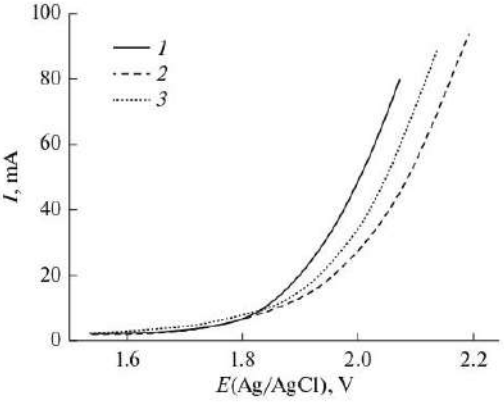

Fig. 2. Quasistationary polarization curves (5 mV/s) of lead dioxide electrodes in 1 M $HClO_4$ prepared at 5 mA/cm^2 from electrolytes of 0.1 M $Pb(NO_3)_2$ + 1.0 M HNO_3 (*1*) containing various amounts of CH_3SO_3Na (M): (*2*) 0.8 and (*3*) 1.2. $S_{electrode}$ = 3 cm^2.

Change in the nature of particles of the disperse phase at their equivalent contents in the composite also changes the overvoltage of OER. One example is that the substitution of ZrO_2 for TiO_2 gives an increase in the overvoltage of oxygen evolution (Fig. 4), which is presumably caused by different binding strength of chemisorbed oxygen-containing particles taking part in OER.

It should also be noted that the overvoltage of oxygen evolution may differ on the composition materials, which are prepared using various approaches (pH

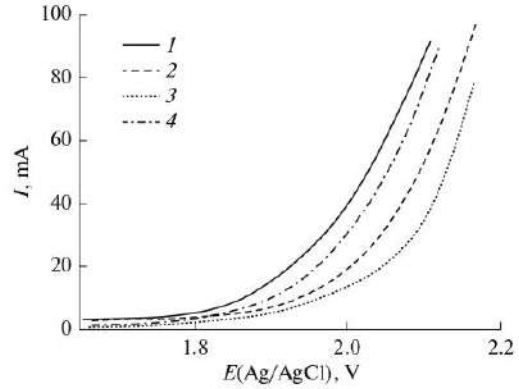

Fig. 3. Quasistationary polarization curves of oxygen evolution in 1 M $HClO_4$ in the case of the electrodes based on lead dioxide prepared from solutions of the following composition: 0.1 M $Pb(CH_3SO_3)_2$ + 0.1 M CH_3SO_3H (*1*) + *X* g/dm^3 TiO_2, where *X* is (*2*) 1.0, (*3*) 2.0, and (*4*) 5.0.

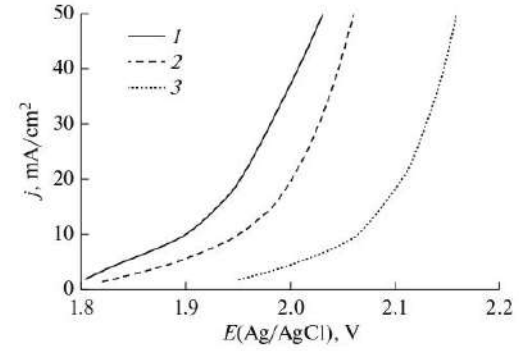

Fig. 4. Quasistationary polarization curves of oxygen evolution in 1 M H_2SO_4 on the materials deposited from electrolytes of the composition 0.1 M $Pb(NO_3)_2$ + 0.1 M HNO_3 + *X* g/dm^3 TiO_2, where *X* is (*1*) 0, (*2*) 2.0, and (*3*) 1.0 g/dm^3 ZrO_2.

of electrolyte, presence of surfactants, and others) at the equivalent contents of the disperse phase in the coating (for example, 9 wt % TiO_2) (Fig. 5).

This phenomenon is caused by the differences in surface morphology, phase composition, and crystallographic orientations of lead dioxide [12–14], that is, manifestation of a structural factor in electrocatalysis.

Unfortunately, at the present time, there are no direct experimental methods which measure the strength of binding of chemisorbed oxygen-containing radicals to the electrode surface. For this reason, various correlation parameters are used in the works on electrocatalysis, which do not directly correlate with OER, as exemplified by the energy of homomolecular isotopic oxygen exchange in oxide or the enthalpy of transition of oxides from a lower to higher oxidation state [12, 15].

In this work, the enthalpy of transition of valve metal oxides from one form to another was used as a correlation parameter, which evaluates the binding strength of chemisorbed oxygen. An increase in enthalpy (Table 1) indicates an increase in the binding strength of OH_{ads} on the electrode surface, which leads to the increase in the overvoltage of OER in the following order: $PbO_2 < PbO_2$-$TiO_2 < PbO_2$-ZrO_2 (Fig. 4).

Thus, upon the inclusion of TiO_2 or ZrO_2 in lead dioxide, an increase in the overvoltage of OER is observed, which is caused by the growth of the strength of binding of chemisorbed oxygen to the electrode surface.

OXIDATION OF ORGANIC COMPOUNDS

Electrochemical destruction of organic substances in wastewater is an important problem. Numerous investigations are devoted to the design of electrode materials employed for wastewater treatment. As electrocatalysts, synthetic boron-doped diamond electrodes (BDD) [16] or PbO_2-based anodes [15] are usually employed. In this case, it is noteworthy that, in the former case, the main problem is high consumption of electric energy owing to the low conductivity of modified synthetic diamonds, which makes them almost inapplicable as anodes under industrial conditions. Thus, the materials based on lead dioxide are more promising, especially that their electrocatalytic activity can be significantly increased through their modification.

It should be considered that the oxidation of organic compounds is not necessarily electrochemical. It is highly probable that the reaction proceeds through oxidizing agents formed during the primary electrochemical reaction of, for example, hydroxyl radicals or ozone. In fact, this process is secondary chemical. It should also be noted that it is not always assumed that the oxygen evolution reaction on the electrode may occur together with other reactions with oxygen transfer, such as oxidation of organic [16, 17] or inorganic compounds [15], which are not necessarily implemented independently.

The efficiency of these processes depends on the ratio of the rates of formation and disappearance of OH radicals. Accumulation of a sufficient amount of these radicals on the electrode surface and in the near-electrode area facilitates their interaction with inorganic and organic compounds, causing their partial or full oxidative destruction. For this reason, a series of investigations was carried out which were aimed at the determination of the number of active forms of oxygen during electrolysis, namely, hydroxyl radicals on lead dioxide electrodes modified with various ionic additives [8]. The results of the studies showed that syn-

thetic boron-doped diamond exhibits the highest activity during electrolysis with respect to the generation of hydroxyl radicals, which is followed by bismuth-modified PbO_2 among lead dioxide electrodes (plating at $T = 282$ K).

Another group of anodic reactions occurring at higher anodic potentials with oxygen-containing particles may include the synthesis of strong oxidizing agents as exemplified by ozone. The ozone evolution reaction occurs in parallel to the oxygen evolution reaction, while the latter significantly affects the ozone current efficiency.

Because ozone is generated along with the oxidation of organic compounds [18, 19], its synthesis during electrolysis may promote the destruction of toxic organic compounds. The results of the studies showed that the ozone current efficiency on the electrodes plated from methanesulfonate electrolytes are on average three times as large as those on the materials deposited from nitrate solutions [6]. Modification with ionic additives slightly increases the ozone current efficiency; however, the latter is characterized by values around 1–3%. An analogous effect was obtained for the composition materials based on lead dioxide containing titania particles in the disperse phase.

This effect is caused by the differences in the chemical and phase composition of the coatings obtained from nitrate and methanesulfonate electrolytes, namely, in the degree of hydroxylation of surface. Because oxygen-containing particles, which are strongly bound to the electrode surface, participate in ozone evolution reaction [1], a decrease in their amount would lead to the decrease in the ozone current efficiency, which is observed in the case of the coatings prepared from methanesulfonate electrolytes.

In order to determine the effect of the method for preparation and the composition of the anodic materials based on lead dioxide on their electrocatalytic activity with respect to the oxidation of organic compounds, 4-nitroaniline and 4-nitrophenol were chosen as model aromatic compounds. This choice is caused by the fact that electrooxidation of phenolic compounds on various electrodes are studied well; therefore, the main attention can be focused only on the determination of the role of anodic material.

In particular, a large number of papers are devoted to electrooxidation of aromatic compounds, where IrO_2 and other noble metal oxides, such as PbO_2 and SnO_2 [8, 14, 20], were used as anodic materials. The choice of the acidity of solution for electrolysis is of a great importance, because it affects the dissociation of acids and bases, as well as individual stages of these reactions. As an example, anodic oxidation of phenols may occur by two routes depending on the pH of the system [21–26]. It should be noted that most oxide materials are chemically and corrosion-resistant only in alkaline solutions; therefore, the choice of anodes for acidic and neutral solutions is limited to noble

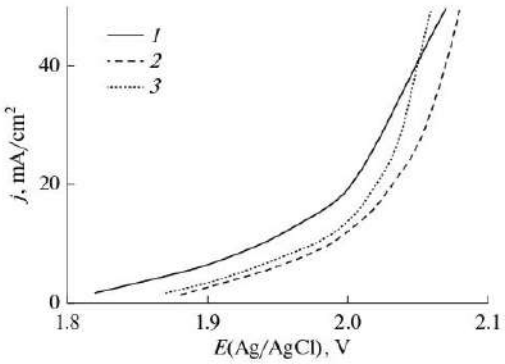

Fig. 5. Quasistationary polarization curves of oxygen evolution in 1 M H_2SO_4 on the materials deposited from electrolytes of the composition 0.1 M $Pb(NO_3)_2$ + 0.1 M HNO_3 + X g/dm^3 TiO_2, where X is (*1*) 2.0 (obtained at i_a = 10 mA/cm^2), (*2*) 2.0 (plated at i_a = 5 mA/cm^2), and (*3*) 2.0 + 7×10^{-4} M surfactant (obtained at $i_a = 7$ mA/cm^2).

metal oxides, as well as lead, tin, and manganese dioxides. In this case, it should be noted that the electrocatalytic activity of noble metal oxides is low with respect to the direct anodic oxidation of phenolic compounds, while lead dioxide exhibits fairly high activity in these processes [1, 26].

Oxidation of *p*-nitroaniline. The choice of *p*-nitroaniline as a model was caused by the necessity to carry out kinetic studies on the initial substance, because its solution is colored. The Lambert–Beer law is fulfilled for it, while the absorbance vs. concentration plot represents a line which crosses the origin of coordinates ($y = 0.1068x + 0.0864$; $r = 0.998$).

It was mentioned in [27] that the general mechanism of oxidation of organic aromatic compounds should involve oxidation of the compound to intermediate products of quinoid structure, aromatic ring opening, and the formation of aliphatic products (mainly acids) and in the ideal case full mineralization to CO_2 and H_2O. According to the published data [28], a fairly large number of intermediate products are formed during anodic oxidation of *p*-nitroaniline, which may include benzoquinone and maleic acid.

Table 1. Enthalpies of transitions from one form to another, which were calculated according to the standard enthalpies of formation of individual oxides

Oxides	Transition	$-\Delta H$, kJ/mol
PbO_2	$Pb_3O_4 \rightarrow PbO_2$	447.15
TiO_2	$Ti_2O_3 \rightarrow TiO_2$	574.47
ZrO_2	$Zr_2O_3 \rightarrow ZrO_2$	707.40

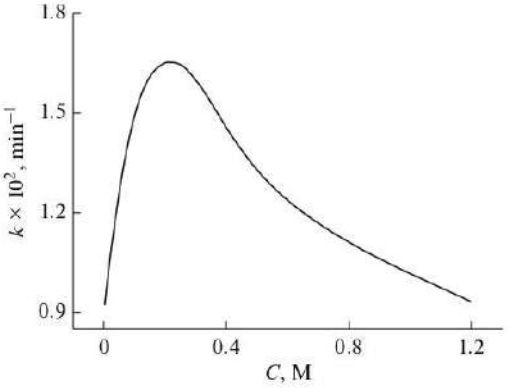

Fig. 6. Dependence of the rate constant of oxidation of *p*-nitroaniline on lead dioxide anodes obtained from electrolyte of 0.1 M $Pb(NO_3)_2$ + 1.0 M HNO_3 + X M CH_3SO_3Na.

As follows from the high-performance liquid chromatography data, 1,4-benzoquinone is the main intermediate aromatic product [8]. During long-term electrolysis in solution, only aliphatic acids are detected.

It should be noted that the electrocatalytic activity of lead dioxide anodes with respect to the oxidation of *p*-nitroaniline depends on the concentration of methanesulfonate ions in electrolyte from which PbO_2 is prepared. The dependence has a critical form with the maximum at the concentrations of CH_3SO_3Na of 0.1–0.3 M. As follows from the results, the chemical composition of lead dioxide hardly changes in this case. However, in this case, as during the oxygen evolution reaction (Figs. 1, 2), structural factors play a significant role. The maximum electrocatalytic activity is achieved with an increase in the fraction of the α phase, on one hand, and the expansion of the crystal zone of oxide, on the other hand, which leads to an increase in the amount of oxygen-containing particles strongly bound to the surface, which participate in electrochemical oxidation of aromatic compounds [8].

On the contrary, the comparison of the data on the overvoltage of OER (Figs. 1, 2) and electrooxidation of *p*-nitroaniline (Fig. 6) indicates the absence of a direct correlation of these two processes. Thus, the statement that an increase in the overvoltage of oxygen evolution necessarily results in a more efficient employment of anodes with respect to other processes with oxygen transfer as exemplified by ozone evolution and electrooxidation of organic and inorganic compounds is not always true.

It is noteworthy that electrooxidation of *p*-nitroaniline on unmodified and modified lead dioxide electrodes proceeds according to a similar mechanism, which allows the correct comparison of their electrocatalytic activity.

According to calculations (Table 2) based on kinetic studies, the rate constant of the destruction of *p*-nitroaniline depends on the composition of the electrode material and changes depending on the nature and the content of ionic additives in lead dioxide.

Bismuth-modified lead dioxide electrodes are of maximum interest for electrochemical destruction of organic compounds, for which the rate constant of the destruction of *p*-nitroaniline increases by the factor of 1.6 as compared to the values obtained when using unmodified PbO_2 electrodes (Fig. 6, Table 2). In other cases, the rate constants are comparable.

Interesting results were obtained in the case of composition electrodes based on lead dioxide obtained from suspension methanesulfonate electrolytes containing nanosized titania particles as a disperse phase. As follows from Table 3, the rate of destruction of *p*-nitroaniline grows with an increase in the content of TiO_2 in the composite, increasing in the limiting case by a factor of 1.8 as compared to the highest values when using unmodified PbO_2 electrodes.

Mixing of the suspension electrolyte during the preparation of the composition material (0.1 M $Pb(CH_3SO_3)_2$ + 0.1 M CH_3SO_3H + 5 g/dm^3 TiO_2, 30 min, 10 mA/cm^2, T = 298 K), which leads to an additional growth of the content of TiO_2, gives a larger rate constant of *p*-nitroaniline, which is 3.56 min^{-1}, while a decrease in the current intensity of the deposition to 5 mA/cm^2 gives 4.45 min^{-1}. In the latter case, the rate constant exceeds by a factor of 2.4 the highest value for PbO_2 electrodes without additives.

Table 2. Kinetic parameters of electrochemical oxidation of *p*-nitroaniline (2×10^{-4} M) on modified PbO_2 anodes

Anodic material	Rate constant of heterogeneous reaction, $k \times 10^2$, min^{-1}
PbO_2	1.68
PbO_2–1.81 wt % Bi	2.76
PbO_2–0.019 wt % Ce	1.36
PbO_2–1.81 wt % Sn	1.38
PbO_2–0.042 wt % Ni; 0.043 wt % F	1.66
PbO_2–1.56 wt % Sn; 0.04 wt % F	1.38

Table 3. Rate constant of electrochemical decomposition of *p*-nitroaniline on various PbO_2-TiO_2 anodes

Electrolyte for plating	Rate constant of heterogeneous reaction, $k \times 10^2$, min^{-1}
0.1 M $Pb(CH_3SO_3)_2$ + 0.1 M CH_3SO_3H	
+ 0.5 g/dm^3 TiO_2	2.32
+ 1 g/dm^3 TiO_2	2.33
+ 2 g/dm^3 TiO_2	2.76
+ 5 g/dm^3 TiO_2	3.02

Conditions of preparation are i_a = 10 mA/cm^2, 30 min, T = 25°C, and $S_{electrode}$ = 3 cm^2.

Table 4. Kinetic parameters of electrochemical oxidation of *p*-nitrophenol (2×10^{-4} M) on modified PbO_2 anodes

Anodic material	Rate constant of heterogeneous reaction, $k \times 10^2$, min^{-1}
PbO_2	0.84
PbO_2–1.81 wt % Bi	0.88
PbO_2–0.019 wt % Ce	0.52
PbO_2–1.87 wt % Sn	0.54
PbO_2–0.042 wt % Ni; 0.043 wt % F	0.82
PbO_2–1.56 wt % Sn; 0.04 wt % F	0.52

The increase in the rate of oxidation of *p*-nitroaniline on composition anodes PbO_2–TiO_2 is caused by the increase in the amount of oxygen-containing particles with high binding strength also owing to their generation according to the photochemical mechanism.

Oxidation of *p*-nitrophenol. It is known that *p*-nitrophenol exists in the ionic form in an acidic medium, where the concentration of hydrogen ions is high. According to the chromophore theory, the molecular structure of *p*-nitrophenol changes with the change in pH due to benzoid–quinoid tautomerism. In addition, *p*-nitrophenols are capable of association owing to the hydrogen bond formation between hydroxyl and nitro groups.

Among the products of electrolysis, maleic acid and a stoichiometric amount of NO_3^- were detected using high-performance liquid chromatography. In this case, the main aromatic intermediate compound was 1,4-benzoquinone; however, its concentration was one order of magnitude higher than during the oxidation of *p*-nitroaniline [8]. The latter fact indicates a more effective destruction of the aromatic ring of *p*-nitroaniline.

The data in Table 4 show that the rate constant of oxidation of *p*-nitrophenol on modified lead dioxide electrodes is slightly less than that of *p*-nitroaniline; however, the order of modifying ions in the series of electrocatalytic activity with respect to the oxidation of organic compounds is preserved (Table 4).

Oxidation of methyl-*tert*-butyl ether. Methyl-*tert*-butyl ether (MTBE) is one of the most widespread additivies to motor fuels. In spite of a significant decrease in hazardous gas release into atmosphere due to the more complete combustion of fuel, the accumulation of MTBE in ground water and water reservoirs cannot be avoided because of the corrosion of fuel containers [29]. Electrochemical conversion and destruction of toxic organic compounds have several advantages as compared to conventional reagent methods, the most important of which are high effectiveness, possibility of the control of the reaction owing to the control of the parameters of electrolysis, reagentlessness, and, consequently, low cost of purification. The processes of anodic conversion of organic compounds include oxygen atom transfer from solvent molecules to the products of oxidation, which are also referred to as oxygen-transfer reactions [1].

It should be noted that there are scarce data on the electrochemical oxidation of MTBE [30–32]. During the electrolysis using PbO_2 anodes in solution, the following main products of electrooxidation of MTBE were detected (gas chromatography): *tert*-butyl alcohol, acetone, acetic acid, and CO_2 [33, 34]. The concentration of *tert*-butyl alcohol becomes maximal after one hour, while the content of acetone and acetic acid (5.5×10^{-3} M) becomes maximal after 3 h of electrolysis. After 6 h of electrolysis, only acetic acid with the concentration of 2.0×10^{-3} M was detected in solution. According to the calculations performed on the basis of kinetic curves, electrochemical oxidation of

Table 5. Kinetic parameters (rate constant of the reaction k and half-life $t_{1/2}$) of electrochemical destruction of MTBE on various PbO_2-TiO_2 anodes

Electrode material	k, min^{-1}	$t_{1/2}$, min
PbO_2	5.5×10^{-3}	125
PbO_2-TiO_2 (6 wt %)	7.0×10^{-3}	99
PbO_2-TiO_2 (16 wt %)	1.0×10^{-2}	69
PbO_2-TiO_2 (6 wt %) upon UV irradiation	1.2×10^{-2}	58
PbO_2-TiO_2 (16 wt %) upon UV irradiation	1.2×10^{-2}	58

MTBE is a pseudo-first-order reaction, the main kinetic parameters of which are given in Table 5.

An increase in the content of TiO_2 in the composite results in an increase in the rate of destruction of MTBE by nearly two times with a decrease in the half-life from 125 to 69 min (Table 5). A higher electrocatalytic activity of composition PbO_2-TiO_2 anodes is presumably caused by the larger amount of tightly bound (inert) forms of chemisorbed oxygen on the electrode surface. Another interesting effect is an increase in the rate of electrooxidation of MTBE upon UV exposure (Table 5). In the case of the composite containing 6 wt % TiO_2, the rate constant of the reaction increases by nearly two times, while the half-life decreases from 99 to 58 min. This effect is caused by the additional formation of hydroxyl radicals during the implementation of the photocatalytic process [33]. Thus, the composition materials PbO_2-TiO_2 significantly exceed conventional lead dioxide anodes in electro- and photocatalytic activity and can be recommended as effective electrodes for electrochemical destruction of MTBE.

CONCLUSIONS

Oxygen evolution on materials based on lead dioxide can be satisfactorily described within the mechanism proposed by Pavlov et al., according to which the second electron transfer (electrochemical desorption) is the limiting step. The composition of the electrolyte for plating significantly affects the overvoltage of OER on the materials based on lead dioxide. A critical dependence of the overvoltage of OER on the content of methanesulfonate ions in the electrolyte for the preparation of PbO_2 is caused by the change in the phase composition and the degree of crystallinity of lead dioxide, which in turn result in the change of the ratio of inert to labile forms of oxygen-containing particles. The inclusion of ionic additives into the materials based on lead dioxides into cationic vacancies or valve metal oxide particles usually leads to the increase in the overvoltage of OER owing to the growth of the number of tightly bound oxygen-containing particles on the electrode surface.

The rate of oxidation of organic substances on the anodic materials is proportional to the number of active forms of oxygen in the near-electrode zone (OH radicals) which are formed during electrolysis as the intermediates of water oxidation and take part in further homogeneous chemical reactions with organic substrates in the solution bulk. For this reason, it is reasonable to employ anode-generated hydroxyl radicals as an evaluation parameter during the prediction of electrocatalytic properties of materials with respect to the oxidation of organic compounds.

The composition materials based on lead dioxide containing titania nanoparticles possess the maximum activity with respect to the oxidative destruction of organic substances of various types owing to the increase in the number of oxygen-containing particles which are strongly bound to the electrode surface, as well as parallel photocatalytic processes on TiO_2 centers, which provides an additional number of oxygen-containing oxidizing agents of radical and peroxide nature.

REFERENCES

1. Trassatti, S. and Lodi, G., in *Electrodes of Conductive Metallic Oxide. Part B*, Amsterdam: Elsevier, 1981, pp. 521–626.
2. Gong, M. and Dai, H., *Nano Res.*, 2015, vol. 8, pp. 23–39.
3. Hao, X., Wuqi, G., Wu, J., Feng, J., Honghui, Y., and Wei, Y., *RSC Adv.*, 2016, vol. 6, pp. 7610–7617.
4. Shmychkova, O., Luk'yanenko, T., Velichenko, A., Meda, L., et al., *Electrochim. Acta*, 2013, vol. 111, pp. 332–338.
5. Shmychkova, O., Luk'yanenko, T., Velichenko, A., and Amadelli, R., *J. Electroanal. Chem.*, 2013, vol. 706, pp. 86–92.
6. Shmychkova, O., Luk'yanenko, T., Amadelli, R., and Velichenko, A., *J. Electroanal. Chem.*, 2014, vols. 717–718, pp. 196–201.
7. Velichenko, A.B., Knysh, V.A., Luk'yanenko, T.V., Danilov, F.I., et al., *Prot. Met. Phys. Chem.*, 2009, vol. 45, pp. 327–332.
8. Shmychkova, O., Luk'yanenko, T., Yakubenko, A., Amadelli, R., et al., *Appl. Catal., B*, 2015, vol. 162, pp. 346–351.
9. Pavlov, D. and Monahov, B., *J. Electrochem. Soc.*, 1998, vol. 145, pp. 70–77.

10. Monahov, B., Pavlov, D., and Petrov, D., *J. Power Sources*, 2000, vol. 85, pp. 59–62.
11. Pavlov, D. and Monahov, B., *J. Electrochem. Soc.*, 1996, vol. 143, pp. 3616–3629.
12. Vargas, R., Borras, C., Mostany, J., and Scharifker, B.R., *Bol. Acad. Cienc. Fis., Mat. Nat.* (Caracas), 2011, vol. 71, pp. 37–56.
13. Low, C.T.J., Pletcher, D., and Walsh, F.C., *Electrochem. Commun.*, 2009, vol. 11, pp. 1301–1304.
14. Liu, Y. and Liu, H., *Electrochim. Acta*, 2008, vol. 53, pp. 5077–5476.
15. Li, X., Pletcher, D., and Walsh, F.C., *Chem. Soc. Rev.*, 2011, vol. 40, pp. 3879–3894.
16. *Electrochemistry for the Environment*, Comninellis, C. and Chen, G., Eds., New York: Springer-Verlag, 2010.
17. Panizza, M. and Cerisola, G., *Chem. Rev.*, 2009, vol. 109, pp. 6541–6569.
18. Babak, A.A., Amadelli, R., De Battisti, A., and Fateev, V.N., *Electrochim. Acta*, 1994, vol. 39, pp. 1597–1602.
19. Babak, A.A., Fateev, V.N., Amadelli, R., and Potapova, G.F., *Russ. J. Electrochem.*, 1994, vol. 30, pp. 739–741.
20. Chaplin, B.P., *Environ. Sci.: Process. Impacts*, 2014, vol. 16, pp. 1182–1203.
21. Kim, J., Korshin, G.V., and Velichenko, A.B., *Water Res.*, 2005, vol. 39, pp. 2527–2534.
22. Cao, J., Zhao, H., Cao, F., Zhang, J., and Cao, C., *Electrochim. Acta*, 2009, vol. 54, pp. 2595–2602.
23. Quiroz, M.A., Reyna, S., Martinez-Huitle, C.A., Ferro, S., et al., *Appl. Catal., B*, 2005, vol. 59, pp. 259–266.
24. Feng, Y.J. and Li, X.Y., *Water Res.*, 2003, vol. 37, pp. 2399–2407.
25. Iniesta, J., Gonzalez-Garsia, J., Exposito, E., and Montiel Aldaz, A., *Water Res.*, 2001, vol. 35, pp. 3291–3300.
26. Kawagoe, K.T. and Johnson, D.C., *J. Electrochem. Soc.*, 1994, vol. 141, pp. 3404–3409.
27. Borras, C., Laredo, T., Mostany, J., and Scharifker, B.R., *Electrochim. Acta*, 2004, vol. 49, pp. 641–648.
28. Widera, J. and Cox, J.A., *Electrochem. Commun.*, 2002, vol. 4, pp. 118–122.
29. Mitani, M.M., Keller, A.A., Golden, S.J., and Hatfield, R., *Appl. Catal., B*, 2001, vol. 34, pp. 87–95.
30. Bergendahl, J.A. and Thies, T.P., *Water Res.*, 2004, vol. 38, pp. 327–334.
31. Johnson, D.C., Feng, J., and Houk, L.L., *Electrochim. Acta*, 2000, vol. 46, pp. 323–330.
32. Amadelli, R., Samiolo, L., De Battisti, A., and Velichenko, A.B., *J. Electrochem. Soc.*, 2011, vol. 158, pp. P87–P92.
33. Graham, J.L., Striebich, R.C., Patterson, C.L., Krishman, E.R., et al., *Chemosphere*, 2004, vol. 54, pp. 1011–1016.
34. Kang, J.W. and Hoffmann, M.R., *Environ. Sci. Technol.*, 1998, vol. 32, pp. 3194–3199.

Translated by A. Muravev

Journal of the Serbian Chemical Society
JSCS-info@shd.org.rs • www.shd.org.rs/JSCS
J. Serb. Chem. Soc. 84 (2) 187–198 (2019) UDC 628.3:546.74'815–31+615.9:544.2.004.12
JSCS–5175 Original scientific paper

Modified lead dioxide for organic wastewater treatment: Physicochemical properties and electrocatalytic activity

OLESIA SHMYCHKOVA[1], TATIANA LUK'YANENKO[1], LARISA DMIRTIKOVA[2] and ALEXANDER VELICHENKO[1]*

[1]*Ukrainian State University of Chemical Technology, 8, Gagarin Ave., 49005 Dnipro, Ukraine and* [2]*Oles Honchar Dnipro National University, 72, Gagarin Ave., 49010 Dnipro, Ukraine*

(Received 12 July, revised 20 September, accepted 26 October 2018)

Abstract: An investigation on lead dioxide electrodeposition from methanesulfonate electrolytes additionally containing Ni^{2+} is reported. It is shown that the lead dioxide electrodes micromodified by nickel have different physicochemical properties *vs.* nonmodified PbO_2-anodes, that are formed during the deposition. The electrocatalytical reactivity of the electrodes involved in comparison to both the oxygen evolution, as well as to the electrooxidation of 2,4-dichlorophenoxyacetic (2,4-D) acid is investigated. The processes of electrochemical oxidation of 2,4-D on various materials occur qualitatively with the same mechanism and differ only in the reaction rate. It is shown that the Ni-PbO_2-anode possesses the highest electrocatalytic activity: the destruction rate of 2,4-D on it increases 1.5 times in comparison with the unmodified lead dioxide. The chemical oxygen demand (*COD*) of a 0.4 mM solution of 2,4-D, determined by the dichromate method, is 90.0 mg dm^{-3} which is 94 % of the theoretical value.

Keywords: methanesulfonate electrolyte; oxygen evolution; 2,4-D; direct anodic oxidation.

INTRODUCTION

Wastewater treatment is recognized as one of the priorities of modern science, particularly in industry, where chemical methods using reagents are widely applied.[1,2] Alternative to the traditional methods of water purification from toxic aromatics are electrochemical technologies, which should be classified as conditionally non-reagent. The electrochemical destruction of toxic pollutants is achieved both by the direct transfer of the electric charge between organic compounds and electrode, and in secondary chemical reactions, where the oxidant is an oxygen-containing radical, which is formed during the electrolysis from water molecules. Such methods are of great advantage for water purification from a

*Corresponding author E-mail: velichenko@ukr.net
https://doi.org/10.2298/JSC180712091S

wide range of organic substances of various types, for example, for phenolic compounds and pesticides.[3–6]

It is recognized,[7,8] that for complex reactions involving organic compounds, the electrode material determines the general direction of the reaction, as well as the nature of intermediates. These two ways of the catalytic action of the electrode material, namely on the rate and selectivity of many reactions, are of great importance for the practical application of such reactions in electrolysis. For most processes, there is a problem of selecting the optimal material for a catalyst electrode, which must satisfy a number of requirements: *i*) to have electronic conductivity; *ii*) to be stable toward corrosion in the conditions of processes; *iii*) not to lose activity for long-term use and, above all, *iv*) to have a low cost. Only a small amount of materials, including metal oxide catalysts, meets the listed requirements. For this purpose, the oxide electrodes, micro-modified with additives of various ions, are of considerable interest for the study, since their activity can vary widely while preserving the basic properties of the material.

As it is well known,[9] there are two zones on PbO_2 surface: hydrated, consisting of Pb^{2+} associated with the corresponding number of hydroxyl ions, and crystalline, in which the ions of Pb^{4+} in the crystal lattice are bound to the O^{2-}.

We believe that the introduction of ions into cation vacancies in the hydrated oxide zone, or at the sites of its crystalline lattice will allow one to control the amount of inert and labile oxygen-containing particles, which in turn will provide the ability to control the electrocatalytic activity and the material selectivity.

The distribution of oxygen-containing particles will depends not only on the electrocatalytic activity of the material in the target process, but also on its selectivity if several reactions are simultaneous. That is, the detection of the relationship between the chemical composition of metal oxide materials, their physicochemical properties and the electrocatalytic activity is of considerable interest in the applied aspect for the creation of efficient materials that will be used in conditional non-reagent systems of the electrochemical wastewater purification from toxic organic compounds.

In a recent work by our group,[10] we have investigated the chemical properties of these systems, deposited from nitrate medium, as well as the nucleation regularities, and kinetics of the electrodeposition of coatings. However, due to the limitations on the mechanical strength, in nitrate solutions it is not possible to obtain coatings with a thickness greater than 100 microns. Considering this, we proposed the methanesulfonate electrolytes in which PbO_2 composite coatings are up to 2 mm thick to be used, with satisfactory mechanical properties that can be prepared.[11]

Herein, we report further important details on the effect of the deposition conditions on the composition, the physicochemical properties and the electrocatalytic activity of Ni modified PbO_2-based materials, obtained from methanesul-

fonate electrolytes. One of the objects of our work was to develop a system with given electrocatalytic properties by changing the quantity of the oxygen-containing particles adsorbed on the electrode surface.

EXPERIMENTAL

Chemicals

The ultrapure acids were obtained from Merck and all other chemicals from Sigma–Aldrich.

Equipment

The determination of the modifying additive in anodic materials was carried out with grafite furnace atomic adsorption spectroscope (GF-AAS) model Analyst 800. The content of nickel in the synthesized PbO_2 does not exceed 0.01 wt.%.

Surface morphology of materials involved was studied by scanning electron microscopy (SEM) with SEM-106I microscope. X-ray powder diffraction data were collected on a STOE STADI P automatic diffractometer equipped with linear PSD detector (transmission mode, $2\theta/\omega$-scan; Cu$K\alpha_1$ radiation, curved germanium (1 1 1) monochromator; 2θ-range 6.000–102.945° with the step of 0.015°; PSD step 0.480°, scan time 50 s/step).

Qualitative and quantitative phase analysis was performed using the PowderCell program. For the selected samples with relatively high degree of crystallinity the Rietveld refinement was carried out using FullProf.2k (version 5.40) program.

The electrooxidation of organic compounds was carried out in a divided cell at j_a = 50 mA cm^{-2}. The formation of coloured compounds during electrolysis was followed by UV–Vis spectroscopy using a Kontron Uvikon 940 spectrophotometer.

Analyses of the reaction products were conducted by HPLC using a Shimadzu RF-10A xL instrument equipped with Ultraviolet SPD-20AV detector and a 30 cm Discovery® C18 column.

Methods

Lead dioxide coatings were electrodeposited on platinized titanium at anodic current density 10 mA cm^{-2} from methanesulfonate electrolytes that contained 0.11M CH_3SO_3H, 0.1 M $Pb(CH_3SO_3)_2$ and 0.1 M $Ni(NO_3)_2$ as dopant.

The volume of anolyte was 130 cm^3. Solution, containing phosphate buffer (0.25 M Na_2HPO_4 + 0.1 M KH_2PO_4)+0.1–0.4 mM organic compound, (pH 6.55) was used as the electrolyte. Stainless steel was used as the cathode. Modified lead dioxide electrodes were used as the anodes. The electrode surface area was 2.5 cm^2. Ag/AgCl reference electrode was used.

The changing of the concentration of the organic substance during the electrolysis was measured by sampling (volume of 5 cm^3) at regular intervals and measuring the optical density of the solution in the ultraviolet and visible region (wavelength range 200–570 nm). Solution, containing phosphate buffer, was used as reference solution.

The chemical oxygen demand (*COD*) was determined by the dichromate method. Samples (5 cm^3) were taken from a cell in a round-bottom flask, 11 cm^3 of water, 1 cm^3 of 0.04 M $HgCl_2$ (to mask chloride ions), 0.8 cm^3 of 0.1 M $AgNO_3$ (as catalyst), 10 cm^3 of H_2SO_4 (concentrated) and 1 cm^3 of 0.1 g-equiv. dm^{-3} of $K_2Cr_2O_7$. The contents of the flask were heated in a sand bath until it was boiling, which was maintained for an hour. After this, the excess of potassium dichromate was measured by the amperometric titration with 0.017 N ammonium iron(II) sulfate, at amperometric titration unit with two indicator platinum electrodes at E = 0.2 V. The reference experiment was conducted the same way, by disposing distilled water instead of organic compound. Concentration of chlorides was determined by the photometric method using mercuric rhodanide.

RESULTS AND DISCUSSION

Phisycochemical properties of Ni–PbO_2 synthesized from methanesulfonate bath

It follows from the above results that the systems based on lead dioxide obtained from methanesulfonate electrolytes are of considerable practical interest and are worth of detailed studies. Considering this, we performed an investigation of the phase composition and the texture of obtained materials. A comparison of the XRD spectra reported in Fig. 1 (a and b) shows that the nickel doping causes some changes in the texture of the PbO_2 coating. Both reflection patterns show that in all cases the deposits consist of a mixture of α- and β-phases of PbO_2. In the doped sample case, the degree of crystallinity of the coatings

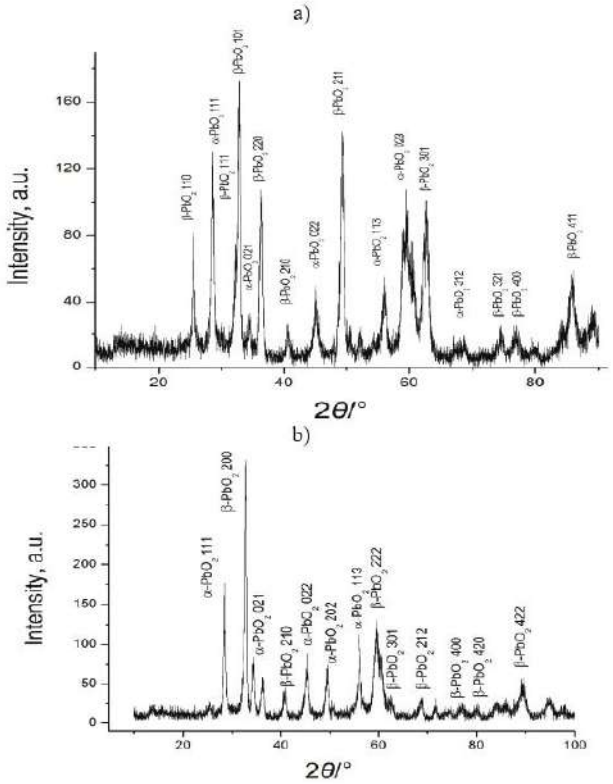

Fig. 1. X-Ray diffractogramms of surfaces of PbO_2, deposited from 0.1 M $Pb(CH_3SO_3)_2$+0.11 M CH_3SO_3H (a) + 0.01 M $Ni(NO_3)_2$ (b).

increases, as evidenced by the increase of the peaks intensity and sharpness on diffractogramms. For the most intensive $\beta(200)$ peak, the average size of particles in Ni–PbO_2, according to Scherrer's equation, yield particle dimensions of 16.5 nm.

The data on the surface morphology of the PbO_2-based materials were obtained by scanning electron microscopy. As one can see from the obtained results (Fig. 2), which are in agreement with XRD results, the morphology of Ni-doped PbO_2 is more regular, with better oriented crystals of bigger size. Typical morphology of lead dioxide electrodeposited from methanesulfonate electrolyte is displayed on Fig. 2a. PbO_2 surface is a mixture of randomly oriented crystals. Polycrystalline clusters sizes vary in the 0.5–4 μm range. A similar morphology was observed during the incorporation of surfactants and polyelectrolytes in the growing PbO_2 deposit.[12]

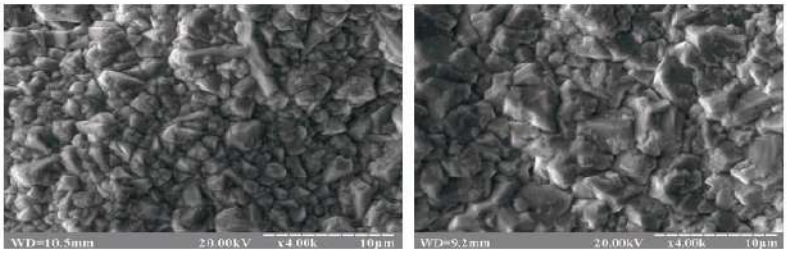

Fig. 2. SEM micrographs of PbO_2-coatings surfaces, obtained electrochemically at $j_a = 10$ mA cm^{-2} from next solution: 0.1 M $Pb(CH_3SO_3)_2$+0.11 M CH_3SO_3H+X M $Ni(NO_3)_2$, where $X = 0$ (a); 0.01 (b);10000×.

As it is seen from Fig. 2b, when lead dioxide is modified by nickel ions the surface crystallinity grows and more marked aggregates can be observed.

We now consider the influence of electrodeposition conditions on the state of lead dioxide surface layer.

SEM/EDAX experiments were performed to evaluate the amount and the distribution of nickel in electrodeposited PbO_2. Unfortunately, it was impossible to reveal nickel because of its low amount in the deposit.

To get further insights in the effect of doping, XPS method was employed. The investigation was focused mainly on the detailed analysis of O1s region. Results are not shown, but the obtained spectra are characterized by two peaks: the one of lower binding energy (528 eV) refers to strongly bound oxygen of the crystal lattice, whereas the one of higher binding energy (530 eV) was assigned to the weakly bound oxygen-containing particles (adsorbed OH-groups and water).

Similar to the Ni-doped coating, obtained from the nitrate bath,[10] the sample synthesized from methanesulfonate medium reveals a significant increase in the

number of labile oxygen-containing particles. Since the amount of adsorbed oxygen-containing particles on the electrode affects the electrocatalytic activity of anodes, the next step of our investigation was to establish the relationship between the composition of the anode material and its electrocatalytic activity in oxygen transfer reactions.

Electrocatalytic activity of nickel-doped lead dioxide

Having in mind that the processes of oxidation of organic substances and the oxygen evolution in most cases proceed simultaneously, we investigated the dependence of the overvoltage of the oxygen evolution reaction on the electrodes involved.

According to the mechanism proposed by Pavlov *et al.*,[13] the oxygen evolution occurs at active sites located in a hydrous layer on PbO_2. Oxygen evolution proceeds through the following elementary steps:

$$PbO(OH)_2 + H_2O \rightarrow PbO(OH)_2\cdots(OH^{\bullet}) + H^+ + e^- \quad (1)$$

$$PbO(OH)_2\cdots(OH^{\bullet}) \rightarrow PbO(OH)_2 + O + H^+ + e^- \quad (2)$$

$$2O \rightarrow O_2 \quad (3)$$

As has been proven by Trasatti and Lodi,[14] if oxygen evolution reaction (OER) is limited by a second electron transfer (electrochemical desorption), an increase of the bond strength of chemisorbed oxygen will lead to an increase of OER overvoltage.

According to our results (Fig. 3), the oxygen overpotential on modified electrodes is practically the same as on non-modified PbO_2-electrode. The Tafel slope is 301.4 and 301.6 mV/dec for non-modified and for Ni-doped PbO_2, respectively. Such phenomenon can be manifested for several reasons, one of which

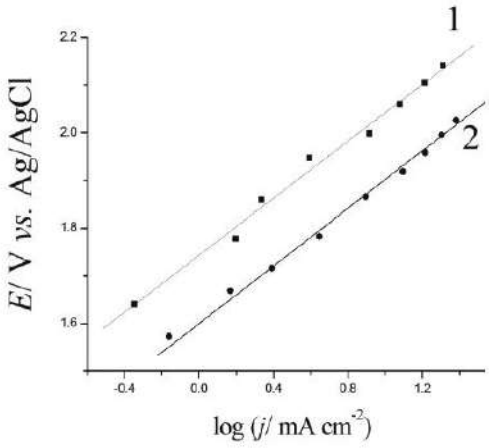

Fig. 3. Polarization curves for oxygen evolution on lead dioxide anodes, electrodeposited from solutions: 1.0–0.1 M $Pb(CH_3SO_3)_2$ + 0.11 M CH_3SO_3H; 2 – 0.1 M $Pb(CH_3SO_3)_2$ + 0.11 M CH_3SO_3H + 0.01 M Ni^{2+} at j_a = 10 mA/cm^2. Supporting electrolyte: 1.0 M $HClO_4$.

is the effect of the semiconductor component of the transition layer. Since the deposition of lead dioxide is carried out on platinized titanium, and the content of platinum is low, the platinum coverage is non-complete, *i.e.*, there is a partial oxidation of the titanium substrate during the deposition of PbO_2, which leads to the formation of TiO_x type oxides, which are n-type semiconductors and contribute to the thickness of the space charge layer. In the case of modified coatings, the additional effect is exerted by Ni active sites, which reduce the degree of filling with the oxygen-containing particles participating in the oxygen evolution process. Since the slope can increase, because of adsorption, as it was observed in the case of bismuth,[15,16] in our case nickel, apparently contributes to the incurporation of $CH_3SO_3^-$ into lead dioxide.[17]

Modification of lead dioxide by Ni^{2+} as in the system[10] reduces the oxygen evolution overpotential, and we did not observe the slope decrease with the increase of Ni^{2+} content in the oxide. This allows one to assume that the reaction of electrochemical desorption (the second electron transfer)[14] remains the rate-limiting step. Since PbO_2 modification by Ni^{2+} leads to a significant increase in the amount of labile surface oxygen-containing species, an increase in the catalytic activity of the oxide, in respect to the oxygen evolution reaction, is quite natural.

We investigated the degradation of aromatic compounds, namely 2,4-dichlorophenoxyacetic acid (2,4-D). This is a pesticide widely used in agriculture because of its low cost and high efficiency. This herbicide belongs to the moderate toxicity class of pesticides. Methods for chemical, photocatalytic and photochemical oxidation[4,6] are used to mineralize 2,4-dichlorophenoxyacetic acid. Electrochemical conversion methods of 2,4-D are also actively used, such as reducing electrochemical dechlorination and direct electrochemical oxidation.[2] A significant number of publications in the last decade are devoted to secondary oxidation of 2,4-D in the process of electro- and photoelectro-Fenton in H_2O_2–Fe^{2+}, H_2O_2–Fe^{2+}–UV systems, which allow the production of OH-radicals in the solution.[3,18–20] The hydroxyl radical is known to be the one of the most effective oxidants for 2,4-D, but in the Fenton process, the oxidation of a pesticide is accompanied by the reaction of formation of complexes of Fe^{3+} with products of 2,4-D oxidation (aliphatic acids), which makes it difficult to completely mineralize the pesticide.

The interaction of $OH^{\bullet}$ with pesticides results in: *i*) reactions with the proton cleavage, *ii*) redox process or *iii*) the electrophilic addition to double bonds. Addition of O_2 to radical organic compounds leads to formation of $OH^{\bullet}$ that initiates further oxidative degradation of pesticides to CO_2 and H_2O.

The simplest and, at the same time, effective electrochemical method of oxidation of 2,4-D by $OH^{\bullet}$ is direct anodic oxidation. In this case, the oxidation of the pesticide occurs through the generation of absorbed on the electrode surface hydroxyl radicals, which are formed by oxidation of water.

The initial solution of 2,4-D is characterized by the absorption maxima at 230 and 285 nm (Fig. 4). At the beginning of electrolysis, the optical density is reduced at 230 nm, while during the formation of the intermediate product 2-chlorobenzoquinone the appearance of the plateau is at 250–270 nm. Further oxidation of the pesticide results in the disappearance of peaks at 230 and 285 nm and the absence of absorption in the region of 250–270 nm, which indicates a complete conversion of 2,4-D and aromatic products of its oxidation into aliphatic compounds, after 3 h of electrolysis. The complete destruction of aromatic compounds, with the formation of only aliphatic products of electrolysis occurs on the Ni–PbO_2 anode after 2 h of electrolysis, and on the unmodified PbO_2-anode after 3 h. Thus, the modification of PbO_2 anodes increases the degradation rate of 2.4-D by 1.5 times. It should also be noted that the processes of the oxidation of a pesticide on the unmodified and modified lead dioxide precede qualitatively the same and differ only in the rate of destruction.

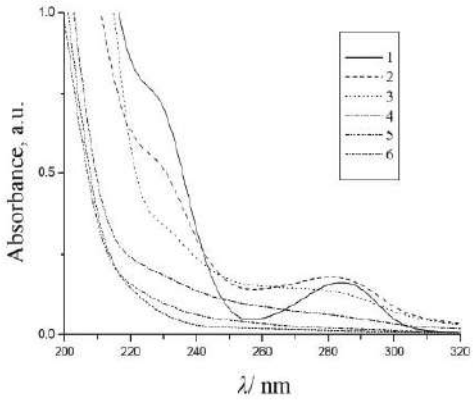

Fig. 4. The absorption spectra of 2,4-D solution (initial concentration 0.1 mM) obtained at different electrolysis duration in a phosphate buffer on Ni–PbO_2 anode. Electrolysis duration, h: 1–0; 2–0.5; 3–1; 4–1.5; 5–2; 6–3.

In most works on wastewater treatment with oxidative methods, not the kinetic parameters of oxidation of the initial organic compounds, but the generalized *COD* index, which reflects the ability to oxidize both the primary substrate and the intermediate products of its degradation, is used to evaluate the efficiency of the processes. The nature of the change in the total amount of the pesticide and its intermediate products in the electrolysis process was determined by the *COD* change (Fig. 5). The theoretically calculated *COD* of 0.4 mM 2,4-D is 96.0 mg dm^{-3} in accordance with the reaction equation:

$$2C_8H_6Cl_2O_3 + 15O_2 \rightarrow 16CO_2 + 4H_2O + 4HCl \quad (4)$$

The *COD* of a 0.4 mM solution of 2,4-D, determined by the dichromate method, is 90.0 mg dm^{-3} which is 94 % of theoretical. It can be seen from Fig. 5,

that during the electrolysis a uniform decrease in the concentration of organic substances in the electrolyte solution occurs. Within 8 h of electrolysis, a complete destruction of the pesticide occurs in a solution containing 0.4 mM 2,4-D, as evidenced by the *COD* value of 24 mg dm^{-3}.

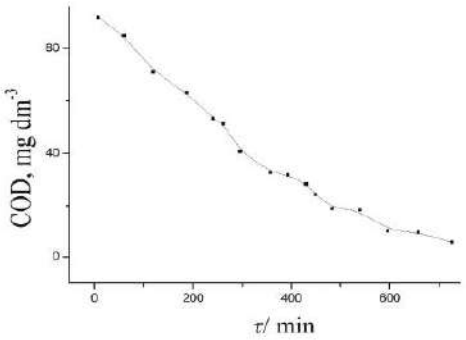

Fig. 5. The *COD versus* the electrolysis duration in a 0.4 mM 2, 4-D on a Ni–PbO_2-anode.

The *COD* data accurately correspond to the electronic absorption spectra of 2,4-D of the same initial concentration (Fig. 6). It is noteworthy that in many cases the oxidation of phenolic organic substances, with an increase in their initial concentration, produces coloured intermediate products during electrolysis. In the UV spectra of solutions, the absorption maxima and the shape of the absorption bands shifts, which slows down the rate of destruction such compounds.[21] As can be seen from Figs. 4 and 6 in the case of 2,4-D, this effect is not observed, *i.e.*, with an increase in the initial content of the pesticide by 4 times, the time of its decomposition to aliphatic acids also increases in 4 times.

Since halogenated derivatives are formed during the decomposition of organic molecules, an important stage in the detoxification of 2,4-D type is the process of their dehalogenation. The character of the change in the concentration of

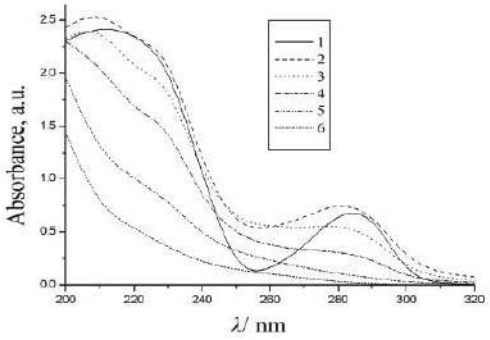

Fig. 6. The absorption spectra of 2,4-D solution (initial concentration 0.4 mM) obtained at different electrolysis duration in a phosphate buffer on Ni–PbO_2 anode. Electrolysis duration, h: 1–0; 2–2; 3–3; 4–4; 5–6; 6–8.

chloride ions over time was studied in the oxidation of 2,4-D on the Ni–PbO_2--anode. The process of destruction of the herbicide to CO_2 and H_2O can be described by the reaction:

$$C_8H_6Cl_2O_3 + 13H_2O \rightarrow 8CO_2 + 2Cl^- + 32H^+ + 30e^- \quad (5)$$

As the herbicide itself and its intermediate aromatic fragments are oxidized, chloride ions are accumulated in the solution and after 2 h of electrolysis, when no more aromatic intermediates are detected on the electronic absorption spectra (see Fig. 4), the concentration of Cl^- reaches a maximum concentration of 0.19 mM, which is 95 % of the value theoretically calculated from the reaction (2). Thus, by the time of the slower process of the destruction of aliphatic acids to CO_2 and H_2O, the dechlorination process is already complete. Further, the concentration of Cl-ions remains constant, which indicates the stability of the chlorides in the solution under the experimental conditions and the absence of their oxidation with the formation of Cl_2.

Analysis of the obtained results suggests that the concentration of 2,4--dichlorophenol, 4,6-dichlororesorcinol, formed at the initial stage of 2,4-D decomposition, decreases rapidly and the main intermediate product, on the decomposition of which is spent most of the time, is 2-chloro-1,4-benzoquinone.

The comparative estimate of the 2,4-D conversion rate is made from the current efficiency (*CE*) value calculated by the formula:[22]

$$CE = \frac{COD_{t_1} - COD_{t_2}}{1000C} \quad (6)$$

where COD_{t_1} and COD_{t_2} are the chemical oxygen demand at the initial and final moment of electrolysis, C is the amount of electricity passed through the cell during this period. Results are displayed in Table I.

TABLE I. The conversion rate of 2,4-D

Compound	Conversion time, h	COD_{t_1}	COD_{t_2}	*CE*
2,4-D	18	90.03	12.2	0.022

The characteristic of the oxidizability of organic compounds in electrochemical methods is the instantaneous current efficiency (*ICE*). We found that during the first two hours of electrolysis the *ICE* value increased sharply. This indicates that the oxidation process proceeds relatively quickly. This period is characterized by the decomposition of 2,4-D with the formation of phenol, resorcinol and hydroquinone, which, as has been found, oxidize much more rapidly on lead dioxide than 2,4-D itself. Therefore, we assume that after the decomposition of 2,4-D with the formation of the above listed intermediates, a large contribution to the process of electrochemical oxidation is the direct adsorption of these compounds on the PbO_2-anode surface. The decrease in the instantaneous current

efficiency indicates the accumulation in the solution of weakly adsorbed and slowly oxidized aliphatic products, which leads to a decrease in the rate of their decomposition.

CONCLUSION

The investigated Ni–PbO_2 anodes, synthesized from methanesulfonate solution are of considerable interest in the applied aspect for the production of efficient materials that will be used in conditional non-reagent systems of electrochemical wastewater purification from toxic organic compounds. It is shown that the lead dioxide electrodes micro-modified by nickel have different physicochemical properties *vs.* unmodified PbO_2-anodes that are formed during the deposition. The obtained deposits consist of the mixture of α- and β-phases of PbO_2. In the doped sample case, the degree of crystallinity of the coatings increases, as evidenced by the increase of the peaks intensity and sharpness on diffractogramms. The morphology of Ni-doped PbO_2 is more regular, with better oriented crystals of bigger size. The coatings revealed a significant increase in the amount of labile oxygen-containing particles on the electrode surface, which in turn enhances the electrocatalytic activity of electrodes. The slope for oxygen evolution is 301.4 and 301.6 mV/dec for the unmodified and for the Ni-doped PbO_2, respectively. The use of the electrocatalysts involved, allows reducing the incineration time of 2,4-D by 1.5 times compared to unmodified anodes. The *COD* of a 0.4 mM solution of herbicide, determined by the dichromate method, is 90.0 mg dm^{-3} which is 94 % of the theoretical.

ИЗВОД

МОДИФИКОВАН ОЛОВО-ДИОКСИД ЗА ТРЕТМАН ОРГАНСКИХ ОТПАДНИХ ВОДА: ФИЗИЧКО–ХЕМИЈСКЕ СВОЈСТВА И ЕЛЕКТРОКАТАЛИТИЧКА АКТИВНОСТ

OLESIA SHMYCHKOVA[1], TATIANA LUK'YANENKO[1], LARISA DMIRTIKOVA[2] и ALEXANDER VELICHENKO[1]

[1]*Ukrainian State University of Chemical Technology, 8, Gagarin Ave., 49005 Dnipro, Ukraine* и [2]*Oles Honchar Dnipro National University, 72, Gagarin Ave., 49010 Dnipro, Ukraine*

Испитивано је електрохемијско таложење олово-диоксида из метансулфонатног електролита коме су били додати Ni^{2+}. Показано је електроде од олово-диоксида микромодификоване никлом (Ni–PbO_2) имају различите физичко–хемијске особине у поређењу са немодификованим анодама које су добијене таложењем олово-диоксида истим поступком. Испитана је електрокаталитичка активност ових електрода за реакције издвајања кисеоника и оксидације 2,4-дихлорфеноксисирћетне киселине (2,4-D). Реакција оксидације 2,4-D на различитим материјалима се одиграва по квалитативно истом механизму, али различитим брзинама. Електроде од Ni–PbO_2 су показале већу електрокаталитичку активност: брзина разлагања 2,4-D на њима је била 1,5 пута већа него на немодификованој електроди. Хемијска потрошња кисеоника (*COD*) раствора 2,4-D концентрације 0,4 mM, одређена дихроматном методом, износила је 90,0 mg dm^{-3}, што је 94 % од теоријске вредности.

(Примљено 12. јула, ревидирано 20. септембра, прихваћено 26. октобра 2018)

REFERENCES

1. S. Cotillas,C. Saez, P. Canizares, I. Cretescu, M. A. Rodrigo, *Sep. Purif. Technol.* **194** (2018) 19 (https://dx.doi.org/10.1016/j.seppur.2017.11.021)
2. F. Islam, J. Wang, M. A. Farooq, S.S. Khan, L.Xu, J. Zhu, M. Zhao, S. Munos, Q. X. Li, W. Zhou, *Environ. Int.* **111** (2018) 332 (https://dx.doi.org/10.1016/j.envint.2017.10.020)
3. V. Iliev, D. Tomova, L. Bilyarska, *J. Photochem. Photobiol. A* **351** (2018) 69 (https://dx.doi.org/10.1016/j.jphotochem.2017.10.022)
4. A. Raschitor, J. Llanos, P.Canizares, M. A. Rodrigo, *Chemosphere* **182** (2017) 85 (https://dx.doi.org/10.1016/j.chemosphere.2017.04.153)
5. S. Zourab, N. Abu Ghalwa, F. R. Zaggout, M.Y. Al-Asqalany, N. Khdear, *J. Dispersion Sci. Technol.* **30** (2009) 712 (https://dx.doi.org/10.1080/01932690802553874)
6. K. H. Hama Aziz , H. Miessner, S. Mueller , A. Mahyar, D. Kalass, D. Moeller, I. Khorshid, M. A. M. Rashid, *J. Hazard. Mater.* **343** (2018) 107 (https://dx.doi.org/10.1016/j.jhazmat.2017.09.025)
7. B. P. Chaplin, *Environ. Sci.: Proc. Impacts* **16** (2014) 1182 (https://dx.doi.org/10.1039/C3EM00679D)
8. R. Vargas, C. Borras, D. Mendez, J. Mostany, B. R. Scharifker, *J. Solid State Electrochem.* **20** (2016) 875 (https://dx.doi.org/10.1007/s10008-015-2984-7)
9. P. Ruetschi, R. Giovanoli, *Power Sources* **13** (1991) 81
10. O. Shmychkova, T. Luk'yanenko, R. Amadelli, A. Velichenko, *J. Electroanal. Chem.* **774** (2016) 88 (https://dx.doi.org/10.1016/j.jelechem.2016.05.017)
11. O. Shmychkova, T. Luk'yanenko, A. Yakubenko, R. Amadelli, A. Velichenko, *Appl. Catal., B* **162** (2015) 346 (https://dx.doi.org/10.1016/j.apcatb.2014.07.011)
12. S. E. Treimer, J. Feng, D. C. Johnson, *J. Electrochem. Soc.* **148** (2001) E321 (https://dx.doi.org/10.1149/1.1378292)
13. D. Pavlov, B. Monahov, D. Petrov, *J. Power Sources* **85** (2000) 59 (https://dx.doi.org/10.1016/S0378-7753(99)00383-3)
14. S. Trasatti, G. Lodi, *Electrodes of conductive metallic oxides, Part B*, Elsevier, Amsterdam, 1981
15. R. Amadelli, A. Maldotti, A. Molinari, F.I. Danilov, A.B. Velichenko, *J. Electroanal. Chem.* **534** (2002) 1 (https://dx.doi.org/10.1016/S0022-0728(02)01152-X)
16. A. Lasia, *Can. J. Chem.* **75** (1997) 1615 (https://dx.doi.org/10.1139/v97-192)
17. B.S. Nielsen, J.L. Davis, P.A. Thiel, *J. Electrochem. Soc.* **137** (1990) 1017 (https://dx.doi.org/10.1149/1.2086596)
18. J. Li, W. Guan, X. Yan, Z. Wu W. Shi, *Catal. Lett.* **148** (2018) 23 (https://dx.doi.org/10.1007/s10562-017-2206-2)
19. F. L. Souza, C. Saez, M. R. V. Lanza, P. Canizares, M. A. Rodrigo, *Sep. Purif. Technol.* **149** (2015) 24 (https://dx.doi.org/10.1016/j.seppur.2015.05.018)
20. O. Garcia, E. Isarain-Chavez, S. Garcia-Segura, E. Brillas, J. M. Peralta-Hernandez, *Electrocatalysis* **4** (2013) 224 (https://dx.doi.org/10.1007/s12678-013-0135-4)
21. R. Amadelli, L. Samiolo, A. De Battisti, A. Velichenko, *J. Electrochem. Soc.* **158** (2011) P87 (https://dx.doi.org/10.1149/1.3589913)
22. M. Panizza, G. Cerisola, *Electrochim. Acta* **48** (2003) 1515 (https://dx.doi.org/10.1016/S0013-4686(03)00028-8).

Таким чином, показано, що зміна фазового складу від α-до β- приводить до збільшення константи швидкості руйнування органічних речовин. За використання запропонованих композитних електрокаталізаторів швидкості руйнування ароматичних забруднювачів зростають у 1,4-2,4 рази. Найефективнішими для використання є електрокаталізатори з флуоровмісними ПАР та полімерами, а також потрійні системи PbO_2-TiO_2-*ПАР.*

Для інтенсифікації процесу електрохімічного руйнування ароматичних забруднювачів були запропоновані проточні системи з електрохімічним комірками коаксіального типу, що дозволило в 10 разів збільшити швидкість руйнування органічних сполук до досягнення ступеня перетворення в 95%. Враховуючи залежність швидкості руйнування органічних сполук від їх природи та складу композиту пропонується послідовно комбінувати окремі електрохімічні комірки в єдиний модуль.

ВИСНОВКИ

У дисертаційній роботі встановлено взаємозв'язок між умовами формування, закономірностями нуклеації, складом, фізико-хімічними властивостями композитів на основі PbO_2 та їх електрокаталітичною активністю та селективністю, що дозволило розв'язати важливу наукову проблему каталізу щодо створення композитних матеріалів металоксид–ПАР(полімер) із заданими функціональними властивостями.

1. Для одержання осадів плюмбум(IV) оксиду, що переважно складаються із α-фази, був рекомендований 1 М метансульфонатний електроліт, а для отримання покриттів, які складаються переважно із β-фази, – 0,1 М $Pb(NO_3)_2$ + 0.1 М HNO_3 або 0.1 М $Pb(CH_3SO_3)_2$ + 0.1 М CH_3SO_3H. Ці електроліти були вибрані як базові для подальших досліджень. Результати досліджень показали, що перспективнішим для створення композитних матеріалів є оксид, збагачений β-фазою. Наявність поверхнево-активних речовин (ПАР) в цих розчинах одночасно впливає на кінетику нуклеації, як α-, так і β-фази, але не приводить до суттєвої зміни фазового складу.

2. Комплексні дослідження впливу ПАР та полімерів на кінетику осадження PbO_2 вказують на пригнічення процесу внаслідок адсорбції. За цього ефект залежить як від природи ПАР, так і довжини флуор-карбонового ланцюга. На відміну від цього, за наявності в електроліті полімера Nafon® спостерігається екстремальна залежність гетерогенної константи швидкості осадження від концентрації добавки, що обумовлено одночасним впливом на кінетику електроосадження ψ` потенціалу та параметру інгібування S.

3. За наявності в електроліті добавок ПАР та полімерів утворюються композитні покриття PbO_2-ПАР та PbO_2-полімер, склад яких залежить від концентрації добавки та густини струму осадження. Варіювання цих параметрів дозволяє змінювати кількість добавок в композиті від 1 до 18 мас.%.

4. Для одержання композитів складу PbO_2-TiO_2-ПАР запропоновано використовувати суспензійні електроліти, де в якості частинок дисперсної фази виступає TiO_2, а в якості добавки – ПАР. Використання таких розчинів створює можливість одержання композиту зі збільшеною кількістю TiO_2 та ПАР, порівняно з подвійними системами.

5. Встановлено, що на покритті, що складається практично із α-фази, перенапруга виділення кисню значно менше в результаті більшої гідратованості покриття порівняно з покриттям із більшим вмістом β-фази. Відмінності в кристалографічній орієнтації за фіксованого фазового складу плюмбум(IV) оксиду практично не впливають на кінетику виділення кисню. За характером впливу на реакцію виділення кисню, композитні матеріали з ПАР можна поділити на дві групи: такі, що зменшують перенапругу виділення кисню (з гідроген карбоновим ланцюгом) та такі, що збільшують перенапругу виділення кисню (з флуоркарбоновим ланцюгом).

6. Показано, що зміна фазового складу від α-до β- приводить до збільшення константи швидкості руйнування органічних речовин. За використання запропонованих композитних електрокаталізаторів швидкості руйнування ароматичних забруднювачів зростають у 1,4-2,4 рази. Найефективнішими для використання є електрокаталізатори з флуоровмісними ПАР та полімерами, а також потрійні системи PbO_2-TiO_2-ПАР.

7. Для інтенсифікації процесу електрохімічного руйнування ароматичних забруднювачів були запропоновані проточні системи з електрохімічним комірками коаксіального типу, що дозволило в 10 разів збільшити швидкість руйнування органічних сполук до досягнення ступеня перетворення в 95%. Враховуючи залежність швидкості руйнування органічних сполук від їх природи та складу композиту пропонується послідовно комбінувати окремі електрохімічні комірки в єдиний модуль.

8. Використання поверхнево-активних речовин та полімерів, які за рахунок гідрофобізації сприяють збільшенню кількості міцнозв’язаних із поверхнею електрода кисеньвмісних частинок на одержаних композитних

матеріалах на основі PbO_2, приводить до зростання парціальної швидкості окиснення органічних сполук. Таким чином, основним фактором керування електрокаталітичною активністю в процесах із перенесенням кисню є хімічний склад матеріалу, а зміна його структурних властивостей має вторинний характер.

ПЕРЕЛІК ВИКОРИСТАНИХ ДЖЕРЕЛ

1. Velichenko, A.B.; Luk'yanenko, T.V.; Shmychkova, O.B.; etc. New approaches to the creation of nanocomposite anode materials based on PbO_2: a review. Theor. Exp. Chem. **2021**, 57(5), 331–342.

2. Электрохимия. Прошедшие тридцать и будущие тридцать лет / [под ред. Г. Блума, Ф. Гутмана]. – М.: Химия, 1982. – 365 с.

3. Velichenko, A.B.; Kovalyov, S.V.; Gnatenko, A.N.; etc. Lead dioxide electrodeposition and its application: influence of fluoride and iron ions. J. Electroanal. Chem. **1998**, 454, 203–208.

4. Основы научных исследований / [под ред. В. И. Крутова, В. В. Попова]. – М.: Высшая школа, 1989. – 400 с.

5. Якість води. Визначання градуювальної характеристики методик кількісного хімічного аналізу. Частина 1. Статистичне оцінювання лінійної градуювальної характеристики (ISO 8466-1:1990, IDT): ДСТУ ISO 8466-1-2001. – [Чинний від 2003-01-01.]. – К.: Держспоживстандарт України, 2003. – 19 с. – (Національний стандарт України).

6. Якість води. Визначання градуювальної характеристики методик кількісного хімічного аналізу. Частина 1. Принцип оцінювання нелінійної градуювальної характеристики другого порядку (ISO 8466-2:1993, IDT): ДСТУ ISO 8466-2-2001. – [Чинний від 2003-01-01.]. – К.: Держспоживстандарт України, 2003. – 16 с. – (Національний стандарт України).

7. Васильев В.П. Аналитическая химия. Гравиметрический и титриметрический методы анализа / В.П. Васильев. – М.: Высшая школа, 1989. – Ч. 1. – 320 с.

8. Sandoval, A.P.; Suarez-Herrera, M.F.; Climent V.; etc. Interaction of water with methanesulfonic acid on Pt single crystal electrode. Electrochem. Commun. **2015**, 50, 47–50.

9. Gernon, M.D.; Wu, M.; Buszta, Th.; etc. Environmental benefits of methane sulfonic acid. Comparative properties and advantages. Green Chem. **1999**, 1, 127–140.

10. Li, X.; Pletcher, D.; Walsh, F. C. Electrodeposited lead dioxide coatings. Chem. Soc. Rev., **2011**, 40, 3879–3894.

11. Velichenko, A.B.; Amadelli, R.; Gruzdeva, E.V.; etc. Electrodeposition of lead dioxide from methanesulfonate solutions. J. Power Sources, **2009**, 191,103–110.

12. Velichenko, A.; Luk'yanenko, T.; Shmychkova, O. Morphology and phase composition of lead dioxide coatings: Influence of methanesulfonate ions. J. Energy Storage. **2020**, 30, 101581/

13. Gonzalez-Garcia, J.; Iniesta, J.; Exposito, E.; etc. Early stages of lead dioxide electrodeposition on rough titanium. Thin Solid Films. **1999**, 352, 49–56.

14. Gonzalez-Garcia, J.; Gallud, F.; Iniesta, J.; etc. Kinetics of electrocrystallisation of PbO_2 on glassy carbon electrodes: influence of ultrasound. New J. Chem. **2001**, 25, 1195–1198.

15. Abyaneh, M.Y.; Saez, V.; Gonzalez-Garcia, J.; etc. Electrocrystallization of lead dioxide: Analysis of the early stages of nucleation and growth. Electrochim. Acta. **2010**, 55, 3572–3579.

16. Gonzalez-Garcia, J.; Gallud, F.; Iniesta, J.; etc. Kinetics of electrocrystallization of PbO_2 on glassy carbon electrodes: partial inhibition of the progressive three-dimensional nucleation and growth. J. Electrochem. Soc. **2000**, 147(8), 2969–2974.

17. Gonzalez-Garcia, J.; Gallud, F.; Iniesta, J.; etc. Kinetics of electrocrystallization of PbO_2 on glassy carbon electrodes: influence of electrode rotation. Electroanalysis. **2001**, 13, 1258–1264.

18. Abyaneh, M.Y. Modelling diffusion controlled electrocrystallisation processes. J. Electroanal. Chem. **2006**, 586, 196–203.

19. Abyaneh, M.Y. Kinetics of two-phase electrocrystallization processes. IV. CTTs associated with the growth of dissimilar geometric shapes J. Electrochem. Soc. **2007**, 154(1), D5–D12.

20. Abyaneh, M.Y. Extracting nucleation rates from current–time transients: Part I: the choice of growth models. J. Electroanal. Chem. **2002**, 530, 82–88.

21. Abyaneh, M.Y.; Fletcher, S. Extracting nucleation rates from current–time transients: Part II: comparing the computer-fit and pre-pulse method. J. Electroanal. Chem. **2002**, 530, 89–95.

22. Abyaneh, M.Y. Extracting nucleation rates from current–time transients: Part III: nucleation kinetics following the application of a pre-pulse. J. Electroanal. Chem. **2002**, 530, 96–104.

23. Shmychkova, O.; Luk'yanenko, T.; Velichenko, A. Lead dioxide electrocrystallization from nitrate and methanesulfonate electrolytes: the influence of various dopants on initial stages. ECS Transactions. 2017, 77(11), 1617–1623.

24. Shmychkova, O.; Luk'yanenko, T.; Piletska, A.; etc. Electrocrystallization of lead dioxide: influence of early stages of nucleation on phase composition. J. Electroanal. Chem. **2015**, 746, 57-61.

25. Velichenko, A.B.; Shmychkova, O.B.; Luk'yanenko, T.V.; etc. The influence of deposition conditions on phase composition of lead dioxide-based materials. Prot. Met. Phys. Chem. Surf. **2015**, 51(4), 593–599.

26. Ruetschi, P.; Giovanoli, R. On the presence of OH^- ions, Pb^{2+} ions and cation vacancies in PbO_2. Power Sources. **1991**, 13, 81–97.

27. Shmychkova, O.; Luk'yanenko, T.; Amadelli, R.; etc. Electrodeposition of Ni^{2+}-doped PbO_2 and physicochemical properties of the coating. J. Electroanal. Chem. **2016**, 774, 88–94.

28. Шмычкова, О.Б.; Лукьяненко, Т.В.; Величенко А.Б. Влияние ионов Ni^{2+} на электроосаждение PbO_2. *Вопр. химии и хим. технологии*. **2016**, 3(107). 40–46.

29. Shmychkova, O.; Luk'yanenko, T.; Velichenko, A. The influence of early stages of PbO_2 nucleation on its phase composition. Chem. Met. Alloys. **2016**, № 3-4, 99–104.

30. Шмычкова, О.Б.; Лукьяненко, Т.В.; Гиренко, Д.В.; та ін. Влияние анионных добавок на закономерности электроосаждения диоксида свинца из нитратных электролитов. *Вопр. химии и хим. технологии*. **2016**, 4(108), 31–37.

31. Shmychkova, O.B.; Luk'yanenko, T.V.; Amadelli, R.; etc. Physicochemical properties of PbO_2 modified with nickel ions. Prot. Met. Phys. Chem. Surf. **2017**, 53, 68–74.

32. **Shmychkova, O.**; Knysh, V.; Luk'yanenko, T.; etc. Electrodeposition of composite PbO_2–TiO_2 materials from colloidal methanesulfonate electrolytes. J. Solid State Electrochem. **2017**, 21, 537–544.

33. Luk'yanenko, T.; Shmychkova, O.; Zahorulko, S.; etc. The influence of surfactants on lead dioxide nucleation and physico-chemical properties. Chem. Met. Alloys. **2020**, 13, 29–35.

34. Wen, T.C.; Wei, M.G.; Lin, K.L. Electrocrystallization of PbO_2 deposits in the presence of additives. J. Electrochem. Soc. **1990**, 137, 2700–2702.

35. Luk'yanenko, T.; **Shmychkova, O.**; Dmitrikova, L.; etc. The composition and electrocatalytic activity of composite PbO_2-surfactant electrodes. Voprosy Khimii i Khimicheskoi Tekhnologii. **2019**, 2019(5), 65–70.

36. Luk'yanenko, T.; **Shmychkova, O.**; Velichenko, A. PbO_2-surfactant composites: electrosynthesis and catalytic activity. J. Solid State Electrochem. **2020**, 24(4), 1045–1056.

37. Velichenko, A.; Luk'yanenko, T.; **Shmychkova, O.** Lead dioxide-SDS composites: design and properties. J. Electroanal. Chem. **2020**, 873, 114412

38. Velichenko, A.; Luk'yanenko, T.; Shmychkova, O.; etc. Electrosynthesis and catalytic activity of PbO_2-fluorinated surfactant composites. J. Chem. Technol. Biotechnol. **2020**, 95(12), 3085–3092.

39. Knysh, V; Shmychkova, O.; Luk'yanenko, T.; etc. Electrosynthesis and characterization of lead dioxide–perfluorobutanesulfonate composite, Voprosy Khimii i Khimicheskoi Tekhnologii, **2021**, 2021(5), 68–76.

40. Velichenko, A.; Luk'yanenko, T.; Nikolenko, N.; Shmychkova, O.; etc. Composite Electrodes PbO_2-Nafion®. J. Electrochem. Soc. **2020**, 167(6), 063501.

41. Fleischmann, M.; Liler, M. The anodic oxidation of solutions of plumbous salts. Part 1. The kinetics of deposition of α-lead dioxide from acetate solutions, Trans. Faraday Soc. **1958**, 54, 1370–1381.

42. Chang, H.; Johnson, D.C. Electrocatalysis of anodic oxygen-transfer reaction. Chronoamperometric and voltammetric studies of the nucleation and electrodeposition of β-lead dioxide at a rotated gold disk electrode in acidic media. J. Electrochem. Soc. **1989**, 136, 17–22.

43. Velicheko, A.B.; Girenko, D.V.; Danilov, F.I. Mechanism of lead dioxide electrodeposition, J. Electroanal. Chem. **1996**, 405(1-2), 127–132.

44. Velichenko, A.B.; Baranova, E.A.; Girenko, D.V.; etc. Mechanism of electrodeposition of lead dioxide from nitrate solutions. Russ. J. Electrochem. **2003**, 39, 615–621.

45. Luk'yanenko, T.V.; Shmychkova, O.B.; Yanova, C.V.; etc. The synthesis and electrocatalytic activity of PbO_2-polyelectrolyte and PbO_2-surfactant composite coatings. J. Chem. Technol. **2019**, 27(1), 92–100.

46. Shmychkova, O.; Luk'yanenko, T.; Amadelli, R.; etc. Physico-chemical properties of PbO_2-anodes doped with $Sn^{4+}$and complex ions. J. Electroanal. Chem. **2014**, 717-718, 196–201.

47. Velichenko, A.; Shmychkova, O.; Samiolo, L.; etc. Reduction of nitroaromatics on cadmium sulfide: further probing the electrochemical model of semiconductor photocatalysis. J. Solid State Electrochem. **2021**, 25(1), 85–92.

48. Pavlov, D.; Monahov, B.; Petrov, D. Influence of Ag as alloy additive on the oxygen evolution reaction on Pb/PbO_2 electrode. J. Power Sources. **2000**, 85, 59–62.

49. Trasatti, S.; Lodi, G. Electrodes of conductive metallic oxides. Part B, Elsevier, Amsterdam, Holland, **1981**.

50. Velichenko, A.B.; Devilliers, D. Electrodeposition of fluorine-doped lead dioxide. J. Fluorine Chem., **2007**, 128(4), 269-276.

51. Shmychkova, O.; Zahorulko, S.; Luk'yanenko, T.; etc. Electrochemical oxidation of chloramphenicol with lead dioxide–surfactant composites, Water Environ. Res. 2021, 93(11) 2716–2726.

52. Shmychkova, O.; Zahorulko, S.; Girenko, D.; etc. Material selection and optimization of conditions for electrooxidation of nitrofurazone: A comparative study of tin and lead dioxides. J. Electrochem. Soc., 2021, 168(8), 086507.

53. Shmychkova, O.; Girenko, D.; Velichenko, A. Noble metals doped tin dioxide for sodium hypochlorite synthesis from low concentrated NaCl solutions. J. Chem. Tech. Biotech. 2021. Article ASAP. DOI: 10.1002/jctb.6973 (accessed 2021-11-04).

54. Shmychkova, O.; Luk'yanenko, T.; Velichenko, A. The electrochemical oxidation of 4-nitroaniline and 4-nitrophenol on modified PbO_2-electrodes. Bull. Dnipr. Univ. Ser. Chem. **2017**, 25(1), 27–35.

55. Shmychkova, O.; Luk'yanenko, T.; Amadelli, R.; etc. The electrochemical oxidation of salicylic acid and its derivatives on modified PbO_2-electrodes. Bull. Dnipr. Univ. Ser. Chem. **2017**, 25(1) 36–44.

56. Velichenko, A.; Knysh, V.; Luk'yanenko, T.; etc. The composition and properties of composite PbO_2–TiO_2 materials electrodeposited from colloidal methanesulfonate electrolytes. Voprosy Khimii i Khimicheskoi Tekhnologii. **2017**, 4, 14–20.

57. Shmychkova, O.B.; Knysh, V.A.; Luk'yanenko, T.V.; etc. Electrocatalytic processes on PbO_2 electrodes at high anodic potentials. Surf. Eng. Appl. Electrochem. **2018**, 54(1), 38–46

58. Shmychkova, O.; Luk'yanenko, T.; Dmitrikova, L.; etc. Modified lead dioxide for organic wastewater treatment: Physicochemical properties and electrocatalytic activity. J. Serb. Chem. Soc. **2019**, 84(2), 187–198.

ДОДАТКИ

Додаток А

Список публікацій здобувача

Наукові праці, що розкривають основні наукові результати дисертації

1. **Shmychkova, O**.; Luk'yanenko, T.; Piletska, A.; etc. Electrocrystallization of lead dioxide: influence of early stages of nucleation on phase composition. J. Electroanal. Chem. **2015**, 746, 57-61. (входить до наукометричних баз, що індексуються Scopus, WoS). Видання віднесене до другого квартилю (**Q2**) відповідно до класифікації SCImago Journal. (*Особистий внесок здобувача: планування і проведення досліджень за використання інверсійної вольтамперометрії*, *аналіз початкових стадій кристалізації з адаптацією модельних уявлень про характер нуклеації плюмбум(*IV*) оксиду, узагальнення та інтерпретація результатів, підготовка рукопису до опублікування*. *Дисертанткою був запропонований експрес-метод напівкількісної оцінки фазового складу покриттів, в основі якого аналіз потенціалу піків відновлення утворюваних осадів на інверсійній вольтамперограмі*).

2. **Shmychkova, O.**; Luk'yanenko, T.; Amadelli, R.; etc. Electrodeposition of Ni^{2+}-doped PbO_2 and physicochemical properties of the coating. J. Electroanal. Chem. **2016**, 774, 88–94. (входить до наукометричних баз, що індексуються Scopus, WoS). Видання віднесене до другого квартилю (**Q2**) відповідно до класифікації SCImago Journal. (*Особистий внесок здобувача: планування і проведення радіохімічних досліджень, узагальнення та інтерпретація результатів, підготовка рукопису до опублікування)*.

3. **Шмычкова, О.Б.**; Лукьяненко, Т.В.; Величенко А.Б. Влияние ионов Ni^{2+} на электроосаждение PbO_2. *Вопр. химии и хим. технологии*. **2016**, 3(107). 40–46. (фахове видання). (*Особистий внесок здобувача: планування і проведення кінетичних досліджень, узагальнення та інтерпретація результатів, підготовка рукопису*).

4. **Shmychkova, O.**; Luk’yanenko, T.; Velichenko, A. The influence of early stages of PbO_2 nucleation on its phase composition. Chem. Met. Alloys. **2016**, № 3-4, 99–104. (фахове видання). (*Особистий внесок здобувача: узагальнення та інтерпретація результатів досліджень стосовно фазового складу покриттів*, *підготовка рукопису*).

5. **Шмычкова, О.Б.**; Лукьяненко, Т.В.; Гиренко, Д.В.; та ін. Влияние анионных добавок на закономерности электроосаждения диоксида свинца из нитратных электролитов. *Вопр. химии и хим. технологии*. **2016**, 4(108), 31–37. (фахове видання). (*Особистий внесок здобувача: планування і проведення експерименту*, *узагальнення та інтерпретація результатів, підготовка рукопису*).

6. **Shmychkova, O.B.**; Luk’yanenko, T.V.; Amadelli, R.; etc. Physicochemical properties of PbO_2 modified with nickel ions. Prot. Met. Phys. Chem. Surf. **2017**, 53, 68–74. (входить до наукометричних баз, що індексуються Scopus, WoS). Видання віднесене до третього квартилю (**Q3**) відповідно до класифікації SCImago Journal. (*Особистий внесок здобувача: планування і проведення експерименту, інтерпретація результатів, підготовка рукопису*).

7. **Shmychkova, O.**; Luk'yanenko, T.; Velichenko, A. Lead dioxide electrocrystallization from nitrate and methanesulfonate electrolytes: the influence of various dopants on initial stages. ECS Transactions. 2017, 77(11), 1617–1623. (входить до наукометричних баз, що індексуються Scopus та WoS). (*Особистий внесок здобувача: планування і проведення експерименту, інтерпретація результатів, підготовка рукопису*).

8. **Shmychkova, O.**; Knysh, V.; Luk’yanenko, T.; etc. Electrodeposition of composite PbO_2–TiO_2 materials from colloidal methanesulfonate electrolytes. J. Solid State Electrochem. **2017**, 21, 537–544. (входить до наукометричних баз, що індексуються. Scopus, WoS). Видання віднесене до другого квартилю (**Q2**) відповідно до класифікації SCImago Journal. (*Особистий внесок здобувача: планування і проведення досліджень стосовно потрійних композитних систем*

PbO_2-TiO_2-*ПАР, узагальнення та інтерпретація результатів, підготовка рукопису до опублікування)*.

9. **Shmychkova, O.**; Luk'yanenko, T.; Velichenko, A. The electrochemical oxidation of 4-nitroaniline and 4-nitrophenol on modified PbO_2-electrodes. Bull. Dnipr. Univ. Ser. Chem. **2017**, 25(1), 27–35. (входить до наукометричних баз, що індексуються WoS). (*Особистий внесок здобувача: планування і проведення експерименту, інтерпретація результатів, підготовка рукопису*).

10. **Shmychkova, O.**; Luk'yanenko, T.; Amadelli, R.; etc. The electrochemical oxidation of salicylic acid and its derivatives on modified PbO_2-electrodes. Bull. Dnipr. Univ. Ser. Chem. **2017**, 25(1), 36–44. (входить до наукометричних баз, що індексуються WoS). (*Особистий внесок здобувача: планування і проведення експерименту, узагальнення та інтерпретація результатів, підготовка рукопису*).

11. Velichenko, A.; Knysh, V.; Luk'yanenko, T.; **Shmychkova, O.** The composition and properties of composite PbO_2–TiO_2 materials electrodeposited from colloidal methanesulfonate electrolytes. Voprosy Khimii i Khimicheskoi Tekhnologii. **2017**, 4, 14–20. (входить до наукометричних баз, що індексуються Scopus). (*Особистий внесок здобувача: інтерпретація результатів, підготовка рукопису*).

12. **Shmychkova, O.B.**; Knysh, V.A.; Luk'yanenko, T.V.; etc. Electrocatalytic processes on PbO_2 electrodes at high anodic potentials. Surf. Eng. Appl. Electrochem. **2018**, 54(1), 38–46 (входить до наукометричних баз, що індексуються Scopus та WoS). (*Особистий внесок здобувача: планування і проведення експерименту, узагальнення та інтерпретація результатів, підготовка рукопису (включаючи змістовний переклад).*

13. **Shmychkova, O.**; Luk'yanenko, T.; Dmitrikova, L.; etc. Modified lead dioxide for organic wastewater treatment: Physicochemical properties and electrocatalytic activity. J. Serb. Chem. Soc., **2019**, 84(2), 187–198. (входить у перелік видань, включених до наукометричних баз Scopus та WoS). (*Особистий*

внесок здобувача: планування і проведення експерименту, узагальнення та інтерпретація результатів, підготовка рукопису).

14. Luk'yanenko, T.; **Shmychkova, O.**; Dmitrikova, L.; etc. The composition and electrocatalytic activity of composite PbO_2-surfactant electrodes. Voprosy Khimii i Khimicheskoi Tekhnologii. **2019**, 2019(5), 65–70. (входить у перелік видань, включених до наукометричних баз Scopus). Видання віднесене до третього квартилю (**Q3**) відповідно до класифікації SCImago Journal. (*Особистий внесок здобувача: планування і проведення експерименту, узагальнення та інтерпретація результатів, підготовка рукопису*).

15. Luk'yanenko, T.V.; **Shmychkova, O.B.**; Yanova, C.V.; etc. The synthesis and electrocatalytic activity of PbO_2-polyelectrolyte and PbO_2-surfactant composite coatings. J. Chem. Technol. **2019**, 27(1), 92–100. (входить у перелік видань, включених до наукометричних баз Scopus та WoS). (*Особистий внесок здобувача: планування і проведення експерименту, узагальнення результатів, підготовка рукопису*).

16. Velichenko, A.; Luk'yanenko, T.; **Shmychkova, O.** Morphology and phase composition of lead dioxide coatings: Influence of methanesulfonate ions. J. Energy Storage. **2020**, 30, 101581 (входить до наукометричних баз, що індексуються Scopus та WoS). Видання віднесене до другого квартилю (**Q2**) відповідно до класифікації SCImago Journal. (*Особистий внесок здобувача: планування і проведення досліджень стосовно вибору оптимальних електролітів для електроосадження композитів із заданим фазовим складом, узагальнення та інтерпретація результатів, підготовка рукопису до опублікування)*.

17. Luk'yanenko, T.; **Shmychkova, O.**; Velichenko, A. PbO_2-surfactant composites: electrosynthesis and catalytic activity. J. Solid State Electrochem. **2020**, 24(4), 1045–1056. (входить до наукометричних баз, що індексуються Scopus та WoS). Видання віднесене до другого квартилю (**Q2**) відповідно до класифікації SCImago Journal. (*Особистий внесок здобувача: планування і проведення досліджень стосовно кінетики електроосадження та фізико-хімічних*

властивостей композитів PbO_2*-натрію лауретсульфат, узагальнення та інтерпретація результатів, підготовка рукопису до опублікування)*.

18. Velichenko, A.; Luk'yanenko, T.; **Shmychkova, O.** Lead dioxide-SDS composites: design and properties. J. Electroanal. Chem. **2020**, 873, 114412 (входить до наукометричних баз, що індексуються Scopus та WoS). Видання віднесене до другого квартилю (**Q2**) відповідно до класифікації SCImago Journal. (*Особистий внесок здобувача: планування і проведення досліджень стосовно електросинтезу та застосування композитів* PbO_2*-натрію додецилсульфат, узагальнення та інтерпретація результатів, підготовка рукопису до опублікування)*.

19. Velichenko, A.; Luk'yanenko, T.; Shmychkova, O.; etc. Electrosynthesis and catalytic activity of PbO_2-fluorinated surfactant composites. J. Chem. Technol. Biotechnol. **2020**, 95(12), 3085–3092. (входить до наукометричних баз, що індексуються Scopus та WoS). Видання віднесене до другого квартилю (**Q2**) відповідно до класифікації SCImago Journal. (*Особистий внесок здобувача: планування і проведення досліджень щодо закономірностей синтезу композитів металоксид-ПАР із флуорокарбоновим ланцюгом, узагальнення та інтерпретація результатів, підготовка рукопису до опублікування)*.

20. Velichenko, A.; Luk'yanenko, T.; Nikolenko, N.; **Shmychkova, O.**; etc. Composite Electrodes PbO_2-Nafion®. J. Electrochem. Soc. **2020**, 167(6), 063501. (входить до наукометричних баз, що індексуються Scopus та WoS). Видання віднесене до першого квартилю (**Q1**) відповідно до класифікації SCImago Journal. (*Особистий внесок здобувача: планування і проведення досліджень стосовно встановлення закономірностей електроосадження та фізико-хімічних властивостей композитів металоксид-поліелектроліт, узагальнення та інтерпретація результатів, підготовка рукопису до опублікування)*.

21. **Shmychkova, O.**; Zahorulko, S.; Luk'yanenko, T.; etc. Electrochemical oxidation of chloramphenicol with lead dioxide–surfactant composites, Water Environ. Res. **2021**, 93(11) 2716–2726 (входить до наукометричних баз, що індексуються Scopus та WoS). Видання віднесене до третього квартилю (**Q3**)

відповідно до класифікації SCImago Journal. (*Особистий внесок здобувача: планування експерименту стосовно електроокиснення модельної сполуки за використання електрокаталізатора* PbO_2*-натрію додецилсульфат у водних розчинах різного складу, узагальнення результатів, підготовка рукопису*).

22. Knysh, V; **Shmychkova, O.**; Luk'yanenko, T.; etc. Electrosynthesis and characterization of lead dioxide–perfluorobutanesulfonate composite, Voprosy Khimii i Khimicheskoi Tekhnologii, **2021**, 2021(5), 68–76. (входить до наукометричних баз, що індексуються Scopus). Видання віднесене до третього квартилю (**Q3**) відповідно до класифікації SCImago Journal. (*Особистий внесок здобувача: планування і проведення експерименту, узагальнення результатів, підготовка рукопису*).

23. **Shmychkova, O.**; Zahorulko, S.; Girenko, D.; etc. Material selection and optimization of conditions for electrooxidation of nitrofurazone: A comparative study of tin and lead dioxides. J. Electrochem. Soc., **2021**, 168(8), 086507. (входить до наукометричних баз, що індексуються Scopus та WoS). Видання віднесене до першого квартилю (**Q1**) відповідно до класифікації SCImago Journal. (*Особистий внесок здобувача: планування експерименту стосовно окиснення фурациліну як модельної сполуки за використання різних електродних матеріалів, узагальнення результатів, підготовка рукопису*).

24. Velichenko, A.; **Shmychkova, O.**; Samiolo, L.; etc. Reduction of nitroaromatics on cadmium sulfide: further probing the electrochemical model of semiconductor photocatalysis. J. Solid State Electrochem. **2021**, 25(1), 85–92. (входить до наукометричних баз, що індексуються Scopus та WoS). Видання віднесене до другого квартилю (**Q2**) відповідно до класифікації SCImago Journal. (*Особистий внесок здобувача: планування експерименту стосовно вибору та можливості застосування фотокаталізаторів для окиснення нітроароматичних сполук, узагальнення та інтерпретація результатів, підготовка рукопису*).

25. Velichenko, A.B.; Luk'yanenko, T.V.; **Shmychkova, O.B.**; etc. New approaches to the creation of nanocomposite anode materials based on PbO_2: a

review. Theor. Exp. Chem. **2021**, 57(5), 331–342. (входить до наукометричних баз, що індексуються Scopus та WoS). Видання віднесене до третього квартилю (**Q3**) відповідно до класифікації SCImago Journal. (*Особистий внесок здобувача: запропоновано оригінальний підхід до створення новітніх нанокомпозитних анодних матеріалів на основі плюмбум(*IV*) оксиду*, *узагальнення результатів, підготовка рукопису*).

26. **Shmychkova, O.**; Girenko, D.; Velichenko, A. Noble metals doped tin dioxide for sodium hypochlorite synthesis from low concentrated NaCl solutions. J. Chem. Tech. Biotech. **2022**, 97(4), 903–913. (входить до наукометричних баз, що індексуються Scopus та WoS). Видання віднесене до другого квартилю (**Q2**) відповідно до класифікації SCImago Journal. (*Особистий внесок здобувача: планування експерименту стосовно дослідження матеріалів для електрохімічного синтезу кисеньвмісних окисників, що утворюються в процесі електролізу водних розчинів різного складу, узагальнення результатів рентгенівської фотоелектронної спектроскопії, підготовка рукопису*).

Публікації, що засвідчують апробацію матеріалів дисертації

1. **Shmychkova, O.**; Luk’yanenko, T.; Velichenko, A. Kinetic regularities of lead dioxide electrocrystallization. In ECS Meeting*: abstracts*, Honolulu, Hawaii (USA), 2016, 3594. (*Здобувач встановила закономірності електрокристалізації*, *підготувала тези до друку)*.

2. **Shmychkova, O.**; Luk’yanenko, T.; Velichenko, A. The influence of ionic dopants on initial stages of lead dioxide electrocrystallisation. *Перспективні матеріали та процеси в технічній електрохімії*: монографія / В. З. Барсуков, Ю. В. Борисенко, О. А. Букет, В. Г. Хоменко; за заг. ред. В. З. Барсукова. – К.: КНУТД, 2016. – С. 199-204. ISBN 978-966-7972-61-5. (*Здобувач встановила закономірності електрокристалізації*, *виступила з доповіддю на конференції*).

3. **Шмичкова, О.**; Лук'яненко, Т.; Величенко, О. Складові малоізношувані аноди з активним шаром на основі PbO_2. В матеріалах Всеукр. наук.-практ. конф. [*«Актуальні проблеми хім. та хім. технол.»*, К.: НУХТ, 2016, 35–36.

(*Здобувач здійснила електрохімічний синтез електродів*, *підготувала тези до друку)*.

4. **Shmychkova, O.**; Luk'yanenko, T.; Velichenko, A. Influence of early stages of PbO_2 nucleation on the phase compostion. In proceedings XIII Intern. conf. on crystal chem. of intermetallic compounds: abstracts, Lviv, 2016, 109. (*Здобувач вивчила нуклеацію покриттів*, *виступила з доповіддю на конференції*).

5. **Шмичкова, О.Б.**; Лук'яненко, Т.В. Електрохімічна руйнація токсичних органічних речовин ароматичної природи − забруднювачів водного середовища. В матеріалах XX міжнар. наук.-техн. конф. [«*Технологія*-2017»], Сєвєродонецьк, 2017, 147–149. (*Здобувач спланувала та провела експеримент*, *підготувала тези до друку)*.

6. **Шмичкова, О.Б.**; Манзюк, М.В.; Мурашевич, Б.В. Електрохімічне окиснення саліцилової кислоти на модифікованих PbO_2-анодах. В матеріалах VIII міжнар. наук.-техн. конф. [«*Хімія та сучасні технології*»], Дніпро, 2017, 56–57. (*Здобувач спланувала та провела експеримент*, *виступила з доповіддю на конференції*).

7. **Shmychkova, O.**; Luk'yanenko, T.; Knysh, V. Electrochemical oxidation of toxic organic aromatic substances. In Promising materials and processes in applied electrochemistry: monograph / editor-in-chief V. Z. Barsukov. – Kyiv: KNUTD, 2017. – Part. – P. 207-213. (ISBN 978-966-7972-79-0). (*Здобувач спланувала та провела експеримент*, *виступила з доповіддю на конференції*).

8. **Shmychkova, O.**; Luk'yanenko, T.; Velichenko, A. Lead dioxide electrocrystallization from nitrate and methanesulfonate electrolytes: the influence of various dopants on initial stages. In ECS Meet. Abstr. – 2017 MA2017-01(38): 1807. (*Здобувач встановила закономірності електрокристалізації*, *підготувала тези до друку)*.

9. **Shmychkova, O.**; Luk'yanenko, T.; Velichenko, A. The influence of various dopants on initial stages of lead dioxide electrocrystallization from nitrate and methanesulfonate electrolytes. In Lead-*Acid Batteries LABAT'2017*, Albena: LabatScience, 2017, 257–290. (входить до наукометричних баз, що індексуються

Scopus). (*Здобувач встановила закономірності електрокристалізації*, *підготувала тези до друку)*.

10. **Shmychkova, O.**; Luk'yanenko, T.; Velichenko, A. Lead dioxide based oxide-surfactant composites. In ECS Meeting: abstracts, Atlanta, GA (USA), 2019, 826. (*Здобувач вивчила властивості покриттів* PbO_2-*ПАР*, *підготувала тези до друку)*.

11. **Шмичкова, О.Б.**; Лук'яненко, Т.В.; Книш, В.О.; та ін. Вплив флуоровмісних поверхнево-активних речовин та поліелектролітів на закономірності електроосадження PbO_2. В *Електрохімія сьогодення: здобутки, проблеми, перспективи*: збірник наукових праць IX Українського з'їзду з електрохімії за участю закордонних вчених, причвячений 90 річниці від дня заснування Інституту загальної та неогрганічної хімії ім В.І. вернадського НАН України, Київ, 2021, 42–43. (*Здобувач встановила вплив довжини флуорокарбонового ланцюга на властивості композитів*, *виступила з доповіддю на конференції*).